BSC

Design Calculation or Analysis Cover Sheet

Complete only applicable items.

1. QA: NA
2. Page 1 of 573

3. System	4. Document Identifier
Geologic Repository Operations Area	000-PSA-MGR0-02200-000-00A

5. Title

Development of Equipment Seismic Fragilities at Yucca Mountain Surface Facilities

6. Group

Bechtel SAIC Company, LLC (BSC), L&NS, Preclosure Safety Analysis (PCSA)

7. Document Status Designation

☐ Preliminary ☒ Committed ☐ Confirmed ☐ Cancelled/Superseded

8. Notes/Comments

Deborah Finney and Steven Carlson provided support for technical product inputs.

Wen H. Tong, Stephen A. Short, and Robert D. Campbell prepared and checked various attachments, see Section 5.0, List of Attachments.

All attachments have been independently reviewed by Robert J. Budnitz.

Attachments	Total Number of Pages
See Section 5.0, List of Attachments	524

RECORD OF REVISIONS

9. No.	10. Reason For Revision	11. Total # of Pgs.	12. Last Pg. #	13. Originator (Print/Sign/Date)	14. Checker (Print/Sign/Date)	15. EGS (Print/Sign/Date)	16. Approved/Accepted (Print/Sign/Date)
00A		573	N-38	Greg S. Hardy 2/22/08	Robert C. Murray 2/22/08	Michael V. Frank Dan'l Moore for 3/07/08	Mark R. Wisenburg 3/05/2008

DISCLAIMER

The calculations contained in this document were developed by ARES Corporation (ARES) and checked by Lawrence Livermore National Laboratory (LLNL), and are intended solely for the use of Bechtel SAIC Company, LLC (BSC) in its work for the Yucca Mountain Project.

CONTENTS

LIST OF FIGURES

Page

LIST OF TABLES

Page

ACRONYMS AND ABBREVIATIONS

ACI	American Concrete Institute
AISC	American Institute of Steel Construction
ANSI	American National Standards Institute
AO	Aging Overpack
APE	Annual Probably of Exceedance
ARES	ARES Corporation
ASCE	American Society of Civil Engineers
ASME	American Society of Mechanical Engineers
BSC	Bechtel SAIC, LLC
BDBGM	Beyond Design Basis Ground Motion at $1x10^{-4}$ APE
CDF	Core Damage Frequency
CDFM	Conservative Deterministic Failure Margin
CFR	Code of Federal Regulation
CHC	Cask Handling Crane
CIP	Cast-in-Place
CRCF	Canister Receipt and Closure Facility
CTM	Canister Transfer Machine
CTT	Cask Transfer Trolley
DBGM-2	Design Basis Ground Motion at $5x10^{-4}$ APE
DL	Dead Load
DOE	U.S. Department of Energy
DOF	Degree of Freedom
DPC	Dual Purpose Canister
EPRI	Electric Power Research Institute
g	Unit of gravitational acceleration (32.2 ft/sec^2)
GROA	Geologic Repository Operations Area
HCLPF	High Confidence of Low Probability of Failure

ACRONYMS AND ABBREVIATIONS (cont.)

HLW	High Level Waste
HVAC	Heating, Ventilation, & Air Conditioning
IEEE	Institute of Electrical and Electronics Engineers
IHF	Initial Handling Facility
IPEEE	Individual Plant Examination for External Events (NRC Program)
ISRS	In-Structure Response Spectra
ITS	Important to Safety
LA	License Application
LBNL	Lawrence Berkeley National Laboratory
LLNL	Lawrence Livermore National Laboratory
MAPE	Mean Annual Probability of Exceedance
NPP	Nuclear Power Plant
NRC	U.S. Nuclear Regulatory Commission
PCSA	Preclosure Safety Analysis
PGA	Peak Ground Acceleration
PRA	Probabilistic Risk Assessment
PSA	Probabilistic Safety Analysis
PSHA	Probabilistic Seismic Hazard Analysis
QA	Quality Assurance
RF	Receipt Facility
RRS	Required Response Spectrum
Sa	Spectral Acceleration
SASSI	System for Analysis of Soil-Structure Interaction
SEL	Seismic Equipment List
SFA	Surface Facilities Area
SFTM	Spent Fuel Transfer Machine
SPCSA	Seismic Preclosure Safety Analysis

ACRONYMS AND ABBREVIATIONS (cont.)

SPRA	Seismic Probabilistic Risk Assessment
SRSS	Square Root of the Sum of Squares
SSE	Safe Shutdown Earthquake (used with NPPs)
SSI	Soil Structure Interaction
SSC	Structure, System, and Component
TAD	Transportation, Aging, and Disposal canister
TEV	Transport and Emplacement Vehicle
TRS	Test Response Spectrum
UHS	Uniform Hazard Spectra
USDOE	United States Department of Energy
USNRC	United States Nuclear Regulatory Commission
WHF	Wet Handling Facility
WP	Waste Package
WPTT	Waste Package Transfer Trolley
YMRP	Yucca Mountain Review Plan
YMSF	Yucca Mountain Surface Facilities
ZPA	Zero Period Acceleration

FRAGILITY TERMINOLOGY

A	Ground Motion Parameter Corresponding to Any Given Frequency of Failure
Am	Median Peak Ground Motion Capacity
β_C	Composite Variability = $(\beta_R^2 + \beta_U^2)^{0.5}$
$\beta_{C\text{-}C}$	Capacity Factor Variability
$\beta_{C\text{-}RS}$	Response Factor Variability
$\beta_{C\text{-}S}$	Strength Composite Variability (typical)
β_R	Log Standard Deviation of Randomness
β_{R_S}	Strength Randomness (typical)

FRAGILITY TERMINOLOGY (cont.)

β_U	Log Standard Deviation of Uncertainty (Lack of Knowledge)
β_{U_S}	Strength Uncertainty (typical)
ε_R	Random Variable with Unit Median and Logarithmic Standard Deviation, β_R
ε_U	Uncertainty Variable with Unit Median and Logarithmic Standard Deviation, β_U
F	Factor of Safety
F_δ	Damping Factor of Safety
F_μ	Inelastic Energy Absorption Factor of Safety
F_C	Capacity Factor
F_{ECC}	Earthquake Component Combination Factor of Safety
F_{GMI}	Ground Motion Incoherence Factor of Safety
F_M	Modeling Factor of Safety
F_{MC}	Modal Combination Factor of Safety
F_{QM}	Qualification Factor of Safety
F_{RE}	Equipment Response Factor of Safety
F_{RS}	Structural Response Factor of Safety
F_S	Strength Factor of Safety
F_{SA}	Spectral Shape Factor of Safety
F_{SSI}	Soil-Structure Interaction Factor of Safety
F_{TOTAL}	Total Factor of Safety
P_N	Normal Operating Loads
P_T	Total Load (Sum of Seismic Load and Normal Operating Load)
S	Strength of Structural Element

INTENTIONALLY LEFT BLANK

1. Purpose

The purpose of this seismic fragility calculation is to support the seismic PCSA approach that the DOE will use to allow the NRC to find, with reasonable assurance, that preclosure seismic design of the surface nuclear facilities satisfies the preclosure performance objectives contained in 10 CFR 63.111 (Reference 2.1.3, Section 63.111(b)(2)). The seismic PCSA approach utilizes seismic fragility analysis methods for the safety-related equipment necessary to demonstrate performance consistent with the risk-informed performance-based framework of the regulation. The methodology for performing the seismic fragility along with the actual fragility results for the key Yucca Mountain Surface Facility (YMSF) equipment is described herein. The fourteen items selected for fragility evaluation were identified by BSC.

2. REFERENCES

This analysis was performed relying on the reference material listed in this section. Its validity is based on an accurate representation of the information in these references. If some of these references have been superseded, that information has not been included in this analysis and it would be inappropriate to reference it.

2.1 PROCEDURES/DIRECTIVES

2.1.1. EG-PRO-3DP-G04B-00037, Rev. 10. *Calculations and Analyses.* Las Vegas, Nevada: Bechtel SAIC Company. ACC: ENG.20071018.0001.

2.1.2. IT-PRO-0011, Rev. 007. *Software Management.* Las Vegas, Nevada: Bechtel SAIC Company. ACC: DOC.20070905.0007.

2.1.3. 10 CFR 63. 2007. *Energy: Disposal of High-Level Radioactive Wastes in a Geologic Repository at Yucca Mountain,* Nevada. Internet Accessible. [DIRS 180319].

2.1.4. NRC (U.S. Nuclear Regulatory Commission) 2006. *Interim Staff Guidelines – HLWRS-ISG-01, Review Methodology for Seismically Initiated Event Sequences*. HLWRS-ISG-01. Washington, D.C. U.S. Nuclear Regulatory Commission. ACC: MOL.20061128.0036, [DIRS 178130].

2.1.5. NRC (U.S. Nuclear Regulatory Commission) 2003. *Yucca Mountain Review Plan, Final Report*. NUREG-1804, Rev. 2. Washington, D.C.: U.S. Nuclear Regulatory Commission, Office of Nuclear Material Safety and Safeguards. TIC: 254568, [DIRS 163274].

2.1.6. ORD (Office of Repository Development) 2007. *Repository Project Management Automation Plan*. 000-PLN-MGR0-00200-000, Rev. 00E. Las Vegas, Nevada: U.S. Department of Energy, Office of Repository Development. ACC: ENG.20070326.0019, [DIRS 182418].

2.2 DESIGN INPUTS

2.2.1 [Reserved]

2.2.2 ASCE/SEI 43-05. 2005. *Seismic Design Criteria for Structures, Systems, and Components in Nuclear Facilities.* Reston, Virginia: American Society of Civil Engineers. TIC:257275. [DIRS 173805].

2.2.3 YMP (Yucca Mountain Site Characterization Project) 1997. *Methodology to Assess Fault Displacement and Vibratory Ground Motion Hazards at Yucca Mountain.* Topical Report YMP/TR-002-NP, REV 1. Las Vegas, Nevada: Yucca Mountain Site Characterization Office. ACC: MOL.19971016.0777. [DIRS 100522].

2.2.4 MO0801HCUHSSFA.001. *Mean Hazard Curves and Mean Uniform Hazard Spectra for the Surface Facilities Area.* Submittal date: 01/11/2008, [DIRS 184802].

2.2.5 DOE (U.S. Department of Energy) 2007. *Preclosure Seismic Design and Performance Demonstration Methodology for a Geologic Repository at Yucca Mountain Topical Report.* YMP/TR-003-NP, Rev 5. Las Vegas, Nevada: U.S. Department of Energy, Office of Civilian Radioactive Waste Management. ACC: DOC.20070625.0013 [DIRS 181572].

2.2.6 EPRI (Electric Power Research Institute) 1994. *Methodology for Developing Seismic Fragilities.* EPRI TR-103959. Palo Alto, California: Electric Power Research Institute. TIC: 253770. [DIRS 161329].

2.2.7 Kennedy, R.P. 2001. "Overview of Methods for Seismic PRA and Margin Analysis Including Recent Innovations." *Proceedings of the OECD/NEA Workshop on Seismic Risk, Committee on the Safety of Nuclear Installations PWG3 and PWG5, Hosted by the Japan Atomic Energy Research Institute under the Sponsorship of the Science Technology Agency, 10-12 August, 1999, Tokyo, Japan. NEA/CSNI/R(99)28, 33-63*. Paris, France: Organization for Economic Co-operation and Development, Nuclear Energy Agency. TIC: 253825 [DIRS 155940].

2.2.8 BSC (Bechtel SAIC Company) 2008. *Supplemental Earthquake Ground Motion Input for a Geologic Repository at Yucca Mountain, NV*. MDL-MGR-GS-000007 REV 00. Las Vegas, Nevada: Bechtel SAIC Company. ACC: DOC.20080221.0001. [DIRS 183776].

Table 1 provides cross references from the main body of this calculation to the attachment references.

2.3 DESIGN CONSTRAINTS

None.

2.4 DESIGN OUTPUTS

This calculation developed the seismic fragilities for selected critical surface facility equipment which will be used within the preclosure safety analysis process.

Table 1. Cross References from Master Document Reference to Attachment References

MASTER DOCUMENT	MASTER DOCUMENT REFERENCE	ATTACHMENT REFERENCES A-N = ATTACHMENTS N.N.N = ATTACHMENT REFERENCE NO.
2.1.3	10 CFR 63. 2007. Energy: Disposal of High-Level Radioactive Wastes in a Geologic Repository at Yucca Mountain, Nevada. Internet Accessible. [DIRS 180319]	
	ACI 349-01. 2001. *Code Requirements for Nuclear Safety Related Concrete Structures (ACI 349-01).* Farmington Hills, Michigan: American Concrete Institute. TIC: 252732. [DIRS 158833]	K2.2.5, L2.2.5
	AISC (American Institute of Steel Construction) 1991. *Manual of Steel Construction, Allowable Stress Design.* 9th Edition, 1st Revision. Chicago, Illinois: American Institute of Steel Construction. TIC: 4254. [DIRS 127579]	A2.2.10, D2.2.10, I2.2.10, K2.2.4, N2.2.13
	ANSI/AISC N690-1994. 1994. *American National Standard Specification for the Design, Fabrication, and Erection of Steel Safety-Related Structures for Nuclear Facilities.* Chicago, Illinois: American Institute of Steel Construction. TIC: 252734. [DIRS 158835]	A2.2.11, D2.2.11, I2.2.11, K2.2.6, L2.2.6, N2.2.6
2.2.2	ASCE/SEI 43-05. 2005. *Seismic Design Criteria for Structures, Systems, and Components in Nuclear Facilities.* Reston, Virginia: American Society of Civil Engineers. TIC: 257275. [DIRS 173805]	C2.2.8, E2.2.7, F2.2.2, G2.2.8, H2.2.2, J2.2.2, K2.2.2, L2.2.2, N2.2.2
	ASME B31.3-2004. 2005. *Process Piping.* New York, New York: American Society of Mechanical Engineers. TIC: 258076. [DIRS 176242]	K2.2.8
	ASME NOG-1-2004. 2005. *Rules for Construction of Overhead and Gantry Cranes (Top Running Bridge, Multiple Girder).* New York, New York: American Society of Mechanical Engineers. TIC: 257672. [DIRS 176239]	A2.2.6, B2.2.2, C2.2.7, D2.2.6, E2.2.5, F2.2.7, G2.2.7, H2.2.9, I2.2.6
	Baltay, P. and Gjelsvik, A. 1990. "Coefficient of Friction for Steel on Concrete at High Normal Stress." *Journal of Materials in Civil Engineering, 2,* (1), 46-49. [New York, New York]: American Society of Civil Engineers. TIC: 260005. [DIRS 184424]	C2.2.13, E2.2.10, G2.2.14
	Blevins, R.D. 2001. *Formulas for Natural Frequency and Mode Shape.* 1st Edition. Malabar, Florida: Krieger Publishing Company. ISBN 1-57524-184-6. 506 pp.	L2.2.13, N2.2.8

MASTER DOCUMENT	MASTER DOCUMENT REFERENCE	ATTACHMENT REFERENCES A-N = ATTACHMENTS N.N.N = ATTACHMENT REFERENCE NO.
	BSC (Bechtel SAIC Company) 2007. *Basis of Design for the TAD Canister-Based Repository Design Concept.* 000-3DR-MGR0-00300-000-001. Las Vegas, Nevada: Bechtel SAIC Company. ACC: ENG.20071002.0042; ENG.20071026.0033; ENG.20071108.0002; ENG.20071109.0001; ENG.20071120.0023; ENG.20071126.0049; ENG.20071214.0009; ENG.20071213.0005; ENG.20071227.0018; ENG.20080207.0004; ENG.20080212.0003. [DIRS 182131]	L2.2.18, N2.2.15
	BSC (Bechtel SAIC Company) 2008. *Canister Receipt and Closure Facility 1 General Arrangement Ground Floor Plan.* 060-P10-CR00-00102-000 REV 00C. Las Vegas, Nevada: Bechtel SAIC Company. ACC: ENG.20080122.0013. [DIRS 184853]	A.2.2.3, C2.2.3, D.2.2.3, F2.2.5, H2.2.5, J2.2.6, K2.2.11, L2.2.15, N2.2.10
	BSC (Bechtel SAIC Company) 2007. *Canister Receipt and Closure Facility 1 General Arrangement Legend and General Notes.* 060-P10-CR00-00101-000 REV 00B. Las Vegas, Nevada: Bechtel SAIC Company. ACC: ENG.20071212.0002. [DIRS 184371]	B2.2.1
	BSC (Bechtel SAIC Company) 2007. *Canister Receipt and Closure Facility Cask Handling Crane Mechanical Equipment Envelope.* 060-MJ0-HM00-00101-000 REV 00A. Las Vegas, Nevada: Bechtel SAIC Company. ACC: ENG.20070304.0009; ENG.20070702.0010; ENG.20070823.0008. [DIRS 178459]	A2.2.8
	BSC (Bechtel SAIC Company) 2006. *Canister Receipt and Closure Facility (CRCF) Seismic Analysis.* 060-SYC-CR00-00400-000-00A. Las Vegas, Nevada: Bechtel SAIC Company. ACC: ENG.20061220.0029. [DIRS 178793]	A2.2.15, L2.2.17, N2.2.12
	BSC (Bechtel SAIC Company) 2007. *Cask Transfer Trolley Mechanical Equipment Envelope.* V0-CY05-QHC4-00459-00033-001 REV 004. Las Vegas, Nevada: Bechtel SAIC Company. ACC: ENG.20071019.0004. [DIRS 183505], [DIRS 184084], [DIRS 184085]	C2.2.2
	BSC (Bechtel SAIC Company) 2008. *CRCF 1 DOE Canister Staging Rack Mechanical Equipment Envelope.* 060-MJ0-HTC0-00501-000 REV 00B. Las Vegas, Nevada: Bechtel SAIC Company. ACC: ENG.20080128.0002. [DIRS 184908]	N2.2.4
	BSC (Bechtel SAIC Company) 2007. *CRCF-1 and IHF WP Transfer Trolley*	F2.2.6

MASTER DOCUMENT	MASTER DOCUMENT REFERENCE	ATTACHMENT REFERENCES A-N = ATTACHMENTS N.N.N = ATTACHMENT REFERENCE NO.
	Mechanical Equipment Envelope Plan & Elevations-Sh 1 of 2. 000-MJ0-HL00-00101-000 REV 00B. Las Vegas, Nevada: Bechtel SAIC Company. ACC: ENG.20071027.0015. [DIRS 183729]	
	BSC (Bechtel SAIC Company) 2007. *CRCF-1 and IHF WP Transfer Trolley Mechanical Equipment Envelope Elevation & Detail - Sheet 2.* 000-MJ0-HL00-00102-000 REV 00B. Las Vegas, Nevada: Bechtel SAIC Company. ACC: ENG.20071027.0017. [DIRS 183730]	F2.2.13
	BSC (Bechtel SAIC Company) 2008. *CRCF 1 TAD Canister Staging Rack Mechanical Equipment Envelope.* 060-MJ0-HTC0-00601-000 REV 00B. Las Vegas, Nevada: Bechtel SAIC Company. ACC: ENG.20080128.0003. [DIRS 184909]	N2.2.5
	BSC (Bechtel SAIC Company) 2006. *CRCF, IHF, RF, and WHF Canister Transfer Machine Mechanical Equipment Envelope.* 000-MJ0-HTC0-00201-000 REV 00A. Las Vegas, Nevada: Bechtel SAIC Company. ACC: ENG.20061120.0011; ENG.20070307.0006; ENG.20070601.0025; ENG.20070823.0002; ENG.20080103.0009. [DIRS 178630]	B2.2.9, D2.2.8
	BSC (Bechtel SAIC Company) 2007. *CRCF Loadout Platforms Mechanical Equipment Envelope Sheet 1 of 2.* 060-MJ0-HL00-00201-000 REV 00A. Las Vegas, Nevada: Bechtel SAIC Company. ACC: ENG.20070315.0009; ENG.20070823.0007. [DIRS 181725]	H2.2.6
	BSC (Bechtel SAIC Company) 2007. *CRCF Tier-1 In-Structure Response Spectra.* 060-SYC-CR00-00900-000-00B. Las Vegas, Nevada: Bechtel SAIC Company. ACC: ENG.20071210.0008. [DIRS 184330]	A2.2.2, B2.2.5, C2.2.10, D2.2.2, F2.2.3, G2.2.10, H2.2.3, J2.2.4, K2.2.3, L2.2.3, N2.2.3
	BSC (Bechtel SAIC Company) 2007. *Emplacement and Retrieval Transport and Emplacement Vehicle Mechanical Equipment Envelope.* 800-MJ0-HE00-00101-000 REV 00B. Las Vegas, Nevada: Bechtel SAIC Company. ACC: ENG.20070918.0041. [DIRS 183353]	H2.2.7
	BSC (Bechtel SAIC Company) 2007. *Initial Handling Facility Cask Transfer Trolley - 265T Mechanical Equipment Envelope*. V0-CY05-QHC4-00459-00072-001 REV 001. Las Vegas, Nevada: Bechtel SAIC Company. ACC: ENG.20071022.0015.	E2.2.2

MASTER DOCUMENT	MASTER DOCUMENT REFERENCE	ATTACHMENT REFERENCES A-N = ATTACHMENTS N.N.N = ATTACHMENT REFERENCE NO.
	[DIRS 183511] [DIRS 184112]	
	BSC (Bechtel SAIC Company) 2007. *Initial Handling Facility General Arrangement Ground Floor Plan.* 51A-P10-IH00-00102-000 REV 00C. Las Vegas, Nevada: Bechtel SAIC Company. ACC: ENG.20071226.0017; ENG.20080121.0016. [DIRS 184529]	E2.2.3
	BSC (Bechtel SAIC Company) 2007. *Initial Handling Facility (IHF): Tier-1 In-Structure Response Spectra.* 51A-SYC-IH00-00600-000 REV 00A. Las Vegas, Nevada: Bechtel SAIC Company. ACC: ENG.20071130.0013. [DIRS 184106]	E2.2.8
	BSC (Bechtel SAIC Company) 2007. *Mechanical Handling Design Report Cask Transfer Trolley (240 Ton & 265 Ton Capacity).* V0-CY05-QHC4-00459-00016-001 REV 006. Las Vegas, Nevada: Bechtel SAIC Company. ACC: ENG.20071018.0017. [DIRS 184122]	C2.2.6, E2.2.4
	BSC (Bechtel SAIC Company) 2007. *Mechanical Handling Design Report for Cranes and Special Lifting Devices.* 000-30R-WHS0-01700-000 REV 001. Las Vegas, Nevada: Bechtel SAIC Company. ACC: ENG.20071101.0026. [DIRS 183727]	B2.2.3
	BSC (Bechtel SAIC Company) 2008. *Mechanical Handling Design Report: Shield Doors, Gates and Windows.* 000-30R-MR00-00100-000 REV 001. Las Vegas, Nevada: Bechtel SAIC Company. ACC: ENG.20080206.0065.	L2.2.4
	BSC (Bechtel SAIC Company) 2007. *Mechanical Handling Design Report – Site Transporter*. 170-30R-HAT0-00100-000-000. Las Vegas, Nevada: Bechtel SAIC Company. ACC: ENG.20071217.0015. [DIRS 184489]	G2.2.6
	BSC (Bechtel SAIC Company). *Mechanical Handling Design Report – Spent Fuel Transfer Machine*. 050-30R-HT00-00100-000 Rev 000. Las Vegas, Nevada: Bechtel SAIC Company. ACC: ENG.20071031.0009. [DIRS 184459]	I2.2.4
	BSC (Bechtel SAIC Company) 2007. *Mechanical Handling Design Report - Waste Package Transfer Trolley.* 000-30R-WHS0-01200-000 REV 000. Las Vegas, Nevada: Bechtel SAIC Company. ACC: ENG.20071006.0001. [DIRS 183209]	F2.2.4

MASTER DOCUMENT	MASTER DOCUMENT REFERENCE	ATTACHMENT REFERENCES A-N = ATTACHMENTS N.N.N = ATTACHMENT REFERENCE NO.
	BSC (Bechtel SAIC Company) 2007. *Mechanical Handling Design Report: Waste Package Transport and Emplacement Vehicle.* 000-30R-HE00-00200-000 REV 001. Las Vegas, Nevada: Bechtel SAIC Company. ACC: ENG.20071205.0002. [DIRS 184221]	H2.2.4
	BSC (Bechtel SAIC Company) 2007. *Nuclear Facilities Buildings Canister Receipt and Closure Facility #1 Details and Sections*. 060-DB0-CR00-00112-000 REV 00B, Las Vegas, Nevada: Bechtel SAIC Company. ACC: ENG.20080117.0036.	F2.2.16
	BSC (Bechtel SAIC Company) 2007. *Nuclear Facilities Equipment Shield Door-Type 1 Mechanical Equipment Envelope.* 000-MJ0-H000-00701-000 REV 00C. Las Vegas, Nevada: Bechtel SAIC Company. ACC: ENG.20071205.0016; ENG.20080213.0003. [DIRS 184352]	L2.2.8
	BSC (Bechtel SAIC Company) 2007. *Nuclear Facilities Equipment Shield Door—Type 2 Mechanical Equipment Envelope.* 000-MJ0-H000-00801-000 REV 00C. Las Vegas, Nevada: Bechtel SAIC Company. ACC: ENG.20071205.0017. [DIRS 184358]	L2.2.9
	BSC (Bechtel SAIC Company) 2007. *Nuclear Facilities Equipment Shield Door-Type 3 Mechanical Equipment Envelope.* 000-MJ0-H000-00901-000 REV 00C. Las Vegas, Nevada: Bechtel SAIC Company. ACC: ENG.20071205.0018. [DIRS 184359]	L2.2.10
	BSC (Bechtel SAIC Company) 2007. *Nuclear Facilities Equipment Shield Door-Type 4 Mechanical Equipment Envelope.* 000-MJ0-H000-01001-000 REV 00B. Las Vegas, Nevada: Bechtel SAIC Company. ACC: ENG.20071205.0019; ENG.20080131.0008. [DIRS 184360]	L2.2.11
	BSC (Bechtel SAIC Company) 2007. *Nuclear Facilities Equipment Shield Door-Type 5 Mechanical Equipment Envelope.* 000-MJ0-H000-01101-000 REV 00B. Las Vegas, Nevada: Bechtel SAIC Company. ENG.20071205.0020. [DIRS 184361]	L2.2.12
	BSC (Bechtel SAIC Company) 2007. *Preliminary Throughput Study for the Canister Receipt and Closure Facility.* 060-30R-CR00-00100-000 REV 001. Las Vegas, Nevada: Bechtel SAIC Company. ACC ENG.20071101.0001.	D.2.2.14

MASTER DOCUMENT	MASTER DOCUMENT REFERENCE	ATTACHMENT REFERENCES A-N = ATTACHMENTS N.N.N = ATTACHMENT REFERENCE NO.
	BSC (Bechtel SAIC Company) 2007. *Project Design Criteria Document.* 000-3DR-MGR0-00100-000-007. Las Vegas, Nevada: Bechtel SAIC Company. ACC: ENG.20071016.0005; ENG.20071108.0001; ENG.20071220.0003; ENG.20080107.0001; ENG.20080107.0002; ENG.20080107.0016; ENG.20080107.0017; ENG.20080131.0006. [DIRS 179641]	A2.2.5, D2.2.5
	BSC (Bechtel SAIC Company) 2005. *Q-List.* 000-30R-MGR0-00500-000-003. Las Vegas, Nevada: Bechtel SAIC Company. ACC: ENG.20050929.0008. [DIRS 175539]	C2.1.2, E2.1.2, G2.1.2
	BSC (Bechtel SAIC Company) 2007. *Quality Management Directive.* QA-DIR-10, Rev. 2. Las Vegas, Nevada: Bechtel SAIC Company. ACC: DOC.20080103.0002. [DIRS 184673]	C2.1.4, E2.1.4, G2.1.4
	BSC (Bechtel SAIC Company) 2006. *Seismic Analysis and Design Approach Document.* 000-30R-MGR0-02000-000 REV 001. Las Vegas, Nevada: Bechtel SAIC Company. ACC: ENG.20071220.0029. [DIRS 184494]	B2.2.13, F2.2.17, J2.2.8, K2.2.13, L2.2.19, N2.2.16
	BSC (Bechtel SAIC Company) 2007. *Site Transporter Mechanical Equipment Envelope.* V0-CY05-QHC4-00459-00032-001 REV 004. Las Vegas, Nevada: Bechtel SAIC Company. ACC: ENG.20071022.0010. [DIRS 183527]	G2.2.2
	BSC (Bechtel SAIC Company) 2007. *Site Transporter Site Interface Drawing.* V0-CY05-QHC4-00459-00054-001 REV 002. Las Vegas, Nevada: Bechtel SAIC Company. ACC: ENG.20071024.0019. [DIRS 184419]	G2.2.4
	BSC (Bechtel SAIC Company) 2007. *Transport and Emplacement Vehicle Envelope Calculation.* 800-MQC-HE00-00100-000 REV 00B. Las Vegas, Nevada: Bechtel SAIC Company. ACC: ENG.20070830.0043. [DIRS 183139]	H2.2.8
	BSC (Bechtel SAIC Company) 2007. *Wet Handling Facility General Arrangement Ground Floor Plan.* 050-P10-WH00-00102-000 REV 00B. Las Vegas, Nevada: Bechtel SAIC Company. ACC: ENG.20071206.0032; ENG.20071226.0001; ENG.20080121.0014; ENG.20080121.0015. [DIRS 184274]	I2.2.3
	BSC (Bechtel SAIC Company) 2006. *Wet Handling Facility Spent Fuel Transfer*	I2.2.8

MASTER DOCUMENT	MASTER DOCUMENT REFERENCE	ATTACHMENT REFERENCES A-N = ATTACHMENTS N.N.N = ATTACHMENT REFERENCE NO.
	Machine Mechanical Equipment Envelope. 050-M90-HT00-00101-000 REV 00A. Las Vegas, Nevada: Bechtel SAIC Company. ACC: ENG.20061120.0016; ENG.20070207.0001; ENG.20070823.0003. [DIRS 178631]	
	BSC (Bechtel SAIC Company) 2007. *WHF Tier-1 In-Structure Response Spectra.* 050-SYC-WH00-01000-000 REV 00A. Las Vegas, Nevada: Bechtel SAIC Company. ACC: ENG.20070924.0046. [DIRS 184254]	I2.2.2
	BSC (Bechtel SAIC Company) 2007. *Yucca Mountain Project Engineering Specification Wet Handling Facility Spent Fuel Transfer Machine.* 050-3PS-HTF0-00100-000 REV 00A. Las Vegas, Nevada: Bechtel SAIC Company. ACC: ENG.20070829.0010.	I2.2.15
	BSC (Bechtel SAIC Company) 2007. *Yucca Mountain Seismic Analysis of 265 Ton Cask Transfer Trolley*. V0-CY05-QHC4-00459-00070-001 REV 001. Las Vegas, Nevada: Bechtel SAIC Company. ACC: ENG.20071018.0021. [DIRS 183501]	E2.2.6
	BSC (Bechtel SAIC Company) 2007. *Yucca Mountain Seismic Analysis of Cask Transfer Trolley*. V0-CY05-QHC4-00459-00020-001 REV 004. Las Vegas, Nevada: Bechtel SAIC Company. ACC: ENG.20071018.0018. [DIRS 183539]	C2.2.14
	BSC (Bechtel SAIC Company) 2007. *Yucca Mountain Site Transporter – Preliminary Seismic Analysis*. V0-CY05-QHC4-00459-00079-001 REV 001. Las Vegas, Nevada: Bechtel SAIC Company. ACC: ENG.20071024.0014. [DIRS 183530]	G2.2.5
2.2.8	BSC (Bechtel SAIC Company) 2007. *Supplemental Earthquake Ground Motion Input for a Geologic Repository at Yucca Mountain, NV.* MDL-MGR-GS-000007 REV 00. Las Vegas, Nevada: Bechtel SAIC Company. ACC: DOC.20080221.0001. [DIRS 183776]	
	Budnitz, R.J.; Lambert, H.E.; Apostolakis, G.; Salas, J.K.; Wu, J.S.; and Ravindra, M.K. 1998. *A Methodology for Analyzing Precursors to Earthquake-Initiated and Fire-Initiated Accident Sequences.* NUREG/CR-6544. Washington, D.C.: U.S. Nuclear Regulatory Commission. ACC: MOL.20080122.0254. [DIRS 184644]	M2.2.2
	Campbell, R.D., Ravindra, M.K., Bhatia, A., and Murray, R.C. 1985. *Compilation of*	M2.2.3

MASTER DOCUMENT	MASTER DOCUMENT REFERENCE	ATTACHMENT REFERENCES A-N = ATTACHMENTS N.N.N = ATTACHMENT REFERENCE NO.
	Fragility Information from Available Probabilistic Risk Assessments. UCID-20571. Livermore, CA: Lawrence Livermore National Laboratory. ACC: MOL.20080207.0023. [DIRS 184646]	
2.2.5	DOE (U.S. Department of Energy) 2007. *Preclosure Seismic Design and Performance Demonstration Methodology for a Geologic Repository at Yucca Mountain Topical Report.* YMP/TR-003-NP, Rev. 5. Las Vegas, Nevada: U.S. Department of Energy, Office of Civilian Radioactive Waste Management. ACC: DOC.20070625.0013. [DIRS 181572]	
	DOE (U.S. Department of Energy) 2007. *Transportation, Aging and Disposal Canister System Performance Specification.* WMO-TADCS-000001, Rev. 0. Washington, D.C.: U.S. Department of Energy, Office of Civilian Radioactive Waste Management. ACC: DOC.20070614.0007. [DIRS 181403]	B2.2.10
2.1.1	EG-PRO-3DP-G04B-00037, Rev. 10. *Calculations and Analyses*. Las Vegas, Nevada: Bechtel SAIC Company. ACC: ENG.20071018.0001.	A2.1.1, B2.1.1, C2.1.1, D2.1.1, E2.1.1, F2.1.1, G2.1.1, H2.1.1, I2.1.1, J2.1.1, K2.1.1, L2.1.1, M2.1.1, N2.1.1
	EPRI (Electric Power Research Institute) 1991. *A Methodology for Assessment of Nuclear Power Plant Seismic Margin (Revision 1).* EPRI NP-6041-SL, Rev. 1. Palo Alto, California: Electric Power Research Institute. TIC: 253771. [DIRS 161330]	F2.2.12, K2.2.7
2.2.6	EPRI (Electric Power Research Institute) 1994. *Methodology for Developing Seismic Fragilities.* EPRI TR-103959. Palo Alto, California: Electric Power Research Institute. TIC: 253770. [DIRS 161329]	A2.2.1, B2.2.4, C2.2.1, D2.2.1, E2.2.1, F2.2.1, G2.2.1, H2.2.1, I2.2.1, J2.2.1, K2.2.1, L2.2.1, M2.2.1, N2.2.1
	Hajje, N. 2007. "FW: Contact Us Form Submittal from Web Site." E-mail from N. Hajje (Fabreeka) to E.C. Blom, November 15, 2007, without attachment. ACC: LLR.20080110.0148. [DIRS 184845]	G2.2.13
	Huang, H.C. and Marsh, L. 2004. "Slack Rope Analysis for Moving Crane System." *13th World Conference on Earthquake Engineering, August 1-6, 2004, Paper 3190.* Tokyo, Japan: International Association for Earthquake Engineering. TIC: 260006. [DIRS 184779]	B2.2.7

MASTER DOCUMENT	MASTER DOCUMENT REFERENCE	ATTACHMENT REFERENCES A-N = ATTACHMENTS N.N.N = ATTACHMENT REFERENCE NO.
	IEEE Std 344-2004. 2005. *IEEE Recommended Practice for Seismic Qualification of Class 1E Equipment for Nuclear Power Generating Stations.* New York, New York: Institute of Electrical and Electronics Engineers. TIC: 258050. [DIRS 176259]	J2.2.3
2.1.2	IT-PRO-0011, Revision 7, ICN 0. *Software Management.* Las Vegas, Nevada: Bechtel SAIC Company. ACC: DOC.20070905.0007.	A2.1.3, B2.1.2, C2.1.3, D2.1.3, E2.1.3, F2.1.2, G2.1.3, H2.1.2, I2.1.2, J2.1.2, K2.1.2, L2.1.2, M2.1.2, N2.1.2
	Jacobsen, L.S. and Ayre, R.S. 1958. *Engineering Vibrations With Applications to Structures and Machinery*. New York, New York: McGraw Hill Book Company. Library of Congress No. 57013334, 564 pp.	B2.2.12
2.2.7	Kennedy, R.P. 2001. "Overview of Methods for Seismic PRA and Margin Analysis Including Recent Innovations." Proceedings of the OECD/NEA Workshop on Seismic Risk, Committee on the Safety of Nuclear Installations PWG3 and PWG5, Hosted by the Japan Atomic Energy Research Institute under the Sponsorship of the Science Technology Agency, 10-12 August, 1999, Tokyo, Japan. NEA/CSNI/R(99)28, 33-63. Paris, France: Organization for Economic Co-operation and Development, Nuclear Energy Agency. TIC: 253825. [DIRS 155940]	
2.2.4	MO0801HCUHSSFA.001. Mean Hazard Curves and Mean Uniform Hazard Spectra for the Surface Facilities Area. Submittal date: 01/11/2008. [DIRS 184802]	A2.2.7, B2.2.6, C2.2.9, D2.2.7, E2.2.9, F2.2.9, G2.2.9, H2.2.10, I2.2.7, J2.2.5, K2.2.10, L2.2.14, N2.2.9
	Moore, D. 2007. "RE: Canister and Cask Physical Dimensions." E-mail from D. Moore to W-H. Tong, October 31, 2007. ACC: LLR.20080128.0003. [DIRS 184927]	A2.2.14
	Moore, D. 2007. "Re: FW: Cranes: Slack Rope Conditions and Pendulum Effects." E-mail from D. Moore to W-H. Tong, December 17, 2007, with attachments. ACC: LLR.20080110.0147. [DIRS 184844]	B2.2.8
	Moore, D. 2007. "Re: WPTT Question." E-mail from D. Moore to R. Campbell (rdc956), October 31, 2007. ACC: LLR.20080110.0146. [DIRS 184843]	F2.2.10
	Moore, D. 2007. "SSI Factor of Safety." E-mail from D. Moore to B. Murray, October 25, 2007. ACC: LLR.20080110.0145. [DIRS 184842]	A2.2.13, B2.2.11, D2.2.13, F2.2.14, H2.2.13, I2.2.13, J2.2.7, K2.2.12, L2.2.16,

MASTER DOCUMENT	MASTER DOCUMENT REFERENCE	ATTACHMENT REFERENCES A-N = ATTACHMENTS N.N.N = ATTACHMENT REFERENCE NO.
		N2.2.11
	Moore, D. 2007. "Staging Racks." E-mail from D. Moore to S. Short (ARES Corp.), November 28, 2007. ACC: LLR.20080128.0004. [DIRS 184928]	N2.2.14
	Newmark, N.M. and Hall, W.J. 1978. *Development of Criteria for Seismic Review of Selected Nuclear Power Plants.* NUREG/CR-0098. Washington, D.C.: U.S. Nuclear Regulatory Commission, Office of Nuclear Reactor Regulation. ACC: NNA.19890327.0045. [DIRS 177216]	F2.2.15, K2.2.9
2.1.4	NRC (U.S. Nuclear Regulatory Commission) 2006. *Interim Staff Guidance HLWRS-ISG-01. Review Methodology for Seismically Initiated Event Sequences.* HLWRS-ISG-01. Washington, D.C.: U.S. Nuclear Regulatory Commission. ACC: MOL.20061128.0036. [DIRS 178130]	
2.1.5	NRC (U.S. Nuclear Regulatory Commission) 2003. *Yucca Mountain Review Plan, Final Report.* NUREG-1804, Rev. 2. Washington, D.C.: U.S. Nuclear Regulatory Commission, Office of Nuclear Material Safety and Safeguards. TIC: 254568. [DIRS 163274]	
2.1.6	ORD (Office of Repository Development) 2007. *Repository Project Management Automation Plan.* 000-PLN-MGR0-00200-000 Rev. 00E. Las Vegas, Nevada: U.S. Department of Energy, Office of Repository Development. ACC: ENG.20070326.0019. [DIRS 182418]	
	SAC Joint Venture 2000. *State of the Art Report on Base Metals and Fracture.* FEMA-355A. Washington, D.C.: Federal Emergency Management Agency. ACC: MOL.20080215.0050. [DIRS 185079]	A2.2.9, D2.2.4, I2.2.9
	Sliger, A. 2007. "Re: WPTT calcs (Document link: David Moore)." E-mail from A. Sliger to D. Moore, October 4, 2007. ACC: LLR.20080128.0002. [DIRS 184926]	F2.2.8
	Timoshenko S., Young D.H., and Weaver W. Jr. 1974. *Vibration Problems in Engineering.* 4th Edition. New York, New York: John Wiley & Sons. ISBN 0-471-87315-2. 522 pp. [DIRS 184110]	A2.2.12, D2.2.12, I2.2.12
2.2.3	YMP (Yucca Mountain Site Characterization Project) 1997. *Methodology to Assess*	

MASTER DOCUMENT	MASTER DOCUMENT REFERENCE	ATTACHMENT REFERENCES A-N = ATTACHMENTS N.N.N = ATTACHMENT REFERENCE NO.
	Fault Displacement and Vibratory Ground Motion Hazards at Yucca Mountain. Topical Report YMP/TR-002-NP, Rev. 1. Las Vegas, Nevada: Yucca Mountain Site Characterization Office. ACC: MOL.19971016.0777. [DIRS 100522]	
2.2.1	Reserved	A2.1.2, A2.2.4, C2.2.4, C2.2.5, C2.2.11, C2.2.12, D2.1.2, D2.2.9, F2.2.11, G2.2.3, G2.2.11, G2.2.12, H2.2.11, H2.2.12, I2.2.5, I2.2.14, L2.2.7, N2.2.7

3. ASSUMPTIONS

The general assumptions used during the seismic fragility analysis of critical surface facility equipment are consistent with standard seismic fragility methodology. In general, the assumptions are compatible with those usually applied within the fragility derivations conducted as part of a seismic PRA. Assumptions unique to each individual calculation are documented in the attachments.

3.1 ASSUMPTIONS REQUIRING VERIFICATION

There are no assumptions requiring verification.

3.2 ASSUMPTIONS NOT REQUIRING VERIFICATION

There are no general assumptions not requiring verification. Assumptions not requiring verification unique to each individual equipment fragility calculation are documented in the attachments.

4. METHODOLOGY

4.1 QUALITY ASSURANCE

This calculation is prepared in accordance with Bechtel SAIC LLC procedure EG-PRO-3DP-G04B-00037, Rev. 10 (Reference 2.1.1). The approved record version of this calculation is designated QA:QA. A pre-job briefing was conducted on January 8 and 9, 2007 by Michael Frank at Las Vegas, Nevada. Key representatives from LLNL and ARES were in attendance.

4.2 USE OF SOFTWARE

Excel 2003 and Word 2003, which are part of the Microsoft Office 2003 suite of programs, were used in this calculation for the generation of tables and word-processing. This software as used in this calculation is classified as Level 2 software usage as defined in IT-PRO-0011 *Software Management* (Ref. 2.1.2) and is listed in *Repository Project Management Automation Plan* (Reference 2.1.6, Table 10-1 and Figure 3-2).

The listed software was installed on personal computers and operated under Microsoft Windows XP Professional operating system, Version 5.1.2600, Service Pack 2, Build 2600.

Mathcad version 14.0 was used in this calculation. The use of this software is classified as Level 2 software per procedure, IT-PRO-0011, Rev. 7, (Reference 2.1.2, Attachment 12) and therefore the software does not need to be qualified. The software is also listed in the Repository Project Management Automation Plan (Reference 2.1.6, Table 6-1).

The accuracy of the resulting graphics and text is verified by visual inspection in compliance with applicable procedures.

4.3 APPROACH

4.3.1 Description of Analysis Methods

Seismic fragilities evaluated for Yucca Mountain Surface Facilities equipment were developed using the separation of variables method where the overall factor of safety is determined from a combination of individual factors of safety from a number of parameters. The factor of safety of a component is defined herein as the resistance capacity for failure modes of interest divided by the response associated with the reference earthquake. The development of seismic safety factors associated with the reference earthquake is based on consideration of several parameters. The two basic considerations for the evaluation of seismic fragilities are the evaluation of dynamic response to the input ground motion and the strength or capacity of the structure or equipment component. Several parameters are involved in determining both the structural response, equipment response and the capacity, and each such parameter has a median factor of safety and variability associated with it. The overall factor of safety is the product of the factors of safety for each parameter. The variabilities of the individual safety factors also combine to determine the variability of the overall safety factor.

Parameters influencing the factor of safety on equipment capacity to withstand earthquake shaking include the strength of the equipment compared to the evaluation or design stress or deformation level and the inelastic energy absorption capacity (ductility) of the equipment defined as its ability to withstand seismic inertial loads beyond elastic limits. Many parameters affect the computed structural response to free field earthquake input ground motion. The more significant parameters, each of which has variability, are (1) ground motion and the associated ground response spectra for a given median spectral acceleration, (2) energy dissipation (damping), (3) structural modeling, (4) method of analysis, (5) combination of modes, (6) combination of earthquake components, and (7) soil-structure interaction including the earthquake ground motion incoherence or spatial variation.

The method of fragility analysis used in this calculation has been used on numerous nuclear power plants, accepted by the U.S. Nuclear Regulatory Commission (NRC), and is documented in detail in Reference 2.2.6.

5 LIST OF ATTACHMENTS

Number of Pages

Total attachment sheets are 524.

All attachments have been independently reviewed by Robert J. Budnitz, LBNL, and Technical Product Inputs have been provided by Deborah Finney and Steven Carlson, LLNL.

6. BODY OF CALCULATION

6.1 METHODOLOGY FOR SEISMIC PRECLOSURE SAFETY ANALYSIS AT YUCCA MOUNTAIN SURFACE FACILITIES

6.1.1 Background and Regulatory Framework for Yucca Mountain Surface Facilities Seismic Program

Bechtel SAIC Company, LLC (BSC) is demonstrating preclosure seismic safety compliance for the Yucca Mountain Surface Facilities based on a seismic safety assessment incorporating probabilistic risk assessment methods. This work is being done to meet the criteria within the Code of Federal Regulations (CFR) related to Preclosure Performance Objectives. The regulatory framework and background associated with the surface facilities seismic program are described in detail within DOE 2007 (Reference 2.2.5, page 2-1), and a summary of that material is presented below.

6.1.2 Code of Federal Regulations Requirements

10 CFR Part 63 (Reference 2.1.3, Section 63.41(c)) states that for a license to be issued for the operation of a high-level radioactive waste (HLW) repository, the U.S. Nuclear Regulatory Commission (NRC) must find that the facility will not constitute an unreasonable risk to the health and safety of the public. 10 CFR 63.21 requires that a preclosure safety analysis (PCSA) be performed to ensure specified preclosure performance objectives have been met. The PCSA is a systematic examination of the site, design, and potential hazards, including a comprehensive identification of potential event sequences. Potential naturally occurring hazards include those event sequences initiated by earthquake ground motions.

In accordance with 10 CFR 63.2 (Reference 2.1.3, Section 63.112(b)), design bases for the repository include consideration of severe natural events, such as earthquakes. The preclosure performance objectives for the geologic repository operations area are given in 10 CFR 63.111 and it is required that the license application (LA) demonstrate that the preclosure performance objectives (10 CFR 63.21[c][3][ii]) have been met. The measure of acceptable risk is expressed in terms of allowable consequences for Category 1 or Category 2 event sequences. Allowable consequences are given as performance objectives (i.e., dose limits) in 10 CFR 63.111.

The PCSA must also include a discussion of the design and how design criteria are related to design bases such that compliance with the preclosure performance objectives is ensured. This calculation defines a methodology that will allow the NRC to find reasonable assurance that the preclosure performance objectives contained in 10 CFR 63.111 are achieved for earthquake ground motion.

10 CFR Part 63 (Reference 2.1.3, Section 63.112(b)) does not prescribe a specific approach to developing seismic design bases. Rather, the regulation is risk-informed and performance-based, which means that the demonstration of compliance with the preclosure performance objectives is the ultimate goal to be used in the establishment of design bases. Therefore, the DOE has developed a preclosure seismic design methodology that consists of two parts: (1) seismic design criteria, including design basis ground motions (DBGM) and codes, standards, and

acceptance criteria that are consistent with applicable regulatory precedents from commercial nuclear licensing, and (2) a compliance demonstration that shows that the preclosure performance objectives in 10 CFR 63.111(a), (b), and (c) have been met. To do so, this preclosure seismic design methodology is integrated with PCSA, and both design methodology and safety analyses are used to demonstrate compliance.

6.1.3 Interim Staff Guidance-Review Methodology for Seismically Initiated Event Sequences

The NRC issued interim staff guidance in 2006 for seismically initiated event sequences (Reference 2.1.4) to supplement the YMRP (Reference 2.1.5). The interim staff guidance document "provides an example methodology to review seismically initiated event sequences, in the context of the preclosure safety analysis, for compliance with performance objectives in 10 CFR 63.111(b)(2)". The suggested methodology is summarized by the following:

- The methodology considers the likelihood of seismic initiating events at the site, and the fragility of structures, systems, and components (SSCs) important to safety (ITS), to estimate probability of failure of SSCs ITS and frequency of occurrence of event sequences. This guidance was developed to take advantage of improvements in probabilistic seismic hazard analyses and performance-based safety assessments, thus differing from the design based on deterministic criteria previously used for licensing of nuclear facilities, especially nuclear power plants.

- This interim staff guidance describes one method that the staff may use to review the seismic performance of SSCs ITS and frequency of occurrence of seismic event sequences, as required by the analysis described in 10 CFR 63.112 to demonstrate compliance with the performance objectives in 10 CFR 63.111(b)(2). This methodology to evaluate seismic performance of an SSC ITS is similar to the one outlined in ASCE/SEI 43-05 (Reference 2.2.2, page 51). The NRC has accepted this methodology to support licensing of the mixed-oxide fuel fabrication facility at the Savannah River Site in South Carolina. Application of the methodology described in ASCE 43-05 (Reference 2.2.2), and the scope of seismic design and analysis for the GROA must be consistent with the Part 63 preclosure safety analysis requirements. The U. S. Department of Energy (DOE) may, however, use alternative methods to demonstrate compliance with the Part 63 preclosure safety analysis requirements for analysis of event sequences.

Examples for exercising the methodology are given in appendices to the interim staff guidance document, including the methodology for computing ITS SSCs probability of failure during a seismic event (Reference 2.1.4, Appendix A) and the methodology for evaluating complete event sequences. The methodology for seismic fragility analyses described in Section 6.2 of this calculation will be integrated into the seismic probabilistic safety analysis and is judged to be consistent with the acceptable methodologies given in the interim staff guidance document.

6.1.4 Yucca Mountain Seismic Design and Demonstration Methodology

The seismic PCSA process can be iterative in its implementation. This means that the first time through the analysis may be conservative relative to later iterations. When this happens, the

analysis used will be re-examined to remove conservatism, or perform additional seismic modeling to get more realistic results. In addition, the seismic design criteria being utilized by BSC for the critical equipment may need to be increased in order to demonstrate compliance with the 10 CFR 63 provisions. The process envisioned for the iterative nature of the seismic PCSA is shown in Figure 1 below. The "component fragilities" box within Figure 1 includes structures, equipment and systems.

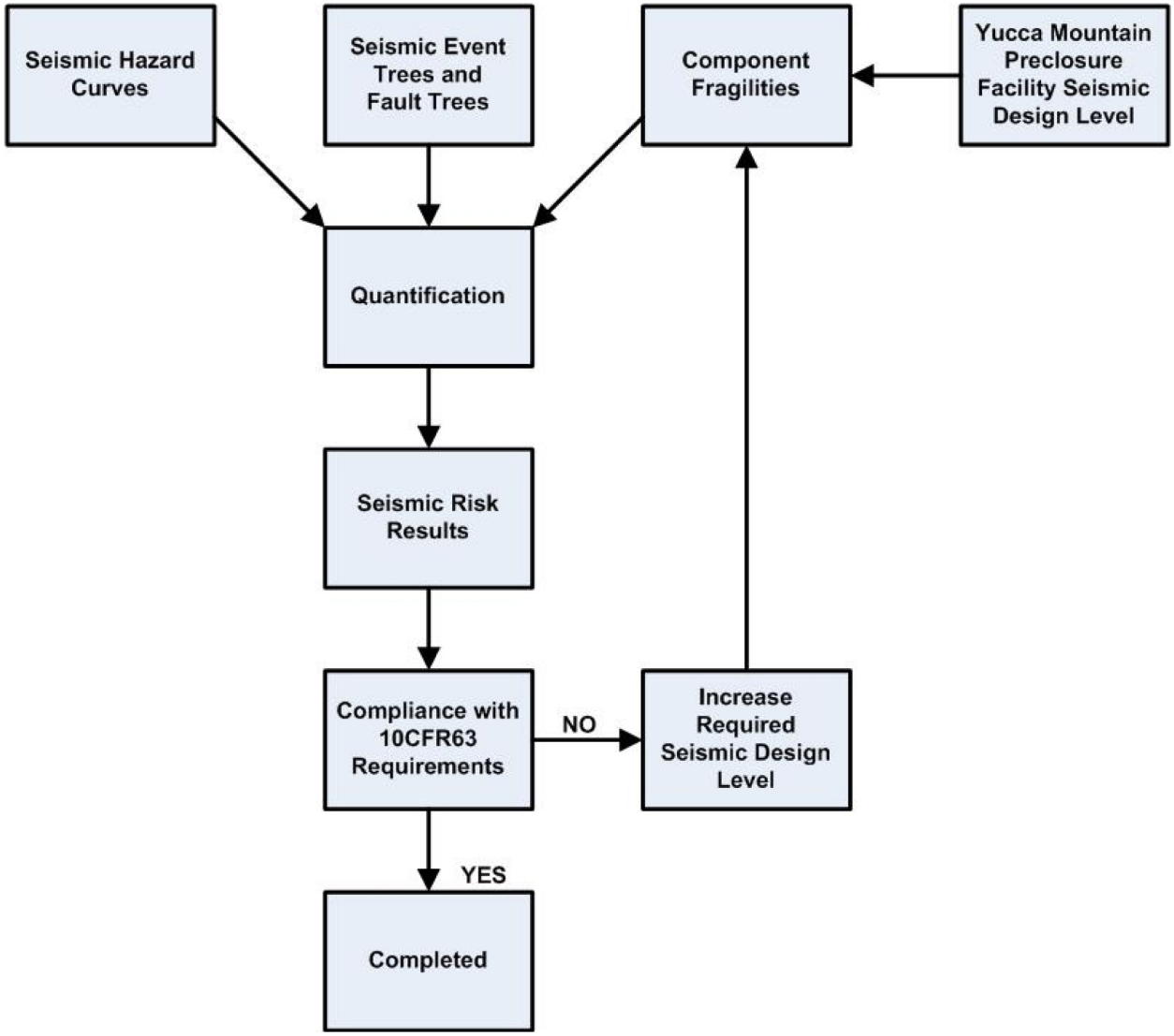

Figure 1. Seismic PCSA Process

6.2 EQUIPMENT SEISMIC FRAGILITY METHODOLOGY

The SPRA methodology is being utilized as a part of the process for preclosure seismic design. The SPRA process is being utilized for Important To Safety (ITS) SSCs. ITS SSCs are credited with preventing the initiation of, or mitigating the consequences of, seismically initiated event sequences. Probabilistic seismic analyses are utilized to assess the probability of seismically initiated event sequences and to demonstrate compliance with 10 CFR 63.111.

6.2.1 SPRA Elements

For the Yucca Mountain Surface Facility equipment, the probabilistic seismic analyses will be conducted to demonstrate compliance with the preclosure performance objectives in 10 CFR 63.111(b)(2) (Reference 2.1.3). The key components of the probabilistic seismic analyses for Yucca Mountain Surface Facilities include:

1. Development of mean hazard curves for pertinent ground motion measures at relevant MAPEs

2. Development of fragility curves for specific ITS SSCs credited in event sequences to demonstrate compliance

3. Development of seismically initiated event sequences

4. Convolution of seismic hazard curves and fragility curves

5. Assessment of probabilities of event sequences

6. Categorization as Category 1, Category 2 or Beyond Category 2 event sequence per 10 CFR 63.2

7. Evaluation of the dose consequences of the seismically initiated event sequences

The probabilistic seismic analyses will:

- Assess whether the probability of seismically initiated event sequences is less than one in 10,000 during the preclosure period, thus allowing Beyond Category 2 event sequences to be screened out, or

- Demonstrate that the radiological dose consequences of each Category 2 event sequence that is not screened out meets the performance objectives of 10 CFR 63.111(b)(2).

Any ITS SSCs that do not lead to compliance will be redesigned to ensure compliance.

6.2.2 Seismic Hazard at Yucca Mountain

To assess the seismic hazards of vibratory ground motion at Yucca Mountain, a Probabilistic Seismic Hazard Assessment (PSHA) was performed. The PSHA provides quantitative hazard results to support assessment of the Repository's long-term performance and to form the basis for developing seismic design criteria for the License Application. The PSHA methodology that the DOE has used for Yucca Mountain is consistent with that documented in *Methodology to Assess Fault Displacement and Vibratory Ground Motion Hazards at Yucca Mountain* (Reference 2.2.3). The seismic hazard characterization at Yucca Mountain is documented in References 2.2.4 and 2.2.8.

The site-specific mean seismic hazard curve is used for quantification of the seismic PCSA model and is considered a critical element in the derivation of consequences and risk resulting

from the seismic PCSA. Seismic hazard curves are typically a family of curves that depict the probability of non-exceedance for each ground acceleration level at various confidence levels. There are usually large uncertainties with regard to seismic hazard estimation. Mean point estimation of a single hazard curve rather than a family of hazard curves will be utilized within the seismic PCSA, in order to obtain insights into potential seismic vulnerabilities. For the purposes of the seismic PCSA study, the mean seismic hazard curves will be utilized for the seismic contribution to plant risk/consequence calculation. The specific curve values that are input into the quantification code are appropriately documented by specifying the seismic hazard curve values used.

The key elements from the seismic hazard study that will be utilized within the seismic fragility assessment of equipment include:

- Spectral Shape of the Uniform Hazard Spectrum used for development of Seismic Design.

- Spectral Shapes of Uniform Hazard Spectra at return periods that significantly contribute to the seismic consequence or seismic risk levels.

6.2.2.1 Design Basis Ground Motions (DBGM) for Yucca Mountain Surface Facilities

The assignment of DBGM levels for the Yucca Mountain Surface Facilities (YMSF) is a risk-informed process. SSCs determined in the PCSA to be more risk-significant will be subjected to more severe seismic design bases.

Two DBGM levels have been defined for the seismic design of ITS SSCs:

DBGM-1 with a MAPE = 10^{-3} (1,000- year return period)

DBGM-2 with a MAPE = 5×10^{-4} (2,000- year return period).

In addition, a higher level Beyond Design Basis Ground Motion (BDBGM) has been defined at the 1×10^{-4} MAPE for purposes of evaluating the effects of larger earthquakes and for demonstrating seismic margin on the design level. The determination of appropriate DBGM levels for specific SSCs depends on their risk significance (i.e., radiological consequences). The ITS SSCs identified in seismically initiated event sequences are identified in the PCSA and, depending on the radiological consequences of the event sequences, are assigned DBGM-2, DBGM-1, or building code seismic design.

Mean Hazard Curves and Mean Uniform Hazard Spectra for the Surface Facilities Area (Reference 2.2.4) contains the mean seismic hazard curves appropriate for the surface facilities area at Yucca Mountain. Reference 2.2.8 describes the models and analyses used to develop these UHS ground motion inputs for the surface facility area. The preceding document (MO0706HCUHSSFA.000, *Mean Hazard Curves and Mean Uniform Hazard Spectra for the Surface Facilities Area*, Submittal Date: 06/11/2007) to Reference 2.2.4 is expected to be superseded by Reference 2.2.4 shortly. The preceding document contains a generally conservative characterization of the surface facility seismic hazard. The UHS for the seismic

hazard from Reference 2.2.4 were plotted together with those from the previous hazard study to demonstrate that conservatism (within engineering accuracy) exists. The comparison of the new and old UHS curves at all frequencies is shown in Figure 2.

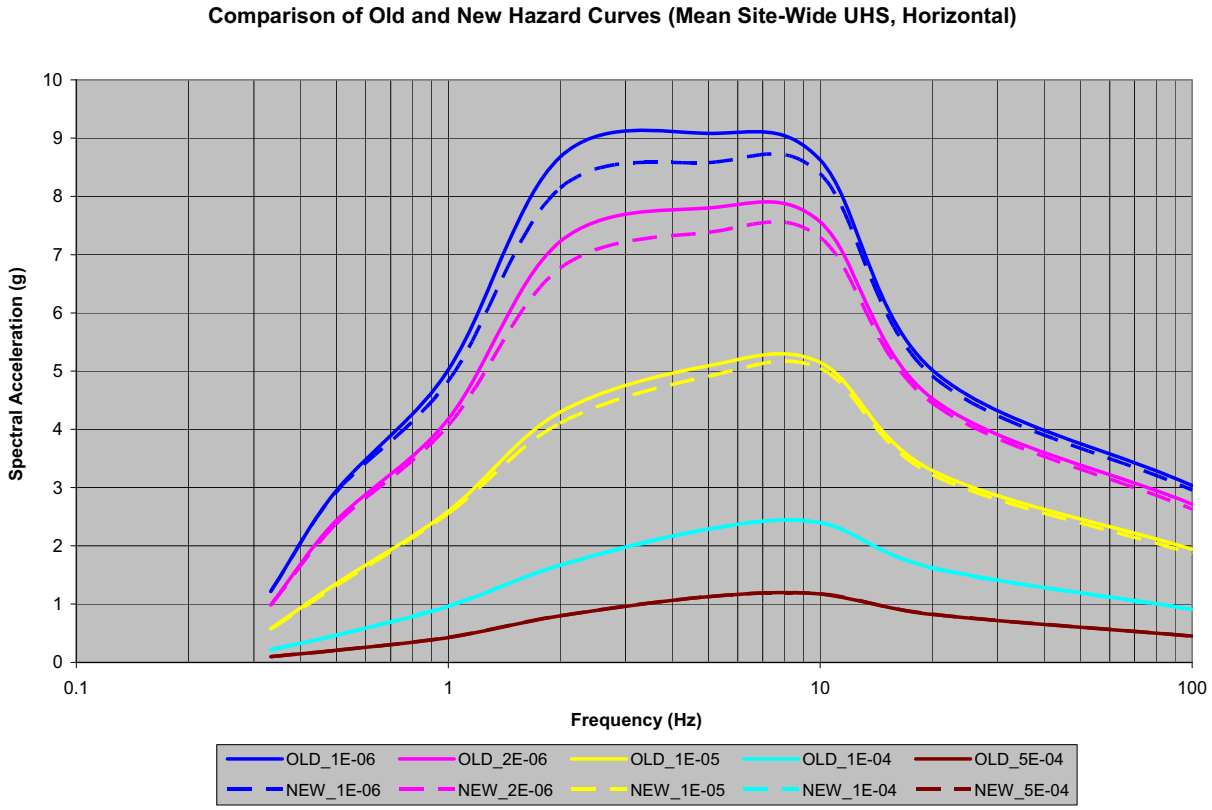

Figure 2. Comparison of YMSF Uniform Hazard Spectra (New = 2008, Old = 2007)

(Note: The solid curve overlaps the dotted curve for the cases of 1E-04 and 5E-04)

These conservative characterizations of the seismic hazard were utilized to develop:

1. The amplitudes of ground motions associated with the DBGM and BDBGM levels depicted in Table 2.

2. The uniform hazard spectra figures and table within the specific fragilities documented within the attachments of this calculation (Figures A6.5-1, C6.5-2, C6.6-2, C6.6-3, D6.5-1, E6.5-2, E6.6-2, F-B-1, G6.5-2, H-B-1, I6.5-1, J-B-1, K-B-1, L-B-1, N-B-1, and Table B-B-1).

3. The BSC calculations to develop design basis ISRS for the YMP surface facilities.

Table 2. Yucca Mountain Surface Facilities Ground Motion

Ground Motion Category	Mean Annual Probability of Exceedance (MAPE)	Horizontal Peak Ground Acceleration (PGA)(g) *
		Surface (Site Wide)
DBGM-1	1.0×10^{-3}	0.325
DBGM-2	5.0×10^{-4}	0.453
BDBGM	1.0×10^{-4}	0.914

* Accelerations from MO0706HCUHSSFA.000, *Mean Hazard Curves and Mean Uniform Hazard Spectra for the Surface Facilities Area,* Submittal Date: 06/11/2007

Reference 2.2.8 developed uniform hazard spectra (UHS) for the Surface Facilities Area (SFA). UHS for both a random horizontal component and a vertical component of motion were developed. They represent the 5%-damped spectral acceleration (Sa) with a given annual frequency of exceedance (APE) as a function of oscillator period. As discussed in Reference 2.2.8 (Section 6.5.2.3), in computing the UHS, data for an oscillator period of 3.3 sec (0.3 Hz) were inadvertently used for an oscillator period of 3 sec (0.33 Hz). Thus, for periods greater than 2.0 sec (frequencies less than 0.5 Hz), the Sa amplitude is lower (has a higher APE) than appropriate for the nominal UHS APE. As a result, the applicability of the UHS for periods greater than 2 sec (frequencies less than 0.5 Hz) is limited.

The UHS for the SFA are associated with data tracking number (DTN) MO0801HCUHSSFA.001. As described in Reference 2.2.8 (Section 6.5.2.3) the value of spectral acceleration given in these data for an oscillator period of 3 sec (0.33 Hz) is actually the value for a period of 3.3 sec (0.3 Hz). Table 3 provides corrected values for the UHS with APEs of 1E-04, 1E-05, and 2E-06.

Table 3. Corrected Uniform Hazard Spectra

Period (sec)	Frequency (Hz)	5%-Damped Spectral Acceleration (g)	
		Horizontal	Vertical
1E-04 APE			
3.3	0.3	2.19E-01	1.18E-01
1E-05 APE			
3.3	0.3	5.63E-01	3.05E-01
2E-06 APE			
3.3	0.3	9.78E-01	5.32E-01

Source: DTN MO0801HCUHSSFA.001

NOTE: Spectral accelerations given in DTN MO0801HCUHSSFA.001 for an oscillator period of 3.0 sec. (0.33 Hz) were erroneously associated with that period, and are the correct values for an oscillator period of 3.3 sec. (0.3 Hz) as indicated in this table (BSC 2008 [DIRS 183776], Section 6.5.2.3).

Most of the calculations in the attachments to this calculation are judged not to be directly impacted by this limitation since they do not involve equipment with periods beyond 2.0 sec (i.e., with frequencies less than 0.5 Hz). However, the following equipment (and associated attachments) do have frequencies in this range and could potentially be impacted. The potential impacts, and associated resolutions, are listed below:

- Attachment B, Fragility for CRCF CTM Hoist: Section B7, canister swing displacement and impact velocity uses 0.163 Hz for the pendulum swinging inside the CTM shield bell. The limitation above could increase the acceleration at this frequency, and thus the impact velocities from swinging displacements. However, the calculation demonstrated that the predicted impact velocities were relatively low, and that the velocity increases with the cube root of the acceleration. Therefore, the resulting impact velocities would also be judged to be relatively low, the overall conclusion from Section B8 would not change, and no change to Attachment B is required.

- Attachment C, Fragility for CRCF Cask Transfer Trolley: Section C6.5.1 includes a frequency of 0.45 Hz for sliding of the CTT in the CRCF. Since this frequency is very close to the 0.5 Hz frequency which is valid, the calculation of sliding would not be significantly impacted by the plotting fault at 0.3 Hz. Therefore, the CTT sliding calculation does not require any change.

  - Sections C6.6.2 and C6.6.3 include frequencies less than 0.5 Hz in the calculation of CTT tipover fragility. In Section C6.6.2, the frequency determined to be the effective rocking frequency is 0.48 Hz, which is very close to the 0.5 Hz frequency which is valid. Therefore, the calculation in Section C6.6.2 would not be significantly impacted by the plotting fault at 0.3Hz, and does not require any change.

  - In Section C6.6.3, the effective rocking frequency is close to 0.3 Hz. To counteract the impact from the plotting fault, the tables in C6.6.3 were revised from Reference 2.2.4 by correcting the 0.3 Hz spectral accelerations before interpolation and calculation.

- Attachment E, Fragility for IHF Cask Transfer Trolley: Section E6.5.1 includes a frequency of 0.45 Hz for sliding of the CTT in the IHF. Since this frequency is very close to the 0.5 Hz frequency which is valid, the calculation of sliding would not be significantly impacted by the plotting fault at 0.3 Hz. In addition, the 0.45 Hz frequency results did not impact the final sliding results. Therefore, the IHF CTT sliding calculation does not require any change.

  - Section E6.6.2 uses a frequency of 0.455 Hz in the calculation of CTT tipover fragility. Since this frequency is very close to the 0.5 Hz frequency which is valid, the calculation of tipover would not be significantly impacted by the plotting fault at 0.3 Hz. Therefore, the IHF CTT tipover calculation does not require any change.

- Attachment F, Fragility for Waste Package Transfer Trolley: Section F6.6.2 includes a frequency of 0.23 Hz in the calculation of WPTT tipover fragility in the CRCF. Rather

than interpolating below 0.3 Hz, the corrected values for 0.3 Hz will be used to bound the WPTT tipover fragility calculation.

- Attachment H, Fragility for Waste Package Transport and Emplacement Vehicle: Section H6.2.4 includes a frequency of 0.476 Hz in the calculation of TEV rocking/tipover. Since this frequency is very close to the 0.5 Hz frequency which is valid, the calculation of tipover would not be significantly impacted by the plotting fault at 0.3 Hz. Therefore, the TEV tipover calculation does not require any change.

6.2.3 Identification of the List of Equipment for Seismic Fragility Assessment

The *Preclosure Seismic Design and Performance Demonstration Methodology for a Geologic Repository at Yucca Mountain Topical Report* (Reference 2.2.5) contains the overall guidance on the identification of specific and representative equipment for which fragility information would be required. The following is a list of equipment and locations that was provided by the Preclosure Safety Analysis Group for the development of seismic fragilities for this project. Since the CRCF in-structure response spectra (ISRS) were available first, and because the equipment fragilities are for representative equipment (i.e., the fragilities are generally based on seismic design criteria since the detailed design of the actual equipment has not been finalized or built for these facilities. Thus, many of the fragility parameters such as the critical failure modes and the design margins will be similar for the same equipment type located in different structures.), most of the fragility calculations were based on the CRCF equipment. Some specific fragility evaluations were made for equipment in other buildings, such as the spent fuel transfer machine in the WHF and the Cask Transfer Trolley in the IHF.

Table 4. Seismic Equipment List for Equipment Fragilities

Calculation Attachment	ITS SSCs	Building
A	Cask Handling Crane	CRCF
B	Hoist System for CTM	CRCF
C	Cask Transfer Trolley	CRCF
D	Canister Transfer Machine	CRCF
E	Cask Transfer Trolley	IHF
F	Waste Package Transfer Trolley	CRCF
G	Site Transporter	CRCF and Site
H	TEV	CRCF and Site
I	Spent Fuel Transfer Machine	WHF
J	Typical NPP type equipment qualified by testing	CRCF

Calculation Attachment	ITS SSCs	Building
K	Typical NPP type equipment qualified by analysis	CRCF
L	Shield Doors	CRCF
M	Offsite Power	Site (free field response)
N	CRCF Canister Staging Racks	CRCF

6.2.4 Equipment Fragility Methods

The definition of seismic fragility of a component is the threshold of seismic response at which the component ceases to perform its intended function. The fragility corresponds to a selected governing failure mode. Fragility is referenced to ground motion input parameters (typically either peak ground acceleration or average spectral acceleration over the frequency range of interest for structure response). For the Yucca Mountain site, the peak ground acceleration (the parameter used in the seismic hazard study) was utilized as the ground motion input parameter for the seismic fragilities.

Fragility is defined as a conditional probability of failure versus the selected ground motion parameter, peak ground acceleration. For calculational convenience, a lognormal distribution is typically assumed and the median ground motion parameter value, A_m, and two variables, β_R and β_U are used to describe randomness and uncertainty about the median. β_R and β_U are logarithmic standard deviations about the median. Figure 3 shows a family of fragility curves for an equipment component. The slope of each curve represents the randomness, β_R, in the prediction of capacity and the family of curves represents the distribution of uncertainty, β_U, in where the true curves lie. The terminology "high confidence of low probability of failure" (HCLPF) is defined as about 95 percent confidence of less than approximately 5 percent probability of failure. The HCLPF is a failure capacity and is typically measured in (g). The HCLPF is also shown in Figure 3 and it is expressed mathematically as:

$$HCLPF = A_m e^{-1.65(\beta_R + \beta_U)} \qquad \text{(Eq. 1)}$$

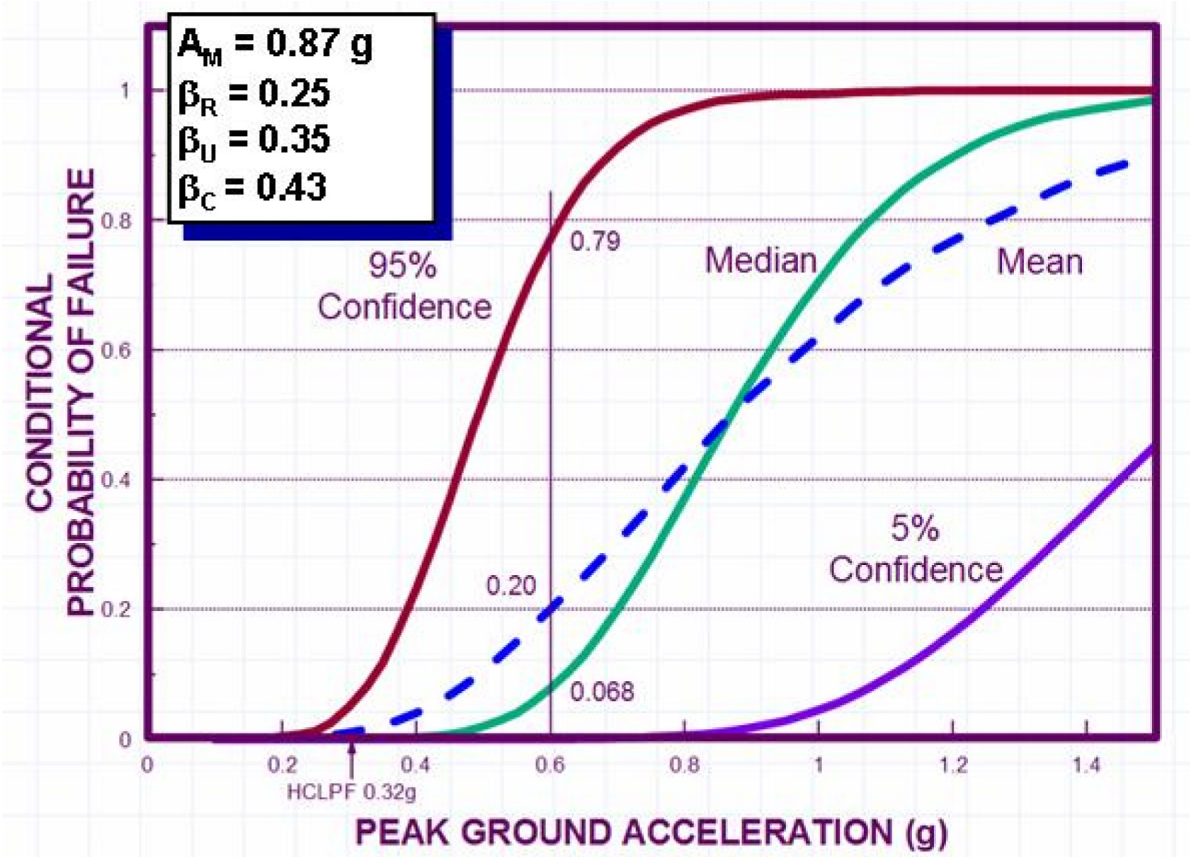

Figure 3. Seismic Fragility Curves

The entire fragility curve and its uncertainty, as shown in Figure 3, can be expressed by three parameters, Am, β_R, and β_U by the following expression:

$$A = A_M \varepsilon_R \varepsilon_U \qquad \text{(Eq. 2)}$$

where: A = ground motion parameter corresponding to any given frequency of failure

A_m = median ground motion capacity of the structure

ε_R, ε_U = random variables with unit median and logarithmic standard deviation, β_R, β_U

ε_R and ε_U represent inherent randomness about the median value and uncertainty in the median value, respectively.

A mean fragility curve (dashed blue curve in Figure 3) can be generated and is a function of the composite variability, βc, which is defined as:

$$\beta_c = (\beta_R^2 + \beta_U^2)^{1/2} \qquad \text{(Eq. 3)}$$

The corresponding value for the HCLPF can be conservatively approximated via the following equation (Reference 2.2.7, Equations 12 and 12b):

$$HCLPF = A_m e^{(-2.33\beta c)} \quad \text{(Eq. 4)}$$

In the NRC IPEEE program, the point estimate (mean value) of the desired risk quantity (CDF) was required, thus the single mean (composite) fragility curve and the mean seismic hazard curve were convolved to calculate the probability of failure of SSCs. The Yucca Mountain project utilizes this point estimate approach as suggested within the Interim Staff Guidance on Seismically Initiated Event Sequences (Reference 2.1.4, page 7) and, thus, median fragility values, A_m, and composite fragilities, β_c, are developed for critical equipment.

Seismic fragilities evaluated for Yucca Mountain equipment are developed using the separation of variables method where the overall factor of safety is determined from a combination of individual factors of safety from a number of parameters. The factor of safety of a component is defined herein as the resistance capacity for failure modes of interest divided by the response associated with the reference earthquake. The development of seismic safety factors associated with the reference earthquake is based on consideration of several parameters. The two basic considerations for the evaluation of equipment fragilities are the evaluation of dynamic response to the input ground motion and the strength or capacity of the equipment component. Several parameters are involved in determining the structural response, equipment response and the capacity, and each such parameter, in turn, has a median factor of safety and variability associated with it. The overall factor of safety is the product of the factors of safety for each parameter. The variabilities of the individual safety factors also combine to determine the variability of the overall safety factor.

Parameters influencing the factor of safety on structural capacity to withstand earthquake shaking include the strength of the structure compared to the evaluation or design stress or deformation level and the inelastic energy absorption capacity (ductility) of the structure defined as its ability to withstand seismic inertial loads beyond elastic limits. Many parameters affect the computed structural response to free field earthquake input ground motion. The more significant parameters, each of which has variability, are (1) ground motion and the associated ground response spectra for a given median spectral acceleration, (2) energy dissipation (damping), (3) structural modeling, (4) method of analysis, (5) combination of modes, (6) combination of earthquake components, and (7) soil-structure interaction including the earthquake ground motion incoherence or spatial variation. The logic structure for the above is shown in Figure 4.

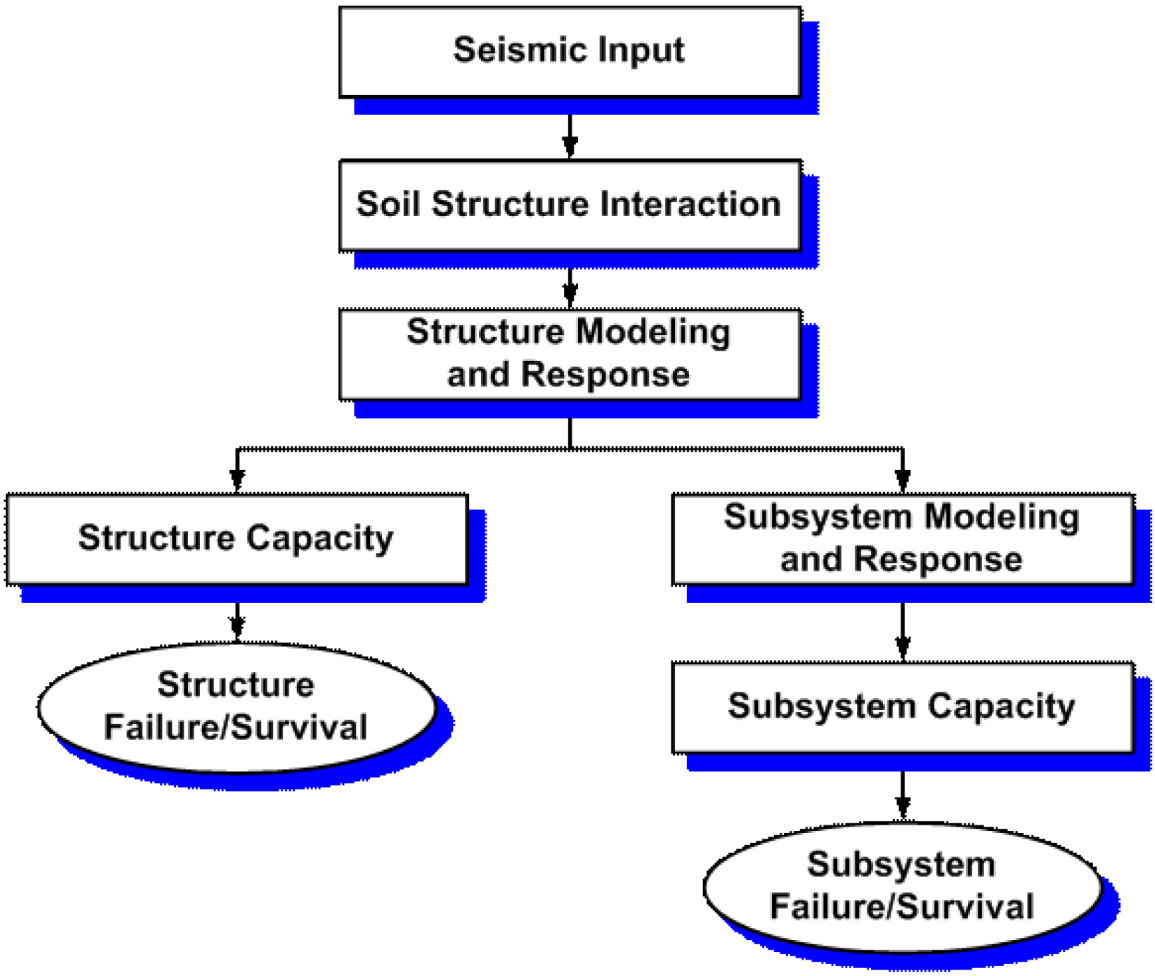

Figure 4. Fragility Logic Structure

Seismic fragilities are evaluated from seismic response analyses of the Yucca Mountain surface facilities structures by quantifying conservatism and variability in the following manner:

$$A_m = F_C F_{RS} PGA \qquad \text{(Eq. 5)}$$

$$\beta_c = (\beta^2_{C\text{-}C} + \beta^2_{C\text{-}RS})^{0.5} \qquad \text{(Eq. 6)}$$

where: F_C = capacity factor accounting for conservatism in strength and ductility

$\beta_{C\text{-}C}$ = capacity factor variability

F_{RS} = response factor accounting for conservatism in response evaluation

$\beta_{C\text{-}RS}$ = response factor variability

PGA = is the peak ground acceleration for the reference earthquake

Most of the effort in structural fragility evaluation resides within the evaluation of capacity factors and the associated variability. Realistic structure and equipment capacities including both strength and inelastic energy absorption capacity are needed. The evaluation of strength factors and variability will be accomplished in the conventional fragility calculation manner in which median strength equations and material strengths are used accounting for changes in material strength with time. For these fragility evaluations, inelastic spectra reduction factors (F_μ) were estimated to characterize the ductility of the equipment in relation to the cyclic nature of the earthquake loading.

6.2.4.1 Seismic Response Analysis

Realistic median-centered response of structures, systems, and components (SSCs) is an essential element of the seismic fragility assessment. Median-centered responses (forces and moments, displacements and accelerations, in-structure response spectra) are defined by conditional probability distributions, i.e., conditional on an earthquake occurring. Two approaches have been used extensively in past seismic PCSAs to estimate median-centered response:

- The factor of safety method – this approach is based on developing a response factor comprised of a number of terms, which when combined and applied to the design calculated seismic responses will estimate a median-centered response conditional on the occurrence of the ground motion. Numerous studies have been performed for generic and site specific conditions over the past 25 years to provide a basis for their development. In addition, studies may be performed to quantify the response factor specifically taking into account the most important of the contributing factors – ground motion characteristics (UHS, PGA, and other parameters), soil-structure interaction, realistic model parameters (damping), and nonlinear response.

- The generation of new seismic response analyses – the generation of a new median centered response using Soil Structure Interaction (SSI) codes and median soil/structure properties is a more exact approach for developing the seismic response. This approach uses best estimate procedures and parameters to model the key elements of the seismic analysis chain. Since BSC has conducted new seismic response analyses incorporating SSI effects (soil-spring models), this approach was utilized for the Yucca Mountain surface facilities.

6.2.4.2 Fragility Development

The basic methodology utilized to develop the equipment seismic fragilities for the Yucca Mountain surface facilities incorporates a separation of variables approach which characterizes the conservatisms/margins and the associated uncertainties involved within each step of the seismic response/design process. These methods are well documented in Reference 2.2.6.

For Yucca Mountain equipment, the median factor of safety between the median ground acceleration capacity and the capacity of the reference earthquake level is evaluated along with its variability in terms of randomness and uncertainty. For structures, the factor of safety can be modeled as the product of three variables:

$$F = F_S F_\mu F_{RS} \quad \text{(Eq. 7)}$$

For equipment, an additional factor (equipment response factor, F_{RE}) exists in addition to the factors in Equation 7 above. The strength factor, F_S, represents the ratio of ultimate strength (or strength at loss of function) to the stress calculated for the reference earthquake. In calculating the value of F_S, the non-seismic portion of the total load acting on the structure/equipment is subtracted from the strength as follows:

$$F_S = \frac{S - P_N}{P_T - P_N} \quad \text{(Eq. 8)}$$

Where S is the strength of the structural element for the specific failure mode considered, P_N is the normal operating load (i.e., dead load), and P_T is the total load acting on the structure (i.e., sum of the seismic load and the normal operating load).

The inelastic energy absorption factor (ductility), F_μ accounts for the fact that an earthquake represents a limited energy source and many structures are capable of absorbing substantial amounts of energy beyond yield without loss of function. The inelastic energy absorption factor, F_μ was evaluated by ductility modified response spectra to determine the de-amplification effect resulting from the inelastic energy dissipation. The de-amplification factor is primarily a function of the ductility ratio μ defined as the ratio of maximum displacement to displacement at yield. This factor is also a function of the system's damping.

The structural response factor, F_{RS}, recognizes the level of conservatism in seismic response analyses. It also accounts for the random nature of seismic response where the actual response may differ substantially from the response evaluated for the reference earthquake.

Based on using the response from these more simplified models, F_{RS} was estimated based on potential conservatisms in the spectral shape, damping, modeling, mode combination, earthquake component combination, spatial variation of ground motion, and soil-structure interaction. The methodology for developing these various factors is summarized in Reference 2.2.6 and was utilized to estimate F_{RS} and its variability.

For the equipment selected to develop fragilities, the strength factor, F_S, was estimated from median centered capacity equations and median material properties including the effects of increases or decreases in strength over time.

6.2.4.3 Design Inputs

Table 5 contains a listing of the various input data/parameters that is useful in order to develop fragilities using the separation of variables approaches. This data, where appropriate and available, was utilized within the fragilities developed and documented within Attachments A through N.

Table 5. Technical Input for Equipment Fragility Evaluations

Item	Description	Input
1	Seismic Hazard	• Seismic Hazard tied to PGA or average peak spectral acceleration • Hazard control point (soil/rock where hazard is defined)
2	Selection of Basic Acceleration Time Histories	• Time histories and their response spectra utilized for structural response analyses (if applicable)
3	Probabilistic Soil Structure Interaction (SSI) Analysis	• Site soil/rock properties (low strain and variability) • Structural models (description of structural sticks, nodes, masses and stiffnesses) • Structural drawings and specifications • Large equipment locations, masses and characteristics • Floor Response Spectra
4	Seismic Response Factor Development for Equipment	Floor Response Spectra • Smoothed/broadened spectra • Unbroadened spectra • Best Estimate, upper bound and lower bound results • Response Methods - Modal and spatial combination approaches - Damping
5	Seismic Capacity Factor Development for Equipment	• Characterization of Critical Failure Modes (Jointly with Systems Analysts) • Seismic Qualification Reports (Similar Components) • Seismic Qualification Criteria (Code criteria, factors of safety, etc.) • Equipment and component drawings • Anchorage details and drawings (if available)

6.3 FUTURE ACTIVITIES RELATED TO EQUIPMENT FRAGILITIES

The seismic fragilities for the Yucca Mountain surface facilities were calculated for inclusion within the repository license submittal. As such, the equipment has not yet been designed in detail, detailed soil structure interaction analyses are underway, and ongoing studies are expected to update the seismic hazard. It is recognized that updates to these equipment seismic fragilities may be desired as additional information becomes available in the future. Areas where future updates may be desired and/or required include:

- Incorporate the new seismic hazard shape into the fragility (Extreme Ground Motion Seismic Hazard study scheduled to be completed December 2008).

- Incorporate the detailed soil-structure interaction analysis (using SASSI) results into the structural response part of the equipment fragilities (Scheduled to be completed in 2008).

- Incorporate design information (following detailed design completion) for critical equipment that contributes to the seismic risk:

  - Seismic design criteria

  - Critical failure modes

  - Seismic analysis results

- Inclusion of walkdown results into the seismic fragilities after facility construction is complete.

  - Seismic interaction review

  - Caveats and restrictions from earthquake and testing experience

7. RESULTS AND CONCLUSIONS

The methodology presented within this calculation was utilized to develop the equipment seismic fragilities that will be utilized by DOE as part of the Yucca Mountain Surface Facilities seismic PCSA. The results of these fragility analyses are contained within Attachments A through N of this calculation and are summarized within Table 6 below.

Table 6. Seismic Fragility Values for YMSF Critical Equipment

Attachment	Component	Failure Mode	Am(g)	β_C	HCLPF(g)
A	CRCF Cask Handling Crane				
		Bridge girders	2.79	0.45	0.98
		Trolley frame	2.79	0.45	0.98
		Trolley seismic restraints	2.11	0.44	0.76
		Hoist	2.28	0.50	0.72
B	CRCF Canister Transfer Machine Hoist				
		Drum	2.28	0.50	0.72
		Swing of Canister Inside Shield Bell (Note 1)	--	--	--
C	CRCF Cask Transfer Trolley				
		Sliding	3.08	0.58	0.79
		Rocking	2.25	0.41	0.87
D	CRCF Canister Transfer Machine				
		Bridge girders & Trolley Frames	2.39	0.45	0.83
		Trolley seismic restraints	1.59	0.42	0.59
E	IHF Cask Transfer Trolley				
		Sliding into wall	1.70	0.44	0.61
		Sliding into column	1.93	0.46	0.66
		Rocking	1.70	0.41	0.65
F	CRCF Waste Package Transfer Trolley				
		Rail Clamp (DBGM-2)	1.47	0.53	0.42
		Impact after Rail Clamp Failure	1.85	0.37	0.78
		Tipover (Note 2)	3.41	--	--
G	Site Transporter (Note 3)				
		Sliding into wall	1.89	0.42	0.71
H	Waste Package TEV				
		Seismic restraints	1.12	0.43	0.41
		Tipover (Note 3)	>4	--	--
I	WHF Spent Fuel Transfer Machine				
		Bridge girders	2.19	0.47	0.72
		Bridge seismic restraints	2.17	0.43	0.8
		Trolley frame	2.19	0.47	0.72
		Trolley seismic restraints	2.17	0.43	0.8
J	Equipment Qualified by Test				
		Function during DBGM-2	1.36	0.44	0.49
		Function after DBGM-2	1.89	0.47	0.63
		Function during BDBGM	2.75	0.44	0.98

Attachment	Component	Failure Mode	Am(g)	β_C	HCLPF(g)
		Function after BDBGM	3.82	0.47	1.27
K	Equipment Qualified by Analysis				
	For DBGM-2 Design	CIP Bolts	0.94	0.44	0.34
		Fillet Weld	1.41	0.46	0.48
		Post Installed Anchors	3.03	0.60	0.75
		Piping Supports	2.24	0.68	0.46
		Cable Tray Supports	3.23	0.68	0.66
		HVAC Supports	2.69	0.66	0.57
	For BDBGM Design	CIP Bolts	1.90	0.44	0.69
		Fillet Weld	2.85	0.46	0.97
		Post Installed Anchors	6.12	0.60	1.51
		Piping Supports	4.52	0.68	0.93
		Cable Tray Supports	6.51	0.68	1.33
		HVAC Supports	5.42	0.66	1.16
L	CRCF Shield Doors				
		CIP Bolts	1.25	0.42	0.47
		Weld	2.92	0.44	1.05
		Door Supports	3.16	0.62	0.75
M	Offsite Power	Switchyard components	0.30	0.54	0.09
N	CRCF Canister Staging Racks				
		Horizontal Supports 1.4 x BDBGM	3.53	0.45	1.25
		Horizontal Supports/ DBGM2	1.25	0.45	0.44

Notes:
1. Impact velocities were calculated for various accelerations and radial gap distances.
2. The reported median seismic capacity for tipover of WPTT in area where tipover could occur.
3. At approximately 4g PGA, the TEV rotates only 23 degrees, whereas the instability angle is about 45 degrees. The site transporter was shown to have similar tip over seismic capacity.

These fragility parameters will be utilized within the seismic PCSA to demonstrate, with reasonable assurance, that preclosure seismic design of the surface facilities satisfies the preclosure performance objectives. The seismic PCSA approach utilizes seismic fragility analysis methods for the safety-related equipment necessary to demonstrate performance consistent with the risk-informed performance-based framework of the regulation.

INTENTIONALLY LEFT BLANK

ATTACHMENT A

FRAGILITY FOR STRUCTURAL FAILURE OF CRCF CASK HANDLING CRANE

Prepared By: Wen H. Tong

ARES Check By: Stephen A. Short

LLNL Check By: Robert C. Murray

TABLE OF CONTENTS

ACRONYMS AND ABBREVIATIONS

ACI	American Concrete Institute
AISC	American Institute of Steel Construction
ANSI	American National Standards Insitute
AO	Aging Overpack
APE	Annual Probability of Exceedance
ASCE	American Society of Civil Engineers
ASME	American Society of Mechanical Engineers
BSC	Bechtel SAIC, LLC
BDBGM	Beyond Design Basis Ground Motion at $1x10^{-4}$ APE
CDFM	Conservative Deterministic Failure Margin
CHC	Cask Handling Crane
CIP	Cast-in-Place
CRCF	Canister Receipt and Closure Facility
CTM	Canister Transfer Machine
CTT	Cask Transfer Trolley
DBGM-2	Design Basis Ground Motion at $5x10^{-4}$ APE
DL	Dead Load
DOF	Degree of Freedom
DPC	Dual Purpose Canister
EPRI	Electric Power Research Institute
HCLPF	High Confidence of Low Probability of Failure
HVAC	Heating, Ventilation, & Air Conditioning
IEEE	Institute of Electrical and Electronics Engineers
IHF	Initial Handling Facility
ISRS	In-Structure Response Spectra

ACRONYMS AND ABBREVIATIONS (cont.)

ITS	Important to Safety
LA	License Application
LLNL	Lawrence Livermore National Laboratory
NPP	Nuclear Power Plant
PGA	Peak Ground Acceleration
RF	Receipt Facility
RRS	Required Response Spectrum
Sa	Spectral Acceleration
SFA	Surface Facilities Area
SFTM	Spent Fuel Transfer Machine
SPRA	Seismic Probabilistic Risk Assessment
SRSS	Square Root of the Sum of Squares
SSE	Safe Shutdown Earthquake (used with NPPs)
SSI	Soil Structure Interaction
SSC	Structure, System, and Component
TAD	Transportation, Aging, and Disposal canister
TEV	Transport and Emplacement Vehicle
TRS	Test Response Spectrum
UHS	Uniform Hazard Spectra
USDOE	United States Department of Energy
USNRC	United States Nuclear Regulatory Commission
WHF	Wet Handling Facility
WP	Waste Package
WPTT	Waste Package Transfer Trolley
YMSF	Yucca Mountain Surface Facilities
ZPA	Zero Period Acceleration

FRAGILITY TERMINOLOGY

Am	Median Peak Ground Motion Capacity
β_R	Log Standard Deviation of Randomness
β_U	Log Standard Deviation of Uncertainty (Lack of Knowledge)
β_C	Composite Variability = $(\beta_R^2 + \beta_U^2)^{0.5}$
F_S	Strength Factor of Safety
β_{R_S}	Strength Randomness (typical)
β_{U_S}	Strength Uncertainty (typical)
β_{C_S}	Strength Composite Variability (typical)
F_μ	Inelastic Energy Absorption Factor of Safety
F_{QM}	Qualification Factor of Safety
F_δ	Damping Factor of Safety
F_M	Modeling Factor of Safety
F_{MC}	Modal Combination Factor of Safety
F_{ECC}	Earthquake Component Combination Factor of Safety
F_{SA}	Spectral Shape Factor of Safety
F_{SSI}	Soil-Structure Interaction Factor of Safety
F_{GMI}	Ground Motion Incoherence Factor of Safety
F_{TOTAL}	Total Factor of Safety
F_{RS}	Structural Response Factor of Safety
F_{RE}	Equipment Response Factor of Safety

A1. PURPOSE

The purpose of this calculation is to estimate seismic fragility of the Cask Handling Crane (CHC) in the Canister Receipt and Closure Facility (CRCF). The mean seismic fragility curve of the CHC will be convolved with the site-specific seismic hazard curves to calculate risk of seismic-induced failure of the CHC.

A2. REFERENCES

A2.1 PROCEDURES/DIRECTIVES

A2.1.1 EG-PRO-3DP-G04B-00037, Rev. 10. *Calculations and Analyses*. Las Vegas, Nevada: Bechtel SAIC Company. ACC: ENG.20071018.0001.

A2.1.2 [Reserved]

A2.1.3 IT-PRO-0011, Revision 7, ICN 0. *Software Management*. Las Vegas, Nevada: Bechtel SAIC Company. ACC: DOC.20070905.0007.

A2.2 DESIGN INPUTS

A2.2.1 EPRI (Electric Power Research Institute) 1994. *Methodology for Developing Seismic Fragilities*. EPRI TR-103959. Palo Alto, California: Electric Power Research Institute. TIC:253770. [DIRS 161329]

A2.2.2 BSC (Bechtel SAIC Company) 2007. *CRCF Tier-1 In-Structure Response Spectra*. 060-SYC-CR00-00900-000-00B. Las Vegas, Nevada: Bechtel SAIC Company. ACC: ENG.20071210.0008. [DIRS 184330]

A2.2.3 BSC (Bechtel SAIC Company) 2008. *Canister Receipt and Closure Facility 1 General Arrangement Ground Floor Plan*. 060-P10-CR00-00102-000 REV 00C. Las Vegas, Nevada: Bechtel SAIC Company. ACC: ENG.20080122.0013. [DIRS 184853]

A2.2.4 [Reserved].

A2.2.5 BSC (Bechtel SAIC Company) 2007. *Project Design Criteria Document*. 000-3DR-MGR0-00100-000-007. Las Vegas, Nevada: Bechtel SAIC Company. ACC: ENG.20071016.0005; ENG.20071108.0001; ENG.20071220.0003; ENG.20080107.0001; ENG.20080107.0002; ENG.20080107.0016; ENG.20080107.0017; ENG.20080131.0006. [DIRS 179641]

A2.2.6 ASME NOG-1-2004. 2005. *Rules for Construction of Overhead and Gantry Cranes (Top Running Bridge, Multiple Girder).* New York, New York: American Society of Mechanical Engineers. TIC: 257672. [DIRS 176239].

A2.2.7 MO0801HCUHSSFA.001. *Mean Hazard Curves and Mean Uniform Hazard Spectra for the Surface Facilities Area*. Submittal date: 01/11/2008. [DIRS 184802]

A2.2.8 BSC (Bechtel SAIC Company) 2007. *Canister Receipt and Closure Facility Cask Handling Crane Mechanical Equipment Envelope.* 060-MJ0-HM00-00101-000 REV 00A. Las Vegas, Nevada: Bechtel SAIC Company. ACC: ENG.20070304.0009; ENG.20070702.0010; ENG.20070823.0008. [DIRS 178459].

A2.2.9 SAC Joint Venture 2000. *State of the Art Report on Base Metals and Fracture.* FEMA-355A. Washington, D.C.: Federal Emergency Management Agency. ACC: MOL.20080215.0050. [DIRS 185079]

A2.2.10 AISC (American Institute of Steel Construction) 1991. *Manual of Steel Construction, Allowable Stress Design.* 9th Edition, 1st Revision. Chicago, Illinois: American Institute of Steel Construction. TIC: 4254. [DIRS 127579]

A2.2.11 ANSI/AISC N690-1994. 1994. *American National Standard Specification for the Design, Fabrication, and Erection of Steel Safety-Related Structures for Nuclear Facilities*. Chicago, Illinois: American Institute of Steel Construction. TIC: 252734. [DIRS 158835]

A2.2.12 Timoshenko S., Young D.H., and Weaver W. Jr. 1974. *Vibration Problems in Engineering.* 4th Edition. New York, New York: John Wiley & Sons. ISBN: 0471873152. [DIRS 184110]

A2.2.13 Moore, D. 2007. "*SSI Factor of Safety.*" E-mail from D. Moore to B. Murray, October 25, 2007. ACC: LLR.20080110.0145. [DIRS 184842]

A2.2.14 Moore, D. 2007. "Canister and Cask Physical Dimensions." E-mail from D. Moore to W-H. Tong, October 31, 2007. ACC: LLR.20080128.0003. [DIRS 184927]

A2.2.15 BSC (Bechtel SAIC Company) 2006. *Canister Receipt and Closure Facility (CRCF) Seismic Analysis.* 060-SYC-CR00-00400-000-00A. Las Vegas, Nevada: Bechtel SAIC Company. ACC: ENG.20061220.0029. [DIRS 178793]

A2.3 DESIGN CONSTRAINTS

There are no design constraints in the performance of this calculation.

A2.4 DESIGN OUTPUTS

The calculated seismic fragility of structural failure of the CHC, expressed in terms of a median seismic capacity and an associated combined variability, will be convolved with the site-specific seismic hazard curve to calculate risk of seismic-induced failure of the CHC. This is performed to support information in the License Application (LA).

A3. ASSUMPTIONS

A3.1 ASSUMPTIONS REQUIRING VERIFICATION

There are no assumptions requiring verification used in this attachment.

A3.2 ASSUMPTIONS NOT REQUIRING VERIFICATION

A3.2.1 Cask Drop

The fragility reported in this calculation is only for failure modes that would result in a drop of the lifted cask and/or structural failure of the CHC itself. Potential results of a cask drop are not addressed here.

Rationale - A separate analysis by others is performed to assess potential of breach of a canister in the event of a lifted cask drop.

A3.2.2 CHC Designed to Code Stress Limits

Structural components of the bridge girders and the trolley will be designed to the stress limits of the NOG-1 code (Reference A2.2.6) for different load combinations specified in the NOG-1.

Rationale - At the time this calculation was prepared, the detailed design calculations of the CHC were not available. Thus, it is not possible to determine the margin between the code limits and the calculated stresses that the designers will use. This is extra margin over the margins in the material strengths, code acceptance criteria and load combinations. Due to lack of a detailed design calculation, it is conservatively assumed that this extra margin is unity.

A3.2.3 Materials Assumed for CHC Bridge Girder and Trolley

The structural steel assumed for the CHC bridge girder and the trolley is A 572.

Rationale - Due to the assumption made in A3.2.2, the strength factor of safety is independent of the material assumed. See Section A6.5.1 for details.

A4. METHODOLOGY

A4.1 QUALITY ASSURANCE

This calculation is prepared in accordance with EG-PRO-3DP-G04B-00037, Calculations and Analyses (Reference A2.1.1).

A4.2 USE OF SOFTWARE

Mathcad version 14 is used in this calculation. The use of this software is classified as Level 2 software per procedure, IT-PRO-0011 (Reference A2.1.3) and therefore the software need not be qualified.

A4.3 APPROACH

The Separation-of-Variable method documented in EPRI TR-103959 (Reference A2.2.1, Section 3) is followed in calculating seismic fragility of this ITS equipment component.

A5. LIST OF APPENDICES

Appendix A-A. Estimate of Vertical Frequency of the Bridge Crane

Appendix A-B. DBGM-2 ISRS at CHC Rail Level (Reference A2.2.2)

A6. FRAGILITY CALCULATION

A6.1 INTRODUCTION

The seismic fragility calculation of the CRCF Cask Handling Crane (CHC) is performed here. The calculation evaluates seismic fragilities of structural failure modes of the CHC that may result in a drop of the lifted cask and/or structural failure of the CHC itself. The scope of this fragility review includes all elements of the CRCF Cask Handling Crane that rest on top of the crane rails. The fragility of the crane rails, the rail supports, the rail anchorage and the structure are addressed by others.

A6.2 CASK HANDLING CRANE

The Cask Handling Crane is an ASME NOG-1 (Reference A2.2.6) Type 1 overhead bridge crane located in the cask preparation rooms of the CRCF. The Cask Handling Crane and the trolley including their respective runway rails are designated ITS (Important to Safety) mechanical handling system equipment per Reference A2.2.8. The rail to rail distance of the CRCF CHC is 87' per Reference A2.2.8. The estimated weights of the CHC and its capacity are provided in Reference A2.2.8 as presented below. A schematic of the CHC is shown in Figure A6.2-1 (Reference A2.2.8).

- Bridge weight = 99 tons
- Trolley weight = 44 tons
- Load Block weight = 10 tons
- TAD-loaded cask w/o impact limiters = 125 tons (Reference A2.2.14)

The general operation of the Cask Handling Crane includes the following:

- Remove the transportation cask personnel barrier (optional)
- Remove the impact limiters from the transportation cask
- Hoist and position the cask handling yokes
- Upend the transportation cask from the horizontal transportation position to the vertical position
- Lift the transportation cask from its conveyance
- Place the cask into the Cask Transfer Trolley

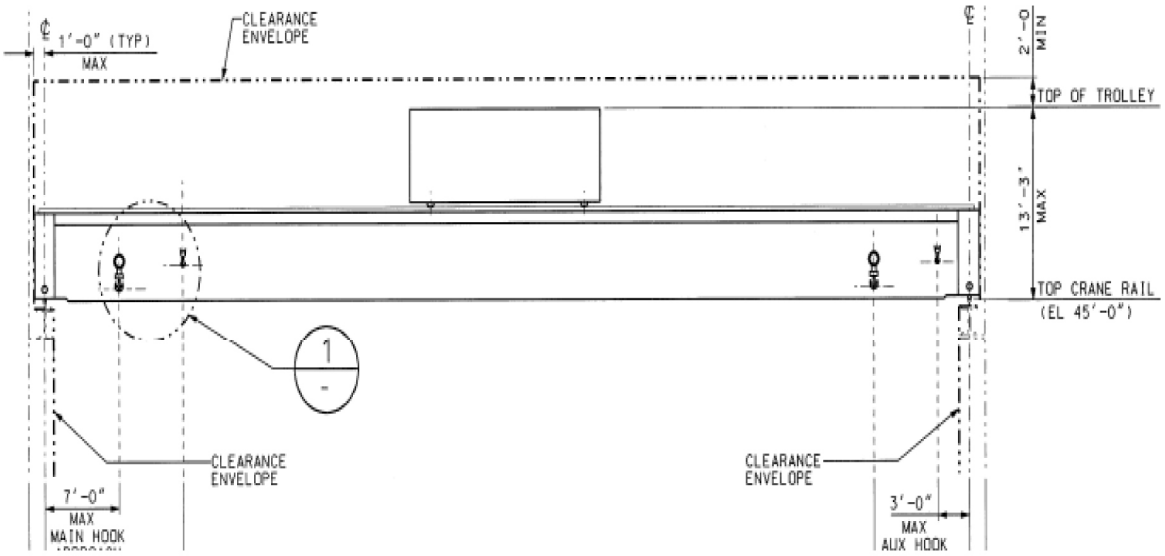

Figure A6.2-1. Schematic of CHC Showing Bridge and Trolley (Reference A2.2.8)

A6.3 STRUCTURAL FAILURE MODES OF CHC

Seismic failure modes that will potentially result in a drop of or damage to a lifted cask are identified below.

- Failure of the bridge crane
- Failure of the trolley
- Failure of seismic restraints of the trolley

A6.4 SEISMIC INPUT MOTION

The DBGM-2 ground motion is defined by the horizontal and vertical site-wide mean uniform hazard spectra (Reference A2.2.7; also Section 6.2.2.1 for source information) at the surface level. The site-wide UHS are the enveloping cases of the surface UHS of 30', 70', 100' and 200' of alluvium over tuff. The alluvium depths under the three CRCF structures vary from 100' to 200'. The Tier 1 analyses (Reference A2.2.2) considered these two depths of alluvium in addition to the three soil properties (upper bound, lower bound, and median cases). The design ISRS are envelopes of these different cases.

The CHC is supported by the CRCF building structure at elevation 45' (elevation at the top of rails per Reference A2.2.8) where the seismic input motion is defined. Since no ISRS was generated at elevation 45', the averaged spectral values of the ISRS at elevations 64' and 32' generated at Nodes 419 and 224 of the CRCF mathematical model (Reference A2.2.15) are used. For this calculation, both the design and the raw (i.e., unbroadened and unsmoothed) ISRS from the BSC Tier 1 analyses (Reference A2.2.2) are utilized.

A6.5 SEISMIC FRAGILITY OF BRIDGE CRANE

A6.5.1 Strength Factor

Per Section 4.8.1 of Mechanical Handling Design Criteria (Reference A2.2.5), the applicable code for the CHC design is ASME NOG-1 2004. The median strength factor of the CHC girder structural failure is estimated based on the NOG-1 design criteria. It is assumed (see Assumption A3.2.2) that the CHC will be designed such that the calculated stresses for the different load combinations in NOG-1 will be at the code allowable.

The basic NOG-1 load combination for crane operational loads (Section 4140 of NOG-1) that is applicable to the CHC is:

LC1 = Dead weight of bridge and trolley + rated load

The NOG-1 load combinations for earthquake loads (SSE) are (Section 4140 of NOG-1):

LC10 = Dead weight of bridge and trolley + SSE loads
LC11 = Dead weight of bridge and trolley + SSE loads + credible critical load with SSE

Per Section 4300 of NOG-1, the basic allowable stress of the operating loading conditions for structural members is 50% of the yield strength for tension and compression. For extreme environmental load combination which includes SSE (Safe Shutdown Earthquake), the allowable stress is 90% of the yield strength (Table 4311-1 of NOG-1). The DBGM-2 is used in the NOG-1 load combinations for SSE.

$$\sigma_{NOL} = 0.5 \cdot F_{y\_min} \qquad \text{Equation A-1}$$

$$\sigma_{NOL} + \sigma_{DBGM} = 0.9 \cdot F_{y\_min} \qquad \text{Equation A-2}$$

where σ_{NOL} and σ_{DBGM} are stresses due to normal operating loads (uniform weight of the bridge crane, the trolley weight and the lifted load) and DBGM-2, respectively and F_{y_min} is the minimum yield strength of the girders.

The CHC bridge girders and the trolley frame are more sensitive to vertical direction input motion since the horizontal inertia load from the suspended load is limited due to pendulum action. The vertical fundamental frequencies of the CHC with the rated load (i.e., 200 ton, Reference A2.2.8) at the mid-span and quarter span are estimated at 2.74 Hz and 3.57 Hz, respectively as presented in Appendix A-A, Section A-A.2. The corresponding 7% damped vertical DBGM-2 spectral accelerations are 0.6g and 0.7g, respectively (Table A-A-1). Also demonstrated in Appendix A-A is that although the vertical acceleration is higher when the trolley is at the quarter point of the span, design of the girders is governed by the case of having the trolley and its rated load at the mid-span (Section A-A.4).

Per Reference A2.2.14, the maximum weight of a cask loaded with a TAD without impact limiters is 250 kips (or 125 tons). This weight is less than the rated capacity of the crane of 200 tons. The vertical fundamental frequency of the CHC with the trolley carrying this weight at the mid-span is calculated to be 3.14 Hz and the corresponding 7% damped DBGM-2 design spectral acceleration is 0.65g (Appendix A-A, Sections A-A.2 and A-A.3).

It is assumed (see A3.2.3) that the bridge girders will be constructed of ASTM 572 Grade 50 steel with a minimum specified yield strength of 50 ksi.

$F_{y\_min} := 50 \cdot ksi$

$F_y := 1.2 \cdot F_{y\_min}$ Median yield strength; the factor to get from minimum specified yield strength to the median value is based on Section 4.6 of Reference A2.2.9.

$F_y = 60 \cdot ksi$

$S_{av\_7\%} := 0.65 \cdot g$ 7% damped DBGM-2 vertical spectral acceleration at the fundamental frequency of the CHC (3.14 Hz) when the trolley loaded with a TAD cask is at the mid-span (See Appendix A-A, mid-span is worst case) . Per Section 4153.8 of NOG-1, a damping value of 7% of critical is used for DBGM-2.

$\sigma_{NOL} := 0.5 \cdot F_{y\_min}$ Normal operating load stress at the mid-span (see Assumption A3.2.2).

$\sigma_{NOL} = 25 \cdot ksi$

$$\sigma_{DBGM} := \frac{S_{av\_7\%}}{g} \cdot \sigma_{NOL} = 16.25 \cdot ksi$$

The median strength factor (F_S) at which a plastic hinge will form at the mid-span is calculated using the equation shown below:

$$(0.78 * \sigma_{NOL}) + (0.78 * \sigma_{NOL} * S_{av\text{-}7\%}) * F_S = (1.1) * F_y$$

where the 0.78 factor determined in Appendix A-A.4 is to account for the fact that the 200-ton crane is not stressed to its full design allowable when it lifts the 125-ton TAD-loaded cask. The 1.1 factor is a conservatively estimated ratio of plastic section modulus to elastic section modulus of a box girder (Reference A2.2.10).

$$F_S := \frac{(1.1)\cdot F_y - \left(\sigma_{NOL}\right)\cdot 0.78}{0.78\cdot \sigma_{DBGM}}$$

$F_S = 3.67$ This is the strength factor when a plastic hinge is formed at the mid-span of the bridge girder.

There is no randomness, only uncertainty associated with the strength factor.

$\beta_{R\_S} := 0$

The uncertainty variability associated with the median yield strength is estimated to be 0.12 based on Table 3-9 of Reference A2.2.1.

$\beta_{U\_S} := 0.12$

$\beta_{c\_S} := \sqrt{\beta_{R\_S}^{\ 2} + \beta_{U\_S}^{\ 2}}$ $\beta_{c\_S} = 0.12$

A6.5.2 Inelastic Energy Absorption Factor

Because the strength factor is calculated based on forming of a plastic hinge of the steel girder (i.e., forming of a mechanism) and the ratcheting effect of the heavy load the crane carries, no further credit is taken for the inelastic energy absorption capability.

$F_\mu := 1.0$

$\beta_{c\_\mu} := 0$

A6.5.3 Equipment Response Factors

A6.5.3.1 Qualification Method

This factor accounts for conservatism in the Tier 1 design ISRS (Reference A2.2.2) relative to the unbroadened and unsmoothed ISRS of the 100-foot best-estimate soil property case. The best-estimate fundamental frequency of the bridge crane in the vertical direction, when the trolley and the TAD-loaded cask are at the mid-span of the span, is 3.14 Hz (Appendix A-A, Section A-A.2).

At 3.14 Hz

$S_{av\_7\%} = 0.65\cdot g$ 7% damped design vertical spectral acceleration from the Tier 1 design ISRS (Appendix A-A, Section A-A.4, Case 2)

$SA_{raw\_224\_7\%} := 0.544\cdot g$ 7% damped raw spectral acceleration of Node 224 (elev. 32'); Figure A-B-2 of Appendix A-B.

$SA_{raw\_419\_7\%} := 0.512\cdot g$ 7% damped raw spectral acceleration of Node 419 (elev. 64'); Figure A-B-4 of Appendix A-B.

$SA_{raw\_7\%} := \frac{1}{2}\left(SA_{raw\_224\_7\%} + SA_{raw\_419\_7\%}\right)$

$SA_{raw\_7\%} = 0.53\cdot g$

$F_{QM} := \frac{S_{av\_7\%}}{SA_{raw\_7\%}}$

$F_{QM} = 1.23$

Since the raw ISRS is used and uncertainties in response due to uncertainty in equipment frequency (i.e., modeling), modal combination, and earthquake component combination are separately calculated below,

$\beta_{c\_QM} := 0$

A6.5.3.2 Equipment Damping

The median and minus one sigma damping values at failure of a welded structure are 7% and 5% , respectively (Table 3-4 of Reference A2.2.1). Since 7% damping will be used for the design per NOG-1, the damping factor of safety is unity.

$F_{\delta\_E} := 1$

$SA_{raw\_5\%\_224} := 0.599 \cdot g$ Raw spectral acceleration at lower bound damping value at the crane frequency; Node 224 raw ISRS (Figure A-B-1 of App. A-B)

$SA_{raw\_5\%\_419} := 0.612 \cdot g$ Raw spectral acceleration at lower bound damping value at the crane frequency; Node 419 raw ISRS (Figure A-B-3 of App. A-B)

$SA_{raw\_5\%} := \frac{1}{2}\left(SA_{raw\_5\%\_224} + SA_{raw\_5\%\_419}\right) = 0.61 \cdot g$

$\beta_{c\_\delta\_E} := \ln\left(\frac{SA_{raw\_5\%}}{SA_{raw\_7\%}}\right)$

$\beta_{c\_\delta\_E} = 0.14$

A6.5.3.3 Equipment Modeling Factor

Since the vertical response of the CHC is a relatively simple system, the frequency calculation is judged to be best-estimate and the modeling factor of safety is unity.

$F_{M\_E} := 1.0$

$\beta_{R\_M\_E} := 0$ No randomness associated with modeling

Reference A2.2.1 provides a range of 0.1 to 0.3 for uncertainty in modal frequencies. Given the relatively simple model of the CHC, a variability of 0.15, which is greater than the 0.1, is judged to be sufficient.

$\beta_f := 0.15$

$f_{v\_m} := 3.14 \cdot Hz$ Best estimate vertical frequency when the trolley with the TAD cask is at the mid-span of the bridge.

$f_u := f_{v\_m} \cdot e^{\beta_f}$ Upper bound frequency

$f_u = 3.65 \cdot Hz$

$SA_{V\_u} := \frac{1}{2}(0.6 \cdot g + 0.595 \cdot g)$ where 0.6g and 0.595g are the 7% damped vertical spectral accelerations from the raw ISRS at Nodes 224 and 419, respectively (Figures A-B-2 and 4 of Appendix A-B).

$SA_{V\_u} = 0.598 \cdot g$

$\beta_{U\_f} := \ln\left(\frac{SA_{V\_u}}{SA_{raw\_7\%}}\right)$

$\beta_{U\_f} = 0.12$

$\beta_{U\_ms} := 0.10$ The uncertainty in response due to uncertainty of mode shape is in the range of 0.05 to 0.15 depending on the complexity of the equipment (Reference A2.2.1). A value of 0.10 is used based on the simple model.

$\beta_{U\_M\_E} := \sqrt{\beta_{U\_f}^2 + \beta_{U\_ms}^2}$

$\beta_{U\_M\_E} = 0.16$

$\beta_{c\_M\_E} := \sqrt{\beta_{R\_M\_E}^2 + \beta_{U\_M\_E}^2}$

$\beta_{c\_M\_E} = 0.16$

A6.5.3.4 Modal Combination

The dynamic response spectrum method is one of the methods described in Section 4153 of NOG-1 for performing seismic analysis for Type 1 cranes. When the response spectrum method is used, closely spaced modes are combined per grouping method, ten-percent method, or double-sum method as per Section 4153.10 of NOG-1. For the failure mode of the bridge girder evaluated here, the response will be predominantly that of the vertical mode. Thus, the modal combination factor of safety is judged to be unity, no conservative or unconservative bias.

$F_{MC\_E} := 1.0$

$\beta_{R\_MC\_E} := 0.05$ For the failure mode evaluated, the fundamental vertical mode is dominant. Thus use the lower bound value of 0.05 in Reference A2.2.1.

$\beta_{U\_MC\_E} := 0$

$\beta_{c\_MC\_E} := \sqrt{\beta_{R\_MC\_E}^2 + \beta_{U\_MC\_E}^2}$

$\beta_{c\_MC\_E} = 0.05$

A6.5.3.5 Earthquake Component Combination

Section 4153.10(c) of NOG-1 requires using the SRSS (Square Root of Sum of the Squares) to

combine contributions for the three components of earthquake motion. This method is considered to be median-centered. Thus,

$F_{ECC\_E} := 1.0$

$\beta_{R\_ECC\_E} := 0.10$ A generic value of 0.18 is suggested in Reference A2.2.1 when responses from each of the three components are not available. A value of 0.10 is used here since the vertical component contributes most significantly to the response of the failure mode evaluated.

$\beta_{U\_ECC\_E} := 0$

$\beta_{c\_ECC\_E} := \sqrt{\beta_{R\_ECC\_E}^2 + \beta_{U\_ECC\_E}^2}$

$\beta_{c\_ECC\_E} = 0.1$

Equipment Response Factors

$F_{RE} := F_{QM} \cdot F_{\delta\_E} \cdot F_{M\_E} \cdot F_{MC\_E} \cdot F_{ECC\_E}$

$F_{RE} = 1.23$

$\beta_{c\_RE} := \sqrt{\beta_{c\_QM}^2 + \beta_{c\_\delta\_E}^2 + \beta_{c\_M\_E}^2 + \beta_{c\_MC\_E}^2 + \beta_{c\_ECC\_E}^2}$

$\beta_{c\_RE} = 0.24$

A6.5.4 Structural Response Factors

A6.5.4.1 Spectral Shape Factor

This factor accounts for conservatism in the site-wide DBGM-2 design spectrum. At the Surface Facilities Area (SFA) the depth of alluvium overlying tuff varies from 30 feet to 200 feet. Uniform hazard spectra at the surface are calculated from site response analyses for alluvium depths of 30', 70', 100' and 200'. The site-wide design ground response spectrum is the envelope of the surface spectra of these four alluvium depths (Reference A2.2.7; also Section 6.2.2.1 for source information).

The dominant frequency of the CRCF soil-structure system in the vertical direction is 6.18 Hz from the Tier 1 ISRS calculation (Reference A2.2.2). Since the vertical UHS for the 100-ft alluvium depth case is not available, the horizontal site-wide and the surface spectrum of the 100-ft alluvium depth case are used to calculate the spectral shape factor. The dominant mode of the CRCF in the horizontal direction has a frequency of 5.2 hz (Reference A2.2.2). At this frequency

$SA_{site} := 1.14g$ 5% damped site-wide spectral acceleration (see Figure A6.5-1).

$SA_{100} := 1.06 \cdot g$ 5% damped spectral acceleration of the 100-foot best-estimate alluvium depth case in the northeast area where the preclosure surface facilities are located.

$F_{SA} := \frac{SA_{site}}{SA_{100}}$

$F_{SA} = 1.08$

Since uncertainty in the UHS is derived from uncertainty in the seismic hazard curves which will be included in the final risk quantification, no uncertainty is included under the spectral shape factor to avoid double-counting the hazard uncertainty, hence

$\beta_{U\_SA} := 0$

$\beta_{R\_SA} := 0.2$ This is random variability to account for peak to valley variability of a smooth ground response spectrum (Reference A2.2.1, Table 3-2)

$\beta_{c\_SA} := \sqrt{\beta_{U\_SA}^2 + \beta_{R\_SA}^2}$

$\beta_{c\_SA} = 0.2$

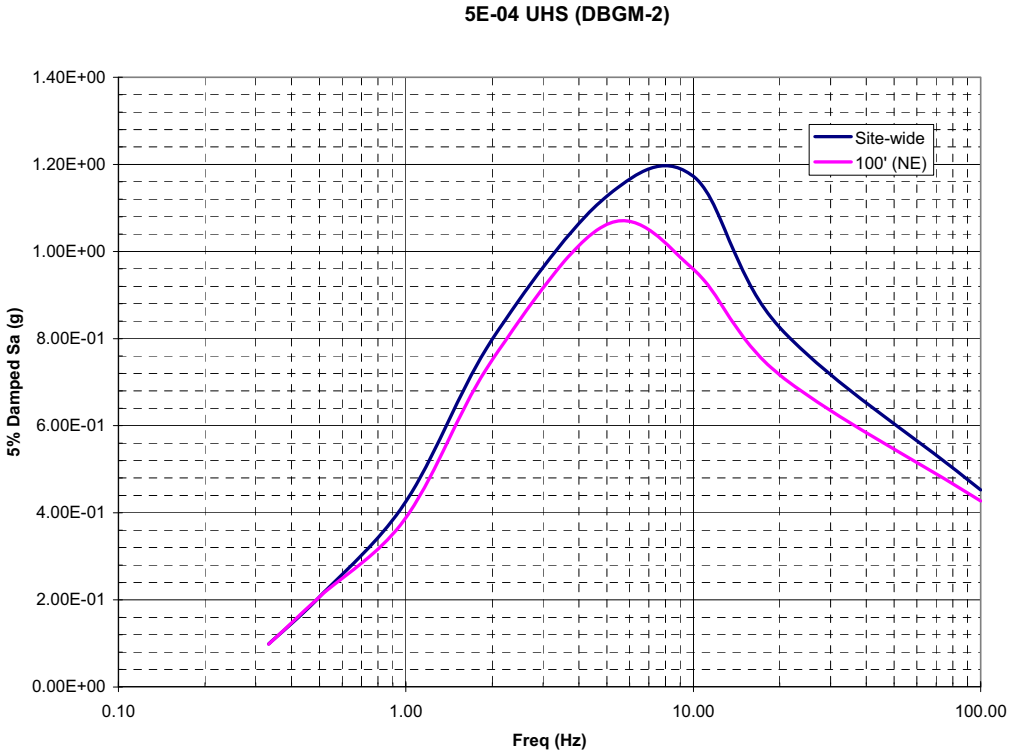

Figure A6.5-1. DBGM-2 (Site-Wide) vs. Horizontal Surface Spectrum of 100-Ft Alluvium Depth Case (See Section 6.2.2.1 for source information)

A6.5.4.2 Damping Factor

This factor is to account for conservatism in the hysteresis damping of the building structure used in the seismic response analysis. Due to the high radiation damping of the foundation media, the effect of structure damping is insignificant. Thus,

$F_\delta := 1.0$

$\beta_{U\_\delta} := 0$

$\beta_{R\_\delta} := 0$

Since a conservative median factor of safety is used for structure damping, no value is assigned to the uncertainty and random logarithmic standard deviations.

$\beta_{c\_\delta} := \sqrt{\beta_{U\_\delta}^{2} + \beta_{R\_\delta}^{2}}$ $\beta_{c\_\delta} = 0$

A6.5.4.3 Modeling Factor

The Tier 1 lumped mass multiple stick model of the CRCF models the stiffness of various reinforced concrete walls and distribution of mass at each floor. The floors are assumed to be rigid diaphragms tying the different sticks together. Torsional response of the structure is captured through modeling eccentricity between the center of mass and center of rigidity of each floor. The foundation media underneath the buildings are modeled with soil springs and dashpots based on elastic half space theory with adjustment to account for the layering effect of alluvium overlying tuff. The model is judged to adequately represent the CRCF structure dynamic characteristics, thus

$F_M := 1.0$

$\beta_{R\_M} := 0$

Uncertainty of structure frequencies predicted from mathematical modeling varies from 0.15 to 0.35 depending on the sophistication of the model (Reference A2.2.1). The value of 0.35 is for a fairly approximate model and the value 0.15 is appropriate for detailed models. Based on the complexity of the CRCF structure and the mathematical model used for the Tier 1 ISRS analysis, it is judged that the calculated CRCF frequency has a logarithmic standard deviation of 0.25.

$\beta_f := 0.25$ Uncertainty in building frequency.

$f_m := 5.2 \cdot Hz$ Best-estimate frequency

$f_{upper} := f_m \cdot e^{\beta_f}$ Upper bound frequency

$f_{upper} = 6.68 \cdot Hz$

$SA_{upper} := 1.05g$ 5% damped spectral acceleration at f_{upper} read off from the mean 5E-4 UHS of the 100-foot alluvium depth case (Figure A6.5-1). This value is less than the value at the best-estimate frequency.

$f_{lower} := f_m \cdot e^{-\beta_f}$ Lower bound frequency

$f_{lower} = 4.05 \cdot Hz$

$SA_{lower} := 1.02 \cdot g$ 5% damped spectral acceleration at f_{lower} read off from the mean 5E-4 UHS of the 100-foot alluvium depth case. This value is less than the value at the best-estimate frequency.

$\beta_{U\_f} := 0$ Since the spectral value at the best-estimate frequency is greater than that at either the lower bound or upper bound frequency.

$\beta_{U\_ms} := 0.10$ Uncertainty of mode shape (Reference A2.2.1, page 3-18); a lower value of 0.10 is used here based on the simple configuration of the bridge girders.

$$\beta_{U\_M} := \sqrt{\beta_{U\_f}^2 + \beta_{U\_ms}^2}$$

$$\beta_{U\_M} = 0.1$$

$$\beta_{c\_M} := \sqrt{\beta_{R\_M}^2 + \beta_{U\_M}^2} \qquad \beta_{c\_M} = 0.1$$

A6.5.4.4 Modal Combination

Since the direct integration time history method was used in the Tier 1 ISRS analysis (Reference A2.2.2), the modal combination method factor of safety is unity and there is no variability associated with modal combination.

$$F_{MC} := 1$$

$$\beta_{R\_MC} := 0$$

$$\beta_{U\_MC} := 0$$

$$\beta_{c\_MC} := \sqrt{\beta_{R\_MC}^2 + \beta_{U\_MC}^2} \qquad \beta_{c\_MC} = 0$$

A6.5.4.5 Soil-Structure Interaction

Two factors are considered, the first one is on the method of treating the SSI effects and the second one is on the effect of soil softening at ground acceleration higher than DBGM-2. The Tier 1 seismic response analyses of the CRCF use the site-wide $5*10^{-4}$ mean uniform hazard spectra as the DBGM-2 input motion. Spectrum compatible time histories are used as the input motion for the time history analyses. The conservatism in the site-wide spectra was accounted for in the spectral shape factor above. Strain compatible soil properties of 100-foot and 200-foot deep alluvium are used to calculate frequency-independent soil springs and soil damping coefficients. Soil radiation damping is introduced into the model by using dashpots. Damping coefficients equal to 75% of the computed values for translational degrees of freedom and to the full computed rotational damping values are used in the response analyses (Reference A2.2.2). Conservatism or unconservatism in SSI will be minimized for final SSI analyses used to develop equipment design seismic input. Before the final SSI analyses are completed, the Tier 1 SSI analysis is taken to represent the best-estimate responses per BSC recommendations in Reference A2.2.13.

$$F_{SSI\_1} := 1$$

$$\beta_{R\_SSI\_1} := 0$$

$\beta_{U\_SSI\_1} := 0.25$ Uncertainty of the median-centered state-of-the-art SSI method based on past probabilistic seismic response analyses using the same method.

It is judged that the median seismic capacity of the structural failure mode of the CHC, expressed in terms of peak ground acceleration, is close to that of BDBGM. Due to soil nonlinearity, amplification of the input ground motion at BDBGM will be different from that of DBGM-2. The second factor of safety is to account for this difference and is estimated using the DBGM-2 raw spectra and the BDBGM raw spectra at the vertical frequency of the CHC which is 3.14 Hz.

At 3.14 Hz

Node 224

$S_{v\_DBGM\_7\%} := 0.544 \cdot g$

$ZPA_{DBGM} := 0.287 \cdot g$

$S_{v\_BDBGM\_10\%} := 1.01 \cdot g$

$ZPA_{BDBGM} := 0.675 \cdot g$

The 7% & 10% damped vertical spectral accelerations and the floor zero period accelerations of DBGM-2 (Figure A-B-2) and BDBGM (Figure A-B-9 of Appendix A-B). Based on that 7% of critical damping will be used for the design of the CHC, the best-estimate damping value at BDBGM is estimated at 10% of critical damping.

$$F_{SSI\_2\_224} := \frac{\frac{S_{v\_DBGM\_7\%}}{ZPA_{DBGM}}}{\frac{S_{v\_BDBGM\_10\%}}{ZPA_{BDBGM}}} = 1.27$$

Node 419

$S_{v\_DBGM\_7\%} := 0.512 \cdot g$

$ZPA_{DBGM} := 0.306 \cdot g$

$S_{v\_BDBGM\_10\%} := 1.02 \cdot g$

$ZPA_{BDBGM} := 0.743 \cdot g$

The 7% & 10% damped vertical spectral accelerations and the floor zero period accelerations of DBGM-2 (Figure A-B-4) and BDBGM (Figure A-B-10 of Appendix A-B). Based on that 7% of critical damping will be used for the design of the CHC, the best-estimate damping value at BDBGM is estimated at 10% of critical damping.

$$F_{SSI\_2\_419} := \frac{\frac{S_{v\_DBGM\_7\%}}{ZPA_{DBGM}}}{\frac{S_{v\_BDBGM\_10\%}}{ZPA_{BDBGM}}} = 1.22$$

$$F_{SSI\_2} := \frac{1}{2}\left(F_{SSI\_2\_224} + F_{SSI\_2\_419}\right)$$

$F_{SSI\_2} = 1.24$

$$\beta_{U\_SSI\_2} := \frac{1}{1.65} \ln\left(F_{SSI\_2}\right) = 0.13$$

$F_{SSI} := F_{SSI\_1} \cdot F_{SSI\_2}$

$F_{SSI} = 1.24$

$\beta_{U\_SSI} := \sqrt{\beta_{U\_SSI\_1}^2 + \beta_{U\_SSI\_2}^2} = 0.28$

$\beta_{c\_SSI} := \sqrt{\beta_{R\_SSI\_1}^2 + \beta_{U\_SSI}^2}$

$\beta_{c\_SSI} = 0.28$

A6.5.4.6 Ground Motion Incoherence

$L1 := 327 \cdot ft$ East-west dimension of CRCF excluding the 49'-6" and 43' extensions at the east and west ends, respectively (Reference A2.2.3).

$L2 := 336 \cdot ft$ North-south dimension of CRCF excluding the 56' extension at the south end.

$L_{eq} := \sqrt{L1 \cdot L2}$ Equivalent foundation dimension of CRCF

$L_{eq} = 331.47\,ft$

The ground motion incoherence reduction factor is a function of foundation size and frequency of response. For a 150 foot plan dimension foundation, the following reduction factors are presented in Reference A2.2.1 in page 3-22. Interpolation or extrapolation may be used to calculate the reduction factor for different dimensions and/or frequencies.

$L_{std} := 150 \cdot ft$ Foundation dimension of which the reduction factors in Reference A2.2.1 are calculated.

$f_5 := 5$ Frequency in cycle/sec (Hz)

$RF_5 := 1$ Reduction factor for response frequency at 5 Hz

$f_{10} := 10$ Frequency in Hz

$RF_{10} := 0.9$ Reduction factor for response frequency at 10 Hz

$RF_{5\_eq} := RF_5$ Reduction factor at 5 Hz, given the CRCF equivalent foundation dimension

$RF_{10\_eq} := 1 - \left[\left(1 - RF_{10}\right) \cdot \frac{L_{eq}}{L_{std}}\right]$ Linear extrapolation

$RF_{10\_eq} = 0.78$ Reduction factor at L_{eq} dimension and 10 Hz frequency of response.

The vertical frequency of the CRCF with 100-ft of median soil with soil properties compatible with DBGM-2 level, is 6.2 Hz. However, the seismic acceleration level at which crane failure is expected is significantly higher than DBGM-2 and even greater than BDBGM. Thus, the vertical frequency of the CRCF with 100-ft of median soil with properties compatible with BDBGM level is considered. This frequency is 5.3 Hz (page 45 of Reference A2.2.2).

$f_6 := 5.3$ Frequency in Hz

Calculate the reduction factor at 5.3 Hz by interpolation

$RF_{6\_eq} := 0.4$ A trial value to initiate the equation solver below.

Given

$$\frac{\log(RF_{10\_eq}) - \log(RF_{5\_eq})}{\log(RF_{6\_eq}) - \log(RF_{5\_eq})} = \frac{\log(f_{10}) - \log(f_5)}{\log(f_6) - \log(f_5)}$$

$a := \text{Find}(RF_{6\_eq})$

$a = 0.98$

Thus, the ground motion incoherence factor of safety is

$$F_{GMI} := \frac{1}{a}$$

$F_{GMI} = 1.02$

$$\beta_{U\_GMI} := \frac{1}{2} \cdot \ln\left(\frac{1}{a}\right)$$

$\beta_{U\_GMI} = 0.01$

A reduction factor of 1.0 (i.e., no reduction) is estimated to be two standard deviation from the calculated median factor of 0.91 (Reference A2.2.1, Page 3-23).

$\beta_{R\_GMI} := 0$

$$\beta_{c\_GMI} := \sqrt{\beta_{R\_GMI}^2 + \beta_{U\_GMI}^2}$$

$\beta_{c\_GMI} = 0.01$

Structural Response Factors

$F_{RS} := F_{SA} \cdot F_{\delta} \cdot F_M \cdot F_{MC} \cdot F_{SSI} \cdot F_{GMI}$

$F_{RS} = 1.36$

$$\beta_{c\_RS} := \sqrt{\beta_{c\_SA}^2 + \beta_{c\_\delta}^2 + \beta_{c\_M}^2 + \beta_{c\_MC}^2 + \beta_{c\_SSI}^2 + \beta_{c\_GMI}^2}$$

$\beta_{c\_RS} = 0.36$

A6.5.5 Overall Factor of Safety

$F_{total} := F_S \cdot F_{\mu} \cdot F_{RS} \cdot F_{RE}$

$F_{total} = 6.16$

$PGA := 0.453g$ Peak ground acceleration of the DBGM-2 design spectrum (Reference A2.2.7; also Section 6.2.2.1 for source information).

$A_m := F_{total} \cdot PGA$

$A_m = 2.79 \cdot g$ Median seismic capacity in terms of PGA

$$\beta_c := \sqrt{\beta_{c\_S}^{\ 2} + \beta_{c\_\mu}^{\ 2} + \beta_{c\_RS}^{\ 2} + \beta_{c\_RE}^{\ 2}}$$

$$\beta_c = 0.45$$

$$HCLPF := A_m \cdot e^{-2.33 \cdot \beta_c} = 0.98 \cdot g$$

A6.6 SEISMIC FRAGILITY OF TROLLEY

Due to high seismicity at the YMP site, it is envisioned that seismic restraints will be provided to the trolleys to prevent the trolleys from uplifting and sliding off the rails in a seismic event. These seismic restraints can be in the form of seismic bumpers to transfer the horizontal seismic inertia load directly to the girders and seismic catchers to transfer the uplift force to the girders. Both the seismic bumpers and catchers can be constructed from structural steel shapes and bolted or welded to the underside of the trolley chassis as schematically depicted in Figure A6.6-1 below.

At this time, detailed design of the trolley and its seismic restraints has not been performed. Structural failure of the trolley frame will have similar generic seismic capacity as the bridge girders since both will be designed to the NOG-1 criteria. Thus, a representative seismic fragility is calculated below for the trolley seismic restraints. Furthermore, because bolted connections in general have lower median capacity than welded connections, when both are designed to the same demand, hence seismic fragility of the bolted connection is calculated here for the seismic restraints.

Conservatively assume A307 bolts will be used for the clamp bolts which have the lowest strength among the acceptable fastener materials in NOG-1, Tables 4221-1 and 4221-2.

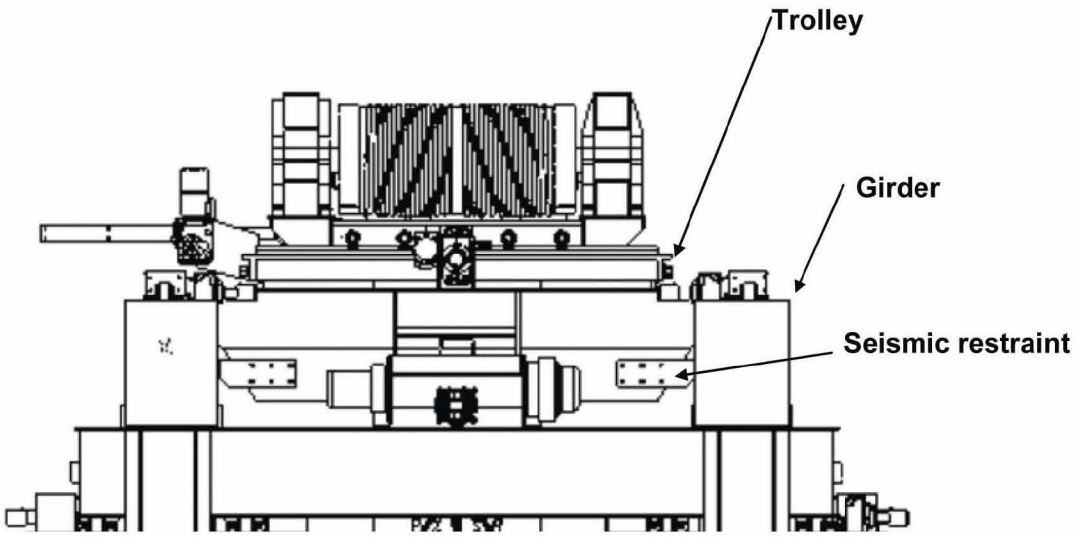

Figure A6.6-1. CHC Hoist Trolley (Schematic)

A6.6.1 Strength Factor

The bolts attaching the seismic restraints to the trolley chassis are subjected to shear.

$f_{u\_min} := 58\text{ksi}$ Minimum ultimate tensile strength of A307 (Table 3-9 of Reference A2.2.1)

$\tau_{design} := 1.4 \cdot (10 \cdot \text{ksi})$ where 10 ksi is the allowable shear stress for bolt steel per AISC and 1.4 is the bump-up factor for DBGM-2 load combination (References A2.2.10 and A2.2.11)

$\tau_{design} = 14 \cdot \text{ksi}$

$f_{u\_m} := 64 \cdot \text{ksi}$ Median ultimate tensile strength of A307 bolt steel (Table 3-9 of Reference A2.2.1)

$\tau_{u\_m} := 0.62 \cdot f_{u\_m}$ Table 3-10 of Reference A2.2.1

$$F_{S\_shear} := \frac{\tau_{u\_m}}{\tau_{design}}$$

$F_{S\_shear} = 2.83$

$\beta_{R\_S} := 0$

$\beta_{U\_S} := 0.10$ Table 3-10 of Reference A2.2.1

$$\beta_{c\_S} := \sqrt{\beta_{R\_S}^2 + \beta_{U\_S}^2}$$

$\beta_{c\_S} = 0.1$

A6.6.2 Inelastic Energy Absorption Factor

The bolt failure mode is localized and the failure of the bolts is based on the ultimate strength , thus there is no inelastic energy absorption factor.

$F_{\mu} := 1.0$

$\beta_{R\_\mu} := 0$

$\beta_{U\_\mu} := 0$

$$\beta_{c\_\mu} := \sqrt{\beta_{R\_\mu}^2 + \beta_{U\_\mu}^2}$$

$\beta_{c\_\mu} = 0$

A6.6.3 Equipment Response Factors

A6.6.3.1 Qualification Method

This factor accounts for conservatism in the Tier 1 design ISRS (Reference A2.2.2) relative to the median ISRS. The median ISRS are the Tier 1 unbroadened and unsmoothed floor response spectra from the median soil case. The fundamental frequency of the bridge crane in the east-west direction (perpendicular to the bridge girder), when the trolley with the lifted cask is at the mid-span of the

bridge, is estimated to be in the range of 2 to 3 Hz.

At 2 Hz

$$SA_{design\_2} := \frac{1}{2}(1.03 \cdot g + 0.98 \cdot g) = 1 \cdot g$$

1.03g and 0.98g are the 7% damped design spectral accelerations of the east-west ISRS of the 100-foot alluvium case at Nodes 224 and 419, respectively (Figures A-B-6 and 8 of Appendix A-B).

$$SA_{raw\_2} := \frac{1}{2}(0.85 \cdot g + 0.86 \cdot g) = 0.86 \cdot g$$

0.85g and 0.86g are the 7% damped spectral accelerations of the median soil case, east-west direction raw spectra of the 100-foot alluvium case (Figures A-B-6 and 8 of Appendix A-B).

$$F_{QM\_2} := \frac{SA_{design\_2}}{SA_{raw\_2}}$$

$$F_{QM\_2} = 1.18$$

At 3 Hz

$$SA_{design\_3} := \frac{1}{2}(1.32 \cdot g + 1.39 \cdot g) = 1.36 \cdot g$$

1.32g and 1.39g are the 7% damped design spectral accelerations of the east-west ISRS of the 100-foot alluvium case at Nodes 224 and 419, respectively (Figures A-B-6 and 8 of Appendix A-B).

$$SA_{raw\_3} := \frac{1}{2}(1.12 \cdot g + 1.16 \cdot g) = 1.14 \cdot g$$

1.12g and 1.16g are the 7% damped spectral accelerations of the median soil case, east-west direction raw spectrum of the 100-foot alluvium case (Figures A-B-6 and 8 of Appendix A-B).

$$F_{QM\_3} := \frac{SA_{design\_3}}{SA_{raw\_3}}$$

$$F_{QM\_3} = 1.19$$

$$F_{QM} := \frac{1}{2} \cdot \left(F_{QM\_2} + F_{QM\_3}\right)$$

$$F_{QM} = 1.18$$

Since the raw ISRS is used and uncertainties in response due to uncertainty in equipment frequency (i.e., modeling), modal combination, and earthquake component combination are separately calculated below,

$$\beta_{c\_QM} := 0$$

A6.6.3.2 Equipment Damping

The median and lower bound damping values at the failure of the bridge crane are 7% and 5%, respectively (Table 3-4 of Reference A2.2.1 for welded steel structures). Since 7% damping is used in the crane design seismic analysis (Section 4153.8 of NOG-1), the factor of safety is unity.

$$F_{\delta\_E} := 1$$

At 2 Hz

$$SA_{raw\_5\%} := \frac{1}{2}(0.991 \cdot g + 1.01 \cdot g) = 1 \cdot g$$

0.991g and 1.01g are the 5% damped spectral accelerations of the median soil case, east-west direction raw spectrum of the 100-foot alluvium case (Figures A-B-5 and 7 of Appendix A-B).

$$\beta_{c\_\delta\_E\_2} := \ln\left(\frac{SA_{raw\_5\%}}{SA_{raw\_2}}\right)$$

$$\beta_{c\_\delta\_E\_2} = 0.16$$

At 3 Hz

$$SA_{raw\_5\%} := \frac{1}{2}(1.31 \cdot g + 1.36 \cdot g) = 1.34 \cdot g$$

1.31g and 1.36g are the 5% damped spectral accelerations of the median soil case, east-west direction raw spectrum of the 100-foot alluvium case (Figures A-B-5 and 7 of Appendix A-B).

$$\beta_{c\_\delta\_E\_3} := \ln\left(\frac{SA_{raw\_5\%}}{SA_{raw\_3}}\right)$$

$$\beta_{c\_\delta\_E\_3} = 0.16$$

$$\beta_{c\_\delta\_E} := \frac{1}{2}\left(\beta_{c\_\delta\_E\_2} + \beta_{c\_\delta\_E\_3}\right)$$

$$\beta_{c\_\delta\_E} = 0.16$$

A6.6.3.3 Equipment Modeling Factor

$$F_{M\_E} := 1.0$$

Since the effect of frequency uncertainty is included in the qualification method factor.

$$\beta_{R\_M\_E} := 0$$

No randomness associated with modeling

$$\beta_{U\_ms} := 0.10$$

The uncertainty in response due to uncertainty of mode shape is in the range of 0.05 to 0.15 depending on the complexity of the equipment (Reference A2.2.1). A value of 0.10 is used.

$$\beta_{U\_M\_E} := \sqrt{\beta_{U\_f}^2 + \beta_{U\_ms}^2} = 0.1$$

$$\beta_{c\_M\_E} := \sqrt{\beta_{R\_M\_E}^2 + \beta_{U\_M\_E}^2} = 0.1$$

A6.6.3.4 Modal Combination

The dynamic response spectrum method is one of the methods described in Section 4153 of NOG-1 for performing seismic analysis for Type 1 cranes. When the response spectrum method is used, closely spaced modes are to be combined per grouping method, ten-percent method, or double-sum method as per Section 4153.10. Thus, the modal combination factor of safety is judged to be unity, no conservative or unconservative bias.

$F_{MC\_E} := 1.0$

$\beta_{R\_MC\_E} := 0.05$ For the failure mode evaluated, the fundamental transverse mode is dominant. Thus use the lower bound value of 0.05 in Reference A2.2.1.

$\beta_{U\_MC\_E} := 0$

$$\beta_{c\_MC\_E} := \sqrt{\beta_{R\_MC\_E}^2 + \beta_{U\_MC\_E}^2} = 0.05$$

A6.6.3.5 Earthquake Component Combination

Section 4153.10(c) of NOG-1 requires using the SRSS (Square Root of Sum of the Squares) to combine contributions for the three components of earthquake motion. This method is considered to be median-centered. Thus,

$F_{ECC\_E} := 1.0$

$\beta_{R\_ECC\_E} := 0.10$ A generic value of 0.18 is suggested in Reference A2.2.1 when responses from each of the three components are not available. A value of 0.10 is used here since the north-south component contributes most significantly to the response of the failure mode evaluated.

$\beta_{U\_ECC\_E} := 0$

$$\beta_{c\_ECC\_E} := \sqrt{\beta_{R\_ECC\_E}^2 + \beta_{U\_ECC\_E}^2} = 0.1$$

Equipment Response Factors

$$F_{RE} := F_{QM} \cdot F_{\delta\_E} \cdot F_{M\_E} \cdot F_{MC\_E} \cdot F_{ECC\_E}$$

$$F_{RE} = 1.18$$

$$\beta_{c\_RE} := \sqrt{\beta_{c\_QM}^2 + \beta_{c\_\delta\_E}^2 + \beta_{c\_M\_E}^2 + \beta_{c\_MC\_E}^2 + \beta_{c\_ECC\_E}^2} = 0.22$$

A6.6.4 Structural Response Factors

A6.6.4.1 Spectral Shape Factor

This factor accounts for conservatism in the site-wide DBGM-2 design spectrum. At the Surface Facilities Area (SFA) the depth of alluvium overlying tuff varies from 30 feet to 200 feet. Uniform hazard spectra at the surface are calculated from site response analyses for alluvium depths of 30', 70', 100' and 200'. The site-wide design ground response spectrum is the envelope of the surface spectra of these four alluvium depths (Reference A2.2.7; also Section 6.2.2.1 for source information).

The dominant frequency of the CRCF soil-structure system in the horizontal direction is 5.2 Hz from the Tier 1 ISRS calculation (Reference A2.2.2). At this frequency

$SA_{site} := 1.14g$ 5% damped site-wide spectral acceleration (see Figure A6.5-1).

$SA_{100} := 1.06 \cdot g$ 5% damped spectral acceleration of the 100-foot best-estimate alluvium depth case in the northeast area where the preclosure surface facilities are located.

$$F_{SA} := \frac{SA_{site}}{SA_{100}}$$

$$F_{SA} = 1.08$$

Since uncertainty in the UHS is derived from uncertainty in the seismic hazard curves which will be included in the final risk quantification, no uncertainty is included under the spectral shape factor to avoid double-counting the hazard uncertainty, hence

$$\beta_{U\_SA} := 0$$

$\beta_{R\_SA} := 0.2$ This is random variability to account for peak to valley variability of a smooth ground response spectrum (Reference A2.2.1, Table 3-2)

$$\beta_{c\_SA} := \sqrt{\beta_{U\_SA}^2 + \beta_{R\_SA}^2} = 0.2$$

A6.6.4.2 Damping Factor

This factor is to account for conservatism in the hysteresis damping of the building structure used in the seismic response analysis. Due to the high radiation damping of the foundation media, the effect of structure damping is insignificant. Thus,

$F_{\delta} := 1.0$

$\beta_{U\_\delta} := 0$

$\beta_{R\_\delta} := 0$

Since a conservative median factor of safety is used for structure damping, no value is assigned to the uncertainty or random logarithmic standard deviation.

$\beta_{c\_\delta} := \sqrt{\beta_{U\_\delta}^{2} + \beta_{R\_\delta}^{2}} = 0$

A6.6.4.3 Modeling Factor

The Tier 1 lumped mass multiple stick model of the CRCF models the stiffness of various reinforced concrete walls and distribution of mass at each floor. The floors are assumed to be rigid diaphragms tying the different sticks together. Torsional response of the structure is captured through modeling eccentricity between the center of mass and center of rigidity of each floor. The foundation media underneath the buildings are modeled with soil springs and dashpots based on elastic half space theory with adjustment to account for the layering effect of alluvium overlying tuff. The model is judged to adequately represent the CRCF structure dynamic characteristics, thus

$F_{M} := 1.0$

$\beta_{R\_M} := 0$

Uncertainty of structure frequencies predicted from mathematical modeling varies from 0.15 to 0.35 depending on the sophistication of the model (Reference A2.2.1). The value of 0.35 is for fairly approximate models and the value 0.15 is appropriate for detailed models. Based on the complexity of the CRCF structure and the mathematical model used for the Tier 1 ISRS analysis, it is judged that the calculated CRCF frequency has a logarithmic standard deviation of 0.25.

$\beta_{f} := 0.25$ Uncertainty in building frequency.

$f_{m} := 5.2 \cdot Hz$ Best-estimate frequency

$f_{upper} := f_{m} \cdot e^{\beta_{f}}$ Upper bound frequency

$f_{upper} = 6.68 \cdot Hz$

$SA_{upper} := 1.05g$ 5% damped spectral acceleration at f_{upper} read off from the mean 5E-4 UHS of the 100-foot alluvium depth case (Figure A6.5-1). This value is less than the value at the best-estimate frequency.

$f_{lower} := f_{m} \cdot e^{-\beta_{f}}$ Lower bound frequency

$f_{lower} = 4.05 \cdot Hz$

$SA_{lower} := 1.02 \cdot g$ 5% damped spectral acceleration at f_{lower} read off from the mean 5E-4 UHS of the 100-foot alluvium depth case. This value is less than the value at the best-estimate frequency.

$\beta_{U\_f} := 0$ Since the spectral value at the best-estimate frequency, (SA_{100}), is greater than that at either the lower bound or upper bound frequency.

$\beta_{U\_ms} := 0.10$ Uncertainty of mode shape (Reference A2.2.1, page 3-18); a lower value of 0.10 is used due to simple geometry of the structure.

$$\beta_{U\_M} := \sqrt{\beta_{U\_f}^2 + \beta_{U\_ms}^2} = 0.1$$

$$\beta_{c\_M} := \sqrt{\beta_{R\_M}^2 + \beta_{U\_M}^2} = 0.1$$

A6.6.4.4 Modal Combination

Since direct integration time history method is used in the Tier 1 ISRS analysis (Reference A2.2.2), the modal combination method factor of safety is unity and there is no variability associated with modal combination.

$F_{MC} := 1$

$\beta_{R\_MC} := 0$

$\beta_{U\_MC} := 0$

$$\beta_{c\_MC} := \sqrt{\beta_{R\_MC}^2 + \beta_{U\_MC}^2} = 0$$

A6.6.4.5 Soil-Structure Interaction

Two factors are considered, the first one is on the method of treating the SSI effects and the second one is on the effect of soil softening at ground acceleration higher than DBGM-2. See discussions in Section A6.5.4.6 for details.

$F_{SSI\_1} := 1$

$\beta_{R\_SSI\_1} := 0$

$\beta_{U\_SSI\_1} := 0.25$

At 2 Hz

$SA_{raw\_2} = 0.86 \cdot g$ See Section A6.6.3.1

$ZPA_{DBGM} := \frac{1}{2}(0.534 \cdot g + 0.647 \cdot g) = 0.59 \cdot g$ where 0.534g and 0.647g are the ZPAs of the raw DBGM-2 E-W ISRS at Nodes 224 and 419 (Figures. A-B-6 and 8 of Appendix A-B)

$S_{v\_BDBGM\_10\%} := \frac{1}{2}(1.35 \cdot g + 1.37 \cdot g) = 1.36 \cdot g$ where 1.35g and 1.37g are the 10% damped spectral accelerations from

the E-W direction raw ISRS at Nodes 224 and 419 (Figures A-B-11 and 12 of Appendix A-B).

$$ZPA_{BDBGM} := \frac{1}{2}(1.08 \cdot g + 1.33 \cdot g) = 1.2 \cdot g$$

where 1.08g and 1.33g are ZPAs of the E-W direction raw ISRS at Nodes 224 and 419 (Figures A-B-11 and 12 of Appendix A-B).

$$F_2 := \frac{\frac{SA_{raw\_2}}{ZPA_{DBGM}}}{\frac{S_{v\_BDBGM\_10\%}}{ZPA_{BDBGM}}} = 1.28$$

At 3 Hz

$$SA_{raw\_3} = 1.14 \cdot g$$

$$ZPA_{DBGM} = 0.59 \cdot g$$

$$S_{v\_BDBGM\_10\%} := \frac{1}{2}(1.75 \cdot g + 1.83 \cdot g) = 1.79 \cdot g$$

where 1.75g and 1.83g are the 10% damped spectral accelerations from the E-W direction raw ISRS at Nodes 224 and 419 (Figures A-B-11 and 12 of Appendix A-B).

$$ZPA_{BDBGM} = 1.2 \cdot g$$

$$F_3 := \frac{\frac{SA_{raw\_3}}{ZPA_{DBGM}}}{\frac{S_{v\_BDBGM\_10\%}}{ZPA_{BDBGM}}} = 1.3$$

$$F_{SSI\_2} := \frac{1}{2} \cdot \left(F_2 + F_3\right)$$

$$F_{SSI\_2} = 1.29$$

$$F_{SSI} := F_{SSI\_1} \cdot F_{SSI\_2}$$

$$F_{SSI} = 1.29$$

$$\beta_{U\_SSI\_2} := \frac{\ln\left(F_{SSI\_2}\right)}{1.65}$$

$$\beta_{U\_SSI\_2} = 0.15$$

$$\beta_{R\_SSI} := 0$$

$$\beta_{U\_SSI} := \sqrt{\beta_{U\_SSI\_1}^2 + \beta_{U\_SSI\_2}^2} \qquad \beta_{U\_SSI} = 0.29$$

$$\beta_{c\_SSI} := \sqrt{\beta_{R\_SSI}^2 + \beta_{U\_SSI}^2}$$

$\beta_{c\_SSI} = 0.29$

A6.6.4.6 Ground Motion Incoherence

The ground motion incoherence reduction factor is a function of foundation size and frequency of response. For a 150 foot plan dimension foundation, the reduction factor is 1.0 (i.e., no reduction) at 5 Hz or less (Reference A2.2.1 in page 3-22). The horizontal fundamental frequencies of the CRCF are calculated to be 5.2 Hz and 4.4 Hz, respectively for DBGM-2 and BDBGM with 100-ft of median soil overlying tuff (Page 45 of Reference A2.2.2). Since the seismic acceleration level at which trolley failure is expected is significantly higher than DBGM-2, the 4.4 Hz horizontal frequency is considered. Furthermore, because this frequency is lower than 5 Hz, the ground motion incoherence reduction factor is 1.0.

$F_{GMI} := 1$

$\beta_{U\_GMI} := 0$

$\beta_{R\_GMI} := 0$

$\beta_{c\_GMI} := \sqrt{\beta_{R\_GMI}^2 + \beta_{U\_GMI}^2}$

$\beta_{c\_GMI} = 0$

Structural Response Factors

$F_{RS} := F_{SA} \cdot F_{\delta} \cdot F_M \cdot F_{MC} \cdot F_{SSI} \cdot F_{GMI} = 1.39$

$\beta_{c\_RS} := \sqrt{\beta_{c\_SA}^2 + \beta_{c\_\delta}^2 + \beta_{c\_M}^2 + \beta_{c\_MC}^2 + \beta_{c\_SSI}^2 + \beta_{c\_GMI}^2}$

$\beta_{c\_RS} = 0.37$

A6.6.5 Overall Factor of Safety

$F_{total} := F_{S\_shear} \cdot F_{\mu} \cdot F_{RS} \cdot F_{RE}$

$F_{total} = 4.65$

$PGA := 0.453g$ Peak ground acceleration of the DBGM-2 design spectrum (Reference A2.2.7; also Section 6.2.2.1 for source information).

$A_m := F_{total} \cdot PGA$

$A_m = 2.11 \cdot g$ Median seismic capacity in terms of PGA

$\beta_c := \sqrt{\beta_{c\_S}^2 + \beta_{c\_\mu}^2 + \beta_{c\_RS}^2 + \beta_{c\_RE}^2} = 0.44$

$$HCLPF := A_m \cdot e^{-2.33 \cdot \beta_c} = 0.76 \cdot g$$

A7. SUMMARY

Three failure modes of the Cask Handling Crane are evaluated above: (1) structural failure of the CHC girders, (2) structural failure of the frame of the trolley, and (3) failure of seismic restraints of the trolley. Since the trolley's frame will also be designed to the NOG-1 criteria for Type 1 cranes, seismic fragility of the CHC bridge girder is reported for the trolley. Hoist fragility from Attachment B is used for the CHC, since both are designed to NOG-1. The seismic fragilities of these failure modes are:

- Failure of bridge girders -

  A_m = 2.79g β_c = 0.45 HCLPF = 0.98g

- Failure of trolley frame -

  A_m = 2.79g β_c = 0.45 HCLPF = 0.98g

- Failure of trolley seismic restraints -

  A_m = 2.11g β_c = 0.44 HCLPF = 0.76g

- Failure of Hoist (from Attachment B) -

  A_m = 2.28g β_c = 0.50 HCLPF = 0.72g

APPENDIX A-A

ESTIMATE OF VERTICAL FREQUENCY OF CHC

A-A.1 DATA OF CHC

$E_s := 30 \cdot 10^6 \cdot psi$ Young's modulus of steel

$L_s := 87 \cdot ft$ Rail to rail distance of the CRCF CHC (Reference A2.2.8)

$Mass_{bridge} := 99 \cdot ton$ Mass of the bridge (Reference A2.2.8)

$W_{bridge} := Mass_{bridge} \cdot g$

$W_{bridge} = 198 \cdot kip$

$Mass_{trolley} := 44 \cdot ton$ Mass of the trolley (Reference A2.2.8)

$W_{trolley} := Mass_{trolley} \cdot g$

$W_{trolley} = 88 \cdot kip$

$Mass_{block} := 10 \cdot ton$ Mass of the block (Reference A2.2.8)

$W_{block} := Mass_{block} \cdot g$

$W_{block} = 20 \cdot kip$

$Mass_{cask} := 200 \cdot ton$ Capacity of the crane (Reference A2.2.8).

$W_{cask} := Mass_{cask} \cdot g$

$W_{cask} = 400 \cdot kip$

A-A.2 Vertical Frequencies of CHC

At the time this calculation was performed, dimensions of the crane girders were not available. However, the vertical frequency of the CHC may be estimated based on the NOG-1 allowable deflections.

$\Delta_{all} := \frac{L_s}{1000}$ Total vertical deflection of the girder under the trolley dead weight and the rated live load is limited to 1/1000 of the span (Section 4341 of A2.2.6).

$\Delta_{all} = 1.04 \cdot in$

$I := 1 \cdot in^4$ An initial value of the bridge girders moment of inertia to initiate the equation solver.

$W_{trolley\_load} := W_{trolley} + W_{block} + W_{cask}$

$W_{trolley\_load} = 508 \cdot kip$ Combined weight of the trolley and its rated loads

Given

$\Delta_{all} = \frac{(W_{trolley\_load}) \cdot L_s^{3}}{48 \cdot E_s \cdot I}$ With the load at the mid-span (Page 2-298 of Reference A2.2.10).

$a := \text{Find}(I)$

$a = 384505.2 \cdot in^4$

$I := a$ Moment of inertia of the bridge girders

Deflection at midspan due to uniform weight of the girders

$w := \frac{W_{bridge}}{L_s}$ $w = 2.28 \cdot \frac{kip}{ft}$ Uniform weight

$\Delta_1 := \frac{5 \cdot w \cdot L_s^{4}}{384 E_s \cdot I}$ Maximum deflection at mid-span due to uniform weight of the girders (Page 2-296 of Reference A2.2.10).

$\Delta_1 = 0.25 \cdot in$

Deflection due to concentrated weight at mid-span

$\Delta_2 := \frac{W_{trolley\_load} \cdot L_s^{3}}{48 \cdot E_s \cdot I}$ $\Delta_2 = 1.04 \cdot in$

$\Delta_{midspan} := \Delta_1 + \Delta_2$

$\Delta_{midspan} = 1.3 \cdot in$

$f_{CHC\_midspan} := \frac{1}{2 \cdot \pi} \cdot \sqrt{\frac{g}{\Delta_{midspan}}}$ where g is the gravitational acceleration (Section 1.1 of Reference A2.2.12)

$f_{CHC\_midspan} = 2.74 \cdot Hz$

Deflection at quarter point when subjected to uniformly distributed load

$\Delta_3 := \frac{w \cdot \left(\frac{1}{4} \cdot L_s\right)}{24 \cdot E_s \cdot I} \left[L_s^{3} - 2 \cdot L_s \cdot \left(\frac{1}{4} \cdot L_s\right)^2 + \left(\frac{1}{4} \cdot L_s\right)^3 \right]$ Page 2-296 of Reference A2.2.10

Deflection at quarter point when the concentrated load is at quarter point

$\Delta_4 := \frac{W_{trolley\_load} \cdot \left(\frac{1}{4} \cdot L_s\right)^2 \cdot \left(\frac{3}{4} \cdot L_s\right)^2}{3 \cdot E_s \cdot I \cdot L_s}$ Page 2-298 of Reference A2.2.10

$\Delta_3 = 0.18 \cdot in$

$\Delta_{quarter} := \Delta_3 + \Delta_4$

$\Delta_{quarter} = 0.77 \cdot in$

$f_{CHC\_quarter} := \frac{1}{2 \cdot \pi} \cdot \sqrt{\frac{g}{\Delta_{quarter}}}$

$f_{CHC\_quarter} = 3.57 \cdot Hz$

A-A.3 SEISMIC INPUT MOTION

The 7% damped DBGM-2 vertical spectral accelerations at the estimated frequencies are presented below (see Figures A-B-2 and 4 of Appendix A-B).

TABLE A-A-1. VERTICAL FREQUENCIES AND DESIGN ACCELERATIONS - TROLLEY LOCATED AT MID-SPAN AND 1/4-SPAN

	Trolley at Mid-Span		Trolley at 1/4 Span	
Elev.	Vert. Freq.	7% Design Spectral Accel (g)	Vert. Freq.	7% Design Spectral Accel (g)
32'	2.74 Hz	0.62g	3.57 Hz	0.73g
64'	2.74 Hz	0.575g	3.57 Hz	0.665g
45'	2.74 Hz	0.6g	3.57 Hz	0.70g
Note: Spectral acceleration at elevation 45' is the average of that at elev. 32' and 64'.				

A-A.4 MOMENTS IN BRIDGE GIRDER

The remaining calculation determines which position of the trolley will govern the design of the girders.

Case 1. Trolley at mid-span

$f_{CHC\_midspan} = 2.74 \cdot Hz$

$S_{v\_7\%\_mid} := 0.6g$ 7% damped DBGM-2 spectral acceleration (Table A-A-1)

$$M_{max\_1} := \frac{w \cdot L_s^{\,2}}{8} \cdot \left(1 + \frac{S_{v\_7\%\_mid}}{g}\right) + \frac{W_{trolley\_load} \cdot L_s}{4}\left(1 + \frac{S_{v\_7\%\_mid}}{g}\right)$$

(Pages 2-296 and 298 of Reference A2.2.10)

$M_{max\_1} = 21123.6 \cdot kip \cdot ft$ Maximum moment at mid-span due to gravity load plus downward acceleration

Case 2. Trolley at quarter point of the span

$f_{CHC\_quarter} = 3.57 \cdot Hz$

$S_{v\_7\%\_qtr} := 0.7 \cdot g$ 7% damped DBGM-2 spectral acceleration (Table A-A-1)

$$M_{max\_2} := \left[\frac{w \cdot L_s^{\,2}}{8} + \frac{W_{trolley\_load} \cdot \frac{L_s}{4}}{L_s} \cdot \left(\frac{L_s}{2} \right) \right] \cdot \left(1 + \frac{S_{v\_7\%\_qtr}}{g} \right)$$

(Pages 2-296 and 298 of Reference A2.2.10)

$M_{max\_2} = 13052.17 \cdot kip \cdot ft$ Moment at the midspan when the trolley is at the quarter point

$$M_{max\_3} := \left[\frac{w \cdot \left(\frac{L_s}{4} \right)}{2} \cdot \left(L_s - \frac{L_s}{4} \right) + \frac{W_{trolley\_load} \cdot \left(\frac{L_s}{4} \right) \cdot \left(\frac{3 \cdot L_s}{4} \right)}{L_s} \right] \cdot \left(1 + \frac{S_{v\_7\%\_qtr}}{g} \right)$$

(Pages 2-296 and 298 of Reference A2.2.10)

$M_{max\_3} = 16832.87 \cdot kip \cdot ft$ Moment at the quarter point when the trolley is at the quarter point.

Based on the above calculation it is clear that though the DBGM-2 vertical acceleration is higher when the loaded trolley is at the quarter point of the span, design of the girders is governed by the case of having the loaded trolley at the midspan. The maximum bending moment for design of girders is

The maximum weight of a TAD-loaded transport cask without impact limiters is 250,000 lbs per Reference A2.2.14. The maximum bending moment in the girders when the trolley carrying this cask is situated at the mid-span is calculated next.

$W_{TAD} := 250 \cdot kip$

$W_{trolley\_load} := W_{trolley} + W_{block} + W_{TAD}$

$W_{trolley\_load} = 358 \cdot kip$ Combined weight of the trolley and the TAD-loaded cask without impact limiters. This is about 70% of the combined trolley weight, block weight, and the rated capacity.

Deflection due to dead weight of the trolley plus the TAD-loaded cask at the mid-span

$$\Delta_4 := \frac{W_{trolley\_load} \cdot L_s^{\,3}}{48 \cdot E_s \cdot I} \qquad \Delta_4 = 0.74 \cdot in$$

$\Delta_{midspan\_TAD} := \Delta_1 + \Delta_4$

$\Delta_{midspan\_TAD} = 0.99 \cdot in$

$$f_{CHC\_midspan\_TAD} := \frac{1}{2 \cdot \pi} \cdot \sqrt{\frac{g}{\Delta_{midspan\_TAD}}}$$

$$f_{CHC\_midspan\_TAD} = 3.14 \cdot Hz$$

$S_{v\_7\%\_TAD\_224} := 0.68 \cdot g$ 7% damped spectral acceleration at 3.14 Hz from the vertical ISRS at Node 224, i.e., elevation 32' (Figure A-B-2 of Appendix A-B)

$S_{v\_7\%\_TAD\_419} := 0.625 \cdot g$ 7% damped spectral acceleration at 3.14 Hz from the ISRS at Node 419, i.e., elevation 64' (Figure A-B-4 of Appendix A-B)

$$S_{v\_7\%\_TAD} := \frac{1}{2}\left(S_{v\_7\%\_TAD\_224} + S_{v\_7\%\_TAD\_419}\right)$$

$$S_{v\_7\%\_TAD} = 0.65 \cdot g$$

$$M_{max\_1\_TAD} := \frac{w \cdot L_s^{\,2}}{8} \cdot \left(1 + \frac{S_{v\_7\%\_TAD}}{g}\right) + \frac{W_{trolley\_load} \cdot L_s}{4}\left(1 + \frac{S_{v\_7\%\_TAD}}{g}\right)$$

(Pages 2-296 and 298 of Reference A2.2.10)

$$M_{max\_1\_TAD} = 16425.44 \cdot kip \cdot ft$$

Maximum moment at mid-span when the trolley with the TAD cask is at the mid-span

Thus, when the 200-ton capacity crane lifts a TAD loaded cask, the maximum stress in the girders will be at $\frac{M_{max\_1\_TAD}}{M_{max\_1}} = 0.78$ of the design allowable of the girders.

APPENDIX A-B

DBGM-2 and BDBGM ISRS AT ELEVATIONS 32' (NODE 224) AND 64' (NODE 419) (REFERENCE A2.2.2)

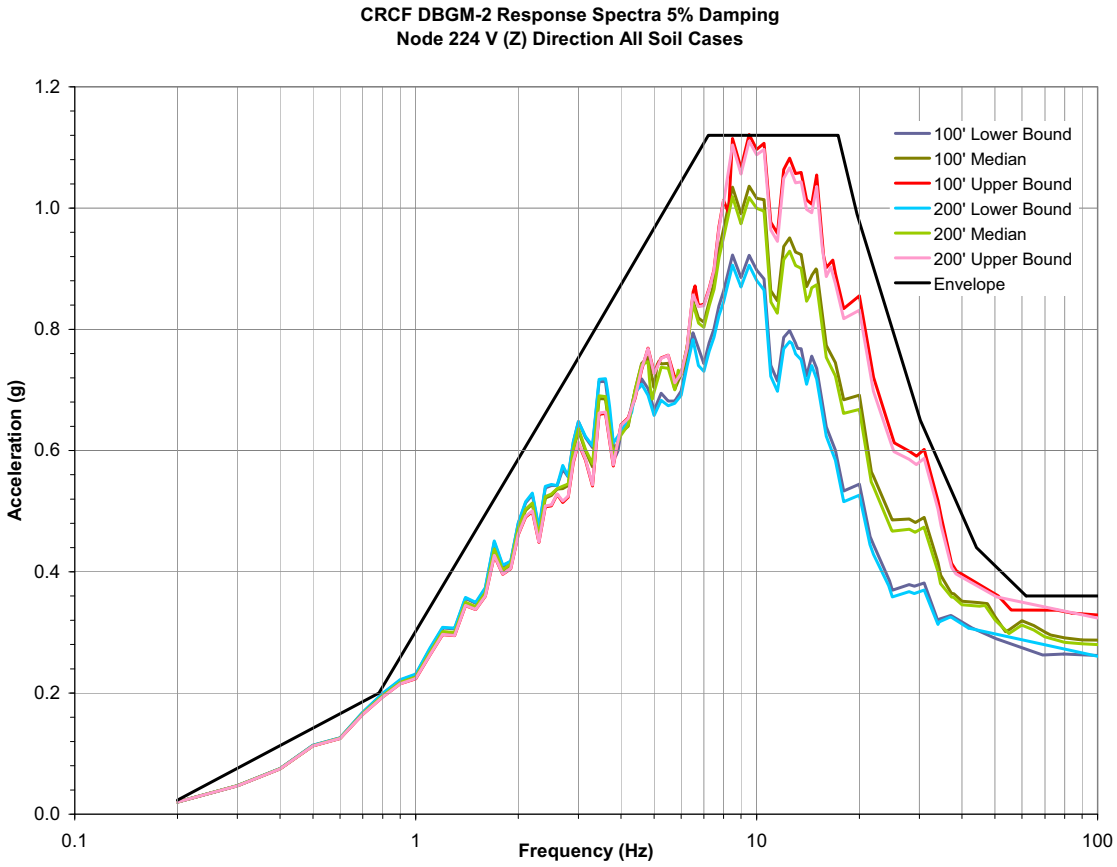

Figure A-B-1. CRCF Vertical DBGM-2 5% Damped ISRS (Both Design and Raw) at Node 224 (Elevation 32')

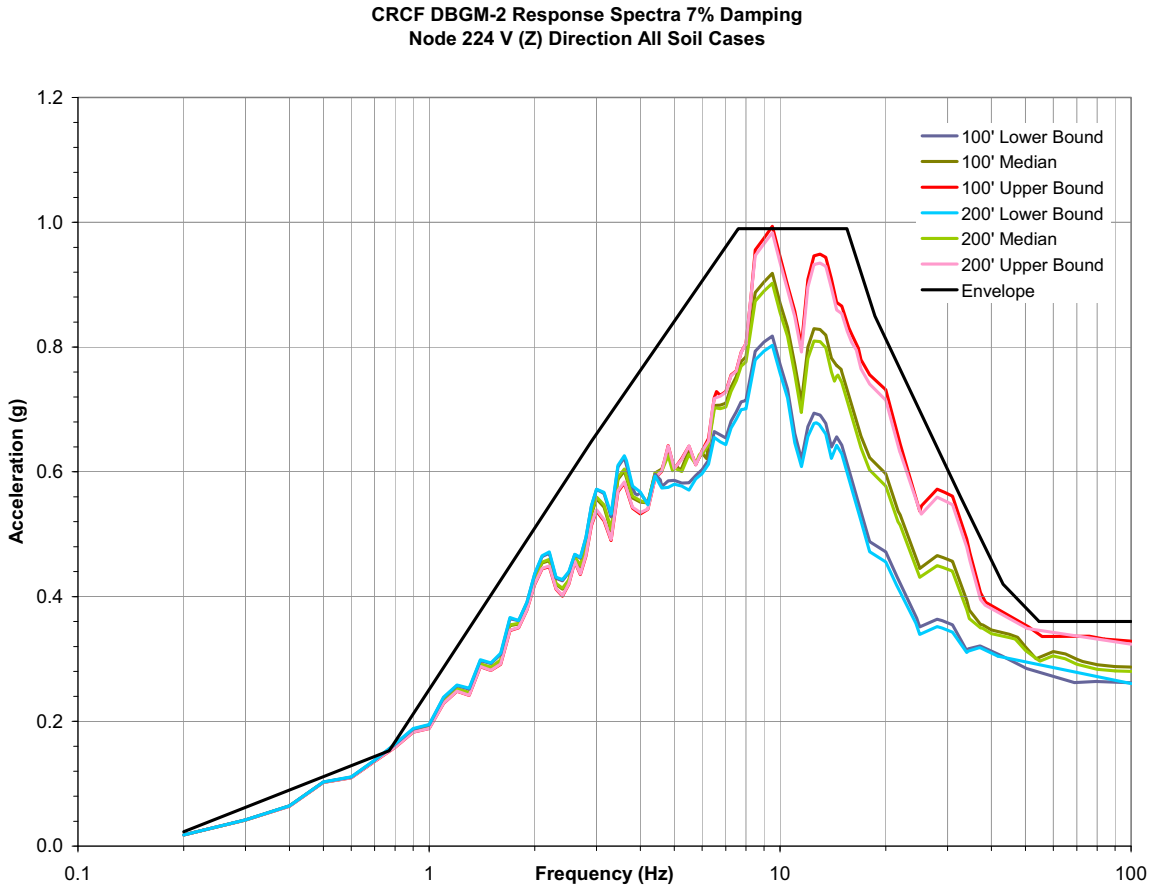

Figure A-B-2. CRCF Vertical DBGM-2 7% Damped ISRS (Both Design and Raw) at Node 224 (Elevation 32')

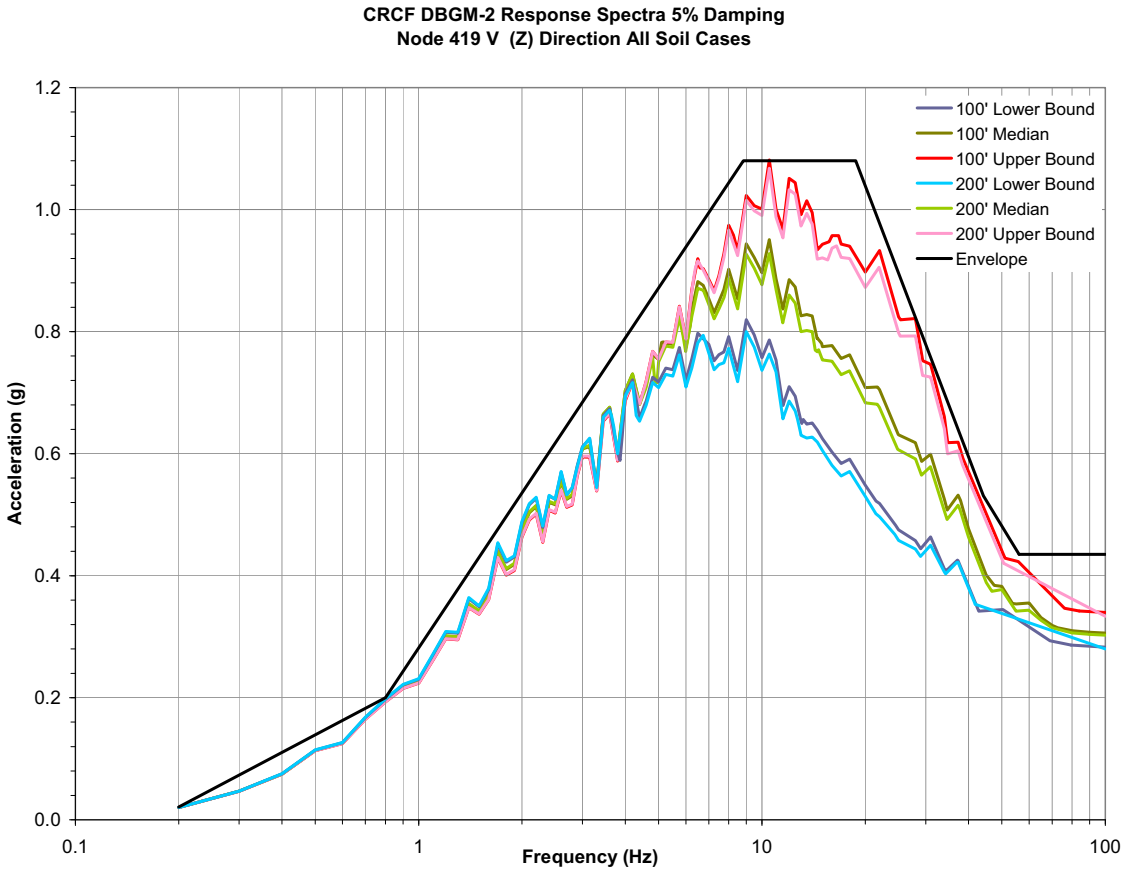

Figure A-B-3. CRCF Vertical DBGM-2 5% Damped ISRS (Both Design and Raw) at Node 419 (Elevation 64')

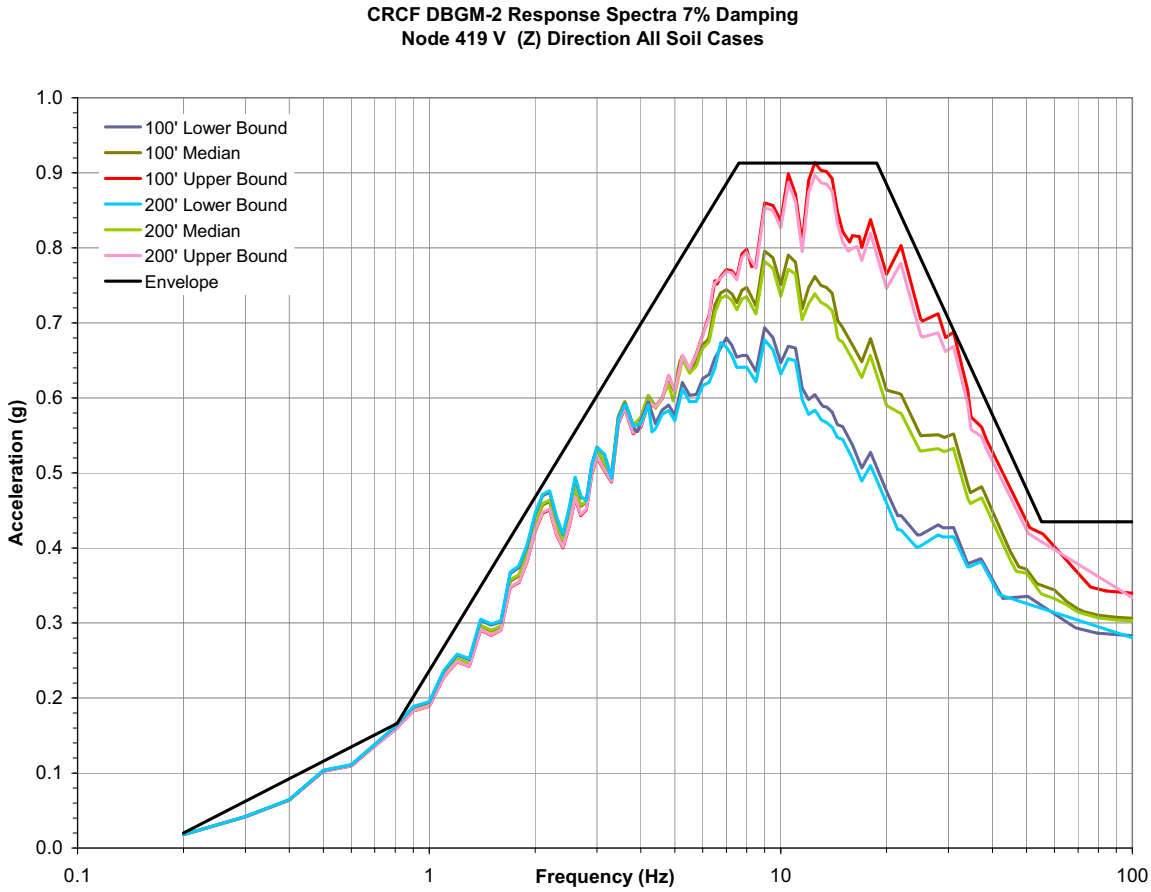

Figure A-B-4. CRCF Vertical DBGM-2 7% Damped ISRS (Both Design and Raw) at Node 419 (Elevation 64')

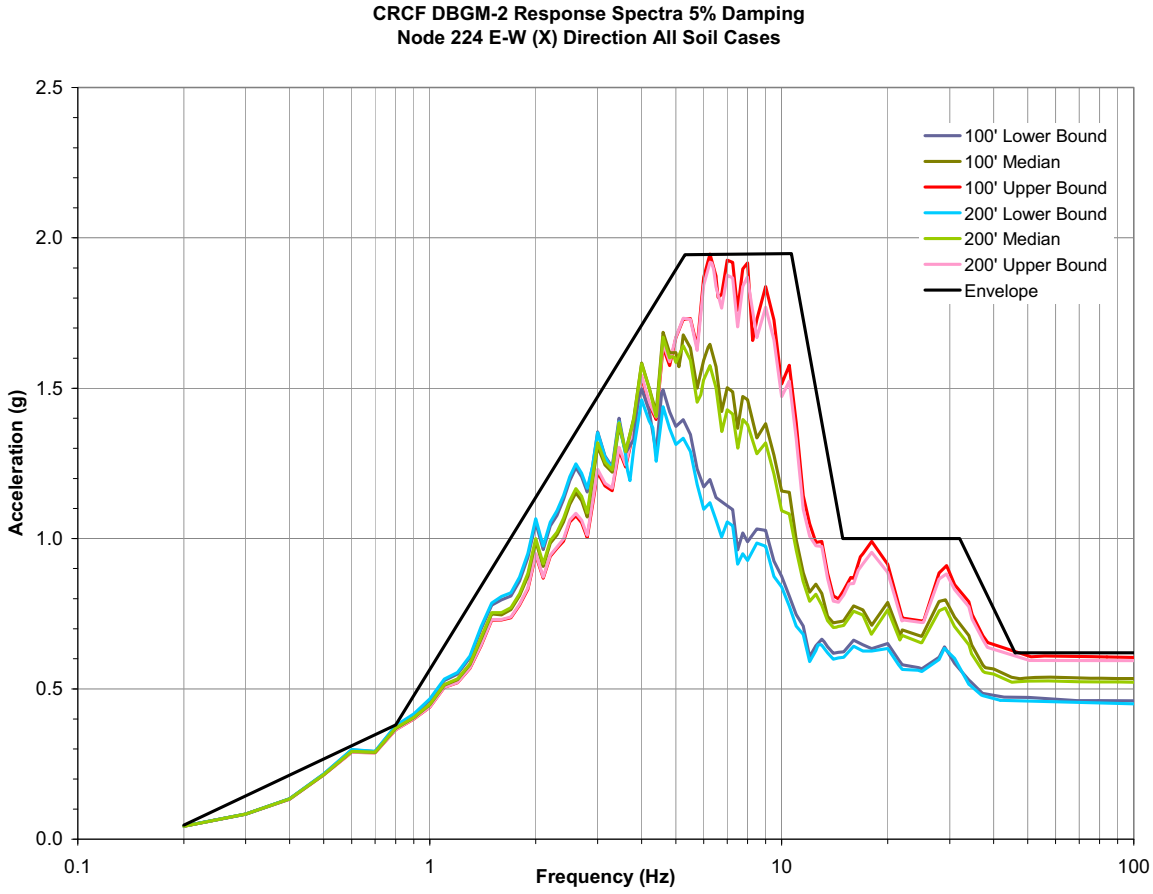

Figure A-B-5. CRCF East-West DBGM-2 5% Damped ISRS (Both Design and Raw) at Node 224 (Elevation 32')

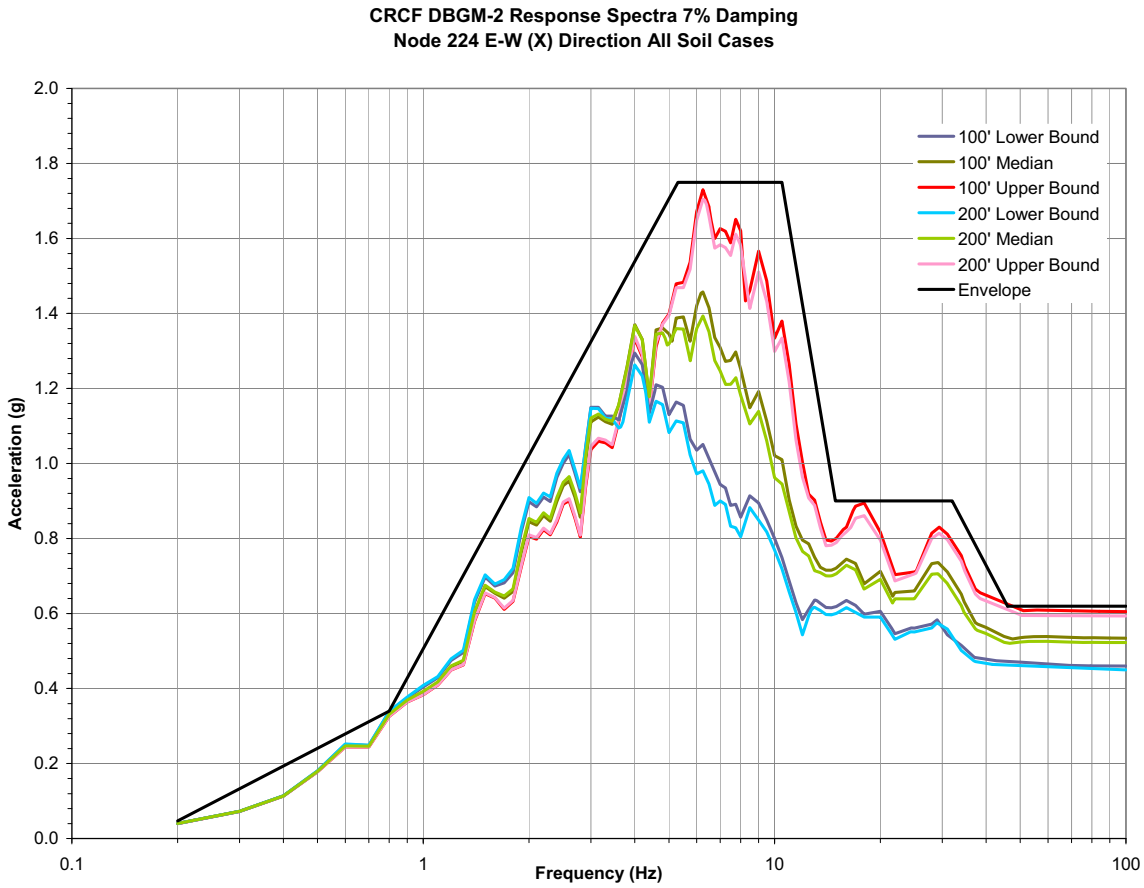

Figure A-B-6. CRCF East-West DBGM-2 7% Damped ISRS (Both Design and Raw) at Node 224 (Elevation 32')

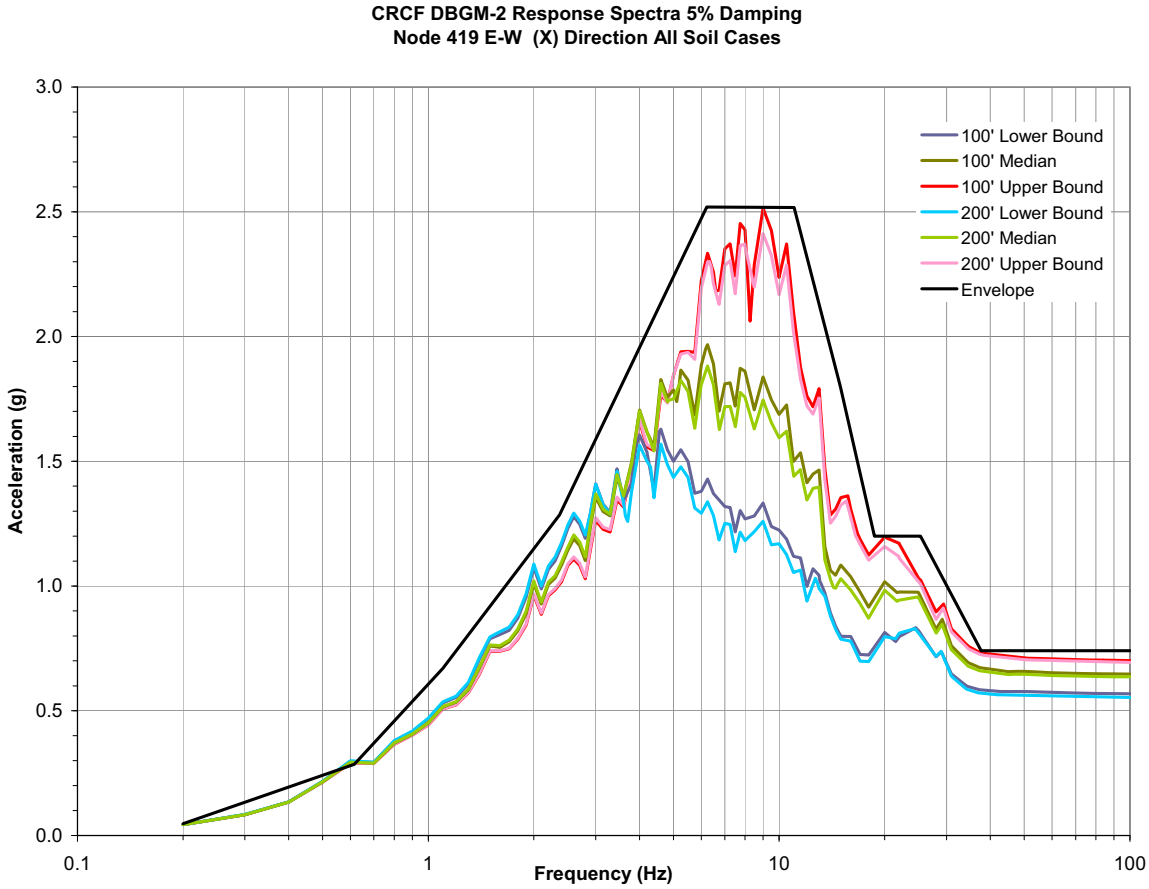

Figure A-B-7. CRCF East-West DBGM-2 5% Damped ISRS (Both Design and Raw) at Node 419 (Elevation 64')

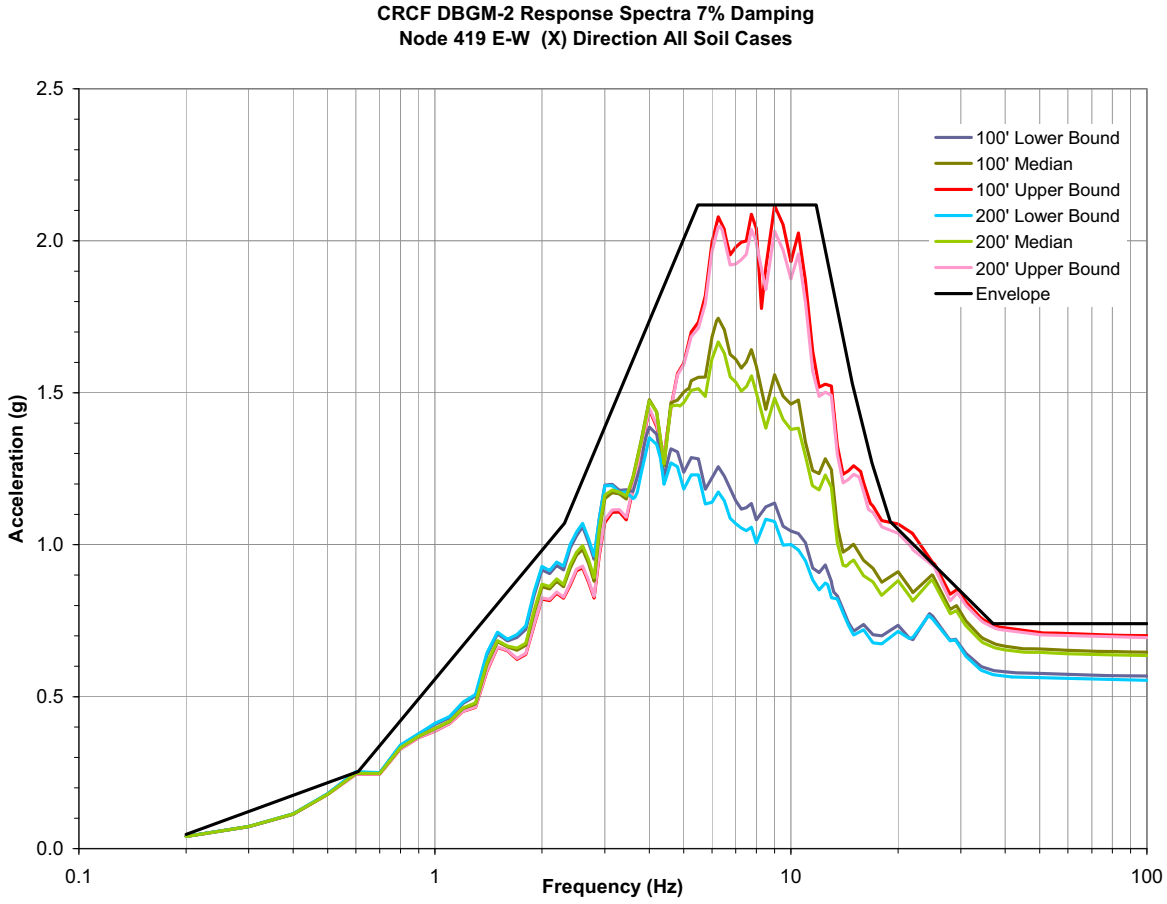

Figure A-B-8. CRCF East-West DBGM-2 7% Damped ISRS (Both Design and Raw) at Node 419 (Elevation 64')

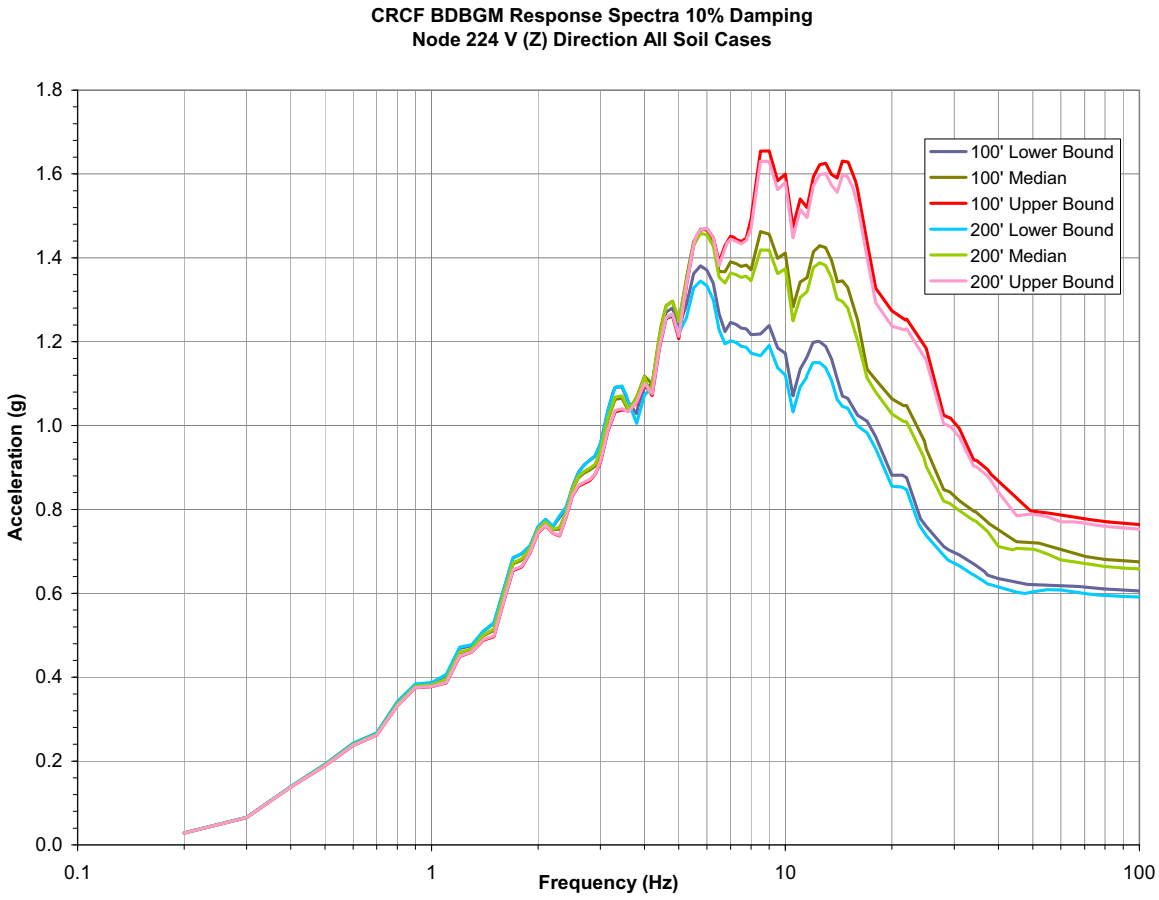

Figure A-B-9. CRCF Vertical BDBGM 10% Damped ISRS at Node 224 (Elevation 32')

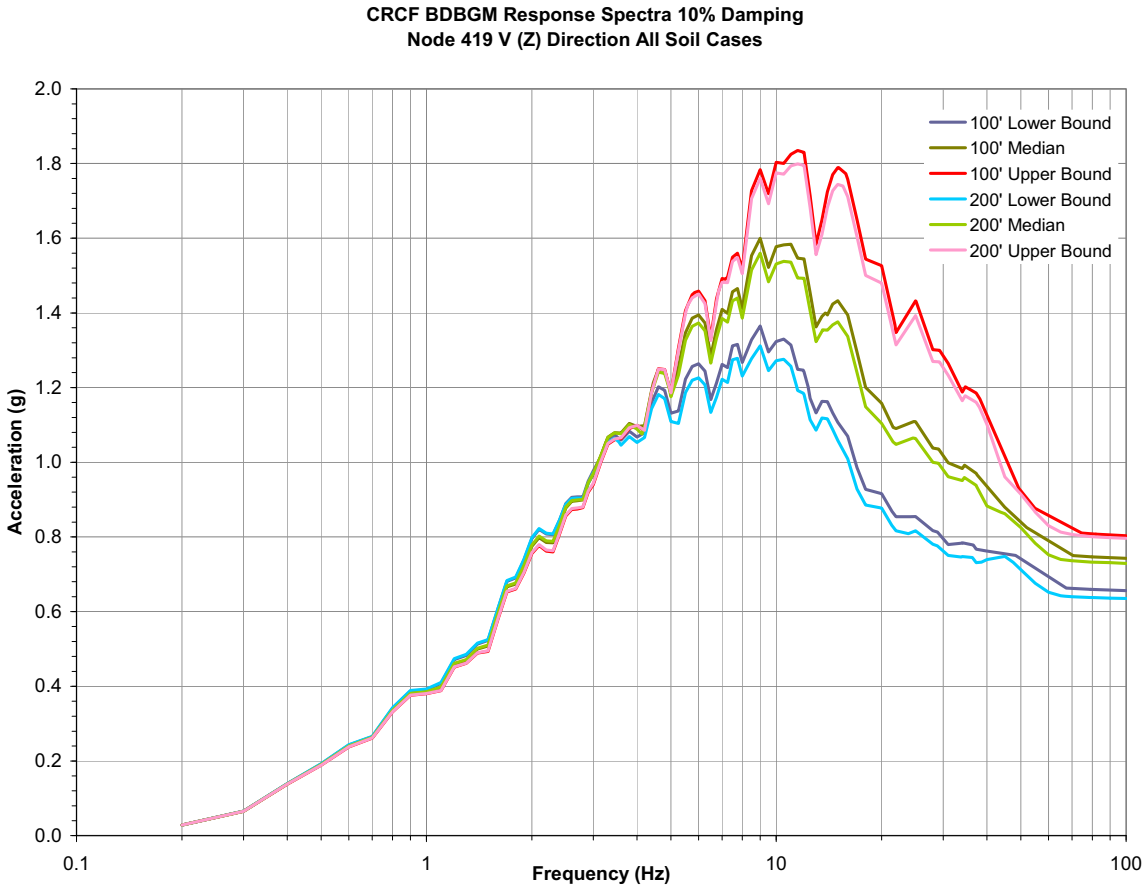

Figure A-B-10. CRCF Vertical BDBGM 10% Damped ISRS at Node 419 (Elevation 64')

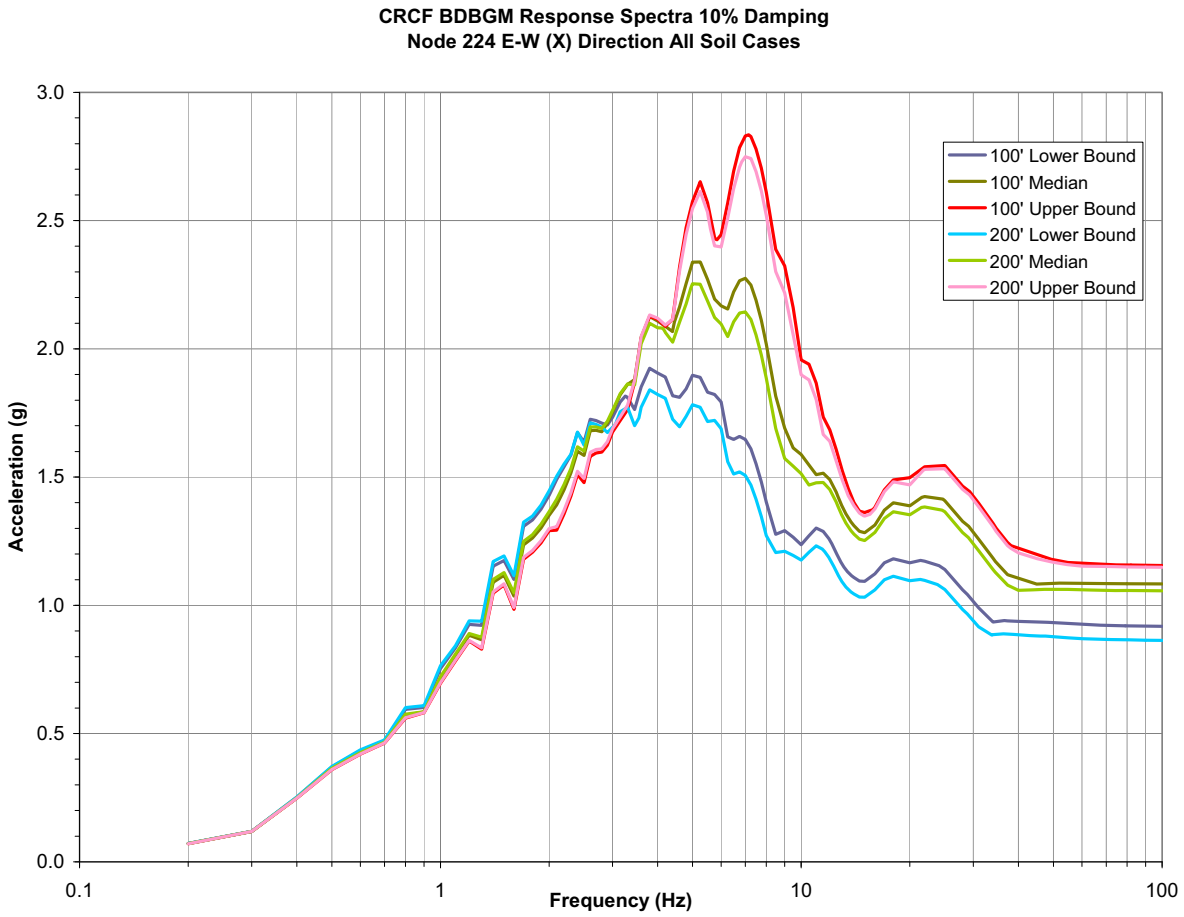

Figure A-B-11. CRCF East-West BDBGM 10% Damped ISRS at Node 224 (Elevation 32')

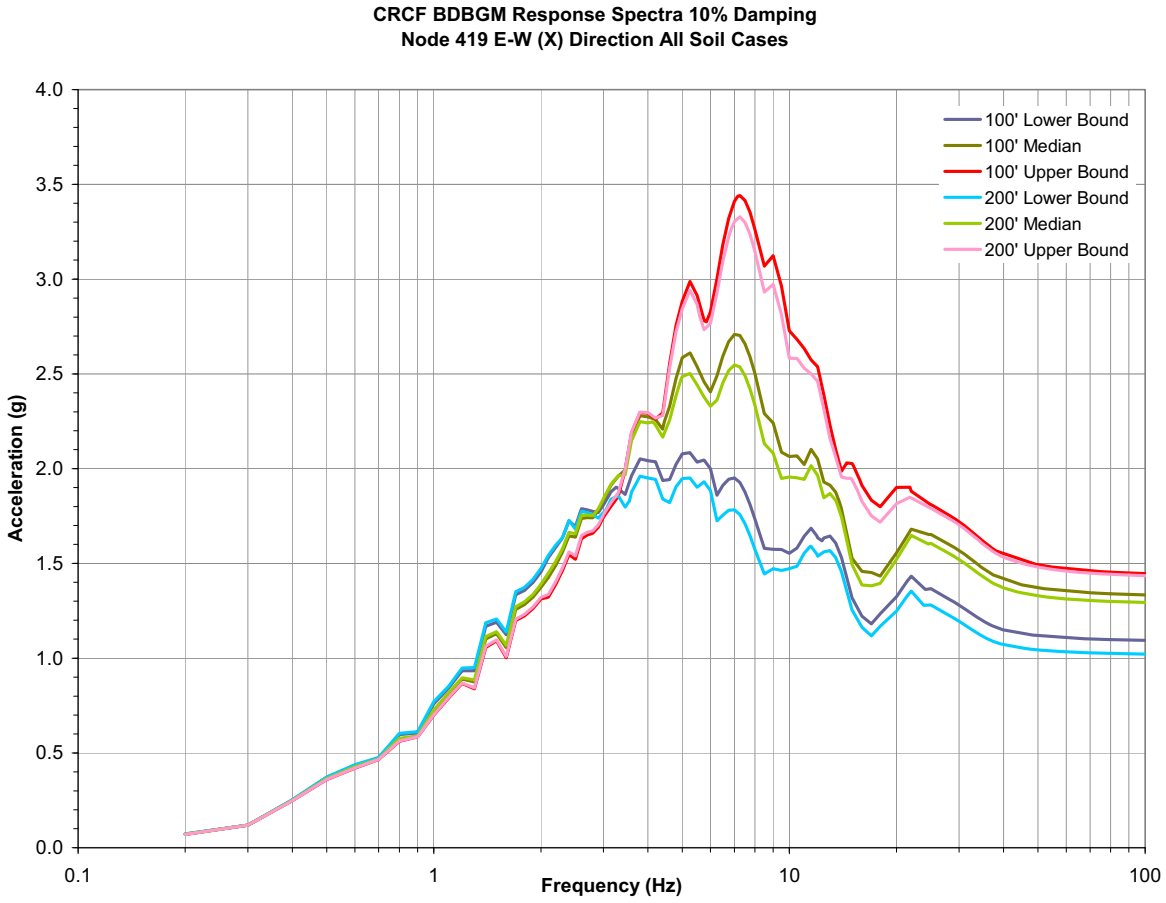

Figure A-B-12. CRCF East-West BDBGM 10% Damped ISRS at Node 419 (Elevation 64')

ATTACHMENT B
FRAGILITY FOR CRCF CANISTER TRANSFER MACHINE HOIST

Prepared By: Robert D. Campbell

ARES Check By: Stephen A. Short

LLNL Check By: Robert C. Murray

TABLE OF CONTENTS

ACRONYMS AND ABBREVIATIONS

ACI	American Concrete Institute
AISC	American Institute of Steel Construction
ANSI	American National Standards Insitute
AO	Aging Overpack
APE	Annual Probability of Exceedance
ASCE	American Society of Civil Engineers
ASME	American Society of Mechanical Engineers
BSC	Bechtel SAIC, LLC
BDBGM	Beyond Design Basis Ground Motion at $1x10^{-4}$ APE
CDFM	Conservative Deterministic Failure Margin
CHC	Cask Handling Crane
CIP	Cast-in-Place
CRCF	Canister Receipt and Closure Facility
CTM	Canister Transfer Machine
CTT	Cask Transfer Trolley
DBGM-2	Design Basis Ground Motion at $5x10^{-4}$ APE
DL	Dead Load
DOF	Degree of Freedom
DPC	Dual Purpose Canister
EPRI	Electric Power Research Institute
HCLPF	High Confidence of Low Probability of Failure
HVAC	Heating, Ventilation, & Air Conditioning
IEEE	Institute of Electrical and Electronics Engineers
IHF	Initial Handling Facility
ISRS	In-Structure Response Spectra

ACRONYMS AND ABBREVIATIONS (cont.)

ITS	Important to Safety
LA	License Application
LLNL	Lawrence Livermore National Laboratory
NPP	Nuclear Power Plant
PGA	Peak Ground Acceleration
RF	Receipt Facility
RRS	Required Response Spectrum
Sa	Spectral Acceleration
SFA	Surface Facilities Area
SFTM	Spent Fuel Transfer Machine
SPRA	Seismic Probabilistic Risk Assessment
SRSS	Square Root of the Sum of Squares
SSE	Safe Shutdown Earthquake (used with NPPs)
SSI	Soil Structure Interaction
SSC	Structure, System, and Component
TAD	Transportation, Aging, and Disposal canister
TEV	Transport and Emplacement Vehicle
TRS	Test Response Spectrum
UHS	Uniform Hazard Spectra
USDOE	United States Department of Energy
USNRC	United States Nuclear Regulatory Commission
WHF	Wet Handling Facility
WP	Waste Package
WPTT	Waste Package Transfer Trolley
YMSF	Yucca Mountain Surface Facilities
ZPA	Zero Period Acceleration

FRAGILITY TERMINOLOGY

Am	Median Peak Ground Motion Capacity
β_R	Log Standard Deviation of Randomness
β_U	Log Standard Deviation of Uncertainty (Lack of Knowledge)
β_C	Composite Variability = $(\beta_R^2 + \beta_U^2)^{0.5}$
F_S	Strength Factor of Safety
β_{R_S}	Strength Randomness (typical)
β_{U_S}	Strength Uncertainty (typical)
β_{C_S}	Strength Composite Variability (typical)
F_μ	Inelastic Energy Absorption Factor of Safety
F_{QM}	Qualification Factor of Safety
F_δ	Damping Factor of Safety
F_M	Modeling Factor of Safety
F_{MC}	Modal Combination Factor of Safety
F_{ECC}	Earthquake Component Combination Factor of Safety
F_{SA}	Spectral Shape Factor of Safety
F_{SSI}	Soil-Structure Interaction Factor of Safety
F_{GMI}	Ground Motion Incoherence Factor of Safety
F_{TOTAL}	Total Factor of Safety
F_{RS}	Structural Response Factor of Safety
F_{RE}	Equipment Response Factor of Safety

B1. PURPOSE

The purpose of this calculation is to develop a seismic fragility for the Canister Transfer Machine (CTM) hoist system while loaded with a design basis load and subjected to a seismic event greater than the DBGM-2. Overall structural failure of the CTM is addressed in Attachment D. Depending upon the failure mode, different consequences may result. This fragility information will be used by the risk analysts to determine the contribution of the Canister Transfer Machine to overall release of radioactivity.

B2. REFERENCES

B2.1. PROCEDURES AND DIRECTIVES

B2.1.1 EG-PRO-3DP-G04B-00037, Rev. 10. *Calculations and Analyses*. Las Vegas, Nevada: Bechtel SAIC Company. ACC: ENG.20071018.0001.

B2.1.2 IT-PRO-0011, Revision 7, ICN 0. *Software Management*. Las Vegas, Nevada: Bechtel SAIC Company. ACC: DOC.20070905.0007.

B2.2 DESIGN INPUTS

B2.2.1 BSC (Bechtel SAIC Company) 2007. *Canister Receipt and Closure Facility 1 General Arrangement Legend and General Notes.* 060-P10-CR00-00101-000 REV 00B. Las Vegas, Nevada: Bechtel SAIC Company. ACC: ENG.20071212.0002. [DIRS 184371].

B2.2.2 ASME NOG-1-2004. 2005 *Rules for Construction of Overhead and Gantry Cranes (Top Running Bridge, Multiple Girder)*. New York, New York: American Society of Mechanical Engineers. TIC: 257672. [DIRS 176239]

B2.2.3 BSC (Bechtel SAIC Company) 2007. *Mechanical Handling Design Report for Cranes and Special Lifting Devices*. 000-30R-WHS0-01700-000 REV 001. Las Vegas, Nevada: Bechtel SAIC Company. ACC: ENG.20071101.0026. ENG.20070910.0001. [DIRS 183727]

B2.2.4 EPRI (Electric Power Research Institute) 1994. *Methodology for Developing Seismic Fragilities*. EPRI TR-103959. Palo Alto, California: Electric Power Research Institute. TIC:253770. [DIRS 161329]

B2.2.5 BSC (Bechtel SAIC Company) 2007. *CRCF Tier-1 In-Structure Response Spectra*. 060-SYC-CR00-00900-000-00B. Las Vegas, Nevada: Bechtel SAIC Company. ACC: ENG.20071210.0008. [DIRS 184330]

.

B2.2.6 MO0801HCUHSSFA.001. *Mean Hazard Curves and Mean Uniform Hazard Spectra for the Surface Facilities Area*. Submittal date: 01/11/2008. [DIRS 184802]

B2.2.7 Huang, H.C. and Marsh, L. 2004. "Slack Rope Analysis for Moving Crane System." *13th World Conference on Earthquake Engineering, August 1-6, 2004, Paper 3190*. Tokyo, Japan: International Association for Earthquake Engineering. TIC: 260006. [DIRS 184779]

B2.2.8 Moore, D. 2007. "Re: FW: Cranes: *Slack Rope Conditions and Pendulum*

Effects." E-mail from D. Moore to W-H. Tong, December 17, 2007, with attachments. ACC: LLR.20080110.0147. [DIRS 184844]

B2.2.9 BSC (Bechtel SAIC Company) 2006. *CRCF, IHF, RF, and WHF Canister Transfer Machine Mechanical Equipment Envelope*. 000-MJ0-HTC0-00201-000 REV 00A. Las Vegas, Nevada: Bechtel SAIC Company. ACC: ENG.20061120.0011; ENG.20070307.0006; ENG.20070601.0025; ENG.20070823.0002; ENG.20080103.0009. [DIRS 178630]

B2.2.10 DOE (U.S. Department of Energy) 2007. *Transportation, Aging and Disposal Canister System Performance Specification.* WMO-TADCS-000001, Rev. 0. Washington, D.C.: U.S. Department of Energy, Office of Civilian Radioactive Waste Management. ACC: DOC.20070614.0007. [DIRS 181403]

B2.2.11 Moore, D. 2007. "*SSI Factor of Safety.*" E-mail from D. Moore to B. Murray, October 25, 2007. ACC: LLR.20080110.0145. [DIRS 184842]

B2.2.12 Jacobsen, L.S. and Ayre, R.S. 1958. *Engineering Vibrations With Applications to Structures and Machinery*. New York, New York: McGraw Hill Book Company. Library of Congress No. 57013334, 564 pp.

B2.2.13 BSC (Bechtel SAIC Company) 2006. *Seismic Analysis and Design Approach Document.* 000-30R-MGR0-02000-000 Rev. 001. Las Vegas, Nevada: Bechtel SAIC Company. ACC: ENG.20071220.0029. [DIRS 184494]

B2.3 DESIGN CONSTRAINTS

There are no design constraints in the performance of this calculation.

B2.4 DESIGN OUTPUTS

The design outputs are seismic fragilities for selected failure modes

B3. ASSUMPTIONS

B3.1 ASSUMPTIONS REQUIRING VERIFICATION

There are no assumptions made that require verification.

B3.2 ASSUMPTIONS NOT REQUIRING VERIFICATION

Assumptions made in the calculation are based on the requirements of References B2.2.13, B2.2.2 and B2.2.3 and are within the guidelines of Reference B2.2.4 for development of fragilities and do not require further verification. Specific assumptions for materials of construction are:

B3.2.1: Per Ref. B2.2.2, the drum must be constructed of rolled plate or centrifugal cast material. Cast SA 216 or SA 352 with similar properties were assumed.

Rationale - The properties of the cast material are very similar to any weldable rolled plate material that would be used.

B3.2.2 Gear material is assumed to be hardened through steel forging with 300 Brinell hardness. The hardness is a mid range of hardness that might be used for gear manufacturing.

Rationale - Since there is a large margin in gear strength, the assumption does not influence any governing results.

B3.2.3 Cable strength and stiffness is taken from a Morris Material Handling calculation (Ref. B2.2.9) to derive an effective modulus of elasticity.

Rationale - The results are consistent with the modulus of elasticity in the slack rope analysis of Ref. B2.2.7.

B4. METHODOLOGY

B4.1 QUALITY ASSURANCE

This calculation is prepared in accordance with Bechtel SAIC LLC procedure EG-PRO-3DP-G04B-00037, Rev. 10, Ref. B2.1.1

B4.2 USE OF SOFTWARE

Mathcad 14 and Excel are used in this calculation. The use of this software is classified as Level 2 software per procedure IT-PRO-0011, Reference B2.1.2. Therefore the software does not require separate qualification.

B5. LIST OF APPENDICES

APPENDIX B-A DBGM-2 Vertical CRCF Spectra for Node 419

APPENDIX B-B BDBGM Vertical UHS

APPENDIX B-C Slack Rope Analysis Data

B6. DEVELOPMENT OF FRAGILITY FOR CTM HOIST

B6.1 INTRODUCTION

The Canister Transfer Machines are bridge cranes and are located in the Canister Receipt and Closure Facility (CRCF). There are two of these machines in the facility, a north and a south machine. They have two trolleys, a shield bell trolley and a hoist trolley. The overall layout in the Canister Receipt and Closure Facility is shown in Reference B2.2.1. The shield bell trolley holds the shield bell while the hoist trolley above lifts the canisters from the ground floor into the shield bell. The focus of this calculation is to develop a fragility for the hoist mechanism to define the conditional probability of failure for dropping of the canister during an earthquake.

In addition, the impact velocity of a TAD canister hanging on the rope within the shield bell is calculated for the DBGM-2 earthquake.

The fragility of the hoisting mechanism will be developed for a representative governing case based on the requirements in BSC "*Mechanical Handling Design Report for Special Lifting Devices*," Reference B2.2.3 , the ASME NOG-1 code, "*Rules for Construction of Overhead and Gantry Cranes,"* Reference B2.2.2 and BSC "*Seismic Analysis and Design Approach Document*," Reference B2.2.13. The hoisting mechanism is to be designed in accordance with ASME NOG-1, Reference B2.2.2, as part of a Type 1 crane. Per Reference B2.2.2, Paragraph 5416, the hoisting mechanism must have single failure proof features such that a single failure of a hoist load mechanism will not result in loss of the lifted load. A braking system is required to prevent the load from falling in the event of a mechanism failure. In addition, per paragraph 5411.7 of ASME NOG-1, provisions must be provided so that failure of the drum shaft or bearing will not result in disengagement of any gearing or brake acting on the drum and preclude disabling of the load-retaining function of these components.

There are options in ASME NOG-1 for meeting the no single failure criterion. A single hoist drive unit with a brake on the drum and a brake on the motor shaft may be used as shown in ASME NOG-1 in Figure 5416.1-1. In this case, if a failure occurs in the gear drive, drum shaft or motor shaft, the brake on the drum can hold the load. The brake is required to have a torque resistance of 125% of the full rated torque load in the hoisting mechanism, however, under seismic loading, the brake would slip and the load would ratchet downward.

A second option is a dual hoist drive unit as shown in ASME NOG-1, Figure 5416.1-2. In this case, the brakes are on the motor shaft but there is redundancy in the drive units and drum shafts so that a single failure of a gear box component or drum shaft will not result in a drop. An example hoisting mechanism design for the CTM by Morris Material Handling, Ref. B2.2.9, has elected to use the dual hoist drive with brakes on the motor shaft due to their experience in reliability issues with the braking system applied on the drum. This type of hoisting system will therefore be chosen for the representative fragility derivation. Figure B6-1 shows the dual hoist system for which a representative fragility will be derived.

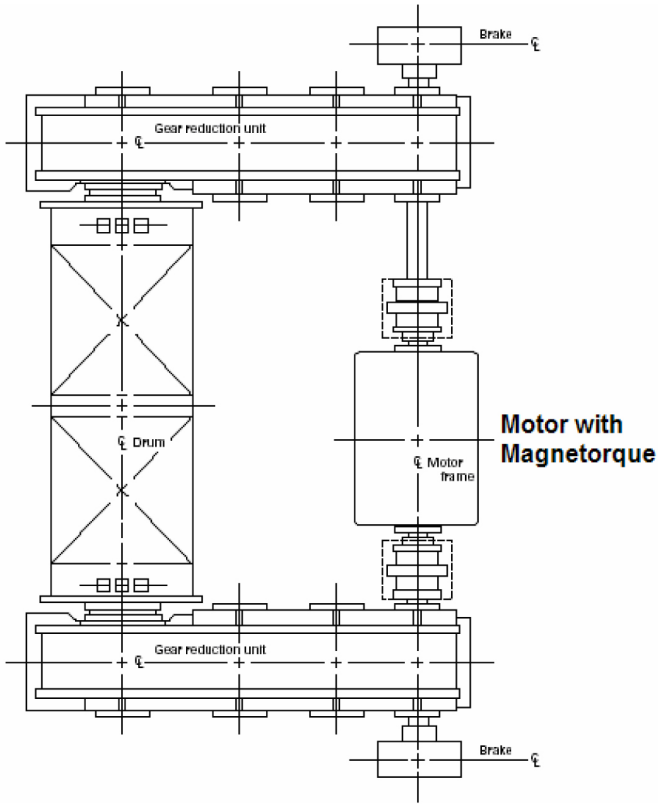

Figure B6-1 Drum, Gearbox and Brake Assembly Reference B2.2.2

In the dual hoist system each gear box must be sized to carry the full motor torque hoisting load, thus there is redundancy in the hoisting system. Two brakes are employed on the motor shafts to keep the load from dropping in the event of a single hoist component failure. Each brake torque setting is required to be 125% of the full load drive torque. However, the two brakes are employed on the drive motor shafts. In a seismic event, both gear boxes carry vertical load but if failure occurs in a gear box, it will potentially be common cause in each gear box and the braking system will not restrict load drop. The focus will therefore be on failure of the gearbox system or on the drum. If no failure occurred in the gearbox, the two brakes would hold 250% of the maximum motor torque load or approximately 250% or more of the load on the hook. Some brake slippage could occur for seismic events higher than the DBGM-2 but a free drop would not occur as long as the gear boxes or drum do not fail.

B6.2 POTENTIAL FAILURE MODES

The total hoisting mechanism consists of several potential failure modes that include:

- Rope
- Hook
- Upper blocks and load blocks
- Lifting yokes
- Drum (as will be shown below, the Drum will dominate)
- Drum shafts

- Gear box shafts
- Gears
- Motor shafts
- Mechanical fasteners

The factors of safety required by design for operating loads will be examined to determine the governing failure mode. At the expected vertical frequency of the crane system, the DBGM-2 vertical acceleration is less than 1.0g as shown later in the calculation, so with the factors of safety required for operating loads, the sizing of components will be controlled by the operating loads and not the seismic loads. We will then examine the factor of safety relative to ultimate failure that is inherent with the static design for operating loads. The governing case will then be examined to determine the scale factor for seismic loads that is required for ultimate failure. This scale factor will be related to a vertical spectral acceleration level at failure. The vertical spectral acceleration level will in turn be related to a peak vertical ground motion level that will become the median PGA capacity of the hoisting system.

B6.2.1 Rope

The rope system must be dual to satisfy the no single failure criterion. Per ASME NOG-1, Paragraph 5425, Reference B2.2.2, the rope is to be sized for the maximum critical load (without impact) with a safety factor of 10 considering all rope parts or a factor of safety of 5 on the maximum loaded dual system. The maximum critical load is the load being lifted plus the weight of the load block. With the dual rope hoisting systems being the same design for each of the dual systems, the factor of safety on ultimate breaking strength of the rope is 10 where the ultimate breaking strength is determined by the manufacturer from tests.

$$FS\_rope := 10$$

B6.2.2 Hook

Per ASME NOG-1, paragraph 5428, and per Reference B2.2.3, the hooks must have single failure proof features. Two attachment points are required with each one capable of carrying the applied load (static and dynamic) with a factor of safety of three on permanent deformation. This implies that the overall factor of safety on yield is 6 for static plus dynamic load. Hooks are typically constructed of high strength material. The ultimate strength to yield strength ratio is typically at least 1.2 for high strength material. The ultimate factor of safety relative to DBGM-2 is then:

$$FS\_hook := 6 \cdot 1.2$$

$$FS\_hook = 7.2$$

Note that this factor of safety includes the DBGM-2 whereas the rope factor of safety is for static load only. The hook has a higher factor of safety.

B6.2.3 Upper Blocks and Load Blocks

Per ASME NOG-1, Paragraph 5421, the upper blocks, in conjunction with the load block shall be designed to maintain a vertical load balance about the center of the lifted load and shall have a reeving system of dual design. Paragraph 5420 (1)(b) requires that each of the dual systems

is able to support a load of three times the static and dynamic load without permanent deformation. This is essentially the same criterion as for the hook design. Thus:

FS_blocks := FS_hook

FS_blocks = 7.2

B6.2.4 Lifting Yokes

Per Reference B2.2.3, paragraph 3.3.1.2, the lifting yokes are to be designed so that each lift point in redundant lift point systems will have a factor of safety of 5 on the ultimate strength for combined static and dynamic load. If no redundancy is incorporated in the design, the required ultimate factor of safety is 10.

FS_liftyoke := 10

B6.2.5 Drum

The design of the hoist drum is specified in ASME NOG-1, Ref. B2.2.2, paragraph 5411. The drum must wind up the redundant cable system in one layer. It is not required to meet the single failure proof features and is an independent item by itself. Consequently, ASME NOG-1 requires in paragraph 5411.7 (b) that in the event of a drum shaft failure or bearing failure, that the drum must be retained on the trolley in a manner which precludes disengagement of any gearing or brake acting on the drum and precludes disablement of the load-retaining function of these components. Allowable stresses are based on crushing stresses in the groove from the rope load, gross bending, local bending, direction shear and torsional shear in the drum cylinder. Per ASME NOG-1, paragraph 5320, allowable stresses for normal operation are based on fatigue life. For Emergency Conditions that include seismic plus operation loads, the allowable stress is 75% of yield. In a typical drum design, the highest stress results from crushing loads from the rope load in the drum grooves and local bending in the cylinder. Equations 1, 2 and 3 in Paragraph 5411.5 of ASME NOG-1 address these stresses and combinations of the stresses. This is not necessarily an ultimate failure criterion. Gross bending, and direct or torsional shear stresses would be more limiting for failure but are typically small. For purposes of estimating the component strength factor of safety relative to normal operating loads, the allowable stress for compression plus bending in the drum groove, which is typically the governing stress for normal operating loads, will be compared to the ultimate tensile strength. ASME NOG-1, paragraph 5476 provides stress equations and allowable fatigue based stresses for different stress combinations. For the case of compression and bending the allowable stress is defined in equation 15 in paragraph 5476 to be:

$$\sigma_{EBN} = \sigma_B + (\sigma_{BA}/\sigma_{NA})\,\sigma_N < \sigma_{BA}$$

In this equation, σ_{EBN} is the allowable combined bending plus compressive stress, σ_{BA} is the allowable fatigue based bending stress defined as a function of the ultimate strength of the material and the stress ratio, R_B, where R_B is the ratio of minimum stress to maximum stress in a stress cycle, σ_B is the bending stress, σ_{NA} is the allowable fatigue based tension or compressive stress and σ_N is the normal tension or compressive stress.

Per Paragraph 5411.3 of ASME NOG-1, the drum shall be constructed of rolled plate or

centrifugal cast steel. Casting material such as SA 216 or SA352 would have a yield strength of 40ksi and an ultimate strength of 70 ksi. From Figure 5474-1 of ASME NOG-1, for a 70ksi ultimate tensile strength, the allowable bending stress, σ_{BA}, is 14.5ksi for an R_B of 0. The ultimate factor of safety of the drum relative to the normal operating stress is:

$$\sigma_{BA} := 14.5\text{ksi}$$

$$FS\_drum := \frac{(70\text{ksi})}{\sigma_{BA}}$$

$$FS\_drum = 4.828$$

B6.2.6 Drum Shafts

With the dual drive design shown in Figure B6-1, there are two drum shafts driving the drum. Each shaft and gear drive must be designed to carry the full operating load. The drum shafts would likely be carbon steel forgings with properties similar to the drum. Per Table 5415.1-1 of ASME NOG-1, the allowable stress for normal operating loads is based on a fatigue allowable and the allowable stress for operating loads and SSE is 0.75 times the yield strength. This is the same situation as for the drum but in this case, there is redundancy in the two independent drive systems so that the overall factor of safety is twice that of the drum.

$$FS\_drumshaft := 2 \cdot FS\_drum$$

$$FS\_drumshaft = 9.655$$

B6.2.7 Gear Box Shafts

The allowable stress criteria is the same as for the drum shafts and the gear shaft materials would likely be similar.

$$FS\_GBshaft := FS\_drumshaft$$

$$FS\_GBshaft = 9.655$$

B6.2.8 Gears

The gears are typically fabricated from higher strength material and designed for fatigue, for maximum motor torque and temporary overload from seismic events. Per ASME NOG-1, Paragraph 5413.1(e), there are three allowable stresses, one for fatigue, one for contact and one for temporary overload. Table 5413.1(e)-1 shows the allowable fatigue stresses and allowable contact stresses as a function of Brinell and Rockwell C hardness. The allowable yield strength is shown in Figure 5413.1(e)-1. As an example, for typical forged and heat treated steel gears hardened through, at 300 Brinell, the allowable fatigue stress from tooth bending is 30 ksi. The allowable contact stress is 120 to 135 ksi. The allowable yield stress is about 112 ksi.

The calculated fatigue stress includes a stress concentration factor whereas the allowable yield stress used in the calculation for temporary overload is based on gross dimensions without stress concentrations. Discounting the difference in calculated stress from stress concentrations, the allowable tooth bending stress is a small fraction of the allowable yield stress. The ultimate strength of a heat treated material with a yield of about 112 ksi would be about 20% higher. Each gear box is designed to carry the full operating load so there is a factor of 2 on the applied stress with both gear boxes engaged. The estimated factor of safety on tooth stress for operating conditions would then be about:

$$FS\_gear := 1.2 \cdot \frac{(112ksi)}{\frac{(30ksi)}{2}}$$

$$FS\_gear = 8.96$$

B6.2.9 Motor Shaft

ASME NOG-1 does not specifically have allowable stresses for motor shafts. The motor shaft and gears should be designed to the same criteria as for the gear box. Motor fasteners design refers to paragraph 5456 of ASME NOG-1 for mechanical component fasteners. Refer to Section B6.2.10 for the mechanical fastener factor of safety.

B6.2.10 Mechanical Fasteners

ASME NOG-1, paragraph 5456.2 provides allowable stresses for mechanical fasteners. The maximum combined stress in mechanical fasteners for normal operating loads (not including preload) is 20% of the ultimate strength. The allowable stress for limiting loads such as seismic is 90% of the yield. The nominal factor of safety for mechanical fasteners for a component that is redundant is twice the factor of safety of a fastener that is not on a redundant component. Since all load paths in the system must be redundant except for the drum, the factor of safety for fasteners of the motor, gear box, upper block, etc. would be:

$$FS\_fastener := \frac{2}{0.2}$$

$$FS\_fastener = 10$$

Any fasteners on the drum would be for the bearing blocks and typical design would not have the fasteners subjected to tension from the rope load. Therefore, the minimum factor of safety for fasteners is as shown above.

B6.2.11 Governing Element

If all components are designed to their limit for normal operating loads, the minimum factor of safety is in the drum. Although the drum is supposed to be retained in the event of a failure of the drum shaft or drum bearings, excessive deformation of the drum itself could cause the gears on the drum shaft to misalign and possibly fail, thus, allowing the drum to rotate freely and release the load. Therefore the results of the above analysis are that the drum will be the focus of the fragility of the hoisting system.

B6.3 CAPACITY FACTORS

The critical drum stress is a combination of gross bending, local bending, torque shear, direct

shear and compression under the rope. The stresses from each source are conservatively combined and compared to the allowable stress. For normal operation, the allowable stress is based on fatigue strength considering any stress concentration factors that are present for changes in geometry. The factor of safety relative to normal operating stress for the drum was determined to be:

$$FS\_drum = 4.828$$

This was based on minimum specified ultimate strength. Median strength would be about 1.1 times the minimum specified (Ref. B2.2.4, Table 3-9).

$$Fult := 1.1 \cdot 70ksi$$

$$Fult = 7.7 \times 10^{4} psi$$

The capacity factor is defined as:

$$F_C = (Fult - \sigma_{BA}) / \sigma_{seis}$$

Where σ_{BA} is the maximum allowable stress due to crushing and bending in the drum due to normal loads and σ_{seis} is the earthquake induced stress in the same location. The total allowable stress for normal loads is conservatively applied.

The seismic stress, σ_{seis}, is a direct function of the vertical acceleration of the load on the hook. The fundamental vertical frequency is a combination of the combined crane girder flexure and the rope stretch. The position of the trolley on the girder determines the frequency of the girder. For purposes of estimating a capacity factor, the 1/4 position of the trolley is used as a point where the lift would likely occur. From Attachment D for the fragility analysis of the CTM crane, Appendix D-A, the vertical frequency is calculated to be between 3.1 Hz and 4.1 Hz with the trolley in the 1/4 position considering only the flexure of the crane girder. The rope is stiffer but would result in a lower first mode frequency that would define the load on the rope. Refer to Section B6.4 for the first mode frequency calculation determined to be about 2.95 Hz. The associated vertical spectral acceleration for the DBGM-2 will be based on 2.95 Hz. The actual demand at failure will be modified later in Section B6.4.1 based on examining a slack rope condition and the resulting dynamic impact factor at the input acceleration level at failure.

ASME NOG-1, Ref. B2.2.2 specifies 7% damping for Type 1 cranes for SSE loading. However BSC in Reference B2.2.13 (Table 7-1) specifies 4% damping which is more applicable for a structural system that remains elastic. Node 419 at 64 feet is applicable for vertical input to the bridge. Use DBGM-2 envelope design spectra for node 419 at 4% damping, 2.95 Hz (See Appendix B-A, Figure B-A-1)

$$Sa_{des} := 0.75g$$

$$\sigma_{seis} := Sa_{des} \cdot \frac{\sigma_{BA}}{1g}$$

$$F_C := \frac{(Fult - \sigma_{BA})}{\sigma_{seis}}$$

$$F_C = 5.747$$

F_C is based on reaching the ultimate strength at which point, there would be large deformation in the drum and it is considered to deform to a point that failure of the ability to hold the load would occur. Alternatively, a ductility factor could be applied to the point of yielding but the development of a ductility factor for a drum does not follow the classic derivation in Reference B2.2.4 so the more practical approach is to use the ultimate strength with no ductility factor.

Uncertainty

The uncertainty in the median ultimate strength is derived from the ratio of median to the specified UTS. The specified UTS value is a 95% confidence value (-1.65 β_U). Median F_{ult} is 1.1 times specified F_{ult}.

$$\beta_{U\_mat} := \frac{1}{1.65} \cdot \ln(1.1) \qquad \beta_{U\_mat} = 0.058$$

There is a large uncertainty in the canister weight but the maximum weight is considered for a bounding case so the weight uncertainty is taken as 0.

Consider additional β_U for uncertainty in failure mechanism (combined bending and crushing of drum, etc.). Ref. B2.2.4, Table 3-10 summarizes uncertainty for common failure modes. For plate bending yield, the combined uncertainty for equation and material is 0.13. However, the failure mechanism considered herein (combined crushing and bending) and the projection to ultimate failure is more complex so the uncertainty in the equation for failure must be greater. Let β_{U_FM} be 0.15.

$$\beta_{U\_FM} := 0.15$$

$$\beta_{U\_C} := \left(\beta_{U\_mat}^{2} + \beta_{U\_FM}^{2}\right)^{0.5}$$

$$\beta_{R\_C} := 0$$

$$\beta_{C\_C} := \beta_{U\_C}$$

$$\beta_{C\_C} = 0.161$$

B6.4 EQUIPMENT RESPONSE FACTOR

A seismic response analysis of the crane and hoisting mechanism, including the rope flexibility, has not been conducted, therefore the conservatism of using the envelope DBGM-2 spectra and the uncertainty in frequency that affects the vertical seismic loading will be estimated from existing information on system dynamics and considering the slack rope impact at the failure level.

Per Attachment D, fragility calculation of the CTM crane, Appendix D-A, the dominant fundamental frequencies of the Canister Transfer Machine crane girder in the vertical direction for the middle span position and the 1/4 span position are dependent on the ratio of trolley and hook load weight to the total weight of the crane system. The calculated frequencies for 50% and 65% trolley/hook load weight to total weight are:

	Center of Span	1/4 Span Position
50% trolley + hook load	2.4 Hz	3.1Hz
65% trolley + hook load	2.7 Hz	4.1 Hz

These frequencies do not consider the rope flexibility. Next the rope frequency is estimated.

Per Reference B2.2.8, the characteristics of rope stretch are portrayed. For a load of 50% of the breaking strength, the elongation is 0.7%. The equivalent modulus of the rope and the stiffness for use in a calculation of vertical frequency vs length of rope are computed next.

$Pult := 299200lbf$

$Length := 22ft$ Minimum rope length with largest canister in bell, Ref. B2.2.9

$P := 0.5 \cdot Pult$

$P = 1.496 \times 10^{5}\ lbf$

$\Delta := 0.007 \cdot Length$

$\Delta = 0.154\ ft$

$k := \frac{P}{\Delta}$

$k := 971429 \frac{lbf}{ft}$

If the normal load on a rope is 1/10 of the ultimate capacity,

$Prope := \frac{Pult}{10}$ rope loaded to full allowable load

$fn := \frac{1}{2 \cdot \pi} \cdot \sqrt{\frac{k \cdot g}{Prope}}$

$fn = 5.144 \cdot Hz$

The first mode frequency of the load on the rope combined with the crane girder flexibility is determined from the Dunkerley equation (Ref. B2.2.12, Page 114). The crane girder frequency is taken as the average of the 50% and 65% trolley weight frequencies for the 1/4 position.

$$f_{gir} := \frac{(3.1Hz + 4.1Hz)}{2}$$

$f_{gir} = 3.6 \cdot Hz$ Girder frequency in Hz based on max deflection limit in ASME NOG-1

$f_{rope} := fn$

$f_{rope} = 5.144 \cdot Hz$ rope frequency in Hz with maximum load

$$Temp := \left(\frac{1}{f_{gir}^{2}} + \frac{1}{f_{rope}^{2}} \right)$$

Dunkerley Equation (Ref. B2.2.12)

$$f_1 := \sqrt{\frac{1}{Temp}}$$

$f_1 = 2.949 \cdot Hz$

The short rope frequency is higher than the crane structural frequency. Longer ropes would have frequency in the ratio of the square root of the length. Thus, when just starting a lift the frequency could be lower than the structural frequency. For purposes of this calculation, the cask spends most of the time in the bell so the short rope case is used with the first mode system frequency of 2.95 Hz.

ASME NOG-1, Ref B2.2.2 specifies 7% damping for type 1 cranes for SSE loading. However BSC specifies 4% damping which is more applicable for a structural system that remains elastic. However, at the point of hoist failure, the crane girder will be highly stressed and the rope and most components will be at 1/2 of the ultimate capacity so 7% damping is used for the median damping value. Node 419 at 64 feet is applicable for vertical input to the bridge. A check to see if the BDBGM will result in a slack rope condition is made first. The quarter position estimated first mode frequency of 2.95 Hz and 7% damping representative of the linear response of the canister on the rope while in the bell is used. The median soil spectra for 100 foot of alluvium is used as a best estimate of the median spectra. From Reference B2.2.5

$Sa_{med} := 1.145g$ Fig. B-A-2 (Digitized value from Ref. B2.2.5 is used)

B6.4.1 Slack Rope Factor

The BDBGM exceeds 1.0g and some slack rope condition will exist that will cause some dynamic impact. Actual failure will not occur until a much larger acceleration than produced by the BDBGM occurs. ASME NOG-1 would require a non-linear dynamic analysis for uplift if it occurs. A non-linear analysis would require at least a 2 DOF model for vertical response and a time history input. The 2 DOF model would consist of the crane girders flexing and the rope stretching. This is not in the scope of a fragility calculation. An estimate will be made of the slack rope impact load based on a study documented in Reference B2.2.7

Appendix B-C shows results of the slack rope analysis of Reference B2.2.7. Figure B-C-1 shows the target input vertical spectrum and the spectra resulting from the 3 time history

input motions. The peak of the input is at about 3 Hz. Table B-C-1 shows the elastic frequencies calculated for the crane and rope system. Note that the crane is much stiffer in this case than calculated for the CTM crane. The rope frequency for a 30 foot rope is 3.57 Hz. Thus, the slack rope analysis of Reference B2.2.7 is more like a single degree of freedom system (a stiff crane girder and a flexible rope). At 3.57 Hz, the slack rope example of Ref. B2.2.7 is in the highly amplified region of the input spectrum shown in Figure B-C-1 and representative of acceleration levels that might be near failure of the CTM hoist. Therefore, the dynamic impact characteristics of Ref. B2.2.7 can be used to make some useful approximations of dynamic load at failure of the CTM hoist system.

Figure B-C-2 shows the results of multiple analyses of both linear cases and non-linear cases. As shown in Figure B-C-2 (Figure 10 of Reference B2.2.7), for 22 feet of rope, the ratio of linear response to non-linear response for the 7% damped case is about 1.7. Within the 16 to 24 foot rope length cases, there is not a lot of difference in this average ratio. Use a dynamic load factor of 1.7 for slack rope at high acceleration levels corresponding to failure.

$$F_{SLK} := \frac{1}{1.7}$$

$$F_{SLK} = 0.588$$

From Figure B-C-2, over the rope length of 16 to 24 feet, the dynamic load factor varies from about 1.5 to 2.4 for the 1/4 span case which is our best estimate of position. Due to the lack of a non-linear analysis for an actual detailed design, this range is considered to be a plus or minus one log standard deviation range.

$$\beta_{U\_SLK} := \frac{1}{2} \cdot \ln\left(\frac{2.4}{1.5}\right)$$

$$\beta_{U\_SLK} = 0.235$$

$$\beta_{C\_SLK} := \beta_{U\_SLK}$$

$$\beta_{C\_SLK} = 0.235$$

B6.4.2 Qualification Method

The crane and rope system will be evaluated for seismic loads by dynamic analysis. The qualification method factor is intended to quantify conservatism in the seismic analysis such as the use of a static coefficient in lieu of conducting a dynamic analysis, use of peak broadened and smoothed spectra versus raw spectra and any conservatism in the time history used to develop in-structure spectra.

The capacity factor was based on a 4% damped envelope response spectrum as shown in Appendix B-A. A median centered spectral shape is considered to be an unbroadened BDBGM spectral shape for a 100 foot depth alluvium median soil profile case as shown in Appendix B-A, Figure B-A-2. The conservatism in spectral shape, including damping, is derived from the ratio of the BDBGM spectral acceleration at 2.95 Hz compared to the smoothed and broadened DBGM-2 spectral acceleration at 2.95 Hz (Figures B-A-1 and B-A-2).

$$F_{SS} := \frac{Sa_{des}}{Sa_{med}}$$

Sa_{des} is the 4% damped DBGM-2 envelope spectral acceleration = 0.75g.
Sa_{med} is the BDBGM 7% damped median soil spectral acceleration = 1.145g

$$F_{SS} = 0.655$$

Note that this is based on the BDBGM so the reference PGA for the fragility will be anchored to the BDBGM PGA of 0.914g from Ref. B2.2.6; also Section 6.2.2.1 for source information.

The variability in the spectral shape factor consists of two parts, the peak broadening and smoothing and the response spectrum that results from the time history input versus the ground motion spectrum defining the BDBGM. The peak broadening and smoothing has been included in the F_{SS} factor above. There is no variability associated with the comparison at a specific frequency. Frequency variation will be addressed in the modeling factor. The Tier 1 report of Reference B2.2.5 has a comparison of the target UHS spectrum to the spectrum resulting from the time history. The match is very close with a plus to minus fluctuation in the 5 Hz frequency range of the structure of less than 10%. The spectral shape factor would be unity. The Beta U is determined based on plus or minus 5% being plus or minus one log standard deviation (1Beta U).

$$F_{QM} := 1.0 F_{SS}$$

$$F_{QM} = 0.655$$

$$\beta_{U\_QM} := \ln(1.05)$$

$$\beta_{C\_QM} := \beta_{U\_QM}$$

$$\beta_{C\_QM} = 0.049$$

B6.4.3 Damping

The difference between median damping and design damping was accounted for in the qualification method factor.

$$F_{\delta} := 1.0$$

Consider that 4% design damping is about a 95% confidence value. From the BDBGM median soil profile for 100 foot alluvium spectra at 2.95 Hz:

$$Sa_{4\%} := 1.47g$$

$$\beta_{U\_\delta} := \frac{1}{1.65} \cdot \ln\left(\frac{Sa_{4\%}}{Sa_{med}}\right)$$

$$\beta_{U\_\delta} = 0.151$$

$\beta_{C\_\delta} := \beta_{U\_\delta}$

$\beta_{C\_\delta} = 0.151$

B6.4.4 Modeling

The model is considered to be a best estimate so:

$F_M := 1.0$

Uncertainty in modeling arises from uncertainty in frequency and uncertainty in mode shape. A canister hanging from a rope has only one mode shape of concern so the uncertainty on mode shape is essentially zero.

$\beta_{U\_MS} := 0$

The first mode frequency of the crane/rope system was calculated to be 2.95 Hz. The crane girder frequency varies by position of the trolley and the percentage of weight of the trolley and hook load. In Attachment D, Fragility of the CTM Crane, Appendix D-A, the crane frequency ranged from 3.1 Hz to 4.1 Hz in the 1/4 span position. Considering that the first mode frequency would be lower due to the rope stretch, the first mode range could shift to a lower frequency, however, the actual range of frequency would be about the same. The range of crane frequency is used to determine the range of design and median spectral accelerations and the range of the spectral shape factor. The range of frequency is on the rising slope of the DBGM-2 and BDBGM spectra. This range will be considered a plus or minus 95 percentile range. From the DBGM-2 spectrum in Appendix B-A, Figure B-A-1:

$Sa_{3.1} := 0.77g$

$Sa_{4.1} := 0.9g$

DBGM-2 design spectra accelerations at 4% damping

The BDBGM spectral accelerations at median damping of 7% are:

$Sa_{med\_3.1} := 1.14g$

$Sa_{med\_4.1} := 1.275g$

The spectral shape factors including damping at 3.1 Hz and 4.1 Hz are:

$$F_{3.1} := \frac{Sa_{3.1}}{Sa_{med\_3.1}}$$

$$F_{4.1} := \frac{Sa_{4.1}}{Sa_{med\_4.1}}$$

$$\beta_{U\_f} := \frac{1}{2 \cdot 1.65} \cdot \ln\left(\frac{F_{4.1}}{F_{3.1}}\right)$$

$\beta_{U\_f} = 0.013$

When β_{U_f} is calculated based on the range of the factor of safety for a representative frequency range, the value is small.

$\beta_{C\_M} := \left(\beta_{U\_MS}^{2} + \beta_{U\_f}^{2}\right)^{0.5}$

$\beta_{C\_M} = 0.013$

B6.4.5 Mode Combination

The model is a two degree of freedom system. For simple systems like this, Reference B2.2.4, page 3-50 suggests a range of 0.05 to 0.15 for Beta R depending on the model complexity. There is no Beta U

$F_{MC} := 1.0$

$\beta_{R\_MC} := 0.1$

$\beta_{C\_MC} := \beta_{R\_MC}$

$\beta_{C\_MC} = 0.1$

B6.4.6 Earthquake Component Combination

The hoist loads are only sensitive to the vertical direction input.

$F_{ECC} := 1.0$

$\beta_{R\_ECC} := 0$

$\beta_{C\_ECC} := \beta_{R\_ECC}$

$\beta_{C\_ECC} = 0$

B6.4.7 Equipment Response Factor

$F_{RE} := F_{SLK} \cdot F_{QM} \cdot F_{\delta} \cdot F_{M} \cdot F_{MC} \cdot F_{ECC}$

$F_{RE} = 0.385$

$$\beta_{C\_RE} := \left(\beta_{C\_SLK}^{2} + \beta_{C\_QM}^{2} + \beta_{C\_\delta}^{2} + \beta_{C\_M}^{2} + \beta_{C\_MC}^{2} + \beta_{C\_ECC}^{2}\right)^{0.5}$$

$$\beta_{C\_RE} = 0.301$$

B6.5 STRUCTURAL RESPONSE FACTOR

The vertical fundamental frequency of the CRCF soil-structure system is 6.177 Hz for the 100 foot alluvium depth median soil properties DBGM-2 earthquake with 99% of the mass participating in the vertical direction, Ref. B2.2.5. As the acceleration increases, the soil softens and the fundamental vertical frequency for BDBGM is 5.26 Hz. The 5.26 Hz frequency is used as a best estimate of vertical frequency at the median capacity level. The 5% damped BDBGM spectral acceleration at this frequency is 1.52g (Ref. B2.2.6; also Section 6.2.2.1 for source information)(See Appendix B-B).

B6.5.1 Spectral Shape

The site wide ground motion UHS is used to develop the various soil stiffness and soil depth cases for development of in-structure spectra. Ref. B2.2.6 (also Section 6.2.2.1 for source information) provides surface UHS for the site wide and for various soil depths and locations (South and Northwest) for the horizontal direction but only the site wide UHS are provided for the vertical direction. As a result, it is necessary to approximate the spectral shape factor using the horizontal 100 foot depth Sa versus the site wide Sa. The CRCF is located in the NE region of the site.

Case	Sa at 5 Hz
Site wide	2.29g
NE	2.07g

$$Sa\_site := 2.29g$$

$$Sa\_NE := 2.07g$$

$$F_{RS\_SA} := \frac{Sa\_site}{Sa\_NE}$$

$$F_{RS\_SA} = 1.106$$

The hazard study only developed mean UHS so the uncertainty in spectral shape must be estimated, From Reference B2.2.4, the Beta R for peak to peak variation is:

$$\beta_{R\_RS\_SA} := 0.2$$

Reference B2.2.4 also recommends a β_U value for cases where the earthquake is referenced to peak ground acceleration and the structural frequency is low. However, this is based on historical uncertainty in spectral amplification. The Yucca Mountain hazard is defined by a probabilistic seismic hazard analysis where the spectral amplification is defined by the mean uniform hazard spectral shape, thus this β_U is considered to be not applicable.

$\beta_{U\_RS\_SA} := 0$

$\beta_{C\_RS\_SA} := \beta_{R\_RS\_SA}$

$\beta_{C\_RS\_SA} = 0.2$

B6.5.2 Structural Damping

This factor is to account for conservatism in the hysteresis damping of the building structure used in the soil-structure interaction seismic response analysis. Because of the high radiation damping of the foundation media, the effect of structure damping is relatively insignificant. Thus:

$F_{RS\_D} := 1.0$

$\beta_{C\_RS\_D} := 0$ The effect of soil damping will be accounted for in the SSI factor

B6.5.3 Modeling

Modeling uncertainty results from uncertainty in mode shape and frequency. The vertical response of the structural system is virtually all in one soil mode, thus mode shape uncertainty is essentially non existent. Frequency is primarily dependent upon the soil stiffness modeling. Consider the lower bound soil stiffness as a 15th percentile confidence value of stiffness (-1 Beta U)

$F_{RS\_M} := 1.0$

From Ref. B2.2.5, the vertical mode 3 frequency for the lower bound soil case, 100 foot depth of alluvium, is 3.83 Hz. From the Ref. B2.2.6 (also Section 6.2.2.1 for source information) digitized spectra for the 100 foot soil depth, the UHS spectral accelerations for the two cases are (Table B-B-1)

$Sa\_lower := 1.265g$ at 3.83 Hz, 5% damping

$Sa\_med := 1.495g$ at 5.26 Hz, 5% damping

$$\beta_{C\_RS\_M} := \ln\left(\frac{Sa\_med}{Sa\_lower}\right)$$

B6.5.4 Mode Combination

Vertical response is 99% in one mode.

$F_{RS\_MC} := 1.0$

$\beta_{C\_RS\_MC} := 0$

B6.5.5 Soil-Structure Interaction

The Tier 1 seismic response analyses of the CRCF uses the site-wide $5*10^{-4}$ mean uniform hazard spectra as the DBGM-2 input motion. Spectrum compatible time histories are used as the input motion for the time history analyses. The conservatism in the site-wide spectra was accounted for in the spectral shape factor above. Strain compatible soil properties of 100-foot and 200-foot deep alluvium are used to calculate frequency-independent soil springs and soil damping coefficients. Soil radiation damping is introduced into the model by using dashpots. Damping coefficients equal to 75% of the computed values for translational degrees of freedom and to the full computed rotational damping values are used in the response analyses (Reference B2.2.5). Conservatism or un-conservatism in SSI will be minimized in the final SSI analysis used to develop equipment design seismic input. Before the final SSI analyses are completed, the Tier 1 SSI analysis is taken to represent the best-estimate responses per BSC recommendations in Reference B2.2.11.

$$F_{SSI} := 1.0$$

There is uncertainty in the SSI analysis that results from the modeling. Uncertainty in soil stiffness was accounted for in the modeling factor. Consider an additional uncertainty for the soil spring and damper analysis details.

$$\beta_{C\_SSI} := 0.25$$

B6.5.6 Ground Motion Incoherence

Large structures are not excited simultaneously in all locations for high frequency input. In Ref. B2.2.4 a correction for ground motion incoherency is given as a function of frequency and plan dimensions of the foundation. At 10 Hz, the ground input motion is reduced by a factor of 0.9. At 5 Hz, there is no reduction. The reduction factors are given for a plan dimension of 150 feet by 150 feet. The reduction factor is interpolated logarithmically for plan dimension and frequency.

$L1 := 337\,ft$ EW direction excluding 49'6" and 43' extensions in East and West directions respectively, Ref. B2.2.1

$L2 := 336\,ft$ NS direction excluding 56' extension at S end. Ref. B2.2.1

$Leq := \sqrt{L1 \cdot L2}$

$Lstd := 150\,ft$

$f5 := 5$ 5 Hz frequency

$f10 := 10$ 10 Hz frequency

$RF_{10} := 0.9$ Reduction at 10 Hz

$RF_{5} := 1.0$ Reduction at 5 Hz

$RF_{5\_eq} := RF_5$ No reduction at 5 Hz for larger plan dimensions.

$RF_{10\_eq} := 1 - \left[\left(1 - RF_{10}\right)\cdot\frac{Leq}{Lstd}\right]$ Reduction at 10 Hz for larger plan dimension

$RF_{10\_eq} = 0.776$

Let RF at 5.26 Hz be defined as RF_{6_eq}

$f6 := 5.26$

Calculate the reduction factor at 5.26 Hz by interpolation

$RF_{6\_eq} := 0.7$ arbitrary value to start the equation solver

Given

$$\frac{\log\left(RF_{10\_eq}\right) - \log\left(RF_{5\_eq}\right)}{\log\left(RF_{6\_eq}\right) - \log\left(RF_{5\_eq}\right)} = \left(\frac{\log(f10) - \log(f5)}{\log(f6) - \log(f5)}\right)$$

$a := \text{Find}\left(RF_{6\_eq}\right)$

$a = 0.982$

$F_{GMI} := \frac{1}{a}$

$F_{GMI} = 1.019$

Let F_{GMI} = 1 be a -2β value

$\beta_{C\_GMI} := \frac{1}{2}\cdot\ln\left(F_{GMI}\right)$

$\beta_{C\_GMI} = 0.01$

B6.5.7 Structural Response Factor

$F_{RS} := F_{RS\_SA}\cdot F_{RS\_D}\cdot F_{RS\_M}\cdot F_{RS\_MC}\cdot F_{SSI}\cdot F_{GMI}$

$F_{RS} = 1.127$

$$\beta_{C\_RS} := \left(\beta_{C\_RS\_SA}^{\ 2} + \beta_{C\_RS\_D}^{\ 2} + \beta_{C\_RS\_M}^{\ 2} + \beta_{C\_RS\_MC}^{\ 2} + \beta_{C\_SSI}^{\ 2} + \beta_{C\_GMI}^{\ 2}\right)^{0.5}$$

$\beta_{C\_RS} = 0.361$

B6.6 FRAGILITY OF HOIST SYSTEM

The median capacity is defined as a peak ground acceleration and is the product of the capacity factor times the equipment response factor times the structural response factor times the BDBGM PGA. BDBGM PGA is the reference input motion since the BDBGM parameters were used in deriving the equipment and structural response factors.

$BDBGM := 0.914g$ Horizontal Reference PGA

$A_m := F_C \cdot F_{RE} \cdot F_{RS} \cdot BDBGM$

$A_m = 2.281 \cdot g$

$\beta_C := \left(\beta_{C\_C}^{\ 2} + \beta_{C\_RE}^{\ 2} + \beta_{C\_RS}^{\ 2} \right)^{0.5}$

$\beta_C = 0.497$

$HCLPF := A_m \cdot e^{-2.33 \cdot \beta_C}$

$HCLPF = 0.716 \cdot g$

B7. CANISTER SWING DISPLACEMENT AND IMPACT VELOCITY

A canister swinging on the rope is essentially a pendulum. When the canister is in the bell, it could swing and impact the bell. The time spent for the canister to enter or leave the bell is much less than the time spent in the bell so the focus will be on the canister in the bell. The bell ID is 72.5 inches maximum, Reference B2.2.9. Maximum canister dimensions are determined from Reference B2.2.10. The diameter, length and weight of the largest TAD canister are:

$Lc := 212in$

$D := 66.5in$

$Wt := 54.25ton$

$$Wt := Wt \cdot g$$

From Reference B2.2.9 the rope length for the tallest TAD canister is estimated to be about 22 feet.

$$Lr := 22ft$$

The effective lateral stiffness, k, of a pendulum is W/L derived as follows.

Taking moments about the point of rotation, the moment due to dead weight is:

$M_{DW} := W \cdot \Delta$ where Δ is the horizontal displacement of the mass

Moment from a lateral force acting on the mass is:

$$M_F := F \cdot L$$

Equating moments:

W*Δ = F*L

$$k := \frac{F}{\Delta}$$

$$k := \frac{W}{L}$$

However, the center of mass of the canister is 106 inches below the attachment point of the hook so the effective length is:

$$Leff := 22ft + 106in$$

$$Leff = 30.833\ ft$$

$$k := \frac{Wt}{Leff}$$

$$k = 1.132 \times 10^5 \frac{lb}{s^2}$$

$$fn := \frac{1}{2\pi} \cdot \sqrt{k \cdot \frac{g}{Wt}}$$

$fn = 0.163 \cdot Hz$ Frequency in Hz

The DBGM-2 spectra at node 419 in the CRCF do not go below 0.2 Hz. At this low of a frequency, the relative displacement of the cask to the crane is essentially the spectral displacement of the ground motion. The ground motion from Reference B2.2.6 (also Section 6.2.2.1 for source information), at 0.163 Hz is used. The 1%

damped horizontal spectral acceleration for DBGM-2 based on log linear interpolation is:

$Sa_{fn} := 0.0395g$

Note that 1% damping is used as there is little damping for a swinging pendulum.

$\omega := 2 \cdot \pi \cdot fn$ circular frequency

$\omega = 1.022 \frac{1}{s}$ radians per second

$Sv := \frac{Sa_{fn}}{\omega}$ maximum spectral velocity

$Sv = 1.244 \frac{ft}{s}$

$Sd := \frac{Sa_{fn}}{\omega^2}$ maximum spectral displacement

$Sd = 1.218\ ft$

This is the estimated maximum velocity and displacement of the center of gravity of the canister. The canister would tend to remain upright due to the weight of gravity so the bottom of the canister would not have much more displacement or velocity than the center of mass.

The ID of the bell is 72.5 inches (Ref. B2.2.9)

$ID := 72.5in$

$\Delta r := \frac{(ID - D)}{2}$

$\Delta r = 0.25\ ft$

Impact would occur at the DBGM-2 acceleration level. Determine velocity at impact. Use rigid body dynamics.

The period of vibration of the pendulum system is:

$p := \frac{1}{fn}$

$p = 6.151\ s$

Alternate acceleration profiles, different values of ground motion acceleration and different radial gaps for smaller diameter canisters will now be examined.

Initially, determine the impact velocity resulting from a DBGM-2 earthquake for the smallest gap of 0.25 feet, using a triangular shaped acceleration profile that is represented by a linear acceleration from zero to a maximum at time p/4, returning to zero at p/2 and then going to a maximum in the opposite direction and returning to zero at the end of the vibration period, p. From rigid body dynamics,

$a = Sa_{fn} \cdot \frac{t}{0.25 \cdot p}$ t is time in seconds

$vel = \frac{Sa_{fn}}{0.25 \cdot p} \cdot \frac{t^2}{2}$

$disp = \frac{Sa_{fn}}{0.25 \cdot p} \cdot \frac{t^3}{6}$

$disp := \Delta r$

$t := 0.01 \cdot s$ An initial trial value to solve the equation

Given

$\Delta r = \frac{Sa_{fn}}{0.25 \cdot p} \cdot \frac{t^3}{6}$

$t := Find(t)$

$t = 1.22\,s$

$v_{impact} := \frac{Sa_{fn}}{0.25 \cdot p} \cdot \frac{t^2}{2}$

$v_{impact} = 0.615 \frac{ft}{s}$

At BDBGM, the acceleration is approximately double that at DBGM-2.

$t1 := .01 \cdot s$ Initial value to solve for time at impact at BDBGM

Given

$\Delta r = 2 \cdot \frac{Sa_{fn}}{0.25 \cdot p} \cdot \frac{t1^3}{6}$

$t1 := Find(t1)$

$t1 = 0.968\,s$

$$v_1 := 2 \cdot \frac{Sa_{fn}}{0.25 \cdot p} \cdot \frac{t1^2}{2}$$

$$v_1 = 0.775 \frac{ft}{s}$$

From the above equations one can observe that, for a fixed displacement, the velocity at impact increases as the cube root of the acceleration. Table B7-1 tabulates impact velocity as a function of PGA at ground surface.

Table B7-1. Impact Velocity as a Function of Ground Motion Acceleration for Fixed Displacement of 0.25 Feet.

Earthquake Ground Motion	PGA (g)	Impact Velocity ft/sec
DBGM-2	0.45	0.615
2 DBGM-2	0.9	0.775
3 DBGM-2	1.35	0.887
4 DBGM-2	1.8	0.976
5 DBGM-2	2.25	1.05

Now consider a sinusoidal input motion to test the sensitivity of impact velocity on shape of input motion. Do a numerical integration for DBGM-2 input spectral acceleration and the radial gap of Δr = 0.25 ft.

$$a := Sa_{fn} \cdot \sin(\omega \cdot t)$$

$$Sa_{max} := Sa_{fn} \qquad Sa_{max} = 0.04 \cdot g$$

$$\text{velocity} = v_o + \frac{(a_o + a_1)}{2} dt$$

$$\text{displacement} = d_o + \frac{(v_o + v_1)}{2} dt$$

a_0 is acceleration at start of time increment
a_1 is acceleration at end of time increment
v_o is velocity at start of time increment
v_1 is velocity at end of time increment
d_o is displacement at start of time increment
dt is time increment

The above equations are input into excel to find the velocity and displacement as a function of time. Table B7-2 is the excel solution for impact velocity at a displacement of 0.25 ft. Figure B7-1 is a plot of acceleration, velocity and distance versus time.

Table B7-2. Numerical Integration for Sine Wave Input Motion DBGM-2 Input and Displacement at Impact of 0.25 Feet.

t (sec)	sin (ωt)	a (ft/sec^2)	v (ft/sec)	d (feet)
0	0	0	0	0
0.05	0.051078	0.064966	0.001624	4.06036E-05
0.1	0.102022	0.129762	0.006492	0.000243516
0.15	0.1527	0.194219	0.014592	0.000770621
0.2	0.20298	0.25817	0.025902	0.001782958
0.25	0.252729	0.321446	0.040392	0.003440299
0.3	0.301819	0.383884	0.058025	0.005900731
0.35	0.350121	0.445319	0.078755	0.009320245
0.4	0.397508	0.505591	0.102528	0.013852329
0.45	0.443858	0.564544	0.129281	0.019647566
0.5	0.48905	0.622022	0.158946	0.026853241
0.55	0.532964	0.677877	0.191443	0.035612956
0.6	0.575487	0.731962	0.226689	0.046066259
0.65	0.616508	0.784137	0.264592	0.058348274
0.7	0.655919	0.834264	0.305052	0.07258935
0.75	0.693618	0.882213	0.347963	0.088914726
0.8	0.729506	0.927859	0.393215	0.107444194
0.85	0.76349	0.971083	0.440689	0.128291797
0.9	0.79548	1.011772	0.49026	0.151565523
0.95	0.825394	1.049819	0.5418	0.177367026
1	0.853153	1.085125	0.595174	0.205791364
1.05	0.878685	1.117599	0.650242	0.236926744
1.06	0.883518	1.123746	0.661448	0.243485195
1.062	0.884473	1.124962	0.663697	0.24481034

Time at impact = 1.06 seconds
Velocity at impact = 0.66 feet per second.

This is very nearly the same result as calculated for a triangular wave form. The results of both solutions are valid for displacements achieved during an impulse rise time of 1/4 of the vibration period or less.

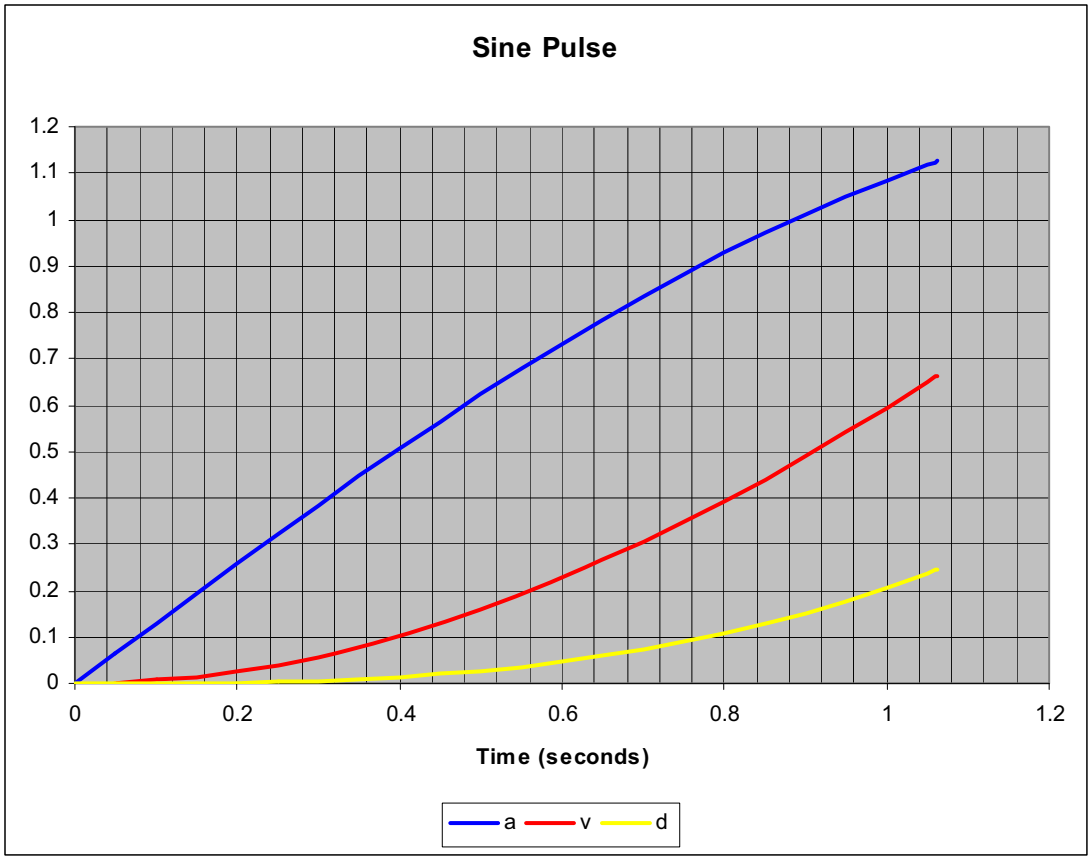

[Note that the vertical axis is acceleration in ft/sec^2; velocity in fps, and displacement in feet]

Figure B7-1
Acceleration, Velocity and Time of Canister Swinging on Rope for DBGM-2 and 0.25 Feet of Radial Clearance to Impact.

For convenience, use the triangular wave form equations for other cases. It has been shown that the impact velocity increases at approximately the cube root of the peak spectral acceleration of the pendulum swing motion for a fixed radial gap of 0.25 feet that represents the gap for the largest diameter canister in a shield bell. Smaller canisters will have larger gaps and potentially larger impact velocities.

From the equation for frequency of a pendulum, it is evident that frequency is independent of mass but is dependent on the square root of rope length. A longer rope that might be more representative of a smaller canister would result in a lower frequency, thus lower spectral acceleration. Therefore the spectral acceleration will conservatively be kept coincidental with the shortest rope for the largest canister.

Let the radial gap be twice the Δr of the largest canister.

$gap := 0.5ft$

For the DBGM-2 case with double the gap.

$t := 0.1s$ initial time to start the equation solver for time for a gap of 0.5 ft.

Given

$$gap = \frac{Sa_{fn}}{0.25 \cdot p} \cdot \frac{t^3}{6}$$

$t := Find(t)$

$t = 1.537\ s$

t = 1.537 seconds corresponds to period/4 so the peak acceleration will occur at this time, but due to phasing, the velocity would continue to increase up to time p/2 at which time the acceleration would reverse.

$$vel_{impact} := \frac{Sa_{fn}}{0.25 \cdot p} \cdot \frac{t^2}{2}$$

$$vel_{impact} = 0.976\ \frac{ft}{s}$$

This velocity is about 60% higher than for the 0.25 foot gap.

Increase the gap to 1 foot and do a numerical integration for 2 times DBGM-2 acceleration (equivalent to BDBGM) with the acceleration beginning to decrease at p/4 if the 1 foot gap is not closed up by time p/4. See Table B7-3 in next page. Equations are the same as for the solution for DBGM-2 with 0.25 foot gap except that the acceleration has doubled.

Table B7-3. Numerical Integration for 2 Times DBGM-2 Acceleration and Gaps up to 1 Foot

Numerical Integration of Canister Swinging on Rope Within Bell					
Triangular Input for 2 Times DBGM-2					
Samax = 2*0.0395g = 2.5438 ft/sec^2					
Period = 6.151 sec					
ω = 1.022 rad/sec					
Acceleration, a, = ((2.5438 ft.sec^2)/(0.25*6.151sec))*dt					
Velocity, v, = vo +((ao+ai)/2)*dt					
Displacement, d, = do+((vo+v1)/2)dt					
t	a	v	d		
0	0	0	0		
0.05	0.08271	0.002068	5.17E-05		
0.1	0.16542	0.008271	0.00031		
0.15	0.24813	0.01861	0.000982		
0.2	0.33084	0.033084	0.002275		
0.25	0.41355	0.051694	0.004394		
0.3	0.49626	0.074439	0.007547		
0.35	0.57897	0.10132	0.011941		
0.4	0.66168	0.132336	0.017783		
0.45	0.74439	0.167488	0.025278		
0.5	0.8271	0.206775	0.034635		
0.55	0.90981	0.250198	0.046059		
0.6	0.99252	0.297756	0.059758		
0.65	1.07523	0.34945	0.075938		
0.7	1.15794	0.405279	0.094806		
0.75	1.24065	0.465244	0.116569		
0.8	1.32336	0.529344	0.141434		
0.85	1.40607	0.59758	0.169607		
0.9	1.48878	0.669951	0.201295		
0.95	1.57149	0.746458	0.236706		
1	1.6542	0.8271	0.276045		
1.05	1.73691	0.911878	0.319519		
1.1	1.81962	1.000791	0.367336		
1.15	1.90233	1.09384	0.419702		
1.2	1.98504	1.191024	0.476823		
1.21	2.001582	1.210957	0.488833		
1.22	2.018124	1.231056	0.501043		
1.25	2.06775	1.292344	0.538894		
1.3	2.15046	1.397799	0.606148		
1.35	2.23317	1.50739	0.678777		
1.4	2.31588	1.621116	0.75699		
1.45	2.39859	1.738978	0.840992		
1.5	2.4813	1.860975	0.930991		
1.53775	2.543746	1.955823	1.003033		

For a gap of 0.5 feet the impact velocity is 1.23 feet per second. For a 1 foot gap, the impact velocity is 1.96 feet per second. The time at impact for a 1 foot gap for BDBGM corresponds exactly with the peak of the acceleration pulse at p/4 so the numerical integration calculations are valid up to this point. For any ground motion accelerations beyond the BDBGM level, the impact velocity varies as the cube root of the peak ground motion acceleration.

B8. CONCLUSIONS

A fragility has been developed for a bounding case of the hoist mechanism of the Canister Transfer Machine in the Cask Receipt and Closure Facility based on the seismic design requirements of Reference B2.2.13, B2.2.3 and the ASME NOG-1 design code of Reference B2.2.2. The resulting fragility is:

$$Am := 2.28g$$

$$\beta_C := 0.50$$

$$HCLPF := 0.72g$$

The calculated median capacity is more that 2 times the BDBGM and the HCLPF is greater than the DBGM-2 and is about 80% of the BDBGM. Different diameters and weights of canisters would result in different fragilities. With lower weight, the median capacity and HCLPF of the Hoist would increase proportionally to the reduced weight.

The canister can swing freely like a pendulum inside the shield bell. For the maximum TAD canister diameter, length and weight, at the 0.453g PGA DBGM-2 earthquake level, the impact velocity would be about 0.62 feet per second based on a triangular shape imput motion and about 0.66 feet per second based on a sine wave input motion. Consequently, the impact velocity is not sensitive to the assumed shape of the imput motion. For a given radial clearance, the impact velocity is a function of the cube root of the maximum spectral acceleration. Additional studies were done to examine the impact velocity for larger gaps for the BDBGM. At a gap of 1 foot, the impact velocity is only 1.96 feet per second. Results of the parametric studies for swinging canisters are summarized in Tables B7-1, B7-2 and B7-3.

APPENDIX B-A
Vertical CRCF Spectra for Node 419
(Reference B2.2.5)

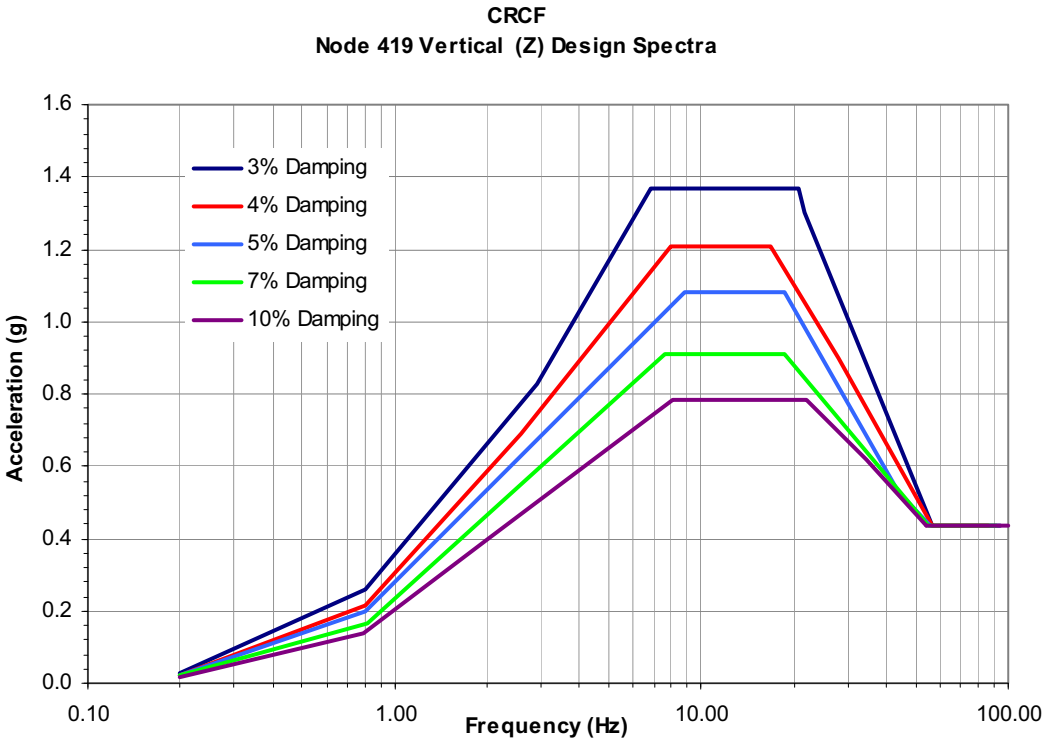

Figure B-A-1
DBGM-2 Vertical Envelope Design Spectra

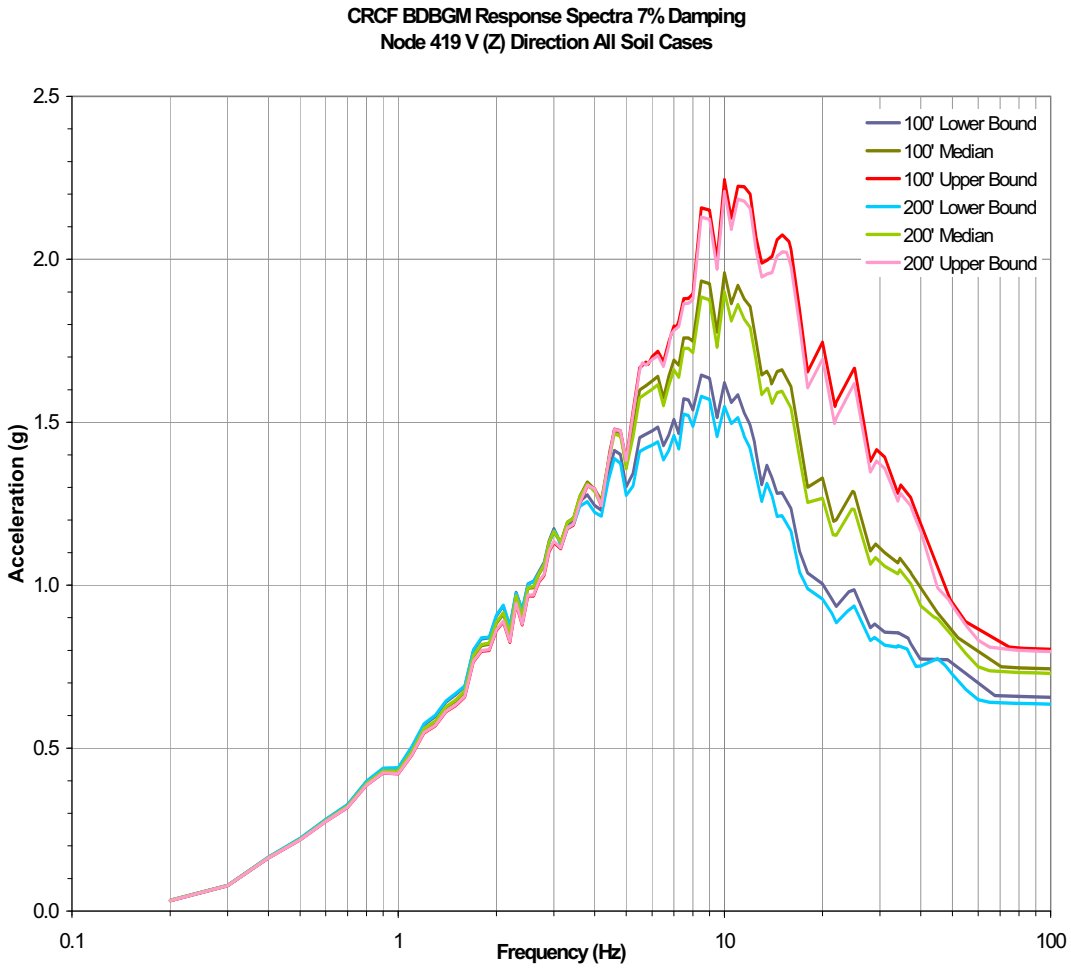

Figure B-A-2
BDBGM Vertical Spectra, 7% Damping

APPENDIX B-B
BDBGM Vertical UHS

Table B-B-1. BDBGM Vertical UHS
(See Section 6.2.2.1 for source information)

Freq (Hz)	SA (3.0%)	SA (5.0%)	SA (7.0%)
100.000	0.7230	0.7230	0.7230
91.116	0.7603	0.7603	0.7603
81.113	0.8130	0.8130	0.8130
70.548	0.9038	0.8828	0.8489
59.948	1.0184	0.9694	0.9153
49.770	1.1597	1.0753	0.9960
40.370	1.3376	1.2086	1.0985
29.837	1.6430	1.4388	1.2782
20.092	2.1057	1.7859	1.5508
10.000	2.6990	2.2060	1.8707
9.112	2.6485	2.1577	1.8263
8.111	2.4935	2.0238	1.7094
7.055	2.2796	1.8431	1.5541
5.995	2.0433	1.6461	1.3860
4.977	1.8200	1.4617	1.2296
4.037	1.6154	1.2945	1.0889
2.984	1.4055	1.1253	0.9476
2.009	1.1487	0.9220	0.7800
1.000	0.6291	0.5125	0.4395
0.890	0.5581	0.4563	0.3926
0.793	0.4935	0.4052	0.3498
0.706	0.4361	0.3597	0.3116
0.600	0.3661	0.3041	0.2649
0.498	0.2954	0.2476	0.2173
0.404	0.1990	0.1687	0.1493
0.298	0.1035	0.0895	0.0804
0.201	0.0425	0.0379	0.0349
0.100	0.0083	0.0080	0.0078

APPENDIX B-C
SLACK ROPE ANALYSIS DATA
(REFERENCE B2.2.7)

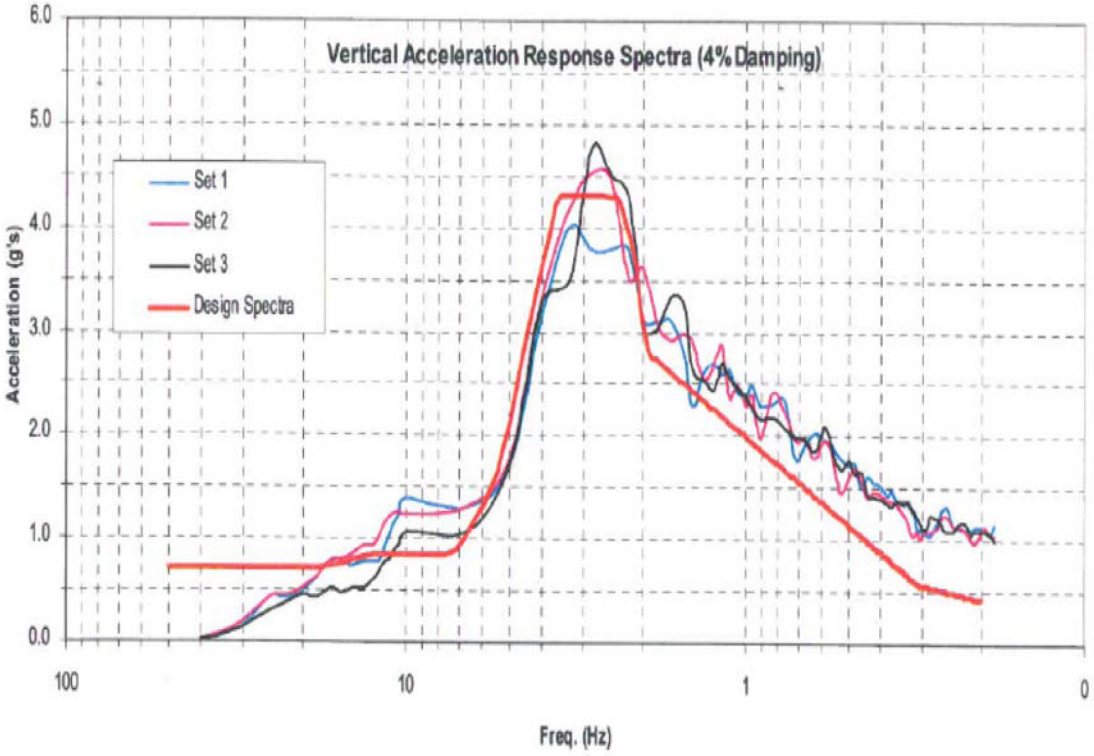

Figure B-C-1
Comparison of Target Response Spectrum to Spectra
From 3 Time History Simulations
(Reference B2.2.7)

Table B-C-1. Eigensolution of 2 DOF Model of Crane and Rope (Reference B2.2.7)

Trolley Position	Crane Frequency Hz	High Hook (L=8.5 ft)		Mid Hook (L=30 ft)		Low Hook (L=71 ft)	
		Rope Freq = 6.72 Hz		Rope Freq = 3.58 Hz		Rope Freq = 2.33 Hz	
		Mode 1	Mode 2	Mode 1	Mode 2	Mode 1	Mode 2
Midspan	12.35	4.97	16.75	3.26	13.62	2.25	12.88
¼ Span	15.05	5.40	18.79	3.36	16.11	2.27	15.50
End span	18.45	5.76	21.59	3.43	19.34	2.30	18.82

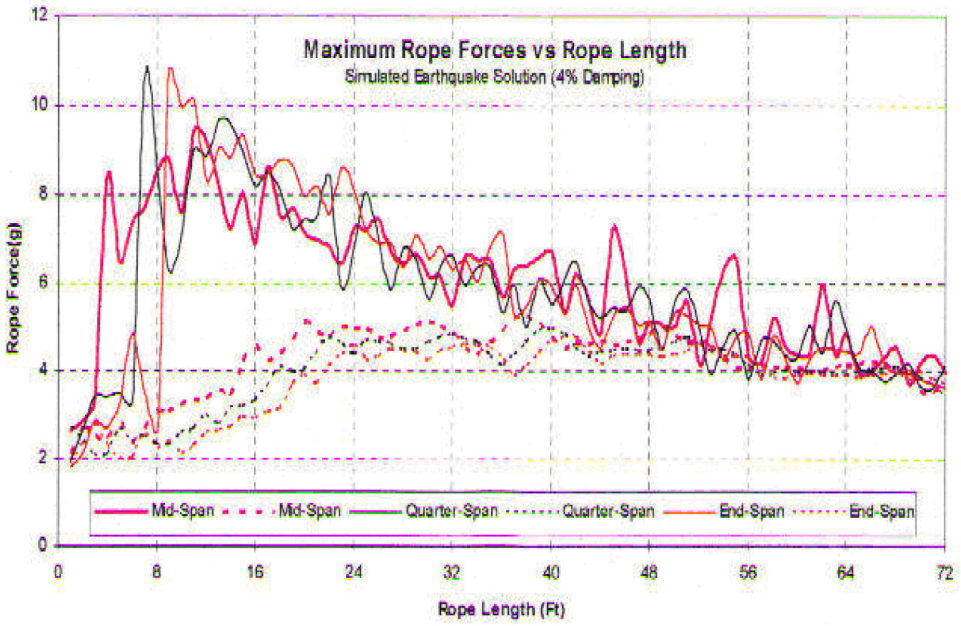

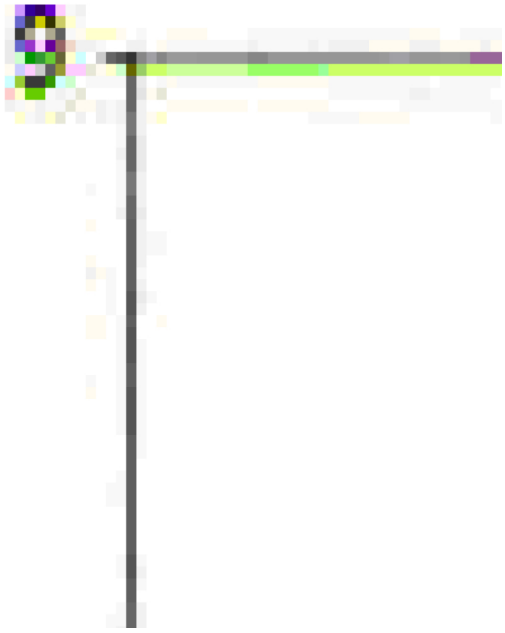

Figure B-C-2
Comparison of Linear and Non-linear Response for Slack Rope Impact
(Reference B2.2.7)

ATTACHMENT C

FRAGILITY FOR CRCF CASK TRANSFER TROLLEY

Prepared By: Wen H. Tong

ARES Check By: Stephen A. Short

LLNL Check By: Robert C. Murray

TABLE OF CONTENTS

ACRONYMS AND ABBREVIATIONS

ACI	American Concrete Institute
AISC	American Institute of Steel Construction
ANSI	American National Standards Insitute
AO	Aging Overpack
APE	Annual Probability of Exceedance
ASCE	American Society of Civil Engineers
ASME	American Society of Mechanical Engineers
BSC	Bechtel SAIC, LLC
BDBGM	Beyond Design Basis Ground Motion at $1x10^{-4}$ APE
CDFM	Conservative Deterministic Failure Margin
CHC	Cask Handling Crane
CIP	Cast-in-Place
CRCF	Canister Receipt and Closure Facility
CTM	Canister Transfer Machine
CTT	Cask Transfer Trolley
DBGM-2	Design Basis Ground Motion at $5x10^{-4}$ APE
DL	Dead Load
DOF	Degree of Freedom
DPC	Dual Purpose Canister
EPRI	Electric Power Research Institute
HCLPF	High Confidence of Low Probability of Failure
HVAC	Heating, Ventilation, & Air Conditioning
IEEE	Institute of Electrical and Electronics Engineers
IHF	Initial Handling Facility
ISRS	In-Structure Response Spectra

ACRONYMS AND ABBREVIATIONS (cont.)

ITS	Important to Safety
LA	License Application
LLNL	Lawrence Livermore National Laboratory
NPP	Nuclear Power Plant
PGA	Peak Ground Acceleration
RF	Receipt Facility
RRS	Required Response Spectrum
Sa	Spectral Acceleration
SFA	Surface Facilities Area
SFTM	Spent Fuel Transfer Machine
SPRA	Seismic Probabilistic Risk Assessment
SRSS	Square Root of the Sum of Squares
SSE	Safe Shutdown Earthquake (used with NPPs)
SSI	Soil Structure Interaction
SSC	Structure, System, and Component
TAD	Transportation, Aging, and Disposal canister
TEV	Transport and Emplacement Vehicle
TRS	Test Response Spectrum
UHS	Uniform Hazard Spectra
USDOE	United States Department of Energy
USNRC	United States Nuclear Regulatory Commission
WHF	Wet Handling Facility
WP	Waste Package
WPTT	Waste Package Transfer Trolley
YMSF	Yucca Mountain Surface Facilities
ZPA	Zero Period Acceleration

FRAGILITY TERMINOLOGY

A_m	Median Peak Ground Motion Capacity
β_R	Log Standard Deviation of Randomness
β_U	Log Standard Deviation of Uncertainty (Lack of Knowledge)
β_C	Composite Variability = $(\beta_R^2 + \beta_U^2)^{0.5}$
F_S	Strength Factor of Safety
β_{R_S}	Strength Randomness (typical)
β_{U_S}	Strength Uncertainty (typical)
β_{C_S}	Strength Composite Variability (typical)
F_μ	Inelastic Energy Absorption Factor of Safety
F_C	Capacity Factor of Safety
F_{QM}	Qualification Factor of Safety
F_δ	Damping Factor of Safety
F_M	Modeling Factor of Safety
F_{MC}	Modal Combination Factor of Safety
F_{ECC}	Earthquake Component Combination Factor of Safety
F_{SA}	Spectral Shape Factor of Safety
F_{SSI}	Soil-Structure Interaction Factor of Safety
F_{GMI}	Ground Motion Incoherence Factor of Safety
F_{TOTAL}	Total Factor of Safety
F_{RS}	Structural Response Factor of Safety
F_{RE}	Equipment Response Factor of Safety

C1. PURPOSE

The purpose of this calculation is to estimate seismic fragility of the Cask Transfer Trolley in the Canister Receipt and Closure Facility (CRCF). The mean seismic fragility curve of the Important to Safety (ITS) Cask Transfer Trolley (CTT) will be convolved with the mean site-specific seismic hazard curve to calculate risk of seismic-induced failure of the trolley.

C2. REFERENCES

C2.1 PROCEDURES/DIRECTIVES

C2.1.1 EG-PRO-3DP-G04B-00037, Rev. 10. *Calculations and Analyses*. Las Vegas, Nevada: Bechtel SAIC Company. ACC: ENG.20071018.0001.

C2.1.2 BSC (Bechtel SAIC Company) 2005. *Q-List*. 000-30R-MGR0-00500-000-003. Las Vegas, Nevada: Bechtel SAIC Company. ACC: ENG.20050929.0008. [DIRS 175539]

C2.1.3 IT-PRO-0011, Revision 7, ICN 0. *Software Management*. Las Vegas, Nevada: Bechtel SAIC Company. ACC: DOC.20070905.0007.

C2.1.4 BSC (Bechtel SAIC Company) 2007. *Quality Management Directive*. QA-DIR-10, Rev. 2. Las Vegas, Nevada: Bechtel SAIC Company. ACC: DOC.20080103.0002. [DIRS 184673]

C2.2 DESIGN INPUTS

C2.2.1 EPRI (Electric Power Research Institute) 1994. *Methodology for Developing Seismic Fragilities*. EPRI TR-103959. Palo Alto, California: Electric Power Research Institute. TIC:253770. [DIRS 161329]

C2.2.2 BSC (Bechtel SAIC Company) 2007. *Cask Transfer Trolley Mechanical Equipment Envelope*. V0-CY05-QHC4-00459-00033-001 REV 004. Las Vegas, Nevada: Bechtel SAIC Company. ACC: ENG.20071019.0004. [DIRS 183505], [DIRS 184084], [DIRS 184085]

C2.2.3 BSC (Bechtel SAIC Company) 2008. *Canister Receipt and Closure Facility 1 General Arrangement Ground Floor Plan*. 060-P10-CR00-00102-000 REV 00C. Las Vegas, Nevada: Bechtel SAIC Company. ACC: ENG.20080122.0013. [DIRS 184853]

C2.2.4 [Reserved]

C2.2.5 [Reserved]

C2.2.6 BSC (Bechtel SAIC Company) 2007. *Mechanical Handling Design Report Cask Transfer Trolley (240 Ton & 265 Ton Capacity)*. V0-CY05-QHC4-00459-00016-001 REV 006. Las Vegas, Nevada: Bechtel SAIC Company. ACC: ENG.20071018.0017. [DIRS 184122]

C2.2.7 ASME NOG-1-2004. 2005 *Rules for Construction of Overhead and Gantry Cranes (Top Running Bridge, Multiple Girder)*. New York, New York: American Society of Mechanical Engineers. TIC: 257672. [DIRS 176239]

C2.2.8 ASCE/SEI 43-05. 2005. *Seismic Design Criteria for Structures, Systems, and Components in Nuclear Facilities*. Reston, Virginia: American Society of Civil Engineers. TIC: 257275. [DIRS 173805]

C2.2.9 MO0801HCUHSSFA.001. *Mean Hazard Curves and Mean Uniform Hazard Spectra for the Surface Facilities Area*. Submittal date: 01/11/2008. [DIRS 184802]

C2.2.10 BSC (Bechtel SAIC Company) 2007. *CRCF Tier-1 In-Structure Response Spectra*. 060-SYC-CR00-00900-000-00B. Las Vegas, Nevada: Bechtel SAIC Company. ACC: ENG.20071210.0008. [DIRS 184330]

C2.2.11 [Reserved]

C2.2.12 [Reserved]

C2.2.13 Baltay, P. and Gjelsvik, A. 1990. "Coefficient of Friction for Steel on Concrete at High Normal Stress." *Journal of Materials in Civil Engineering, 2*, (1), 46-49. [New York, New York]: American Society of Civil Engineers. TIC: 260005. [DIRS 184424]

C2.2.14 BSC (Bechtel SAIC Company) 2007. *Yucca Mountain Seismic Analysis of Cask Transfer Trolley*. V0-CY05-QHC4-00459-00020-001 REV 004. Las Vegas, Nevada: Bechtel SAIC Company. ACC: ENG.20071018.0018. [DIRS 183539]

C2.3 DESIGN CONSTRAINTS

There are no design constraints in the performance of this calculation.

C2.4 DESIGN OUTPUTS

The calculation is performed to calculate seismic fragility of the Cask Transfer Trolley which will be convolved with the site-specific seismic hazard curve to calculate risk of seismic-induced failure of the trolley. This is performed to support information in the License Application.

C3. ASSUMPTIONS

C3.1 ASSUMPTIONS REQUIRING VERIFICATION

There are no assumptions made in the calculation that require verification.

C3.2 ASSUMPTIONS NOT REQUIRING VERIFICATION

There are no assumptions not requiring verification.

C4. METHODOLOGY

C4.1 QUALITY ASSURANCE

This calculation is prepared in accordance with EG-PRO-3DP-G04B-00037, Calculations and Analyses (Reference C2.1.1). The Cask Transfer Trolley is classified as Important to Safety on the Q List (Reference C2.1.2), Table A-1. Therefore, this document is subject to the appropriate requirements for the BSC Quality Management Directive (Reference C2.1.4, Section 2.1.C.1.1), and the approved record version is designated as "QA:QA".

C4.2 USE OF SOFTWARE

Mathcad version 14 is used in this calculation. The use of this software is classified as Level 2 software per procedure IT-PRO-0011 (Reference C2.1.3) and therefore the software need not be qualified.

C4.3 APPROACH

The Separation-of-Variable method (Section 3 of Reference C2.2.1) is followed in calculating seismic fragility of the ITS equipment component.

C5. LIST OF APPENDICES

There are no appendices to this calculation.

C6. FRAGILITY CALCULATION

C6.1 INTRODUCTION

Seismic fragility calculation of the CRCF Cask Transfer Trolley (CTT) is presented in this section. The trolley is located at the ground floor (elevation 0') of the CRCF.

C6.2 CASK TRANSFER TROLLEY

The Cask Transfer Trolley is required to support a loaded transportation cask and to transfer the cask to the canister transfer station. The CRCF Cask Transfer Trolley has overall dimensions of 16' by 16' at the base by 22'-6" high (Reference C2.2.2). The top of the cask after being mounted on the trolley is at 27'-3" from the bottom face of the trolley.

The trolley is mounted on air modules and is propelled by an air motor and travels on the concrete floor at elevation 0' from the cask preparation area to the canister transfer cell. Transfer of the canister from the transportation cask to the waste package is done by the overhead Canister Transfer Machine (CTM) which is supported by the building structure.

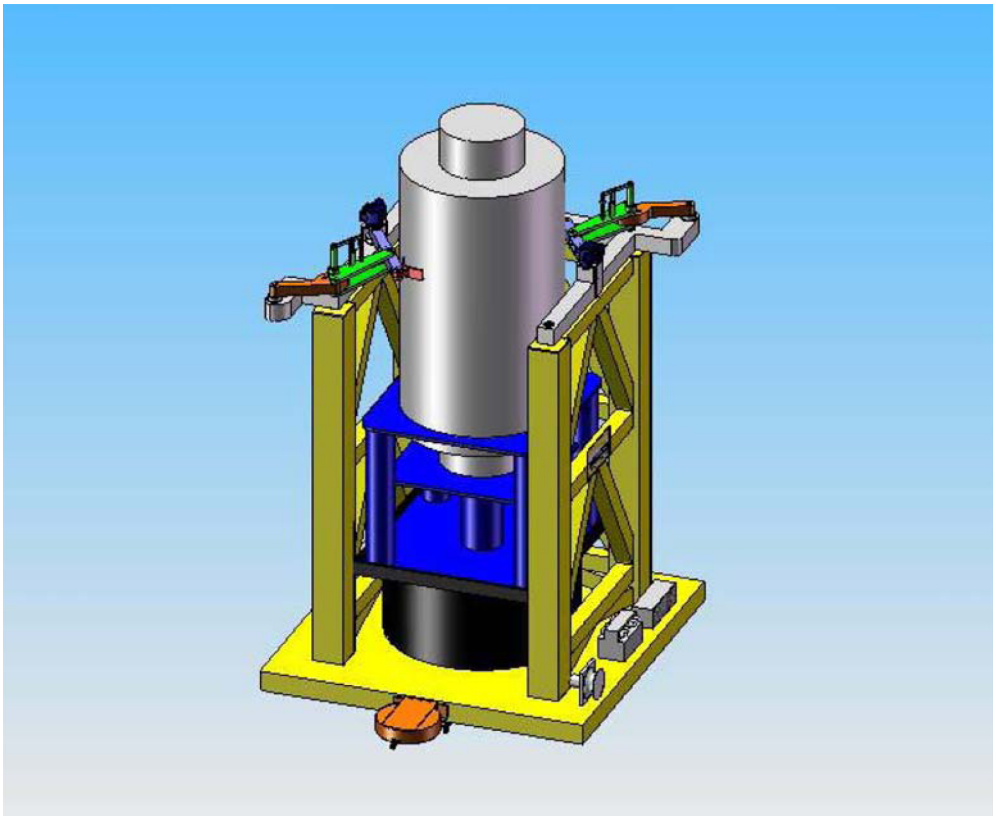

Figure C6.2-1. Cask Transfer Trolley (Reference C2.2.6)

C6.3 POTENTIAL FAILURE MODES

Potential failure modes of the Cask Transfer Trolley that may impact performance goals of the Yucca Mountain Project are presented below based on our understanding of safety functions and operation of the trolley.

C6.3.1 Transfer of Cask from Railcar to Trolley

This is addressed separately in the fragility calculation of the cask handling crane.

C6.3.2 During Transit to Canister Transfer Cell

The air-powered trolley travels on the concrete floor slab. In the event of loss of power during an earthquake, the air modules will depressurize such that the trolley will rest on the floor. The free-standing Cask Transfer Trolley is subject to seismic-induced sliding or tip over. A potential consequence of sliding or tip over of the trolley is impact of the Cask Transfer Trolley with the steel columns at the ground floor. However damage of the steel columns will not lead to local collapse because the concrete wall above these columns will behave as a deep beam spanning between the concrete walls along column lines E and G.

C6.3.3 Parked in the Canister Transfer Cell

Upon entering the transfer cell, the CTT will be guided directly below the transfer port by floor guides that are bolted to the floor slab. Since these floor guides are not intended to be seismic stops, they are not strong enough to prevent the trolley from sliding in a seismic event. Upon sliding or rocking and impacting a 4-foot thick cell wall, breach of a canister inside a transportation cask with impact limiters removed is taken to be a credible failure mode. The probability of canister breach given trolley impact is not included in this calculation.

C6.3.4 Trolley Structural Failure

Reference C2.2.6 provides design analyses of the Cask Transfer Trolley for load combinations including DBGM-2 and BDBGM. The stresses in the trolley due to DBGM-2 load combination are found to be lower than the NOG-1 stress limits (Table 4311-1 of Reference C2.2.7). The BDBGM stresses are calculated to be 84% of the ultimate tensile strength of the trolley. These calculated design stresses are overly conservative for the reasons given below:

- The trolley is modeled as fixed at the base. The horizontal fundamental frequencies are calculated to be 12 to 13 Hz which are near the peak of the horizontal response spectrum used in the analysis (Reference C2.2.6). In reality, sliding of the trolley will initiate at a low acceleration level. The trolley will slide as a rigid body and the equivalent system frequency is much lower than 12 Hz and the spectral acceleration will be much less than half that at 12 to 13 Hz.
- The maximum trolley stresses due to the three components of earthquake were assumed to all occur at the same location in the trolley. This results in conservative seismic stresses in the trolley.

The abovementioned conservatism in the P&H design analysis is acceptable for design purpose. However, using these stresses will result in conservatively biased (unrealistic) seismic fragility estimates. Since rocking and sliding dominate, the failure mode due to seismic-induced stresses in the CTT is not further considered in this calculation.

C6.3.5 Governing Failure Mode

Based on the above discussions, either sliding or tip over of the CTT is a credible failure mode. The governing failure mode is evaluated below.

The center of gravity of the trolley loaded with the heaviest cask is at (Section 5.5 of Reference C2.2.14):

$H_{cg} := 177 \cdot in$	Height measured from the bottom of the trolley
$X_{cg} := 96 \cdot in$	From the edge of the trolley base in the X-direction (horizontal) which is parallel to the open face of the trolley (Figure C6.2.1)
$Y_{cg} := 95.4 \cdot in$	From the edge of the trolley base in the Y-direction (horizontal).
$W_t := 644.6 \cdot kip$	Total weight of the loaded trolley

When an earthquake occurs, the air supply to the air modules will stop and the trolley will rest on the concrete floor. The best-estimate coefficient of friction between the steel trolley base and the concrete

floor slab is 0.47.

$\mu := 0.47$ Figure 3, Reference C2.2.13

Based on the above given center of gravity, the acceleration level at which one edge of the trolley base will lift up is determined.

$$S_{a\_liftup} := \left(\frac{Y_{cg}}{H_{cg}}\right) \cdot g$$

$$S_{a\_liftup} = 0.54 \cdot g$$

At this acceleration level, the seismic inertia load of the trolley is

$$V_{trolley} := W_t \cdot \frac{S_{a\_liftup}}{g}$$

$$V_{trolley} = 347.43 \cdot kip$$

Frictional resistance at the base of the trolley

$$V_{friction} := \mu \cdot W_t$$

$V_{friction} = 302.96 \cdot kip$ Less than the seismic inertia load at uplift

Since the acceleration levels at which trolley sliding and lifting at one edge are not very different, seismic fragility of both failure modes are evaluated.

C6.4 SEISMIC INPUT MOTION

The Cask Transfer Trolley operates at the ground floor of the CRCF. Therefore seismic input motion to the trolley is defined by the CRCF ISRS at elevation 0'. Note that there will be three identical CRCFs on site. The depth of alluvium under these CRCFs varies from 100 feet to 200 feet. The 100-ft alluvium case yields slightly higher ISRS than the 200-ft alluvium case. The 5% and 10% damped BDBGM ISRS in the two horizontal directions and the vertical direction for the 100-foot alluvium case are presented in Figures C6.4-1, C6.4-2, and C6.4-3. Also presented in the figures are the 5% damped site-wide UHS. The 10% damped BDBGM ($1x10^{-4}$ annual exceedance frequency) will be used in the calculations.

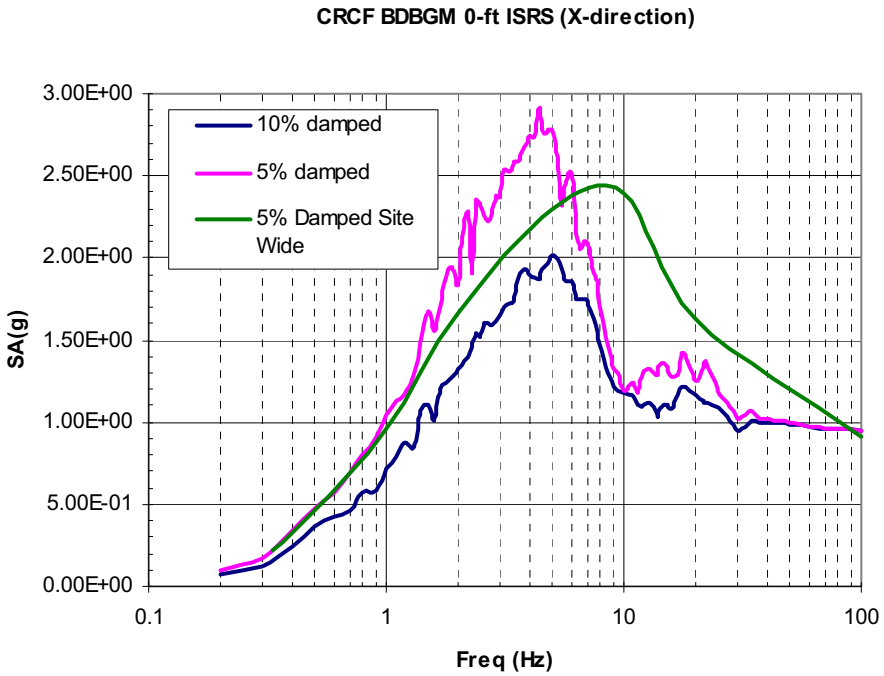

Figure C6.4-1. X-Direction BDBGM ISRS at 0' Floor - Median Soil Case (Plotted from Data in Reference C2.2.10)

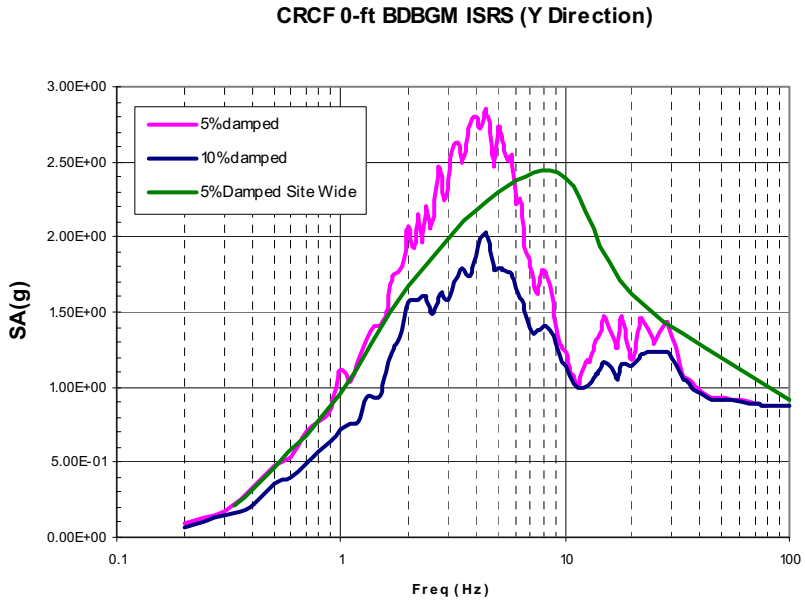

Figure C6.4-2. Y-Direction BDBGM ISRS at 0' Floor - Median Soil Case (Plotted from Data in Reference C2.2.10)

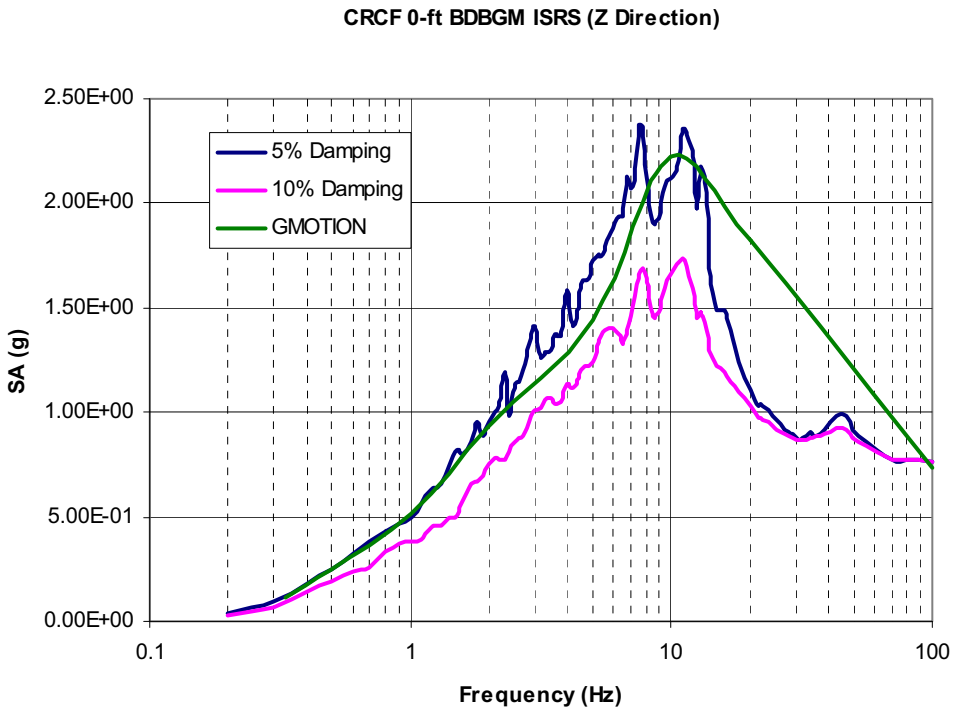

Figure C6.4-3. Z-Direction (Vertical) BDBGM ISRS at 0' Floor - Median Soil Case (Plotted from Data in Reference C2.2.10)

C6.5 SEISMIC FRAGILITY OF SEISMIC-INDUCED SLIDING OF TROLLEY

The approach presented in Appendix A.1 of ASCE 43-05 (Reference C2.2.8) is used to calculate the best-estimate seismic-induced sliding displacement of the Cask Transfer Trolley at which impact between the trolley and the transfer cell walls would occur.

C6.5.1 Strength Factor

The displacement limit of the Cask Transfer Trolley is determined based on the clearance between the trolley and the walls of the transfer cell. The center to center spacing of the CRCF building columns in the transfer cell is 32' per Reference C2.2.3. The clearance between the trolley base and the end wall of the transfer cell is 4' based on the trolley being directly underneath the transfer port as shown in Reference C2.2.3. Given the trolley base dimensions of 16' by 16', the column spacing of 32,' and the cell walls being 4-foot thick, the clearance between the CTT base and the side walls of the transfer cell is greater than 4' (Reference C2.2.3).

$$\delta_{limit} := 4 \cdot ft$$

Next the rigid body displacement of the trolley is calculated using the reserve energy method in Appendix A of Reference C2.2.8. This method treats the nonlinear problem of rigid body sliding using an equivalent linear model. The rigid-body displacements are calculated for input motion of different annual probabilities of exceedance and the motion which yields a displacement closest to the limit is used for the strength factor calculation.

$\mu_e := \mu$ The effective coefficient of sliding friction does not account for the vertical component of ground motion for a "best-estimate" sliding displacement. This is because the vertical acceleration will oscillate several times during the time the rigid body displaces from 0 to a finite displacement.

$\mu_e = 0.47$

The force-displacement curve of a rigid body sliding is shown in Figure C6.5-1, where F_{RS} is the resisting force and δ_s is the displacement to be estimated. Based on the reserve energy method, an equivalent linear system is used to estimate the displacement. This equivalent system has a stiffness of K_e and a displacement of $_s$.

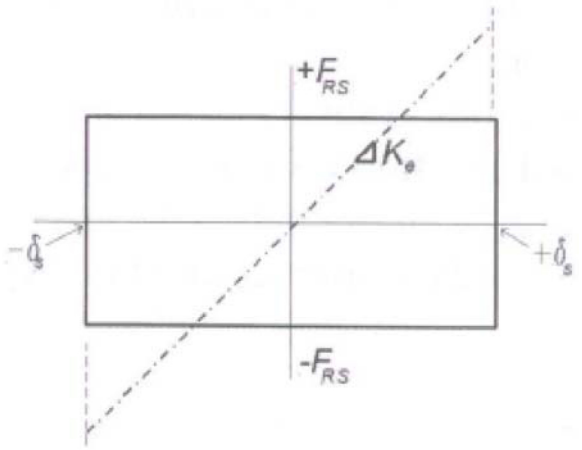

Figure C6.5-1. Sliding Force-Displacement Diagram (Reference C2.2.8, Appendix B)

Next define sliding coefficient as shown below

$c_s := 2 \cdot \mu_e \cdot g$ Equation A-2 of Reference C2.2.8, where g is the gravitational acceleration.

$c_s = 0.94 \cdot g$

Based on the reserve energy method, the sliding displacement of the rigid body is estimated by Equation B-5 of Reference C2.2.8 in which f_{eS} is the lowest natural frequency at which the vector horizontal spectral acceleration equals c_s.

$SA_H := 0.1 \cdot g$ Initial trial value of SA_H (i.e., spectral acceleration in one horizontal direction) to solve the equation below so that the vector horizontal spectral acceleration is equal to c_s

Given

$\sqrt{SA_H^2 + 0.16 SA_H^2} = c_s$ The two horizontal components of earthquake have essentially the same spectral shape. Equation A-4 of Reference C2.2.8.

$SA_H := \text{Find}(SA_H)$

$SA_H = 0.87 \cdot g$

The lowest natural frequency (f_{eS}) at which the vector spectral acceleration equals c_s is determined from the 10% damped ISRS at the ground floor which has an annual exceedance frequency of 10^{-4} as shown in Figure C6.4-1.

$f_{es} := 1.2 \cdot Hz$ at which the spectral acceleration in one direction is 0.87g.

$\delta_s := \frac{c_s}{(2 \cdot \pi \cdot f_{es})^2}$ Sliding distance as given in Equation A-3 of Reference C2.2.8

$\delta_s = 0.53 \cdot ft$ This BDBGM-induced displacement will not result in impact with the cell wall.

Next the lowest natural frequency (f_{eS}) at which the vector spectral acceleration equals c_s is determined from the ISRS at the ground floor which has an annual exceedance frequency of 10^{-5}. Though the 10^{-5} ISRS are not available, f_{eS} can be estimated from the 1E-5 site-wide ground response spectrum as shown in Table C6.5-1. Figures C6.4-1 and 2 show that the in-structure spectra are essentially same as the ground response spectrum in the frequency range less than 1 Hz. Thus, the 5% damped 1E-5 UHS is scaled to 10% UHS using the 5% and 10% BDBGM ISRS in Figures C6.4-1 and C6.4-2.

Table C6.5-1 10% Damped 1E-5 UHS Scaled From 5% Damped 1E-5 Site-Wide UHS

Frequency (Hz)	5% Damped BDBGM Sa (g)	10% Damped BDBGM Sa (g)	Ratio	5% Damped 1E-5 Sa (g);Figure C6.5-2	Scaled 10% Damped 1E-5 Sa (g)
0.3	1.72E-01	1.18E-01	0.69	0.48	0.33
0.4	3.45E-01	2.49E-01	0.72	0.9	0.65
0.5	4.75E-01	3.62E-01	0.76	1.35	1.03
0.6	5.73E-01	4.23E-01	0.74	1.7	1.26
0.7	6.94E-01	4.64E-01	0.67	1.94	1.30
0.8	7.96E-01	5.71E-01	0.72	2.2	1.58
0.9	9.15E-01	5.79E-01	0.63	2.4	1.52

$f_{es} := 0.45 \cdot Hz$

At this frequency the 10% damped 1E-5 spectral acceleration is equal to 0.87g.

$$\delta_s := \frac{c_s}{\left(2 \cdot \pi \cdot f_{es}\right)^2}$$

Sliding distance as given in Equation A-3 of Reference C2.2.8

$\delta_s = 3.78 \cdot ft$

When the trolley slides more than 4 feet and impact the transfer cell wall, the canister will be assumed breached.

$$F_S := \frac{\delta_{limit}}{\delta_s}$$

$F_S = 1.06$

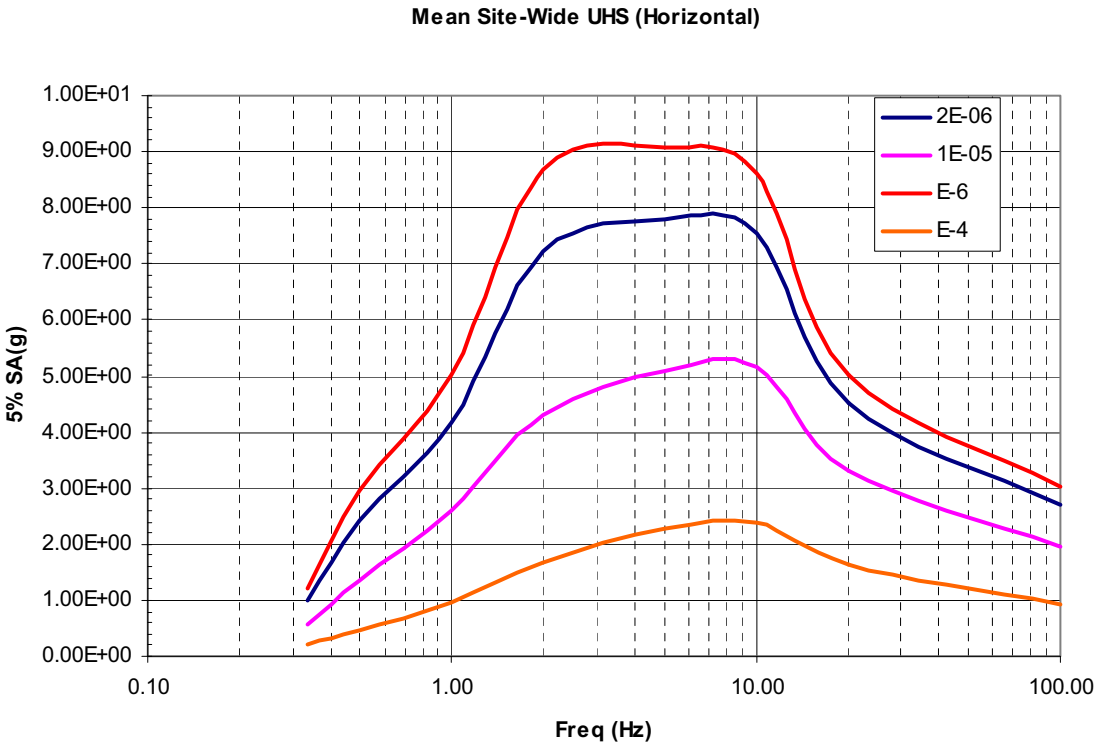

Figure C6.5-2. 5% Damped Mean Site-Wide Horizontal Uniform Hazard Spectra at E-4, E-5, 2E-6 and E-6 APE (See Section 6.2.2.1 for source information)

C6.5.1.1 Uncertainty in Equation

A factor of safety of 2 is recommended for the calculated rigid body displacement for design purposes (Appendix A.1 of Reference C2.2.8). Based on common design practice, a design value typically represents at least a 98% non-exceedance value. Based on this, uncertainty associated with the best-estimate displacement is calculated.

$\beta_{U\_S\_1} := \frac{1}{2}\cdot\ln(2)$ The 98% non-exceedance value is two (2) standard deviation from the mean. The second value of 2 in the equation is the factor of safety recommended for design value.

$\beta_{U\_S\_1} = 0.35$

$\beta_{R\_S} := 0$ There is no randomness associated with the strength factor.

C6.5.1.2 Uncertainty in Coeff. of Friction

A median value of 0.47 is used for coefficient friction between steel and concrete based on Reference C2.2.13. A -1σ value of 0.40 is estimated based on the same reference for normal stress in the range of 50 to 100 psi (Figure 4 of Reference C2.2.13)

$\mu_{1\sigma} := 0.4$

$c_{s\_1\sigma} := 2\cdot\mu_{1\sigma}\cdot g$

$c_{s\_1\sigma} = 0.8\cdot g$

Based on the reserve energy method, the sliding displacement of the rigid body is estimated by Equation B-5 of Reference C2.2.8 in which f_{eS} is the lowest natural frequency at which the vector horizontal spectral acceleration equals to c_s.

$SA_H := 0.1\cdot g$ Initial guess of SA_H value (i.e., spectral acceleration in one horizontal direction) to solve the equation below so that the vector horizontal spectral acceleration is equal to c_s

Given

$\sqrt{SA_H^2 + 0.16SA_H^2} = c_{s\_1\sigma}$ Assuming the two horizontal components of earthquake have the same spectral shape. Equation A-4 of Reference C2.2.8.

$SA_H := \text{Find}(SA_H)$

$SA_H = 0.74\cdot g$

The lowest natural frequency (f_{eS}) at which the vector spectral acceleration equals c_s is determined from the 10% damped $1*10^{-5}$ UHS.

$f_{es} := 0.41\cdot Hz$

$$\delta_{s\_1\sigma} := \frac{c_{s\_1\sigma}}{\left(2\cdot\pi\cdot f_{es}\right)^2}$$ Equation A-3 of Reference C2.2.8

$$\delta_{s\_1\sigma} = 3.88\cdot ft$$

$$\beta_{U\_S\_2} := \ln\left(\frac{\delta_{s\_1\sigma}}{\delta_s}\right)$$

$$\beta_{U\_S\_2} = 0.02$$

$$\beta_{U\_S} := \sqrt{\beta_{U\_S\_1}^2 + \beta_{U\_S\_2}^2}$$

$$\beta_{U\_S} = 0.35$$

C6.5.2 Inelastic Energy Absorption Factor

For rigid body sliding, there is no inelastic energy absorption capability. Thus,

$$F_\mu := 1.0$$

$$\beta_{R\_\mu} := 0$$

$$\beta_{U\_\mu} := 0$$

C6.5.3 Structural Response Factors

As shown in Figures C6.4-1 and C6.4-2, the BDBGM ISRS in the frequency range from 0.2 Hz to 1 Hz is essentially same as the site-wide BDBGM UHS. Since the seismic-induced sliding of the Cask Transfer Trolley is responding in this low frequency range as shown above, the trolley is treated as a structure founded at grade.

C6.5.3.1 Spectral Shape Factor

$F_{SA} := 1.0$ The median strength factor is calculated based on input motion of mean $1*10^{-5}$ site-wide ground response spectrum.

Since uncertainty in the UHS is derived from uncertainty in the seismic hazard curves which will be included in the final risk quantification, no additional uncertainty is included under the spectral shape factor to avoid double-counting the hazard uncertainty, hence

$$\beta_{U\_SA} := 0$$

$\beta_{R\_SA} := 0.2$ This is random variability to account for peak to valley variability of a smooth ground response spectrum (Reference C2.2.1).

C6.5.3.2 Damping Factor

A damping value of 10% is suggested in Reference C2.2.8 (page 33 of Reference C2.2.8) for the rigid body sliding calculation. Since 10% damped spectrum was used in the strength factor calculation, thus

$F_{\delta} := 1.0$

$\beta_{U\_\delta} := 0.05$ Nominal value used to account for the fact that a scaling approach was used in getting the 10% damped UHS from the 5% damped UHS.

$\beta_{R\_\delta} := 0$

C6.5.3.3 Modeling Factor

The reserve energy method used in calculating the sliding displacement above is a conservatively biased "best estimate" method (Section A.1 of Reference C2.2.8). Using this method, a factor of safety of 2.0 is recommended to obtain design value of sliding (Reference C2.2.8). When time history analysis is used to determine the best estimate sliding distance, a factor of safety of 3 is recommended (Section 7.1 of Reference C2.2.8) to obtain design value. Therefore, the modeling factor of safety is equal to the ratio of the factors of safety associated with these two methods.

$F_M := \frac{3}{2}$

$\beta_{R\_M} := 0$

$\beta_{U\_M} := \frac{1}{1} \cdot \ln\left(\frac{3}{2}\right)$ The conservatively bias best estimate sliding is judged to be one standard deviation from the best estimate results from time history analyses.

$\beta_{U\_M} = 0.41$

C6.5.3.4 Modal Combination

Since it is single mode response,

$F_{MC} := 1$

$\beta_{R\_MC} := 0.05$ A nominal value.

$\beta_{U\_MC} := 0$

C6.5.3.5 Earthquake Component Combination

In the strength factor calculation above, the best-estimate vector spectral acceleration is the combination of S_{AH} and $0.4*S_{AH}$. The vector of 100% of both horizontal components is at 3 sigma from the median case.

$F_{EC} := 1.0$ Since the best-estimate earthquake component combination is used in the above strength factor calculation.

$SA_H := 0.1 \cdot g$ Initial trial value of SA_H value (i.e., spectral acceleration in one horizontal direction) to solve the equation below so that the vector horizontal spectral acceleration is equal to c_s

Given

$$\sqrt{SA_H^2 + SA_H^2} = c_s$$

$$a_{3\sigma} := \text{Find}(SA_H)$$

$$a_{3\sigma} = 0.66 \cdot g$$

The lowest natural frequency (f_{eS}) at which the vector spectral acceleration equals c_s is determined from the 10% damped mean horizontal UHS at annual exceedance frequency of $1*10^{-5}$.

$$f_{es} := 0.4 \cdot Hz$$

$$\delta_{s\_3\sigma} := \frac{c_s}{(2 \cdot \pi \cdot f_{es})^2}$$

$$\delta_{s\_3\sigma} = 4.79 \cdot ft$$

$$\beta_{R\_EC} := \frac{1}{3} \cdot \ln\left(\frac{\delta_{s\_3\sigma}}{\delta_s}\right)$$

$$\beta_{R\_EC} = 0.08$$

$$\beta_{U\_EC} := 0$$

C6.5.3.6 Soil-Structure Interaction

The soil-structure interaction effects were considered in the BSC Tier 1 CRCF seismic response analysis (Reference C2.2.10) using frequency independent soil springs and soil damping coefficients based on an elastic half space. The calculated translational soil damping coefficients were reduced by 25% to account for layering effects. Three soil properties were considered in the BSC SSI analysis, i.e., lower bound, median, and upper bound. It is seen from Figure C6.5-3 below that in the frequency range of sliding of the CTT, there is practically no difference in the response due to difference in soil properties.

At the frequency of the equivalent linear model (<1 Hz) the SSI effects are minimal as shown in Figure C6.5-3, the factor of safety of the soil-structure interaction analysis is set as unity.

$$F_{SSI} := 1.0$$

$$\beta_{R\_SSI} := 0$$

$\beta_{U\_SSI} := 0.05$ Nominal value used

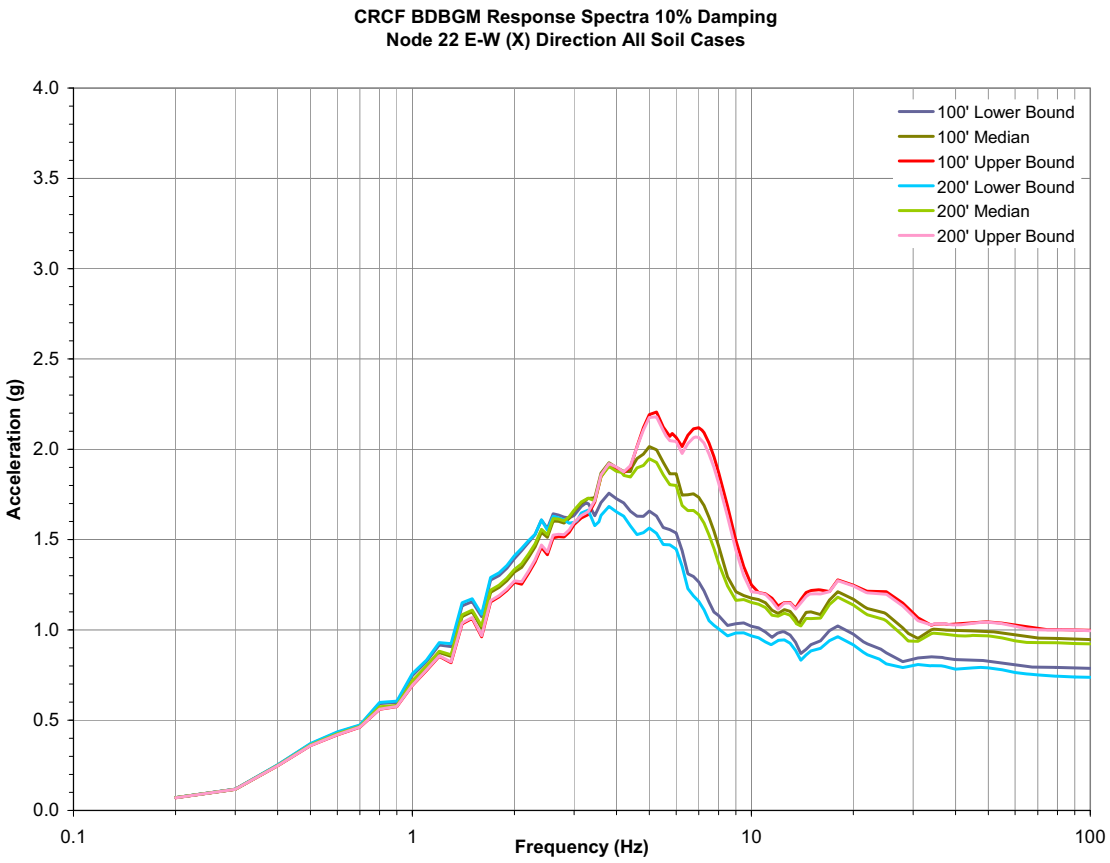

Figure C6.5-3 BDBGM Elevation 0 Feet In-Structure Response Spectra (Reference C2.2.10)

C6.5.4 Overall Factor of Safety of CTT Sliding

$F_{total} := F_S \cdot F_\mu \cdot F_{SA} \cdot F_\delta \cdot F_M \cdot F_{MC} \cdot F_{EC} \cdot F_{SSI}$

$F_{total} = 1.59$

$PGA := 1.94g$ Peak ground acceleration of the 1E-05 APE site-wide UHS (Ref. C2.2.9; also Section 6.2.2.1 for source information)

$A_m := F_{total} \cdot PGA$

$A_m = 3.08 \cdot g$ Median seismic capacity in terms of PGA

$$\beta_R := \sqrt{\beta_{R\_S}^2 + \beta_{R\_\mu}^2 + \beta_{R\_SA}^2 + \beta_{R\_\delta}^2 + \beta_{R\_M}^2 + \beta_{R\_MC}^2 + \beta_{R\_EC}^2 + \beta_{R\_SSI}^2}$$

$\beta_R = 0.22$

$$\beta_U := \sqrt{\beta_{U\_S}^2 + \beta_{U\_\mu}^2 + \beta_{U\_SA}^2 + \beta_{U\_\delta}^2 + \beta_{U\_M}^2 + \beta_{U\_MC}^2 + \beta_{U\_EC}^2 + \beta_{U\_SSI}^2}$$

$\beta_U = 0.54$

$\beta_c := \sqrt{\beta_R^2 + \beta_U^2}$

$\beta_c = 0.58$

$HCLPF := A_m \cdot e^{-2.33 \cdot \beta_c}$

$HCLPF = 0.79 \cdot g$

C6.6 SEISMIC FRAGILITY OF SEISMIC-INDUCED ROCKING OF TROLLEY

The approach presented in Appendix A.2 of Reference C2.2.8 is used to calculate the median seismic capacity of trolley tipover in a seismic event. The approach accounts for frequency shift when an unanchored rigid body is subjected to ground motion of a seismic event and initiates rocking. As the rocking angle increases, the equivalent frequency of the rocking block becomes less. Instability (i.e., tipover) occurs when the center of gravity of the rigid block is directly over point B shown in Figure C6.6-1. This occurs when the rocking angle is equal to the instability angle defined by arctan(a) where a is the ratio of b to h (see Figure C6.6-1 for definition of b and h).

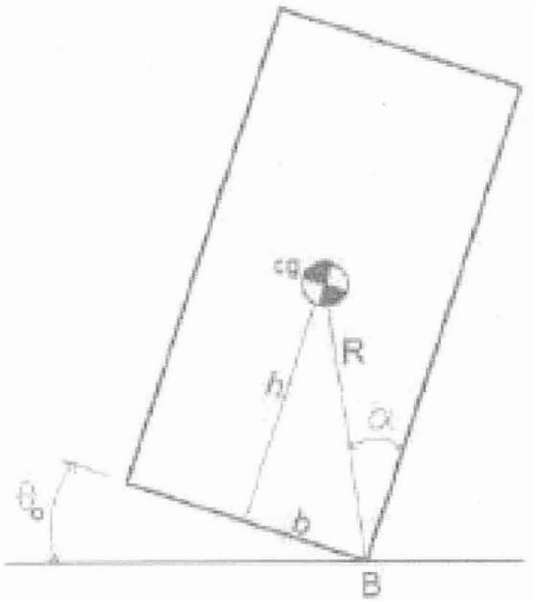

Figure C6.6-1. Rigid Body Rocking Definitions (Figure 7-1 of Ref. C2.2.8)
NOTE: Legibility of figure does not affect the technical content of the document.
See source for detail

The weights of an empty Cask Transfer Trolley and the heaviest transportation cask are 165 kips and 480 kips, respectively per Section 5.5 of Reference C2.2.14. The center of gravity of this loaded Cask Transfer Trolley is 177 inches from the floor. The base of the trolley is 16' square. Data required for the tipover analysis are summarized below.

$h_{cg} := 177 \cdot in$	Center of gravity height measured from the floor
$b := 95.4 \cdot in$	Minimum horizontal distance from the edge of the rigid body to the center of gravity. This value is taken from Section 5.5 of Reference C2.2.14.

$$a := \frac{b}{h_{cg}}$$

$a = 0.54$

$C_l := \frac{4}{3} \cdot \left(1 + a^2\right)$ Equation A-6(f) of Reference C2.2.8

$C_l = 1.721$

$C_R := 1 - \frac{2 \cdot a^2}{C_l}$ Equation A-6(e) of Reference C2.2.8

$\gamma := -2 \cdot \ln\left(C_R\right)$ Equation A-6(d) of Reference C2.2.8

$\beta_e := \frac{\gamma}{\sqrt{4 \cdot \pi^2 + \gamma^2}}$ Effective damping, Equation A-6(b) of Reference C2.2.8

$\beta_e = 0.13$ Note that the Tier 1 ISRS (DBGM-2 and BDBGM) are plotted only up to 10% of critical damping case.

$\beta_e := 0.1$

The rigid body rocking of the trolley is evaluated for the following earthquakes: BDBGM (1E-4 APE), 1E-5 APE, and 2E-6 APE.

6.6.1 BDBGM Earthquake

For BDBGM, the 10% damped ISRS at the ground floor are used (see Figures C6.4-1 to C6.4-3).

Table C6.6-1 Seismic-Induced Rocking Analysis of CTT for BDBGM

Rocking angle (radians)	Rocking angle (deg.)	fe (Hz), Note 5	SAV	SAH	SAV/SAH, Note 7	BDBGM Demand (g)	$F_{V,}$ Note 8	SAH capacity (g), Note 9	Cap/Dem
0.0025	0.14	3.72	1.06	1.93	0.55	1.93	1.04	1.03	0.54
0.005	0.29	2.63	0.88	1.62	0.54	1.62	1.04	1.03	0.64
0.01	0.57	1.85	0.67	1.25	0.54	1.25	1.04	1.03	0.82
0.015	0.86	1.51	0.53	1.11	0.48	1.11	1.03	1.03	0.93
0.017	0.97	1.42	0.49	1.03	0.48	1.03	1.03	1.03	1.00
0.02	1.15	1.30	0.48	0.86	0.56	0.86	1.04	1.01	1.18
0.025	1.43	1.16	0.40	0.78	0.51	0.78	1.04	1.02	1.30
1. Instability angle is 28.5 degrees (0.5 radians)									
2. Effective damping is 10% of critical.									
3. Center of gravity		177	inches						
4. C_I =	1.721								
5. Equation A-6(a) of Ref. C2.2.8									
6. Effective damping is 10% of critical.									
7. Ratio of vertical to horizontal spectral acceleration at the effective rocking frequency and da									
8. Equation A-5 (c) of Ref. C2.2.8.									
9. Equation A-5 of Ref. C2.2.8.									

The best-estimate angle of rocking is 0.97 degrees.

C6.6.2 1E-5 APE Earthquake

Since the Tier-1 seismic response analyses were performed only for DBGM-2 and BDBGM, there are no ISRS for 1E-5 and 2E-6 APE earthquakes. However, as shown in Figure C6.4-1, the difference between the UHS and the ISRS at the ground floor in the low frequency range (<1 Hz) is not significant. Therefore, the site-wide UHS are used for the 1E-5 and 2E-6 APE earthquakes with adjustment for 10% damping value as shown in the table below.

Table C6.6-2 Seismic-Induced Rocking Analysis of CTT for 1E-5 APE Earthquake

Rocking angle (radians)	Rocking angle (deg.)	fe (Hz), Note 4	SAV, Notes 5& 9	SAH, Notes 5& 9	SAV/SAH, Notes 5&6	1E-5 APE Demand (g), Note 10	F_V, Note 7	SAH capacity (g), Note 8	Cap/Dem
0.01	0.57	1.85	2.3	4.2	0.55	2.96	1.04	1.03	-0.35
0.02	1.15	1.30	1.9	3.4	0.56	2.39	1.04	1.01	0.42
0.03	1.72	1.06	1.50	2.80	0.54	1.97	1.04	1.01	0.51
0.05	2.86	0.81	1.20	2.20	0.55	1.55	1.04	0.99	0.64
0.08	4.58	0.63	0.90	1.80	0.50	1.27	1.04	0.96	0.76
0.1	5.73	0.56	0.85	1.60	0.53	1.13	1.04	0.94	0.83
0.13	7.45	0.48	0.68	1.28	0.53	0.90	1.04	0.91	1.01
0.15	8.59	0.45	0.60	1.20	0.50	0.85	1.04	0.89	1.06

1. Instability angle, given trolley's dimensions and center of gravity, is 28.5 degrees (0.5 radians)
2. Center of gravity 177 inches
3. C_I = 1.721 Equation A-6 (c) of Ref. C2.2.8.
4. Equation A-6(a) of Ref. C2.2.8
5. Spectral values of 5% of critical damping are used.
6. Ratio of vertical to horizontal spectral acceleration (E-5 APE) at the effective rocking frequency and effective damping
7. Equation A-5 (c) of Ref. C2.2.8.
8. Equation A-5 of Ref. C2.2.8.
9. See Figure C6.6-2 for 5% damped 1E-5 APE horizontal and vertical UHS.
10. The seismic demand is divided by a factor of 1.42 to convert the 5% damped spectral acceleration to the 10% damped spectral values. See table below for the factor of 1.42.

The best-estimate angle of rocking as determined above is 7.45 degrees. The corresponding effective frequency is 0.48 Hz which is very close to the 0.5 Hz which is valid. Thus, the calculated rocking angle would not be significantly impacted by the plotting fault at 0.3 Hz (see Section 6.2.2.1 for details).

Table C6.6-3 Determination of Scale Factor to Estimate 10% Damped 1E-5 UHS

Scale Factor to Get 10% Damped 1E-5 UHS from 5% Damped UHS						
Frequency (Hz)	5% Damped BDBGM Sa (g), Column A	10% Damped BDBGM Sa (g), Column B	Ratio of Column B to Column A	5% Damped 1E-5 Sa (g), Column C	Scaled 10% Damped 1E-5 Sa (g), Column D	Ratio of Column C to Column D
0.3	1.72E-01	1.18E-01	0.69	0.4	0.28	1.45
0.4	3.45E-01	2.49E-01	0.72	0.94	0.68	1.39
0.5	4.75E-01	3.62E-01	0.76	1.37	1.04	1.31
0.6	5.73E-01	4.23E-01	0.74	1.7	1.26	1.35
0.7	6.94E-01	4.64E-01	0.67	1.94	1.30	1.50
0.8	7.96E-01	5.71E-01	0.72	2.2	1.58	1.39
0.9	9.15E-01	5.79E-01	0.63	2.4	1.52	1.58
					Average ratio	**1.42**
Note: See Figure C6.4-1 for the 5% and 10% damped ISRS.						

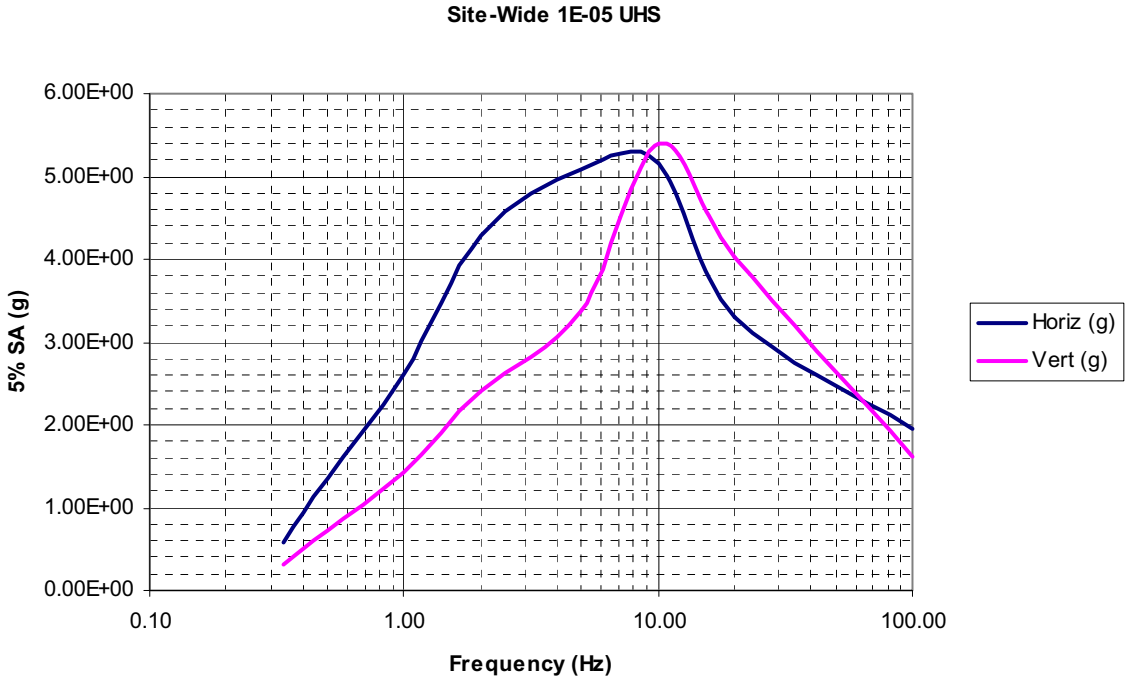

Figure C6.6-2. 5% Damped 1E-5 APE UHS (See Section 6.2.2.1 for source information)

C6.6.3 2E-6 APE Earthquake

The effective system frequency of the rigid body rocking of the trolley when subjected to 1E-05 earthquake is close to 0.5 Hz as shown in Table C6.6-2. At 2E-6 earthquake, the frequency is expected to lower to 0.3 Hz where the UHS plotting fault was identified (see Section 6.2.2.1 for details). Hence it is necessary to use the corrected 5% damped spectral acceleration values given in Table 3 of Section 6.2.2.1, i.e., 0.978g horizontal and 0.532g vertical at 0.3 Hz. The corrected values are scaled to 10% damping. Between 0.3 and 0.5 Hz, linear interpolation is done.

Table C6.6-4 Seismic-Induced Rocking Analysis of CTT for 2E-6 APE Earthquake

Rocking angle (radians)	Rocking angle (deg.)	fe (Hz), Note 4	SAV, Notes 5& 9	SAH, Notes 5& 9	SAV/SAH, Notes 5&6	2E-6 APE Demand (g), Note 10	F_V, Note 7	SAH capacity (g), Note 8	Cap/Dem
0.03	1.72	1.06	2.50	4.60	0.54	3.24	1.04	1.01	0.31
0.05	2.86	0.81	2.00	3.60	0.56	2.54	1.04	0.99	0.39
0.08	4.58	0.63	1.64	3.00	0.55	2.11	1.04	0.96	0.45
0.1	5.73	0.56	1.50	2.80	0.54	1.97	1.04	0.94	0.48
0.15	8.59	0.45	1.09	2.02	0.54	1.42	1.04	0.89	0.63
0.2	11.46	0.37	0.79	1.47	0.54	1.04	1.04	0.84	0.81
0.24	13.75	0.33	0.64	1.19	0.54	0.84	1.04	0.80	0.95
0.25	14.32	0.32	0.61	1.12	0.54	0.79	1.04	0.79	1.00
0.27	15.47	0.31	0.57	1.05	0.54	0.74	1.04	0.77	1.04
0.3	17.19	0.29	0.49	0.91	0.54	0.64	1.04	0.74	1.15
1. Instability angle, given trolley's dimensions and center of gravity, is 28.5 degrees (0.5 radians)									
2. Center of gravity		177	inches						
3. C_I =	1.721	Equation A-6 (c) of Ref. C2.2.8.							
4. Equation A-6(a) of Ref. C2.2.8									
5. Spectral values of 5% of critical damping are used.									
6. Ratio of vertical to horizontal spectral acceleration (2E-6 APE) at the effective rocking frequency and effective damping									
7. Equation A-5 (c) of Ref. C2.2.8.									
8. Equation A-5 of Ref. C2.2.8.									
9. See Figure C6.6-3 for 2E-6 APE horizontal and vertical UHS. Values at frequencies between 0.3 Hz and 0.5 Hz are interpolated as discussed above.									
10. The seismic demand is divided by a factor of 1.42 to convert the 5% damped spectral acceleration to the 10% damped spectral values. See Table C6.6-5 for the factor of 1.42.									

The best estimate of angle of rocking is 14.32 degrees.

Table C6.6-5 Determination of Scale Factor to Estimate 10% Damped 2E-6 UHS

Scale Factor to Get 10% Damped 2E-6 UHS from 5% Damped UHS						
Frequency (Hz)	5% Damped BDBGM Sa (g), Column A	10% Damped BDBGM Sa (g), Column B	Ratio of Column B to Column A	5% Damped 2E-6 Sa (g), Column C	Scaled 10% Damped 2E-6 Sa (g), Column D	Ratio of Column C to Column D
0.3	1.72E-01	1.18E-01	0.69	0.66	0.45	1.45
0.4	3.45E-01	2.49E-01	0.72	1.7	1.23	1.39
0.5	4.75E-01	3.62E-01	0.76	2.45	1.87	1.31
0.6	5.73E-01	4.23E-01	0.74	2.9	2.14	1.35
0.7	6.94E-01	4.64E-01	0.67	3.23	2.16	1.50
0.8	7.96E-01	5.71E-01	0.72	3.56	2.55	1.39
0.9	9.15E-01	5.79E-01	0.63	3.85	2.44	1.58
					Average ratio	**1.42**

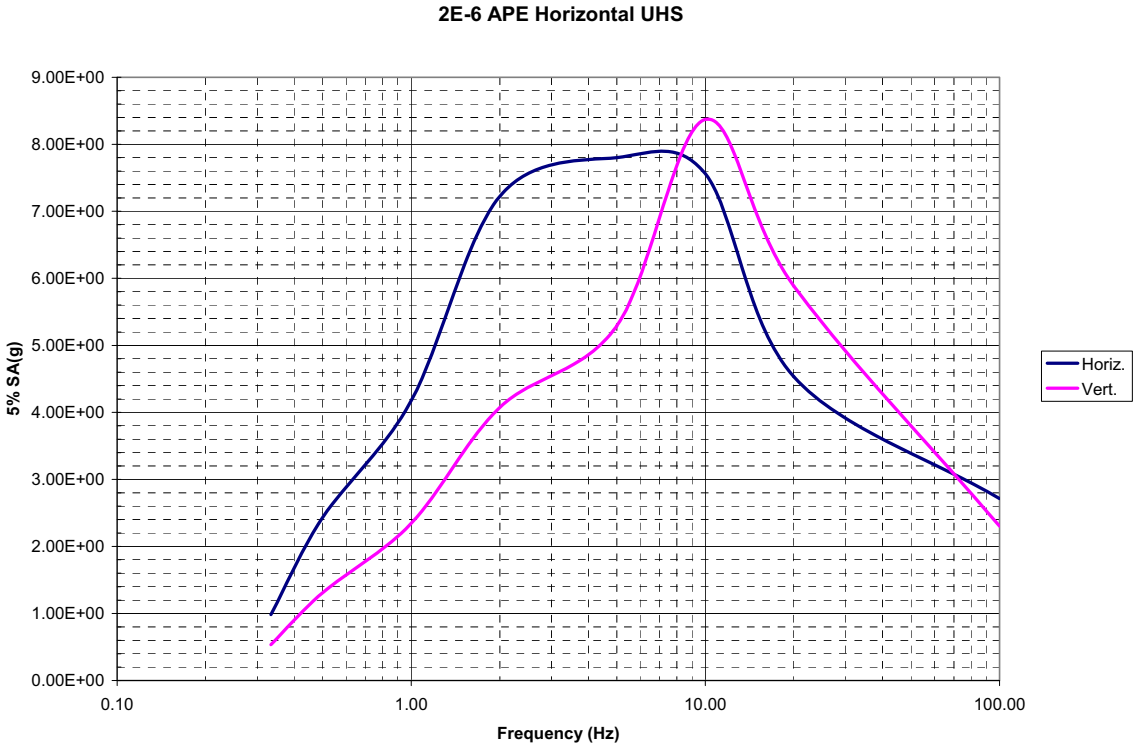

Figure C6.6-3. 2E-06 APE 5% Damped Site-Wide Horizontal and Vertical UHS (See Section 6.2.2.1 for source information)

Based on the above tabulated results, it is seen that trolley tipover is not expected when the trolley is subjected to the 2E-06 APE site-wide ground motion. Next, the lateral displacement at the top of the trolley at each of the best-estimate angle of rocking is calculated.

As shown in Reference C2.2.2, the overall heights measured from the top of the cask and from the top of the trolley to the base of the trolley are 327 inches and 270 inches, respectively. Impact to the adjacent reinforced concrete walls due to rigid body rocking of the trolley will occur between the top of the trolley frame and the walls. Because the cask is recessed from the perimeter of the trolley frame, there will be no direct impact between the top of the cask and the cell walls.

$h_{trolley} := 270 \cdot in$ Measured from the bottom of the trolley to the top of the trolley frame (Reference C2.2.2).

BDBGM $PGA_{BDBGM} := 0.91 \cdot g$ Reference C2.2.9; also Section 6.2.2.1 for source information

$\theta_{BE\_BDBGM} := 0.97 \cdot deg$

$\Delta_{BDBGM} := h_{trolley} \cdot \sin\left(\theta_{BE\_BDBGM}\right)$

$\Delta_{BDBGM} = 4.57 \cdot in$

1E-05 APE

$PGA_1 := 1.94 \cdot g$ Peak ground acceleration of the 1E-05 UHS (Reference C2.2.9; also Section 6.2.2.1 for source information)

$\theta_{BE\_1} := 7.45 \cdot deg$

$\Delta_{1E05} := h_{trolley} \cdot \sin\left(\theta_{BE\_1}\right)$

$\Delta_{1E05} = 2.92 \cdot ft$

2E-06 APE

$PGA_2 := 2.71 \cdot g$ Peak ground acceleration of the 2E-6 UHS (Reference C2.2.9; also Section 6.2.2.1 for source information)

$\theta_{BE\_2} := 14.3239 \cdot deg$

$\Delta_{2E06} := h_{trolley} \cdot \sin\left(\theta_{BE\_2}\right)$

$\Delta_{2E06} = 5.57 \cdot ft$ Greater than the 4-foot gap

Interpolate between 1E-5 and 2E-6 APE PGA to estimate the PGA at impact.

$$PGA_{impact} := PGA_1 + \frac{4ft - \Delta_{1E05}}{\left(\Delta_{2E06} - \Delta_{1E05}\right)} \cdot \left(PGA_2 - PGA_1\right)$$

$$PGA_{impact} = 2.25 \cdot g$$

$$F_S := \frac{PGA_{impact}}{PGA_{BDBGM}}$$

$$F_S = 2.48$$

Uncertainty in Equation

A factor of safety of 2 is recommended for the calculated rigid body rocking angle for design purposes (Section 7.1 of Reference C2.2.8). Based on common design practice, a design value typically represents at lease a 98% non-exceedance value. Based on this, uncertainty associated with the best-estimate displacement is calculated.

$\beta_{U\_S\_1} := \frac{1}{2} \cdot \ln(2)$

$\beta_{U\_S\_1} = 0.35$

The 98% non-exceedance value is two (2) standard deviation from the mean. The second value of 2 in the equation is the factor of safety recommended for design value.

$\beta_{R\_S} := 0$

There is no randomness associated with the strength factor.

C6.6.4 Inelastic Energy Absorption Factor

For rigid body rocking, there is no inelastic energy absorption capability. Thus,

$$F_\mu := 1.0$$

$$\beta_{R\_\mu} := 0$$

$$\beta_{U\_\mu} := 0$$

C6.6.5 Structural Response Factors

As shown in Figures C6.4-1 and C6.4-2, the BDBGM ISRS in the frequency range from 0.2 Hz to 1 Hz is essentially same as the site-wide BDBGM UHS. Thus, the trolley may be treated as a structure at grade.

C6.6.5.1 Spectral Shape Factor

$F_{SA} := 1.0$ The median strength factor is calculated based on input motion of mean $1*10^{-5}$ and 2*10-6 APE site-wide ground response spectra.

Since uncertainty in the UHS is derived from uncertainty in the seismic hazard curves which will be included in the final risk quantification, no additional uncertainty is included under the spectral shape factor to avoid double-counting the hazard uncertainty, hence

$\beta_{U\_SA} := 0$

$\beta_{R\_SA} := 0.2$ This is random variability to account for peak to valley variability of a smooth ground response spectrum (Reference C2.2.1).

C6.6.5.2 Damping Factor

An effective damping value of 13% is calculated using the approximate method in Reference C2.2.8 for the rigid body rocking calculation. 10% damped spectral acceleration was used in the strength factor calculation the factor of safety is set to unity, which is slightly conservative.

$F_{\delta} := 1$

$\beta_{U\_\delta} := 0.0$ Since conservative damping value is used in the rocking calculation.

$\beta_{R\_\delta} := 0$

C6.6.5.3 Modeling Factor

The rigid body rocking is a single degree-of-freedom response. Uncertainty of this approximate method is already accounted for in the uncertainty of the strength factor, thus

$F_{M} := 1$

$\beta_{R\_M} := 0$

$\beta_{U\_M} := 0$

C6.6.5.4 Modal Combination

Since the approximate method of rocking calculation is essentially a single mode response,

$F_{MC} := 1$

$\beta_{R\_MC} := 0.05$ A nominal value.

$\beta_{U\_MC} := 0$

C6.6.5.5 Earthquake Component Combination

$F_{EC} := 1.0$ Since the best-estimate earthquake component combination is used in the above strength factor calculation.

As shown in the above rocking calculation, the factor F_V (correction for probabilistically combined vertical ground motion) has only a small effect on rocking. Thus,

$\beta_{R\_EC} := 0.05$ A nominal value

$\beta_{U\_EC} := 0$

C6.6.5.6 Soil-Structure Interaction

The soil-structure interaction effects were considered in the BSC Tier 1 CRCF seismic response analysis (Reference C2.2.10) using frequency independent soil springs and soil damping coefficients based on elastic half space. The calculated translational soil damping coefficients were reduced by 25% to account for layering effects. Three soil properties were considered in the BSC SSI analysis, i.e., lower bound, median, and upper bound. It is seen from Figure C6.5-3 that in the frequency range of sliding of the CTT, there is practically no difference in the response due to difference in soil properties.

At the frequency of the equivalent linear rocking model (<1 Hz) the SSI effects are minimal as shown in Figure C6.5-3, the factor of safety of the soil-structure interaction analysis is set as unity.

$F_{SSI} := 1.0$

$\beta_{R\_SSI} := 0$

$\beta_{U\_SSI} := 0.05$ Nominal value assumed

C6.6.6 Overall Factor of Safety of CTT Rocking

$F_{total} := F_S \cdot F_\mu \cdot F_{SA} \cdot F_\delta \cdot F_M \cdot F_{MC} \cdot F_{EC} \cdot F_{SSI}$

$F_{total} = 2.48$

$PGA_{BDBGM} := 0.91g$ Peak ground acceleration of the BDBGM site-wide UHS (Ref. C2.2.9; also Section 6.2.2.1 for source information)

$A_m := F_{total} \cdot PGA_{BDBGM}$

$A_m = 2.25 \cdot g$ Median seismic capacity in terms of PGA

$$\beta_R := \sqrt{\beta_{R\_S}^2 + \beta_{R\_\mu}^2 + \beta_{R\_SA}^2 + \beta_{R\_\delta}^2 + \beta_{R\_M}^2 + \beta_{R\_MC}^2 + \beta_{R\_EC}^2 + \beta_{R\_SSI}^2}$$

$\beta_R = 0.21$

$$\beta_U := \sqrt{\beta_{U\_S}^2 + \beta_{U\_\mu}^2 + \beta_{U\_SA}^2 + \beta_{U\_\delta}^2 + \beta_{U\_M}^2 + \beta_{U\_MC}^2 + \beta_{U\_EC}^2 + \beta_{U\_SSI}^2}$$

$$\beta_U = 0.35$$

$$\beta_c := \sqrt{\beta_R^2 + \beta_U^2}$$

$$\beta_c = 0.41$$

$$HCLPF := A_m \cdot e^{-2.33 \cdot \beta_c}$$

$$HCLPF = 0.87 \cdot g$$

C7 SUMMARY

The seismic-induced failure of the Cask Transfer Trolley due to rigid body sliding or rocking is evaluated and seismic fragilities are calculated. The governing failure mode is taken to be that when the trolley impacts the transfer cell walls, the canister could be breached. Seismic fragilities of the Cask Transfer Trolley are shown below:

Sliding: Cask Transfer Trolley slides and impacts the transfer cell wall

A_m = 3.08g β_c = 0.58 HCLPF = 0.79g

Rocking: Impact of the Trolley with the cell walls due to rocking

A_m = 2.25g β_c = 0.41 HCLPF = 0.87g

ATTACHMENT D

FRAGILITY FOR STRUCTURAL FAILURE OF CRCF CANISTER TRANSFER MACHINE

Prepared By: Wen H. Tong

ARES Check By: Stephen A. Short

LLNL Check By: Robert C. Murray

TABLE OF CONTENTS

ACRONYMS AND ABBREVIATIONS

ACI	American Concrete Institute
AISC	American Institute of Steel Construction
ANSI	American National Standards Insitute
AO	Aging Overpack
APE	Annual Probability of Exceedance
ASCE	American Society of Civil Engineers
ASME	American Society of Mechanical Engineers
BSC	Bechtel SAIC, LLC
BDBGM	Beyond Design Basis Ground Motion at $1x10^{-4}$ APE
CDFM	Conservative Deterministic Failure Margin
CHC	Cask Handling Crane
CIP	Cast-in-Place
CRCF	Canister Receipt and Closure Facility
CTM	Canister Transfer Machine
CTT	Cask Transfer Trolley
DBGM-2	Design Basis Ground Motion at $5x10^{-4}$ APE
DL	Dead Load
DOF	Degree of Freedom
DPC	Dual Purpose Canister
EPRI	Electric Power Research Institute
HCLPF	High Confidence of Low Probability of Failure
HVAC	Heating, Ventilation, & Air Conditioning
IEEE	Institute of Electrical and Electronics Engineers
IHF	Initial Handling Facility
ISRS	In-Structure Response Spectra

ACRONYMS AND ABBREVIATIONS (cont.)

ITS	Important to Safety
LA	License Application
LLNL	Lawrence Livermore National Laboratory
NPP	Nuclear Power Plant
PGA	Peak Ground Acceleration
RF	Receipt Facility
RRS	Required Response Spectrum
Sa	Spectral Acceleration
SFA	Surface Facilities Area
SFTM	Spent Fuel Transfer Machine
SPRA	Seismic Probabilistic Risk Assessment
SRSS	Square Root of the Sum of Squares
SSE	Safe Shutdown Earthquake (used with NPPs)
SSI	Soil Structure Interaction
SSC	Structure, System, and Component
TAD	Transportation, Aging, and Disposal canister
TEV	Transport and Emplacement Vehicle
TRS	Test Response Spectrum
UHS	Uniform Hazard Spectra
USDOE	United States Department of Energy
USNRC	United States Nuclear Regulatory Commission
WHF	Wet Handling Facility
WP	Waste Package
WPTT	Waste Package Transfer Trolley
YMSF	Yucca Mountain Surface Facilities
ZPA	Zero Period Acceleration

FRAGILITY TERMINOLOGY

Am	Median Peak Ground Motion Capacity
β_R	Log Standard Deviation of Randomness
β_U	Log Standard Deviation of Uncertainty (Lack of Knowledge)
β_C	Composite Variability = $(\beta_R^2 + \beta_U^2)^{0.5}$
F_S	Strength Factor of Safety
β_{R_S}	Strength Randomness (typical)
β_{U_S}	Strength Uncertainty (typical)
β_{C_S}	Strength Composite Variability (typical)
F_μ	Inelastic Energy Absorption Factor of Safety
F_{QM}	Qualification Factor of Safety
F_δ	Damping Factor of Safety
F_M	Modeling Factor of Safety
F_{MC}	Modal Combination Factor of Safety
F_{ECC}	Earthquake Component Combination Factor of Safety
F_{SA}	Spectral Shape Factor of Safety
F_{SSI}	Soil-Structure Interaction Factor of Safety
F_{GMI}	Ground Motion Incoherence Factor of Safety
F_{TOTAL}	Total Factor of Safety
F_{RS}	Structural Response Factor of Safety
F_{RE}	Equipment Response Factor of Safety

D1. PURPOSE

The purpose of this calculation is to estimate seismic fragility of the Canister Transfer Machine (CTM) in the Canister Receipt and Closure Facility (CRCF). The mean seismic fragility curve of the CTM will be convolved with the mean site-specific seismic hazard curve to calculate risk of seismic-induced failure of the CTM.

D2. REFERENCES

D2.1 PROCEDURES/DIRECTIVES

D2.1.1 EG-PRO-3DP-G04B-00037, Rev. 10. *Calculations and Analyses*. Las Vegas, Nevada: Bechtel SAIC Company. ACC: ENG.20071018.0001.

D2.1.2 [Reserved]

D2.1.3 IT-PRO-0011, Revision 7, ICN 0. *Software Management*. Las Vegas, Nevada: Bechtel SAIC Company. ACC: DOC.20070905.0007.

D2.2 DESIGN INPUTS

D2.2.1 EPRI (Electric Power Research Institute) 1994. *Methodology for Developing Seismic Fragilities*. EPRI TR-103959. Palo Alto, California: Electric Power Research Institute. TIC:253770. [DIRS 161329]

D2.2.2 BSC (Bechtel SAIC Company) 2007. *CRCF Tier-1 In-Structure Response Spectra*. 060-SYC-CR00-00900-000-00B. Las Vegas, Nevada: Bechtel SAIC Company. ACC: ENG.20071210.0008. [DIRS 184330]

D2.2.3 BSC (Bechtel SAIC Company) 2008. *Canister Receipt and Closure Facility 1 General Arrangement Ground Floor Plan*. 060-P10-CR00-00102-000 REV 00C. Las Vegas, Nevada: Bechtel SAIC Company. ACC: ENG.20080122.0013. [DIRS 184853]

D2.2.4 SAC Joint Venture 2000. *State of the Art Report on Base Metals and Fracture.* FEMA-355A. Washington, D.C.: Federal Emergency Management Agency. ACC: MOL.20080215.0050. [DIRS 185079]

D2.2.5 BSC (Bechtel SAIC Company) 2007. *Project Design Criteria Document*. 000-3DR-MGR0-00100-000-007. Las Vegas, Nevada: Bechtel SAIC Company. ACC: ENG.20071016.0005; ENG.20071108.0001; ENG.20071220.0003; ENG.20080107.0001; ENG.20080107.0002; ENG.20080107.0016; ENG.20080107.0017; ENG.20080131.0006. [DIRS 179641]

D2.2.6 ASME NOG-1-2004. 2005 *Rules for Construction of Overhead and Gantry Cranes (Top Running Bridge, Multiple Girder)*. New York, New York: American Society of Mechanical Engineers. TIC: 257672. [DIRS 176239]

D2.2.7 MO0801HCUHSSFA.001. *Mean Hazard Curves and Mean Uniform Hazard Spectra*

for the Surface Facilities Area. Submittal date: 01/11/2008. [DIRS 184802]

D2.2.8 BSC (Bechtel SAIC Company) 2006. *CRCF, IHF, RF, and WHF Canister Transfer Machine Mechanical Equipment Envelope*. 000-MJ0-HTC0-00201-000 REV 00A. Las Vegas, Nevada: Bechtel SAIC Company. ACC: ENG.20061120.0011; ENG.20070307.0006; ENG.20070601.0025; ENG.20070823.0002; ENG.20080103.0009. [DIRS 178630]

D2.2.9 [Reserved].

D2.2.10 AISC (American Institute of Steel Construction) 1991. *Manual of Steel Construction, Allowable Stress Design.* 9th Edition, 1st Revision. Chicago, Illinois: American Institute of Steel Construction. TIC: 4254. [DIRS 127579]

D2.2.11 ANSI/AISC N690-1994. 1994. *American National Standard Specification for the Design, Fabrication, and Erection of Steel Safety-Related Structures for Nuclear Facilities*. Chicago, Illinois: American Institute of Steel Construction. TIC: 252734. [DIRS 158835]

D2.2.12 Timoshenko S, D.H. Young, and W. Weaver, Jr. *Vibration Problems in Engineering*, 4th Edition. New York, New York: John Wiley & Sons. [DIRS 184110]

D2.2.13 Moore, D. 2007. "*SSI Factor of Safety.*" E-mail from D. Moore to B. Murray, October 25, 2007. ACC: LLR.20080110.0145. [DIRS 184842]

D2.2.14 BSC (Bechtel SAIC Company) 2007. *Preliminary Throughput Study for the Canister Receipt and Closure Facility*. 060-30R-CR00-00100-000 REV 001. Las Vegas, Nevada: Bechtel SAIC Company. ACC ENG.20071101.0001.

D2.3 DESIGN CONSTRAINTS

None

D2.4 DESIGN OUTPUTS

The calculated seismic fragility of structural failure of the CTM, expressed in terms of a median seismic capacity and an associated combined variability, will be convolved with the site-specific seismic hazard curve to calculate risk of seismic-induced failure of the CTM. This is performed to support information in the License Application (LA).

D3. ASSUMPTIONS

D3.1 ASSUMPTIONS REQUIRING VERIFICATION

There are no assumptions requiring verification used in this attachment.

D3.2 ASSUMPTIONS NOT REQUIRING VERIFICATION

D3.2.1 Canister Drop

The fragility reported in this calculation is only for failure modes that would result in a drop of the lifted canister. Potential results of a canister drop are not addressed here.

Rationale - A separate analysis by others is performed to assess potential of breach of a canister

in the event of a lifted load drop.

D3.2.2 CTM Designed to Code Stress Limits

Structural components of the bridge girders and the trolleys are designed up to the stress limits of the NOG-1 code (Reference D2.2.6) for different load combinations specified in NOG-1.

Rationale - At the time this calculation was prepared, the design calculations of the CTM were not available. Thus, it is not possible to determine the margin between the code limits and the calculated stresses that the designers will use. This is extra margin over the margins in the material strengths, code acceptance criteria and load combinations. Due to lack of a design calculation, it is conservatively assumed that this extra margin is unity.

D4. METHODOLOGY

D4.1 QUALITY ASSURANCE

This calculation is prepared in accordance with EG-PRO-3DP-G04B-00037, Calculations and Analyses (Reference D2.1.1).

D4.2 USE OF SOFTWARE

Mathcad version 14 is used in this calculation. The use of this software is classified as Level 2 software per procedure, IT-PRO-0011 (Reference D2.1.3) and therefore the software need not be qualified.

D4.3 APPROACH

The Separation-of-Variable method documented in EPRI TR-103959 (Reference D2.2.1, Section 3) is followed in calculating seismic fragility of this ITS equipment component.

D5. LIST OF APPENDICES

Appendix D-A. Estimate of Vertical Frequency of the Bridge Crane

Appendix D-B. DBGM-2 ISRS at CTM Level (Reference D2.2.2)

D6. FRAGILITY CALCULATION

D6.1 INTRODUCTION

The seismic fragility calculation of the CRCF Canister Transfer Machine (CTM) is performed here. The calculation evaluates seismic fragilities of structural failure modes of the CTM that may result in a drop of the lifted canister and/or structural failure of the CTM itself. A separate calculation is prepared for the hoist system of the CTM (Attachment B). The scope of this fragility review includes all elements of the CRCF Cask Handling Crane that rest on top of the crane rails. The fragility of the crane rails, the rail supports, the rail anchorage and the structure are addressed by others.

D6.2 CANISTER TRANSFER MACHINE

The CRCF Canister Transfer Machine (CTM) which is an ITS (Important to Safety) item consists of (1) a double-box girder bridge crane running along the plant north-south direction at column lines 6 and 9, (2) a shield bell trolley that runs along the girders of the bridge crane, (3) a radiation shield bell supported by the shield bell trolley, (4) a canister hoist trolley that runs along the girders, (5) a canister hoist assembly supported by the canister hoist trolley (Reference D2.2.8). The rail to rail distance of the CRCF CTM is 86'-4 per Reference D2.2-8. The estimated weight of the heaviest canister is 61 tons (Note 3 of Reference D2.2-8). A schematic of the CTM is shown in Figure D6.2-1 (Reference D2.2.8). The CTM will be designed per 2004 ASME NOG-1 requirements for Type 1 cranes (Section 4.8.1 of Reference D2.2.5).

The general operation of the CTM consists of:

- Position the shield bell and the canister hoist over the cask transfer trolley in the transfer cell
- Attach the grapple to the canister through a lifting device
- Lift the canister out of the transportation cask into the shield bell
- Transfer the canister over to the Waste Package (WP) cell
- Lower the canister into the WP in the WP cell

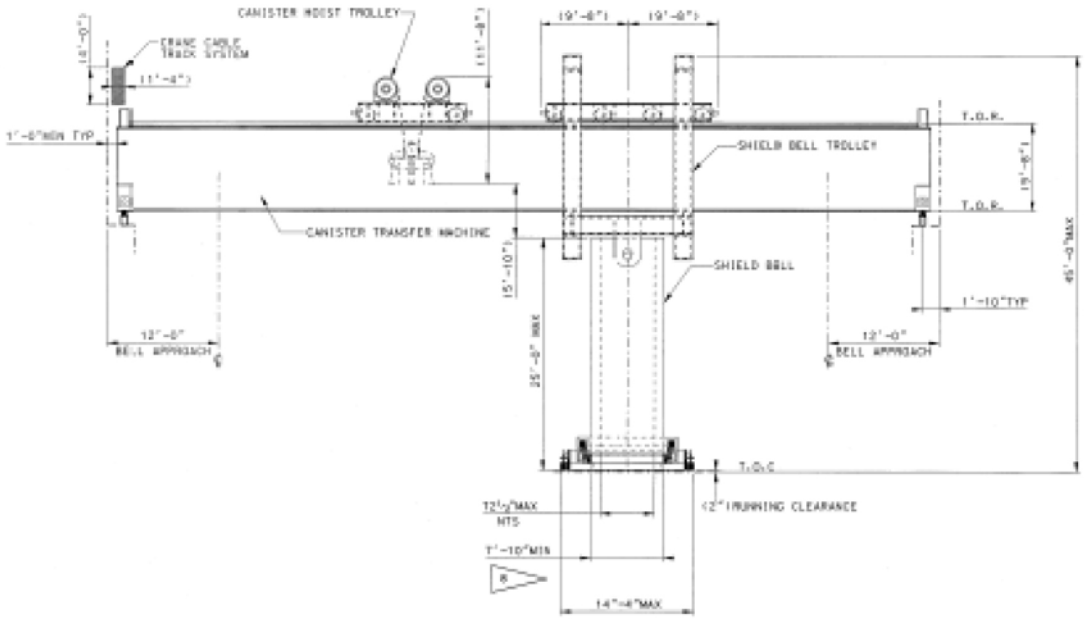

Figure D6.2-1. Sketch of CTM Showing Canister Hoist Trolley (Left), Shield Bell Support Trolley (Middle), Shield Bell, and the Bridge Girder (Reference D2.2.8)
NOTE: Legibility of the figure does not affect the technical content of the document. See source for detail

D6.3 STRUCTURAL FAILURE MODES OF CTM

Seismic failure modes that will potentially result in a drop of or damage to a lifted canister are identified below.

- Failure of the bridge crane
- Failure of the trolleys
- Failure of seismic restraints of the trolleys
- Sliding of the bridge or trolleys while lifting a canister

The fourth potential failure mode, sliding of the bridge or trolleys while lifting a canister, could cause breach of the canister due to impact with the cask transfer trolley, waste package transfer trolley, floor slab, or port slide gate. However, the canister would be in a partially raised or lowered position only 20 minutes (per canister processed as per Reference D2.2.14), which results in a very short exposure time for this potential scenario. Rather than evaluating the potential for seismic-induced sliding and subsequent canister impact, this scenario will be directly included in the seismic event sequence quantification.

D6.4 SEISMIC INPUT MOTION

The DBGM-2 ground motion is defined by the horizontal and vertical site-wide mean uniform hazard spectra (Reference D2.2.7; also Section 6.2.2.1 for source information) at the surface level. The site-wide UHS are the enveloping cases of the surface UHS of 30', 70', 100' and 200' of alluvium over tuff. The alluvium depths under the three CRCF structures vary from 100' to 200'. The Tier 1 analyses (Reference D2.2.2) considered these two depths of alluvium in addition to the three soil properties (upper, lower, and median cases). The design ISRS are envelopes of these different cases.

The CTM is supported by the CRCF building structure at elevation 60' (elevation at the top of rails per Reference D2.2.3, Section E). The seismic input motion to the CTM is defined by the in-structure response spectra (ISRS) at that elevation. For this calculation, both the design and the raw (i.e., unbroadened and unsmoothed) floor response spectra from the BSC Tier 1 analyses (Reference D2.2.2) are utilized.

D6.5 SEISMIC FRAGILITY OF BRIDGE CRANE

Each of the bridge girders is a welded steel box section with heavy top and bottom horizontal cover plates and stiffened vertical web plates. Full depth diaphragms are typically designed to keep the box section square and to provide resistance to torsional forces. Longitudinal stiffeners are added to the web plates in the compression area to prevent web buckling between the diaphragms.

D6.5.1 Strength Factor

Per Section 4.8.1 of Mechanical Handling Design Criteria (Reference D2.2.5), the applicable code for the CTM design is ASME NOG-1 2004. The median strength factor of the CTM girder structural failure is estimated based on the NOG-1 design criteria. It is assumed (see Assumption D3.2.2) that the CTM will be designed such that the calculated stresses for different load combinations will be at the code allowable.

The basic NOG-1 load combination for crane operational loads (Section 4140 of NOG-1) that is applicable to the CTM is:

LC1 = Dead weight of bridge and trolleys + rated load

The NOG-1 load combinations for earthquake loads (SSE) are (Section 4140 of NOG-1):

LC10 = Dead weight of bridge and trolleys + SSE loads
LC11 = Dead weight of bridge and trolleys + SSE loads + credible critical load with SSE

Per Section 4300 of NOG-1, the basic allowable stress of the operating loading conditions for structural members is 50% of yield strength for tension and compression. For extreme environmental load combination which includes SSE, the allowable stress is 90% of the yield strength (Table 4311-1 of NOG-1). The DBGM-2 is used in the NOG-1 load combinations for SSE.

$$\sigma_{NOL} = 0.5 \cdot F_{y\_min} \qquad \text{Equation D-1}$$

$$\sigma_{NOL} + \sigma_{DBGM} = 0.9 \cdot F_{y\_min} \qquad \text{Equation D-2}$$

where σ_{NOL} and σ_{DBGM} are stresses due to normal operating loads and DBGM-2, respectively and F_{y_min} is the minimum yield strength of steel of the girders.

Following the NOG-1 requirement, the CTM design will consider trolleys at different locations of the bridge, i.e., end, quarter, and middle of the crane span. Based on the locations of the transfer cell and the waste package cell relative to the walls that support the CTM (i.e., walls along column lines 6 and 9, Reference D2.2.3), seismic fragility is calculated for the case when the trolleys are at the quarter point of the span. This is the location where canister lifting/lowering will take place. The risk of seismic failure when the trolleys are at the mid-span will be lower because the duration in which the trolleys will be at the mid-span is short compared to the time to lift or insert the canister.

The CTM bridge girders and the trolley frames are more sensitive to the vertical direction input motion since the horizontal inertia load from the lifted load is limited due to pendulum action. The vertical fundamental frequencies of the CTM with rated loads at the mid-span and quarter point are estimated as shown in Appendix D-A. The vertical frequencies when both the trolleys and their rated loads are at the midspan and quarter point of the span are estimated to be 2.7 Hz and 4.1 Hz, respectively (Appendix D-A). The corresponding 7% damped vertical DBGM-2 spectral accelerations are 0.56g and 0.71g, respectively (Figure D-B-3). Also demonstrated in Appendix D-A is that although the vertical acceleration is higher when the trolleys are at the quarter point of the span, design of the girders is governed by the case of having trolleys and their rated loads at the midspan.

It is assumed that the bridge girders will be constructed of ASTM 572 Grade 50 steel with a minimum specified yield strength of 50 ksi.

$F_{y\_min} := 50 \cdot ksi$

$F_y := 1.2 \cdot F_{y\_min}$ Median yield strength; the factor to get from minimum specified yield strength to the median value is based on Section 4.6 of Reference D2.2.4.

$S_{av\_7\%} := 0.71 \cdot g$ 7% damped DBGM-2 vertical spectral acceleration (Figure D-B-3). Per Section 4153.8 of NOG-1, a damping value of 7% of critical is used for DBGM-2.

$\sigma_{NOL} := 0.5 \cdot F_{y\_min}$ Normal operating load stress at the midspan (see Assumption D3.2.2).

$$\sigma_{DBGM} := \frac{S_{av\_7\%}}{g} \cdot \sigma_{NOL}$$

Given (1) the stress at the midspan (σ_{NOL}) due to uniform weight of the crane girders and combined weight of the two trolleys and their rated loads at the midspan and (2) vertical acceleration of 0.71g when the trolleys and their loads are at the quarter point, the median strength factor (F_S) at which a plastic hinge will form at the quarter point can be calculated using the equation shown below:

$$(0.82 * \sigma_{NOL}) + (0.82 * \sigma_{NOL} * S_{av\text{-}7\%}) * F_S = (1.1) * F_y$$

where the 0.82 factor is to account for the fact that design of the girders is governed by the case when both trolleys are at the midspan (see Appendix D-A) and the 1.1 factor is the estimated ratio of plastic section modulus to elastic section modulus of a box girder.

$$F_S := \frac{(1.1)\cdot F_y - (\sigma_{NOL})\cdot 0.82}{0.82\cdot \sigma_{DBGM}}$$

$F_S = 3.13$ This is the strength factor when a plastic hinge is formed at the quarter point of the bridge girder.

There is no randomness, only uncertainty associated with the strength factor.

$$\beta_{R\_S} := 0$$

The uncertainty variability associated with the median yield strength is estimated to be 0.12 based on Table 3-9 of Reference D2.2.1.

$$\beta_{U\_S} := 0.12$$

$$\beta_{c\_S} := \sqrt{\beta_{R\_S}^2 + \beta_{U\_S}^2} \qquad \beta_{c\_S} = 0.12$$

D6.5.2 Inelastic Energy Absorption Factor

Because the strength factor is calculated based on forming of a plastic hinge of the steel girder (i.e., forming of a mechanism) and the ratcheting effect of the heavy load the crane carries, no further credit is taken for the inelastic energy absorption capability.

$$F_\mu := 1.0$$

$$\beta_{c\_\mu} := 0$$

D6.5.3 Equipment Response Factors

D6.5.3.1 Qualification Method

This factor accounts for conservatism in the Tier 1 design ISRS (Reference D2.2.2) relative to the unbroadened and unsmoothed ISRS of the 100-foot best-estimate soil property case. The best-estimate fundamental frequency of the bridge crane in the vertical direction, when the trolleys and the rated loads are at the quarter point of the span, is 4.1 Hz

At 4.1 Hz

$SA_{design} := 0.71\cdot g$ 7% damped acceleration from the Tier 1 design vertical ISRS

$SA_{raw} := 0.6g$ 7% damped acceleration from the raw DBGM-2 vertical ISRS at the elevation where the CTM rails are (Reference D2.2.2)

$$F_{QM} := \frac{SA_{design}}{SA_{raw}}$$

$$F_{QM} = 1.18$$

Since the raw ISRS is used and uncertainties in response due to uncertainty in equipment frequency (i.e., modeling), modal combination, and earthquake component combination are separately calculated below,

$$\beta_{c\_QM} := 0$$

D6.5.3.2 Equipment Damping

The median and minus one sigma damping values at failure of a welded structure are 7% and 5% , respectively (Table 3-4 of Reference D2.2.1). Since 7% damping will be used for design per NOG-1, the damping factor of safety is unity.

$$F_{\delta\_E} := 1$$

$SA_{raw\_5\%} := 0.71 \cdot g$ Raw spectral acceleration at lower bound damping value at the crane frequency

$$\beta_{c\_\delta\_E} := \ln\left(\frac{SA_{raw\_5\%}}{SA_{raw}}\right)$$

$$\beta_{c\_\delta\_E} = 0.17$$

D6.5.3.3 Equipment Modeling Factor

Since the vertical response of the CTM is a relatively simple system, the frequency calculation is judged to be best-estimate and the modeling factor of safety is unity.

$$F_{M\_E} := 1.0$$

$\beta_{R\_M\_E} := 0$ No randomness associated with modeling

Reference D2.2.1 provides a range of 0.1 to 0.3 for uncertainty in modal frequencies. Given the relatively simple model of the CTM, a variability of 0.15, which is greater than the 0.1, is judged to be sufficient.

$$\beta_f := 0.15$$

$f_{v\_m} := 4.1 \cdot Hz$ Best estimate vertical frequency when the trolleys with their rated loads are at the quarter span of the bridge.

$f_u := f_{v\_m} \cdot e^{\beta_f}$ Upper bound frequency

$$f_u = 4.76 \cdot Hz$$

$SA_{V\_u} := 0.62 \cdot g$ 7% damped vertical spectral acceleration at the upper bound frequency.

$$\beta_{U\_f} := \ln\left(\frac{SA_{V\_u}}{SA_{raw}}\right)$$

$$\beta_{U\_f} = 0.03$$

$\beta_{U\_ms} := 0.10$ The uncertainty in response due to uncertainty of mode shape is in the range of 0.05 to 0.15 depending on the complexity of the equipment (Reference D2.2.1). A value of 0.10 is used based on the simple model.

$$\beta_{U\_M\_E} := \sqrt{\beta_{U\_f}^2 + \beta_{U\_ms}^2}$$

$$\beta_{U\_M\_E} = 0.11$$

$$\beta_{c\_M\_E} := \sqrt{\beta_{R\_M\_E}^2 + \beta_{U\_M\_E}^2}$$

$$\beta_{c\_M\_E} = 0.11$$

D6.5.3.4 Modal Combination

The dynamic response spectrum method is one of the methods described in Section 4153 of NOG-1 for performing seismic analysis for Type 1 cranes. When the response spectrum method is used, closely spaced modes are combined per grouping method, ten-percent method or double-sum method as per Section 4153.10 of NOG-1. For the failure mode of the bridge girder evaluated here, the response will be predominantly that of the vertical mode. Thus, the modal combination factor of safety is judged to be unity, no conservative or unconservative bias.

$F_{MC\_E} := 1.0$

$\beta_{R\_MC\_E} := 0.05$ For the failure mode evaluated, the fundamental vertical mode is dominant. Thus use the lower bound value of 0.05 in Reference D2.2.1.

$\beta_{U\_MC\_E} := 0$

$$\beta_{c\_MC\_E} := \sqrt{\beta_{R\_MC\_E}^2 + \beta_{U\_MC\_E}^2}$$

$$\beta_{c\_MC\_E} = 0.05$$

D6.5.3.5 Earthquake Component Combination

Section 4153.10(c) of NOG-1 requires using the SRSS (Square Root of Sum of the Squares) to combine contributions for the three components of earthquake motion. This method is considered to be median-centered. Thus,

$F_{ECC\_E} := 1.0$

$\beta_{R\_ECC\_E} := 0.10$ A generic value of 0.18 is suggested in Reference D2.2.1 when responses from each of the three components are not available. A value of 0.10 is used here since the vertical component contributes most significantly to the response of the failure mode evaluated.

$$\beta_{U\_ECC\_E} := 0$$

$$\beta_{c\_ECC\_E} := \sqrt{\beta_{R\_ECC\_E}^2 + \beta_{U\_ECC\_E}^2}$$

$$\beta_{c\_ECC\_E} = 0.1$$

Equipment Response Factors

$$F_{RE} := F_{QM} \cdot F_{\delta\_E} \cdot F_{M\_E} \cdot F_{MC\_E} \cdot F_{ECC\_E}$$

$$F_{RE} = 1.18$$

$$\beta_{c\_RE} := \sqrt{\beta_{c\_QM}^2 + \beta_{c\_\delta\_E}^2 + \beta_{c\_M\_E}^2 + \beta_{c\_MC\_E}^2 + \beta_{c\_ECC\_E}^2}$$

$$\beta_{c\_RE} = 0.23$$

D6.5.4 Structural Response Factors

D6.5.4.1 Spectral Shape Factor

This factor accounts for conservatism in the site-wide DBGM-2 design spectrum. At the Surface Facilities Area (SFA) the depth of alluvium overlying tuff varies from 30 feet to 200 feet. Uniform hazard spectra at the surface are calculated from site response analyses for alluvium depths of 30', 70', 100' and 200'. The site-wide design ground response spectrum is the envelope of the surface spectra of these four alluvium depths (Reference D2.2.7; also Section 6.2.2.1 for source information).

The dominant frequency of the CRCF soil-structure system in the vertical direction is 6.18 Hz from the Tier 1 ISRS calculation (Reference D2.2.2). Since the vertical UHS for the 100-ft alluvium depth case is not available, the horizontal site-wide and the surface spectrum of the 100-ft alluvium depth case are used to calculate the spectral shape factor. The dominant mode of the CRCF in the horizontal direction has a frequency of 5.2 Hz (Reference D2.2.2). At this frequency

$SA_{site} := 1.14g$ 5% damped site-wide spectral acceleration (see Figure D6.5-1).

$SA_{100} := 1.06 \cdot g$ 5% damped spectral acceleration of the 100-foot best-estimate alluvium depth case in the northeast area where the preclosure surface facilities are located.

$$F_{SA} := \frac{SA_{site}}{SA_{100}}$$

$$F_{SA} = 1.08$$

Since uncertainty in the UHS is derived from uncertainty in the seismic hazard curves which will be included in the final risk quantification, no uncertainty is included under the spectral shape factor to avoid double-counting the hazard uncertainty, hence

$$\beta_{U\_SA} := 0$$

$\beta_{R\_SA} := 0.2$ This is random variability to account for peak to valley variability of a smooth ground response spectrum (Reference D2.2.1, Table 3-2)

$$\beta_{c\_SA} := \sqrt{\beta_{U\_SA}^{2} + \beta_{R\_SA}^{2}}$$

$\beta_{c\_SA} = 0.2$

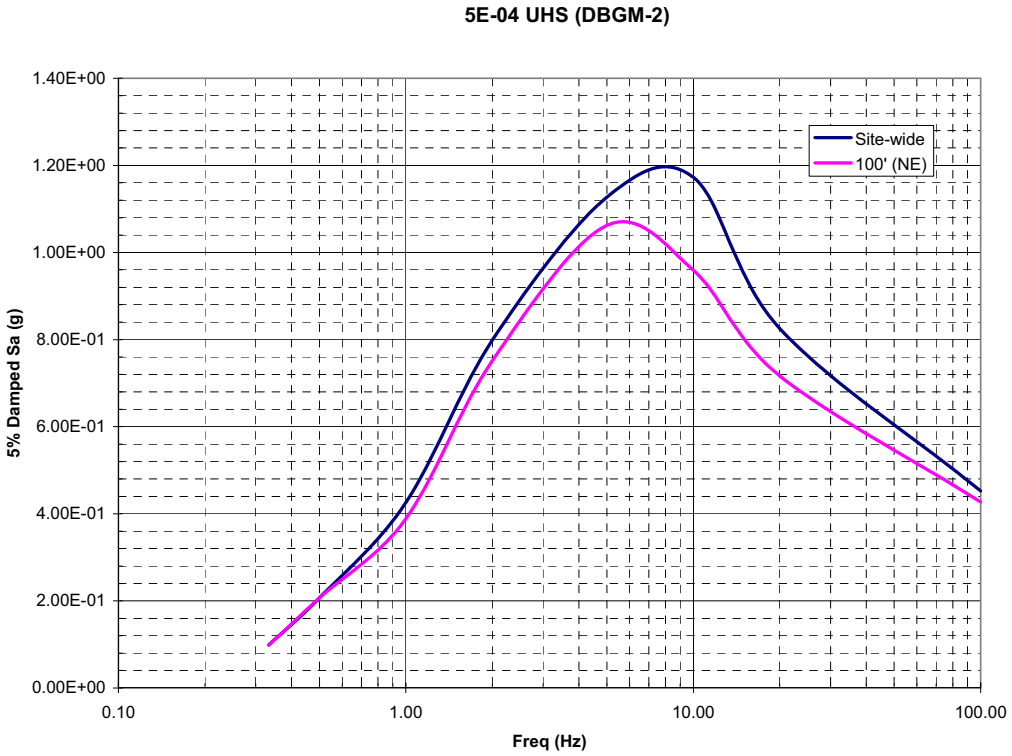

Figure D6.5-1. DBGM-2 (Site-Wide) vs. Surface Spectrum of 100-Ft Alluvium Depth Case (See Section 6.2.2.1 for source information)

D6.5.4.2 Damping Factor

This factor is to account for conservatism in the hysteresis damping of the building structure used in the seismic response analysis. Due to the high radiation damping of the foundation media, the effect of structure damping is insignificant. Thus,

$F_{\delta} := 1.0$

$\beta_{U\_\delta} := 0$ Since a conservative median factor of safety is used for structure damping, no value is assigned to the uncertainty logarithmic standard deviation.

$\beta_{R\_\delta} := 0$

$\beta_{c\_\delta} := \sqrt{\beta_{U\_\delta}^2 + \beta_{R\_\delta}^2}$ $\beta_{c\_\delta} = 0$

D6.5.4.3 Modeling Factor

The Tier 1 lumped mass multiple stick model of CRCF models the stiffness of various reinforced concrete walls and distribution of mass at each floor. The floors are assumed to be rigid diaphragms tying the different sticks together. Torsional response of the structure is captured through modeling eccentricity between the center of mass and center of rigidity of each floor. The foundation media underneath the buildings are modeled with soil springs and dashpots based on elastic half space theory with adjustment to account for the layering effect of alluvium overlying tuff. The model is judged to adequately represent the CRCF structure dynamic characteristics, thus

$F_M := 1.0$

$\beta_{R\_M} := 0$

Uncertainty of structure frequencies predicted from mathematical modeling varies from 0.15 to 0.35 depending on the sophistication of the model (Reference D2.2.1). The value of 0.35 is for fairly approximate model and the value 0.15 is appropriate for detailed models. Based on the complexity of the CRCF structure and the mathematical model used for the Tier 1 ISRS analysis, it is judged that the calculated CRCF frequency has a logarithmic standard deviation of 0.25.

$\beta_f := 0.25$ Uncertainty in building frequency.

$f_m := 5.2 \cdot Hz$ Best-estimate frequency

$f_{upper} := f_m \cdot e^{\beta_f}$ Upper bound frequency

$f_{upper} = 6.68 \cdot Hz$

$SA_{upper} := 1.05g$ 5% damped spectral acceleration at f_{upper} read off from the mean 5E-4 UHS of the 100-foot alluvium depth case (Figure D6.5-1). This value is less than the value at the best-estimate frequency.

$f_{lower} := f_m \cdot e^{-\beta_f}$ Lower bound frequency

$f_{lower} = 4.05 \cdot Hz$

$SA_{lower} := 1.02 \cdot g$ 5% damped spectral acceleration at f_{lower} read off from the mean 5E-4 UHS of the 100-foot alluvium depth case. This value is less than the value at the best-estimate frequency.

$\beta_{U\_f} := 0$ Since the spectral value at the best-estimate frequency is greater than that at either the lower bound or upper bound frequency.

$\beta_{U\_ms} := 0.10$ Uncertainty of mode shape (Reference D2.2.1, page 3-18); a lower value of 0.10 is used here based on the simple configuration of the bridge girders.

$\beta_{U\_M} := \sqrt{\beta_{U\_f}^2 + \beta_{U\_ms}^2}$

$\beta_{U\_M} = 0.1$

$\beta_{c\_M} := \sqrt{\beta_{R\_M}^2 + \beta_{U\_M}^2}$ $\beta_{c\_M} = 0.1$

D6.5.4.4 Modal Combination

Since the direct integration time history method was used in the Tier 1 ISRS analysis (Reference D2.2.2), the modal combination method factor of safety is unity and there is no variability associated with modal combination.

$F_{MC} := 1$

$\beta_{R\_MC} := 0$

$\beta_{U\_MC} := 0$

$\beta_{c\_MC} := \sqrt{\beta_{R\_MC}^2 + \beta_{U\_MC}^2}$ $\beta_{c\_MC} = 0$

D6.5.4.5 Soil-Structure Interaction

Two factors are considered, the first one is on the method of treating the SSI effects and the second one is on the effect of soil softening at ground acceleration higher than DBGM-2. The Tier 1 seismic response analyses of the CRCF use the site-wide $5*10^{-4}$ mean uniform hazard spectra as the DBGM-2 input motion. Spectrum compatible time histories are used as the input motion for the time history analyses. The conservatism in the site-wide spectra was accounted for in the spectral shape factor above. Strain compatible soil properties of 100-foot and 200-foot deep alluvium are used to calculate frequency-independent soil springs and soil damping coefficients. Soil radiation damping is introduced into the model by using dashpots. Damping coefficients equal to 75% of the computed values for translational degrees of freedom and to the full computed rotational damping values are used in the response analyses (Reference D2.2.2). This treatment of soil radiation damping has unknown bias. Conservatism or unconservatism in SSI will be minimized for final SSI analyses used to develop equipment design seismic input. Before the final SSI analyses are completed, the Tier 1 SSI analysis is taken to represent the best-estimate responses per BSC recommendations in Reference D2.2.13.

$F_{SSI\_1} := 1$

$\beta_{R\_SSI\_1} := 0$

$\beta_{U\_SSI\_1} := 0.25$ Uncertainty of the median-centered state-of-the-art SSI method based on past probabilistic seismic response analyses using the same method.

It is judged that the median seismic capacity of the structural failure mode of the CTM, expressed in terms of peak ground acceleration, is close to that of BDBGM. Due to soil nonlinearity, amplification of the input ground motion at BDBGM will be different from that of DBGM-2. The second factor of safety is to account for this difference and is estimated using the DBGM-2 raw spectra and the BDBGM raw spectra at the vertical frequency of the CTM which is 4.1 Hz.

At 4.1 Hz

$S_{v\_DBGM\_7\%} := 0.5885 \cdot g$ The 7% & 10% damped vertical spectral accelerations and the floor zero period accelerations of DBGM-2 and

$ZPA_{DBGM} := 0.306 \cdot g$

$S_{v\_BDBGM\_10\%} := 1.1 \cdot g$

$ZPA_{BDBGM} := 0.743 \cdot g$

BDBGM are read from the digitized raw floor response spectra of Reference D2.2.2. Based on that 7% of critical damping is used for design of the CTM, the best-estimate damping value at BDBGM is estimated at 10% of critical damping.

$$F_{SSI\_2} := \frac{\frac{S_{v\_DBGM\_7\%}}{ZPA_{DBGM}}}{\frac{S_{v\_BDBGM\_10\%}}{ZPA_{BDBGM}}}$$

$F_{SSI\_2} = 1.3$

$\beta_{U\_SSI\_2} := \frac{1}{1.65} \ln\left(F_{SSI\_2}\right)$

$F_{SSI} := F_{SSI\_1} \cdot F_{SSI\_2}$

$F_{SSI} = 1.3$

$\beta_{U\_SSI} := \sqrt{\beta_{U\_SSI\_1}^{2} + \beta_{U\_SSI\_2}^{2}}$

$\beta_{c\_SSI} := \sqrt{\beta_{R\_SSI\_1}^{2} + \beta_{U\_SSI}^{2}}$

$\beta_{c\_SSI} = 0.3$

D6.5.4.6 Ground Motion Incoherence

$L1 := 327 \cdot ft$ East-west dimension of CRCF excluding the 49'-6" and 43' extensions at the east and west ends, respectively (Reference D2.2.3).

$L2 := 336 \cdot ft$ North-south dimension of CRCF excluding the 56' extension at the south end.

$L_{eq} := \sqrt{L1 \cdot L2}$ Equivalent foundation dimension of CRCF

$L_{eq} = 331.47\,ft$

The ground motion incoherence reduction factor is a function of foundation size and frequency of response. For a 150 foot plan dimension foundation, the following reduction factors are presented in Reference D2.2.1 in page 3-22. Interpolation or extrapolation may be used to calculate the reduction factor for different dimensions and/or frequencies.

$L_{std} := 150 \cdot ft$ Foundation dimension of which the reduction factors in Reference D2.2.1 are calculated.

$f_5 := 5$ Frequency in cycle/sec (Hz)

$RF_5 := 1$ Reduction factor for response frequency at 5 Hz

$f_{10} := 10$ Frequency in Hz

$RF_{10} := 0.9$ Reduction factor for response frequency at 10 Hz

$RF_{5\_eq} := RF_5$ Reduction factor at 5 Hz, given the CRCF equivalent foundation dimension

$$RF_{10\_eq} := 1 - \left[\left(1 - RF_{10}\right)\cdot\frac{L_{eq}}{L_{std}}\right]$$ Linear extrapolation

$RF_{10\_eq} = 0.78$ Reduction factor at L_{eq} dimension and 10 Hz frequency of response.

The vertical frequency of the CRCF with 100-ft of median soil with soil properties compatible with DBGM-2 level, is 6.2 Hz. However, the seismic acceleration level at which crane failure is expected is significantly higher than DBGM-2 and even greater than BDBGM. Thus, the vertical frequency of the CRCF with 100-ft of median soil with properties compatible with BDBGM level is considered. This frequency is 5.3 Hz (page 45 of Reference D2.2.2).

$f_6 := 5.3$ Frequency in Hz

Calculate the reduction factor at 5.3 Hz by interpolation

$RF_{6\_eq} := 0.4$ An arbitrary value to initiate the equation solver below.

Given

$$\frac{\log\left(RF_{10\_eq}\right) - \log\left(RF_{5\_eq}\right)}{\log\left(RF_{6\_eq}\right) - \log\left(RF_{5\_eq}\right)} = \frac{\log\left(f_{10}\right) - \log\left(f_5\right)}{\log\left(f_6\right) - \log\left(f_5\right)}$$

$a := \text{Find}\left(RF_{6\_eq}\right)$

$a = 0.98$

Thus, the ground motion incoherence factor of safety is

$$F_{GMI} := \frac{1}{a}$$

$F_{GMI} = 1.02$

$$\beta_{U\_GMI} := \frac{1}{2}\cdot\ln\left(\frac{1}{a}\right)$$

$\beta_{U\_GMI} = 0.01$

A reduction factor of 1.0 (i.e., no reduction) is estimated to be two standard deviation from the calculated median factor of 0.91 (Reference D2.2.1, Page 3-23).

$\beta_{R\_GMI} := 0$

$$\beta_{c\_GMI} := \sqrt{\beta_{R\_GMI}^{2} + \beta_{U\_GMI}^{2}}$$

$\beta_{c\_GMI} = 0.01$

Structural Response Factors

$F_{RS} := F_{SA}\cdot F_{\delta}\cdot F_{M}\cdot F_{MC}\cdot F_{SSI}\cdot F_{GMI}$

$F_{RS} = 1.43$

$\beta_{c\_RS} := \sqrt{\beta_{c\_SA}^2 + \beta_{c\_\delta}^2 + \beta_{c\_M}^2 + \beta_{c\_MC}^2 + \beta_{c\_SSI}^2 + \beta_{c\_GMI}^2}$

$\beta_{c\_RS} = 0.37$

D6.5.5 Overall Factor of Safety

$F_{total} := F_S \cdot F_\mu \cdot F_{RS} \cdot F_{RE}$

$F_{total} = 5.28$

$PGA := 0.453g$ Peak ground acceleration of the DBGM-2 design spectrum (Reference D2.2.7; also Section 6.2.2.1 for source information).

$A_m := F_{total} \cdot PGA$

$A_m = 2.39 \cdot g$ Median seismic capacity in terms of PGA

$\beta_c := \sqrt{\beta_{c\_S}^2 + \beta_{c\_\mu}^2 + \beta_{c\_RS}^2 + \beta_{c\_RE}^2}$

$\beta_c = 0.45$

$HCLPF := A_m \cdot e^{-2.33 \cdot \beta_c}$

$HCLPF = 0.83 \cdot g$

D6.6 SEISMIC FRAGILITY OF TROLLEYS

Due to high seismicity at the YMP site, it is envisioned that seismic restraints will be provided to the trolleys to prevent the trolleys from uplifting and sliding off the rails in a seismic event. These seismic restraints can be in the form of seismic bumpers to transfer the horizontal seismic inertia load directly to the girders and seismic catchers to transfer the uplift force to the girders. Both the seismic bumpers and catchers can be constructed from structural steel shapes and bolted or welded to the underside of the trolley chassis as schematically depicted in Figure D6.6-1 below.

At this time, detailed design of the trolleys and their seismic restraints has not been performed. Structural failure of the trolley frame will have similar generic seismic capacity as the bridge girders since both will be designed to the NOG-1 criteria. Thus a representative seismic fragility is calculated below for the trolley seismic restraints. Furthermore, because bolted connections in general have lower median capacity than welded connections, when both are designed to the same demand, hence seismic fragility of the bolted connection is calculated here for the seismic restraints.

Conservatively assume A307 bolts are used for the clamp bolts which have the lowest strength among the acceptable fastener materials in NOG-1, Tables 4221-1 and 4221-2.

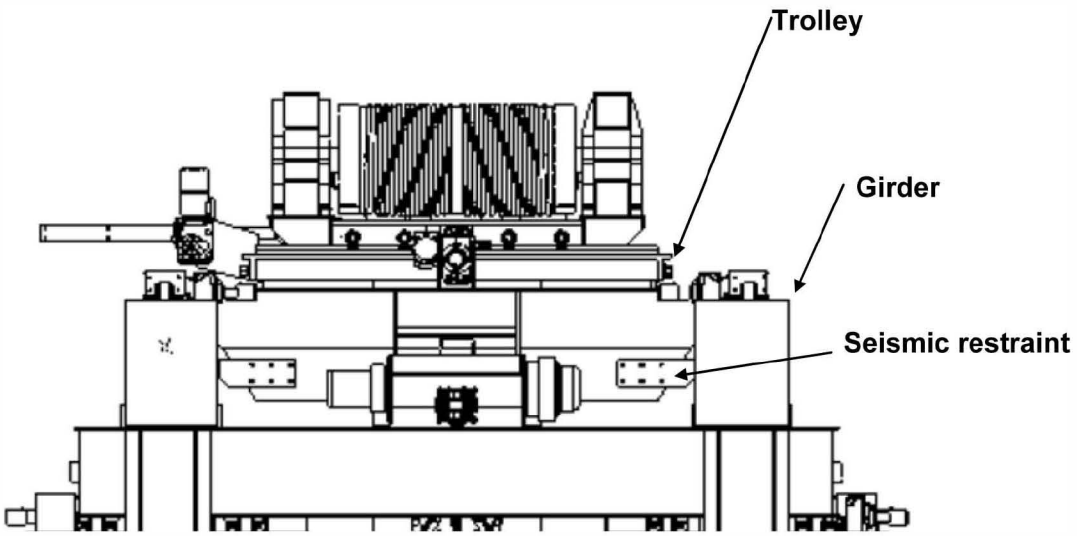

Figure D6.6-1. CTM Hoist Trolley (Schematic)

D6.6.1 Strength Factor

The bolts attaching the seismic restraints to the trolley chassis are subjected to shear.

$f_{u\_min} := 58\text{ksi}$ Minimum ultimate tensile strength of A307 (Table 3-9 of Reference D2.2.1)

$\tau_{design} := 1.4 \cdot (10 \cdot \text{ksi})$ where 10 ksi is the allowable shear stress for bolt steel per AISC and 1.4 is the bump-up factor for DBGM-2 load combination (References D2.2.10 and D2.2.11)

$\tau_{design} = 14 \cdot \text{ksi}$

$f_{u\_m} := 64 \cdot \text{ksi}$ Median ultimate tensile strength of A307 bolt steel (Table 3-9 of Reference D2.2.1)

$\tau_{u\_m} := 0.62 \cdot f_{u\_m}$ Table 3-10 of Reference D2.2.1

$F_{S\_shear} := \frac{\tau_{u\_m}}{\tau_{design}}$

$F_{S\_shear} = 2.83$

$\beta_{R\_S} := 0$

$\beta_{U\_S} := 0.10$ Table 3-10 of Reference D2.2.1

$\beta_{c\_S} := \sqrt{\beta_{R\_S}^2 + \beta_{U\_S}^2}$

$\beta_{c\_S} = 0.1$

D6.6.2 Inelastic Energy Absorption Factor

The bolt failure mode is localized, thus there is no inelastic energy absorption factor.

$F_{\mu} := 1.0$

$\beta_{R\_\mu} := 0$

$\beta_{U\_\mu} := 0$

$\beta_{c\_\mu} := \sqrt{\beta_{R\_\mu}^2 + \beta_{U\_\mu}^2}$

$\beta_{c\_\mu} = 0$

D6.6.3 Equipment Response Factors

D6.6.3.1 Qualification Method

This factor accounts for conservatism in the Tier 1 design ISRS (Reference D2.2.2) relative to the median ISRS. The median ISRS are the Tier 1 unbroadened and unsmoothed floor response spectra from the median soil case. The horizontal fundamental frequencies of the bridge crane in the north-south direction (perpendicular to the bridge girder), when the trolleys and the rated loads are at the quarter point of the bridge, is estimated to be in the range of 2 to 3 Hz.

At 2 Hz

$SA_{design} := 0.93 \cdot g$ 7% damped design spectral acceleration of the north-south ISRS of the 100-foot alluvium case (Figure D-B-1 of Appendix D-B)

$SA_{raw\_2} := 0.81g$ 7% damped spectral acceleration of the median soil case north-south direction raw spectrum of the 100-foot alluvium case

$F_{QM\_2} := \frac{SA_{design}}{SA_{raw\_2}}$

$F_{QM\_2} = 1.15$

At 3 Hz

$SA_{design} := 1.18 \cdot g$ 7% damped design spectral acceleration of the north-south ISRS of the 100-foot alluvium case

$SA_{raw\_3} := 1.1g$ 7% damped spectral acceleration of the median soil case north-south direction raw spectrum of the 100-foot alluvium case

$$F_{QM\_3} := \frac{SA_{design}}{SA_{raw\_3}}$$

$F_{QM\_3} = 1.07$

$$F_{QM} := \frac{1}{2} \cdot \left(F_{QM\_2} + F_{QM\_3}\right)$$

$F_{QM} = 1.11$

Since the raw ISRS is used and uncertainties in response due to uncertainty in equipment frequency (i.e., modeling), modal combination, and earthquake component combination are separately calculated below,

$\beta_{c\_QM} := 0$

D6.6.3.2 Equipment Damping

The median and lower bound damping values at the failure of the bridge crane are 7% and 5%, respectively (Table 3-4 of Reference D2.2.1 for welded steel structures). Since 7% damping is used in the crane design seismic analysis (Section 4153.8 of NOG-1), the factor of safety is unity.

$F_{\delta\_E} := 1$

At 2 Hz

$SA_{raw\_5\%} := 0.96 \cdot g$ See Figure D-B-2 of Appendix D-B.

$$\beta_{c\_\delta\_E\_2} := \ln\left(\frac{SA_{raw\_5\%}}{SA_{raw\_2}}\right)$$

$\beta_{c\_\delta\_E\_2} = 0.17$

At 3 Hz

$SA_{raw\_5\%} := 1.35 \cdot g$

$$\beta_{c\_\delta\_E\_3} := \ln\left(\frac{SA_{raw\_5\%}}{SA_{raw\_3}}\right)$$

$\beta_{c\_\delta\_E\_3} = 0.2$

$$\beta_{c\_\delta\_E} := \frac{1}{2}\left(\beta_{c\_\delta\_E\_2} + \beta_{c\_\delta\_E\_3}\right)$$

$\beta_{c\_\delta\_E} = 0.19$

D6.6.3.3 Equipment Modeling Factor

$F_{M\_E} := 1.0$ Since the effect of frequency uncertainty is included in the qualification method factor.

$\beta_{R\_M\_E} := 0$ No randomness associated with modeling

$\beta_{U\_ms} := 0.10$ The uncertainty in response due to uncertainty of mode shape is in the range of 0.05 to 0.15 depending on the complexity of the equipment. A value of 0.10 is used.

$$\beta_{U\_M\_E} := \sqrt{\beta_{U\_f}^2 + \beta_{U\_ms}^2}$$

$\beta_{U\_M\_E} = 0.1$

$$\beta_{c\_M\_E} := \sqrt{\beta_{R\_M\_E}^2 + \beta_{U\_M\_E}^2}$$

$\beta_{c\_M\_E} = 0.1$

D6.6.3.4 Modal Combination

The dynamic response spectrum method is one of the methods described in Section 4153 of NOG-1 for performing seismic analysis for Type 1 cranes. When the response spectrum method is used, closely spaced modes are to be combined per grouping method, ten-percent method or double-sum method as per Section 4153.10. Thus, the modal combination factor of safety is judged to be unity, no conservative or unconservative bias.

$F_{MC\_E} := 1.0$

$\beta_{R\_MC\_E} := 0.05$ For the failure mode evaluated, the fundamental transverse mode is dominant. Thus use the lower bound value of 0.05 in Reference D2.2.1.

$\beta_{U\_MC\_E} := 0$

$$\beta_{c\_MC\_E} := \sqrt{\beta_{R\_MC\_E}^2 + \beta_{U\_MC\_E}^2}$$

$\beta_{c\_MC\_E} = 0.05$

D6.6.3.5 Earthquake Component Combination

Section 4153.10(c) of NOG-1 requires using the SRSS (Square Root of Sum of the Squares) to combine contributions for the three components of earthquake motion. This method is considered to be median-centered. Thus,

$F_{ECC\_E} := 1.0$

$\beta_{R\_ECC\_E} := 0.10$ A generic value of 0.18 is suggested in Reference D2.2.1 when responses from each of the three components are not available. A value of 0.10 is used here since the north-south component contributes most significantly to the response of the failure mode evaluated.

$\beta_{U\_ECC\_E} := 0$

$\beta_{c\_ECC\_E} := \sqrt{\beta_{R\_ECC\_E}^2 + \beta_{U\_ECC\_E}^2}$

$\beta_{c\_ECC\_E} = 0.1$

Equipment Response Factors

$F_{RE} := F_{QM} \cdot F_{\delta\_E} \cdot F_{M\_E} \cdot F_{MC\_E} \cdot F_{ECC\_E}$

$F_{RE} = 1.11$

$\beta_{c\_RE} := \sqrt{\beta_{c\_QM}^2 + \beta_{c\_\delta\_E}^2 + \beta_{c\_M\_E}^2 + \beta_{c\_MC\_E}^2 + \beta_{c\_ECC\_E}^2}$

$\beta_{c\_RE} = 0.24$

D6.6.4 Structural Response Factors

D6.6.4.1 Spectral Shape Factor

This factor accounts for conservatism in the site-wide DBGM-2 design spectrum. At the Surface Facilities Area (SFA) the depth of alluvium overlying tuff varies from 30 feet to 200 feet. Uniform hazard spectra at the surface are calculated from site response analyses for alluvium depths of 30', 70', 100' and 200'. The site-wide design ground response spectrum is the envelope of the surface spectra of these four alluvium depths (Reference D2.2.7; also Section 6.2.2.1 for source information).

The dominant frequency of the CRCF soil-structure system in the horizontal direction is 5.2 Hz from the Tier 1 ISRS calculation (Reference D2.2.2). At this frequency

$SA_{site} := 1.14g$ 5% damped site-wide spectral acceleration (see Figure D6.5-1).

$SA_{100} := 1.06 \cdot g$ 5% damped spectral acceleration of the 100-foot best-estimate alluvium depth case in the northeast area where the preclosure surface facilities are located.

$F_{SA} := \frac{SA_{site}}{SA_{100}}$

$F_{SA} = 1.08$

Since uncertainty in the UHS is derived from uncertainty in the seismic hazard curves which will be included in the final risk quantification, no uncertainty is included under the spectral shape factor to avoid double-counting the hazard uncertainty, hence

$\beta_{U\_SA} := 0$

$\beta_{R\_SA} := 0.2$ This is random variability to account for peak to valley variability of a smooth ground response spectrum (Reference D2.2.1, Table 3-2)

$\beta_{c\_SA} := \sqrt{\beta_{U\_SA}^2 + \beta_{R\_SA}^2}$ $\beta_{c\_SA} = 0.2$

D6.6.4.2 Damping Factor

This factor is to account for conservatism in the hysteresis damping of the building structure used in the seismic response analysis. Due to the high radiation damping of the foundation media, the effect of structure damping is insignificant. Thus,

$F_\delta := 1.0$

$\beta_{U\_\delta} := 0$ Since a conservative median factor of safety is used for structure damping, no value is assigned to the uncertainty logarithmic standard deviation.

$\beta_{R\_\delta} := 0$

$\beta_{c\_\delta} := \sqrt{\beta_{U\_\delta}^2 + \beta_{R\_\delta}^2}$ $\beta_{c\_\delta} = 0$

D6.6.4.3 Modeling Factor

The Tier 1 lumped mass multiple stick model of CRCF models the stiffness of various reinforced concrete walls and distribution of mass at each floor. The floors are assumed to be rigid diaphragms tying the different sticks together. Torsional response of the structure is captured through modeling eccentricity between the center of mass and center of rigidity of each floor. The foundation media underneath the buildings are modeled with soil springs and dashpots based on elastic half space theory with adjustment to account for the layering effect of alluvium overlying tuff. The model is judged to adequately represent the CRCF structure dynamic characteristics, thus

$F_M := 1.0$

$\beta_{R\_M} := 0$

Uncertainty of structure frequencies predicted from mathematical modeling varies from 0.15 to 0.35 depending on the sophistication of the model (Reference D2.2.1). The value of 0.35 is for fairly approximate models and the value 0.15 is appropriate for detailed models. Based on the complexity of the CRCF structure and the mathematical model used for the Tier 1 ISRS analysis, it is judged that the calculated CRCF frequency has a logarithmic standard deviation of 0.25.

$\beta_f := 0.25$ Uncertainty in building frequency.

$f_m := 5.2 \cdot Hz$ Best-estimate frequency

$f_{upper} := f_m \cdot e^{\beta_f}$ Upper bound frequency

$f_{upper} = 6.68 \cdot Hz$

$SA_{upper} := 1.05g$ 5% damped spectral acceleration at f_{upper} read off from the mean 5E-4 UHS of the 100-foot alluvium depth case (Figure D6.5-1). This value is less than the value at the best-estimate frequency.

$f_{lower} := f_m \cdot e^{-\beta_f}$ Lower bound frequency

$f_{lower} = 4.05 \cdot Hz$

$SA_{lower} := 1.02 \cdot g$ 5% damped spectral acceleration at f_{lower} read off from the mean 5E-4 UHS of the 100-foot alluvium depth case. This value is less than the value at the best-estimate frequency.

$\beta_{U\_f} := 0$ Since the spectral value at the best-estimate frequency is greater than that at either the lower bound or upper bound frequency.

$\beta_{U\_ms} := 0.10$ Uncertainty of mode shape (Reference D2.2.1, page 3-18); a lower value of 0.10 is used due to simple geometry of the structure.

$\beta_{U\_M} := \sqrt{\beta_{U\_f}^2 + \beta_{U\_ms}^2}$

$\beta_{U\_M} = 0.1$

$\beta_{c\_M} := \sqrt{\beta_{R\_M}^2 + \beta_{U\_M}^2}$ $\beta_{c\_M} = 0.1$

D6.6.4.4 Modal Combination

Since direct integration time history method is used in the Tier 1 ISRS analysis (Reference D2.2.2), the modal combination method factor of safety is unity and there is no variability associated with modal combination.

$F_{MC} := 1$

$\beta_{R\_MC} := 0$

$\beta_{U\_MC} := 0$

$\beta_{c\_MC} := \sqrt{\beta_{R\_MC}^2 + \beta_{U\_MC}^2}$ $\beta_{c\_MC} = 0$

D6.6.4.5 Soil-Structure Interaction

Two factors are considered, the first one is on the method of treating the SSI effects and the second one is on the effect of soil softening at ground acceleration higher than DBGM-2. See discussions in Section D6.5.4.6 for details.

$F_{SSI\_1} := 1$

$\beta_{R\_SSI\_1} := 0$

$\beta_{U\_SSI\_1} := 0.25$

At 2 Hz

$S_{v\_DBGM\_7\%} := 0.81 \cdot g$

The 7% damped north-south spectral accelerations and the floor zero period accelerations of DBGM-2 and BDBGM are read from the digitized raw floor response spectra of Reference D2.2.2.

$ZPA_{DBGM} := 0.591 \cdot g$

$S_{v\_BDBGM\_10\%} := 1.64 \cdot g$

$ZPA_{BDBGM} := 1.09 \cdot g$

$$F_2 := \frac{\frac{S_{v\_DBGM\_7\%}}{ZPA_{DBGM}}}{\frac{S_{v\_BDBGM\_10\%}}{ZPA_{BDBGM}}}$$

$F_2 = 0.91$

At 3 Hz

$S_{v\_DBGM\_7\%} := 1.11 \cdot g$

$ZPA_{DBGM} := 0.591 \cdot g$

$S_{v\_BDBGM\_10\%} := 1.76 \cdot g$

$ZPA_{BDBGM} := 1.09 \cdot g$

$$F_3 := \frac{\frac{S_{v\_DBGM\_7\%}}{ZPA_{DBGM}}}{\frac{S_{v\_BDBGM\_10\%}}{ZPA_{BDBGM}}}$$

$F_3 = 1.16$

$F_{SSI\_2} := \frac{1}{2} \cdot (F_2 + F_3)$

$F_{SSI\_2} = 1.04$

$F_{SSI} := F_{SSI\_1} \cdot F_{SSI\_2}$

$F_{SSI} = 1.04$

$$\beta_{U\_SSI\_2} := \frac{\ln(F_{SSI\_2})}{1.65}$$

$\beta_{U\_SSI\_2} = 0.02$

$\beta_{R\_SSI} := 0$

$\beta_{U\_SSI} := \sqrt{\beta_{U\_SSI\_1}^2 + \beta_{U\_SSI\_2}^2}$ $\beta_{U\_SSI} = 0.25$

$\beta_{c\_SSI} := \sqrt{\beta_{R\_SSI}^2 + \beta_{U\_SSI}^2}$

$\beta_{c\_SSI} = 0.25$

D6.6.4.6 Ground Motion Incoherence

The ground motion incoherence reduction factor is a function of foundation size and frequency of response. For a 150 foot plan dimension foundation, the reduction factor is 1.0 (i.e., no reduction) at 5 Hz or less (Reference D2.2.1 in page 3-22). The horizontal fundamental frequencies of the CRCF are calculated to be 5.2 Hz and 4.4 Hz, respectively for DBGM-2 and BDBGM with 100-ft of median soil overlying tuff (Page 45 of Reference D2.2.2). Since the seismic acceleration level at which trolley failure is expected is significantly higher than DBGM-2, the 4.4 Hz horizontal frequency is considered. Furthermore, because this frequency is lower than 5 Hz, the ground motion incoherence reduction factor is 1.0.

$F_{GMI} := 1$

$\beta_{U\_GMI} := 0$

$\beta_{R\_GMI} := 0$

$\beta_{c\_GMI} := \sqrt{\beta_{R\_GMI}^2 + \beta_{U\_GMI}^2}$

$\beta_{c\_GMI} = 0$

Structural Response Factors

$F_{RS} := F_{SA} \cdot F_{\delta} \cdot F_M \cdot F_{MC} \cdot F_{SSI} \cdot F_{GMI}$

$F_{RS} = 1.12$

$\beta_{c\_RS} := \sqrt{\beta_{c\_SA}^2 + \beta_{c\_\delta}^2 + \beta_{c\_M}^2 + \beta_{c\_MC}^2 + \beta_{c\_SSI}^2 + \beta_{c\_GMI}^2}$

$\beta_{c\_RS} = 0.34$

D6.6.5 Overall Factor of Safety

$F_{total} := F_{S\_shear} \cdot F_{\mu} \cdot F_{RS} \cdot F_{RE}$

$F_{total} = 3.51$

$PGA := 0.453g$ Peak ground acceleration of the DBGM-2 design spectrum (Reference D2.2.7; also Section 6.2.2.1 for source information).

$A_m := F_{total} \cdot PGA$

$A_m = 1.59 \cdot g$ Median seismic capacity in terms of PGA

$$\beta_c := \sqrt{\beta_{c\_S}^2 + \beta_{c\_\mu}^2 + \beta_{c\_RS}^2 + \beta_{c\_RE}^2}$$

$\beta_c = 0.42$

$HCLPF := A_m \cdot e^{-2.33 \cdot \beta_c}$

$HCLPF = 0.59 \cdot g$

D7. SUMMARY

Three failure modes of the canister transfer machine are evaluated above: (1) structural failure of the CTM girders, (2) structural failure of the frames of the trolleys, and (3) failure of seismic restraints of the trolleys. Since the trolleys' frames will also be designed to the NOG-1 criteria for Type 1 cranes, seismic fragility of the CTM bridge girder is reported for the trolleys. The seismic fragilities of these failure modes are:

- Failure of bridge girders -

  A_m = 2.39g β_c = 0.45 HCLPF = 0.83g

- Failure of trolley frames

  A_m = 2.39g β_c = 0.45 HCLPF = 0.83g

- Failure of trolley seismic restraints -

  A_m = 1.59g β_c = 0.42 HCLPF = 0.59g

  Note that it would be cost-effective to increase the seismic capacity of the trolleys' seismic restraints such that its seismic fragility is equivalent to the other CTM failure modes.

APPENDIX D-A

ESTIMATE OF VERTICAL FREQUENCY OF CTM

$E_s := 30 \cdot 10^6 \cdot psi$ Young's modulus of steel

$L_s := 86.33 \cdot ft$ Rail to rail distance of the CRCF CTM (Reference D2.2.8)

$Mass_{CTM} := 500 \cdot ton$ Mass of the CTM (Reference D2.2.8)

$W_{CTM} := Mass_{CTM} \cdot g$

$W_{CTM} = 1000 \cdot kip$

At the time this calculation is performed, dimensions of the crane girders are not available. However, the vertical frequency of the CTM may be estimated based on the NOG-1 allowable deflections.

$\Delta_{all} := \frac{L_s}{1000}$ Total vertical deflection of the girder under the trolley dead weight and the rated live load is limited to 1/1000 of the span (Section 4341 of NOG-1).

$\Delta_{all} = 1.04 \cdot in$

$I := 1 \cdot in^4$ An initial trial value of the girder moment of inertia

Since there is not a detailed design of the CTM at the time this calculation is prepared, it is necessary to assume the weight of the trolleys and their rated loads relative to the total weight of the CTM. This relative weight will affect the frequency estimates. Based on designs of similar bridge cranes, the combined weight of the trolleys and their rated loads is estimated to be between 50% and 65% of the total CTM weight.

<u>At 50% of the total CTM weight</u>

$W_{trolley\_load} := 0.5 \cdot W_{CTM}$ Combined weight of the trolleys and their rated loads

Given

$\Delta_{all} = \frac{(W_{trolley\_load}) \cdot L_s^3}{48 \cdot E_s \cdot I}$ With the load at the mid-span (Page 2-298 of Reference D2.2.10).

$a := Find(I)$

$a = 372643.45 \cdot in^4$

$I := a$ Moment of inertia of the bridge girders

Deflection at midspan due to uniform weight of the girders

$w := \frac{W_{CTM} - W_{trolley\_load}}{L_s}$ $w = 5.79 \cdot \frac{kip}{ft}$ Uniform weight

$$\Delta_1 := \frac{5 \cdot w \cdot L_s^{\,4}}{384 E_s \cdot I}$$ Maximum deflection at mid-span due to uniform weight (Page 2-296 of Reference D2.2.10).

Deflection due to concentrated weight at mid-span

$$\Delta_2 := \frac{W_{trolley\_load} \cdot L_s^{\,3}}{48 \cdot E_s \cdot I} \quad \Delta_2 = 1.04 \cdot in$$

$$\Delta_{midspan} := \Delta_1 + \Delta_2$$

$$\Delta_{midspan} = 1.68 \cdot in$$

$$f_{CTM\_midspan} := \frac{1}{2 \cdot \pi} \cdot \sqrt{\frac{g}{\Delta_{midspan}}}$$ where g is the gravitational acceleration (Section 1.1 of Reference D2.2.12)

$$f_{CTM\_midspan} = 2.41 \cdot Hz$$

Deflection at quarter point when subjected to uniformly distributed load

$$\Delta_3 := \frac{w \cdot \left(\frac{1}{4} \cdot L_s\right)}{24 \cdot E_s \cdot I} \left[L_s^{\,3} - 2 \cdot L_s \cdot \left(\frac{1}{4} \cdot L_s\right)^2 + \left(\frac{1}{4} \cdot L_s\right)^3 \right]$$ Page 2-296 of Reference D2.2.10

Deflection at quarter point when the concentrated load is at quarter point

$$\Delta_4 := \frac{W_{trolley\_load} \cdot \left(\frac{1}{4} \cdot L_s\right)^2 \cdot \left(\frac{3}{4} \cdot L_s\right)^2}{3 \cdot E_s \cdot I \cdot L_s}$$ Page 2-298 of Reference D2.2.10

$$\Delta_3 = 0.46 \cdot in$$

$$\Delta_{quarter} := \Delta_3 + \Delta_4$$

$$\Delta_{quarter} = 1.04 \cdot in$$

$$f_{CTM\_quarter} := \frac{1}{2 \cdot \pi} \cdot \sqrt{\frac{g}{\Delta_{quarter}}}$$

$$f_{CTM\_quarter} = 3.06 \cdot Hz$$

At 65% of the total crane weight.

$$W_{trolley\_load} := 0.65 \cdot W_{CTM}$$

Given

$$\Delta_{all} = \frac{\left(W_{trolley\_load}\right)\cdot L_s^{\,3}}{48\cdot E_s\cdot I}$$

$a := \text{Find}(I)$

$a = 484436.48\cdot in^4$

$I := a$ Moment of intertia of the bridge crane

Deflection due to uniform weight

$$w := \frac{W_{CTM} - W_{trolley\_load}}{L_s}$$

$$\Delta_1 := \frac{5\cdot w\cdot L_s^{\,4}}{384 E_s\cdot I}$$ Maximum deflection at mid-span due to uniform weight

Deflection due to concentrated weight at mid-span

$$\Delta_2 := \frac{W_{trolley\_load}\cdot L_s^{\,3}}{48\cdot E_s\cdot I}$$

$\Delta_{midspan} := \Delta_1 + \Delta_2$ $\Delta_{midspan} = 1.38\cdot in$

$$f_{CTM\_midspan} := \frac{1}{2\cdot\pi}\cdot\sqrt{\frac{g}{\Delta_{midspan}}}$$

$f_{CTM\_midspan} = 2.66\cdot Hz$

Deflection due to concentrated load at quarter point

$$\Delta_3 := \frac{w\cdot\left(\frac{1}{4}\cdot L_s\right)}{24\cdot E_s\cdot I}\left[L_s^{\,3} - 2\cdot L_s\cdot\left(\frac{1}{4}\cdot L_s\right)^2 + \left(\frac{1}{4}\cdot L_s\right)^3\right]$$

$\Delta_3 = 0.25\cdot in$

$$\Delta_4 := \frac{W_{trolley\_load}\cdot\left(\frac{1}{4}\cdot L_s\right)^2\cdot\left(\frac{3}{4}\cdot L_s\right)^2}{3\cdot E_s\cdot I\cdot L_s}$$

$\Delta_{quarter} := \Delta_1 + \Delta_3$ $\Delta_{quarter} = 0.6\cdot in$

$$f_{CTM\_quarter} := \frac{1}{2\cdot\pi}\cdot\sqrt{\frac{g}{\Delta_{quarter}}}$$

$$f_{CTM\_quarter} = 4.05\cdot Hz$$

The 7% damped DBGM-2 vertical spectral accelerations at the estimated frequencies are presented below (see Figures D-B-3 of Attachment DB)

% of Trolley Weight Plus Rated Load	Trolleys at Mid-Span		Trolleys at 1/4 Span	
	Vert. Frequency (Hz)	7% Design Spectral Accel	Vert. Frequency (Hz)	7% Design Spectral Accel
50%	2.4 Hz	0.52g	3.1 Hz	0.61g
65%	2.7 Hz	0.56g	4.1 Hz	0.71g

It is clear that the vertical seismic load will be higher for the case that combined trolley dead weight plus their rated loads amount to 65% of the total CTM weight.

The remaining calculation determines which position of the trolleys will govern the design of the girders.

Case 1. Trolleys at the mid-span

$$f_{CTM\_midspan} = 2.66\cdot Hz$$

$S_{v\_7\%\_mid} := 0.56g$ 7% damped DBGM-2 spectral acceleration (Figure D-B-3)

$$M_{max\_1} := \frac{w\cdot L_s^{\,2}}{8}\cdot\left(1+\frac{S_{v\_7\%\_mid}}{g}\right)+\frac{W_{trolley\_load}\cdot L_s}{4}\left(1+\frac{S_{v\_7\%\_mid}}{g}\right)$$

(Pages 2-296 and 298 of Reference D2.2.10)

$M_{max\_1} = 27776.68\cdot kip\cdot ft$ Maximum moment at **midspan** due to dead weight plus downward acceleration

Case 2. Trolleys at the quarter point of the span

$$f_{CTM\_quarter} = 4.05\cdot Hz$$

$S_{v\_7\%\_qtr} := 0.71\cdot g$ 7% damped DBGM-2 spectral acceleration (Figure D-B-3)

$$M_{max\_2} := \left[\frac{w\cdot L_s^{\,2}}{8}+\frac{W_{trolley\_load}\cdot\frac{L_s}{4}}{L_s}\cdot\left(\frac{L_s}{2}\right)\right]\cdot\left(1+\frac{S_{v\_7\%\_qtr}}{g}\right)$$

(Pages 2-296 and 298 of Reference D2.2.10)

$M_{max\_2} = 18453.04\cdot kip\cdot ft$ Moment at midspan when the trolleys are at the quarter point

$$M_{max\_3} := \left[\frac{w \cdot \left(\frac{L_s}{4} \right)}{2} \cdot \left(L_s - \frac{L_s}{4} \right) + \frac{W_{trolley\_load} \cdot \left(\frac{L_s}{4} \right) \cdot \left(\frac{3 \cdot L_s}{4} \right)}{L_s} \right] \cdot \left(1 + \frac{S_{v\_7\%\_qtr}}{g} \right)$$

(Pages 2-296 and 298 of Reference D2.2.10)

$M_{max\_3} = 22835.63 \cdot kip \cdot ft$ Moment at the quarter point when the trolleys are at the quarter point.

Thus, when both trolleys and their rated loads are at quarter point of the span, the maximum bending moment in the girder is $\frac{M_{max\_3}}{M_{max\_1}} = 0.82$ of the design maximum moment.

Based on the above calculations it becomes clear that though the vertical acceleration is higher when the trolleys are at the quarter point of the span, design of the girders is governed by the case of having trolleys and their rated loads at the midspan.

APPENDIX D-B

DBGM-2 ISRS AT CTM LEVEL (REFERENCE D2.2.2)

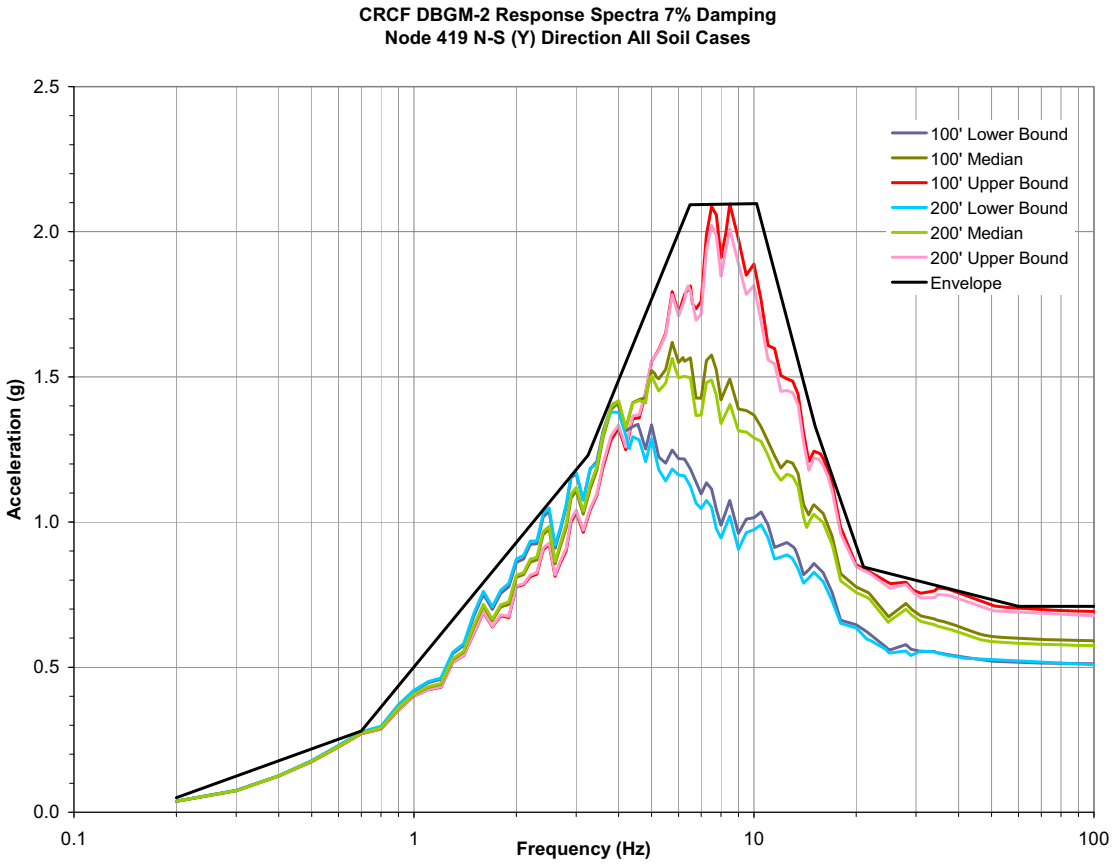

Figure D-B-1. CRCF DBGM-2 7% Damped Node 419 N-S (Y)

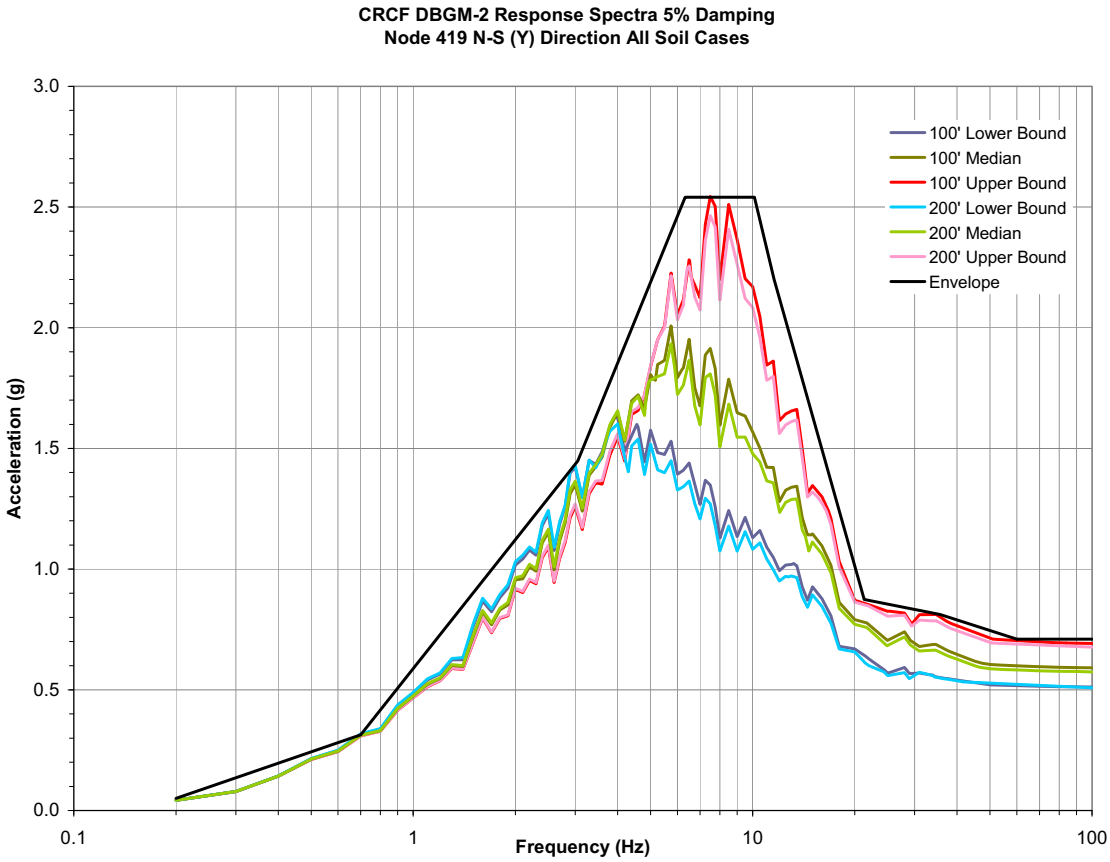

Figure D-B-2. CRCF DBGM-2 5% Damped Node 419 N-S (Y)

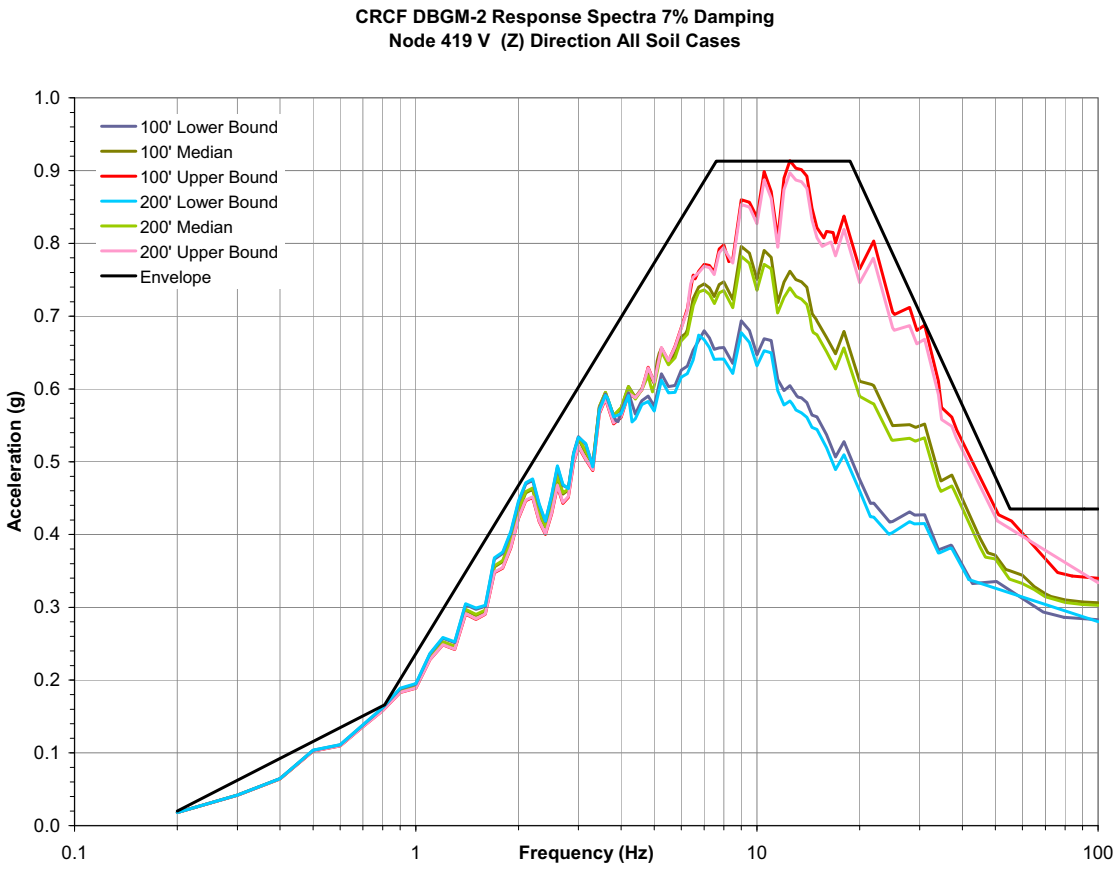

Figure D-B-3. CRCF DBGM-2 7% Damped Node 419 Vertical (Z)

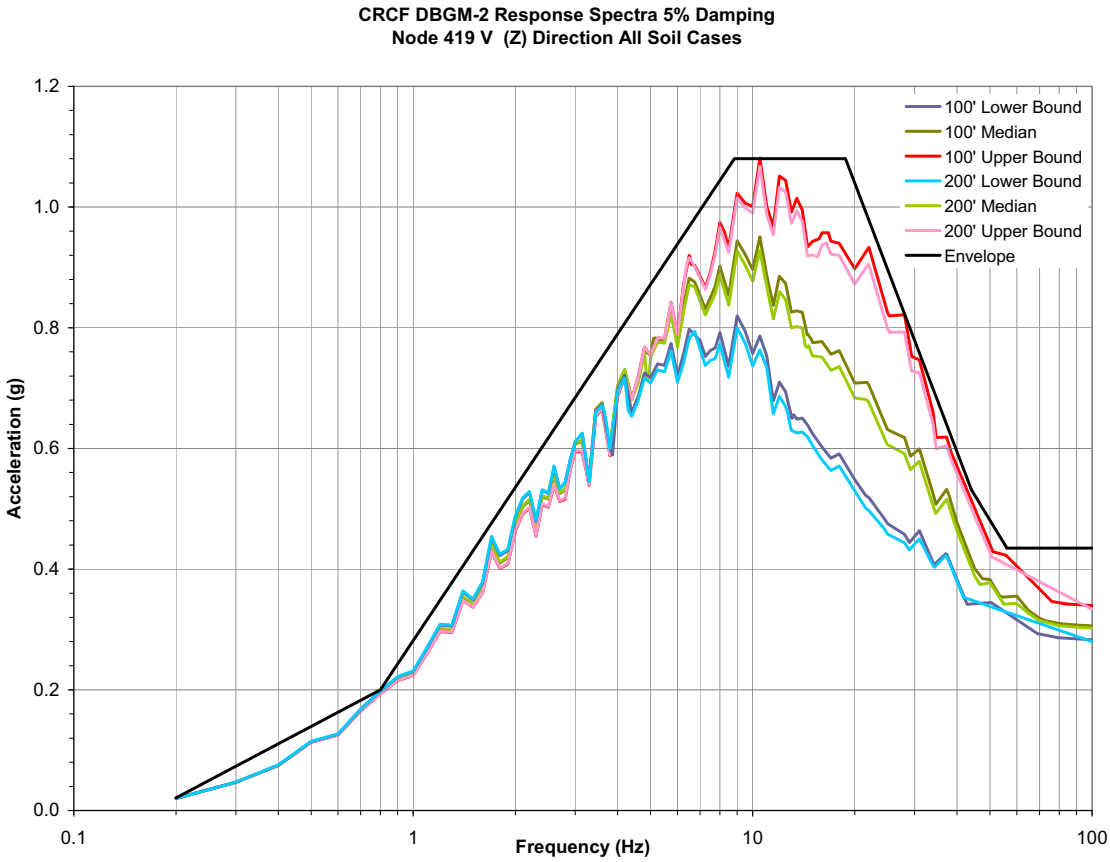

Figure D-B-4. CRCF DBGM-2 5% Damped Node 419 Vertical (Z)

ATTACHMENT E

FRAGILITY FOR IHF CASK TRANSFER TROLLEY

Prepared By: Wen H. Tong

ARES Check By: Robert D. Campbell

LLNL Check By: Robert C. Murray

TABLE OF CONTENTS

ACRONYMS AND ABBREVIATIONS

ACI	American Concrete Institute
AISC	American Institute of Steel Construction
ANSI	American National Standards Insitute
AO	Aging Overpack
APE	Annual Probability of Exceedance
ASCE	American Society of Civil Engineers
ASME	American Society of Mechanical Engineers
BSC	Bechtel SAIC, LLC
BDBGM	Beyond Design Basis Ground Motion at $1x10^{-4}$ APE
CDFM	Conservative Deterministic Failure Margin
CHC	Cask Handling Crane
CIP	Cast-in-Place
CRCF	Canister Receipt and Closure Facility
CTM	Canister Transfer Machine
CTT	Cask Transfer Trolley
DBGM-2	Design Basis Ground Motion at $5x10^{-4}$ APE
DL	Dead Load
DOF	Degree of Freedom
DPC	Dual Purpose Canister
EPRI	Electric Power Research Institute
HCLPF	High Confidence of Low Probability of Failure
HVAC	Heating, Ventilation, & Air Conditioning
IEEE	Institute of Electrical and Electronics Engineers
IHF	Initial Handling Facility
ISRS	In-Structure Response Spectra

ACRONYMS AND ABBREVIATIONS (cont.)

ITS	Important to Safety
LA	License Application
LLNL	Lawrence Livermore National Laboratory
NPP	Nuclear Power Plant
PGA	Peak Ground Acceleration
RF	Receipt Facility
RRS	Required Response Spectrum
Sa	Spectral Acceleration
SFA	Surface Facilities Area
SFTM	Spent Fuel Transfer Machine
SPRA	Seismic Probabilistic Risk Assessment
SRSS	Square Root of the Sum of Squares
SSE	Safe Shutdown Earthquake (used with NPPs)
SSI	Soil Structure Interaction
SSC	Structure, System, and Component
TAD	Transportation, Aging, and Disposal canister
TEV	Transport and Emplacement Vehicle
TRS	Test Response Spectrum
UHS	Uniform Hazard Spectra
USDOE	United States Department of Energy
USNRC	United States Nuclear Regulatory Commission
WHF	Wet Handling Facility
WP	Waste Package
WPTT	Waste Package Transfer Trolley
YMSF	Yucca Mountain Surface Facilities
ZPA	Zero Period Acceleration

FRAGILITY TERMINOLOGY

Am	Median Peak Ground Motion Capacity
β_R	Log Standard Deviation of Randomness
β_U	Log Standard Deviation of Uncertainty (Lack of Knowledge)
β_C	Composite Variability = $(\beta_R^2 + \beta_U^2)^{0.5}$
F_S	Strength Factor of Safety
β_{R_S}	Strength Randomness (typical)
β_{U_S}	Strength Uncertainty (typical)
β_{C_S}	Strength Composite Variability (typical)
F_μ	Inelastic Energy Absorption Factor of Safety
F_{QM}	Qualification Factor of Safety
F_δ	Damping Factor of Safety
F_M	Modeling Factor of Safety
F_{MC}	Modal Combination Factor of Safety
F_{ECC}	Earthquake Component Combination Factor of Safety
F_{SA}	Spectral Shape Factor of Safety
F_{SSI}	Soil-Structure Interaction Factor of Safety
F_{GMI}	Ground Motion Incoherence Factor of Safety
F_{TOTAL}	Total Factor of Safety
F_{RS}	Structural Response Factor of Safety
F_{RE}	Equipment Response Factor of Safety

E1. PURPOSE

The purpose of this calculation is to calculate seismic fragility of the Cask Transfer Trolley (CTT) in the Initial Handling Facility (IHF). The mean seismic fragility curve of the Cask Transfer Trolley (CTT) will be convolved with the mean site-specific seismic hazard curve to calculate risk of seismic-induced failure of the trolley.

E2. REFERENCES

E2.1 PROCEDURES/DIRECTIVES

E2.1.1 EG-PRO-3DP-G04B-00037, Rev. 10. *Calculations and Analyses*. Las Vegas, Nevada: Bechtel SAIC Company. ACC: ENG.20071018.0001.

E2.1.2 BSC (Bechtel SAIC Company) 2005. *Q-List*. 000-30R-MGR0-00500-000-003. Las Vegas, Nevada: Bechtel SAIC Company. ACC: ENG.20050929.0008. [DIRS 175539]

E2.1.3 IT-PRO-0011, Revision 7, ICN 0. *Software Management*. Las Vegas, Nevada: Bechtel SAIC Company. ACC: DOC.20070905.0007.

E2.1.4 BSC (Bechtel SAIC Company) 2007. *Quality Management Directive*. QA-DIR-10, Rev. 2. Las Vegas, Nevada: Bechtel SAIC Company. ACC: DOC.20080103.0002. [DIRS 184673]

E2.2 DESIGN INPUTS

E2.2.1 EPRI (Electric Power Research Institute) 1994. *Methodology for Developing Seismic Fragilities*. EPRI TR-103959. Palo Alto, California: Electric Power Research Institute. TIC:253770. [DIRS 161329]

E2.2.2 BSC (Bechtel SAIC Company) 2007. *Initial Handling Facility Cask Transfer Trolley - 265T Mechanical Equipment Envelope*. V0-CY05-QHC4-00459-00072-001 REV 001. Las Vegas, Nevada: Bechtel SAIC Company. ACC: ENG.20071022.0015. [DIRS 183511] [DIRS 184112]

E2.2.3 BSC (Bechtel SAIC Company) 2007. *Initial Handling Facility General Arrangement Ground Floor Plan*. 51A-P10-IH00-00102-000 REV 00C. Las Vegas, Nevada: Bechtel SAIC Company. ACC: ENG.20071226.0017; ENG.20080121.0016. [DIRS 184529]

E2.2.4 BSC (Bechtel SAIC Company) 2007. *Mechanical Handling Design Report Cask Transfer Trolley (240 Ton & 265 Ton Capacity).* V0-CY05-QHC4-00459-00016-001 REV 006. Las Vegas, Nevada: Bechtel SAIC Company. ACC: ENG.20071018.0017. [DIRS 184122]

E2.2.5 ASME NOG-1-2004. 2005. *Rules for Construction of Overhead and Gantry Cranes (Top Running Bridge, Multiple Girder).* New York, New York: American Society of Mechanical Engineers. TIC: 257672. [DIRS 176239].

E2.2.6 BSC (Bechtel SAIC Company) 2007. *Yucca Mountain Seismic Analysis of 265 Ton Cask Transfer Trolley*. V0-CY05-QHC4-00459-00070-001 REV 001. Las Vegas, Nevada: Bechtel SAIC Company. ACC: ENG.20071018.0021. [DIRS 183501]

E2.2.7 ASCE/SEI 43-05. 2005. *Seismic Design Criteria for Structures, Systems, and Components in Nuclear Facilities*. Reston, Virginia: American Society of Civil Engineers. TIC: 257275. [DIRS 173805]

E2.2.8 BSC (Bechtel SAIC Company) 2007. *Initial Handling Facility (IHF): Tier-1 In-Structure Response Spectra.* 51A-SYC-IH00-00600-000-00A. Las Vegas, Nevada: Bechtel SAIC Company. ACC: ENG.20071130.0013. [DIRS 184106]

E2.2.9 MO0801HCUHSSFA.001. *Mean Hazard Curves and Mean Uniform Hazard Spectra for the Surface Facilities Area*. Submittal date: 01/11/2008. [DIRS 184802]

E2.2.10 Baltay, P. and Gjelsvik, A. 1990. "Coefficient of Friction for Steel on Concrete at High Normal Stress." *Journal of Materials in Civil Engineering, 2*, (1), 46-49. [New York, New York]: American Society of Civil Engineers. TIC: 260005. [DIRS 184424]

E2.3 DESIGN CONSTRAINTS

None.

E2.4 DESIGN OUTPUTS

The calculation is performed to calculate seismic fragility of the Cask Transfer Trolley in the IHF which will be convolved with the site-specific seismic hazard curve to calculate risk of seismic-induced failure of the trolley. This is performed to support information in the License Application.

E3. ASSUMPTIONS

E3.1 ASSUMPTIONS REQUIRING VERIFICATION

There are no assumptions made in the calculation that require verification.

E3.2 ASSUMPTIONS NOT REQUIRING VERIFICATION

There are no assumptions not requiring verification that have been used in this calculation.

E4. METHODOLOGY

E4.1 QUALITY ASSURANCE

This calculation is prepared in accordance with EG-PRO-3DP-G04B-00037, Calculations and Analyses (Reference E2.1.1). The Cask Transfer Trolley is classified as Important to Safety on the Q List (Reference E2.1.2), Table A-1. Therefore, this document is subject to the appropriate requirements for the BSC Quality Management Directive (Reference E2.1.4, Section 2.1.C.1.1), and the approved record version is designated as "QA:QA".

E4.2 USE OF SOFTWARE

Mathcad version 14 is used in this calculation. The use of this software is classified as Level 2 software per procedure IT-PRO-0011 (Reference E2.1.3) and therefore the software need not be qualified.

E4.3 APPROACH

The Separation-of-Variable method (Section 3 of Reference E2.2.1) is followed in calculating seismic fragility of the ITS equipment component.

E5. LIST OF APPENDICES

There are no appendices to this calculation.

E6. FRAGILITY CALCULATION

E6.1 INTRODUCTION

Seismic fragility calculation of the IHF Cask Transfer Trolley (CTT) is presented in this section. The trolley is located at the ground floor (elevation 0') of the IHF.

E6.2 CASK TRANSFER TROLLEY

The Cask Transfer Trolley is required to support a loaded transportation cask and to transfer the cask to the canister transfer cell. The IHF Cask Transfer Trolley shown in Figure E6.2-1 has overall dimensions of 18' by 18' at the landing pad by 25'-1" high at the top of the trolley frame (Reference E2.2.2). The top of the cask after being mounted on the trolley is 32'-3" from the bottom face of the trolley (Reference E2.2.2).

The trolley is mounted on air modules and is propelled by an air motor and travels on the concrete floor at elevation 0' from the cask preparation area to the canister transfer cell. Transfer of the canister from the transportation cask to the waste package is done by the overhead Canister Transfer Machine (CTM) which is supported by the building structure.

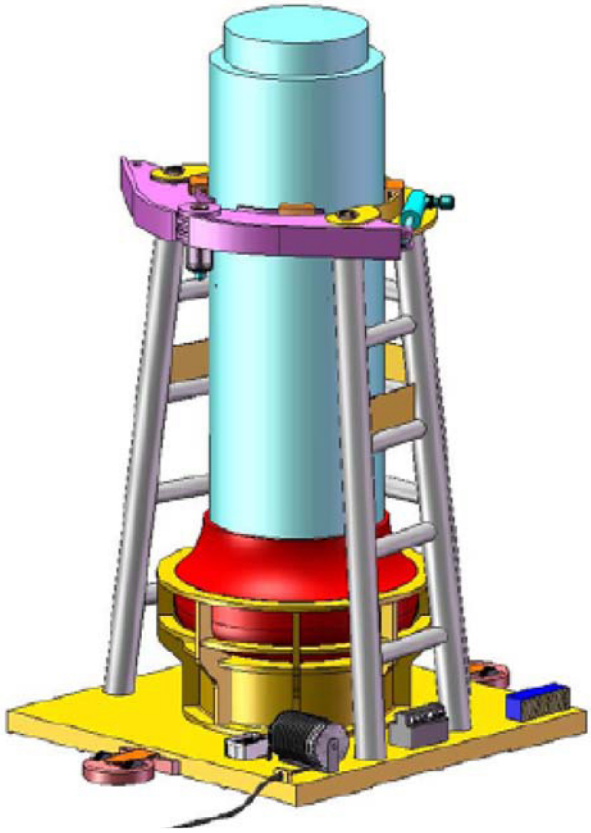

Figure E6.2-1. IHF Cask Transfer Trolley (Reference E2.2.6)

E6.3 POTENTIAL FAILURE MODES

The potential failure modes of the Cask Transfer Trolley that may impact performance goals of the Yucca Mountain Project are presented below based on our understanding of safety functions and operation of the trolley.

E6.3.1 Transfer of Cask from Railcar to Trolley

This is addressed separately in the fragility calculation of the Cask Handling Crane.

E6.3.2 Transit to Canister Transfer Cell

The air-powered trolley travels on the concrete floor slab. In the event of loss of power during an earthquake, the air modules will depressurize such that the trolley will rest on the floor. The free-standing Cask Transfer Trolley is subject to seismic-induced sliding or tip over which may result in impact of the Cask Transfer Trolley with the steel columns that support the Cask Handling Crane (see Reference E2.2.3 for locations of these steel columns) or impact with the concrete cell walls.

E6.3.3 Parked in the Canister Transfer Cell

Upon entering the transfer cell, the CTT will be guided directly below the transfer port by floor guides that are bolted to the floor slab. Since these floor guides are not intended to be seismic stops, they are not strong enough to prevent the trolley from sliding in a seismic event. Upon sliding or rocking and impacting the 4-foot thick cell wall, breach of the canister inside the transportation cask is taken to be a credible failure mode. The probability of canister breach given trolley impact is not included in this calculation.

E6.3.4 Trolley Structural Failure

Reference E2.2.4 provides design analyses of the Cask Transfer Trolley for load combinations including both DBGM-2 and BDBGM. The stresses in the trolley including the cask restraint assembly due to the DBGM-2 load combination are found to be lower than the NOG-1 stress limits (Table 4311-1 of Reference E2.2.5). These calculated design stresses are overly conservative for the reasons given below:

- The trolley is modeled as fixed at the base. The horizontal fundamental frequencies are calculated to be 8 Hz which is near the peak of the horizontal response spectrum used in the analysis (Reference E2.2.6, Section 5.2). In reality, sliding of the trolley will initiate at a low acceleration level. The trolley will slide as a rigid body and the equivalent system frequency will be much lower than 8 Hz such that the spectral acceleration will be significantly lower.

- The maximum trolley stresses due to the three components of earthquake were assumed to all occur at the same location in the trolley. This results in conservative seismic stresses in the trolley.

The abovementioned conservatism in the design analysis is acceptable for design purpose. However, using these stresses will result in conservatively biased seismic fragility estimates. Since rocking and sliding will dominate as shown in Sections E6.5 and E6.6, the failure mode due to seismic-induced stresses in the CTT is not further considered in this calculation.

E6.3.5 Governing Failure Mode

Based on the above discussions, either sliding or tip over of the CTT will be a credible failure mode. The governing failure mode is evaluated below.

The center of gravity of the trolley loaded with the cask is at (Section 5.5 of Reference E2.2.6):

$H_{cg} := 210 \cdot in$	Height measured from the bottom of the trolley
$X_{cg} := 108 \cdot in$	From the edge of the trolley base in the X-direction (horizontal) which is parallel to the open face of the trolley (Figure E6.2.1)
$Y_{cg} := 107 \cdot in$	From the edge of the trolley base in the Y-direction (horizontal).
$W_t := 684 \cdot kip$	Total weight of the loaded trolley

When an earthquake occurs, a seismic safety switch will provide a signal to shut off the air supply to the trolley and the trolley will rest on the concrete floor (Ref. E2.2.4, Section 3.3). The best-estimate coefficient of friction between the steel trolley base and the concrete floor slab is 0.47 (Reference E2.2.10).

$\mu := 0.47$

Based on the location of the center of gravity, the acceleration level at which one edge of the trolley base will lift up is determined.

$$S_{a\_liftup} := \left(\frac{Y_{cg}}{H_{cg}}\right) \cdot g$$

$$S_{a\_liftup} = 0.51 \cdot g$$

At this acceleration level, the seismic inertia load of the trolley is

$$V_{trolley} := W_t \cdot \frac{S_{a\_liftup}}{g}$$

$$V_{trolley} = 348.514 \cdot kip$$

Frictional resistance at the base of the trolley

$$V_{friction} := \mu \cdot W_t$$

$V_{friction} = 321.48 \cdot kip$ Less than the seismic inertia load at uplift

Since the acceleration levels at which trolley sliding and lifting at one edge are not very different, seismic fragility of both failure modes are evaluated (Sections E6.5 and E6.6).

E6.4 SEISMIC INPUT MOTION

The Cask Transfer Trolley operates at the ground floor of the IHF. Thus, the seismic input motion to the trolley is defined by the IHF ISRS at elevation 0'. The 5% and 10% damped BDBGM ISRS in the two horizontal directions for the four boundary conditions considered in the IHF seismic response analyses (Reference E2.2.8) are presented in Figures E6.4-1and E6.4-2. The four boundary conditions are: 30 feet deep of median alluvium, 30 feet deep of upper bound alluvium, 100 feet deep of lower bound alluvium, and 100 feet deep of median alluvium. The alluvium depth underneath the IHF varies from 30' at the west end to 90' at the east end.

Also presented in Figures E6.4-1 and E6.4-2 is the overplot of the 5% damped site-wide UHS (Reference E2.2.9; also Section 6.2.2.1 for source information). As shown in these figures, the ISRSs of the four boundary conditions and the site-wide UHS are practically the same at frequencies below 1.2 Hz. The system frequency of sliding or rocking of the trolley falls within this frequency range as shown in Sections E6.5 and E6.6 below.

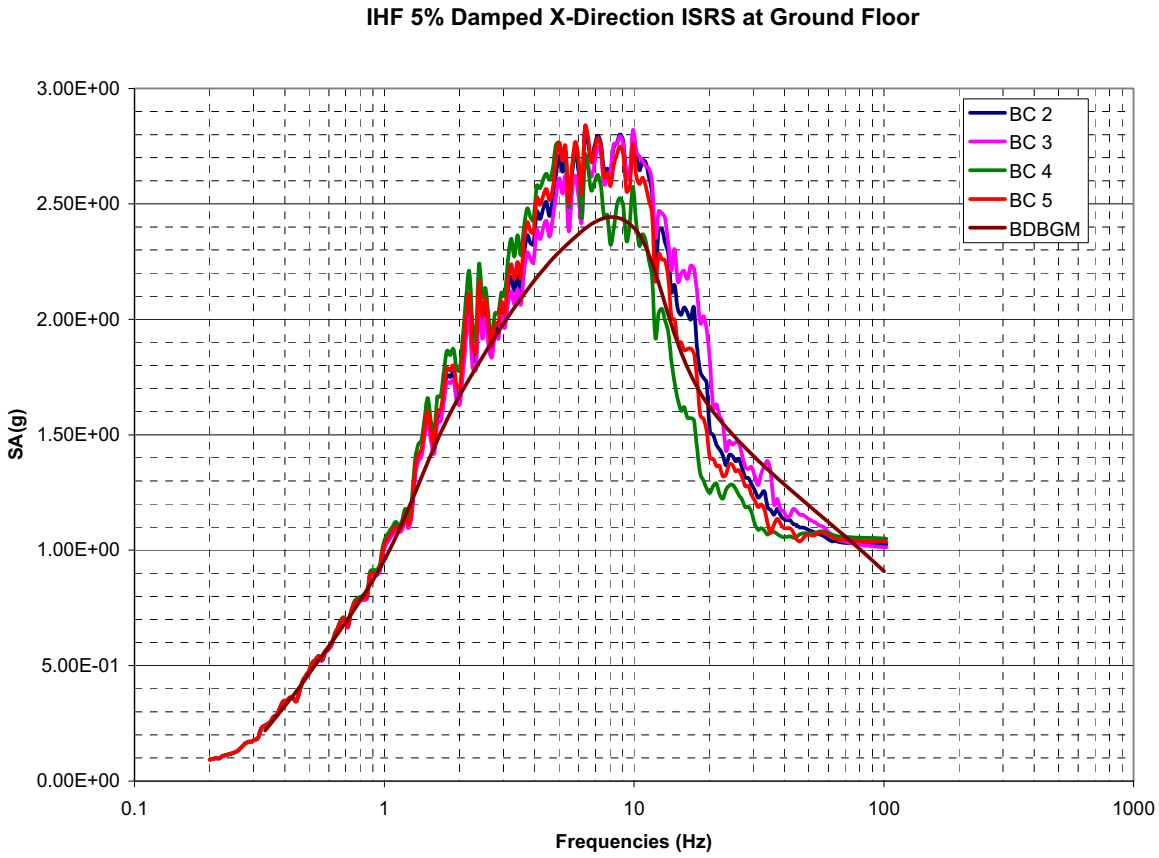

Figure E6.4-1. X-Direction 5% Damped BDBGM ISRS at 0' Floor of IHF - Four Boundary Conditions (Plotted from Data in Reference E2.2.8)

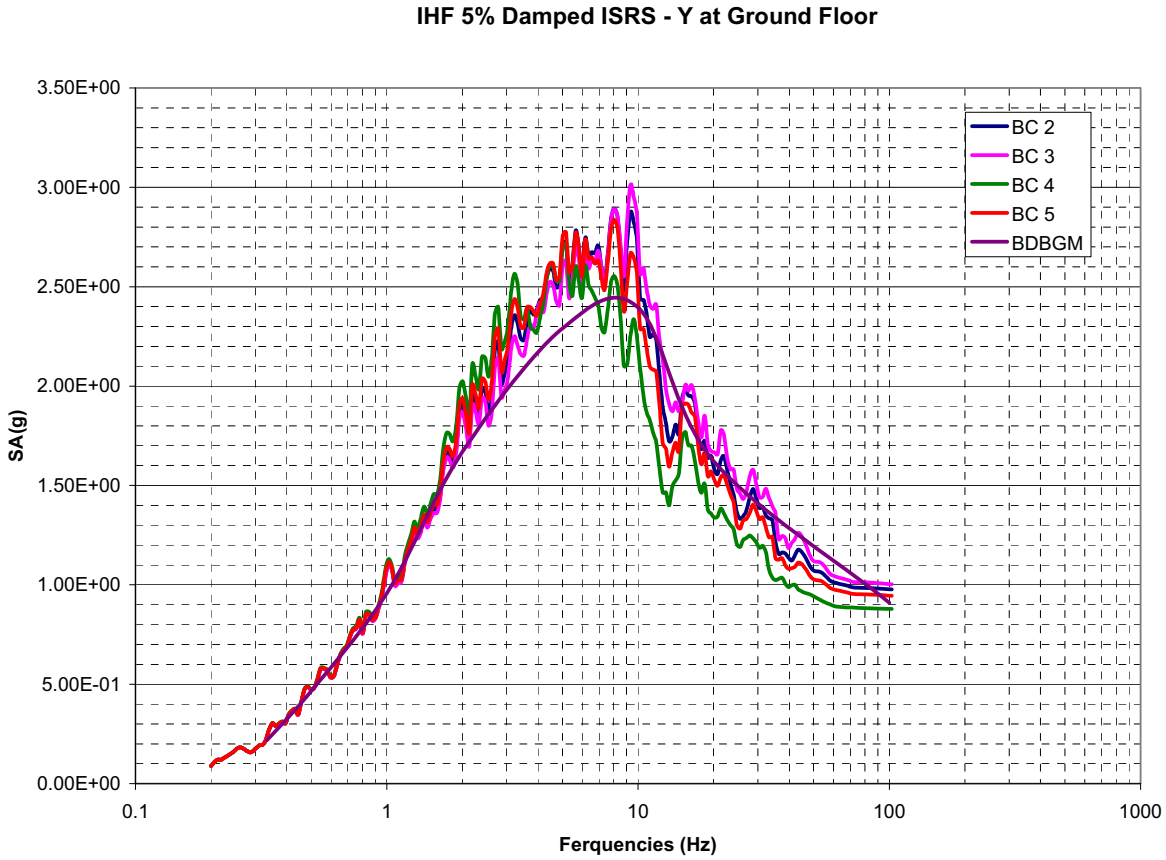

Figure E6.4-2. Y-Direction 5% Damped BDBGM ISRS at 0' Floor of IHF - Four Boundary Conditions (Plotted from Data in Reference E2.2.8)

E6.5 SEISMIC FRAGILITY OF SEISMIC-INDUCED SLIDING OF TROLLEY

The approach presented in Appendix A.1 of ASCE 43-05 (Reference E2.2.7) is used to calculate the best-estimate seismic-induced sliding displacement of the Cask Transfer Trolley at which impact between the trolley and the IHF structure would occur.

E6.5.1 Strength Factor

The center to center spacing of the IHF steel columns along column lines 7 and 8 is 25' (Reference E2.2.3). Given that the trolley base is 18' by 18', the clearance between the trolley base and the steel columns which support the Cask Handling Crane is estimated at 2.5 feet, i.e., . Note that one-foot is subtracted from the 3.5 ft measured from the centerline of the steel column to the edge of the trolley base to account for dimensions of the steel columns. Similarly, the clearance between the trolley base and the canister transfer cell wall (4-foot thick) is estimated at 1.5 feet (see Reference E2.2.3), i.e., .

Next the rigid body displacement of the trolley is calculated using the reserve energy method in Appendix A of Reference E2.2.7. This method treats the nonlinear problem of rigid body sliding using an equivalent linear model. The rigid-body displacements are calculated for input motion of different annual probabilities of exceedance and the motion which yields a displacement closest to the limit is used for the strength factor calculation.

$\mu_e := \mu$	The effective coefficient of sliding friction does not account for the vertical component of ground motion for a "best-estimate" sliding displacement. This is because the vertical acceleration will oscillate several times during the time the rigid body displaces from 0 to a finite displacement.
$\mu_e = 0.47$	Best-estimate friction coefficient between concrete and steel (Reference E2.2.10)

The force-displacement curve of a rigid body sliding is shown in Figure E6.5-1, where F_{RS} is the resisting force and δ_s is the displacement to be estimated. Based on the reserve energy method, an equivalent linear system is used to estimate the displacement. This equivalent system has a stiffness of K_e and a displacement of $_s$.

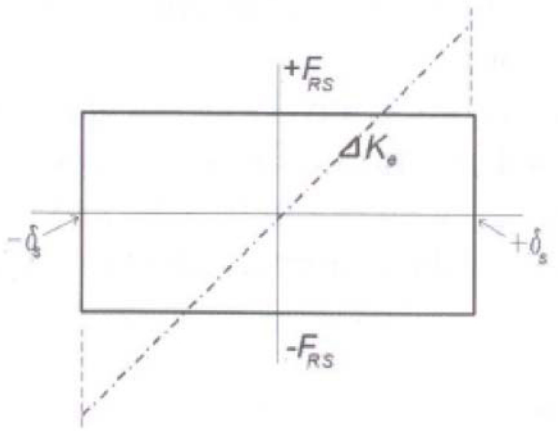

Figure E6.5-1. Sliding Force-Displacement Diagram (Reference E2.2.7, Appendix B)

Next, the sliding coefficient (c_s) is defined below:

$c_s := 2 \cdot \mu_e \cdot g$ Equation A-2 of Reference E2.2.7, where g is the gravitational acceleration.

$c_s = 0.94 \cdot g$

The sliding displacement of the rigid body is estimated using Equation A-3 of Reference E2.2.7 in which f_{eS} is the lowest natural frequency at which the vector horizontal spectral acceleration equals c_s.

$SA_H := 0.1 \cdot g$ Initial trial value of SA_H (i.e., spectral acceleration in one horizontal direction) to solve the equation below so that the vector horizontal spectral acceleration is equal to c_s

Given

$\sqrt{SA_H^2 + 0.16 SA_H^2} = c_s$ The two horizontal components of earthquake have essentially the same spectral shape. Equation A-4 of Reference E2.2.7.

$SA_H := \text{Find}(SA_H)$

$SA_H = 0.87 \cdot g$

The lowest natural frequency (f_{eS}) at which the vector spectral acceleration equals c_s is determined from the 10% damped ISRS at the ground floor which has an annual exceedance frequency of 1×10^{-4} (BDBGM). The 10% damping value is used per Equation B-7 of Reference E2.2.7.

$f_{es} := 1.17 \cdot Hz$ at this frequency the 10% damped spectral acceleration in one direction is 0.87g (Digitized IHF X - direction ISRS at ground floor in Reference E2.2.8).

$\delta_s := \frac{c_s}{\left(2 \cdot \pi \cdot f_{es}\right)^2}$ Sliding distance as given in Equation A-3 of Reference E2.2.7

$\delta_s = 0.56 \cdot ft$

Thus, at BDBGM there will be no impact between the Cask Transfer Trolley and the steel columns that support the Cask Handling Crane (2.5 feet clearance) nor impact with the canister transfer cell wall (1.5 feet clearance).

Next the lowest natural frequency (f_{eS}) at which the vector spectral acceleration equals c_s is determined from the ISRS at the ground floor which has an annual exceedance frequency of 10^{-5}. Though the 10^{-5} ISRS are not available, f_{eS} can be estimated from the 1E-5 site-wide ground response spectrum as shown in Table E6.5-1. Figures E6.4-1 and E6.4-2 show that the BDBGM ISRSs are essentially the same as the ground response spectrum in the frequency range less than 1 Hz. Thus, the 10% damped 1E-5 UHS is scaled from the 5% UHS using the 5% and 10% BDBGM ISRS provided in digitized ISRSs in Reference E2.2.8.

Table E6.5-1 10% Damped 1E-5 UHS Scaled From 5% Damped 1E-5 Site-Wide UHS (Horizontal)

Frequency (Hz)	5% Damped BDBGM Sa (g)	10% Damped BDBGM Sa (g)	Ratio	5% Damped 1E-5 UHS Sa (g);Figure E6.5-2	Scaled 10% Damped 1E-5 UHS Sa (g)
0.3	1.79E-01	1.27E-01	0.71	0.48	0.34
0.4	3.50E-01	2.60E-01	0.74	0.9	0.67
0.5	4.80E-01	3.70E-01	0.77	1.35	1.04
0.6	5.70E-01	4.30E-01	0.75	1.7	1.28
0.7	7.00E-01	4.70E-01	0.67	1.94	1.30
0.8	8.00E-01	5.80E-01	0.73	2.2	1.60
0.9	9.10E-01	6.00E-01	0.66	2.4	1.58

$f_{es} := 0.45 \cdot Hz$ At this frequency the 10% damped 1E-5 spectral acceleration is 0.87g.

$\delta_s := \frac{c_s}{\left(2 \cdot \pi \cdot f_{es}\right)^2}$ Sliding distance as given in Equation A-3 of Reference E2.2.7

$\delta_s = 3.783 \cdot ft$

This sliding displacement exceeds the clearances of 1.5 feet between the trolley and the transfer cell and the 2.5 feet clearance between the trolley and the steel columns.

Next, the BDBGM spectra will be scaled up to calculate the trolley sliding distance until the clearance is closed.

1.5 times the BDBGM

At the frequency of 0.80 Hz, 1.5 times the 10% damped BDBGM floor spectral acceleration is equal to SA_H (0.87g). This is determined from the digitized IHF X - direction ISRS at the ground floor in Reference E2.2.8.

$$f_{es} := 0.8 \cdot Hz$$

$$\delta_s := \frac{c_s}{\left(2 \cdot \pi \cdot f_{es}\right)^2} = 1.197 \cdot ft$$ Less than the 1.5 feet clearance

1.74 times the BDBGM

At the frequency of 0.74 Hz, 1.74 times the 10% damped BDBGM floor spectral acceleration is equal to SA_H (0.87g). This is determined from the digitized IHF X - direction ISRS at the ground floor in Reference E2.2.8.

$$f_{es} := 0.74 \cdot Hz$$

$$\delta_s := \frac{c_s}{\left(2 \cdot \pi \cdot f_{es}\right)^2} = 1.4 \cdot ft$$ This approximately equals 1.5 feet.

$$\delta_{wall\_slide} := \delta_s = 1.399 \cdot ft$$

$$F_{S\_wall} := \frac{\Delta_{wall}}{\delta_{wall\_slide}} = 1.072$$

Note that this strength factor is relative to 1.74 times the BDBGM.

2.3 times the BDBGM

At the frequency of 0.53 Hz, 2.3 times the 10% damped BDBGM floor spectral acceleration is equal to SA_H (0.87g).

$$f_{es} := 0.53 \cdot Hz$$

$$\delta_s := \frac{c_s}{\left(2 \cdot \pi \cdot f_{es}\right)^2} = 2.73 \cdot ft$$ This slightly exceeds the 2.5 feet clearance.

$$\delta_{col\_slide} := \delta_s = 2.727 \cdot ft$$

$$F_{S\_col} := \frac{\Delta_{col}}{\delta_{col\_slide}} = 0.917$$

Note that this strength factor is relative to 2.3 times the BDBGM.

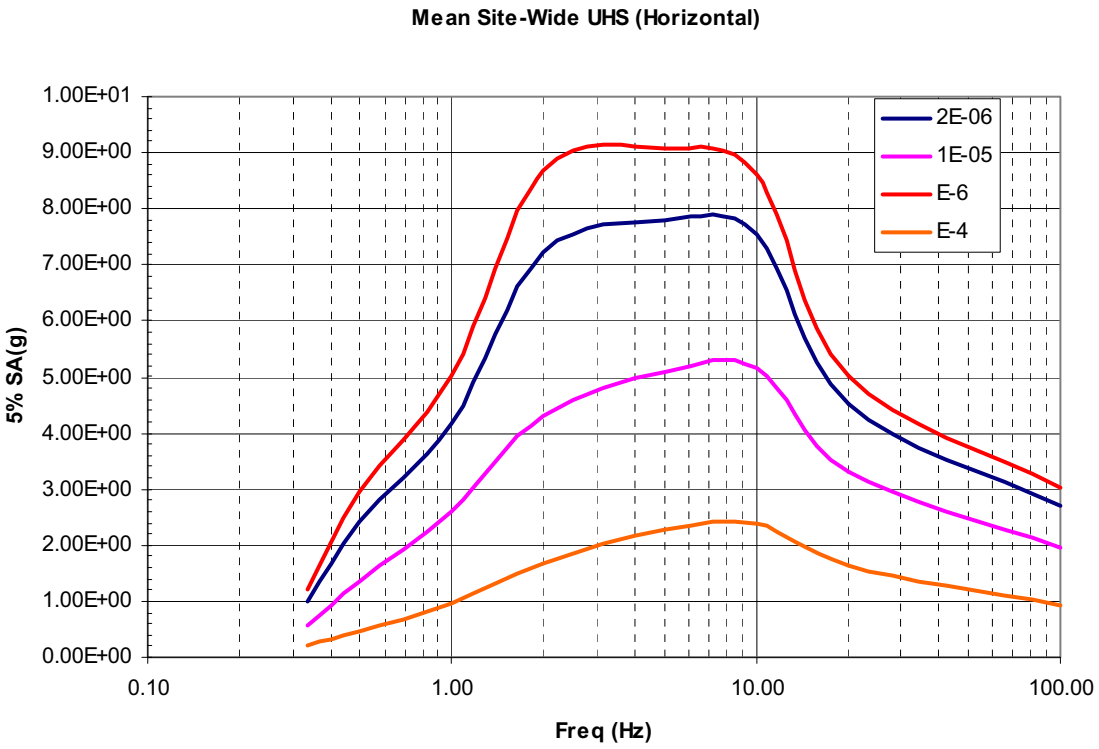

Figure E6.5-2. 5% Damped Mean Site-Wide Horizontal Uniform Hazard Spectra at E-4, E-5, 2E-6 and E-6 APE (See Section 6.2.2.1 for source information)

E6.5.1.1 Uncertainty in Equation

A factor of safety of 2 is recommended for the calculated rigid body displacement for design purposes (Appendix A.1 of Reference E2.2.7). Based on common design practice, a design value typically represents at least a 98% non-exceedance value. Based on this, uncertainty associated with the best-estimate displacement is calculated.

$\beta_{U\_S\_1} := \frac{1}{2} \cdot \ln(2)$

$\beta_{U\_S\_1} = 0.35$

The 98% non-exceedance value is two (2) standard deviation from the mean. The second value of 2 in the equation is the factor of safety recommended for the design value.

$\beta_{R\_S} := 0$

There is no randomness associated with the strength factor.

E6.5.1.2 Uncertainty in Coeff. of Friction

A median value of 0.47 is used for coefficient friction between steel and concrete based on Reference E2.2.10. A -1σ value of 0.40 is estimated based on the same reference for normal stress in the range of 50 to 100 psi (Figure 4 of Reference E2.2.10).

$\mu_{1\sigma} := 0.4$

$c_{s\_1\sigma} := 2 \cdot \mu_{1\sigma} \cdot g$

$c_{s\_1\sigma} = 0.8 \cdot g$

Based on the reserve energy method, the sliding displacement of the rigid body is estimated by Equation A-3 of Reference E2.2.7 in which f_{eS} is the lowest natural frequency at which the vector horizontal spectral acceleration equals to c_s.

$SA_H := 0.1 \cdot g$ Initial trial value of SA_H (i.e., spectral acceleration in one horizontal direction) to solve the equation below so that the vector horizontal spectral acceleration is equal to c_s

Given $\sqrt{SA_H^2 + 0.16 SA_H^2} = c_{s\_1\sigma}$ Assuming the two horizontal components of earthquake have the same spectral shape. Equation A-4 of Reference E2.2.7.

$SA_H := \text{Find}(SA_H)$

$SA_H = 0.74 \cdot g$

Impact with Transfer Cell Walls

The lowest natural frequency (f_{eS}) at which the vector spectral acceleration equals c_s is determined from the **1.5** times the 10% damped BDBGM ISRS at the ground floor.

$f_{es} := 0.653 \cdot Hz$

$\delta_{s\_1\sigma} := \frac{c_{s\_1\sigma}}{(2 \cdot \pi \cdot f_{es})^2}$ Equation A-3 of Reference E2.2.7

$\delta_{s\_1\sigma} = 1.529 \cdot ft$ Approximately equals the 1.5 feet clearance

$\beta_{U\_S\_2} := -\ln\left(\frac{1.5}{1.74}\right)$ See Section E6.5.1 for the scale factor 1.74 applied to the BDBGM to reach a sliding displacement of 1.5 feet.

$\beta_{U\_S\_2} = 0.148$

$\beta_{U\_S\_wall} := \sqrt{\beta_{U\_S\_1}^2 + \beta_{U\_S\_2}^2}$

$\beta_{U\_S\_wall} = 0.377$

Impact with Steel Columns

The lowest natural frequency (f_{eS}) at which the vector spectral acceleration equals c_s is determined from the **1.9** times the 10% damped BDBGM ISRS at the ground floor.

$f_{es} := 0.515 \cdot Hz$

$\delta_{s\_1\sigma} := \frac{c_{s\_1\sigma}}{\left(2 \cdot \pi \cdot f_{es}\right)^2}$ Equation A-3 of Reference E2.2.7

$\delta_{s\_1\sigma} = 2.458 \cdot ft$ Close to the 2.5 feet clearance between the trolley and the steel columns.

$\beta_{U\_S\_2} := -\ln\left(\frac{1.9}{2.3}\right)$ See Section E6.5.1 for the scale factor 2.3 applied to the BDBGM to reach a sliding displacement of 2.5 feet.

$\beta_{U\_S\_2} = 0.191$

$\beta_{U\_S\_col} := \sqrt{\beta_{U\_S\_1}^2 + \beta_{U\_S\_2}^2}$

$\beta_{U\_S\_col} = 0.396$

E6.5.2 Inelastic Energy Absorption Factor

For rigid body sliding, there is no inelastic energy absorption capability. Thus,

$F_\mu := 1.0$

$\beta_{R\_\mu} := 0$

$\beta_{U\_\mu} := 0$

E6.5.3 Structural Response Factors

Figures E6.4-1 and E6.4-2 show that the BDBGM ISRS in the frequency range from 0.2 Hz to 1 Hz is essentially the same as the site-wide BDBGM UHS. Since the seismic-induced sliding of the Cask Transfer Trolley is responding in this low frequency range, the trolley is treated as a structure founded at grade.

E6.5.3.1 Spectral Shape Factor

$F_{SA} := 1.0$ The mean BDBGM UHS was used.

Since uncertainty in the UHS is derived from uncertainty in the seismic hazard curves which will be

included in the final risk quantification, no additional uncertainty is included under the spectral shape factor to avoid double-counting the hazard uncertainty, hence

$\beta_{U\_SA} := 0$

$\beta_{R\_SA} := 0.2$ This is random variability to account for peak to valley variability of a smooth ground response spectrum (Reference E2.2.1).

E6.5.3.2 Damping Factor

A damping value of 10% is suggested in Reference E2.2.7 for the rigid body sliding calculation. Since 10% damped spectrum was used in the strength factor calculation, thus

$F_{\delta} := 1.0$

$\beta_{U\_\delta} := 0.05$ Nominal value

$\beta_{R\_\delta} := 0$

E6.5.3.3 Modeling Factor

The reserve energy method used in calculating the sliding displacement above is a conservatively biased "best estimate" method (Section A.1 of Reference E2.2.7). Using this method, a factor of safety of 2.0 is recommended to obtain design value of sliding (Reference E2.2.7). Thus, the modeling factor of safety is assigned a value of unity.

$F_M := 1$

$\beta_{R\_M} := 0$

$\beta_{U\_M} := 0$ Since the modeling uncertainty is already included in the uncertainty of equation in Section E6.5.1.1.

E6.5.3.4 Modal Combination

Since it is a single mode response,

$F_{MC} := 1$

$\beta_{R\_MC} := 0.05$ A nominal value.

$\beta_{U\_MC} := 0$

E6.5.3.5 Earthquake Component Combination

In the strength factor calculation above, the best-estimate vector spectral acceleration is the combination of S_{AH} and 0.4*S_{AH}. The vector of 100% of both horizontal components is at 3 sigma from the median case.

$F_{EC} := 1.0$ Since the best-estimate earthquake component combination is used in the above strength factor calculation.

$SA_H := 0.1 \cdot g$ Initial trial value of SA_H (i.e., spectral acceleration in one horizontal direction) to solve the equation below so that the vector horizontal spectral acceleration is equal to c_s

Given

$$\sqrt{SA_H^2 + SA_H^2} = c_s$$

$$a_{3\sigma} := \text{Find}(SA_H)$$

$$a_{3\sigma} = 0.66 \cdot g$$

The lowest natural frequency (f_{eS}) at which the vector spectral acceleration equals c_s is determined from the **1.4** times the 10% damped BDBGM ISRS at the ground floor.

$$f_{es} := 0.72 \cdot Hz$$

$$\delta_{s\_3\sigma} := \frac{c_s}{\left(2 \cdot \pi \cdot f_{es}\right)^2}$$

$$\delta_{s\_3\sigma} = 1.478 \cdot ft$$

$\beta_{R\_EC} := \frac{-1}{3} \cdot \ln\left(\frac{1.4}{1.74}\right)$ See Section E6.5.1 for the scale factor 1.74 applied to the BDBGM to reach a sliding displacement of 1.5 feet.

$$\beta_{R\_EC} = 0.072$$

$$\beta_{U\_EC} := 0$$

E6.5.3.6 Soil-Structure Interaction

The soil-structure interaction effects were considered in the BSC Tier 1 IHF seismic response analysis (Reference E2.2.8) using frequency independent soil springs and soil damping coefficients based on an elastic half space. The calculated translational soil damping coefficients were reduced by 25% to account for layering effects. Four boundary conditions were considered in the BSC SSI analysis (Section E6.4). It is seen from Figures E6.4-1 and E6.4-2 that in the frequency range of sliding of the CTT, there is practically no difference in the response due to difference in soil depth and soil

properties. Thus, the factor of safety of the soil-structure interaction analysis is set as unity.

$F_{SSI} := 1.0$

$\beta_{R\_SSI} := 0$

$\beta_{U\_SSI} := 0.05$ Nominal value used

E6.5.4 Overall Factor of Safety of CTT Sliding

CTT Slides and Impacts Transfer Cell Walls

$F_{total} := F_{S\_wall} \cdot F_{\mu} \cdot F_{SA} \cdot F_{\delta} \cdot F_{M} \cdot F_{MC} \cdot F_{EC} \cdot F_{SSI}$

$F_{total} = 1.072$

$PGA := (1.74) \cdot 0.914g$ Peak ground acceleration is 1.74 times the PGA of the BDBGM site-wide UHS since the strength factor was calculated relative to 1.74 times the BDBGM (Section E6.4).

$A_{m\_wall} := F_{total} \cdot PGA$

$A_{m\_wall} = 1.705 \cdot g$ Median seismic capacity in terms of PGA

$$\beta_R := \sqrt{\beta_{R\_S}^2 + \beta_{R\_\mu}^2 + \beta_{R\_SA}^2 + \beta_{R\_\delta}^2 + \beta_{R\_M}^2 + \beta_{R\_MC}^2 + \beta_{R\_EC}^2 + \beta_{R\_SSI}^2}$$

$\beta_R = 0.219$

$$\beta_U := \sqrt{\beta_{U\_S\_wall}^2 + \beta_{U\_\mu}^2 + \beta_{U\_SA}^2 + \beta_{U\_\delta}^2 + \beta_{U\_M}^2 + \beta_{U\_MC}^2 + \beta_{U\_EC}^2 + \beta_{U\_SSI}}$$

$\beta_U = 0.384$

$\beta_c := \sqrt{\beta_R^2 + \beta_U^2}$

$\beta_c = 0.441$

$HCLPF\_wall := A_{m\_wall} \cdot e^{-2.33 \cdot \beta_c}$

$HCLPF\_wall = 0.61 \cdot g$

CTT Slides and Impacts Steel Columns

$F_{total} := F_{S\_col} \cdot F_{\mu} \cdot F_{SA} \cdot F_{\delta} \cdot F_{M} \cdot F_{MC} \cdot F_{EC} \cdot F_{SSI} = 0.917$

$PGA := (2.3) \cdot 0.914g$ Peak ground acceleration is 2.3 times the PGA of the BDBGM site-wide UHS since the strength factor was calculated relative to 2.3 times the BDBGM (Section E6.4).

$$\beta_U := \sqrt{\beta_{U\_S\_col}^2 + \beta_{U\_\mu}^2 + \beta_{U\_SA}^2 + \beta_{U\_\delta}^2 + \beta_{U\_M}^2 + \beta_{U\_MC}^2 + \beta_{U\_EC}^2 + \beta_{U\_SSI}^2}$$

$$\beta_c := \sqrt{\beta_R^2 + \beta_U^2}$$

$A_{m\_col} := F_{total} \cdot PGA = 1.927 \cdot g$ Median seismic capacity in terms of PGA

$\beta_c = 0.458$

$HCLPF\_col := A_{m\_col} \cdot e^{-2.33 \cdot \beta_c}$

$HCLPF\_col = 0.664 \cdot g$

E6.6 SEISMIC FRAGILITY OF SEISMIC-INDUCED ROCKING OF TROLLEY

The approach in Appendix A.2 of Reference E2.2.7 is used to calculate the median seismic capacity of trolley tipover in a seismic event. The approach accounts for a frequency shift when an unanchored rigid body is subjected to a seismic event and initiates rocking. As the rocking angle increases, the equivalent frequency of the rocking block becomes less. Instability (i.e., tipover) occurs when the center of gravity of the rigid block is directly over point B shown in Figure E6.6-1. This occurs when the rocking angle is equal to the instability angle defined by arctan(a) where a is the ratio of b to h (see Figure E6.6-1 for definition of b and h).

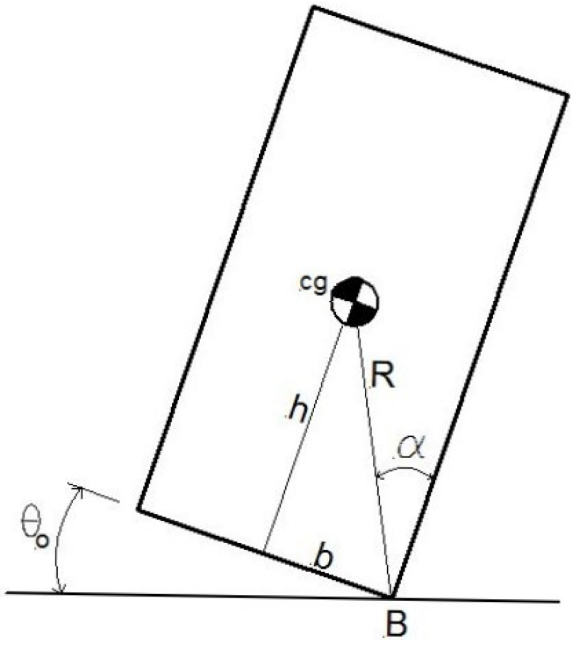

Figure E6.6-1. Rigid Body Rocking Definitions (Figure 7-1 of Ref. E2.2.7)

The center of gravity of a loaded Cask Transfer Trolley is 210 inches from the floor (see Section E6.3.5). The base of the trolley is 18' square. Data required for the tipover analysis are presented below.

$h_{cg} := 210 \cdot in$	Center of gravity height measured from the floor
$b := 107 \cdot in$	Minimum horizontal distance from the edge of the rigid body to the center of gravity (see Section E6.3.5).

$a := \frac{b}{h_{cg}} = 0.51$

$\alpha := \text{atan}(a) = 0.471$ instability angle in radians (equals 27 degrees)

$C_I := \frac{4}{3}\cdot\left(1 + a^2\right)$ Equation A-6(f) of Reference E2.2.7

$C_I = 1.679$

$C_R := 1 - \frac{2\cdot a^2}{C_I}$ Equation A-6(e) of Reference E2.2.7

$\gamma := -2\cdot\ln\left(C_R\right)$ Equation A-6(d) of Reference E2.2.7

$\beta_e := \frac{\gamma}{\sqrt{4\cdot\pi^2 + \gamma^2}}$ Effective damping, Equation A-6(b) of Reference E2.2.7

$\beta_e = 0.117$ Note that the Tier 1 ISRS (DBGM-2 and BDBGM) are plotted only up to 10% of critical damping case. Thus, use 10% damping in the calculation below.

$\beta_e := 0.1$

The rigid body rocking of the trolley is evaluated for the following earthquakes: BDBGM (1E-4 APE) and 1E-5 APE.

E6.6.1 BDBGM Earthquake

$\theta_0 := 0.0155\cdot\text{rad}$ This angle of rocking is determined after a few iterations by assuming an angle and compare the seismic demand (SAH) with the seismic capacity (SAH_{CAP}). A converged solution is obtained when SAH is equal to SAH_{CAP} (Ref. E2.2.7).

$\theta_0 = 0.888\cdot\text{deg}$

$f_1 := \cos\left(\theta_0\right) + a\cdot\sin\left(\theta_0\right) = 1.008$ Equation A-5(a) of Ref. E2.2.7

$f_e := \frac{1}{2\cdot\pi}\cdot\left[\frac{2\cdot\left(f_1 - 1\right)\cdot g}{C_I\cdot\theta_0^{\,2}\cdot h_{cg}}\right]^{0.5} = 1.34\cdot\text{Hz}$ Effective rocking frequency, Equation A-6(a) of Ref. E2.2.7

At this frequency, the 10% damped BDBGM ISRSs are:

$SAH := 0.984g$ Digitized ISRS at ground floor of IHF (Ref. E2.2.8). Note that difference of accelerations of the four boundary conditions is insignificant such that the enveloping accelerations are used.

$SAV := 0.495\cdot g$

$F_H := 1$ No correction is made for vertical and horizontal masses and their respective distances from center of rotation for small angle of rocking.

$$F_V := \left[1 + \left(\frac{a \cdot SAV}{F_H \cdot SAH}\right)^2\right]^{0.5}$$ Equation A-5(c) of Ref. E2.2.7

$F_V = 1.032$

$$SAH_{CAP} := \frac{2 \cdot g \cdot (f_1 - 1)}{F_H \cdot F_V \cdot \theta_0}$$ Equation A-5 of Ref. E2.2.7

$SAH_{CAP} = 0.972 \cdot g$

$\theta_{BE\_BDBGM} := \theta_0 = 0.888 \cdot deg$

The capacity approximately equals the demand. Thus, the best-estimate maximum rocking angle when the trolley is subjected to the BDBGM is . Since this angle is less than instability angle, the trolley will not tip over.

E6.6.2 1E-5 APE Earthquake

Since the Tier-1 seismic response analyses were performed only for DBGM-2 and BDBGM, there are no ISRS for 1E-5. As shown in Figure E6.4-1, the difference between the UHS and the ISRS at the ground floor in the low frequency range (<1 Hz) is not significant. Therefore, the site-wide UHS are used for the 1E-5 APE earthquake.

$\theta_0 := 0.12 \cdot rad$ This angle of rocking is determined after a few iterations by assuming an angle and compare the seismic demand (SAH) with the seismic capacity (SAH_{CAP}). A converged solution is obtained when SAH is equal to SAH_{CAP}.

$\theta_0 = 6.875 \cdot deg$

$f_1 := \cos(\theta_0) + a \cdot \sin(\theta_0) = 1.054$

$$f_e := \frac{1}{2 \cdot \pi} \cdot \left[\frac{2 \cdot (f_1 - 1) \cdot g}{C_I \cdot {\theta_0}^2 \cdot h_{cg}}\right]^{0.5} = 0.455 \cdot Hz$$ Effective rocking frequency

At this frequency, the 10% damped spectral accelerations from the 1E-5 APE UHS are:

$SAH_{5\%} := 1.148 \cdot g$ Interpolated from the 5% damped 1E-5 UHS accelerations of 0.3 and 0.4 Hz in Table E6.5-1.

$SAH := 0.874g$ Interpolated from the 10% damped 1E-5 UHS accelerations of 0.3 and 0.4 Hz in Table E6.5-1.

$SAV_{5\%} := 0.65 \cdot g$ Figure E6.6-2

$$SAV := SAV_{5\%} \cdot \left(\frac{SAH}{SAH_{5\%}} \right)$$

$SAV = 0.495 \cdot g$

$F_H := 1$ No correction is made for vertical and horizontal masses and their respective distances from center of rotation for small angle of rocking.

$$F_V := \left[1 + \left(\frac{a \cdot SAV}{F_H \cdot SAH} \right)^2 \right]^{0.5}$$

$F_V = 1.041$

$$SAH_{CAP} := \frac{2 \cdot g \cdot \left(f_1 - 1 \right)}{F_H \cdot F_V \cdot \theta_0}$$

$SAH_{CAP} = 0.862 \cdot g$

$\theta_{BE\_1} := \theta_0 = 6.875 \cdot deg$

The capacity is slightly lower than the demand. Thus, the best-estimate maximum rocking angle when the trolley is subjected to the 1E-5 UHS is . Since this angle is less than the instability angle, the trolley will not tip over.

Based on the above result for the 1E-5 APE earthquake, tipover is not expected when the trolley is subjected to the 2E-06 APE site-wide ground motion.

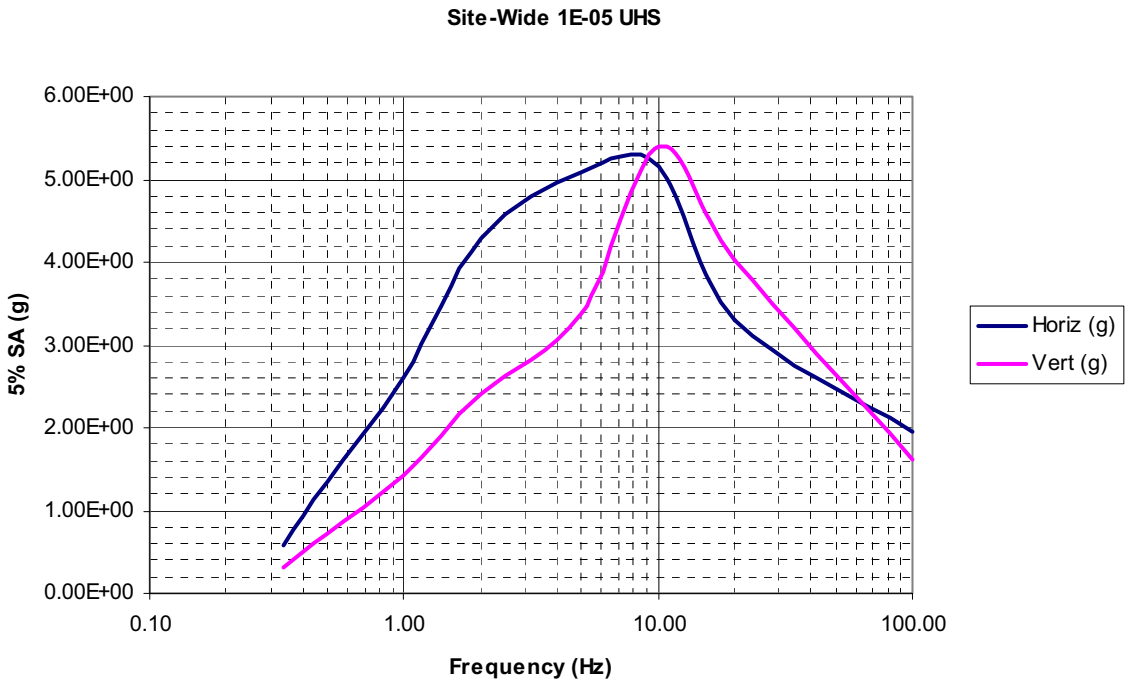

Figure E6.6-2. 5% Damped 1E-5 APE UHS (See Section 6.2.2.1 for source information)

Next, the lateral displacement at the top of the trolley at each of the best-estimate angles of rocking is calculated.

As discussed in Section E6.2, the overall heights measured from the top of the cask and from the top of the trolley frame to the base of the trolley are 387 inches and 301 inches, respectively. Impact to the adjacent reinforced concrete walls due to rigid body rocking of the trolley will occur between the top of the trolley ring frame and the walls. Because the 92" diameter cask (Reference E2.2.2) is recessed from the perimeter of the trolley frame, there will be no direct impact between the top of the cask and the cell walls.

Also shown in Reference E2.2.2, the trolley ring frame tapers off near the top. However, the clearance between the cask restraint assembly at the top of the ring frame is only 1.5 feet estimated from Reference E2.2.2. Thus, the limiting rocking displacement is 1.5 feet.

$$\Delta_{rocking} := 1.5 \cdot ft$$

$h_{trolley} := 301 \cdot in$ Measured from the bottom of the trolley to the top of the trolley ring frame (Section E6.2).

BDBGM (1E-4 APE)

$\Delta_{BDBGM} := h_{trolley} \cdot \sin(\theta_{BE\_BDBGM})$

$\Delta_{BDBGM} = 0.389 \cdot ft$

This rocking displacement is much less than the 1.5 feet gap between the the top of the trolley ring frame and the cask restraint assembly. Thus no impact will occur at BDBGM.

1E-05 APE

$\Delta_{1E05} := h_{trolley} \cdot \sin(\theta_{BE\_1})$

$\Delta_{1E05} = 3.003 \cdot ft$

Thus impact of the trolley to the transfer cell wall will occur at ground motion between BDBGM and 1E-05 APE.

Next, the capacity factor at the occurrence of the impact is calculated.

$$\theta_i := \operatorname{atan}\left(\frac{\Delta_{rocking}}{h_{trolley}}\right)$$

$\theta_i = 3.422 \cdot deg$

$f_1 := \cos(\theta_i) + a \cdot \sin(\theta_i) = 1.029$ Equation A-5(a) of Ref. E2.2.7

$$f_e := \frac{1}{2 \cdot \pi} \cdot \left[\frac{2 \cdot (f_1 - 1) \cdot g}{C_l \cdot \theta_i^{\,2} \cdot h_{cg}}\right]^{0.5} = 0.667 \cdot Hz$$ Effective rocking frequency, Equation A-6(a) of Ref. E2.2.7

At 1.75 times BDBGM Ground Motion

$SF := 1.75$

At f_e frequency, the 10% damped BDBGM ISRSs are:

$SAH := SF \cdot (0.497g)$ where 0.497g and 0.259g are 10% damped horizontal and vertical BDBGM floor spectral accelerations, respectively, from

$SAH = 0.87 \cdot g$

$SAV := SF \cdot (0.259 \cdot g)$

$SAV = 0.453 \cdot g$

the digitized ISRS at the ground floor of the IHF (Ref. E2.2.8). Note that difference of accelerations of the four boundary conditions is insignificant such that the enveloping accelerations are used here.

$F_H := 1$

No correction is made for vertical and horizontal masses and their respective distances from center of rotation for small angle of rocking.

$$F_V := \left[1 + \left(\frac{a \cdot SAV}{F_H \cdot SAH}\right)^2\right]^{0.5}$$

Equation A-5(c) of Ref. E2.2.7

$F_V = 1.035$

$$SAH_{CAP} := \frac{2 \cdot g \cdot (f_1 - 1)}{F_H \cdot F_V \cdot \theta_i}$$

Equation A-5 of Ref. E2.2.7

$SAH_{CAP} = 0.927 \cdot g$ The capacity is greater than the demand.

At 1.86 times BDBGM Ground Motion

$SF := 1.86$

At f_e frequency, the 10% damped BDBGM ISRSs are:

$SAH := SF \cdot (0.497g)$

$SAH = 0.924 \cdot g$

$SAV := SF \cdot (0.259 \cdot g)$

$SAV = 0.482 \cdot g$

$F_H := 1$

No correction is made for vertical and horizontal masses and their respective distances from center of rotation for small angle of rocking.

$$F_V := \left[1 + \left(\frac{a \cdot SAV}{F_H \cdot SAH}\right)^2\right]^{0.5}$$

Equation A-5(c) of Ref. E2.2.7

$F_V = 1.035$

$$SAH_{CAP} := \frac{2 \cdot g \cdot (f_1 - 1)}{F_H \cdot F_V \cdot \theta_i}$$

Equation A-5 of Ref. E2.2.7

$SAH_{CAP} = 0.927 \cdot g$ The capacity equals the demand.

$F_{S\_rocking} := SF = 1.86$ Capacity factor

Uncertainty in Equation

A factor of safety of 2 is recommended for the calculated rigid body rocking angle for design purposes (Section 7.1 of Reference E2.2.7). Based on common design practice, a design value typically represents at lease a 98% non-exceedance value. Based on this, uncertainty associated with the best-estimate displacement is calculated.

$\beta_{U\_S} := \frac{1}{2} \cdot \ln(2)$ The 98% non-exceedance value is two (2) standard deviation from the mean. The second value of 2 in the equation is the factor of safety recommended for design value.

$\beta_{U\_S} = 0.35$

$\beta_{R\_S} := 0$ There is no randomness associated with the strength factor.

E6.6.4 Inelastic Energy Absorption Factor

For rigid body rocking, there is no inelastic energy absorption capability. Thus,

$F_{\mu} := 1.0$

$\beta_{R\_\mu} := 0$

$\beta_{U\_\mu} := 0$

E6.6.5 Structural Response Factors

As shown in Figures E6.4-1 and E6.4-2, the BDBGM ISRS in the frequency range from 0.2 Hz to 1 Hz is essentially same as the site-wide BDBGM UHS. Thus, the trolley may be treated as a structure at grade.

E6.6.5.1 Spectral Shape Factor

$F_{SA} := 1.0$

Since uncertainty in the UHS is derived from uncertainty in the seismic hazard curves which will be included in the final risk quantification, no additional uncertainty is included under the spectral shape factor to avoid double-counting the hazard uncertainty, hence

$\beta_{U\_SA} := 0$

$\beta_{R\_SA} := 0.2$ This is random variability to account for peak to valley variability of a smooth ground response spectrum (Reference E2.2.1).

E6.6.5.2 Damping Factor

An effective damping value of 11.7% was calculated above using the approximate method in Reference E2.2.7 for the rigid body rocking calculation. 10% damped spectral acceleration was used in the strength factor calculation. In the frequency range of the rocking response, the spectral accelerations are not particularly sensitive to the damping values. Thus, the factor of safety is set to unity with slight conservative bias.

$F_{\delta} := 1$

$\beta_{U\_\delta} := 0.0$ Since conservative damping value is used in the rocking calculation.

$\beta_{R\_\delta} := 0$

E6.6.5.3 Modeling Factor

The rigid body rocking is a single degree-of-freedom response. Uncertainty of this approximate method is already accounted for in the uncertainty of the strength factor, thus

$F_M := 1$

$\beta_{R\_M} := 0$

$\beta_{U\_M} := 0$

E6.6.5.4 Modal Combination

Since the approximate method of rocking calculation is essentially a single mode response,

$F_{MC} := 1$

$\beta_{R\_MC} := 0.05$ A nominal value.

$\beta_{U\_MC} := 0$

E6.6.5.5 Earthquake Component Combination

$F_{EC} := 1.0$ Since the best-estimate earthquake component combination is used in the above strength factor calculation.

As shown in the above rocking calculation, the factor F_V (correction for probabilistically combined vertical ground motion) has only a small effect on rocking. Thus,

$\beta_{R\_EC} := 0.05$ A nominal value

$\beta_{U\_EC} := 0$

E6.6.5.6 Soil-Structure Interaction

The soil-structure interaction effects were considered in the BSC Tier 1 IHF seismic response analysis (Reference E2.2.8) using frequency independent soil springs and soil damping coefficients based on elastic half space. The calculated translational soil damping coefficients were reduced by 25% to account for layering effects. Four boundary conditions were considered in the BSC SSI analysis (Section E6.4). It is seen from Figures E6.4-1 and E6.4-2 that in the frequency range of rocking of the CTT, there is practically no difference in the response due to the differences in soil properties. Thus, the factor of safety of the soil-structure interaction analysis is set as unity.

$F_{SSI} := 1.0$

$\beta_{R\_SSI} := 0$

$\beta_{U\_SSI} := 0.05$ Nominal value assumed

E6.6.6 Overall Factor of Safety of CTT Rocking

$F_{total} := F_{S\_rocking} \cdot F_{\mu} \cdot F_{SA} \cdot F_{\delta} \cdot F_{M} \cdot F_{MC} \cdot F_{EC} \cdot F_{SSI}$

$F_{total} = 1.86$

$PGA_{BDBGM} := 0.914g$ Peak ground acceleration of the 1E-4 site-wide UHS is used in the capacity factor calculation.

$A_m := F_{total} \cdot PGA_{BDBGM}$

$A_m = 1.7 \cdot g$ Median seismic capacity in terms of PGA

$$\beta_R := \sqrt{\beta_{R\_S}^2 + \beta_{R\_\mu}^2 + \beta_{R\_SA}^2 + \beta_{R\_\delta}^2 + \beta_{R\_M}^2 + \beta_{R\_MC}^2 + \beta_{R\_EC}^2 + \beta_{R\_SSI}^2}$$

$\beta_R = 0.212$

$$\beta_U := \sqrt{\beta_{U\_S}^2 + \beta_{U\_\mu}^2 + \beta_{U\_SA}^2 + \beta_{U\_\delta}^2 + \beta_{U\_M}^2 + \beta_{U\_MC}^2 + \beta_{U\_EC}^2 + \beta_{U\_SSI}^2}$$

$\beta_U = 0.35$

$$\beta_c := \sqrt{\beta_R^2 + \beta_U^2}$$

$\beta_c = 0.409$

$HCLPF := A_m \cdot e^{-2.33 \cdot \beta_c} = 0.655 \cdot g$

E7. SUMMARY

The seismic-induced failures of the Cask Transfer Trolley due to rigid body sliding or rocking were evaluated and their seismic fragilities are presented below:

Sliding 1: The Cask Transfer Trolley slides and impacts the transfer cell wall (Section E6.5). The impact velocity is expected to be low due to the small gap of 1.5 feet.

A_m = 1.7g β_c = 0.44 HCLPF = 0.61g

Sliding 2: The Cask Transfer Trolley slides while in the cask preparation area and impacts the steel columns supporting the Cask Handling Crane (Section E6.5).

A_m = 1.93g β_c = 0.46 HCLPF = 0.66g

Rocking: Impact of the cask seismic restraint assembly with the cell walls due to rocking of the trolley (Section E6.6). Failure of the seismic restraint assembly could result in slapdown of the cask.

A_m = 1.7g β_c = 0.41 HCLPF = 0.65g

No tipover is expected at 2E-06 APE earthquake when the trolley is in the cask preparation area.

At the median and the HCLPF capacities, the impact velocity due to sliding or rocking of the Cask Transfer Trolley is zero. It would require a significantly higher ground motion acceleration to cause significant impact damage.

ATTACHMENT F
FRAGILITY FOR CRCF WASTE PACKAGE TRANSFER TROLLEY

Prepared by: Robert D. Campbell

ARES Check By: Wen H. Tong

LLNL Check By: Robert C. Murray

TABLE OF CONTENTS

ACRONYMS AND ABBREVIATIONS

ACI	American Concrete Institute
AISC	American Institute of Steel Construction
ANSI	American National Standards Insitute
AO	Aging Overpack
APE	Annual Probability of Exceedance
ASCE	American Society of Civil Engineers
ASME	American Society of Mechanical Engineers
BSC	Bechtel SAIC, LLC
BDBGM	Beyond Design Basis Ground Motion at $1x10^{-4}$ APE
CDFM	Conservative Deterministic Failure Margin
CHC	Cask Handling Crane
CIP	Cast-in-Place
CRCF	Canister Receipt and Closure Facility
CTM	Canister Transfer Machine
CTT	Cask Transfer Trolley
DBGM-2	Design Basis Ground Motion at $5x10^{-4}$ APE
DL	Dead Load
DOF	Degree of Freedom
DPC	Dual Purpose Canister
EPRI	Electric Power Research Institute
HCLPF	High Confidence of Low Probability of Failure
HVAC	Heating, Ventilation, & Air Conditioning
IEEE	Institute of Electrical and Electronics Engineers
IHF	Initial Handling Facility
ISRS	In-Structure Response Spectra

ACRONYMS AND ABBREVIATIONS (cont.)

ITS	Important to Safety
LA	License Application
LLNL	Lawrence Livermore National Laboratory
NPP	Nuclear Power Plant
PGA	Peak Ground Acceleration
RF	Receipt Facility
RRS	Required Response Spectrum
Sa	Spectral Acceleration
SFA	Surface Facilities Area
SFTM	Spent Fuel Transfer Machine
SPRA	Seismic Probabilistic Risk Assessment
SRSS	Square Root of the Sum of Squares
SSE	Safe Shutdown Earthquake (used with NPPs)
SSI	Soil Structure Interaction
SSC	Structure, System, and Component
TAD	Transportation, Aging, and Disposal canister
TEV	Transport and Emplacement Vehicle
TRS	Test Response Spectrum
UHS	Uniform Hazard Spectra
USDOE	United States Department of Energy
USNRC	United States Nuclear Regulatory Commission
WHF	Wet Handling Facility
WP	Waste Package
WPTT	Waste Package Transfer Trolley
YMSF	Yucca Mountain Surface Facilities
ZPA	Zero Period Acceleration

FRAGILITY TERMINOLOGY

Am	Median Peak Ground Motion Capacity
β_R	Log Standard Deviation of Randomness
β_U	Log Standard Deviation of Uncertainty (Lack of Knowledge)
β_C	Composite Variability = $(\beta_R^2 + \beta_U^2)^{0.5}$
F_S	Strength Factor of Safety
β_{R_S}	Strength Randomness (typical)
β_{U_S}	Strength Uncertainty (typical)
β_{C_S}	Strength Composite Variability (typical)
F_μ	Inelastic Energy Absorption Factor of Safety
F_{QM}	Qualification Factor of Safety
F_δ	Damping Factor of Safety
F_M	Modeling Factor of Safety
F_{MC}	Modal Combination Factor of Safety
F_{ECC}	Earthquake Component Combination Factor of Safety
F_{SA}	Spectral Shape Factor of Safety
F_{SSI}	Soil-Structure Interaction Factor of Safety
F_{GMI}	Ground Motion Incoherence Factor of Safety
F_{TOTAL}	Total Factor of Safety
F_{RS}	Structural Response Factor of Safety
F_{RE}	Equipment Response Factor of Safety

F1. PURPOSE

The purpose of this calculation is to develop a seismic fragility for the CRCF Waste Package Transfer Trolley (WPTT) when it is loaded with a Waste Package (WP). The WPTT may be in the upright or horizontal position.

F2. REFERENCES

F2.1 PROCEDURES AND DIRECTIVES

F2.1.1 EG-PRO-3DP-G04B-00037, Rev. 10. *Calculations and Analyses*. Las Vegas, Nevada: Bechtel SAIC Company. ACC: ENG.20071018.0001.

F2.1.2 IT-PRO-0011, Revision 7, ICN 0. *Software Management*. Las Vegas, Nevada: Bechtel SAIC Company. ACC: DOC.20070905.0007.

F2.2 DESIGN INPUTS

F2.2.1 EPRI (Electric Power Research Institute) 1994. *Methodology for Developing Seismic Fragilities*. EPRI TR-103959. Palo Alto, California: Electric Power Research Institute. TIC:253770. [DIRS 161329].

F2.2.2 ASCE/SEI 43-05. 2005. *Seismic Design Criteria for Structures, Systems, and Components in Nuclear Facilities*. Reston, Virginia: American Society of Civil Engineers. TIC: 257275. [DIRS 173805]

F2.2.3 BSC (Bechtel SAIC Company) 2007. *CRCF Tier-1 In-Structure Response Spectra*. 060-SYC-CR00-00900-000-00B. Las Vegas, Nevada: Bechtel SAIC Company. ACC: ENG.20071210.0008. [DIRS 184330]

F2.2.4 BSC (Bechtel SAIC Company) 2007. *Mechanical Handling Design Report - Waste Package Transfer Trolley.* 000-30R-WHS0-01200-000 REV 000. Las Vegas, Nevada: Bechtel SAIC Company. ACC: ENG.20071006.0001. [DIRS 183209]

F2.2.5 BSC (Bechtel SAIC Company) 2008. *Canister Receipt and Closure Facility 1 General Arrangement Ground Floor Plan*. 060-P10-CR00-00102-000 REV 00C. Las Vegas, Nevada: Bechtel SAIC Company. ACC: ENG.20080122.0013. [DIRS 184853]

F2.2.6 BSC (Bechtel SAIC Company) 2007. *CRCF-1 and IHF WP Transfer Trolley Mechanical Equipment Envelope Plan & Elevations-Sh 1 of 2.* 000-MJ0-HL00-00101-000 REV 00B. Las Vegas, Nevada: Bechtel SAIC Company. ACC: ENG.20071027.0015. [DIRS 183729]

F2.2.7 ASME NOG-1-2004. 2005 *Rules for Construction of Overhead and Gantry Cranes (Top Running Bridge, Multiple Girder)*. New York, New York: American Society of Mechanical Engineers. TIC: 257672. [DIRS 176239]

F2.2.8 Sliger, A. 2007. "Re: WPTT calcs (Document Link: David Moore." E-mail from A. Sliger to D. Moore, October 4, 2007. ACC: LLR.20080128.0002. [DIRS 184926]

F2.2.9 MO0801HCUHSSFA.001. *Mean Hazard Curves and Mean Uniform Hazard Spectra for the Surface Facilities Area*. Submittal date: 01/11/2008. [DIRS 184802]

F2.2.10 Moore, D. 2007. "*Re: WPTT Question*." E-mail from D. Moore to R. Campbell (rdc956), October 31, 2007. ACC: LLR.20080110.0146. [DIRS 184843]

F2.2.11 [Reserved]

F2.2.12 EPRI (Electric Power Research Institute) 1991. *A Methodology for Assessment of Nuclear Power Plant Seismic Margin (Revision 1).* EPRI NP-6041-SL, Rev. 1. Palo Alto, California: Electric Power Research Institute. TIC: 253771. [DIRS 161330]

F2.2.13 BSC (Bechtel SAIC Company) 2007. *CRCF-1 and IHF WP Transfer Trolley Mechanical Equipment Envelope Elevation & Detail - Sheet 2.* 000-MJ0-HL00-00102-000 REV 00B. Las Vegas, Nevada: Bechtel SAIC Company. ACC: ENG.20071027.0017. [DIRS 183730].

F2.2.14 Moore, D. 2007. "*SSI Factor of Safety.*" E-mail from D. Moore to B. Murray, October 25, 2007. ACC: LLR.20080110.0145. [DIRS 184842]

F2.2.15 Newmark, N.M. and Hall, W.J. 1978. *Development of Criteria for Seismic Review of Selected Nuclear Power Plants*. NUREG/CR-0098. Washington, D.C.: U.S. Nuclear Regulatory Commission, Office of Nuclear Reactor Regulation. ACC: NNA.19890327.0045. [DIRS 177216]

F2.2.16 BSC (Bechtel SAIC Company) 2007. *Nuclear Facilities Buildings Canister Receipt and Closure Facility #1 Details and Sections*. 060-DB0-CR00-00112-000 REV. 00B, Las Vegas, Nevada: Bechtel SAIC Company. ACC: ENG.20080117.0036.

F2.2.17 BSC (Bechtel SAIC Company) 2006. *Seismic Analysis and Design Approach Document.* 000-30R-MGR0-02000-000 Rev. 001. Las Vegas, Nevada: Bechtel SAIC Company. ACC: ENG.20071220.0029. [DIRS 184494]

F2.3 DESIGN CONSTRAINTS

None.

F2.4 DESIGN OUTPUTS

The design outputs are the seismic fragilities for selected failure modes that could result in damage to a waste package and release of radioactive material.

F3. ASSUMPTIONS

F3.1 ASSUMPTIONS REQUIRING VERIFICATION

None.

F3.2 ASSUMPTIONS NOT REQUIRING VERIFICATION

F3.2.1 Detailed designs are not completed so the fragilities are based on Mechanical Equipment Layout Drawings (References F2.2.6 and F2.2.13) and the Mechanical Handling Design Report, (Reference F2.2.4).

F3.2.2 The development of representative fragilities is based on the methodology in Reference F2.2.1. The methodology is well established and quoted in Reference F2.2.17 and does not require any further verification.

F3.2.3 Rocking calculations are performed in accordance with ASCE/SEI 43-05, Reference F2.2.2. This is a consensus standard and is quoted in Reference F2.2.17 and does not require any further verification.

F3.2.4 Other standards used are quoted in Reference F2.2.17 and are industry standards that do not require any further verification.

F4. METHODOLOGY

F4.1 QUALITY ASSURANCE

This calculation is prepared in accordance with Bechtel SAIC LLC procedure EG-PRO-3DP-GO4B-00037, Rev. 10, Reference F2.1.1

F4.2 USE OF SOFTWARE

Mathcad 14 is used in this calculation. The use of this software is classified as Level 2 software per procedure IT-PRO-0011, Rev. 7, Ref. F2.1.2. Therefore the software does not require separate qualification.

F4.3 APPROACH

The standard methodology of Reference F2.2.1 is used for development of a fragility of the rail clamps. The methodology in Reference F2.2.2 is used to perform rocking calculations after failure of the rail clamps.

F5. LIST OF APPENDICES

APPENDIX F-A In-Structure Response Spectra for Base Mat of CRCF

APPENDIX F-B Comparison of Site-Wide DBGM-2 UHS with 100-Foot Alluvium Median Soil UHS

F6. DEVELOPMENT OF FRAGILITY

F6.1 DESCRIPTION OF EQUIPMENT AND OPERATION

The Waste Package Transfer Trolley (WPTT) is shown in Figure F6-1, extracted from Reference F2.2.6. There are two WPTTs in the CRCF and one in the IHF. The CRCF location will be the focus of this fragility calculation. The WPTTs are part of the load out system which also consists of the waste package (WP) transfer carriage docking station. The WPTTs transports an empty WP to the WP positioning room in the CRCF as shown in Ref. F2.2.5 where the WP is loaded with a sealed TAD or DPC which contains spent fuel or high level waste. The WPTT then transports the full WP to the WP sealing location below the WP closure room in the CRCF where the WP is sealed and welds are inspected. Once the WP has been sealed, the WPTT transports the WP to the WP load out room where the WP is loaded onto a Transport and Emplacement Vehicle (TEV) via the WP transfer carriage docking station.

As shown in Figure F6-1, the shield enclosure is in an upright position when it receives a canister from the CTM and is moved to a location under the opening in the WP closure room. After the sealing process, the shield enclosure is rotated to a horizontal position before loading the WP onto the TEV.

Per Reference F2.2.4, the WP is supported both axially and laterally in the shield enclosure by a shield ring on top and a pedestal at the bottom.

Per Reference F2.2.4, the trolley is on a rail system with seismic hold down clamps to the rail to prevent overturning during an earthquake. The rail clamps, rail anchorage and rails are designed to the requirements of ASME-NOG-1, Reference F2.2.7, to assure an adequate seismic design.

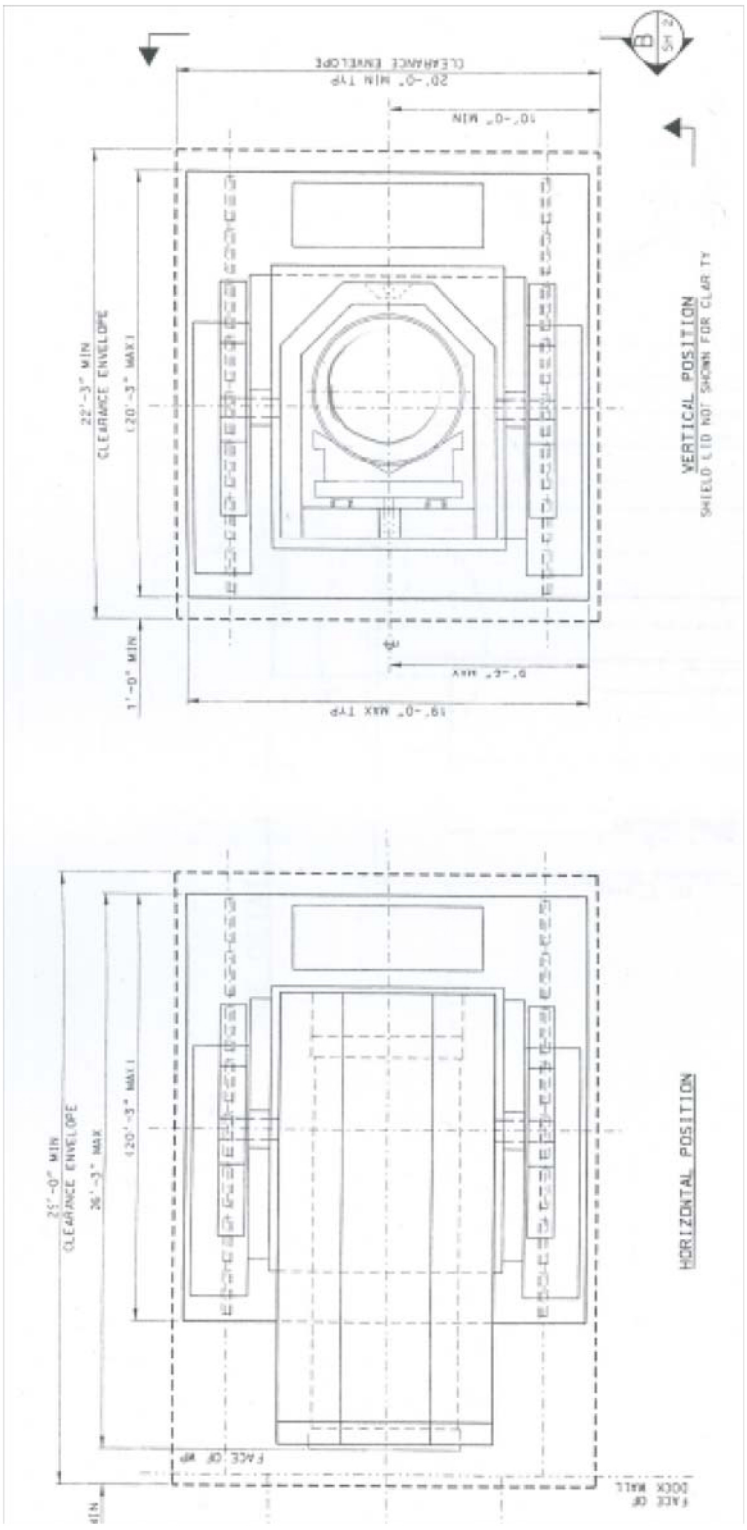

Figure F6-1(a)
Waste Package Transfer Trolley With Waste Package and Canister (Ref. F2.2.6)
NOTE: Legibility of the figure does not affect the technical content of the document. See source for detail

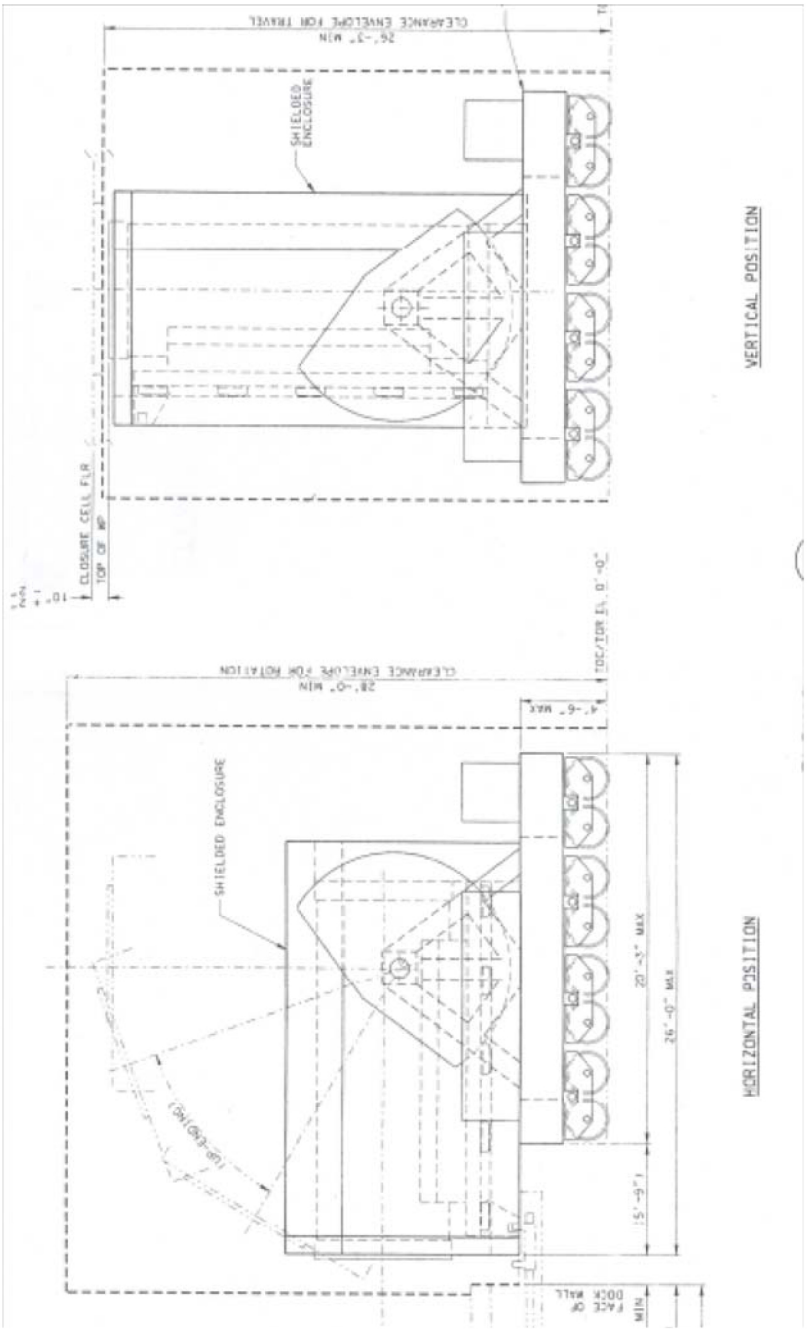

Figure F6-1(b)
Waste Package Transfer Trolley with Waste Package and Canister (Ref. F2.2.6)
NOTE: Legibility of figure does not affect technical content of the document. See source for detail

F6.2 FAILURE MODES AND DESIGN CAPACITIES

The WPTT spends most of its time in the upright position while the waste package is being sealed shut by welding and is inspected. The vertical position is also the most vulnerable during a seismic event due to the fact that the center of gravity is highest in this position and the seismic loads causing overturning moment are highest. In accordance with Reference F2.2.4, there are to be clamps on the rails to resist overturning during a seismic events. The rails are to be secured to resist seismic loads. Per assumption F3.1.1, the rails and anchorage are not yet designed and are not included in this calculation on the basis that they will be stronger than the equipment.

The potential failure modes to be considered are:

1. Failure of the clamps between the trolley and rails that resist overturning.

2. Rocking and impact with the CRCF structure after failure of the rail clamps.

3. Failure of the trolley rotating mechanism when the WPTT is in the vertical position.

4. Sliding in the direction of the rails and impacting the shield door at column line 5 shown in Ref. F2.2.5.

Failure mode 4 is ruled out due to the large distance between the end of the trolley and the shield door when the trolley is in the position where the waste package is being sealed.

The scope of this fragility review includes all elements of the CRCF Cask Handling Crane that rest on top of the crane rails. The fragility of the crane rails, the rail supports, the rail anchorage and the structure are addressed by others.

F6.2.1 Failure of the Clamps Between the Trolley and the Rails

The clamps could fail in bending or by failure of the fasteners to the trolley. For practical construction and maintenance purposes, the clamps would likely be bolted to the trolley and the bolts would be subjected primarily to shear. Per Reference F2.2.4, the rail clamp design would be to ASME NOG-1. The allowable bending stress for the load combination that includes SSE would be 0.9 times the specified yield strength, Fy, (Table 4311-1 in Ref. F2.2.4). The allowable shear stress, τ, for bolting per Table 4315-1 in Ref. F2.2.4, is 0.26 times the ultimate tensile strength of the bolt, Ftu. In the upright position, there would be no load on the clamps until gravity is overcome.

$$\sigma_{bend\text{—}all} = 0.9Fy$$

$$\tau_{all} = 0.26Ftu$$

Per Ref. F2.2.4, the WPTT moves by itself from the WP docking transfer station to the area where the canister is loaded and then to the WP sealing location. Even if there are brakes on the wheels, the WPTT can slide along the rails and would not contribute to uplift load on the rail clamps. Therefore, the rail clamps would only be subjected to seismic loading from overturning in the direction normal to the rails and from the vertical earthquake.

Per References F2.2.8 and F2.2.10, the weight and center of gravity of the fully loaded WPTT are:

$Wt := 680000lbm$ mass of the fully loaded WPTT

$h := 14.06ft$ Height from top of rail to center of gravity

$w := 15ft$ Distance between rails, Ref. F2.2.6, DCN-2

The WPTT would be a fairly stiff design with a fundamental frequency in the two horizontal directions estimated to be greater than 10 Hz. The vertical fundamental frequency would be much higher and is taken as 30 Hz. From Ref. F2.2.3, (see Appendix F-A) the corresponding spectral accelerations for the DBGM-2 horizontal and vertical site wide design spectra at 4% damping for node 24 on the base mat would be:

$Sa_x := 1.2g$ EW

$Sa_y := 1.17g$ NS

$Sa_z := 0.44g$ Vert

Note that it is immaterial what frequencies are estimated in this calculation since the loading of the WPTT in the vertical position is all seismic and the design would be conducted for the corresponding spectral acceleration.

Rails are oriented in the EW direction. Use 1.2g as a maximum design input for the lateral direction and 40% of 0.44g for the vertical direction per the Ref. F2.2.17 and F2.2.15 100-40-40 earthquake component combination design rule. 4% damping is used for design per Ref. F2.2.17. If there is a rail clamp at each outboard wheel location, two clamps resist overturning and 4 clamps resist vertical uplift. The load on a clamp is then:

$$P_{clamp} := \frac{\left(Sa_x \cdot h \cdot Wt\right)}{2 \cdot w} + \frac{\left(0.4 \cdot Sa_z \cdot Wt\right)}{4} - Wt \cdot \frac{g}{4}$$

$P_{clamp} = 2.424 \times 10^5 lbf$ Demand on the clamp

If P_{clamp} results in 0.9Fy in bending or a fastener shear stress of 0.26Ftu, determine the governing failure mode and the factor to failure.

Bending Failure

For structural steel such as A-36, Fy is 36ksi and median Fy is 44ksi (Ref. F2.2.1, Table 3-9). A plastic hinge would form at 1.5 times median yield for a rectangular section in bending. When a hinge forms, the uplift load resistance is lost.

$$\sigma_{hinge} := 36ksi \cdot 1.2 \cdot 1.5$$

$$\sigma_{hinge} = 6.48 \times 10^{4}\ psi$$

$$P_{ult} := P_{clamp} \cdot \left[\frac{\left(\sigma_{hinge}\right)}{0.9 \cdot 36ksi} \right]$$ Ultimate clamp load at failure

$$P_{ult} = 4.847 \times 10^{5}\ lbf$$

$$F_S := \frac{\left(P_{ult} + Wt \cdot \frac{g}{4} \right)}{Wt \cdot \left[\frac{\left(Sa_x \cdot h\right)}{2 \cdot w} + 0.4 \cdot \frac{Sa_z}{4} \right]}$$

$$F_S = 1.588$$

$$\beta_{U\_S} := 0.12$$ Ref. F2.2.1, Table 3-9

This is a ductile failure mode. Per Ref. 2.2.2, Table 8-1, for limit state A, for mechanical equipment supports, a ductility factor of 2 is recommended. For limit state C, essentially elastic response, the ductility factor is 1.25. This is consistent with Ref. F2.2.12 , Table 2-5, for calculating a HCLPF by the CDFM method where ductility can be taken as 1.25. Let the limit state C ductility be a 95th percentile value (Consistent with Ref. F2.2.12, Table 2-5).

$$F_\mu := 2.0$$

$$\beta_{U\_F\mu} := \frac{1}{1.65} \cdot \ln\left(\frac{2}{1.25} \right)$$

$$\beta_{U\_F\mu} = 0.285$$

$$F_{C\_bend} := F_S \cdot F_\mu$$

$$F_{C\_bend} = 3.175$$

$$\beta_{c\_C} := \left(\beta_{U\_S}^{2} + \beta_{U\_F\mu}^{2} \right)^{0.5}$$

$$\beta_{c\_C} = 0.309$$

Shear Failure in Rail Clamp Attachment Fasteners

Now look at the capacity of attachment bolts in shear. The DBGM-2 load at the design limit is P_{clamp} which was previously calculated. This is based on a shear stress of 26% of the specified ultimate tensile strength. The shear ultimate strength is taken as 62% of the ultimate tensile strength (Ref. F2.2.1, Table 3-10) with a median ultimate strength of 1.1 times specified (Ref. F2.2.1, Table 3-9)

$$V_{ult} := P_{clamp} \cdot \left(\frac{0.62 \cdot 1.1}{0.26} \right)$$ Ultimate shear capacity

$$V_{ult} = 6.357 \times 10^5 \text{ lbf}$$

From the above equation for computing the seismic scale factor for bending failure, substitute Vult for Pult to compute the seismic scale factor to shear failure.

$$SF := \frac{\left(V_{ult} + Wt \cdot \frac{g}{4} \right)}{Wt \cdot \left[\frac{\left(Sa_x \cdot h \right)}{2 \cdot w} + 0.4 \cdot \frac{Sa_z}{4} \right]}$$

$$SF = 1.954$$

There is no ductility with this failure mode so fasteners for the rail clamps will govern clamp failure, e.g. $1.954 < F_{C\_bend} = 3.175$.

F6.2.2 Failure of Shield Enclosure Rotating Mechanism

The WPTT mechanism that rotates the shield enclosure, waste package and canister must be designed for earthquake and dead weight in any position. When it is in the vertical position, the moment tending to rotate the shield enclosure at the rotation point is governed totally by earthquake in the longitudinal direction of the trolley. If the trolley is rigidly clamped to the rails, the moment can be calculated as the spectral acceleration times the weight at the CG times the distance from the rotation point to the CG. From the center of gravity locations in the horizontal and vertical position from Ref. F2.2.8, the following information about the location of the center of gravity is provided.

CG in vertical position is 14.06 feet above rail and -9.84 feet from back of trolley

CG in horizontal position is 9.72 feet from top of rail and -15.38 feet from back of trolley.

Then the distance from the point of rotation to the Center of gravity (CG) can be estimated from these dimensions.

$d_{CG1} := 15.38\,ft - 9.84\,ft$

$d_{CG1} = 5.54\,ft$

$d_{CG2} := 14.06\,ft - 9.72\,ft$

$d_{CG2} = 4.34\,ft$

The centers of gravity cited in Ref. F2.2.8 include the weight of the trolley as well as the weights of the shield enclosure, WP and canister, thus do not pin point the location of the rotation hinge.

Dimensions are not given on the Ref. F2.2.6 and F2.2.13 drawings. Scaling of the drawings results in the rotation point being about 58 inches from center of the shield enclosure. An average of the locations determined from center of gravity dimensions is:

$$d_{CG} := \frac{\left(d_{CG1} + d_{CG2}\right)}{2}$$

$d_{CG} = 4.94\,ft$

This is close to the dimension determined from scaling of the drawings. Use 5 feet as a reasonable estimate.

$D_{CG} := 5\,ft$

Let Wt_{se} be the mass to be rotated with an arbitrary value of 1/2 Wt. This estimate does not affect results since it is used for a comparison of design moments in the horizontal and vertical positions where both moment equations include D_{CG} and Wt_{se}.

$Wt_{se} := 0.5 \cdot Wt$

$$M_V := \frac{\left(Sa_y \cdot d_{CG} \cdot Wt_{se}\right)}{g}$$

Moment about rotation point when in vertical position where Wt_{se} is the mass of the shield enclosure plus WP plus canister.

$M_V = 1.965 \times 10^6\,ft \cdot lb$

When in the horizontal position, the dead weight plus vertical acceleration from DBGM-2 results in M_H

$$M_H := \frac{\left[\left(Sa_Z + g\right) \cdot D_{CG} \cdot Wt_{se}\right]}{g}$$

$M_H = 2.448 \times 10^6\,ft \cdot lb$

Total demand in the horizontal position is greatest but is governed by dead weight.

Per Ref. F2.2.4, paragraph 3.3.2, the gear drive mechanism for rotating the shield enclosure must be a dual system with each designed for the full torque load. The drive system is a worm gear such that upon loss of power, tilting cannot occur unless both drive mechanisms fail structurally. The gear drive system itself would have a high margin since the system would likely be designed for fatigue and normal operating stresses would be low. Since a detailed design does not exist, the fragility will be developed as a representative fragility for a structural failure as was done for the rail clamp. In that case, fasteners were shown to have the governing failure margin. Per ASME NOG-1, Ref. F2.2.7, Table 4315-1, the shear allowable for normal operating loads is 0.17 times the ultimate tensile strength, Ftu, and the shear allowable for extreme environment is 0.26 times Ftu. With a dual drive system, the effective moments acting on the drive mechanism are 1/2 of the full moment for which each drive mechanism is designed. The vertical acceleration for DBGM-2 is 0.44g so the strength design would potentially be governed by dead weight since the allowable stress for extreme environment loads is 1.5 times the allowable for normal operating loads, equivalent to 1.5g vertical.

Ultimate shear capacity of a fastener is 1.1 times 0.62% of the ultimate specified tensile strength, Ftu, Ref. F2.2.1, Table 3-10. Let Ftu be the strength of an A325 bolt = 120ksi, Ref. F2.2.1, Table 3-9. It does not matter what the selected strength is as everything is relative to the ultimate tensile strength, Ftu.

$Ftu := 120ksi$

$\tau_{ult} := 1.1 \cdot 0.62 \cdot Ftu$ ultimate shear strength

$\tau_{ult} = 8.184 \times 10^{4} psi$

$\tau_n := 0.17 \cdot \frac{Ftu}{2}$ normal shear stress per drive mechanism

$\tau_n = 1.02 \times 10^{4} psi$

$\tau_{EQ} := 0.44 \cdot \tau_n$ DBGM-2 earthquake shear stress per drive mechanism

$\tau_{EQ} = 4.488 \times 10^{3} psi$

$SF_H := \frac{(\tau_{ult} - \tau_n)}{\tau_{EQ}}$

$SF_H = 15.963$

This is not a governing failure mode in the horizontal position. Next the scale factor when the shield enclosure is in the vertical position is checked. In this case all load is from the earthquake.

$\tau_V := 0.26 \cdot \frac{Ftu}{2}$ Two mechanisms take load with each designed to the limit of 0.26 Ftu for shear stress on a fastener.

$\tau_V = 1.56 \times 10^4 \text{ psi}$

$SF_V := \frac{\tau_{ult}}{\tau_V}$

$SF_V = 5.246$

The vertical position would govern if the rotation mechanism were designed to the limit for normal operating plus extreme environment DBGM-2 loads. However, the rail hold down clamps were shown to have a much lower scale factor to failure of:

F6.2.3 Governing Capacity Factor

$SF = 1.954$ Failure of rail clamps

$F_C := SF$

$F_C = 1.954$ governing capacity factor based on rail clamp failure

The uncertainty for material strength, equation and fabrication is 0.1 per Ref. F2.2.1, Table 3-10.

$\beta_{C\_C} := 0.1$

F6.3 EQUIPMENT RESPONSE FACTOR

F6.3.1 Qualification Method

A dynamic analysis to determine the fundamental frequency will likely be conducted. The capacity factor was based on an estimated fundamental frequency of greater than 10 Hz, however, since the capacity factor was based on the demand being entirely seismic and reaching the allowable stress for extreme environment loads, the estimate of fundamental frequency is immaterial since the design would be based on the spectral acceleration at whatever frequency was calculated. The qualification method factor will determine the conservatism in using the broadened and smoothed spectra versus best estimate spectra for the median response case for 100 feet of alluvium with median soil properties. The 4% damped design spectra are shown in Appendix F-A. At the acceleration level of failure, the best estimate of the in-structure amplification and spectral shape would be from the BDBGM input. The X direction design spectra were used to compare to the X direction BDBGM at 10 Hz. BDBGM digitized spectra from Ref. F2.2.3 are shown in Appendix F-A, Table F-A-1.

$Sa_{BDBGM} := 1.19g$

In this case, the BDBGM spectral acceleration is slightly lower than the DBGM-2 spectral acceleration for direction X because of the broadening of the DBGM-2 spectra and the particular frequency chosen. Since the WPTT is believed to be stiffer than 10 Hz, compare the spectra at a higher frequency. From Appendix F-A, Fig. F-A-1, for the X direction the DBGM-2 broadened spectra are flat from about 11 to 17 Hz with a 4% damped design spectral acceleration of 0.99g (taken from the digitized spectra). The 4% damped BDBGM spectra shown in Appendix F-A, Table F-A-3, vary from 1.27g to 1.48 g in this range. Use the average value for comparison to the DBGM spectra and consider the range as a plus to minus 95 percentile range (plus or minus $1.65\beta_U$)

$$Sa_{BDBGM} := \frac{(1.27 + 1.48)}{2} g$$

$$Sa_{BDBGM} = 1.375 \cdot g$$

$$F_{QM} := \frac{(0.99g)}{Sa_{BDBGM}}$$

$$F_{QM} = 0.72$$

Because the qualification method (QM) factor is based on BDBGM, the reference earthquake for fragility will be the BDBGM PGA of 0.914g.

The uncertainties in response will be addressed for frequency uncertainty so:

$$\beta_{c\_QM} := 0.0$$

F6.3.2 Damping

Four percent damping is used for design. At failure of the rail clamps, 5% damping would be more median centered, Ref. F2.2.1, Table 3-8. Compare 4% and 5% damped design spectra from Appendix F-A, Figure F-A-1 in the flat 11 to 17 Hz range. Sa at 5% damping is 0.93g and is 0.99g at 4% damping

$$F_{\delta} := \frac{0.99}{0.93}$$

$$F_{\delta} = 1.065$$

Let this difference in spectral acceleration be 1β.

$$\beta_{c\_\delta} := \ln\left(\frac{0.99}{0.93}\right)$$

$$\beta_{c\_\delta} = 0.063$$

F6.3.3 Modeling

Modeling is affected by mode shape and frequency. There is no deliberate conservatism in modeling

$$F_M := 1.0$$

Per Ref. F2.2.1, page 3-50, the uncertainty in mode shape varies from 0.05 to 0.15. For a simple relatively stiff model, the mode shape uncertainty is estimated to be about 0.10.

$$\beta_{U\_MS} := 0.1$$

The uncertainty in frequency varies from about 0.1 to 0.30 per Ref. F2.2.1, page 3-49. For the relatively simple model use 0.15. The 10 Hz frequency used in the capacity factor calculation is near the flat portion of the design spectra beyond 11 Hz. The maximum uncertainty would occur if the fundamental frequency is lower.

$$f\_\beta := 10e^{-0.15}$$

$$f\_\beta = 8.607$$

$$Sa\_\beta := 1.53g$$

Figure F-A-1

$$\beta_{U\_f} := \ln\left(1.53\frac{g}{Sa_x}\right)$$

$$\beta_{U\_f} = 0.243$$

$$\beta_{c\_M} := \left(\beta_{U\_MS}^{\ 2} + \beta_{U\_f}^{\ 2}\right)^{0.5}$$

$$\beta_{c\_M} = 0.263$$

F6.3.4 Mode Combination

Mode combination would be conducted per the requirements of Ref. F2.2.17 and are median centered.

$$F_{MC} := 1.0$$

The massive WPTT is fairly rigid and a single mode would likely govern in each direction. Use a lower bound value suggested in Ref. F2.2.1, page 3-50.

$$\beta_{c\_MC} := 0.05$$

F6.3.5 Earthquake Component Combination

The SRSS or 100-40-40 rule would be used for design per Ref. F2.2.17. These methods are median centered.

$$F_{ECC} := 1.0$$

The governing failure mode was controlled by one horizontal plus the vertical direction of earthquake. Per Ref. F2.2.1, page 3-50. with the components in phase, this would be about a $3\beta_R$ extreme. From the governing capacity scale factor calculation in F6.2.1,

$$SF_{3\beta} := \frac{\left(V_{ult} + Wt \cdot \frac{g}{4}\right)}{Wt \cdot \left[\frac{\left(Sa_x \cdot h\right)}{2 \cdot w} + \frac{Sa_z}{4}\right]}$$

$$SF_{3\beta} = 1.762$$

$$\beta_{R\_ECC} := \frac{1}{3} \cdot \ln\left(\frac{SF}{SF_{3\beta}}\right)$$

$$\beta_{R\_ECC} = 0.034$$

$$\beta_{c\_ECC} := \beta_{R\_ECC}$$

$$\beta_{c\_ECC} = 0.034$$

F6.3.6 Equipment Response Factor

$$F_{RE} := F_{QM} \cdot F_{\delta} \cdot F_M \cdot F_{MC} \cdot F_{ECC}$$

$F_{RE} = 0.766$ This is relative to BDBGM PGA of 0.914g

$$\beta_{c\_RE} := \left(\beta_{c\_QM}^{2} + \beta_{c\_\delta}^{2} + \beta_{c\_M}^{2} + \beta_{c\_MC}^{2} + \beta_{c\_ECC}^{2}\right)^{0.5}$$

$$\beta_{c\_RE} = 0.277$$

F6.4 STRUCTURAL RESPONSE FACTOR

F6.4.1 Spectral Shape Factor

This factor accounts for conservatism in the site-wide DBGM-2 design spectrum. At the Surface Facilities Area (SFA) the depth of alluvium overlying tuff varies from 30 feet to 200 feet. Uniform hazard spectra at the surface are calculated from site response analyses for alluvium depths of 30', 70', 100' and 200'. The site-wide design ground response spectrum is the

envelope of the surface spectra of these four alluvium depths (Reference F2.2.9; also Section 6.2.2.1 for source information). The median site response is considered to be the 100 foot depth median soil property case.

The dominant frequency of the CRCF soil-structure system in the horizontal direction is 5.2 Hz from the Tier 1 ISRS calculation (Reference F2.2.3). At this frequency:

$SA_{site} := 1.14g$ Appendix F-B

$SA_{med} := 1.06g$

$F_{SA} := \frac{SA_{site}}{SA_{med}}$

$F_{SA} = 1.075$

Reference F2.2.1 recommends a β_U of about 0.24 if the fundamental frequency is about 5 Hz and the fragility is anchored to PGA. This is to account for uncertainty in amplification of the PGA as observed from statistical data when using a standard spectral shape. However, the Yucca Mountain surface facility UHS is derived probabilistically and this uncertainty is not applicable.

$\beta_{U\_SA} := 0$

$\beta_{R\_SA} := 0.2$ Ref. F2.2.1, Table 3-2 to account for peak to peak variation.

$\beta_{c\_SA} := \beta_{R\_SA}$

$\beta_{c\_SA} = 0.2$

F6.4.2 Damping

This factor is to account for conservatism in the hysteresis damping of the building structure used in the seismic response analysis. Due to the high radiation damping of the foundation media, the effect of structure damping is insignificant. Thus,

$F_{\delta\_s} := 1.0$

$\beta_{c\_\delta\_s} := 0$

F6.4.3 Modeling

The Tier 1 lumped mass multiple stick model of the CRCF models the stiffness of various reinforced concrete walls and distribution of mass at each floor. The floors are assumed to be rigid diaphragms tying the different sticks together. Torsional response of the structure is captured through modeling eccentricity between the center of mass and center of rigidity of each floor. The foundation media underneath the buildings are modeled with soil springs and dashpots based on elastic half space theory with adjustment to account for the layering effect of alluvium overlying tuff. The model is judged to adequately represent the CRCF structure

dynamic characteristics, thus

$$F_{M\_s} := 1.0$$

Uncertainty of structure frequencies predicted from mathematical modeling varies from 0.15 to 0.35 depending on the sophistication of the model (Reference F2.2.1, Page 3-18). The value of 0.35 is for fairly approximate models and the value 0.15 is appropriate for detailed models. Based on the complexity of the CRCF structure and the mathematical model used for the Tier 1 ISRS analysis, it is judged that the calculated CRCF frequency has a logarithmic standard deviation of 0.25.

$$\beta f := 0.25$$

$$f_m := 5.25\text{Hz}$$

$$f_{upper} := f_m \cdot e^{\beta f}$$

$$f_{upper} = 6.741 \cdot \text{Hz}$$

$$f_{lower} := f_m \cdot e^{-\beta f}$$

$$f_{lower} = 4.089 \cdot \text{Hz}$$

$SA_{upper} := 1.05g$ 5% damped Sa at f_{upper} from Figure F-B-1 for the 100 foot alluvium case

$SA_{lower} := 1.02g$ 5% damped Sa at f_{lower} from Figure F-B-1 for the 100 foot alluvium case.

Both values are less than the response at 5.2 Hz, thus there is no uncertainty penalty.

$$\beta_{U\_f} := 0$$

The mode shape uncertainty is taken as a lower value of the range suggested in Ref. F2.2.1, page 3-18, due to the detail in the modeling of the fairly simple rectangular concrete structure.

$$\beta_{U\_MS} := 0.1$$

$$\beta_{c\_M\_s} := \left(\beta_{U\_f}^2 + \beta_{U\_MS}^2\right)^{0.5}$$

$$\beta_{c\_M\_s} = 0.1$$

F6.4.4 Mode Combination

Since the direct integration time history method is used in the Tier 1 ISRS analysis (Reference F2.2.3), the modal combination method factor of safety is unity and there is no variability associated with modal combination.

$$F_{MC\_s} := 1.0$$

$$\beta_{c\_MC\_s} := 0$$

F6.4.5 Soil-Structure Interaction

Two factors are considered, the first one is on the method of treating the SSI effects and the second one is on the effect of soil softening at ground acceleration higher than DBGM-2. The Tier 1 seismic response analyses of the CRCF use the site-wide $5*10^{-4}$ mean uniform hazard spectra as the DBGM-2 input motion. Spectrum compatible time histories are used as the input motion for the time history analyses. The conservatism in the site-wide spectra was accounted for in the spectral shape factor above. Strain compatible soil properties of 100-foot and 200-foot deep alluvium are used to calculate frequency-independent soil springs and soil damping coefficients. Soil radiation damping is introduced into the model by using dashpots. Damping coefficients equal to 75% of the computed values for translational degrees of freedom and to the full computed rotational damping values are used in the response analyses (Reference F2.2.3). Conservatism or un-conservatism in SSI will be minimized for final SSI analyses used to develop equipment design seismic input. Before the final SSI analyses are completed, the Tier 1 SSI analysis is taken to represent the best-estimate responses per BSC recommendations in Reference F2.2.14.

$$F_{SSI\_1} := 1.0$$

$$\beta_{R\_SSI\_1} := 0$$

$\beta_{U\_SSI\_1} := 0.25$ Estimated uncertainty in spring damper soil modeling from past experience.

The second effect of soil softening has already been taken into effect in the equipment qualification method factor where BDBGM response is compared to DBGM-2 response. Therefore this contribution is not used here.

$$F_{SSI} := 1.0$$

$$\beta_{c\_SSI} := \beta_{U\_SSI\_1}$$

$$\beta_{c\_SSI} = 0.25$$

F6.4.6 Ground Motion Incoherence

For large structures the foundation cannot be excited uniformly thus the practice of applying the ground motion time histories uniformly across the base mat can be conservative. In Ref.

F2.2.1, page 3-22 it is shown that above 5 Hz some reduction can be made to the input motion. The horizontal fundamental frequency from Ref. F2.2.3 is about 5.2 Hz for DBGM-2 input, however, at the failure level, the BDBGM response characteristics of the structure are more appropriate. From Ref. F2.2.3, the first two horizontal modes of structural response are 4.39 Hz and 4.46 Hz respectively, thus there is no reduction for ground motion incoherence.

$$F_{GMI} := 1.0$$

$$\beta_{c\_GMI} := 0$$

F6.4.7 Structural Response Factor

$$F_{RS} := F_{SA} \cdot F_{\delta\_s} \cdot F_{M\_s} \cdot F_{MC\_s} \cdot F_{SSI} \cdot F_{GMI}$$

$$F_{RS} = 1.075$$

$$\beta_{c\_RS} = 0.335$$

F6.5 FRAGILITY OF RAIL CLAMPS

The equipment response factor was developed relative to the BDBGM PGA of 0.914g and the equipment response factor was less than unity due to the comparison of the DBGM-2 spectra to the BDBGM spectra, therefore the fragility must be referenced to the BDBGM.

$$BDBGM := 0.914g$$

$$A_m := F_C \cdot F_{RE} \cdot F_{RS} \cdot BDBGM$$

$$A_m = 1.472 \cdot g$$

$$\beta_c := \left(\beta_{c\_C}^{\,2} + \beta_{c\_RE}^{\,2} + \beta_{c\_RS}^{\,2} \right)^{0.5}$$

$$\beta_c = 0.534$$

$$HCLPF := A_m \cdot e^{-2.33 \cdot \beta_c}$$

$$HCLPF = 0.425 \cdot g$$

This HCLPF is less than the DBGM-2 PGA of 0.453g. This appears to arise from large uncertainties applied in the calculation due to the fact that the derivation is generic and is a bounding case where the design stresses of brittle components are equated to the maximum allowable stress.

F6.6 ROCKING OF WPTT AFTER FAILURE OF RAIL CLAMPS

Two cases will be considered; rocking while in the WP closure position where the WPTT shielding enclosure can impact an opening in the concrete floor above and rocking in an area where complete tip over could happen.

F6.6.1 WPTT in Closure Area

As shown in Section D of Ref. F2.2.5, and in Ref. F2.2.13, when the WPTT trolley is under the WP closure room gate, there is not much clearance between the shield enclosure and the concrete floor opening above. Once the rail clamps fail, the trolley is free to rock and will likely impact the floor opening. The minimum clearance for the shield enclosure to pass through is 12 feet as shown in Ref. F2.2.13. From Ref. F2.2.16, the floor opening distance is 14 feet from Ref. F2.2.6, the estimated WPTT shield width is about 130 inches. The clearance between the shield enclosure and concrete floor opening is then about:

$$\Delta := \frac{(14\text{ft} - 130\text{in})}{2} = 1.583\ \text{ft}$$ clearance between shield enclosure and concrete floor opening.

Ref. F2.2.2, Appendix A, Section A-2 has equations for rocking rotations. The rocking angle is less than 0.4 radians based on the height of the WPTT and the 19 inch clearance so the approximate equations A-5(d) and A-5(e) can be used in the solution to find the spectral acceleration SAH_{CAP} at impact. A rigid body rocking is shown in Figure F6-2.

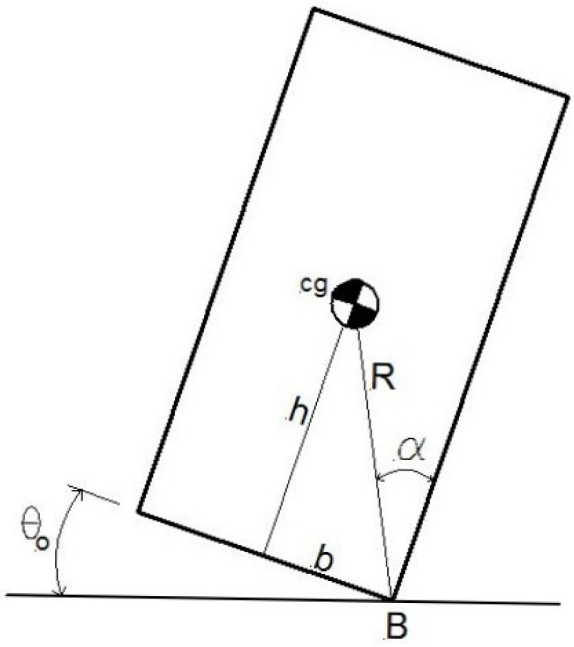

Figure F6-2

Rigid Body Rocking Model

The following parameters and equations are from Ref. F2.2.2.

$b := \frac{w}{2}$ Half the distance between the rails

The top of the shield enclosure is 26' 10" from the top of the rails. (Ref. F2.2.13 and DCN-1)

$h_{encl} := 322in$

$a := \frac{b}{h}$ Eq. 7-2(b) Ref. F2.2.2

$a = 0.533$

$R := \left(h^2 + b^2\right)^{0.5}$ Fig. F6-2

$R = 15.935\,ft$ Distance from rail to center of gravity of WPTT

$\theta := \operatorname{asin}\left(\frac{\Delta}{h_{encl}}\right)$ Rigid body rotation angle at impact

$\theta = 0.059$ radians

$I_b := (Wt)\cdot R^2$

$I_b = 1.727 \times 10^8 \cdot ft^2 \cdot lbm$ mass moment of inertia of the rigid block about point B in Figure F6-2

$C_I := \frac{I_b}{Wt \cdot h^2}$ Eq A-6(c) of Ref. F2.2.2

$C_I = 1.285$

$fi\_\theta := 1 + \theta\cdot\left(a - \frac{\theta}{2}\right)$

$fi\_\theta - 1 = 0.03$ Eq A-5(d) of Ref. F2.2.2

$fe := \frac{1}{2\cdot\pi}\cdot\frac{[2(fi\_\theta - 1)\cdot g]^{0.5}}{\left(C_I\cdot\theta^2\cdot h\right)^{0.5}}$ Eq. A-6(a) of Ref. F2.2.2

$fe = 0.878\cdot Hz$ Effective frequency.

$$C_R := 1 - \frac{\left(2 \cdot a^2\right)}{C_I}$$ Eq, A-6(e) of Ref. F2.2..2

$C_R = 0.557$

$\gamma := -2 \cdot \ln\left(C_R\right)$ Eq. A6(d) of Ref F2.2.2

$\gamma = 1.17$

$$\beta e := \frac{\gamma}{\left(4 \cdot \pi^2 + \gamma^2\right)^{0.5}}$$ Effective damping, Eq A-6(b) Ref. F2.2.2

$\beta e = 0.183$ 18.3% effective damping

$F_H := 1.0$ Eq. A-5(b) of Ref. F2.2.2. No correction is made for vertical versus horizontal mass and respective distances from center of rotation

$SAH := 0.577g$ Appendix F-A, Table F-A-1 for 10% damping, at frequency, fe, for BDBGM (highest damping available)

$SAV := 0.366g$ Appendix F-A, Table F-A-2 for 10% damping at effective frequency, fe, for BDBGM.

$$F_V := \left[1 + \left(a \cdot \frac{SAV}{F_H \cdot SAH}\right)^2\right]^{0.5}$$ Eq. A-5(c) of Ref. F2.2.2

$F_V = 1.056$

$$SAH_{CAP} := \left[\frac{g}{F_H \cdot F_V} \cdot (2 \cdot a - \theta)\right]$$

$SAH_{CAP} = 0.95 \cdot g$

When rail clamps fail the elastic spectral acceleration level is higher than this so impact can only occur after rail clamp failure.

With the high effective damping, βe, the spectral acceleration at the effective

frequency is estimated. From Ref. F2.2.15, equations are given for median spectral amplification for different damping. These amplification factors are for ground motion and a standard spectral shape but the values can be used to estimate the amplification of in-structure spectra. At fe = 0.878 Hz, the spectral amplification is in the amplified velocity region. Compare the ratio of velocity amplification at 10% damping and βe of 18.3% damping.

$Amp_{18} := 2.31 - 0.41 \cdot \ln(18.3)$ Ref. F2.2.15, where βe = 18.3 is in percent damping

$Amp_{18} = 1.118$ 18.3 % damping

$Amp_{10} := 2.31 - 0.41 \cdot \ln(10)$ 10 % damping

$Amp_{10} = 1.366$

Spectral acceleration is spectral velocity times ω (rad/sec circular frequency) so the ratio of spectra acceleration at fe = 0.878 Hz is the same as the spectral velocity ratio.

$$SAH_{18} := \frac{Amp_{18}}{Amp_{10}} \cdot SAH$$

$SAH_{18} = 0.472 \cdot g$

$$SAV_{18} := \frac{Amp_{18}}{Amp_{10}} SAV$$

$SAV_{18} = 0.3 \cdot g$

$$F_{V18} := \left[1 + \left(a \cdot \frac{SAV_{18}}{F_H \cdot SAH_{18}} \right)^2 \right]^{0.5}$$

$F_{V18} = 1.056$ No change as ratio of SAV and SAH is the same.

$$SAH_{CAP18} := \left[\frac{g}{F_H \cdot F_{V18}} \cdot (2 \cdot a - \theta) \right]$$

$SAH_{CAP18} = 0.95 \cdot g$

This is the same as computed for 10% damping since the values of F_H and F_V did not change. The failure of the rail clamp occurs at a higher acceleration level so when the rail clamp fails, rocking will occur. However, the rocking frequency and resulting spectral acceleration is less than SAH_{CAP18}. Determine PGA at impact. SAH_{18} is referenced to BDBGM.

$BDBGM_{PGA} := 0.914g$

$$PGA_{impact} := \frac{SAH_{CAP18}}{SAH_{18}} \cdot BDBGM_{PGA} = 1.847 \cdot g$$

Since the gap will just close at this ground motion acceleration level, the velocity at impact will be zero.

The rigid body rocking equations provide a best estimate of rocking angle and SAH_{CAP} for the rocking angle. Consider that the the SAH_{CAP} could be associated with an angle of rotation a factor of 2 lower than used in the calculation. Recompute the PGA at impact for half the angle of rotation. Consider this to be a 99% lower bound case. For this case, the effective Δr is 1/2 of Δ.

$$\Delta r := \frac{\Delta}{2} = 0.792\ ft$$

$$\theta r := \operatorname{asin}\left(\frac{\Delta r}{h_{encl}}\right) = 0.03 \qquad \text{angle in radians}$$

$$fi\_\theta r := 1 + \theta r \cdot \left(a - \frac{\theta r}{2}\right) = 1.015$$

$$fi\_\theta r - 1 = 0.015$$

$$fe := \frac{\frac{1}{2 \cdot \pi}\left[2 \cdot (fi\_\theta r - 1) \cdot g\right]^{0.5}}{\left(C_I \theta r^2 \cdot h\right)^{0.5}} = 1.26 \cdot Hz \qquad \text{effective frequency}$$

$SAH_r := 0.862g$ 10% damped BDBGM from Table F-A-1

$SAV_r := 0.457g$ 10% damped BDBGM from Table F-A-2

$$SAH_{r18} := \frac{Amp_{18}}{Amp_{10}} \cdot SAH_r = 0.706 \cdot g$$

$$SAV_{r18} := \frac{Amp_{18}}{Amp_{10}} \cdot SAV_r = 0.374 \cdot g$$

$$F_{Vr18} := \left[1 + \left(a \cdot \frac{SAV_{r18}}{F_H \cdot SAH_{r18}}\right)^2\right]^{0.5} = 1.039$$

$$SAH_{CAPr} := \left[\frac{g}{F_H \cdot F_{Vr18}} (2 \cdot a - \theta r) \right] = 0.998 \cdot g$$

$$PGA_{r\_impact} := \frac{SAH_{CAPr}}{SAH_{r18}} \cdot BDBGM = 1.293 \cdot g$$

$$\beta_{U\_eq} := \frac{1}{2.33} \cdot \ln\left(\frac{PGA_{impact}}{PGA_{r\_impact}} \right) = 0.153$$

$$\beta_{c\_eq} := \beta_{U\_eq} = 0.153$$

From the structural response factor calculation

$$\beta_{c\_RS} = 0.335$$

The plus 1β SAH is then:

$$SAH_{\beta} := SAH_{18} \cdot e^{\beta_{c\_RS}} = 0.661 \cdot g$$

SAH_{CAP} is not affected by SAH as long as FV does not change much.

$$PGA_{impact\_\beta} := \frac{SAH_{CAP18}}{SAH_{\beta}} \cdot BDBGM = 1.321 \cdot g$$

$$\beta_{c\_FRS} := \ln\left(\frac{PGA_{impact}}{PGA_{impact\_\beta}} \right) = 0.335$$

$$\beta_{c\_impact} := \left(\beta_{c\_eq}^{\ 2} + \beta_{c\_FRS}^{\ 2} \right)^{0.5} = 0.369$$

The minimum ground motion acceleration at impact is then:

$$PGA_{impact\_min} := PGA_{impact} \cdot e^{-2.33 \cdot \beta_{c\_impact}} = 0.782 \cdot g$$

This is greater than the HCLPF value of 0.425g for failure of the rail clamps. Thus, the rail clamps, if designed to their maximum allowable capacity are not effective in keeping the WP from impact. The calculation of impact velocity beyond the point of

first contact was not calculated.

F6.6.2 WPTT in Area Where Tip Over Could Occur

Instability could occur when the center of gravity rotates beyond Point B in Figure F6-2.

$\theta_{stab} := \operatorname{atan}\left(\frac{b}{h}\right) = 0.49$ instability angle in radians

Note that equations used are approximate up to an angle of 0.4 radians but are considered adequate for an approximation of the acceleration required to tip over the WPTT.

$$fi\_\theta_{stab} := 1 + \theta_{stab}\cdot\left(a - \frac{\theta_{stab}}{2}\right) = 1.141$$

$$fi\_\theta_{stab} - 1 = 0.141$$

$$fe_{stab} := \frac{1}{2\cdot\pi}\cdot\frac{\left[2\cdot\left(fi\_\theta_{stab} - 1\right)\cdot g\right]^{0.5}}{\left(C_I\cdot\theta_{stab}{}^{2}\cdot h\right)^{0.5}} = 0.23\cdot Hz$$

The in-structure spectral acceleration in Reference F 2.2.3 and the ground motion spectral acceleration in Reference F2.2.9 are based on extrapolations below 0.5Hz. Per discussions in Section 6.2.2.1, corrected ground motion accelerations at 0.3Hz have been calculated. These values are only available for 5% damping. At low frequency, there is virtually no difference between the in-structure spectral acceleration on the base slab and the ground motion spectral acceleration. Therefore the ground motion spectral acceleration from Section 6.2.2.1 at 0.3 Hz will conservatively be used as the demand at 0.23 Hz. The 5% damped spectral acceleration will be adjusted for the higher 18.3% effective damping using the equations in Reference F2.2.15.

$SAH_{stab} := 0.219g$ 5% damped BDBGM spectra (Section 6.2.2.1)

$SAV_{stab} := 0.118g$ 5% damped BDBGM spectra (Section 6.2.2.1)

0.3 Hz is in the amplified velocity region per Ref. 2.2.15. Adjust the 5% damped spectral accelerations for 18.3% effective damping.

$Amp_5 := 1.65$ Ref. F2.2.15 spectral amplification in velocity region.

$$SAH_{stab18} := \frac{Amp_{18}}{Amp_5} \cdot SAH_{stab} = 0.148 \cdot g$$

$$SAV_{stab18} := \frac{Amp_{18}}{Amp_5} \cdot SAV_{stab} = 0.08 \cdot g$$

$$F_{Vstab} := \left[1 + \left(a \cdot \frac{SAV_{stab18}}{F_H \cdot SAH_{stab18}} \right)^2 \right]^{0.5} = 1.04$$

$$SAH_{CAP\_stab} := \left[\frac{g}{F_H \cdot F_{Vstab}} \cdot \left(2 \cdot a - \theta_{stab} \right) \right] = 0.554 \cdot g$$

$$PGA_{stab} := \frac{SAH_{CAP\_stab}}{SAH_{stab18}} \cdot BDBGM = 3.414 \cdot g$$

The WPTT could not tip over under any credible ground motion.

7. SUMMARY OF RESULTS AND CONCULUSIONS

The WPTT spends most of its time in the vertical position while the WP is being sealed by welding and is subsequently inspected. This is also the most vulnerable position for seismic loading. Therefore the fragility derivation for the seismic rail clamps is based on the WPTT being in this position.

A representative fragility has been derived for the WPTT based on a brittle failure mode in the rail clamp fasteners. Since the design has not progressed to a point where detailed dynamic response analyses and detailed stress analyses are available, the resulting capacity factor is based on the rail clamp fasteners being stressed to the maximum allowable stress and failing in a brittle mode. At the acceleration level that the rail clamps fail, the WPTT would rock and at some level of acceleration the shield enclosure of the WPTT could impact the structure, thus imparting shock loads into the waste package and the canister contained within. However it was shown that the median ground motion PGA where impact could occur is 1.85g. At this ground motion acceleration, the gap between the WPTT shield enclosure and the floor opening is just closed and the velocity at impact would be zero. A minimum ground motion acceleration at which impact could occur was calculated to be 0.78g. There would be zero impact velocity at this minimum ground motion level. Velocity at impact at higher ground motion acceleration levels was not computed.

A calculation was conducted to find the median ground motion PGA where tip over could occur when the WPTT is not in the closure position. The median instability ground motion

acceleration level was calculated to be 3.41g, thus there is no credible possibility of tip over.

When the rail clamps fail while the WPTT is in the closure position, any equipment involved with welding the closure would likely be damaged but it is unclear if there could be a breach of a canister from this. Also, if the rail clamps fail when the WPTT is in the loadout position, and the WP is in the process of being transferred to the TEV, it is not clear if misalignment between the WPTT and TEV could result in damage to the WP. In this latter case, the WPTT is in the horizontal position and failure of the rail clamps would not occur until a higher ground motion is achieved. The calculation of rail clamp capacity for the TEV in Attachment H would govern this case. The alternative to trying to address consequences while the WPTT is in the closure position is to design the rails and rail clamps for BDBGM. In this case the rail clamp failure would double to 2.94g. At 2.94g pga, the spectral acceleration at 0.3Hz and 18.3% damping would exceed the impact spectral acceleration capacity so if the rail clamps failed, impact would occur.

In Summary:

For failure of the rail clamps and possible damage to the WP from unknown vulnerabilities when the WPTT is in the closure position and being welded closed:

$A_m := 1.47g$ Rail clamps designed for DBGM-2

$\beta_c = 0.534$

$HCLPF := 0.42g$

$Am := 2.94g$ Rail clamps designed for BDBGM

$HCLPF := 0.84g$

.

If the rail clamps are designed for the DBGM-2 earthquake, after the rail clamps fail, while the WPTT is in the closure position, initial impact with the floor opening above the closure area would not occur until a ground motion acceleration of 1.85g is experienced.

$A\_impact := 1.85g$

$\beta_{c\_impact} := 0.37$

$HCLPF\_impact := 0.78g$

At initial impact, the velocity is zero so a considerably higher acceleration is required for damage to the Waste Package.

If the rail clamps are designed for BDBGM, upon their failure at 2.94g pga, impact would occur when the WPTT is in the closure position.

When the WPTT is vertical and not in the closure position, the median ground motion acceleration at tip over was calculated to be:

$$A_{m\_tip} := 3.41g$$

Tipping over does not appear to be a credible failure mode.

APPENDIX F-A

IN-STRUCTURE RESPONSE FOR BASE MAT OF CRCF

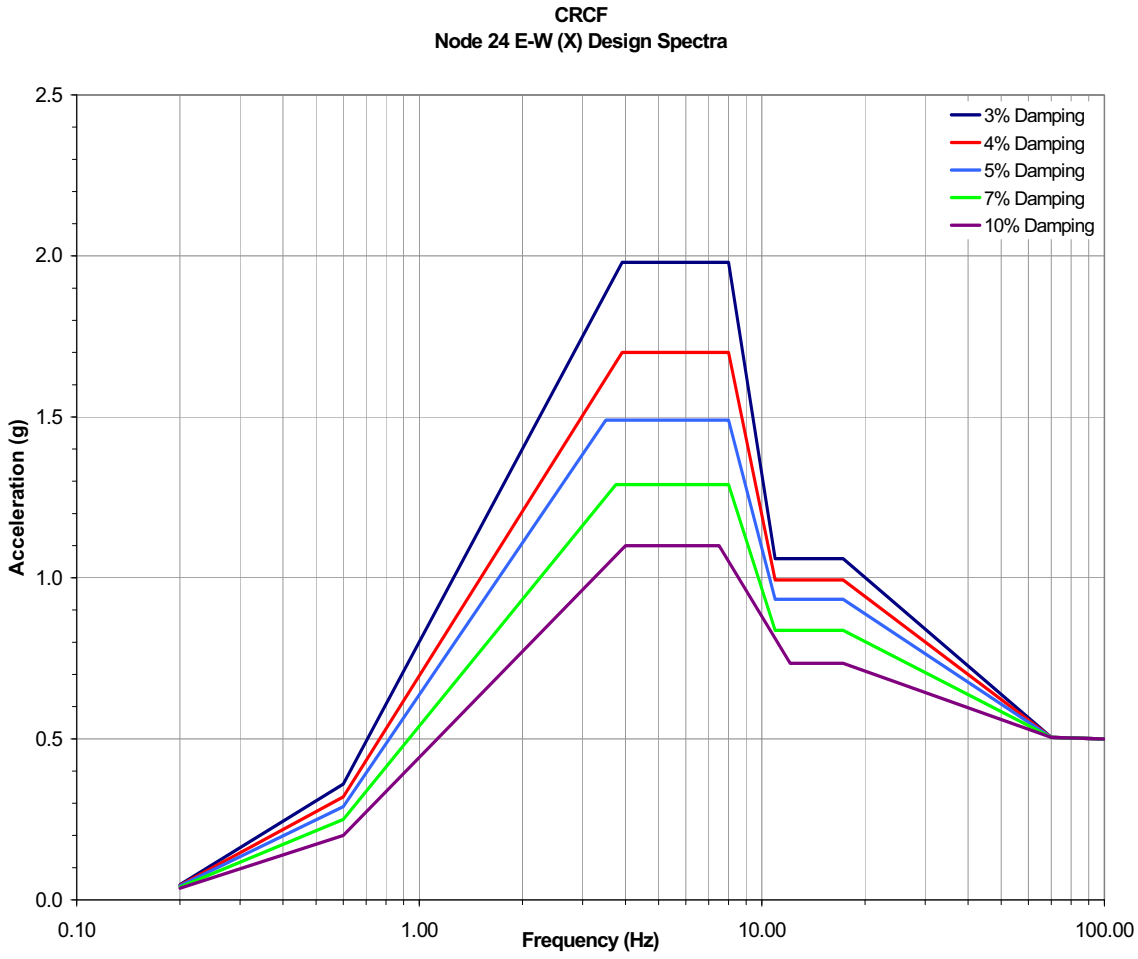

Figure F-A-1
Envelope DBGM-2 Design Spectra for CRCF Ground Floor
Direction X

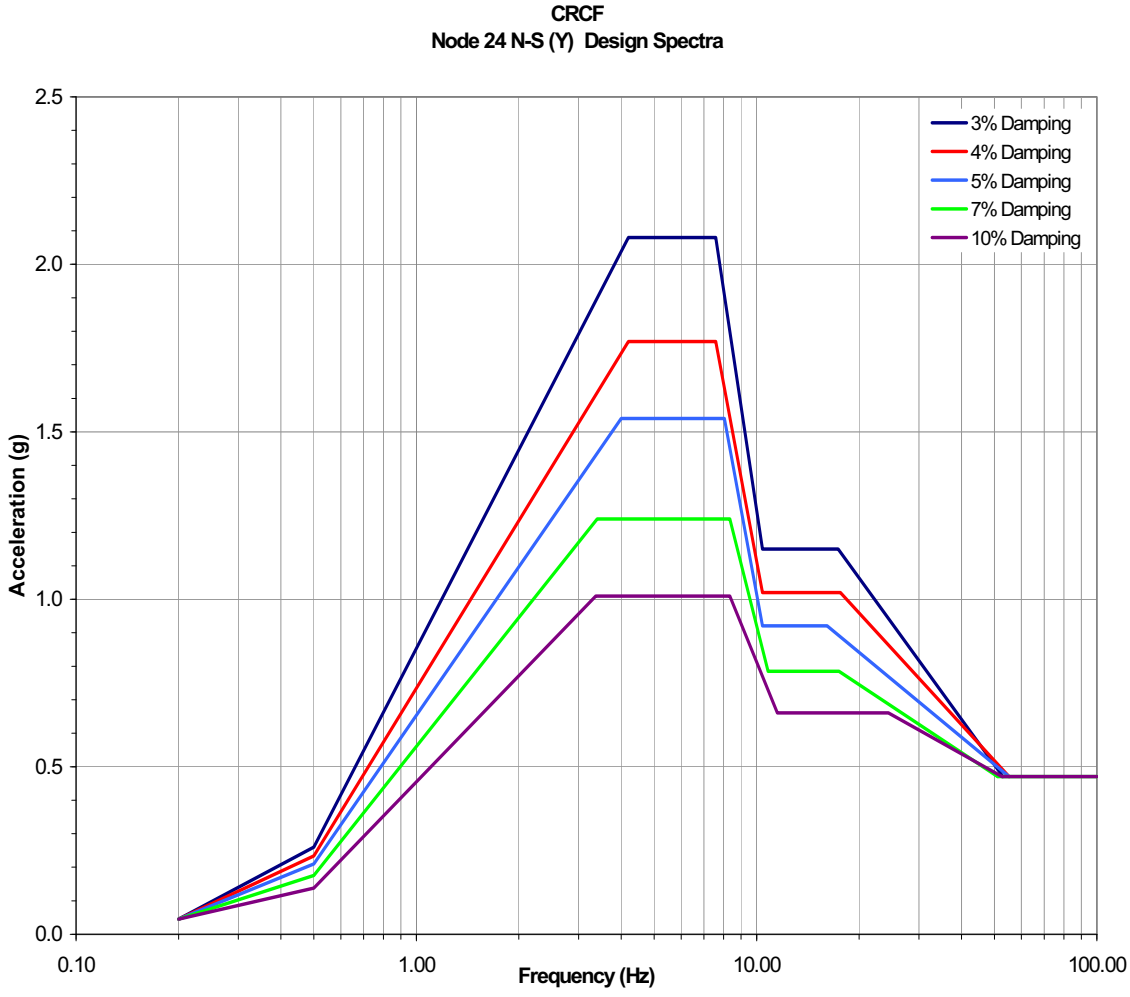

Figure F-A-2
Envelope DBGM-2 Design Spectra for CRCF Ground Floor Direction Y

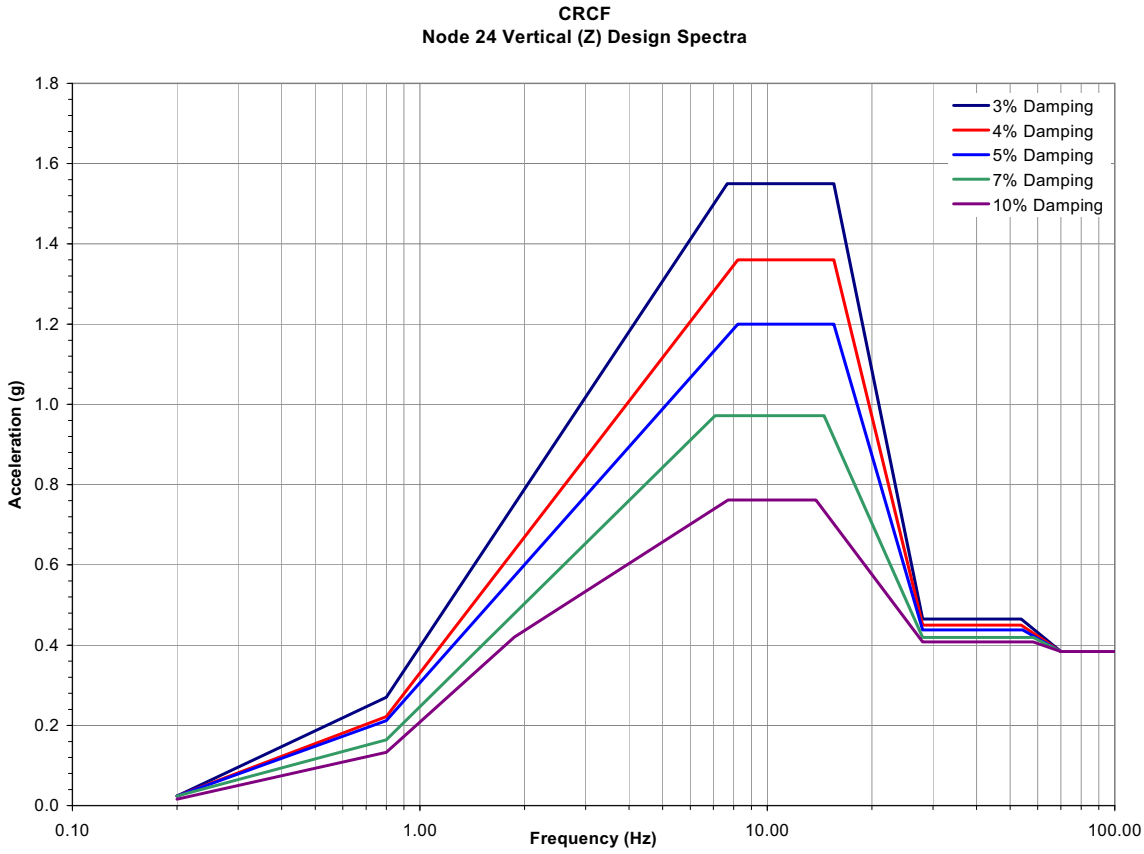

Figure F-A-3
Envelope DBGM-2 Design Spectra for CRCF Ground Floor Direction Z

Table F-A-1
BDBGM 100 Foot Alluvium Spectra for Node 24 of CRCF
Ground Floor, Direction X, Low Frequency Range

Freq	DAMPING	DAMPING	DAMPING	DAMPING	DAMPING
	0.03	0.04	0.05	0.07	0.1
0.2	1.15E-01	1.02E-01	9.14E-02	8.04E-02	7.08E-02
0.3	2.14E-01	1.89E-01	1.72E-01	1.45E-01	1.18E-01
0.4	4.08E-01	3.70E-01	3.45E-01	3.01E-01	2.49E-01
0.5	5.41E-01	5.10E-01	4.75E-01	4.24E-01	3.62E-01
0.6	6.93E-01	6.05E-01	5.73E-01	5.08E-01	4.23E-01
0.7	8.89E-01	7.68E-01	6.94E-01	5.81E-01	4.64E-01
0.8	9.15E-01	8.55E-01	7.96E-01	6.91E-01	5.71E-01
0.9	1.21E+00	1.03E+00	9.15E-01	7.46E-01	5.79E-01
1	1.24E+00	1.13E+00	1.04E+00	8.86E-01	7.12E-01
1.1	1.31E+00	1.21E+00	1.13E+00	9.74E-01	7.95E-01
1.2	1.39E+00	1.27E+00	1.17E+00	1.02E+00	8.75E-01
1.3	1.65E+00	1.45E+00	1.29E+00	1.06E+00	8.53E-01
1.4	1.64E+00	1.56E+00	1.49E+00	1.31E+00	1.07E+00
1.5	2.22E+00	1.91E+00	1.67E+00	1.37E+00	1.10E+00
1.6	2.20E+00	1.81E+00	1.56E+00	1.25E+00	1.01E+00
1.7	2.37E+00	1.98E+00	1.71E+00	1.45E+00	1.21E+00
1.8	2.41E+00	2.12E+00	1.88E+00	1.53E+00	1.24E+00
1.9	2.66E+00	2.24E+00	1.94E+00	1.54E+00	1.27E+00
2	2.30E+00	2.04E+00	1.83E+00	1.53E+00	1.32E+00
2.1	2.59E+00	2.36E+00	2.13E+00	1.74E+00	1.35E+00
2.2	3.12E+00	2.62E+00	2.28E+00	1.81E+00	1.40E+00
2.3	2.66E+00	2.20E+00	1.91E+00	1.69E+00	1.46E+00
2.4	3.25E+00	2.73E+00	2.36E+00	1.91E+00	1.54E+00
2.5	3.05E+00	2.63E+00	2.32E+00	1.89E+00	1.51E+00
2.6	2.77E+00	2.48E+00	2.26E+00	1.93E+00	1.60E+00
2.7	2.94E+00	2.54E+00	2.23E+00	1.81E+00	1.60E+00
2.8	3.09E+00	2.60E+00	2.27E+00	1.84E+00	1.59E+00
2.9	3.21E+00	2.70E+00	2.38E+00	1.98E+00	1.62E+00
3	3.01E+00	2.63E+00	2.37E+00	2.01E+00	1.66E+00

Table F-A-2
BDBGM 100 Foot Alluvium Spectra for Node 24 of CRCF
Ground Floor, Direction Z, Low Frequency Range

Freq	DAMPING	DAMPING	DAMPING	DAMPING	DAMPING
	0.03	0.04	0.05	0.07	0.1
0.2	4.23E-02	3.90E-02	3.64E-02	3.25E-02	2.85E-02
0.3	1.21E-01	1.07E-01	9.50E-02	7.83E-02	6.55E-02
0.4	2.11E-01	1.98E-01	1.86E-01	1.64E-01	1.39E-01
0.5	3.16E-01	2.68E-01	2.47E-01	2.20E-01	1.90E-01
0.6	3.97E-01	3.57E-01	3.24E-01	2.77E-01	2.39E-01
0.7	4.85E-01	4.28E-01	3.85E-01	3.21E-01	2.62E-01
0.8	4.65E-01	4.49E-01	4.30E-01	3.90E-01	3.35E-01
0.9	5.25E-01	4.95E-01	4.66E-01	4.22E-01	3.75E-01
1	6.07E-01	5.48E-01	5.00E-01	4.23E-01	3.81E-01
1.1	6.86E-01	6.17E-01	5.63E-01	4.82E-01	3.91E-01
1.2	7.21E-01	6.71E-01	6.25E-01	5.46E-01	4.50E-01
1.3	8.13E-01	7.11E-01	6.61E-01	5.70E-01	4.61E-01
1.4	9.29E-01	8.23E-01	7.40E-01	6.18E-01	4.94E-01
1.5	1.15E+00	9.62E-01	8.24E-01	6.40E-01	5.06E-01
1.6	1.12E+00	9.10E-01	8.02E-01	6.65E-01	5.84E-01
1.7	1.09E+00	9.26E-01	8.59E-01	7.69E-01	6.57E-01
1.8	1.21E+00	1.06E+00	9.55E-01	8.06E-01	6.68E-01
1.9	1.13E+00	9.71E-01	8.86E-01	7.98E-01	7.01E-01
2	1.17E+00	1.04E+00	9.55E-01	8.64E-01	7.57E-01
2.1	1.22E+00	1.10E+00	1.00E+00	8.93E-01	7.81E-01
2.2	1.40E+00	1.18E+00	1.03E+00	8.52E-01	7.69E-01
2.3	1.61E+00	1.37E+00	1.19E+00	9.58E-01	7.69E-01
2.4	1.41E+00	1.15E+00	9.80E-01	8.84E-01	8.09E-01
2.5	1.46E+00	1.27E+00	1.14E+00	9.66E-01	8.56E-01
2.6	1.44E+00	1.27E+00	1.15E+00	9.84E-01	8.77E-01
2.7	1.52E+00	1.34E+00	1.20E+00	1.01E+00	8.84E-01
2.8	1.44E+00	1.36E+00	1.27E+00	1.11E+00	9.29E-01
2.9	1.72E+00	1.53E+00	1.38E+00	1.19E+00	9.86E-01
3	1.69E+00	1.53E+00	1.41E+00	1.22E+00	1.01E+00

Table F-A-3
BDBGM 100 Foot Alluvium Spectra for Node 24 of CRCF
Ground Floor, Direction Z, Higher Frequency Range

Freq	DAMPING 0.03	DAMPING 0.04	DAMPING 0.05	DAMPING 0.07	DAMPING 0.1
6	3.06E+00	2.75E+00	2.52E+00	2.18E+00	1.86E+00
6.25	2.70E+00	2.34E+00	2.20E+00	1.98E+00	1.75E+00
6.5	2.51E+00	2.24E+00	2.05E+00	1.92E+00	1.75E+00
6.75	2.35E+00	2.21E+00	2.11E+00	1.95E+00	1.76E+00
7	2.28E+00	2.16E+00	2.09E+00	1.93E+00	1.73E+00
7.25	2.32E+00	2.17E+00	2.05E+00	1.88E+00	1.69E+00
7.5	2.01E+00	1.96E+00	1.91E+00	1.79E+00	1.62E+00
7.75	2.05E+00	1.92E+00	1.83E+00	1.70E+00	1.54E+00
8	1.99E+00	1.75E+00	1.69E+00	1.59E+00	1.46E+00
8.5	1.66E+00	1.55E+00	1.47E+00	1.38E+00	1.29E+00
9	1.52E+00	1.42E+00	1.34E+00	1.25E+00	1.21E+00
9.5	1.41E+00	1.35E+00	1.31E+00	1.25E+00	1.20E+00
10	1.33E+00	1.19E+00	1.19E+00	1.20E+00	1.18E+00
10.5	1.28E+00	1.25E+00	1.23E+00	1.20E+00	1.17E+00
11	1.32E+00	1.27E+00	1.24E+00	1.19E+00	1.15E+00
11.5	1.29E+00	1.20E+00	1.17E+00	1.13E+00	1.11E+00
12	1.42E+00	1.33E+00	1.27E+00	1.18E+00	1.09E+00
12.5	1.43E+00	1.37E+00	1.31E+00	1.21E+00	1.11E+00
13	1.43E+00	1.37E+00	1.31E+00	1.21E+00	1.10E+00
13.5	1.45E+00	1.36E+00	1.29E+00	1.17E+00	1.06E+00
13.8113	1.55E+00	1.40E+00	1.29E+00	1.15E+00	1.03E+00
13.9416	1.58E+00	1.43E+00	1.33E+00	1.17E+00	1.05E+00
14	1.59E+00	1.44E+00	1.34E+00	1.18E+00	1.06E+00
14.5	1.65E+00	1.48E+00	1.36E+00	1.22E+00	1.10E+00
15	1.66E+00	1.47E+00	1.35E+00	1.21E+00	1.11E+00
16	1.43E+00	1.32E+00	1.28E+00	1.19E+00	1.11E+00
17	1.51E+00	1.39E+00	1.31E+00	1.26E+00	1.20E+00
18	1.69E+00	1.56E+00	1.46E+00	1.35E+00	1.25E+00
20	1.34E+00	1.31E+00	1.29E+00	1.25E+00	1.21E+00

APPENDIX F-B
COMPARISON OF SITE WIDE DBGM-2 UHS WITH 100 FOOT ALLUVIUM MEDIAN SOIL UHS

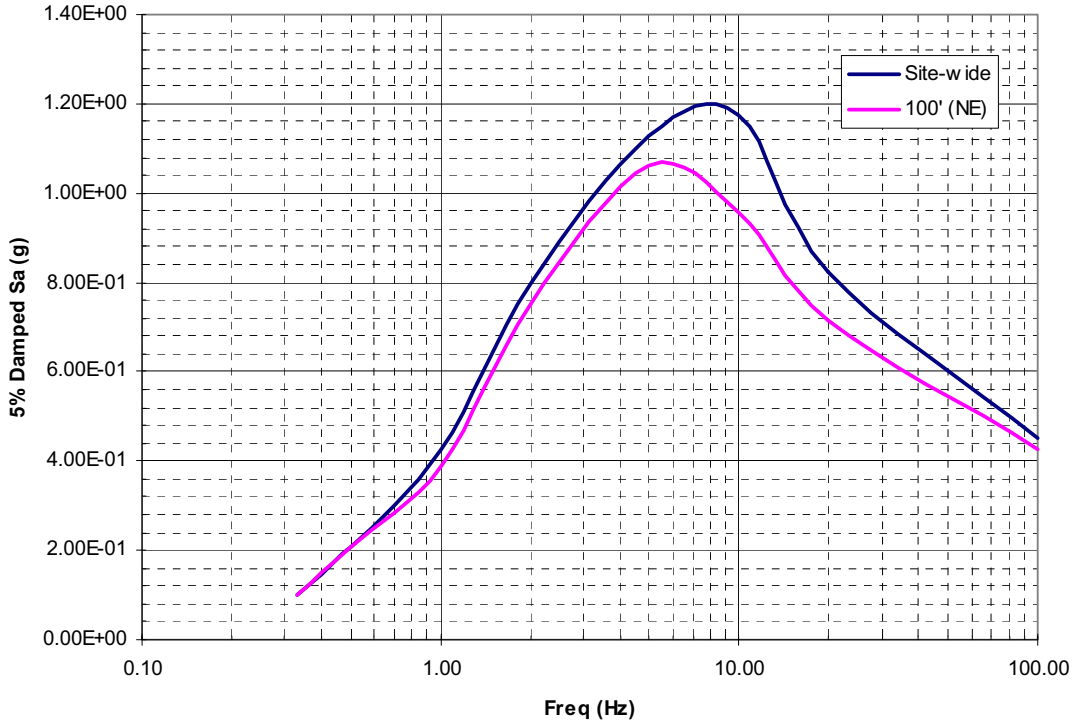

Figure F-B-1
Comparison of Site Wide Horizontal DBGM-2 UHS to 100-Foot Alluvium Median Soil Case (See Section 6.2.2.1 for source information)

ATTACHMENT G

SEISMIC FRAGILITY OF THE SITE TRANSPORTER IN THE CANISTER RECEIPT AND CLOSURE FACILITY

Prepared By: Stephen A. Short

ARES Check By: Wen H. Tong

LLNL Check By: Robert C. Murray

TABLE OF CONTENTS

ACRONYMS AND ABBREVIATIONS

ACI	American Concrete Institute
AISC	American Institute of Steel Construction
ANSI	American National Standards Insitute
AO	Aging Overpack
APE	Annual Probability of Exceedance
ASCE	American Society of Civil Engineers
ASME	American Society of Mechanical Engineers
BSC	Bechtel SAIC, LLC
BDBGM	Beyond Design Basis Ground Motion at $1x10^{-4}$ APE
CDFM	Conservative Deterministic Failure Margin
CHC	Cask Handling Crane
CIP	Cast-in-Place
CRCF	Canister Receipt and Closure Facility
CTM	Canister Transfer Machine
CTT	Cask Transfer Trolley
DBGM-2	Design Basis Ground Motion at $5x10^{-4}$ APE
DL	Dead Load
DOF	Degree of Freedom
DPC	Dual Purpose Canister
EPRI	Electric Power Research Institute
HCLPF	High Confidence of Low Probability of Failure
HVAC	Heating, Ventilation, & Air Conditioning
IEEE	Institute of Electrical and Electronics Engineers
IHF	Initial Handling Facility
ISRS	In-Structure Response Spectra

ACRONYMS AND ABBREVIATIONS (cont.)

ITS	Important to Safety
LA	License Application
LLNL	Lawrence Livermore National Laboratory
NPP	Nuclear Power Plant
PGA	Peak Ground Acceleration
RF	Receipt Facility
RRS	Required Response Spectrum
Sa	Spectral Acceleration
SFA	Surface Facilities Area
SFTM	Spent Fuel Transfer Machine
SPRA	Seismic Probabilistic Risk Assessment
SRSS	Square Root of the Sum of Squares
SSE	Safe Shutdown Earthquake (used with NPPs)
SSI	Soil Structure Interaction
SSC	Structure, System, and Component
TAD	Transportation, Aging, and Disposal canister
TEV	Transport and Emplacement Vehicle
TRS	Test Response Spectrum
UHS	Uniform Hazard Spectra
USDOE	United States Department of Energy
USNRC	United States Nuclear Regulatory Commission
WHF	Wet Handling Facility
WP	Waste Package
WPTT	Waste Package Transfer Trolley
YMSF	Yucca Mountain Surface Facilities
ZPA	Zero Period Acceleration

FRAGILITY TERMINOLOGY

Am	Median Peak Ground Motion Capacity
β_R	Log Standard Deviation of Randomness
β_U	Log Standard Deviation of Uncertainty (Lack of Knowledge)
β_C	Composite Variability = $(\beta_R^2 + \beta_U^2)^{0.5}$
F_S	Strength Factor of Safety
β_{R_S}	Strength Randomness (typical)
β_{U_S}	Strength Uncertainty (typical)
β_{C_S}	Strength Composite Variability (typical)
F_μ	Inelastic Energy Absorption Factor of Safety
F_{QM}	Qualification Factor of Safety
F_δ	Damping Factor of Safety
F_M	Modeling Factor of Safety
F_{MC}	Modal Combination Factor of Safety
F_{ECC}	Earthquake Component Combination Factor of Safety
F_{SA}	Spectral Shape Factor of Safety
F_{SSI}	Soil-Structure Interaction Factor of Safety
F_{GMI}	Ground Motion Incoherence Factor of Safety
F_{TOTAL}	Total Factor of Safety
F_{RS}	Structural Response Factor of Safety
F_{RE}	Equipment Response Factor of Safety

G1. PURPOSE

The purpose of this calculation is to estimate seismic fragility of the Site Transporter as it is loaded with an Aging Overpack in the Canister Receipt and Closure Facility (CRCF) and as it shuttles loaded Aging Overpacks between the handling facilities and the Aging Pad. The mean seismic fragility curve of the Important to Safety (ITS) Site Transporter will be convolved with the mean site-specific seismic hazard curve to calculate risk of seismic-induced failure of the transporter.

G2. REFERENCES

G2.1 PROCEDURES/DIRECTIVES

G2.1.1 EG-PRO-3DP-G04B-00037, Rev. 10. *Calculations and Analyses*. Las Vegas, Nevada: Bechtel SAIC Company. ACC: ENG.20071018.0001.

G2.1.2 BSC (Bechtel SAIC Company) 2005. *Q-List*. 000-30R-MGR0-00500-000-003. Las Vegas, Nevada: Bechtel SAIC Company. ACC: ENG.20050929.0008. [DIRS 175539]

G2.1.3 IT-PRO-0011, Revision 7, ICN 0. *Software Management*. Las Vegas, Nevada: Bechtel SAIC Company. ACC: DOC.20070905.0007.

G2.1.4 BSC (Bechtel SAIC Company) 2007. *Quality Management Directive*. QA-DIR-10, Rev. 2. Las Vegas, Nevada: Bechtel SAIC Company. ACC: DOC.20080103.0002. [DIRS 184673]

G2.2 DESIGN INPUTS

G2.2.1 EPRI (Electric Power Research Institute) 1994. *Methodology for Developing Seismic Fragilities*. EPRI TR-103959. Palo Alto, California: Electric Power Research Institute. TIC:253770. [DIRS 161329]

G2.2.2 BSC (Bechtel SAIC Company) 2007. *Site Transporter Mechanical Equipment Envelope*. V0-CY05-QHC4-00459-00032-001REV004. Las Vegas, Nevada: Bechtel SAIC Company. ACC: ENG.20071022.0010. [DIRS 183527]

G2.2.3 [Reserved]

G2.2.4 BSC (Bechtel SAIC Company) 2007. Site Transporter Site Interface Drawing. V0-CY05-QHC4-00459-00054-001 REV 002. Las Vegas, Nevada: Bechtel SAIC Company. ACC: ENG.20071024.0019. [DIRS 184419]

G2.2.5 BSC (Bechtel SAIC Company) 2007. *Yucca Mountain Site Transporter – Preliminary Seismic Analysis*. V0-CY05-QHC4-00459-00079-001 REV 001. Las Vegas, Nevada: Bechtel SAIC Company. ACC: ENG.20071024.0014. [DIRS 183530]

G2.2.6 BSC (Bechtel SAIC Company) 2007. *Mechanical Handling Design Report – Site Transporter*. 170-30R-HAT0-00100-000-000. Las Vegas, Nevada: Bechtel SAIC Company. ACC: ENG.20071217.0015. [DIRS 184489]

G2.2.7 ASME NOG-1-2004. 2005 *Rules for Construction of Overhead and Gantry Cranes (Top Running Bridge, Multiple Girder)*. New York, New York: American Society of Mechanical Engineers. TIC: 257672. [DIRS 176239]

G2.2.8 ASCE/SEI 43-05. 2005. *Seismic Design Criteria for Structures, Systems, and Components in Nuclear Facilities*. Reston, Virginia: American Society of Civil Engineers. TIC: 257275. [DIRS 173805]

G2.2.9 MO0801HCUHSSFA.001. *Mean Hazard Curves and Mean Uniform Hazard Spectra for the Surface Facilities Area*. Submittal date: 01/11/2008. [DIRS 184802]

G2.2.10 BSC (Bechtel SAIC Company) 2007. *CRCF Tier-1 In-Structure Response Spectra*. 060-SYC-CR00-00900-000-00B. Las Vegas, Nevada: Bechtel SAIC Company. ACC: ENG.20071210.0008. [DIRS 184330]

G2.2.11 [Reserved].

G2.2.12 [Reserved]

G2.2.13 Hajje, N. 2007. "FW: Contact Us Form Submittal from Web Site." E-mail from N. Hajje (Fabreeka) to E.C. Blom, November 15, 2007, without attachment. ACC: LLR.20080110.0148. [DIRS 184845]

G2.2.14 Baltay, P. and Gjelsvik, A. 1990. "Coefficient of Friction for Steel on Concrete at High Normal Stress." *Journal of Materials in Civil Engineering, 2*, (1), 46-49. [New York, New York]: American Society of Civil Engineers. TIC: 260005. [DIRS 184424]

G2.3 DESIGN CONSTRAINTS

None.

G2.4 DESIGN OUTPUTS

The calculation is performed to calculate seismic fragility of the Site Transporter which will be convolved with the site-specific seismic hazard curve to calculate risk of seismic-induced failure of the transporter. This is performed to support information in the License Application.

G3. ASSUMPTIONS

G3.1 ASSUMPTIONS REQUIRING VERIFICATION

There are no assumptions made in the calculation that require verification.

G3.2 ASSUMPTIONS NOT REQUIRING VERIFICATION

There are no assumptions not requiring verification that have been used in this calculation.

G4. METHODOLOGY

G4.1 QUALITY ASSURANCE

This calculation is prepared in accordance with EG-PRO-3DP-G04B-00037, Calculations and Analyses (Reference G2.1.1). The Site Transporter is classified as Important to Safety on the Q List (Reference G2.1.2), Table A-1. Therefore, this document is subject to the appropriate requirements for the BSC Quality Management Directive (Reference G2.1.4, Section 2.1.C.1.1), and the approved record version is designated as "QA:QA".

G4.2 USE OF SOFTWARE

Mathcad version 14 is used in this calculation. The use of this software is classified as Level 2 software per procedure IT-PRO-0011 (Reference G2.1.3) and therefore the software need not be qualified.

G4.3 APPROACH

The Separation-of-Variable method (Section 3 of Reference G2.2.1) is followed in calculating seismic fragility of the ITS equipment component.

G5. LIST OF APPENDICES

There are no appendices to this calculation.

G6. FRAGILITY CALCULATION

G6.1 INTRODUCTION

Seismic fragility calculation of the Site Transporter in the CRCF and between the CRCF and the Aging Pad is presented in this section. The transporter can be located at the ground floor (elevation 0') of the CRCF. The transporter can also be located outside all facilities on a roadway of compacted aggregate.

G6.2 SITE TRANSPORTER

The Site Transporter is an diesel/electric self-propelled tracked vehicle (Figure G6.2-1) that is designed to transport a concrete and steel ventilated Aging Overpack (AO). The Site Transporter is described in References G2.2.2 and G2.2.6. When loaded, the AO is in the vertical position with a lid on the top. The interface between the Site Transporter and the AO is via two lifting forks that pass through the AO at its lower end. In addition, the AO is held in the transporter by front support arms and by a cask restraint system applied near the top end of the AO. The Site Transporter operated on diesel power when outdoors between handling facilities and the Aging Pad. It is operated through an electrical umbilical when it is located within the CRCF or other facilities.

While in the CRCF, the site transporter sets on the concrete ground floor and has clearances to adjacent walls as shown in Figure G6.2-2 (Reference G2.2.4). Minimum clearance is 19.42 inches from the edge of the transporter to the back wall and 51 inches to the side wall.

While on the road outdoors, the Site Transporter may be on a slope of as much as 5 % grade in the direction of travel and as much as 2 % grade transversely as shown in Figure G6.2-3 (References G2.2.2 and G2.2.6).

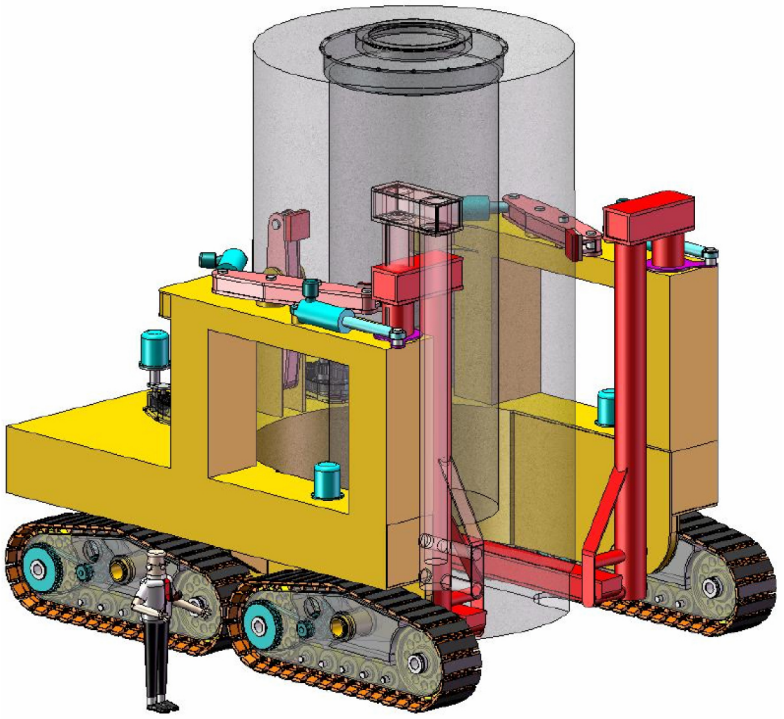

Figure G6.2-1. Site Transporter (Reference G2.2.6)

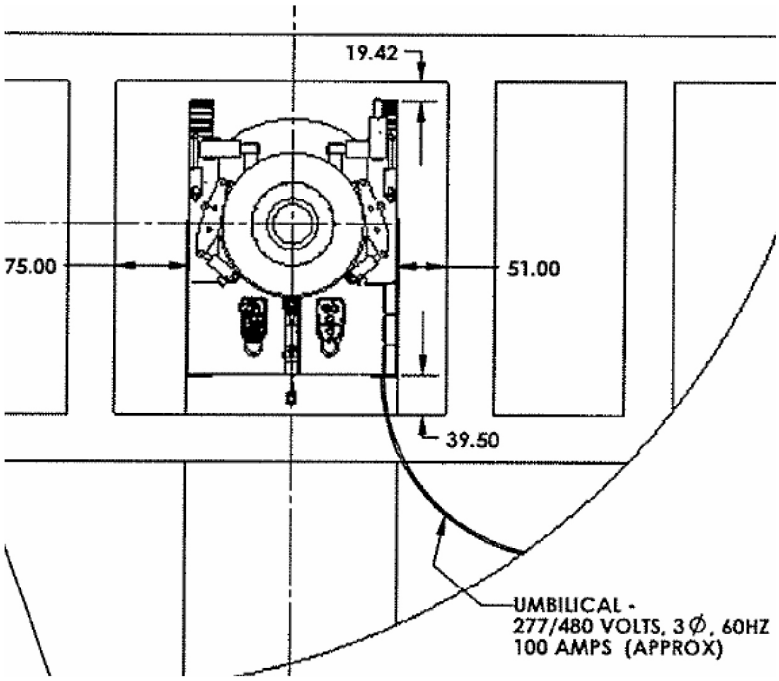

Figure G6.2-2. Site Transporter Clearances (in) within the CRCF (Reference G2.2.4)

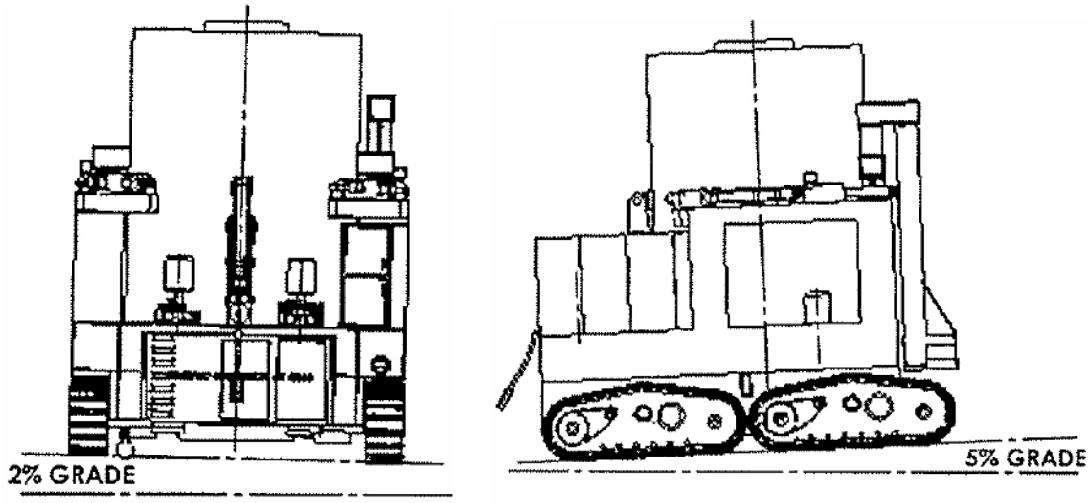

Figure G6.2-3. Site Transporter Maximum Slopes on Outdoor Roadways (Reference G2.2.2)

G6.3 POTENTIAL FAILURE MODES

Potential failure modes of the Site Transporter that may impact performance goals of the Yucca Mountain Project are presented below based on our understanding of safety functions and operation of the transporter.

G6.3.1 Transporter Structural Failure

Reference G2.2.5 provides design analyses of the Site Transporter for load combinations including DBGM-2 and BDBGM. The stresses in the transporter due to BDBGM load combination are found to be lower than the NOG-1 stress limits (Table 4311-1 of Reference G2.2.7). The DBGM-2 stresses are calculated to be much lower that the NOG-1 stress limits. These calculated design stresses are overly conservative for the reasons given below:

The transporter is modeled as fixed at the base. The horizontal fundamental frequencies are calculated to be between 13 and 18 Hz. The vertical fundamental frequency is calculated to be about 10 Hz. At these frequencies, response is in the highly amplified region of the input response spectrum used in the analysis (Reference G2.2.5). In reality, sliding and or rocking of the transporter will initiate at a low acceleration level. The transporter is not fixed at its base and will slide or rock as a rigid body and the equivalent system frequency will be much lower than that computed in Ref. G2.2.5 and the spectral acceleration will be much less than that used in Ref. G2.2.5.

The maximum transporter stresses due to the three components of earthquake were assumed to all occur at the same location in the transporter. This results in conservative seismic stresses in the transporter.

The abovementioned conservatism in the P&H design analysis is acceptable for design purpose. However, using these stresses will result in conservatively biased (unrealistic) seismic fragility

estimates. Because there is margin for the BDBGM to NOG-1 stress limits with very conservative analyses, the failure mode due to seismic-induced stresses in the Site Transporter is not considered to be governing. Rocking and sliding of the Site Transporter govern the seismic fragility,

G6.3.2 Inside the CRCF

The electric-powered transporter travels on the concrete floor slab. The free-standing Site Transporter is subject to seismic-induced sliding or tip over. A potential consequence of sliding or tip over of the trolley is impact of the transporter with CRCF concrete walls. Upon sliding or rocking and impacting a CRCF cell wall, breach of a canister inside an Aging Overpack is taken to be a credible failure mode. The probability of breach given transporter impact is not included in this calculation.

G6.3.3 During Transit to the Aging Pad

The diesel-powered transporter travels on a compacted aggregate roadway. The Site Transporter could be subject to seismic-induced sliding or tip over. There are no adverse consequences of sliding or rocking as there are no nearby surfaces to impact. However, upon overturning of the Site Transporter during an earthquake, breach of a canister inside an Aging Overpack is taken to be a credible failure mode. However, sliding of the Site Transporter within the CRCF will occur at a much lower earthquake acceleration level for this relatively low profile vehicle as shown in Section G6.3.4.

Overturning of the low profile Site Transporter will not occur at credible acceleration levels even considering the sloping grades during transit to the aging pads (Figure G6.2-3) as demonstrated in Section 6 of Reference G2.2.5. It is also demonstrated that overturning will not occur based on overturning calculations for the TEV as presented in Attachment H. Reference G2.2.8 shows that overturning depends on the ratio b/h and the earthquake ground motion (b = horizontal distance from c.g. to edge of body; h = height of the c.g.). The TEV experiences the motion of the ground floor within the building while the Site Transporter during transit experiences free field motion. At low rocking frequencies these motions are the same as demonstrated in Attachment H.

TEV: b = 66 inches; h = 65 inches; b/h = 1.015 per Attachment H
Site Transporter: b = 105 inches; h = 109 inches; b/h = 0.96 as shown below (transverse)

Attachment H concludes that the TEV will not overturn at any credible ground motion. The same conclusion is applicable for the Site Transporter that has similar aspect ratio and ground motion.

Hence, overturning during transit to the aging pad is not considered to be a governing failure mode.

G6.3.4 Governing Failure Mode

Based on the above discussions, either sliding or tip over of the Site Transporter is a credible failure mode. The governing failure mode is evaluated below.

The center of gravity of the transporter loaded with the heaviest AO is at (Reference G2.2.5):

$H_{cg} := 109.07 \cdot in$ Height measured from the bottom of the transporter

$X_{cg} := 153.23 \cdot in$ From the edge of the transporter tracks in the longitudinal direction of the transporter)

$Y_{cg} := 105 \cdot in$ From the edge of the transporter tracks in the transverse direction.

$W_t := 800 \cdot kip$ Total weight of the loaded transporter (Ref. G2.2.2)

When an earthquake occurs, the track pads of the transporter will rest on the concrete floor. The track pads include a resilient pad made of a material called Fabreeka (Ref. G2.2.6). According to Reference G2.2.13, the best-estimate coefficient of friction between the Fabreeka pads on the steel tracks and the concrete floor slab is 0.65.

$\mu := 0.65$ Reference G2.2.13

Based on the above given center of gravity, the acceleration level at which one edge of the transporter base will lift up is determined.

$$S_{a\_liftupT} := \left(\frac{Y_{cg}}{H_{cg}}\right) \cdot g \qquad S_{a\_liftupL} := \left(\frac{X_{cg}}{H_{cg}}\right) \cdot g$$

$S_{a\_liftupT} = 0.96 \cdot g$ $S_{a\_liftupL} = 1.4 \cdot g$

At this acceleration level, the seismic inertia load of the transporter is

$$V_{uplift\_transverse} := W_t \cdot \frac{S_{a\_liftupT}}{g} \qquad V_{uplift\_longitudinal} := W_t \cdot \frac{S_{a\_liftupL}}{g}$$

$V_{uplift\_transverse} = 770.15 \cdot kip$ $V_{uplift\_longitudinal} = 1123.9 \cdot kip$

Frictional resistance at the base of the transporter

$V_{friction} := \mu \cdot W_t$

$V_{friction} = 520 \cdot kip$ Much less than the seismic inertia load at uplift

Since the acceleration level at which transporter sliding occurs is so much less than the acceleration level for lifting at one edge, seismic fragility of only the sliding failure mode is evaluated.

G6.4 SEISMIC INPUT MOTION

The Site Transporter operates at the ground floor of the CRCF. Therefore seismic input motion to the transporter is defined by the CRCF ISRS at elevation 0'. Note that there will be three identical CRCFs on site. The depth of alluvium under these CRCFs varies from 100 feet to 200 feet. The 100-ft alluvium case yields slightly higher ISRS than the 200-ft alluvium case. The 5% and 10% damped BDBGM ISRS in the two horizontal directions and the vertical direction for the 100-foot alluvium case are presented in Figures G6.4-1, G6.4-2, and G6.4-3. Also presented in the figures are the 5% damped site-wide UHS (Reference G2.2.9; also Section 6.2.2.1 for source information). The 10% damped BDBGM ($1x10^{-4}$ annual exceedance frequency) will be used in the calculations.

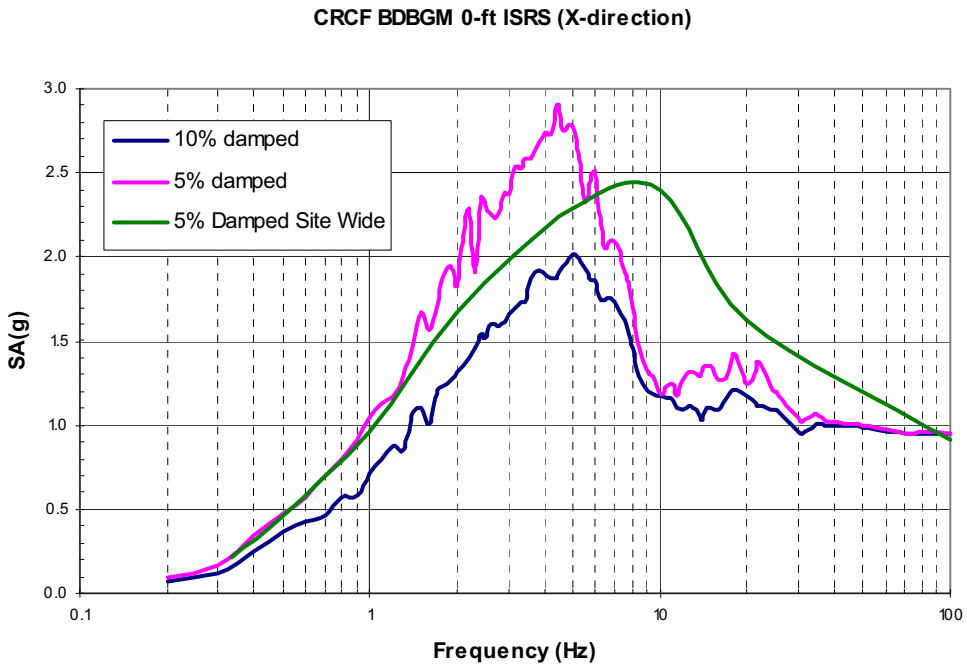

Figure G6.4-1. X-Direction BDBGM ISRS at 0' Floor - Median Soil Case (Plotted from Data in Reference G2.2.10)

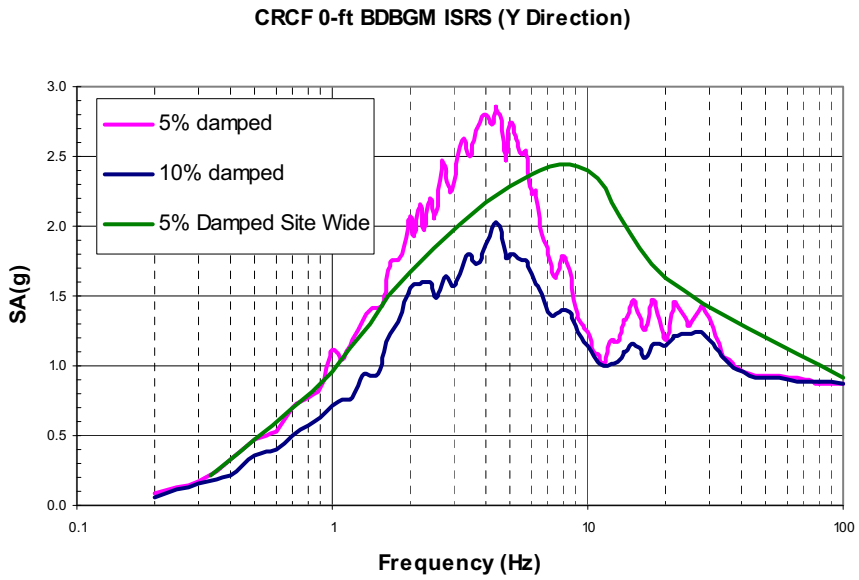

Figure G6.4-2. Y-Direction BDBGM ISRS at 0' Floor - Median Soil Case (Plotted from Data in Reference G2.2.10)

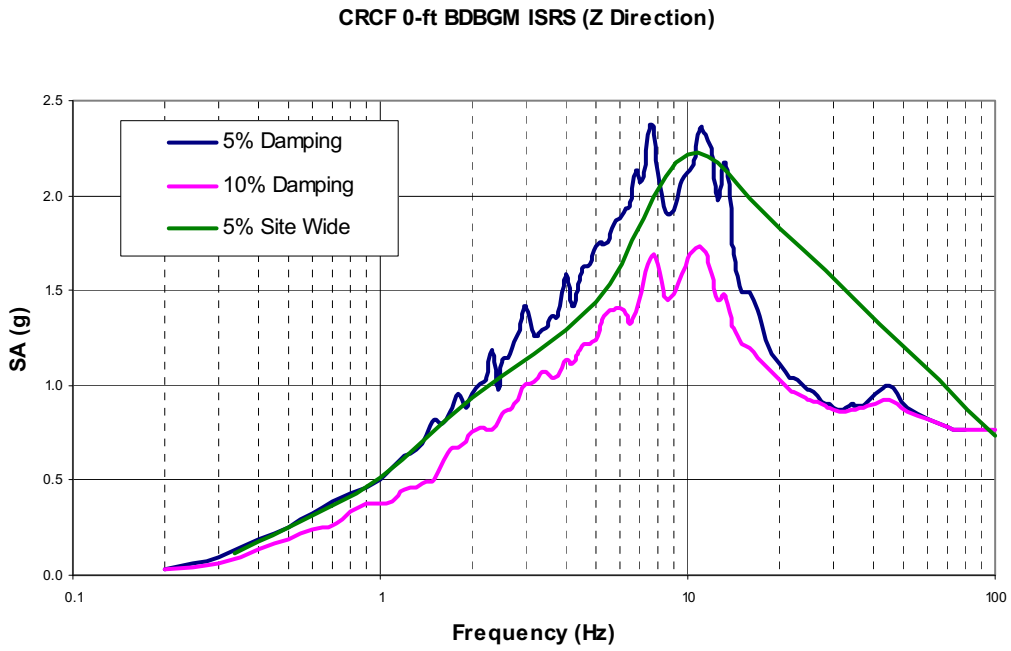

Figure G6.4-3. Z-Direction (Vertical) BDBGM ISRS at 0' Floor - Median Soil Case (Plotted from Data in Reference G2.2.10)

G6.5 FRAGILITY OF SEISMIC-INDUCED SLIDING OF THE SITE TRANSPORTER

The approach presented in Appendix A.1 of ASCE 43-05 (Reference G2.2.8) is used to calculate the best-estimate seismic-induced sliding displacement of the Site Transporter at which impact between the transporter and the transfer cell walls would occur.

G6.5.1 Strength Factor

The displacement limit of the Site Transporter is determined based on the clearance between the transporter and the walls of the transfer cell. As shown in Figure G6.2-2. the closest distance from the transporter to the cell wall is 19.42 inches (Reference G2.2.4).

$$\delta_{limit} := 19.42 \cdot in$$

Next the rigid body displacement of the transporter is calculated using the reserve energy method in Appendix A of Reference G2.2.8. This method treats the nonlinear problem of rigid body sliding using an equivalent linear model. The rigid-body displacements are calculated for input motion of different annual probabilities of exceedance and the motion which yields a displacement closest to the limit is used for the strength factor calculation.

$\mu_e := \mu$ The effective coefficient of sliding friction does not account for the vertical component of ground motion for a "best-estimate" sliding displacement. This is because the vertical acceleration will oscillate several times during the time the rigid body displaces from 0 to a finite displacement.

$\mu_e = 0.65$ Friction coefficient between resilient pads of the site transporter and concrete per Reference G2.2.13.

The force-displacement curve of a rigid body sliding is shown in Figure G6.5-1, where F_{RS} is the resisting force and δ_S is the displacement to be estimated. Based on the reserve energy method, an equivalent linear system is used to estimate the displacement. This equivalent system has a stiffness of K_e and a displacement of

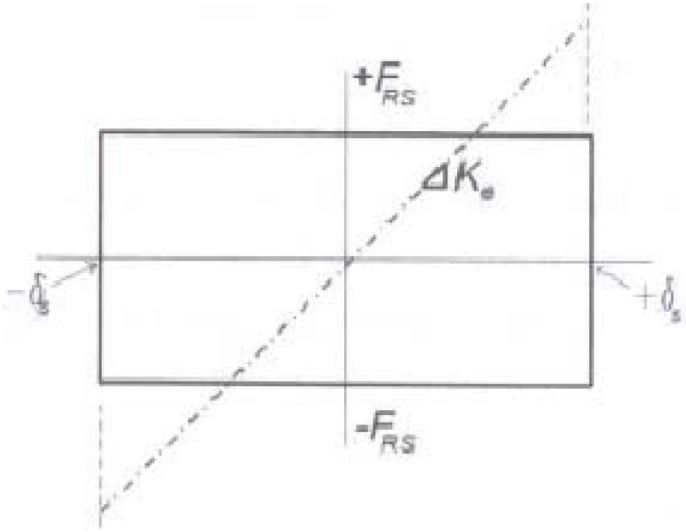

Figure G6.5-1. Sliding Force-Displacement Diagram (Reference G2.2.8, Appendix B)

Next define sliding coefficient as shown below

$c_s := 2 \cdot \mu_e \cdot g$ Equation A-2 of Reference G2.2.8, where g is the gravitational acceleration.

$c_s = 1.3 \cdot g$

Based on the reserve energy method, the sliding displacement of the rigid body is estimated by Equation B-5 of Reference G2.2.8 in which f_{eS} is the lowest natural frequency at which the vector horizontal spectral acceleration equals c_s.

$SA_H := 0.1 \cdot g$ Initial trial value of SA_H (i.e., spectral acceleration in one horizontal direction) to solve the equation below so that the vector horizontal spectral acceleration is equal to c_s.

Given

$\sqrt{SA_H^2 + 0.16SA_H^2} = c_s$ The two horizontal components of earthquake have essentially the same spectral shape. Equation A-4 of Reference G2.2.8.

$SA_H := \text{Find}(SA_H)$

$SA_H = 1.21 \cdot g$

The lowest natural frequency (f_{eS}) at which the vector spectral acceleration equals c_s is determined from the 10% damped BDBGM ISRS at the ground floor which has an annual exceedance frequency of 10^{-4} as shown in Figure G6.4-1.

$f_{es} := 1.7 \cdot Hz$ at which the spectral acceleration in one direction is 1.21g.

$\delta_s := \frac{c_s}{(2 \cdot \pi \cdot f_{es})^2}$ Sliding distance as given in Equation A-3 of Reference G2.2.8

$\delta_s = 4.4 \cdot in$ This BDBGM-induced displacement will not result in impact with the cell wall. When the transporter slides more than 19.42 inches and impacts the CRCF wall, a breach is assumed.

$F_S := \frac{\delta_{limit}}{\delta_s}$ Because sliding is a nonlinear seismic response it is necessary to consider ground motion for which the factor of safety is near unity.

$F_S = 4.41$

Next the lowest natural frequency (f_{eS}) at which the vector spectral acceleration equals c_s is determined from the ISRS at the ground floor which has an annual exceedance frequency of 10^{-5}. Though the 10^{-5} ISRS are not available, f_{eS} can be estimated from the 1E-5 site-wide ground response spectrum as shown in Table G6.5-1. Figures G6.4-1 and 2 show that the in-structure spectra are essentially the same as the ground response spectrum in the frequency range less than 1 Hz. Thus, the 5% damped 1E-5 UHS is scaled to 10% UHS using the 5% and 10% BDBGM ISRS in Figures G6.4-1 and G6.4-2.

Table G6.5-1 10% Damped 1E-5 UHS Scaled From 5% Damped 1E-5 Site-Wide UHS

Frequency (Hz)	5% Damped BDBGM Sa (g)	10% Damped BDBGM Sa (g)	Ratio	5% Damped 1E-5 Sa (g);Figure C6.5-2	Scaled 10% Damped 1E-5 Sa (g)
0.3	1.72E-01	1.18E-01	0.69	0.48	0.33
0.4	3.45E-01	2.49E-01	0.72	0.9	0.65
0.5	4.75E-01	3.62E-01	0.76	1.35	1.03
0.6	5.73E-01	4.23E-01	0.74	1.7	1.26
0.7	6.94E-01	4.64E-01	0.67	1.94	1.30
0.8	7.96E-01	5.71E-01	0.72	2.2	1.58
0.9	9.15E-01	5.79E-01	0.63	2.4	1.52

$f_{es} := 0.58 \cdot Hz$

At this frequency the 10% damped 1E-5 spectral acceleration is equal to 1.21g.

$$\delta_s := \frac{c_s}{\left(2 \cdot \pi \cdot f_{es}\right)^2}$$

Sliding distance as given in Equation A-3 of Reference G2.2.8

$\delta_s = 3.15 \cdot ft$

This sliding distance is greater than the distance from the transporter to the wall of 19.42 inches.

$$F_S := \frac{\delta_{limit}}{\delta_s}$$

$F_S = 0.51$

This factor of safety is also not sufficiently close to unity to account for sliding nonlinearity properly.

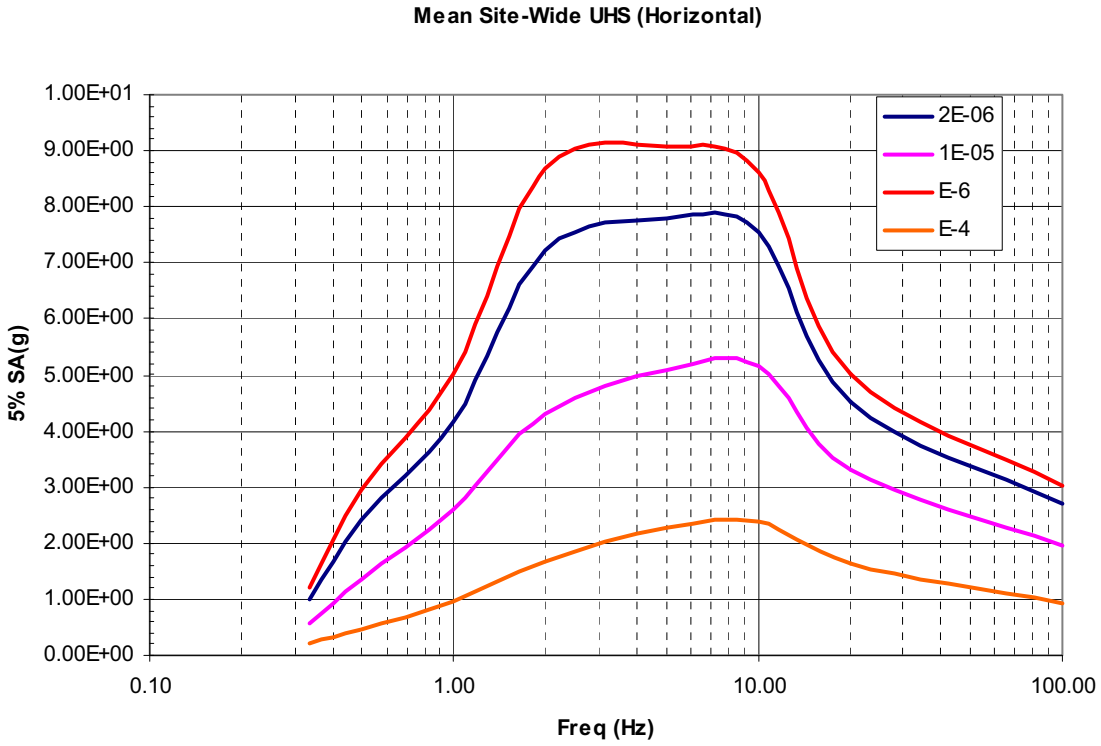

Figure G6.5-2. 5% Damped Mean Site-Wide Horizontal Uniform Hazard Spectra at E-4, E-5, 2E-6 and E-6 APE (See Section 6.2.2.1 for source information)

Next, the BDBGM spectra will be scaled up to calculate the transporter sliding distance until the clearance of 19.42 inches is closed.

1.5 times the BDBGM

At the frequency of 1.11 Hz, 1.5 times the 10% damped BDBGM floor spectral acceleration is equal to SA_H (1.21g). This is determined from the digitized CRCF X - direction ISRS at the ground floor in Reference G2.2.10.

$$f_{es} := 1.11 \cdot Hz$$

$$\delta_s := \frac{c_s}{\left(2 \cdot \pi \cdot f_{es}\right)^2} = 10.32 \cdot in$$ Less than the 19.42 inch clearance

2.12 times the BDBGM

At the frequency of 0.8 Hz, 2.12 times the 10% damped BDBGM floor spectral acceleration is equal to SA_H (1.21g). This is determined from the digitized CRCF X - direction ISRS at the ground floor in Reference G2.2.10.

$f_{es} := 0.8 \cdot Hz$

$\delta_s := \frac{c_s}{\left(2 \cdot \pi \cdot f_{es}\right)^2} = 19.87 \cdot in$ This approximately equals the distance to the wall of 19.42 inches.

$F_S := \frac{\delta_{limit}}{\delta_s}$ $F_S = 0.98$

Note that this strength factor is relative to 2.12 times the BDBGM.

G6.5.1.1 Uncertainty in Equation

A factor of safety of 2 is recommended for the calculated rigid body displacement for design purposes (Appendix A.1 of Reference G2.2.8). Based on common design practice, a design value typically represents at least a 98% non-exceedance value. Based on this, uncertainty associated with the best-estimate displacement is calculated.

$\beta_{U\_S\_1} := \frac{1}{2} \cdot \ln(2)$ The 98% non-exceedance value is two (2) standard deviation from the mean. The second value of 2 in the equation is the factor of safety recommended for design value.

$\beta_{U\_S\_1} = 0.35$

$\beta_{R\_S} := 0$ There is no randomness associated with the strength factor.

G6.5.1.2 Uncertainty in Coeff. of Friction

A median value of 0.65 is used for coefficient friction between the transporter track resilient pads and concrete based on Reference G2.2.13. A -1σ value of 0.55 is estimated based on the variation of friction for steel on concrete (Figure 4 of Reference G2.2.14) and scaled to match the Fabreeka friction.

$\mu_{1\sigma} := 0.55$

$c_{s\_1\sigma} := 2 \cdot \mu_{1\sigma} \cdot g$

$c_{s\_1\sigma} = 1.1 \cdot g$

Based on the reserve energy method, the sliding displacement of the rigid body is estimated by Equation B-5 of Reference G2.2.8 in which f_{eS} is the lowest natural frequency at which the vector horizontal spectral acceleration equals to c_s.

$SA_H := 0.1 \cdot g$ Initial trial value of SA_H (i.e., spectral acceleration in one horizontal direction) to solve the equation below so that the vector horizontal spectral acceleration is equal to c_s

Given

$\sqrt{SA_H^2 + 0.16 SA_H^2} = c_{s\_1\sigma}$ Assuming the two horizontal components of earthquake have the same spectral shape. Equation A-4 of Reference G2.2.8.

$SA_H := \text{Find}(SA_H)$

$SA_H = 1.02 \cdot g$

The lowest natural frequency (f_{eS}) at which the vector spectral acceleration equals c_s is determined from **2.0** times the 10% damped BDBGM ISRS.

$f_{es} := 0.74 \cdot Hz$

$\delta_{s\_1\sigma} := \frac{c_{s\_1\sigma}}{(2 \cdot \pi \cdot f_{es})^2}$ Equation A-3 of Reference G2.2.8

$\delta_{s\_1\sigma} = 19.65 \cdot in$ Approximately equals the 19.42 clearance distance

$\beta_{U\_S\_2} := -\ln\left(\frac{2.0}{2.12}\right)$ See Section G6.5.1 for the scale factor 2.12 applied to the BDBGM to reach a sliding displacement of 19.42 inches

$\beta_{U\_S\_2} = 0.06$

$\beta_{U\_S} := \sqrt{\beta_{U\_S\_1}^2 + \beta_{U\_S\_2}^2}$

$\beta_{U\_S} = 0.35$

G6.5.2 Inelastic Energy Absorption Factor

For rigid body sliding, there is no inelastic energy absorption capability. Thus,

$F_\mu := 1.0$

$\beta_{R\_\mu} := 0$

$\beta_{U\_\mu} := 0$

G6.5.3 Structural Response Factors

As shown in Figures G6.4-1 and G6.4-2, the 5% damped BDBGM ISRS at frequencies near 1 Hz is essentially same as the site-wide 5% damped BDBGM UHS. Since the seismic-induced sliding of the Site Transporter is responding in this low frequency range as shown above, the transporter is treated as a structure founded at grade.

G6.5.3.1 Spectral Shape Factor

$F_{SA} := 1.0$ The median strength factor is calculated based on input motion of mean BDBGM site-wide ground response spectrum.

Since uncertainty in the UHS is derived from uncertainty in the seismic hazard curves which will be included in the final risk quantification, no additional uncertainty is included under the spectral shape factor to avoid double-counting the hazard uncertainty, hence

$\beta_{U\_SA} := 0$

$\beta_{R\_SA} := 0.2$ This is random variability to account for peak to valley variability of a smooth ground response spectrum (Reference G2.2.1).

G6.5.3.2 Damping Factor

A damping value of 10% is suggested in Reference G2.2.8 (page 33 of Reference G2.2.8) for the rigid body sliding calculation. Since the 10% damped spectrum was used in the strength factor calculation, thus

$F_{\delta} := 1.0$

$\beta_{U\_\delta} := 0.05$ A nominal value

$\beta_{R\_\delta} := 0$

G6.5.3.3 Modeling Factor

The reserve energy method used in calculating the sliding displacement above is a conservatively biased "best estimate" method (Section A.1 of Reference G2.2.8). Using this method, a factor of safety of 2.0 is recommended to obtain the design value of sliding (Reference G2.2.8). Thus, the modeling factor of safety is assigned a value of unity.

$F_M := 1$

$\beta_{R\_M} := 0$

$\beta_{U\_M} := 0$ Since the modeling uncertainty is already included in the uncertainty of equation in Section G6.5.1.1.

G6.5.3.4 Modal Combination

Since it is single mode response,

$F_{MC} := 1$

$\beta_{R\_MC} := 0.05$ A nominal value

$\beta_{U\_MC} := 0$

G6.5.3.5 Earthquake Component Combination

In the strength factor calculation above, the best-estimate vector spectral acceleration is the combination of S_{AH} and $0.4*S_{AH}$. The vector of 100% of both horizontal components is at 3 sigma from the median case.

$F_{EC} := 1.0$ Since the best-estimate earthquake component combination is used in the above strength factor calculation.

$SA_H := 0.1 \cdot g$ Initial trial value of SA_H (i.e., spectral acceleration in one horizontal direction) to solve the equation below so that the vector horizontal spectral acceleration is equal to c_s

Given

$$\sqrt{SA_H^2 + SA_H^2} = c_s$$

$a_{3\sigma} := \text{Find}(SA_H)$

$a_{3\sigma} = 0.92 \cdot g$

The lowest natural frequency (f_{eS}) at which the vector spectral acceleration equals c_s is determined from **1.6** times the 10% damped mean BDBGM ISRS.

$f_{es} := 0.81 \cdot Hz$

$$\delta_{s\_3\sigma} := \frac{c_s}{(2 \cdot \pi \cdot f_{es})^2}$$

$\delta_{s\_3\sigma} = 19.38 \cdot in$

$\beta_{R\_EC} := \frac{-1}{3} \cdot \ln\left(\frac{1.6}{2.12}\right)$ See Section G6.5.1 for the scale factor 2.12 applied to the BDBGM to reach a sliding displacement of 19.42 inches.

$\beta_{R\_EC} = 0.09$

$\beta_{U\_EC} := 0$

G6.5.3.6 Soil-Structure Interaction

The soil-structure interaction effects were considered in the BSC Tier 1 CRCF seismic response analysis (Reference G2.2.10) using frequency independent soil springs and soil damping coefficients based on an elastic half space. The calculated translational soil damping coefficients were reduced by 25% to account for layering effects. Three soil properties were considered in the BSC SSI analysis, i.e., lower bound, median, and upper bound. It is seen from Figure G6.5-3 below that in the frequency range of sliding of the Site Transporter, there is practically no difference in the response due to difference in soil properties.

At the frequency of the equivalent linear model (<1 Hz) the SSI effects are minimal as shown in Figure G6.5-3, the factor of safety of the soil-structure interaction analysis is set as unity.

$F_{SSI} := 1.0$

$\beta_{R\_SSI} := 0$

$\beta_{U\_SSI} := 0.05$ Nominal value used

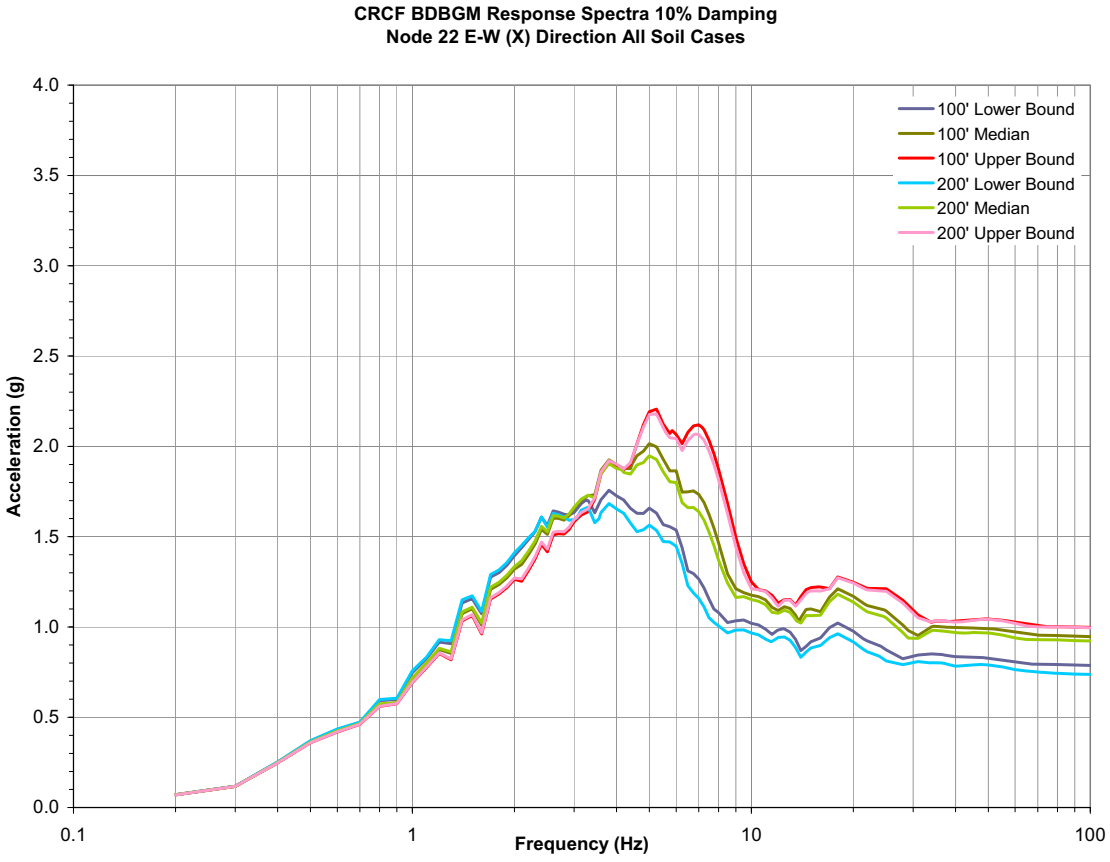

Figure G6.5-3 BDBGM Elevation 0 Feet In-Structure Response Spectra (Reference G2.2.10)

G6.5.4 Overall Factor of Safety of Site Transporter Sliding

$F_{total} := F_S \cdot F_\mu \cdot F_{SA} \cdot F_\delta \cdot F_M \cdot F_{MC} \cdot F_{EC} \cdot F_{SSI}$

$F_{total} = 0.98$

$PGA := (2.12) \cdot 0.914g$

Peak ground acceleration of the BDBGM site-wide UHS (Ref. G2.2.10) multiplied by a factor of 2.12 to be compatible with the strength factor per Section G6.5.

$PGA = 1.94 \cdot g$

$A_m := F_{total} \cdot PGA$

$A_m = 1.89 \cdot g$ Median seismic capacity in terms of PGA

$\beta_R := \sqrt{\beta_{R\_S}^2 + \beta_{R\_\mu}^2 + \beta_{R\_SA}^2 + \beta_{R\_\delta}^2 + \beta_{R\_M}^2 + \beta_{R\_MC}^2 + \beta_{R\_EC}^2 + \beta_{R\_SSI}^2}$

$\beta_R = 0.23$

$\beta_U := \sqrt{\beta_{U\_S}^2 + \beta_{U\_\mu}^2 + \beta_{U\_SA}^2 + \beta_{U\_\delta}^2 + \beta_{U\_M}^2 + \beta_{U\_MC}^2 + \beta_{U\_EC}^2 + \beta_{U\_SSI}^2}$

$\beta_U = 0.36$

$\beta_c := \sqrt{\beta_R^2 + \beta_U^2}$

$\beta_c = 0.42$

$HCLPF := A_m \cdot e^{-2.33 \cdot \beta_c}$

$HCLPF = 0.71 \cdot g$

G7 SUMMARY

The seismic-induced failure of the Site Transporter due to rigid body sliding is evaluated and seismic fragility is calculated. The governing failure mode is taken to be that when the transporter impacts the CRCF walls, and a breach could occur. It is shown that transporter structural failure and transporter rocking or overturning would occur at higher earthquake shaking levels

Seismic fragilities of the Site Transporter are shown below:

Sliding: Site Transporter slides and impacts the CRCF concrete wall

$A_m = 1.89 \cdot g$ $\beta_c = 0.42$ HCLPF $= 0.71 \cdot g$

Overturning: The Site Transporter will not overturn during transit from the handling facilities to the Aging Pad at any credible earthquake ground shaking level.

ATTACHMENT H

FRAGILITY FOR WASTE PACKAGE TRANSPORT AND EMPLACEMENT VEHICLE (TEV)

Prepared by: Robert D. Campbell

ARES Check by: Wen H. Tong

LLNL Check by: Robert C. Murray

TABLE OF CONTENTS

ACRONYMS AND ABBREVIATIONS

ACI	American Concrete Institute
AISC	American Institute of Steel Construction
ANSI	American National Standards Insitute
AO	Aging Overpack
APE	Annual Probability of Exceedance
ASCE	American Society of Civil Engineers
ASME	American Society of Mechanical Engineers
BSC	Bechtel SAIC, LLC
BDBGM	Beyond Design Basis Ground Motion at $1x10^{-4}$ APE
CDFM	Conservative Deterministic Failure Margin
CHC	Cask Handling Crane
CIP	Cast-in-Place
CRCF	Canister Receipt and Closure Facility
CTM	Canister Transfer Machine
CTT	Cask Transfer Trolley
DBGM-2	Design Basis Ground Motion at $5x10^{-4}$ APE
DL	Dead Load
DOF	Degree of Freedom
DPC	Dual Purpose Canister
EPRI	Electric Power Research Institute
HCLPF	High Confidence of Low Probability of Failure
HVAC	Heating, Ventilation, & Air Conditioning
IEEE	Institute of Electrical and Electronics Engineers
IHF	Initial Handling Facility
ISRS	In-Structure Response Spectra

ACRONYMS AND ABBREVIATIONS (cont.)

ITS	Important to Safety
LA	License Application
LLNL	Lawrence Livermore National Laboratory
NPP	Nuclear Power Plant
PGA	Peak Ground Acceleration
RF	Receipt Facility
RRS	Required Response Spectrum
Sa	Spectral Acceleration
SFA	Surface Facilities Area
SFTM	Spent Fuel Transfer Machine
SPRA	Seismic Probabilistic Risk Assessment
SRSS	Square Root of the Sum of Squares
SSE	Safe Shutdown Earthquake (used with NPPs)
SSI	Soil Structure Interaction
SSC	Structure, System, and Component
TAD	Transportation, Aging, and Disposal canister
TEV	Transport and Emplacement Vehicle
TRS	Test Response Spectrum
UHS	Uniform Hazard Spectra
USDOE	United States Department of Energy
USNRC	United States Nuclear Regulatory Commission
WHF	Wet Handling Facility
WP	Waste Package
WPTT	Waste Package Transfer Trolley
YMSF	Yucca Mountain Surface Facilities
ZPA	Zero Period Acceleration

FRAGILITY TERMINOLOGY

Am	Median Peak Ground Motion Capacity
β_R	Log Standard Deviation of Randomness
β_U	Log Standard Deviation of Uncertainty (Lack of Knowledge)
β_C	Composite Variability = $(\beta_R^2 + \beta_U^2)^{0.5}$
F_S	Strength Factor of Safety
β_{R_S}	Strength Randomness (typical)
β_{U_S}	Strength Uncertainty (typical)
β_{C_S}	Strength Composite Variability (typical)
F_μ	Inelastic Energy Absorption Factor of Safety
F_{QM}	Qualification Factor of Safety
F_δ	Damping Factor of Safety
F_M	Modeling Factor of Safety
F_{MC}	Modal Combination Factor of Safety
F_{ECC}	Earthquake Component Combination Factor of Safety
F_{SA}	Spectral Shape Factor of Safety
F_{SSI}	Soil-Structure Interaction Factor of Safety
F_{GMI}	Ground Motion Incoherence Factor of Safety
F_{TOTAL}	Total Factor of Safety
F_{RS}	Structural Response Factor of Safety
F_{RE}	Equipment Response Factor of Safety

H1. PURPOSE

The purpose of this calculation is to develop the seismic fragility for the Waste Package Transport and Emplacement Vehicle (TEV) when it is loaded with a Waste Package and either at the waste package loadout station or in transit to the emplacement drifts.

H2. REFERENCES

H2.1 PROCEDURES AND DIRECTIVES

H2.1.1 EG-PRO-3DP-G04B-00037, Rev. 10. *Calculations and Analyses*. Las Vegas, Nevada: Bechtel SAIC Company. ACC: ENG.20071018.0001.

H2.1.2 IT-PRO-0011, Revision 7, ICN 0. *Software Management*. Las Vegas, Nevada: Bechtel SAIC Company. ACC: DOC.20070905.0007.

H2.2 DESIGN INPUTS

H2.2.1 EPRI (Electric Power Research Institute) 1994. *Methodology for Developing Seismic Fragilities*. EPRI TR-103959. Palo Alto, California: Electric Power Research Institute. TIC:253770. [DIRS 161329]

H2.2.2 ASCE/SEI 43-05. 2005. *Seismic Design Criteria for Structures, Systems, and Components in Nuclear Facilities*. Reston, Virginia: American Society of Civil Engineers. TIC: 257275. [DIRS 173805]

H2.2.3 BSC (Bechtel SAIC Company) 2007. *CRCF Tier-1 In-Structure Response Spectra*. 060-SYC-CR00-00900-000-00B. Las Vegas, Nevada: Bechtel SAIC Company. ACC: ENG.20071210.0008. [DIRS 184330]

H2.2.4 BSC (Bechtel SAIC Company) 2007. *Mechanical Handling Design Report: Waste Package Transport and Emplacement Vehicle.* 000-30R-HE00-00200-000 REV 001. Las Vegas, Nevada: Bechtel SAIC Company. ACC:ENG20071205.0002. [DIRS 184221].

H2.2.5 BSC (Bechtel SAIC Company) 2008. *Canister Receipt and Closure Facility 1 General Arrangement Ground Floor Plan*. 060-P10-CR00-00102-000 REV 00C. Las Vegas, Nevada: Bechtel SAIC Company. ACC: ENG.20080122.0013. [DIRS 184853]

H2.2.6 BSC (Bechtel SAIC Company) 2007. *CRCF Loadout Platforms Mechanical Equipment Envelope Sheet 1 of 2.* 060-MJ0-HL00-00201-000 REV 00A. Las Vegas, Nevada: Bechtel SAIC Company. ACC: ENG.20070315.0009; ENG20070823.0007. [DIRS 181725]

H2.2.7 BSC (Bechtel SAIC Company) 2007. *Emplacement and Retrieval Transport and Emplacement Vehicle Mechanical Equipment Envelope.* 800-MJ0-HE00-00101-000 REV 00B. Las Vegas, Nevada: Bechtel SAIC Company. ACC: ENG.20070918.0041. [DIRS 183353]

H2.2.8 BSC (Bechtel SAIC Company) 2007. *Transport and Emplacement Vehicle Envelope Calculation.* 800-MQC-HE00-00100-000-00B. Las Vegas, Nevada: Bechtel SAIC Company. ACC: ENG.20070830.0043. [DIRS 183139]

H2.2.9 ASME NOG-1-2004. 2005 *Rules for Construction of Overhead and Gantry Cranes (Top Running Bridge, Multiple Girder)*. New York, New York: American Society of Mechanical Engineers. TIC: 257672. [DIRS 176239]

H2.2.10 MO0801HCUHSSFA.001. *Mean Hazard Curves and Mean Uniform Hazard Spectra for the Surface Facilities Area*. Submittal date: 01/11/2008. [DIRS 184802]

H2.2.11 [Reserved]

H2.2.12 [Reserved]

H2.2.13 Moore, D. 2007. "*SSI Factor of Safety.*" E-mail from D. Moore to B. Murray, October 25, 2007. ACC: LLR.20080110.0145. [DIRS 184842]

H2.3 DESIGN CONSTRAINTS

None.

H2.4 DESIGN OUTPUTS

The design outputs are the seismic fragilities for selected failure modes of the TEV that could result in damage to a waste package and release of radioactive material.

H3. ASSUMPTIONS

H3.1 ASSUMPTIONS REQUIRING VERIFICATION

There are no assumptions requiring verification used in this attachment.

H3.2 ASSUMPTIONS NOT REQUIRING VERIFICATION

H3.2.1 Detailed designs are not completed so the fragilities are based on Mechanical Equipment Envelope Drawings (Reference H2.2.6 and H2.2.7), the Mechanical Handling Design Report, Reference H2.2.4 and the TEV Vehicle Envelope Calculations in H2.2.8.

H4. METHODOLOGY

H4.1 QUALITY ASSURANCE

This calculation is prepared in accordance with Bechtel SAIC LLC procedure EG-PRO-3DP-G04B-00037, Rev. 10, Reference H2.1.1.

H4.2 USE OF SOFTWARE

Mathcad 14 is used in this calculation. The use of this software is classified as Level 2 software per procedure IT-PRO-0011, Rev. 7, Ref. H2.1.2. Therefore the software does not require separate qualification.

H5. LIST OF APPENDICES

APPENDIX H-A DBGM-2 Design Response Spectra for CRCF Ground Floor

APPENDIX H-B Site- Wide DBGM-2 UHS Versus 100 Foot Alluvium Median Soil UHS

APPENDIX H-C BDBGM Response Spectra for CRCF Ground Floor

H6. DEVELOPMENT OF FRAGILITIES

H6.1 DESCRIPTION OF EQUIPMENT AND OPERATIONS

The TEV transports waste packages from the CRCF or IHF to the emplacement drifts. The focus of this calculation will be on the TEV being in the loadout area of the CRCF and in transit to the drifts.

After a WP in the WPTT shield enclosure is sealed and inspected with the WP in the vertical position, the WPTT moves the full WP to a docking station in the loadout area in the CRCF. The shield enclosure of the WPTT is then rotated into the horizontal position so that the WP and the pallet can be transferred to the TEV. Figure H6-1 shows the TEV and major component identification.

When the TEV reaches the docking station in the loadout area, several mechanical movements of components must take place in order to receive the WP and emplacement pallet. The front and rear shield doors must be opened and the base plate must be extended. Then, the shielded enclosure is lowered from its transport position via the shielded enclosure jack screw lifting system. The WP and pallet are then placed into the shielded enclosure so that the TEV integral shielded enclosure lifting features are positioned under the emplacement pallet lifting points. The WP is then lifted into place and the TEV shielded enclosure is raised by jack screws to the transportation height where shot bolts are placed to carry the load during transportation. The lifting jacks are then raised so that they are no longer supporting the shielded enclosure. The base plate extension, which is a shield, is then retracted. The shield doors are then closed and the TEV is ready to transport a WP to the drifts.

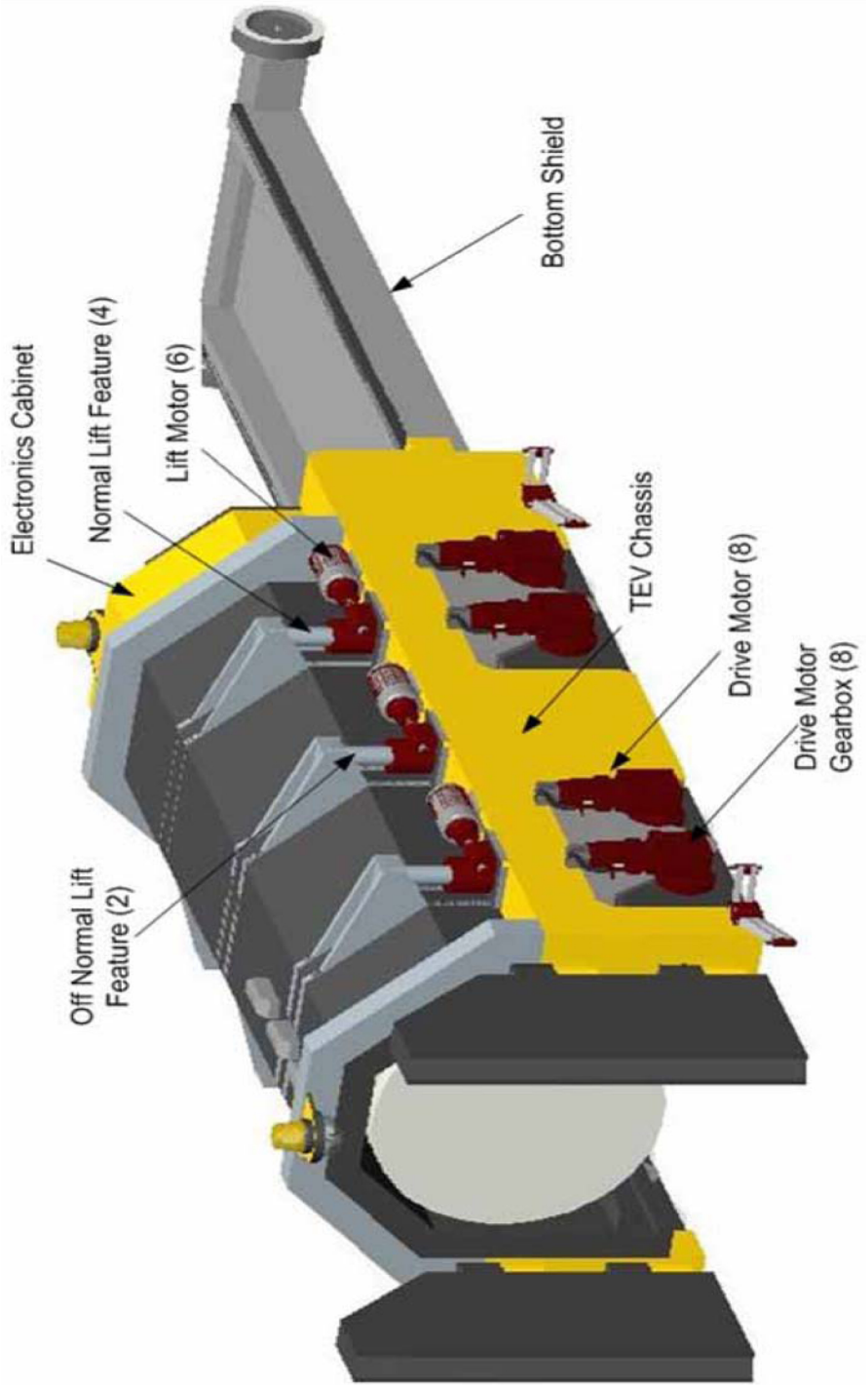

Figure H6-1
TEV and Major Components

H6.2 FAILURE MODES AND DESIGN CAPACITIES

Important features of the TEV to consider for seismic events are:

1. The front and rear wheels are double flanged on one side of the TEV and the remaining wheels on both sides are flangeless, Ref. H2.2.4, page 10 and 27.

2. On loss of power, rail brakes are activated to prevent runaway, Ref. H2.2.4, pages 17, 28 and 29.

3. The gear drive motors on the wheels are a high ratio such that the wheels cannot back drive the motors, Ref. H2.2.4, page 15.

4. The screw jack shielded enclosure lifting devices are self locking to prevent a drop during a shielded enclosure lifting operation and there are redundant lifting devices, Ref. H2.2.4, pages 27 and 32.

5. The screw jack shielded enclosure lifting devices are protected from lateral loading with a roller assembly between the TEV frame and the shielding enclosure, Ref. H2.2.4 page 27.

6. ASME NOG-1 is specified for design of mechanical components so that all drive systems and lifting devices have no single failure features and are individually sized for the design loads, thus the safety factor to failure of all drive systems and lifting devices are higher than for the structural components, or any rail clamps that may be present. Ref. H2.2.4, page 20.

7. Seismic anti lift restraints are not specifically required, but may be added as the design progresses, Ref. H2.2.4, page 15. This calculation will determine if they are required for DBGM-2 and develop a representative fragility for them if they are included.

8. Per Reference H2.2.4, page 18, the maximum lift height for a WP, when in a horizontal orientation, is 6.5 feet. The TEV design limits the maximum lift height of the emplacement pallet base to 20 inches so a drop during a lift does not fail the WP. The shielded enclosure straddles the WP and pallet. The bottom edges of the shielded enclosure are within 2 inches of any surface and the distance between the shielded enclosure internal top faces and a maximum diameter WP is 4 inches so a failure of the shielded enclosure support will not impact the WP.

9. Per Section 3.3.8 of Ref H2.2.4, the load bearing shot bolts are engaged to provide position confirmation that the shielded enclosure has achieved maximum height. In addition, these bolts will provide the shielded enclosure positive support during vehicle movement (transportation or seismic).

10. From Ref. H2.2.4, page 46**,** the TEV, when fully loaded with a waste package, has a center of gravity of less than 65 inches from the top of the rails, the fully loaded maximum weight is 600,000 pounds and the distance between rails is 132 inches. Depending on the fundamental frequencies of the TEV in the horizontal and vertical directions, the TEV could tip when subjected to a DBGM-2 earthquake. One possible failure mode is tipping and/or jumping the rails although this does not necessarily result in failure of a WP.

From the above discussions on design features and redundancy, it appears that the only failure modes of concern are failure of the seismic anti lift restraints and subsequent derailment of the TEV which would result in sliding or tipping of the derailed TEV.

The scope of this fragility review includes all elements of the CRCF Cask Handling Crane that rest on top of the crane rails. The fragility of the crane rails, the rail supports, the rail anchorage and the structure are addressed by others.

H6.2.1 Failure of the Shielded Enclosure

The shielded enclosure is a composite structure constructed of type 316 stainless steel and neutron and gamma shielding. Total weight is 77 tons, Ref. H2.2.8. page 29. There is lateral support provided by a vertical roller assembly that guides the lifting frame during jacking operations as shown in Figure H6-2 and when in the transportation height position, shot bolts as shown in Figure H6-3 also provide stabilization.

Figure H6-2
Roller Guides Providing Lateral Support of Shielding Assembly

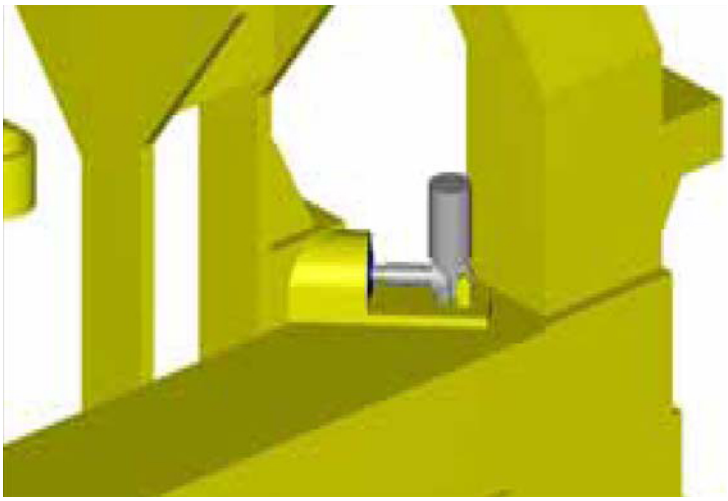

Figure H6-3
Shot Bolts Tying Lifting Frame to TEV Chassis

Per Ref. H2.2.4, page 33, the lateral static capacity of the guide rollers is 96,000 pounds total. This is a design rated capacity and the ultimate failure capacity would be much higher. The shot bolt capacity is not stated but the design should be for DBGM-2 since the shot bolts are to support the WP and pallet during transport to the drifts. The shot bolts take both longitudinal and lateral load but the longitudinal seismic load is limited by the brake force on the rails so most load is lateral. Both the guide rollers and the shot bolts take lateral load so there is redundancy in the support of the lifting frames shielded enclosure assembly. This is not considered to be a credible failure mode that would damage the WP.

H6.2.2 Failure of the Rail Clamps

Per Ref. H2.2.4, page 15, seismic anti lift restraints may be considered. Depending upon the dynamic characteristics of the TEV, there may or may not be any uplift during a DBGM-2 seismic event. Consider three cases. In one case, the TEV is considered rigid and only the ZPA in the horizontal and vertical directions are applied. In the second case consider that the peak spectral acceleration is used for design. In the third case, the fundamental frequency of the TEV is greater than 10 Hz but not rigid.

Case 1: Rigid in horizontal and vertical directions.

From Ref. H2.2.4, Page 46

$Wt := 600000lbm$	Total mass of the TEV
$h := 65in$	Maximum height to center of gravity
$w := 132in$	Width between rails.

From Ref. H2.2.3 for DBGM-2, node 24 on the CRCF ground floor and Appendix H-A

$Sa_x := 0.5g$

$Sa_y := 0.47g$

$Sa_z := 0.39g$

Use max horizontal for uplift.

Let F_{vert} be the down force on the outboard wheels. Use the 100-40-40 earthquake component phasing, Ref. H2.3.4. Use max horizontal acceleration, Sa_x.

$$F_{vert} := \left(Sa_x \cdot Wt \cdot \frac{h}{w} + 0.4 \cdot Sa_z \cdot \frac{Wt}{2} \right) - \frac{1g \cdot Wt}{2}$$

$F_{vert} = -1.055 \times 10^5 \text{ lbf}$

No uplift occurs at DBGM-2 if the TEV is considered rigid and no seismic anti lift restraints would be required.

Case 2: TEV is flexible and designed for peak Sa horizontal and vertical. Specified damping would be 4% per Ref. H2.3.4.

From Ref H2.2.3 and Appendix H-A

$Sa_{x\_peak} := 1.7g$

$Sa_{y\_peak} := 1.77g$

$Sa_{z\_peak} := 1.36g$

$$F_{vert\_peak} := Sa_{y\_peak} \cdot Wt \cdot \frac{h}{w} + 0.4 \cdot Sa_{z\_peak} \cdot \frac{Wt}{2} - 1g \cdot \frac{Wt}{2}$$

$F_{vert\_peak} = 3.862 \times 10^5 \text{ lbf}$

Seismic restraints are required for Case 2.

Case 3: Dynamic analysis is conducted and fundamental frequencies horizontal and vertical are greater than 10 Hz but less than rigid. This is considered to be the most realistic case.

From Ref. H2.2.3 and Appendix H-A, the horizontal spectral acceleration is flat between about 11 Hz and 17 Hz. The vertical spectral acceleration is flat between

about 7.7 Hz and 15.5 Hz. The vertical fundamental frequency is expected to fall into this range due to flexure of the TEV frame and the lifting frames. Use the 4% damped spectra acceleration in these ranges.

$$Sa_{x\_best} := 1.0g$$

$$Sa_{y\_best} := 1.02g$$

$$Sa_{z\_best} := 1.36g$$

$$F_{vert\_best} := Sa_{y\_best} \cdot Wt \cdot \frac{h}{w} + 0.4 \cdot Sa_{z\_best} \cdot \frac{Wt}{2} - 1g \cdot \frac{Wt}{2}$$

$$F_{vert\_best} = 1.646 \times 10^5 \text{ lbf}$$

Check 100% vertical and 40% horizontal

$$F_{vert\_100} := 0.4 \cdot Sa_{y\_best} \cdot Wt \cdot \frac{h}{w} + Sa_{z\_best} \cdot \frac{Wt}{2} - 1g \cdot \frac{Wt}{2}$$

$$F_{vert\_100} = 2.285 \times 10^5 \text{ lbf}$$

This case governs and seismic restraints are required for the best estimate case. Base seismic restraint capacity on this case.

A conceptual seismic restraint from Ref. H2.2.4 is shown in Figure H6-4.

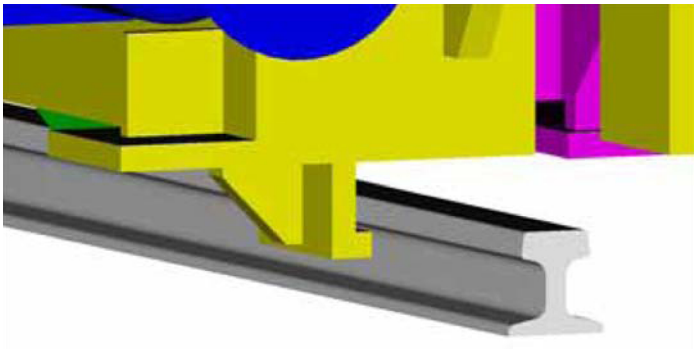

Figure H6-4
Conceptual Seismic Restraint

For maintenance purposes, the restraint would have to be bolted to the TEV chassis. Fasteners would be designed to ASME NOG-1, Ref. H2.2.9. The stiffened design shown in Figure H6-4 would most likely fail in the fasteners. There would be no ductility in fasteners in tension or shear. The flanged wheels would initially take lateral load so only uplift would act on the seismic restraints and the fasteners would be in tension. Fasteners in tension have an allowable stress of 0.5 of the ultimate tensile strength for extreme environmental loads, Ref. H2.2.9, Table 4315-1. Determine the scale factor on DBGM-2 for failure of the seismic restraints.

Median bolt tensile strength is 1.1 times specified. Ref. H2.2.1, Table 3-9. With the best estimate uplift load being equal to the allowable stress:

$$F_{ult} := 0.9 \cdot \left(F_{vert\_100} \cdot \frac{1.1}{0.5} \right)$$

median capacity of bolting where 0.9 is a reduction factor for threads, Ref. H2.2.1, Table 3-10

$$F_{ult} = 4.525 \times 10^{5}\ \text{lbf}$$

$$F = SF \cdot \left(0.4 Sa_{y\_best} \cdot Wt \cdot \frac{h}{w} + Sa_{z\_best} \cdot \frac{Wt}{2} \right) - 1g \cdot \frac{Wt}{2}$$

F = bolt load at the failure capacity, F_{ult}

$$SF := \frac{\left(F_{ult} + 1g \cdot \frac{Wt}{2} \right)}{\left(0.4 Sa_{y\_best} \cdot Wt \cdot \frac{h}{w} + Sa_{z\_best} \cdot \frac{Wt}{2} \right)}$$

$$SF = 1.424$$

$$F_C := SF$$

$$F_C = 1.424$$

From Ref. H2.2.1, Table 3-10, the uncertainty for failure equation, material strength and fabrication is:

$$\beta_{c\_C} := 0.13$$

The seismic margin is small because the design would consider the dead weight negating overturning and when this weight resistance is overcome, the bolting load rapidly rises from increased acceleration. The design of seismic anti lift restraints for DBGM-2 would not assure a large margin above DBGM-2 and would only assure that the TEV would not jump the rail at DBGM-2. However, the consequences of jumping the rail may not be serious enough to result in a release of radioactive material.

Per Ref. H2.2.4, page 45, if the TEV derails, the maximum drop of the TEV is limited to 2 inches plus the 1 inch height of the wheel flange. The 3 inch drop is much less than the drop height limit of 6.5 feet, Ref. H2.2.4, page 18, so derailment is not considered to be an event that fails a WP. Overturning or sliding into a rigid body would be the only

credible failure modes that could fail a WP.

H6.2.3 Sliding Failure

There are large clearances between the TEV and adjacent structures or equipment when it is in the loadout area. Per Ref H2.2.5, The TEV centerline is about 30 feet from a side wall and the two TEVs side by side are 34 feet apart. The TEV minimum clearance envelope for width is 16 feet, Ref. H2.2.6. Thus, there is 22 feet to a structural wall in the lateral direction. There would be18 feet between TEVs parked side by side. If they became derailed during an earthquake, they would likely move in the same direction so side to side sliding impact is not a credible failure mode while in the loadout position. If an earthquake were to occur when the TEV is moving in a doorway, then a sliding impact is credible but the time involved in that position is very small.

When the TEV is being loaded, it is in close proximity to the WPTT as shown in Ref. H2.2.6. During the transfer operation, derailment of the TEV or the WPTT could result in an impact between the WP and the TEV shielded enclosure or the WPTT shield enclosure. This could potentially result in damage to the WP. The risk analysis team will need to determine if the time spent in this position and the probability of derailment of the TEV is within the limits imposed for release of radioactive material. The TEV and WPTT are restrained in the axial position by rail brakes. When the braking resistance is overcome, the WP could be damaged by axial sliding of the TEV or WPTT. Again, the time the WP spends in this position is limited and the risk analysts will need to determine if this is a critical failure mode.

When the TEV leaves the CRCF it travels at a slow speed. The maximum grade that the TEV is subjected to is 2.5 %, Ref. H2.2.4, Page 10. If it were to derail in a seismic event, it would slide but with the shallow grade, the sliding would not be much different than calculated below for a level surface. Tunnel clearances are unknown. Derailment within a tunnel could result in impact and possible damage to the WP. Upon any derailment the wheels would be gouging into the surface and the effective coefficient of friction would be high. A typical sliding distance will be determined for steel on concrete based on the BDBGM spectral shape for surface facilities. The ground motion deep in the tunnel is lower and sliding distances would be lower.

Reference H2.2.2 has equations for conservative biased estimates of sliding distance for a rigid body sliding on a level surface.

$\mu := 0.6$ Estimate of coefficient of friction of steel wheels gouging into concrete surface. Design values are as low as 0.4 but are based on flat contact, with a low probability of sliding and not a gouging situation. As will be shown, the final conclusions are not sensitive to this estimate.

$\mu e := \mu$ For a best estimate of sliding distance, the vertical acceleration is ignored since it oscillates both up and down and the average vertical acceleration is zero.

$\mu e = 0.6$

$c_s := 2 \cdot \mu e \cdot g$ Equation A-2 of Ref. H2.2.2

$c_s = 1.2 \cdot g$

The sliding displacement of the rigid body is estimated by Equation A-3 of Ref. H2.2.2 in which f_{es} is the lowest natural frequency at which the 10% damped vector of horizontal spectral acceleration equals c_s. Determine horizontal acceleration vector, Sa_H.

$Sa_H := 1.25g$ Initial trial value of vector Sa_H to initiate the equation solver

Given

$\sqrt{\left(Sa_H^2 + 0.16 \cdot Sa_H^2\right)} = c_s$ Eq. A-4 Ref. H2.2.2

$a := \text{Find}\left(Sa_H\right)$

$a = 1.114 \cdot g$

$Sa_H := a$

$Sa_H = 1.114 \cdot g$

Sliding during the journey to the drifts would be less of a concern than when in the CRCF, therefore use the higher CRCF spectral acceleration to determine sliding distance.

The lowest natural frequency (f_{es}) at which the vector spectral acceleration equals c_s is determined from CRCF ISRS at the ground floor for DBGM-2. See Ref. H2.2.3 and Appendix H-A for DBGM-2 spectrum. Use 100 foot median soil as a median spectrum from Appendix H-A, Figure H-A-4.

The 100 foot median spectrum does not go beyond 1.03g at 4 Hz for DBGM-2. Use 4 Hz for f_{es} as an approximate effective frequency.

$f_{es} := 4Hz$

$\Delta_s := \dfrac{c_s}{\left(2 \cdot \pi \cdot f_{es}\right)^2}$ Eq. A-3, Ref H2.2.2

$\Delta_s = 0.061 \text{ ft}$

There is virtually no sliding at DBGM-2. The BDBGM spectra in Appendix H-C, for 100 foot alluvium, median soil, are used next.

$f_{es2} := 1.64Hz$

$$\Delta_2 := \frac{c_s}{\left(2 \cdot \pi \cdot f_{es2}\right)^2}$$

$\Delta_2 = 0.364\ ft$

The displacement at 1.5 times BDBGM is estimated by scaling up the BDBGM spectra in Appendix H-C to find f_{es} at acceleration C_s.

$f_{es3} := 1.14Hz$

$$\Delta_3 := \frac{c_s}{\left(2 \cdot \pi \cdot f_{es3}\right)^2}$$

$\Delta_3 = 0.753\ ft$

Next, twice the BDBGM spectra are used to obtain an increased sliding distance.

$f_{es4} := 0.79Hz$

$$\Delta_4 := \frac{c_s}{\left(2 \cdot \pi \cdot f_{es4}\right)^2}$$

$\Delta_4 = 1.567\ ft$

These are best estimates of sliding distance. Per Ref. H2.2.2 page 33, the displacement should be increased by a factor of 2 for design. This is considered to be an upper bound HCLPF value of 2.33 βc.

$$\beta_{c\_\Delta} := \frac{1}{2.33} \cdot \ln(2)$$

$\beta_{c\_\Delta} = 0.297$

The other variable is the coefficient of friction μ.

Let μ = 0.4 be a lower bound 95% confidence value, which is consistent with design values.

$c_{s\_\beta} := 2 \cdot 0.4 \cdot g$

$c_{s\_\beta} = 0.8 \cdot g$

$f_{es\beta} := 0.56Hz$ From Appendix H-C with BDBGM spectra scaled by a factor of 2 to be consistent with calculation for Δ_4.

$$\Delta_{ub} := \frac{c_{s\_\beta}}{\left(2 \cdot \pi \, f_{es\beta}\right)^2}$$

$\Delta_{ub} = 2.079$ ft

$$\beta_{c\_\mu} := \frac{1}{1.65} \cdot \ln\left(\frac{\Delta_{ub}}{\Delta_4}\right)$$

$\beta_{c\_\mu} = 0.171$

$$\beta_{c\_slide} := \left(\beta_{c\_\Delta}{}^2 + \beta_{c\_\mu}{}^2\right)^{0.5}$$

$\beta_{c\_slide} = 0.343$

Table H6-1 and Figure H6-5 show the sliding displacement as a function of ground motion PGA assuming that the TEV is not derailed at DBGM-2 and is derailed at BDGBM and beyond. The upper bound displacement (less than 1% probability of exceedance) is calculated as:

$$\Delta_{ub} = \Delta_{best} \cdot e^{2.33 \cdot \beta_{c\_slide}}$$

$$\Delta_{ub} = 2.224 \cdot \Delta_{best}$$

Table H6-1
Sliding Distance as a Function of PGA

EQ	PGA	Median Δ ft	Upper Bound Δ ft
DBGM-2	0.45	0	0
BDBGM	0.91	0.364	0.809
1.5 BDBGM	1.37	0.753	1.67
2.0 BDBGM	1.82	1.567	3.48

The sliding distances at BDBGM is not large but increases at a non linear rate as the ground motion increases.

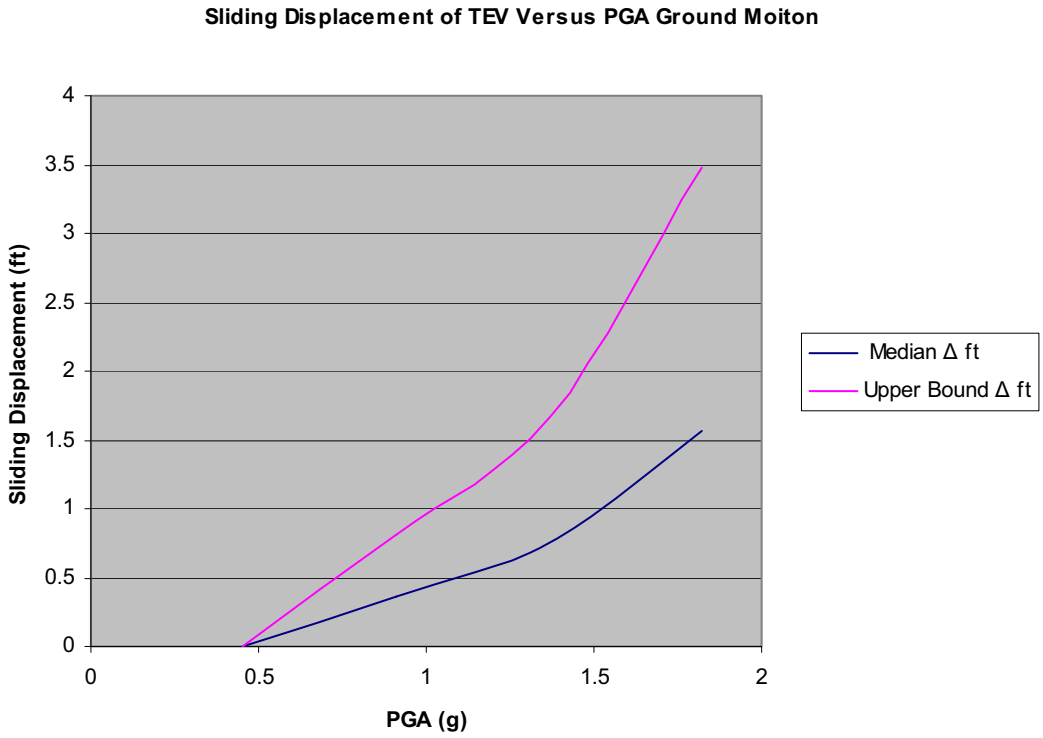

Figure H6-5
Sliding Distance as a Function of PGA

H6.2.4 Rocking

The TEV can rock if the wheels gouge into the concrete and create a rotation point. Figure H6-6 shows a rigid body rocking. Reference H2.2.2 contains equations for rigid body rocking. The most critical location for rocking is in the CRCF. Also, the CRCF ISRS are higher than the free field ground motion that would be applicable to the time the TEV is in transit to the drifts so the CRCF ISRS for the ground floor are conservatively used for the rocking calculations.

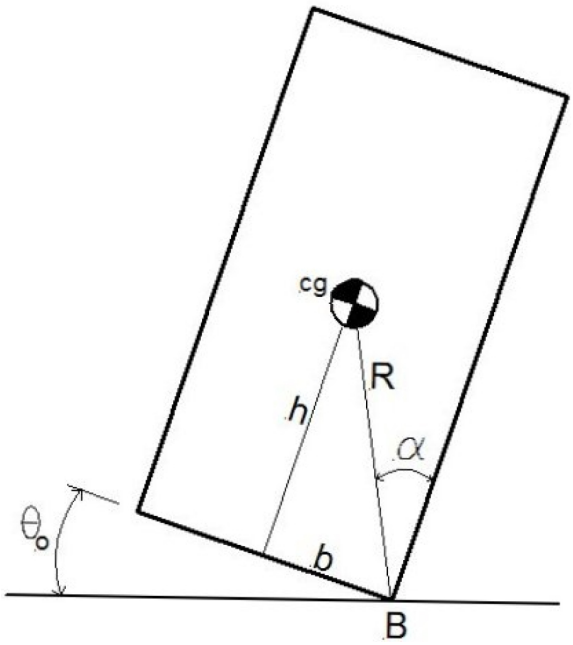

Figure H6-6
Rigid Body Rocking

$h := 65in$ Ref. H2.2.4,page 46

$b := \frac{w}{2}$ w is track width from Ref. H2.2.4, page 46

$b = 5.5\,ft$

$a := \frac{b}{h}$ Eq. 7-2(b) of Ref. H2.2.2

$a = 1.015$

$\alpha := atan(a) = 0.793 \cdot rad$ (45.4 degrees, Eq. 7.2(a) of Ref. H2.2.2)

Let the rocking angle θ be 0.2 radians (11.46 degrees)

$\theta_{0.2} := 0.2rad$

If the center of gravity is at the center of the rigid body and the lateral inertial mass

and the vertical resistance mass are equal and uniformly distributed:

$C_I := \frac{4}{3}\cdot\left(1 + a^2\right)$ Eq. A-6(f) Ref. H2.2.2

$C_I = 2.708$

$fi_{\theta.0.2} := 1 + \theta_{0.2}\cdot\left(a - \frac{\theta_{0.2}}{2}\right) = 1.183$

$fi_{\theta.0.2} - 1 = 0.183$ Eq. A-5(d) of Ref. H2.2.2

$fe_{0.2} := \frac{1}{2\cdot\pi}\frac{\left[2\cdot\left(fi_{\theta.0.2} - 1\right)\cdot g\right]^{0.5}}{\left(C_I\cdot\theta_{0.2}{}^2\cdot h\right)^{0.5}}$ Eq. A-6(a) Ref. H2.2.2

$fe_{0.2} = 0.713\cdot Hz$

$C_R := 1 - \frac{\left(2\cdot a^2\right)}{C_I}$ Eq. A-6(e) of Ref H2.2.2

$C_R = 0.239$

$\gamma := -2\cdot\ln\left(C_R\right)$ Eq. A-6(d) of Ref H2.2.2

$\gamma = 2.866$

$\beta e := \frac{\gamma}{\left(4\cdot\pi^2 + \gamma^2\right)^{0.5}}$ Eq. A-6(b) Ref. H2.2.2

$\beta e = 0.415$ 41.5% damping

At $fe_{0.2}$ = 0.713 Hz, the Sa is not particularly sensitive to damping. Use max available damping of 10% in Appendix H-C. This is conservative.

$SAH_{0.2} := 0.478g$ Appendix H-C 100 foot median soil case, direction X

$SAV_{0.2} := 0.271g$

$F_H := 1$ No correction made for vertical and horizontal masses and their respective distances from center of rotation for small angle.

$$F_V := \left[1 + \left(a \cdot \frac{SAV_{0.2}}{F_H \cdot SAH_{0.2}}\right)^2\right]^{0.5}$$ Eq. A-5(c) of Ref. H2.2.2

$F_V = 1.154$

$$SAH_{CAP0.2} := \left[\frac{g}{F_H \cdot F_V} \cdot \left(2 \cdot a - \theta_{0.2}\right)\right]$$ Eq. A-5(e) of Ref. H2.2.2

$SAH_{CAP0.2} = 1.587 \cdot g$

$SAH_{CAP0.2}$ exceeds $SAH_{0.2}$

The PGA at 0.2 radians rotation is now determined.

All parameters remain the same so scale the demand and capacity relative to the BDBGM

$BDBGM_{PGA} := 0.914g$ Ref. H2.2.3

$$PGA_{0.2} := \frac{SAH_{CAP0.2}}{SAH_{0.2}} \cdot BDBGM_{PGA}$$

$PGA_{0.2} = 3.034 \cdot g$ PGA for 0.2 radians rotation

Next, the PGA required for 0.3 radians rotation is determined.

$\theta_{0.3} := 0.3rad$

$$fi_{\theta 0.3} := 1 + \theta_{0.3} \cdot \left(a - \frac{\theta_{0.3}}{2}\right)$$

$fi_{\theta 0.3} - 1 = 0.26$

$$fe_{\theta 0.3} := \frac{1}{2 \cdot \pi} \frac{\left[2 \cdot \left(fi_{\theta 0.3} - 1\right) \cdot g\right]^{0.5}}{\left(C_I \cdot {\theta_{0.3}}^2 \cdot h\right)^{0.5}}$$

$fe_{\theta 0.3} = 0.566 \cdot Hz$

βe remains the same. From Appendix H-C at 0.566 Hz, conservatively use 10% damping.

$SAH_{0.3} := 0.402g$

$SAV_{0.3} := 0.222g$

$$F_{V0.3} := \left[1 + \left(a \cdot \frac{SAV_{0.3}}{F_H \cdot SAH_{0.3}}\right)^2\right]^{0.5}$$

$F_{V0.3} = 1.146$

$$SAH_{CAP0.3} := \left[\frac{g}{F_H \cdot F_{V0.3}} \cdot \left(2 \cdot a - \theta_{0.3}\right)\right]$$

$SAH_{CAP0.3} = 1.51 \cdot g$

$$SAH_{03} := \frac{SAH_{CAP0.3}}{SAH_{0.3}} \cdot BDBGM_{PGA}$$

$SAH_{03} = 3.432 \cdot g$ PGA for 0.3 radians rotation.

At 0.4 rad rotation (22.9 degrees)

$\theta_4 := 0.4rad$

$$fi_{\theta.4} := 1 + \theta_4 \cdot \left(a - \frac{\theta_4}{2}\right)$$

$fi_{\theta.4} - 1 = 0.326$

$$fe_4 := \frac{1}{2 \cdot \pi} \cdot \frac{\left[2 \cdot \left(fi_{\theta.4} - 1\right) \cdot g\right]^{0.5}}{\left(C_I \cdot {\theta_4}^2 \cdot h\right)^{0.5}}$$

$fe_4 = 0.476 \cdot Hz$

From 10% damped spectra in Appendix H-C

$SAH_4 := 0.335g$

$$SAV_4 := 0.177g$$

$$F_{V.4} := \left[1 + \left(a \cdot \frac{SAV_4}{F_H \cdot SAH_4}\right)^2\right]^{0.5}$$

$$F_{V.4} = 1.135$$

$$SAH_{CAP.4} := \left[\frac{g}{F_H \cdot F_{V.4}} \cdot \left(2 \cdot a - \theta_4\right)\right] = 46.235 \frac{ft}{s^2}$$

$$SAH_{CAP.4} = 1.437 \cdot g$$

$$SAH_{4rad} := \frac{SAH_{CAP.4}}{SAH_4} \cdot BDBGM_{PGA}$$

$$SAH_{4rad} = 3.921 \cdot g$$

We are up to almost 4g PGA and the TEV has rotated only 0.4 radians (22.9 degrees whereas the instability point is about 45 degrees. It is concluded that the TEV cannot tip over at any credible ground motion. The only credible failure mode is sliding after the failure of the seismic anti lift restraints. In that case, the sliding is nearly as shown in Figure H6-6 but there will be some additional uncertainty due to the uncertainty in the structural response.

H6.3 EQUIPMENT RESPONSE FACTOR

The equivalent of the equipment response factor and uncertainty is included in the sliding and rocking calculations.

$$F_{RE\_S} := 1.0$$

$$\beta_{c\_RE\_S} := 0$$

For the initial failure of the seismic anti lift restraints, an Equipment Response Factor and Uncertainty will be calculated.

H6.3.1 Qualification Method

A dynamic analysis to determine the fundamental frequency will likely be conducted. The capacity factor was based on an estimated fundamental frequency of greater than 10 Hz which is considered to be a realistic range. The qualification method factor will determine the conservatism in using the broadened and smoothed spectra versus best estimate spectra for the median response case for 100 feet of alluvium with median soil properties.

The 4% damped DBGM-2 design spectra are shown in Appendix H-A. At the acceleration level of failure, the best estimate of the in-structure amplification and spectral shape would be from the BDBGM input. The X direction design spectra are used to compare to the X direction BDBGM. BDBGM digitized spectra from Ref. H2.2.3 are shown in Appendix H-C, Table H-C-1.

From Appendix H-A, Fig. H-A-1, for the X direction the broadened spectra are flat from about 11 to 17 Hz with a 4% damped design spectral acceleration of 1.0g. The 4% damped BDBGM spectra shown in Appendix H-C, Table H-C-1, vary from 1.20g to 1.48 g in this range. Use the average value for comparison to the DBGM-2 spectra and consider the range as a plus to minus 95 percentile range (plus or minus 1.65β)

$$Sa_{BDBGM} := \frac{(1.20 + 1.48)g}{2}$$

$$Sa_{BDBGM} = 1.34 \cdot g$$

$$F_{QM} := 1.0 \frac{g}{Sa_{BDBGM}}$$

$$F_{QM} = 0.746$$

Note that the factor is less than unity since the BDBGM PGA is twice the DBGM-2 PGA. The fragility will be derived relative to the BDBGM PGA.

Let the range of BDBGM Sa be a plus or minus 95% confidence bound (plus and minus 1.65β)

$$\beta_{c\_QM} := \frac{1}{2 \cdot 1.65} \cdot \ln\left(\frac{1.48}{1.20}\right)$$

$$\beta_{c\_QM} = 0.064$$

H6.3.2 Damping

Four percent damping is used for design. At failure of the rail clamps, 5% damping would be more median centered, Ref. H2.2.1, Table 3-8. Compare 4% and 5% damped design spectra from Appendix H-A, Figure H-A-1 in the flat 11 to 17 Hz range. Sa at 5% damping is 0.93g and is 1.0g at 4% damping.

$$F_{\delta\_e} := \frac{1.0}{0.93}$$

$$F_{\delta\_e} = 1.075$$

Let this difference be a 1β value

$$\beta_{c\_\delta\_e} := \ln\left(\frac{1.0}{0.93}\right)$$

$$\beta_{c\_\delta\_e} = 0.073$$

H6.3.3 Modeling

Modeling uncertainty is affected by mode shape and frequency uncertainty. There is no deliberate conservatism in modeling.

$$F_{M\_e} := 1.0$$

Per Ref. H2.2.1, page 3-50, the uncertainty in mode shape varies from 0.05 to 0.15. For a simple relatively stiff model, the mode shape uncertainty is estimated to be about 0.10.

$$\beta_{U\_MS\_e} := 0.1$$

The estimated frequency is in the flat portion of the design spectrum. Thus, a shift in frequency would not change the design response unless the calculated frequency is near a corner point in the design spectrum. Therefore a modest uncertainty will be estimated.

$$\beta_{U\_f\_e} := 0.15$$

$$\beta_{c\_M\_e} := \left(\beta_{U\_MS\_e}^{2} + \beta_{U\_f\_e}^{2}\right)^{0.5}$$

$$\beta_{c\_M\_e} = 0.18$$

H6.3.4 Mode Combination

Mode combination would be conducted in accordance with the requirements of H2.3.4. These requirements are median centered.

$$F_{MC\_e} := 1.0$$

The TEV is massive and fairly rigid and a single mode would likely dominate in each direction. Use a lower bound value suggested in Ref. H2.2.1, page 3-50.

$$\beta_{R\_MC\_e} := 0.05$$

$$\beta_{c\_MC\_e} := \beta_{R\_MC\_e}$$

$\beta_{c\_MC\_e} = 0.05$

H6.3.5 Earthquake Component Combination

The SRSS or 100-40-40 rule would be used per requirements in Ref. H2.3.4. These methods are median centered.

$F_{ECC\_e} := 1.0$

The governing failure mode is governed by one horizontal plus the vertical direction of earthquake. Per Ref. H2.2.1, page 3-50, for components in phase, this would be about a $3\beta_R$ combination. From the governing capacity scale factor calculation equation in H6.2.2:

$$SF\_ECC := \frac{\left(F_{ult} + 1g \cdot \frac{Wt}{2}\right)}{\left(Sa_{y\_best} \cdot Wt \cdot \frac{h}{w} + Sa_{z\_best} \cdot \frac{Wt}{2}\right)}$$

$SF\_ECC = 1.061$

$$\beta_{R\_ECC} := \frac{1}{3} \cdot \ln\left(\frac{SF}{SF\_ECC}\right)$$

$\beta_{R\_ECC} = 0.098$

$\beta_{c\_ECC} := \beta_{R\_ECC}$

$\beta_{c\_ECC} = 0.098$

H6.3.6 Equipment Response Factor

$F_{RE} := F_{QM} \cdot F_{\delta\_e} \cdot F_{M\_e} \cdot F_{MC\_e} \cdot F_{ECC\_e}$

$F_{RE} = 0.802$ This is relative to BDBGM PGA

$$\beta_{c\_RE} := \left(\beta_{c\_QM}^2 + \beta_{c\_\delta\_e}^2 + \beta_{c\_M\_e}^2 + \beta_{c\_MC\_e}^2 + \beta_{c\_ECC}^2\right)^{0.5}$$

$\beta_{c\_RE} = 0.232$

H6.4 STRUCTURAL RESPONSE FACTOR

H6.4.1 Spectral Shape Factor

This factor accounts for conservatism in the site-wide DBGM-2 design spectrum. At the Surface Facilities Area (SFA) the depth of alluvium overlying tuff varies from 30 feet to 200 feet. Uniform hazard spectra at the surface are calculated from site response analyses for alluvium depths of 30', 70', 100' and 200'. The site-wide design ground response spectrum is the envelope of the surface spectra of these four alluvium depths (Reference H2.2.10; also Section 6.2.2.1 for source information). The median site response is considered to be the 100 foot depth median soil property case.

The dominant frequency of the CRCF soil-structure system in the horizontal direction is 5.2 Hz from the Tier 1 ISRS calculation (Reference H2.2.3). At this frequency, the site wide horizontal ground motion spectrum is slightly higher than the 100 foot alluvium depth spectrum as shown in Appendix H-B.

$SA_{site} := 1.14g$

$SA_{med} := 1.06g$

$F_{SA} := \frac{SA_{site}}{SA_{med}}$

$F_{SA} = 1.075$

Reference H2.2.1 recommends a β_U of about 0.24 if the fundamental frequency is about 5 Hz and the fragility is anchored to PGA. This is to account for uncertainty in amplification of the PGA as observed from statistical data when using a standard spectral shape. However, the Yucca Mountain surface facility UHS is derived probabilistically and this uncertainty is not applicable.

$\beta_{U\_SA} := 0$

$\beta_{R\_SA} := 0.2$ Ref H2.2.1, Table 3-2 to account for peak to valley variation

$\beta_{c\_SA} := \beta_{R\_SA}$

$\beta_{c\_SA} = 0.2$

H6.4.2 Damping

This factor is to account for conservatism in the hysteresis damping of the building structure used in the seismic response analysis. Due to the high radiation damping of the foundation media, the effect of structure damping at the ground floor level is insignificant. Thus,

$F_{\delta} := 1.0$

$\beta_{c\_\delta} := 0$

H6.4.3 Modeling

The Tier 1 lumped mass multiple stick model of the CRCF models the stiffness of various reinforced concrete walls and distribution of mass at each floor. The floors are assumed to be rigid diaphragms tying the different sticks together. Torsional response of the structure is captured through modeling eccentricity between the center of mass and center of rigidity of each floor. The foundation media underneath the buildings are modeled with soil springs and dashpots based on elastic half space theory with adjustment to account for the layering effect of alluvium overlying tuff. The model is judged to adequately represent the CRCF structural dynamics characteristics, thus

$F_M := 1.0$

Uncertainty of structure frequencies predicted from mathematical modeling varies from 0.15 to 0.35 depending on the sophistication of the model (Reference H2.2.1, Page 3-18). The value of 0.35 is for fairly approximate models and the value 0.15 is appropriate for detailed models. Based on the complexity of the CRCF soil-structure system and the mathematical model used for the Tier 1 ISRS analysis, it is judged that the calculated CRCF fundamental frequency has a logarithmic standard deviation of 0.25.

$\beta_f := 0.25$

$f_m := 5.2Hz$

$f_{upper} := f_m \cdot e^{\beta_f}$

$f_{upper} = 6.677 \cdot Hz$

$f_{lower} := f_m \cdot e^{-\beta_f}$

$f_{lower} = 4.05 \cdot Hz$

$SA_{upper} := 1.05g$ Fig H-B-1 for 100 foot alluvium case

$SA_{lowr} := 1.02g$ Fig. H-B-1 for 100 foot alluvium case

Both values are less than SA_{med} at 5.2 Hz. Therefore there is no uncertainty penalty.

$\beta_{U\_f} := 0$

The mode shape uncertainty for the CRCF ground floor response is taken as a lower value of the range suggested in Ref. H2.2.1, page 3-18, due to the fact that the response is primarily rigid body translation and rotation in the soil.

$\beta_{U\_MS} := 0.1$

$\beta_{c\_M} := \left(\beta_{U\_f}^{2} + \beta_{U\_MS}^{2}\right)^{0.5}$

$\beta_{c\_M} = 0.1$

H6.4.4 Mode Combination

Since the direct integration time history method is used in the Tier 1 ISRS analysis (Reference H2.2.3), the modal combination method factor of safety is unity and there is no variability associated with modal combination.

$F_{MC} := 1.0$

$\beta_{c\_MC} := 0$

H6.4.5 Soil-Structure Interaction

Two factors are considered, the first one is on the method of treating the SSI effects and the second one is on the effect of soil softening at ground acceleration higher than DBGM-2. The Tier 1 seismic response analyses of the CRCF use the site-wide $5*10^{-4}$ mean uniform hazard spectra as the DBGM-2 input motion. Spectrum compatible time histories are used as the input motion for the time history analyses. The conservatism in the site-wide spectra was accounted for in the spectral shape factor above. Strain compatible soil properties of 100-foot and 200-foot deep alluvium are used to calculate frequency-independent soil springs and soil damping coefficients. Soil radiation damping is introduced into the model by using dashpots. Damping coefficients equal to 75% of the computed values for translational degrees of freedom and equal to the full computed rotational damping values are used in the response analyses (Reference H2.2.3). Conservatism or unconservatism in SSI will be minimized for the final SSI analyses used to develop equipment design seismic input. Before the final SSI analyses are completed, the Tier 1 SSI analysis is taken to represent the best-estimate responses per BSC recommendations in Reference H2.2.13.

$F_{SSI\_1} := 1.0$

$\beta_{R\_SSI} := 0$

$\beta_{U\_SSI\_1} := 0.25$ Estimated uncertainty in spring damper soil modeling

The second effect of soil softening has already been taken into account in the failure of the seismic uplift restraints and the sliding and rocking evaluations since all demands were referenced to the BDBGM median soil 100 foot alluvium spectra in Appendix H-C.

$F_{SSI} := 1.0$

$\beta_{c\_SSI} := \beta_{U\_SSI\_1}$

$\beta_{c\_SSI} = 0.25$

H6.4.6 Ground Motion Incoherence

For large structures the foundation cannot be excited uniformly thus the practice of applying the ground motion time histories uniformly across the base mat can be conservative. In Ref. H2.2.1, page 3-22 it is shown that above 5 Hz some reduction can be made to the input motion. The horizontal fundamental frequency from Ref. H2.2.3 is about 5.2 Hz for DBGM-2 input, however, at the failure level, the BDBGM response characteristics of the structure are more appropriate. From Ref. H2.2.3, the first two horizontal modes of structural response are 4.39 Hz and 4.46 Hz respectively, thus there is no reduction for ground motion incoherence.

$F_{GMI} := 1.0$

$\beta_{c\_GMI} := 0$

F6.4.7 Structural Response Factor

$F_{RS} := F_{SA} \cdot F_{\delta} \cdot F_{M} \cdot F_{MC} \cdot F_{SSI} \cdot F_{GMI}$

$F_{RS} = 1.075$

$\beta_{c\_RS} := \left(\beta_{c\_SA}^{2} + \beta_{c\_\delta}^{2} + \beta_{c\_M}^{2} + \beta_{c\_MC}^{2} + \beta_{c\_SSI}^{2} + \beta_{c\_GMI}^{2}\right)^{0.5}$

$\beta_{c\_RS} = 0.335$

6.5 FRAGILITY

The first mode of failure would be the failure of the seismic uplift restraints.

$BDBGM := 0.914g$

$A_m := F_C \cdot F_{RE} \cdot F_{RS} \cdot BDBGM$

$$A_m = 1.123 \cdot g$$

$$\beta_c := \left(\beta_{c\_C}^{2} + \beta_{c\_RE}^{2} + \beta_{c\_RS}^{2}\right)^{0.5}$$

$$\beta_c = 0.428$$

$$HCLPF := A_m \cdot e^{-2.33 \cdot \beta_c}$$

$$HCLPF = 0.414 \cdot g$$

The median is greater than the BDBGM but the HCLPF is slightly less than DBGM-2. The calculations have shown that if seismic uplift restraints are designed for the DBGM-2 earthquake, and are designed to the stress limits of ASME-NOG-1, Ref. H2.2.9, that they would have a 50% probability of failure just after reaching the BDBGM level. This occurs because, the dead weight restoring moment resists much of the uplift force at DBGM-2 but once this dead weight resistance is overcome, the load on the uplift restraints builds up quickly. However, it has been shown that the TEV cannot tip over for earthquakes exceeding over 4 times the BDBGM so tip over is not a credible failure mode. When the seismic uplift restraints fail, the TEV will become derailed and slide. While in the loadout docking station, some damage could occur to the WP if an earthquake occurred and the TEV were to slide. This is not so much of an impact problem. The more serious issue would be a gross misalignment with the mating WPTT where lateral movement of either the TEV or WPTT upon failure of their seismic uplift restraints could jam a WP and subject it to point loads and large bending moments. This type of failure should be postulated to occur upon failure of the seismic anti lift restraints during the time that the WP is being transferred from the WPTT to the TEV, which should be a short time.

Once the WP is secured in the TEV, it would be virtually impossible for the WP to fail. In the event of derailment during an earthquake, the TEV could impact an adjacent shielding doorway, tunnel entrance doorway or any structural object that would be in close proximity to the TEV. However, the safe drop height of a WP is stated to be 6.5 feet onto an unyielding surface in Reference H2.2.4. This equates to an impact velocity of about 20 feet per second. When the WP is in the TEV, it is surrounded by the shielding enclosure and a sharp impact to the TEV shielding enclosure would have about the same effect as a WP free drop onto an unyielding surface. The sliding acceleration would be limited by the coefficient of friction and would never exceed the acceleration of gravity, nor could the velocity build up as in a free drop, thus the sliding velocity would not exceed the 20 feet per second limit for impact.

In the event the TEV becomes derailed during transit, the steepest grade is 2.5 %, thus, it can not roll over a steep embankment. The sliding resistance on a 2.5% grade would hardly be affected from that on a flat surface.

Consequently the only credible failure mode appears to be a failure of the seismic anti lift restraints during the process of transferring the WP from the WPTT to the TEV. For consideration of the risk analysts, the sliding displacements as a function of PGA are tabulated..

The upper bound on sliding distance shown in Figure H6-5 would increase due to the uncertainty in structural response. Table H6-2 and Figure H6-7 shows this sliding distance with the increased uncertainty from structural response included.

$$\beta_{c\_disp} := \left(\beta_{c\_slide}^{2} + \beta_{c\_RS}^{2}\right)^{0.5}$$

$$\beta_{c\_disp} = 0.48$$

Table H6-2
Median and Upper Bound (less than 1% probability of exceedance)
Sliding Versus PGA

EQ	PGA	Median Δ ft	Upper Bound Δ ft
DBGM-2	0.45	0	0
BDBGM	0.91	0.364	1.11
1.5 BDBGM	1.37	0.753	2.3
2.0 BDBGM	1.82	1.567	4.79

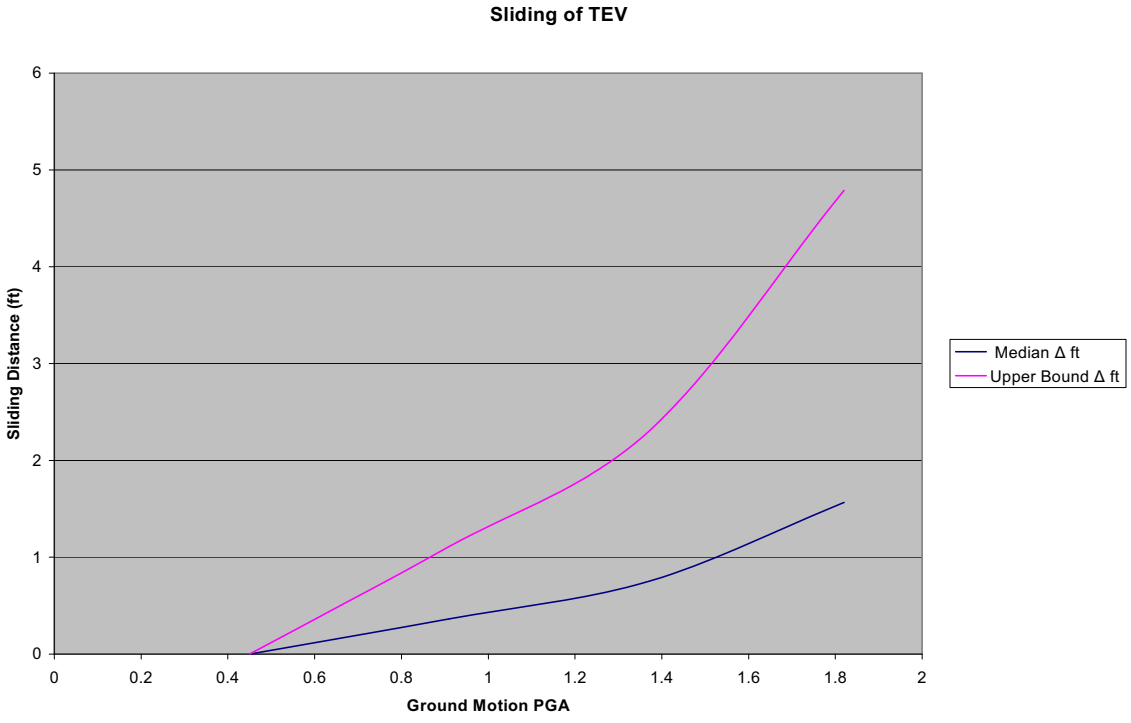

Figure H6-7
Median and Upper Bound Sliding Versus Ground Motion PGA

In the Table H6-2 and Figure H6-7and plot, the displacement has been set at 0 for DBGM-2 since the probability of failure at that level is very low. At BDBGM and beyond, the plot is based on free sliding after failure of the seismic anti lift restraints.

7. SUMMARY OF RESULTS AND CONCLUSIONS

A representative calculation has been conducted for the TEV when subjected to earthquake loading. If the seismic anti lift restraints are designed to the limits of ASME NOG-1, Reference H2.2.9, the median capacity of the clamps is 1.12g and is slightly greater than the BDBGM. The HCLPF capacity is 0.41g and is slightly less than DBGM-2. This low capacity arises from the fact that the dead weight provides a good portion of the anti tipping restraint for the DBGM-2 but, when the seismic load overcomes this dead weight, the forces in the anti lift restraints build up quickly.

Upon failure of the anti lift restraints, the TEV will likely derail and slide or rock. It was shown that the best estimate rocking was only about 23 degrees at about 4 times the BDBGM. This high capacity results from the center of gravity being less than half of the width of the rails and due to the fact that the effective frequency for large rocking motion is low and the resulting demand is low (the spectral acceleration at the effective frequency is much lower than the PGA). Thus, it is concluded that a TEV cannot tip over at any credible ground motion level and that the HCLPF capacity would be significantly greater than the BDBGM.

If the TEV is at the docking station in the loadout area and the WP is in the process of being transferred from the WPTT to the TEV, any sliding could possibly damage the WP. This is a short period in time but is the only credible condition where it appears likely that the WP could be seriously damaged in a seismic event. Once the WP is secured in the TEV it is protected from direct impact by the shielded enclosure. A sliding impact on the shielded enclosure would be analogous to the shock from a free drop. The WP can survive a free drop of 6.5 feet which relates to a 20 fps impact velocity. A sliding velocity that could be achieved would be lower than the 20 fps so impact of a sliding TEV with an adjacent structure should not breach the WP.

Other failure modes were examined qualitatively and found not to govern.

APPENDIX H-A
DBGM-2 DESIGN RESPONSE SPECTRA FOR CRCF GROUND FLOOR

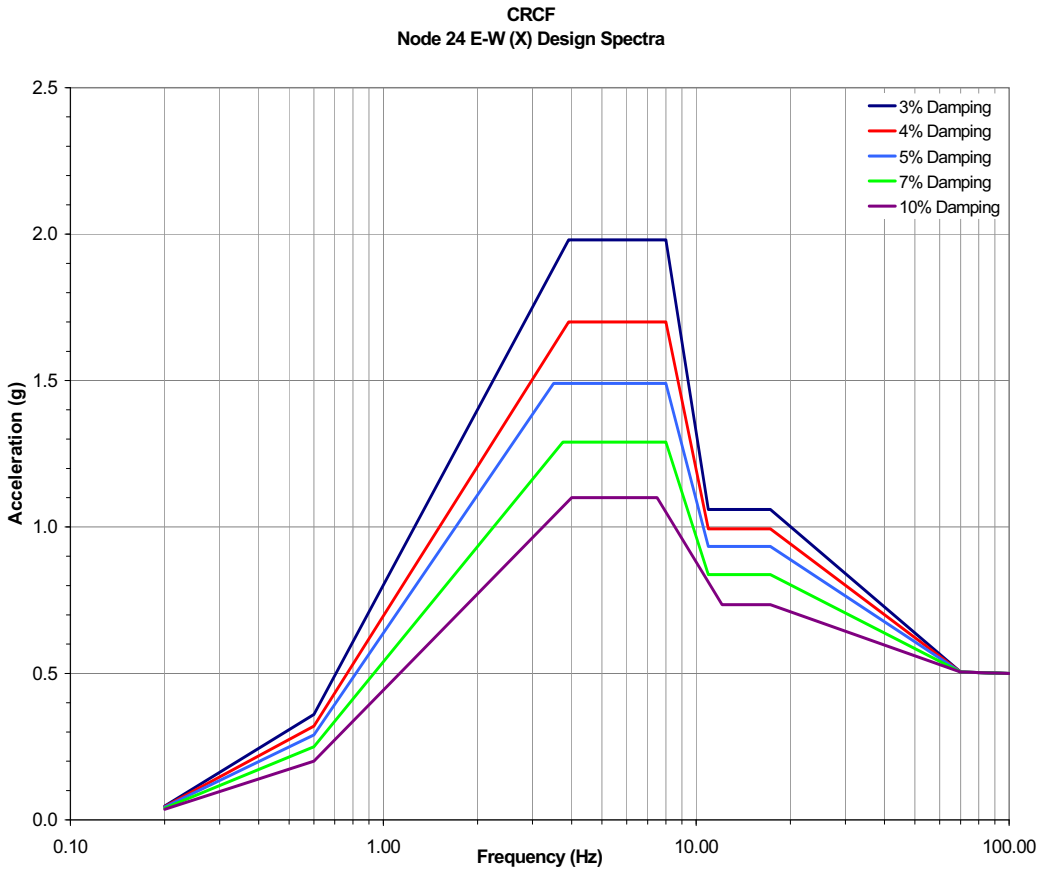

Figure H-A-1
DBGM-2 Design Spectra for CRCF Ground Floor Direction X

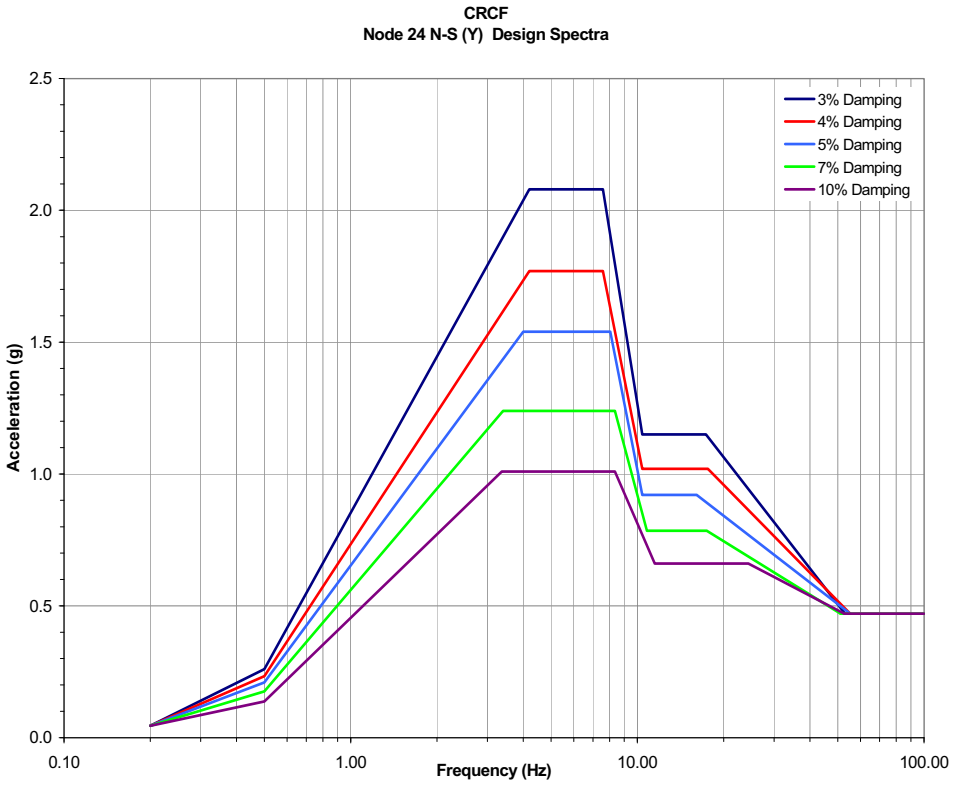

Figure H-A-2
DBGM-2 Design Spectra for CRCF Ground Floor Direction Y

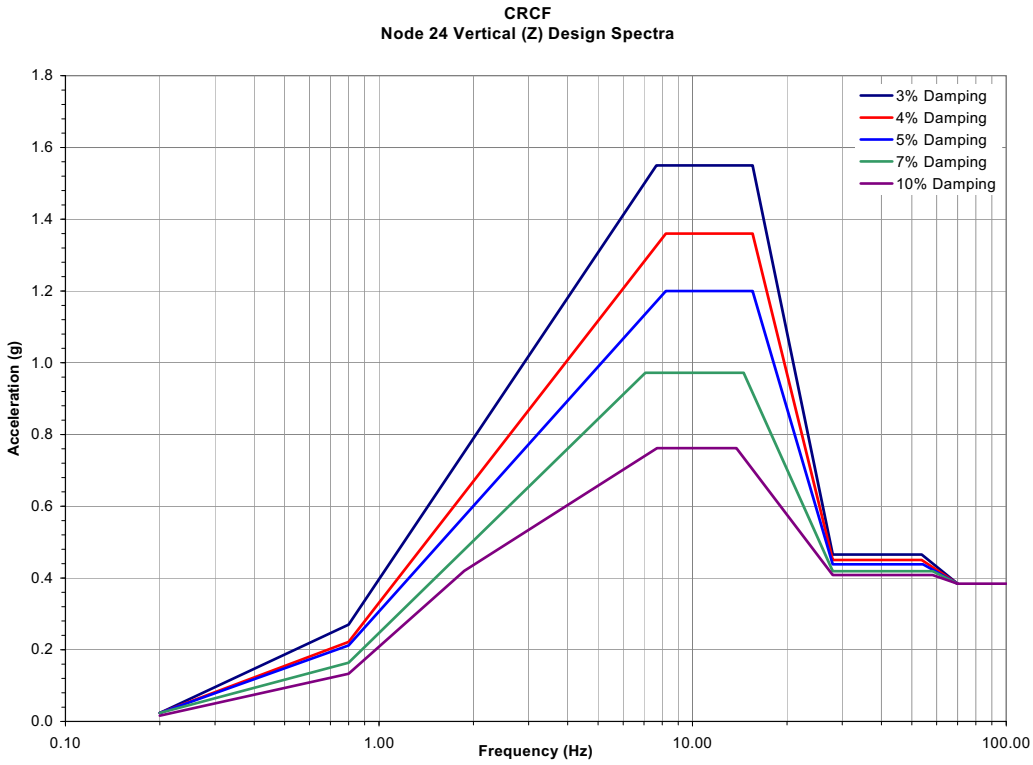

Figure H-A-3
DBGM-2 Design Spectra for CRCF Ground Floor Direction Z

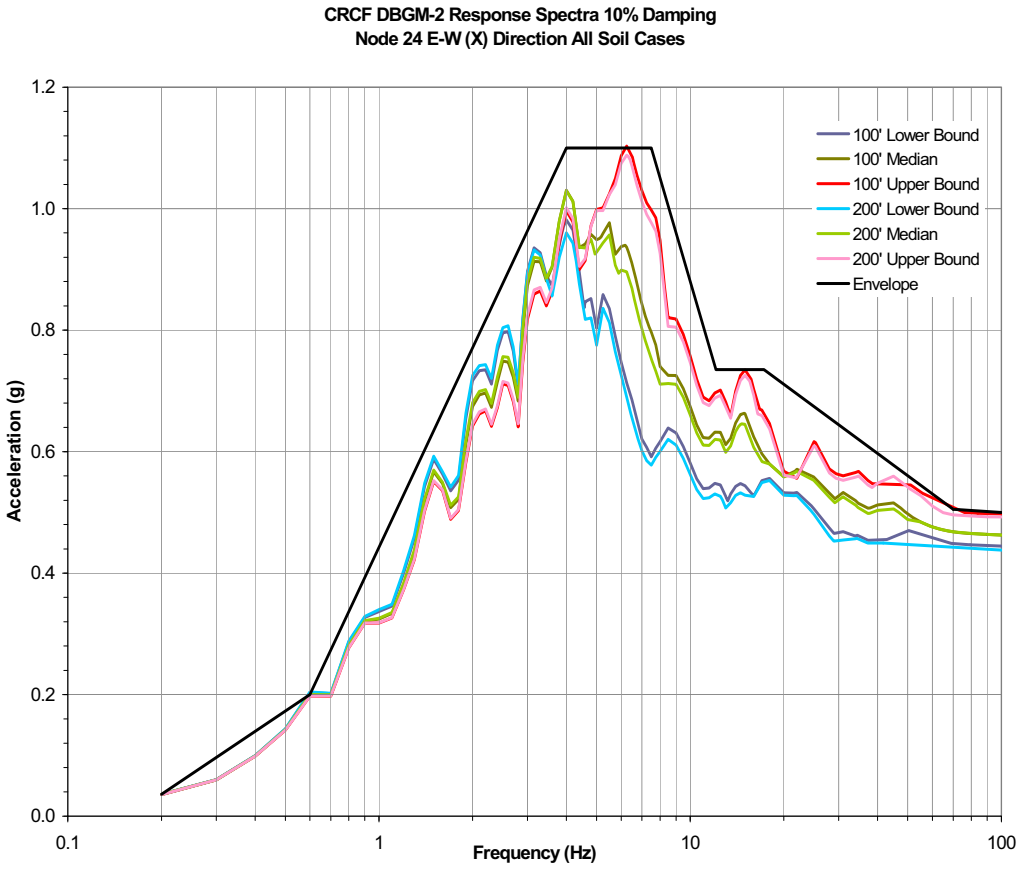

Figure H-A-4
DBGM-2 Spectra for CRCF Ground Floor Direction X, All Soil Cases, 10% Damping

APPENDIX H-B
SITE WIDE DBGM-2 UHS VERSUS 100 FOOT ALLUVIUM MEDIAN SOIL UHS

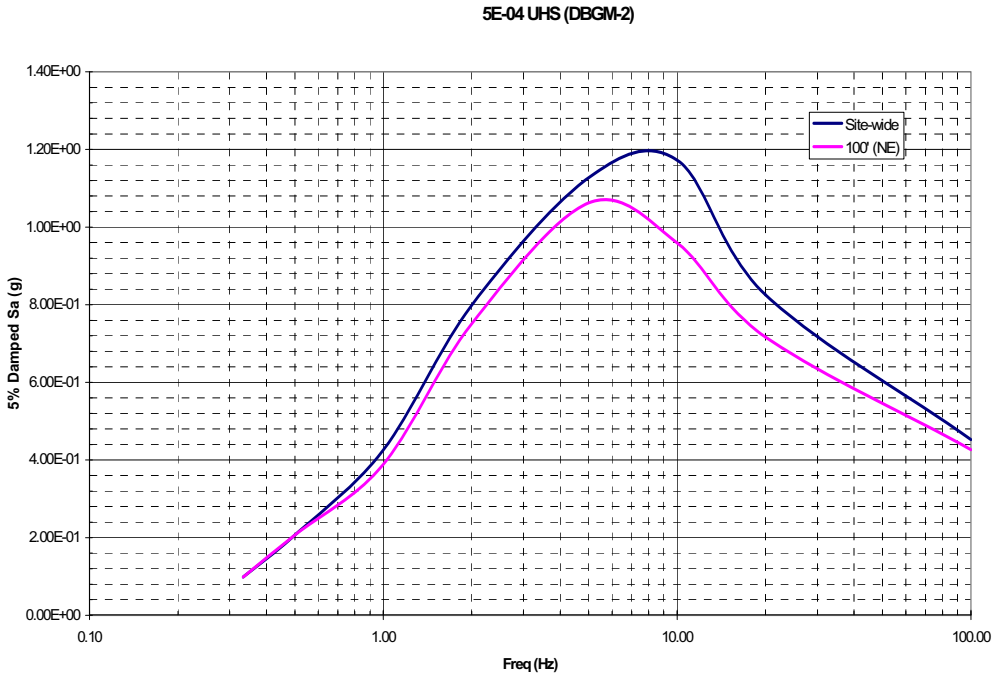

Figure H-B-1
Comparison of Site Wide DBGM-2 UHS to 100-Foot Alluvium Median Soil Case (See Section 6.2.2.1 for source information)

APPENDIX H-C
BDBGM RESPONSE SPECTRA FOR CRCF GROUND FLOOR

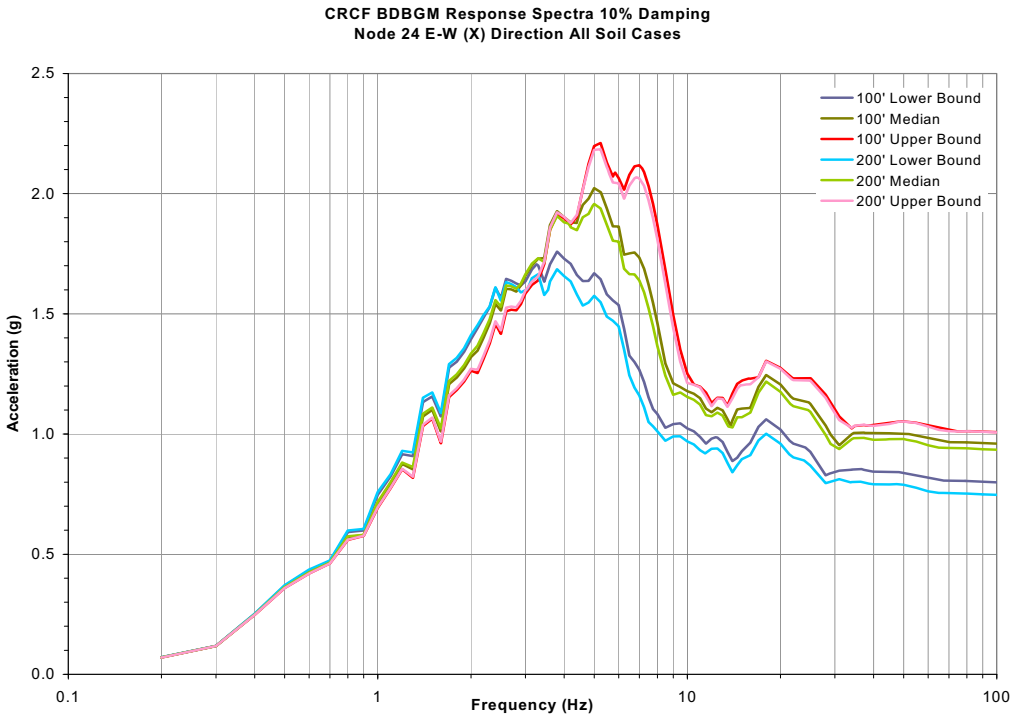

Figure H-C-1
BDBGM Spectra All Soil Cases, 10% Damping, Direction X

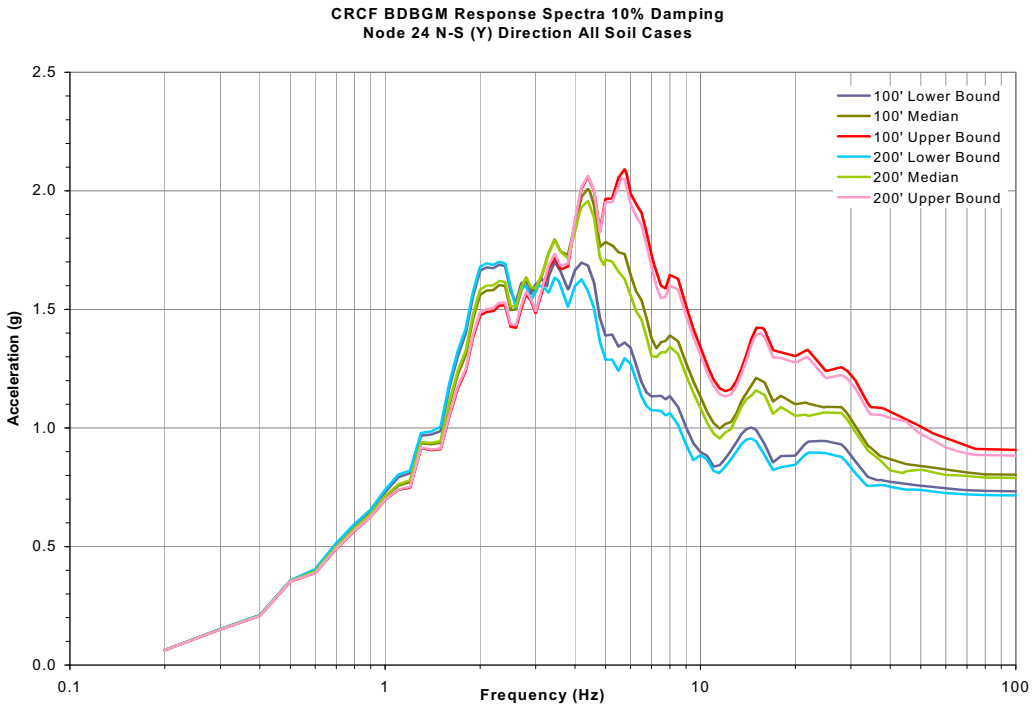

Figure H-C-2
BDBGM Spectra All Soil Cases, 10% Damping, Direction Y

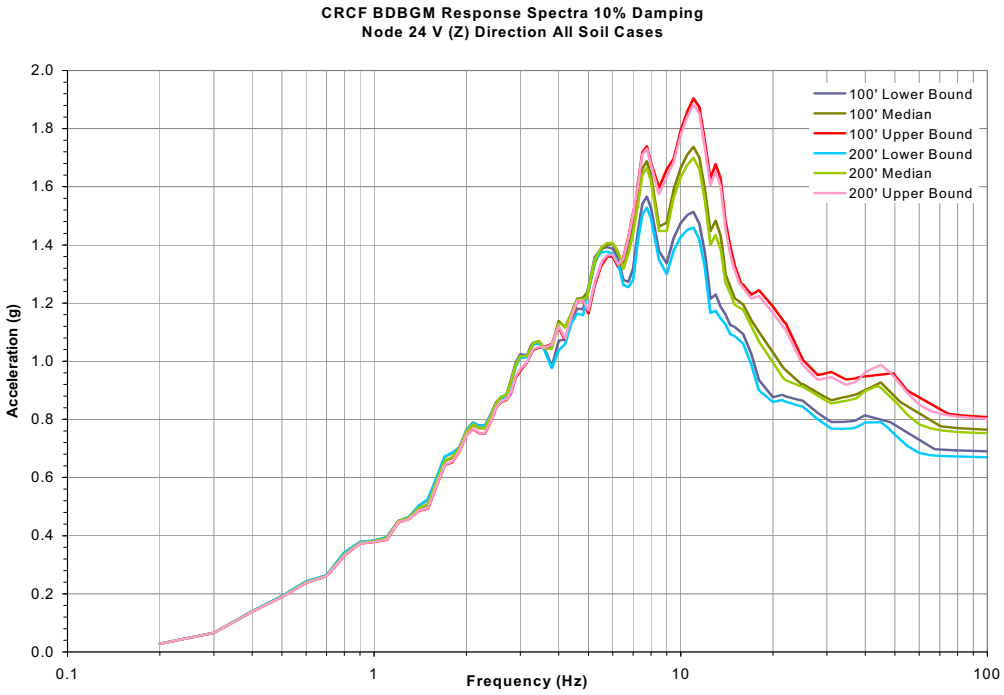

Figure H-C-3
BDBGM Spectra All Soil Cases, 10% Damping, Direction Z

Table H-C-1
BDBGM 100 Foot Alluvium Spectra for CRCF Ground Floor, Direction X

Frequency	DAMPING 0.03	DAMPING 0.04	DAMPING 0.05	DAMPING 0.07	DAMPING 0.1
8	1.99E+00	1.75E+00	1.69E+00	1.59E+00	1.46E+00
8.5	1.66E+00	1.55E+00	1.47E+00	1.38E+00	1.29E+00
9	1.52E+00	1.42E+00	1.34E+00	1.25E+00	1.21E+00
9.5	1.41E+00	1.35E+00	1.31E+00	1.25E+00	1.20E+00
10	1.33E+00	1.19E+00	1.19E+00	1.20E+00	1.18E+00
10.5	1.28E+00	1.25E+00	1.23E+00	1.20E+00	1.17E+00
11	1.32E+00	1.27E+00	1.24E+00	1.19E+00	1.15E+00
11.5	1.29E+00	1.20E+00	1.17E+00	1.13E+00	1.11E+00
12	1.42E+00	1.33E+00	1.27E+00	1.18E+00	1.09E+00
12.5	1.43E+00	1.37E+00	1.31E+00	1.21E+00	1.11E+00
13	1.43E+00	1.37E+00	1.31E+00	1.21E+00	1.10E+00
13.5	1.45E+00	1.36E+00	1.29E+00	1.17E+00	1.06E+00
13.8113	1.55E+00	1.40E+00	1.29E+00	1.15E+00	1.03E+00
13.9416	1.58E+00	1.43E+00	1.33E+00	1.17E+00	1.05E+00
14	1.59E+00	1.44E+00	1.34E+00	1.18E+00	1.06E+00
14.5	1.65E+00	1.48E+00	1.36E+00	1.22E+00	1.10E+00
15	1.66E+00	1.47E+00	1.35E+00	1.21E+00	1.11E+00
16	1.43E+00	1.32E+00	1.28E+00	1.19E+00	1.11E+00
17	1.51E+00	1.39E+00	1.31E+00	1.26E+00	1.20E+00
18	1.69E+00	1.56E+00	1.46E+00	1.35E+00	1.25E+00
20	1.34E+00	1.31E+00	1.29E+00	1.25E+00	1.21E+00

ATTACHMENT I

FRAGILITY OF SPENT FUEL TRANSFER MACHINE IN WET HANDLING FACILITY

Prepared By: Wen H. Tong

ARES Check By: Stephen A. Short

LLNL Check By: Robert C. Murray

TABLE OF CONTENTS

ACRONYMS AND ABBREVIATIONS

ACI	American Concrete Institute
AISC	American Institute of Steel Construction
ANSI	American National Standards Insitute
AO	Aging Overpack
APE	Annual Probability of Exceedance
ASCE	American Society of Civil Engineers
ASME	American Society of Mechanical Engineers
BSC	Bechtel SAIC, LLC
BDBGM	Beyond Design Basis Ground Motion at $1x10^{-4}$ APE
CDFM	Conservative Deterministic Failure Margin
CHC	Cask Handling Crane
CIP	Cast-in-Place
CRCF	Canister Receipt and Closure Facility
CTM	Canister Transfer Machine
CTT	Cask Transfer Trolley
DBGM-2	Design Basis Ground Motion at $5x10^{-4}$ APE
DL	Dead Load
DOF	Degree of Freedom
DPC	Dual Purpose Canister
EPRI	Electric Power Research Institute
HCLPF	High Confidence of Low Probability of Failure
HVAC	Heating, Ventilation, & Air Conditioning
IEEE	Institute of Electrical and Electronics Engineers
IHF	Initial Handling Facility
ISRS	In-Structure Response Spectra

ACRONYMS AND ABBREVIATIONS (cont.)

ITS	Important to Safety
LA	License Application
LLNL	Lawrence Livermore National Laboratory
NPP	Nuclear Power Plant
PGA	Peak Ground Acceleration
RF	Receipt Facility
RRS	Required Response Spectrum
Sa	Spectral Acceleration
SFA	Surface Facilities Area
SFTM	Spent Fuel Transfer Machine
SPRA	Seismic Probabilistic Risk Assessment
SRSS	Square Root of the Sum of Squares
SSE	Safe Shutdown Earthquake (used with NPPs)
SSI	Soil Structure Interaction
SSC	Structure, System, and Component
TAD	Transportation, Aging, and Disposal canister
TEV	Transport and Emplacement Vehicle
TRS	Test Response Spectrum
UHS	Uniform Hazard Spectra
USDOE	United States Department of Energy
USNRC	United States Nuclear Regulatory Commission
WHF	Wet Handling Facility
WP	Waste Package
WPTT	Waste Package Transfer Trolley
YMSF	Yucca Mountain Surface Facilities
ZPA	Zero Period Acceleration

FRAGILITY TERMINOLOGY

Am	Median Peak Ground Motion Capacity
β_R	Log Standard Deviation of Randomness
β_U	Log Standard Deviation of Uncertainty (Lack of Knowledge)
β_C	Composite Variability = $(\beta_R^2 + \beta_U^2)^{0.5}$
F_S	Strength Factor of Safety
β_{R_S}	Strength Randomness (typical)
β_{U_S}	Strength Uncertainty (typical)
β_{C_S}	Strength Composite Variability (typical)
F_μ	Inelastic Energy Absorption Factor of Safety
F_{QM}	Qualification Factor of Safety
F_δ	Damping Factor of Safety
F_M	Modeling Factor of Safety
F_{MC}	Modal Combination Factor of Safety
F_{ECC}	Earthquake Component Combination Factor of Safety
F_{SA}	Spectral Shape Factor of Safety
F_{SSI}	Soil-Structure Interaction Factor of Safety
F_{GMI}	Ground Motion Incoherence Factor of Safety
F_{TOTAL}	Total Factor of Safety
F_{RS}	Structural Response Factor of Safety
F_{RE}	Equipment Response Factor of Safety

I1. PURPOSE

The purpose of this calculation is to estimate seismic fragility of the Spent Fuel Transfer Machine (SFTM) in the Wet Handling Facility (WHF). The mean seismic fragility curve of the SFTM will be convolved with the site-specific seismic hazard curves to calculate risk of seismic-induced failure of the SFTM.

I2. REFERENCES

I2.1 PROCEDURES/DIRECTIVES

I2.1.1 EG-PRO-3DP-G04B-00037, Rev. 10. *Calculations and Analyses*. Las Vegas, Nevada: Bechtel SAIC Company. ACC: ENG.20071018.0001.

I2.1.2 IT-PRO-0011, Revision 7, ICN 0. *Software Management*. Las Vegas, Nevada: Bechtel SAIC Company. ACC: DOC.20070905.0007.

I2.2 DESIGN INPUTS

I2.2.1 EPRI (Electric Power Research Institute) 1994. *Methodology for Developing Seismic Fragilities*. EPRI TR-103959. Palo Alto, California: Electric Power Research Institute. TIC:253770. [DIRS 161329]

I2.2.2 BSC (Bechtel SAIC Company) 2007. *WHF Tier-1 In-Structure Response Spectra.* 050-SYC-WH00-01000-000 REV 00A. Las Vegas, Nevada: Bechtel SAIC Company. ACC: ENG.20070924.0046. [DIRS 184254]

I2.2.3 BSC (Bechtel SAIC Company) 2007. *Wet Handling Facility General Arrangement Ground Floor Plan*. 050-P10-WH00-00102-000 REV 00B. Las Vegas, Nevada: Bechtel SAIC Company. ACC: ENG.20071206.0032; ENG.20071226.0001; ENG.20080121.0014; ENG.20080121.0015. [DIRS 184274]

I2.2.4 BSC (Bechtel SAIC Company). *Mechanical Handling Design Report - Spent Fuel Transfer Machine*. 050-30R-HT00-00100-000 Rev 000. Las Vegas, Nevada: Bechtel SAIC Company. ACC: ENG.20071031.0009. [DIRS 184459]

I2.2.5 [Reserved]

I2.2.6 ASME NOG-1-2004. 2005 *Rules for Construction of Overhead and Gantry Cranes (Top Running Bridge, Multiple Girder)*. New York, New York: American Society of Mechanical Engineers. TIC: 257672. [DIRS 176239]

I2.2.7 MO0801HCUHSSFA.001. *Mean Hazard Curves and Mean Uniform Hazard Spectra for the Surface Facilities Area*. Submittal date: 01/11/2008. [DIRS 184802]

I2.2.8 BSC (Bechtel SAIC Company) 2006. *Wet Handling Facility Spent Fuel Transfer Machine Mechanical Equipment Envelope.* 050-M90-HT00-00101-000 REV 00A. Las Vegas, Nevada: Bechtel SAIC Company. ACC: ENG.20061120.0016; ENG.20070207.0001; ENG.20070823.0003. [DIRS 178631]

I2.2.9 SAC Joint Venture 2000. *State of the Art Report on Base Metals and Fracture.* FEMA-355A. Washington, D.C.: Federal Emergency Management Agency. ACC: MOL.20080215.0050. [DIRS 185079]

I2.2.10 AISC (American Institute of Steel Construction) 1991. *Manual of Steel Construction, Allowable Stress Design.* 9th Edition, 1st Revision. Chicago, Illinois: American Institute of Steel Construction. TIC: 4254. [DIRS 127579]

I2.2.11 ANSI/AISC N690-1994. 1994. *American National Standard Specification for the Design, Fabrication, and Erection of Steel Safety-Related Structures for Nuclear Facilities*. Chicago, Illinois: American Institute of Steel Construction. TIC: 252734. [DIRS 158835]

I2.2.12 Timoshenko S., Young D.H., and Weaver W. Jr. 1974. *Vibration Problems in Engineering.* 4th Edition. New York, New York: John Wiley & Sons. ISBN: 0471873152 [DIRS 184110]

I2.2.13 Moore, D. 2007. "*SSI Factor of Safety.*" E-mail from D. Moore to B. Murray, October 25, 2007. ACC: LLR.20080110.0145. [DIRS 184842]

I2.2.14 [Reserved].

I2.2.15 BSC (Bechtel SAIC Company) 2007. *Yucca Mountain Project Engineering Specification Wet Handling Facility Spent Fuel Transfer Machine*. 050-3PS-HTF0-00100-000, Rev. 00A. Las Vegas, Nevada: Bechtel SAIC Company. ACC: ENG.20070829.0010.

I2.3 DESIGN CONSTRAINTS

None.

I2.4 DESIGN OUTPUTS

The calculated seismic fragility of structural failure of the SFTM, expressed in terms of a median seismic capacity and an associated combined variability, will be convolved with the site-specific seismic hazard curve to calculate risk of seismic-induced failure of the SFTM. This is performed to support information in the License Application (LA).

I3. ASSUMPTIONS

I3.1 ASSUMPTIONS REQUIRING VERIFICATION

There are no assumptions requiring verification used in this attachment.

I3.2 ASSUMPTIONS NOT REQUIRING VERIFICATION

I3.2.1 Drop of Lifted Load

The fragility reported in this calculation is only for those failure modes that would result in gross structural failure or falling of the SFTM. Drop of a lifted spent fuel assembly is not a concern, either for release or criticality.

Rationale - The only concern is to have the crane or the trolley fall into the pool and damage several spent fuel racks or tip over the casks (criticality concern, not release).

I3.2.2 SFTM Designed to Code Stress Limits

Structural components of the bridge girders and the trolley are designed to the stress limits of the NOG-1 code (Reference I2.2.6) for different load combinations specified in the NOG-1.

Rationale - At the time this calculation is prepared, the detailed design is not complete. Thus, it is not possible to determine the margin between the code limits and the calculated stresses that the designers will use. This is extra margin over the margins in the material strengths, code acceptance criteria and load combinations. Due to lack of a design calculation, it is conservatively assumed that this extra margin does not exist.

I3.2.3 Materials Assumed for SFTM Bridge and Trolley

The structural steel assumed for the SFTM bridge girder and the trolley is A 572.

Rationale - Due to the assumption made in I3.2.2, the strength factor of safety is independent of the material assumed. See Section I6.5.1 for details.

I4. METHODOLOGY

I4.1 QUALITY ASSURANCE

This calculation is prepared in accordance with EG-PRO-3DP-G04B-00037, Calculations and Analyses (Reference I2.1.1).

I4.2 USE OF SOFTWARE

Mathcad version 14 is used in this calculation. The use of this software is classified as Level 2 software per procedure, IT-PRO-0011 (Reference I2.1.2) and therefore the software need not be qualified.

I4.3 APPROACH

The Separation-of-Variable method documented in EPRI TR-103959 (Reference I2.2.1, Section 3) is followed in calculating seismic fragility of this ITS equipment component.

I5. LIST OF APPENDICES

Appendix I-A. Estimate of Vertical Frequency of the Bridge Crane
Appendix I-B. DBGM-2 and BDBGM ISRS at SFTM Rail Level (Reference I2.2.2)

I6. FRAGILITY CALCULATION

I6.1 INTRODUCTION

The seismic fragility calculation of the Spent Fuel Transfer Machine (SFTM) in the Wet Handling Facility is performed here. The calculation evaluates seismic fragilities of structural failure modes of the SFTM that may result in gross structural failure or falling of the SFTM. The scope of this fragility review includes all elements of the CRCF Cask Handling Crane that rest on top of the crane rails. The fragility of the crane rails, the rail supports, the rail anchorage and the structure are addressed by others.

I6.2 SPENT FUEL TRANSFER MACHINE

The SFTM is located above the pool in the cask preparation area in the WHF. It is used for transferring spent nuclear fuel elements arriving in transportation casks and dual-purpose canisters into transportation, aging, and disposal canisters. Per Reference I2.2.4, the SFTM is classified as a Type 1 crane in accordance with ASME NOG-1 (Reference I2.2.6). The SFTM is a rectilinear bridge and trolley system with a vertical mast that extends down into the pool. The SFTM including the bridge and the trolley and their respective runway rails are designated ITS (Important to Safety) mechanical handling system equipment per Reference I2.2.8. The bridge spans the pool and runs on rails on the edge of the pool. The trolley runs on a set of rails on the bridge.

The estimate weights of the SFTM and its lifting capacity are provided in References I2.2.4 and I2.2.8 as presented below. A schematic of the SFTM is shown in Figure I6.2-1 (Reference I2.2.8).

- Fully loaded crane weight = 15 tons (Note 3 of Reference I2.2.8)
- Lifted load no more than 2000 pounds (Section 3.10 of Reference I2.2.15)

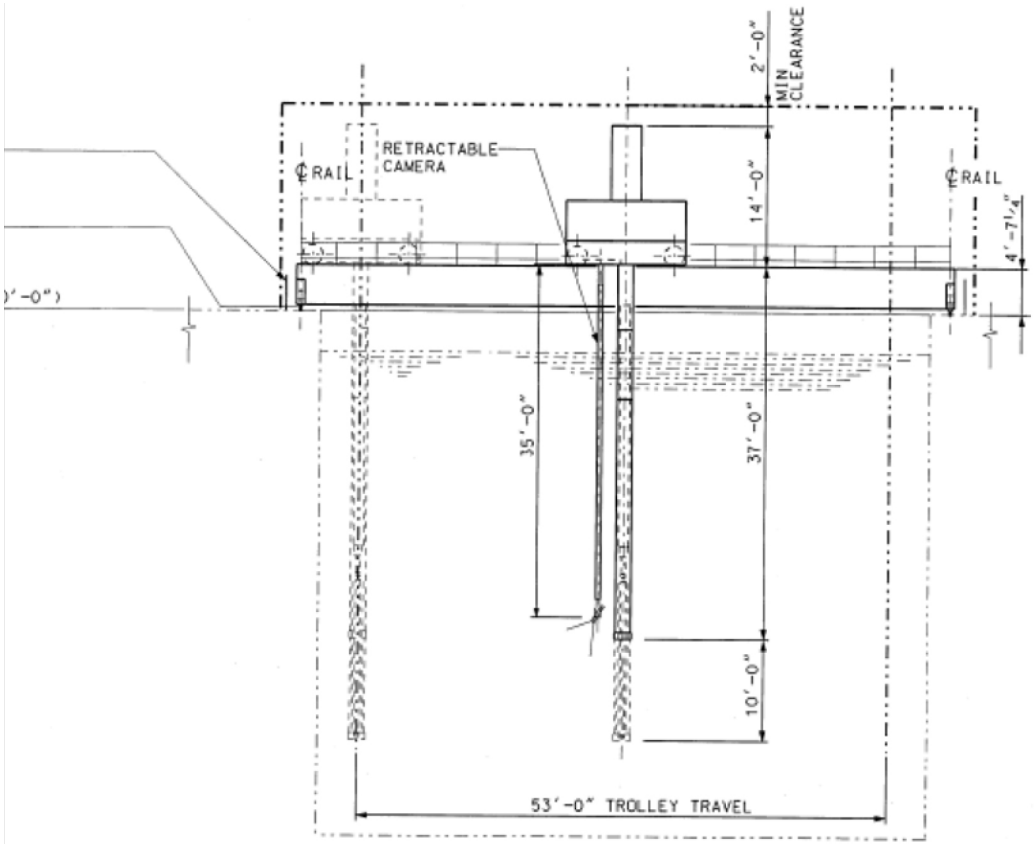

Figure I6.2-1. Schematic of SFTM Showing Bridge and Trolley (Reference I2.2.8)

I6.3 STRUCTURAL FAILURE MODES OF SFTM

The only failure modes of concern are the ones that could result in gross structural failure or falling of the SFTM. Falling of the bridge or the trolley into the pool could potentially damage several spent fuel racks or tip over the casks. Drop of a spent fuel assembly is not a concern, either for release or criticality. Per Section 3.1.2 of Reference I2.2.4, the SFTM bridge and the trolley are provided with devices so that they remain on their respective runways during and after a seismic event. The restraint device and resisting structure are designed for the maximum load.

The design and the associated fragility analyses of the crane rails, rail support, and rail anchorage will be addressed in the detailed design by others. During the detailed design, the rails and rail anchorage will be designed for the DBGM-2 with margin such that the HCLPF is greater than the BDBGM (see Assumption I3.1.1). Thus, seismic fragility of the following failure modes are evaluated in this calculation.

- Failure of the bridge crane and its seismic restraint
- Failure of the trolley and its seismic restraint

I6.4 SEISMIC INPUT MOTION

The DBGM-2 ground motion is defined by the horizontal and vertical site-wide mean uniform hazard spectra (Reference I2.2.7; also Section 6.2.2.1 for source information) at the surface level. The site-wide UHS are the enveloping cases of the surface UHS of 30', 70', 100' and 200' of alluvium over tuff.

The Tier 1 analyses (Reference I2.2.2) considered two depths of alluvium (30 and 100 feet) in addition to three soil properties (upper bound, lower bound, and median cases). The design ISRS are envelopes of these different cases.

The SFTM is supported by the WHF structure at elevation 0' and the seismic input motions of the SFTM are defined by the floor response spectra generated at Node 2099 per Reference I2.2.2. The alluvium depths under the WHF is between 60 and 70 feet. The median input motion to the SFTM is defined by the raw ISRS of the 100-foot alluvium case (median soil properties). At the frequency range of the SFTM there is no significant difference between the 30 and 100 feet ISRS.

I6.5 SEISMIC FRAGILITY OF SFTM BRIDGE AND TROLLEY

I6.5.1 Strength Factor

Per Section 2.1 of the Mechanical Handling Design Report of the SFTM (Reference I2.2.4), the applicable code for the SFTM design is ASME NOG-1 2004. The median strength factor of the SFTM bridge structural failure is estimated based on the NOG-1 design criteria. It is assumed (see Assumption I3.2.2) that the SFTM will be designed such that the calculated stresses for the different load combinations in NOG-1 will be at the corresponding code allowable.

The basic NOG-1 load combination for crane operational loads (Section 4140 of NOG-1) that is applicable to the SFTM is:

LC1 = Dead weight of bridge and trolley + rated load

The NOG-1 load combinations for earthquake loads (SSE) are (Section 4140 of NOG-1):

LC10 = Dead weight of bridge and trolley + SSE loads
LC11 = Dead weight of bridge and trolley + SSE loads + credible critical load with SSE

Per Section 4300 of NOG-1, the basic allowable stress of the operating loading conditions for structural members is 50% of the yield strength for tension and compression. For extreme environmental load combination which includes SSE (Safe Shutdown Earthquake), the allowable stress is 90% of the yield strength (Table 4311-1 of NOG-1). The DBGM-2 is used in the NOG-1 load combinations for SSE.

$\sigma_{NOL} = 0.5 \cdot F_{y\_min}$ Operating loading condition

$\sigma_{NOL} + \sigma_{DBGM} = 0.9 \cdot F_{y\_min}$ Extreme load combination

where σ_{NOL} and σ_{DBGM} are stresses due to normal operating loads (uniform weight of the bridge crane, the trolley weight, the mast, and the lifted load) and DBGM-2, respectively and F_{y_min} is the minimum yield strength of the SFTM.

The SFTM bridge and the trolley frame are sensitive to the vertical direction input motion since the horizontal inertia load from the suspended load is limited due to pendulum action. The vertical fundamental frequency of the SFTM with the rated load at the mid-span is estimated at 2.57 Hz as presented in Appendix I-A, Section I-A.2. The corresponding 7% damped vertical DBGM-2 spectral acceleration is 0.64g (Figure I-B-2 of Appendix I-B).

It is assumed (see I3.2.3) that the bridge girders will be constructed of ASTM 572 Grade 50 steel with a minimum specified yield strength of 50 ksi.

$F_{y\_min} := 50 \cdot ksi$

$F_y := 1.2 \cdot F_{y\_min}$ Median yield strength; the factor to get from minimum specified yield strength to the median value is based on Section 4.6 of Reference I2.2.9.

$F_y = 60 \cdot ksi$

$S_{av\_7\%} := 0.64 \cdot g$ 7% damped DBGM-2 vertical spectral acceleration (design) at the fundamental frequency (2.57 Hz) of the SFTM when the loaded trolley is at the mid-span (See Appendix I-A) . Per Section 4153.8 of NOG-1, a damping value of 7% of critical is used for DBGM-2.

$\sigma_{NOL} := 0.5 \cdot F_{y\_min}$ Normal operating load stress at the mid-span (see Assumption I3.2.2).

$\sigma_{NOL} = 25 \cdot ksi$

$$\sigma_{DBGM} := \frac{S_{av\_7\%}}{g} \cdot \sigma_{NOL}$$

$\sigma_{DBGM} = 16 \cdot ksi$

The median strength factor (F_S) at which a plastic hinge will form at the mid-span is calculated using the equation shown below:

$(\sigma_{NOL}) + (\sigma_{NOL} * S_{av\text{-}7\%}) * F_S = (1.1) * F_y$

where the 1.1 factor is a conservatively estimated ratio of plastic section modulus to elastic section modulus of a box girder.

$$F_S := \frac{(1.1)\cdot F_y - (\sigma_{NOL})}{\sigma_{DBGM}}$$

$F_S = 2.56$ This is the strength factor when a plastic hinge is formed at the mid-span of the bridge girder.

There is no randomness, only uncertainty associated with the strength factor.

$$\beta_{R\_S} := 0$$

The uncertainty variability associated with the median yield strength is estimated to be 0.12 based on Table 3-9 of Reference I2.2.1.

$$\beta_{U\_S} := 0.12$$

$$\beta_{c\_S} := \sqrt{\beta_{R\_S}^2 + \beta_{U\_S}^2} \qquad \beta_{c\_S} = 0.12$$

I6.5.2 Inelastic Energy Absorption Factor

Because the strength factor is calculated based on forming of a plastic hinge of the steel girder (i.e., forming of a mechanism) and the ratcheting effect of the heavy load the crane carries, no further credit is taken for the inelastic energy absorption capability.

$$F_\mu := 1.0$$

$$\beta_{c\_\mu} := 0$$

I6.5.3 Equipment Response Factors

I6.5.3.1 Qualification Method

This factor accounts for conservatism in the Tier 1 design ISRS (Reference I2.2.2) relative to the unbroadened and unsmoothed ISRS of the 100-foot best-estimate soil property case. The best-estimate fundamental frequency of the bridge crane in the vertical direction, when the trolley, the mast and the rated load are at the mid-span, is 2.57 Hz (Appendix I-A, Section I-A.2).

At 2.57 Hz

$S_{av\_7\%} = 0.64\cdot g$ 7% damped design vertical spectral acceleration from the Tier 1 design ISRS (Figure I-B-2 of Appendix I-B)

$SA_{raw\_7\%} := 0.474\cdot g$ 7% damped raw spectral acceleration of the ground floor (Figure I-B-2 of Appendix I-B).

$$F_{QM} := \frac{S_{av\_7\%}}{SA_{raw\_7\%}}$$

$F_{QM} = 1.35$

Since the raw ISRS is used and uncertainties in response due to uncertainty in equipment frequency (i.e., modeling), modal combination, and earthquake component combination are separately calculated below,

$\beta_{c\_QM} := 0$

I6.5.3.2 Equipment Damping

The median and minus one sigma damping values at failure of a welded structure are 7% and 5% , respectively (Table 3-4 of Reference I2.2.1). Since 7% damping will be used for the design per NOG-1, the damping factor of safety is unity.

$F_{\delta\_E} := 1$

$SA_{raw\_5\%} := 0.556 \cdot g$ Raw spectral acceleration at lower bound damping value at the crane frequency; Node 2099 5% damped raw ISRS (Figure I-B-1 of App. I-B)

$\beta_{c\_\delta\_E} := \ln\left(\frac{SA_{raw\_5\%}}{SA_{raw\_7\%}}\right)$

$\beta_{c\_\delta\_E} = 0.16$

I6.5.3.3 Equipment Modeling Factor

Since the vertical response of the SFTM is a relatively simple system, the frequency calculation is judged to be best-estimate and the modeling factor of safety is unity.

$F_{M\_E} := 1.0$

$\beta_{R\_M\_E} := 0$ No randomness associated with modeling

Reference I2.2.1 provides a range of 0.1 to 0.3 for uncertainty in modal frequencies. Given the relatively simple model of the SFTM, a variability of 0.15, which is greater than the 0.1, is judged to be sufficient.

$\beta_f := 0.15$

$f_{v\_m} := 2.57 \cdot Hz$ Best estimate vertical frequency when the mast and the trolley with the rated load is at the mid-span of the bridge.

$f_u := f_{v\_m} \cdot e^{\beta_f}$ Upper bound frequency

$f_u = 2.99 \cdot Hz$

$SA_{V\_u} := 0.566 \cdot g$ where 0.566g is the 7% damped vertical spectral acceleration at f_u from the raw ISRS at 0 foot (Figure I-B-1 of Appendix I-B).

$\beta_{U\_f} := \ln\left(\frac{SA_{V\_u}}{SA_{raw\_7\%}}\right)$

$\beta_{U\_f} = 0.18$

$\beta_{U\_ms} := 0.10$ The uncertainty in response due to uncertainty of mode shape is in the range of 0.05 to 0.15 depending on the complexity of the equipment (Reference I2.2.1). A value of 0.10 is used based on the simple model.

$\beta_{U\_M\_E} := \sqrt{\beta_{U\_f}^2 + \beta_{U\_ms}^2}$

$\beta_{U\_M\_E} = 0.2$

$\beta_{c\_M\_E} := \sqrt{\beta_{R\_M\_E}^2 + \beta_{U\_M\_E}^2}$

$\beta_{c\_M\_E} = 0.2$

I6.5.3.4 Modal Combination

The dynamic response spectrum method is one of the methods described in Section 4153 of NOG-1 for performing seismic analysis for Type 1 cranes. When the response spectrum method is used, closely spaced modes are combined per grouping method, ten-percent method or double-sum method as per Section 4153.10 of NOG-1. For the failure mode of the bridge girder evaluated here, the response will be predominantly that of the vertical mode. Thus, the modal combination factor of safety is judged to be unity.

$F_{MC\_E} := 1.0$

$\beta_{R\_MC\_E} := 0.05$ For the failure mode evaluated, the fundamental vertical mode is dominant. Thus use the lower bound value of 0.05 in Reference I2.2.1.

$\beta_{U\_MC\_E} := 0$

$\beta_{c\_MC\_E} := \sqrt{\beta_{R\_MC\_E}^2 + \beta_{U\_MC\_E}^2}$

$\beta_{c\_MC\_E} = 0.05$

I6.5.3.5 Earthquake Component Combination

Section 4153.10(c) of NOG-1 requires using the SRSS (Square Root of Sum of the Squares) to combine contributions for the three components of earthquake motion. This method is considered to be median-centered. Thus,

$F_{ECC\_E} := 1.0$

$\beta_{R\_ECC\_E} := 0.10$ A generic value of 0.18 is suggested in Reference I2.2.1 when responses from each of the three components are not available. A value of 0.10 is used here since the vertical component contributes most significantly to the response of the failure mode evaluated.

$\beta_{U\_ECC\_E} := 0$

$\beta_{c\_ECC\_E} := \sqrt{\beta_{R\_ECC\_E}^2 + \beta_{U\_ECC\_E}^2}$

$\beta_{c\_ECC\_E} = 0.1$

Equipment Response Factors

$F_{RE} := F_{QM} \cdot F_{\delta\_E} \cdot F_{M\_E} \cdot F_{MC\_E} \cdot F_{ECC\_E}$

$F_{RE} = 1.35$

$\beta_{c\_RE} := \sqrt{\beta_{c\_QM}^2 + \beta_{c\_\delta\_E}^2 + \beta_{c\_M\_E}^2 + \beta_{c\_MC\_E}^2 + \beta_{c\_ECC\_E}^2}$

$\beta_{c\_RE} = 0.28$

I6.5.4 Structural Response Factors

I6.5.4.1 Spectral Shape Factor

This factor accounts for conservatism in the site-wide DBGM-2 design spectrum. At the Surface Facilities Area (SFA) the depth of alluvium overlying tuff varies from 30 feet to 200 feet. Uniform hazard spectra at the surface are calculated from site response analyses for alluvium depths of 30', 70', 100' and 200'. The site-wide design ground response spectrum is the envelope of the surface spectra of these four alluvium depths (Reference I2.2.7; also Section 6.2.2.1 for source information).

The dominant frequency of the WHF soil-structure system in the vertical direction is 6.8 Hz from the Tier 1 ISRS calculation (Reference I2.2.2, Table B6). Since the vertical UHS for the 100-ft alluvium depth case is not available, the horizontal site-wide and the surface spectrum of the 100-ft alluvium depth case are used to calculate the spectral shape factor. The dominant mode of the WHF in the horizontal direction has a frequency of about 5 hz (Reference I2.2.2, Table B6). At this frequency

$SA_{site} := 1.13g$ 5% damped site-wide spectral acceleration (see Figure I6.5-1).

$SA_{100} := 1.06 \cdot g$ 5% damped spectral acceleration of the 100-foot best-estimate alluvium depth case in the northeast area where the preclosure surface facilities are located.

$F_{SA} := \frac{SA_{site}}{SA_{100}}$

$F_{SA} = 1.07$

Since uncertainty in the UHS is derived from uncertainty in the seismic hazard curves which will be included in the final risk quantification, no uncertainty is included under the spectral shape factor to avoid double-counting the hazard uncertainty, hence

$\beta_{U\_SA} := 0$

$\beta_{R\_SA} := 0.2$ This is random variability to account for peak to valley variability of a smooth ground response spectrum (Reference I2.2.1, Table 3-2)

$$\beta_{c\_SA} := \sqrt{\beta_{U\_SA}^{2} + \beta_{R\_SA}^{2}} = 0.2$$

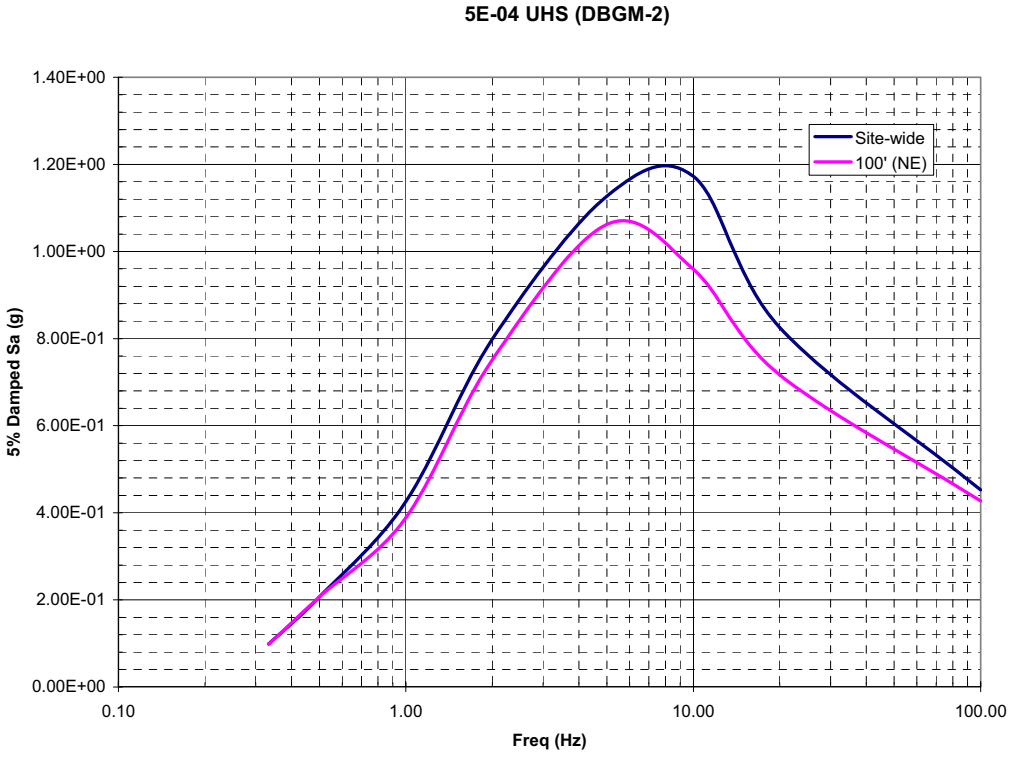

Figure I6.5-1. 5% Damped DBGM-2 (Site-Wide) vs. Surface Spectrum of 100-Ft Alluvium Depth Case (See Section 6.2.2.1 for source information)

I6.5.4.2 Damping Factor

This factor is to account for conservatism in the hysteresis damping of the building structure used in the seismic response analysis. Due to the high radiation damping of the foundation media, the effect of structure damping is insignificant. Thus,

$$F_{\delta} := 1.0$$

$$\beta_{U\_\delta} := 0$$

$$\beta_{R\_\delta} := 0$$

Since a conservative median factor of safety is used for structure damping, no value is assigned to the uncertainty logarithmic standard deviation.

$$\beta_{c\_\delta} := \sqrt{\beta_{U\_\delta}^{2} + \beta_{R\_\delta}^{2}} \qquad \beta_{c\_\delta} = 0$$

I6.5.4.3 Modeling Factor

The Tier 1 lumped mass multiple stick model of the WHF models the stiffness of various reinforced concrete walls and distribution of mass at each floor. The floors are assumed to be rigid diaphragms tying the different sticks together. Torsional response of the structure is captured through modeling eccentricity between the center of mass and center of rigidity of each floor. The foundation media underneath the buildings are modeled with soil springs and dashpots based on elastic half space theory with adjustment to account for the layering effect of alluvium overlying tuff. The model is judged to adequately represent the WHF structure dynamic characteristics, thus

$F_M := 1.0$

$\beta_{R\_M} := 0$

Uncertainty of structure frequencies predicted from mathematical modeling varies from 0.15 to 0.35 depending on the sophistication of the model (Reference I2.2.1). The value of 0.35 is for fairly approximate model and the value 0.15 is appropriate for detailed models. Based on the complexity of the WHF structure and the mathematical model used for the Tier 1 ISRS analysis, it is judged that the calculated WHF frequency has a logarithmic standard deviation of 0.25.

$\beta_f := 0.25$ Uncertainty in building frequency.

$f_m := 5 \cdot Hz$ Best-estimate frequency

$f_{upper} := f_m \cdot e^{\beta_f}$ Upper bound frequency

$f_{upper} = 6.42 \cdot Hz$

$SA_{upper} := 1.06g$ 5% damped spectral acceleration at f_{upper} read off from the mean 5E-4 UHS of the 100-foot alluvium depth case (Figure I6.5-1). This value is less than the value at the best-estimate frequency.

$f_{lower} := f_m \cdot e^{-\beta_f}$ Lower bound frequency

$f_{lower} = 3.89 \cdot Hz$

$SA_{lower} := 1.02 \cdot g$ 5% damped spectral acceleration at f_{lower} read off from the mean 5E-4 UHS of the 100-foot alluvium depth case. This value is less than the value at the best-estimate frequency.

$\beta_{U\_f} := 0$ Since the spectral value at the best-estimate frequency is greater than that at either the lower bound or upper bound frequency.

$\beta_{U\_ms} := 0.10$ Uncertainty of mode shape (Reference I2.2.1, page 3-18); a lower value of 0.10 is used here based on the simple configuration of the bridge girders.

$\beta_{U\_M} := \sqrt{\beta_{U\_f}^2 + \beta_{U\_ms}^2}$

$\beta_{U\_M} = 0.1$

$\beta_{c\_M} := \sqrt{\beta_{R\_M}^2 + \beta_{U\_M}^2}$ $\beta_{c\_M} = 0.1$

I6.5.4.4 Modal Combination

Since the direct integration time history method was used in the Tier 1 ISRS analysis (Reference I2.2.2), the modal combination method factor of safety is unity and there is no variability associated with modal combination.

$F_{MC} := 1$

$\beta_{R\_MC} := 0$

$\beta_{U\_MC} := 0$

$\beta_{c\_MC} := \sqrt{\beta_{R\_MC}^2 + \beta_{U\_MC}^2}$ $\beta_{c\_MC} = 0$

I6.5.4.5 Soil-Structure Interaction

Two factors are considered, the first one is on the method of treating the SSI effects and the second one is on the effect of soil softening at ground acceleration higher than DBGM-2. The Tier 1 seismic response analyses of the WHF use the site-wide $5*10^{-4}$ mean uniform hazard spectra as the DBGM-2 input motion. Spectrum compatible time histories are used as the input motion for the time history analyses. The conservatism in the site-wide spectra was accounted for in the spectral shape factor above. Strain compatible soil properties of 30-foot and 100-foot deep alluvium are used to calculate frequency-independent soil springs and soil damping coefficients. Soil radiation damping is introduced into the model by using dashpots. Damping coefficients equal to 75% of the computed values for translational degrees of freedom and to the full computed rotational damping values are used in the response analyses (Reference I2.2.2). Conservatism or unconservatism in SSI will be minimized for final SSI analyses used to develop equipment design seismic input. Before the final SSI analyses are completed, the Tier 1 SSI analysis is taken to represent the best-estimate responses per BSC recommendations in Reference I2.2.13.

$F_{SSI\_1} := 1$

$\beta_{R\_SSI\_1} := 0$

$\beta_{U\_SSI\_1} := 0.25$ Uncertainty of the median-centered state-of-the-art SSI method based on past probabilistic seismic response analyses using the same method.

It is judged that the median seismic capacity of the structural failure mode of the SFTM, expressed in terms of peak ground acceleration, is close to the BDBGM. Due to soil nonlinearity, amplification of the input motion of the BDBGM will be different from that of the DBGM-2. The second factor of safety is to account for this difference and is estimated using the DBGM-2 raw spectra and the BDBGM raw spectra at the vertical frequency of the SFTM which is 2.57 Hz.

$S_{v\_DBGM\_7\%} := SA_{raw\_7\%}$ 7% damped vertical spectral accelerations and the floor zero period accelerations of DBGM-2 (Figure I-B-1 of Appendix I-B)

$S_{v\_DBGM\_7\%} = 0.474 \cdot g$

$ZPA_{DBGM} := 0.282 \cdot g$

$S_{v\_BDBGM\_10\%} := 0.928 \cdot g$ 10% damped BDBGM (Figure I-B-5 of Appendix I-B) raw spectra. Based on that 7% of critical damping will be used for the design of the SFTM, the best-estimate damping value at BDBGM is estimated at 10% of critical damping.

$ZPA_{BDBGM} := 0.692 \cdot g$

$$F_{SSI\_2} := \frac{\frac{S_{v\_DBGM\_7\%}}{ZPA_{DBGM}}}{\frac{S_{v\_BDBGM\_10\%}}{ZPA_{BDBGM}}} = 1.25$$

$F_{SSI\_2} = 1.25$

$$\beta_{U\_SSI\_2} := \frac{1}{1.65} \ln\left(F_{SSI\_2}\right) = 0.14$$

$F_{SSI} := F_{SSI\_1} \cdot F_{SSI\_2}$

$F_{SSI} = 1.25$

$$\beta_{U\_SSI} := \sqrt{\beta_{U\_SSI\_1}^{2} + \beta_{U\_SSI\_2}^{2}} = 0.29$$

$$\beta_{c\_SSI} := \sqrt{\beta_{R\_SSI\_1}^{2} + \beta_{U\_SSI}^{2}}$$

$\beta_{c\_SSI} = 0.29$

I6.5.4.6 Ground Motion Incoherence

$L1 := 266 \cdot ft$ East-west dimension of the WHF excluding the 50'-6" and 33' extensions at the west and east ends, respectively (Reference I2.2.3).

$L2 := 210 \cdot ft$ North-south dimension of the WHF excluding the extensions at the north and south ends.

$L_{eq} := \sqrt{L1 \cdot L2}$ Equivalent foundation dimension of the WHF

$L_{eq} = 236.35\,ft$

The ground motion incoherence reduction factor is a function of foundation size and frequency of response. For a 150 foot plan dimension foundation, the following reduction factors are presented in Reference I2.2.1 in page 3-22. Interpolation or extrapolation may be used to calculate the reduction factor for different dimensions and/or frequencies.

$L_{std} := 150 \cdot ft$ Foundation dimension of which the reduction factors in Reference I2.2.1 are calculated.

$f_5 := 5$ Frequency in cycle/sec (Hz)

$RF_5 := 1$ Reduction factor for response frequency at 5 Hz

$f_{10} := 10$ Frequency in Hz

$RF_{10} := 0.9$ Reduction factor for response frequency at 10 Hz

$RF_{5\_eq} := RF_5$ Reduction factor at 5 Hz, given the WHF equivalent foundation dimension

$RF_{10\_eq} := 1 - \left[\left(1 - RF_{10}\right) \cdot \frac{L_{eq}}{L_{std}} \right]$ Linear extrapolation

$RF_{10\_eq} = 0.84$ Reduction factor at L_{eq} dimension and 10 Hz frequency of response.

The vertical frequency of the WHF with 100-ft of median soil with soil properties compatible with DBGM-2 level, is 6.8 Hz. However, the seismic acceleration level at which crane failure is expected is significantly higher than DBGM-2. Thus, the vertical frequency of the WHF with 100-ft of median soil with properties compatible with the BDBGM level is considered. This frequency is 6 Hz (page B5 of Reference I2.2.2).

$f_6 := 6$ Frequency in Hz

Calculate the reduction factor at 6 Hz by interpolation

$RF_{6\_eq} := 0.4$ A trial value to initiate the equation solver below.

Given

$$\frac{\log\left(RF_{10\_eq}\right) - \log\left(RF_{5\_eq}\right)}{\log\left(RF_{6\_eq}\right) - \log\left(RF_{5\_eq}\right)} = \frac{\log\left(f_{10}\right) - \log\left(f_5\right)}{\log\left(f_6\right) - \log\left(f_5\right)}$$

$a := \text{Find}\left(RF_{6\_eq}\right)$

$a = 0.96$

Thus, the ground motion incoherence factor of safety is

$F_{GMI} := \frac{1}{a}$

$F_{GMI} = 1.05$

$\beta_{U\_GMI} := \frac{1}{2} \cdot \ln\left(\frac{1}{a}\right)$ A reduction factor of 1.0 (i.e., no reduction) is estimated to be two standard deviation from the calculated median factor of 0.91 (Reference I2.2.1, Page 3-23).

$\beta_{U\_GMI} = 0.02$

$\beta_{R\_GMI} := 0$

$$\beta_{c\_GMI} := \sqrt{\beta_{R\_GMI}^2 + \beta_{U\_GMI}^2}$$

$$\beta_{c\_GMI} = 0.02$$

Structural Response Factors

$$F_{RS} := F_{SA} \cdot F_{\delta} \cdot F_M \cdot F_{MC} \cdot F_{SSI} \cdot F_{GMI}$$

$$F_{RS} = 1.4$$

$$\beta_{c\_RS} := \sqrt{\beta_{c\_SA}^2 + \beta_{c\_\delta}^2 + \beta_{c\_M}^2 + \beta_{c\_MC}^2 + \beta_{c\_SSI}^2 + \beta_{c\_GMI}^2}$$

$$\beta_{c\_RS} = 0.36$$

I6.5.5 Overall Factor of Safety

$$F_{total} := F_S \cdot F_{\mu} \cdot F_{RS} \cdot F_{RE}$$

$$F_{total} = 4.84$$

$PGA := 0.453g$ Peak ground acceleration of the DBGM-2 design spectrum (Reference I2.2.7; also Section 6.2.2.1 for source information).

$$A_m := F_{total} \cdot PGA$$

$A_m = 2.19 \cdot g$ Median seismic capacity in terms of PGA

$$\beta_c := \sqrt{\beta_{c\_S}^2 + \beta_{c\_\mu}^2 + \beta_{c\_RS}^2 + \beta_{c\_RE}^2}$$

$$\beta_c = 0.47$$

$$HCLPF := A_m \cdot e^{-2.33 \cdot \beta_c}$$

$$HCLPF = 0.72 \cdot g$$

The above seismic fragility is calculated for structural failure of the bridge girders of the SFTM. Seismic fragility of the trolley is similar since both will be designed to the NOG-1 criteria.

I6.6 SEISMIC FRAGILITY OF SEISMIC RESTRAINTS

Due to high seismicity at the YMP site, the SFTM bridge and the trolley will be provided with devices so that they will remain on their respective runways during and after a design seismic event. These seismic restraints can be in the form of rail clamps to resist seismic uplift force and seismic bumpers to transfer horizontal seismic inertia load. Both the seismic bumpers and the rail clamps can be constructed from structural steel shapes and bolted or welded to the chassis of the bridge end trucks and the trolley as schematically depicted in Figure I6.6-1 below.

At this time, detailed designs of the bridge and the trolley and their seismic restraints have not been performed. Thus, a representative seismic fragility is calculated below for the trolley seismic restraints. Furthermore, because bolted connections in general have lower median capacity than welded connections, when both are designed to the same demand, hence seismic fragility of the bolted connection is calculated here for the seismic restraints.

Conservatively assume that A307 bolts will be used for attaching the seismic restraints to the trolley chassis. A307 bolts have the lowest strength among the acceptable fastener materials in NOG-1, Tables 4221-1 and 4221-2.

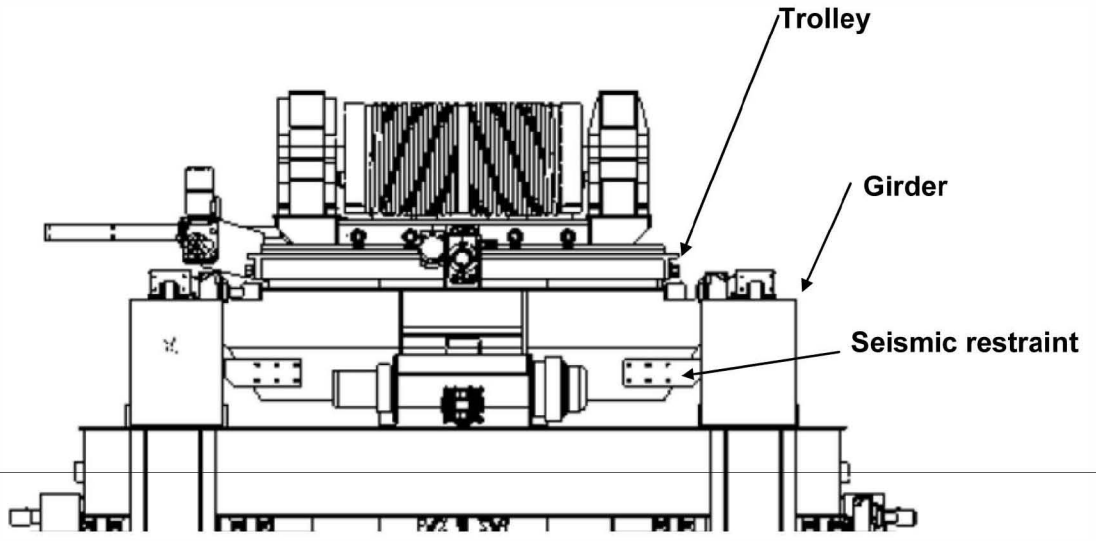

Figure I6.6-1. SFTM Trolley Seismic Restraints (Schematic)

I6.6.1 Strength Factor

The bolts attaching the seismic restraints to the trolley chassis are subjected to shear.

$f_{u\_min} := 58\text{ksi}$ Minimum ultimate tensile strength of A307 (Table 3-9 of Reference I2.2.1)

$\tau_{design} := 1.4 \cdot (10 \cdot \text{ksi})$ where 10 ksi is the allowable shear stress for bolt steel per AISC and 1.4 is the bump-up factor for DBGM-2 load combination (References I2.2.10 and I2.2.11)

$\tau_{design} = 14 \cdot \text{ksi}$

$f_{u\_m} := 64 \cdot ksi$ Median ultimate tensile strength of A307 bolt steel (Table 3-9 of Reference I2.2.1)

$\tau_{u\_m} := 0.62 \cdot f_{u\_m}$ Table 3-10 of Reference I2.2.1

$$F_{S\_shear} := \frac{\tau_{u\_m}}{\tau_{design}}$$

$F_{S\_shear} = 2.83$

$\beta_{R\_S} := 0$

$\beta_{U\_S} := 0.10$ Table 3-10 of Reference I2.2.1

$$\beta_{c\_S} := \sqrt{\beta_{R\_S}^2 + \beta_{U\_S}^2}$$

$\beta_{c\_S} = 0.1$

I6.6.2 Inelastic Energy Absorption Factor

The bolt failure mode is localized and the failure of the bolts is based on the ultimate strength , thus there is no inelastic energy absorption factor.

$F_{\mu} := 1.0$

$\beta_{R\_\mu} := 0$

$\beta_{U\_\mu} := 0$

$$\beta_{c\_\mu} := \sqrt{\beta_{R\_\mu}^2 + \beta_{U\_\mu}^2}$$

$\beta_{c\_\mu} = 0$

I6.6.3 Equipment Response Factors

I6.6.3.1 Qualification Method

This factor accounts for conservatism in the Tier 1 design ISRS (Reference I2.2.2) relative to the median ISRS. The median ISRS are the Tier 1 unbroadened and unsmoothed floor response spectra from the 100-ft alluvium median soil case. The fundamental frequency of the bridge crane in the east-west direction (perpendicular to the bridge girder), when the trolley with the lifted load is at the mid-span of the bridge, is estimated to be in the range of 2 to 3 Hz.

At 2 Hz

$SA_{design\_2} := 1.12 \cdot g$ 1.1g is the 7% damped design spectral acceleration of the east-west ISRS of the 100-foot alluvium case at the ground floor (Figures I-B-4 of Appendix I-B).

$SA_{raw\_2} := 0.854g$ 0.854g is the 7% damped spectral acceleration of the east-west direction raw spectra of the 100-foot alluvium case at the ground floor (Figures I-B-4 and 8 of Appendix I-B).

$$F_{QM\_2} := \frac{SA_{design\_2}}{SA_{raw\_2}}$$

$F_{QM\_2} = 1.31$

At 3 Hz

$SA_{design\_3} := 1.51 \cdot g$ 1.5g is the 7% damped design spectral acceleration of the east-west ISRS of the 100-foot alluvium case at the ground floor (Figures I-B-4 of Appendix I-B).

$SA_{raw\_3} := 1.2 \cdot g$ 1.2g is the 7% damped spectral acceleration of the east-west direction raw spectrum of the 100-foot alluvium case (Figure I-B-4 of Appendix I-B).

$$F_{QM\_3} := \frac{SA_{design\_3}}{SA_{raw\_3}}$$

$F_{QM\_3} = 1.26$

$$F_{QM} := \frac{1}{2} \cdot \left(F_{QM\_2} + F_{QM\_3}\right)$$

$F_{QM} = 1.28$

Since the raw ISRS is used and uncertainties in response due to uncertainty in equipment frequency (i.e., modeling), modal combination, and earthquake component combination are separately calculated below,

$\beta_{c\_QM} := 0$

I6.6.3.2 Equipment Damping

The median and lower bound damping values at the failure of the bridge crane are 7% and 5%, respectively (Table 3-4 of Reference I2.2.1 for welded steel structures). Since 7% damping is used in the crane design seismic analysis (Section 4153.8 of NOG-1), the factor of safety is unity.

$F_{\delta\_E} := 1$

At 2 Hz

$SA_{raw\_5\%} := 1.0 \cdot g$ 1.0g is the 5% damped raw spectral acceleration of the east-west direction raw spectrum of the 100-foot alluvium case at the ground floor (Figures I-B-3 of Appendix I-B).

$$\beta_{c\_\delta\_E\_2} := \ln\left(\frac{SA_{raw\_5\%}}{SA_{raw\_2}}\right)$$

$\beta_{c\_\delta\_E\_2} = 0.16$

At 3 Hz

$SA_{raw\_5\%} := 1.4 \cdot g$ 1.4g is the 5% damped spectral acceleration of the east-west direction raw spectrum of the 100-foot alluvium case at the ground floor (Figures I-B-3 of Appendix I-B).

$$\beta_{c\_\delta\_E\_3} := \ln\left(\frac{SA_{raw\_5\%}}{SA_{raw\_3}}\right)$$

$\beta_{c\_\delta\_E\_3} = 0.15$

$$\beta_{c\_\delta\_E} := \frac{1}{2}\left(\beta_{c\_\delta\_E\_2} + \beta_{c\_\delta\_E\_3}\right)$$

$\beta_{c\_\delta\_E} = 0.16$

I6.6.3.3 Equipment Modeling Factor

$F_{M\_E} := 1.0$ Since the effect of frequency uncertainty is included in the qualification method factor.

$\beta_{R\_M\_E} := 0$ No randomness associated with modeling

$\beta_{U\_ms} := 0.10$ The uncertainty in response due to uncertainty of mode shape is in the range of 0.05 to 0.15 depending on the complexity of the equipment (Reference I2.2.1). A value of 0.10 is used.

$$\beta_{U\_M\_E} := \sqrt{\beta_{U\_f}^{2} + \beta_{U\_ms}^{2}}$$

$\beta_{U\_M\_E} = 0.1$

$$\beta_{c\_M\_E} := \sqrt{\beta_{R\_M\_E}^{2} + \beta_{U\_M\_E}^{2}}$$

$\beta_{c\_M\_E} = 0.1$

I6.6.3.4 Modal Combination

The dynamic response spectrum method is one of the methods described in Section 4153 of NOG-1 for performing seismic analysis for Type 1 cranes. When the response spectrum method is used, closely spaced modes are to be combined per grouping method, ten-percent method or double-sum method as per Section 4153.10. Thus, the modal combination factor of safety is judged to be unity, no conservative or unconservative bias.

$F_{MC\_E} := 1.0$

$\beta_{R\_MC\_E} := 0.05$ For the failure mode evaluated, the fundamental transverse mode is dominant. Thus use the lower bound value of 0.05 in Reference I2.2.1.

$\beta_{U\_MC\_E} := 0$

$\beta_{c\_MC\_E} := \sqrt{\beta_{R\_MC\_E}^2 + \beta_{U\_MC\_E}^2}$

$\beta_{c\_MC\_E} = 0.05$

I6.6.3.5 Earthquake Component Combination

Section 4153.10(c) of NOG-1 requires using the SRSS (Square Root of Sum of the Squares) to combine contributions for the three components of earthquake motion. This method is considered to be median-centered. Thus,

$F_{ECC\_E} := 1.0$

$\beta_{R\_ECC\_E} := 0.10$ A generic value of 0.18 is suggested in Reference I2.2.1 when responses from each of the three components are not available. A value of 0.10 is used here since the north-south component contributes most significantly to the response of the failure mode evaluated.

$\beta_{U\_ECC\_E} := 0$

$\beta_{c\_ECC\_E} := \sqrt{\beta_{R\_ECC\_E}^2 + \beta_{U\_ECC\_E}^2}$

$\beta_{c\_ECC\_E} = 0.1$

Equipment Response Factors

$F_{RE} := F_{QM} \cdot F_{\delta\_E} \cdot F_{M\_E} \cdot F_{MC\_E} \cdot F_{ECC\_E}$

$F_{RE} = 1.28$

$\beta_{c\_RE} := \sqrt{\beta_{c\_QM}^2 + \beta_{c\_\delta\_E}^2 + \beta_{c\_M\_E}^2 + \beta_{c\_MC\_E}^2 + \beta_{c\_ECC\_E}^2}$

$\beta_{c\_RE} = 0.22$

I6.6.4 Structural Response Factors

I6.6.4.1 Spectral Shape Factor

This factor accounts for conservatism in the site-wide DBGM-2 design spectrum. At the Surface Facilities Area (SFA) the depth of alluvium overlying tuff varies from 30 feet to 200 feet. Uniform hazard

spectra at the surface are calculated from site response analyses for alluvium depths of 30', 70', 100' and 200'. The site-wide design ground response spectrum is the envelope of the surface spectra of these four alluvium depths (Reference I2.2.7; also Section 6.2.2.1 for source information).

The dominant frequency of the WHF soil-structure system in the horizontal direction is about 5 Hz from the Tier 1 ISRS calculation (Reference I2.2.2). At this frequency

$SA_{site} := 1.13g$ 5% damped site-wide spectral acceleration (see Figure I6.5-1).

$SA_{100} := 1.06 \cdot g$ 5% damped spectral acceleration of the 100-foot best-estimate alluvium depth case in the northeast area where the preclosure surface facilities are located.

$$F_{SA} := \frac{SA_{site}}{SA_{100}}$$

$F_{SA} = 1.07$

Since uncertainty in the UHS is derived from uncertainty in the seismic hazard curves which will be included in the final risk quantification, no uncertainty is included under the spectral shape factor to avoid double-counting the hazard uncertainty, hence

$\beta_{U\_SA} := 0$

$\beta_{R\_SA} := 0.2$ This is random variability to account for peak to valley variability of a smooth ground response spectrum (Reference I2.2.1, Table 3-2)

$\beta_{c\_SA} := \sqrt{\beta_{U\_SA}^2 + \beta_{R\_SA}^2}$ $\beta_{c\_SA} = 0.2$

I6.6.4.2 Damping Factor

This factor is to account for conservatism in the hysteresis damping of the building structure used in the seismic response analysis. Due to the high radiation damping of the foundation media, the effect of structure damping is insignificant. Thus,

$F_{\delta} := 1.0$

$\beta_{U\_\delta} := 0$ Since a conservative median factor of safety is used for structure damping, no value is assigned to the uncertainty logarithmic standard deviation.

$\beta_{R\_\delta} := 0$

$\beta_{c\_\delta} := \sqrt{\beta_{U\_\delta}^2 + \beta_{R\_\delta}^2}$ $\beta_{c\_\delta} = 0$

I6.6.4.3 Modeling Factor

The Tier 1 lumped mass multiple stick model of the WHF models the stiffness of various reinforced concrete walls and distribution of mass at each floor. The floors are assumed to be rigid diaphragms tying the different sticks together. Torsional response of the structure is captured through modeling eccentricity between the center of mass and center of rigidity of each floor. The foundation media

underneath the buildings are modeled with soil springs and dashpots based on elastic half space theory with adjustment to account for the layering effect of alluvium overlying tuff. The model is judged to adequately represent the WHF structure dynamic characteristics, thus

$F_M := 1.0$

$\beta_{R\_M} := 0$

Uncertainty of structure frequencies predicted from mathematical modeling varies from 0.15 to 0.35 depending on the sophistication of the model (Reference I2.2.1). The value of 0.35 is for fairly approximate models and the value 0.15 is appropriate for detailed models. Based on the complexity of the WHF structure and the mathematical model used for the Tier 1 ISRS analysis, it is judged that the calculated WHF frequency has a logarithmic standard deviation of 0.25.

$\beta_f := 0.25$ Uncertainty in building frequency.

$f_m := 5.0 \cdot Hz$ Best-estimate frequency

$f_{upper} := f_m \cdot e^{\beta_f}$ Upper bound frequency

$f_{upper} = 6.42 \cdot Hz$

$SA_{upper} := 1.06g$ 5% damped spectral acceleration at f_{upper} read off from the mean 5E-4 UHS of the 100-foot alluvium depth case (Figure I6.5-1). This value is less than the value at the best-estimate frequency.

$f_{lower} := f_m \cdot e^{-\beta_f}$ Lower bound frequency

$f_{lower} = 3.89 \cdot Hz$

$SA_{lower} := 1.02 \cdot g$ 5% damped spectral acceleration at f_{lower} read off from the mean 5E-4 UHS of the 100-foot alluvium depth case. This value is less than the value at the best-estimate frequency.

$\beta_{U\_f} := 0$ Since the spectral value at the best-estimate frequency is greater than that at either the lower bound or upper bound frequency.

$\beta_{U\_ms} := 0.10$ Uncertainty of mode shape (Reference I2.2.1, page 3-18); a lower value of 0.10 is used due to simple geometry of the structure.

$\beta_{U\_M} := \sqrt{\beta_{U\_f}^2 + \beta_{U\_ms}^2}$

$\beta_{U\_M} = 0.1$

$\beta_{c\_M} := \sqrt{\beta_{R\_M}^2 + \beta_{U\_M}^2}$ $\beta_{c\_M} = 0.1$

I6.6.4.4 Modal Combination

Since the direct integration time history method is used in the Tier 1 ISRS analysis (Reference I2.2.2), the modal combination method factor of safety is unity and there is no variability associated with modal combination.

$F_{MC} := 1$

$\beta_{R\_MC} := 0$

$\beta_{U\_MC} := 0$

$\beta_{c\_MC} := \sqrt{\beta_{R\_MC}^{2} + \beta_{U\_MC}^{2}}$ $\beta_{c\_MC} = 0$

I6.6.4.5 Soil-Structure Interaction

Two factors are considered, the first one is on the method of treating the SSI effects and the second one is on the effect of soil softening at ground acceleration higher than DBGM-2. See discussions in Section I6.5.4.5 for details.

$F_{SSI\_1} := 1$

$\beta_{R\_SSI\_1} := 0$

$\beta_{U\_SSI\_1} := 0.25$

At 2 Hz

$SA_{raw\_2} = 0.854 \cdot g$ See Section I6.6.3.1

$ZPA_{DBGM} := 0.545 \cdot g$ where 0.545g is the ZPA of the raw DBGM-2 E-W ISRS at the ground floor

$S_{v\_BDBGM\_10\%} := 1.36 \cdot g$ where 1.36g is the 10% damped spectral acceleration from the E-W direction raw ISRS at the ground floor (Figure I-B-6 and of Appendix I-B).

$ZPA_{BDBGM} := 1.09 \cdot g$ where 1.09g is ZPA of the E-W direction raw ISRS at the ground floor (Figure I-B-6 of Appendix I-B).

$$F_2 := \frac{\frac{SA_{raw\_2}}{ZPA_{DBGM}}}{\frac{S_{v\_BDBGM\_10\%}}{ZPA_{BDBGM}}}$$

$F_2 = 1.26$

At 3 Hz

$SA_{raw\_3} = 1.2 \cdot g$ See Section I6.6.3.1

$ZPA_{DBGM} = 0.545 \cdot g$

$S_{v\_BDBGM\_10\%} := 1.98 \cdot g$ where 1.98g is the 10% damped spectral acceleration from the E-W direction raw ISRS at the ground floor (Figure I-B-6 of Appendix I-B).

$ZPA_{BDBGM} = 1.09 \cdot g$

$$F_3 := \frac{\frac{SA_{raw\_3}}{ZPA_{DBGM}}}{\frac{S_{v\_BDBGM\_10\%}}{ZPA_{BDBGM}}}$$

$F_3 = 1.21$

$$F_{SSI\_2} := \frac{1}{2} \cdot \left(F_2 + F_3\right)$$

$F_{SSI\_2} = 1.23$

$F_{SSI} := F_{SSI\_1} \cdot F_{SSI\_2}$

$F_{SSI} = 1.23$

$$\beta_{U\_SSI\_2} := \frac{\ln\left(F_{SSI\_2}\right)}{1.65}$$

$\beta_{U\_SSI\_2} = 0.13$

$\beta_{R\_SSI} := 0$

$\beta_{U\_SSI} := \sqrt{\beta_{U\_SSI\_1}^2 + \beta_{U\_SSI\_2}^2}$ $\beta_{U\_SSI} = 0.28$

$\beta_{c\_SSI} := \sqrt{\beta_{R\_SSI}^2 + \beta_{U\_SSI}^2}$

$\beta_{c\_SSI} = 0.28$

I6.6.4.6 Ground Motion Incoherence

The ground motion incoherence reduction factor is a function of foundation size and frequency of response. For a 150 foot plan dimension foundation, the reduction factor is 1.0 (i.e., no reduction) at 5 Hz or less (Reference I2.2.1 in page 3-22). The horizontal fundamental frequencies of the WHF are calculated to be 5 Hz and 4.4 Hz, respectively for DBGM-2 and BDBGM with 100-ft of median soil overlying tuff (Pages B3 and B5 of Reference I2.2.2). Since the seismic acceleration level at which trolley failure is expected is significantly higher than DBGM-2, the 4.4 Hz horizontal frequency is considered. Furthermore, because this frequency is lower than 5 Hz, the ground motion incoherence reduction factor is 1.0.

$F_{GMI} := 1$

$\beta_{U\_GMI} := 0$

$\beta_{R\_GMI} := 0$

$\beta_{c\_GMI} := \sqrt{\beta_{R\_GMI}^2 + \beta_{U\_GMI}^2}$

$\beta_{c\_GMI} = 0$

Structural Response Factors

$F_{RS} := F_{SA} \cdot F_{\delta} \cdot F_M \cdot F_{MC} \cdot F_{SSI} \cdot F_{GMI}$

$F_{RS} = 1.32$

$\beta_{c\_RS} := \sqrt{\beta_{c\_SA}^2 + \beta_{c\_\delta}^2 + \beta_{c\_M}^2 + \beta_{c\_MC}^2 + \beta_{c\_SSI}^2 + \beta_{c\_GMI}^2}$

$\beta_{c\_RS} = 0.36$

I6.6.5 Overall Factor of Safety

$F_{total} := F_{S\_shear} \cdot F_{\mu} \cdot F_{RS} \cdot F_{RE}$

$F_{total} = 4.79$

$PGA := 0.453g$ Peak ground acceleration of the DBGM-2 design spectrum (Reference I2.2.7; also Section 6.2.2.1 for source information).

$A_m := F_{total} \cdot PGA$

$A_m = 2.17 \cdot g$ Median seismic capacity in terms of PGA

$\beta_c := \sqrt{\beta_{c\_S}^2 + \beta_{c\_\mu}^2 + \beta_{c\_RS}^2 + \beta_{c\_RE}^2}$

$\beta_c = 0.43$

$HCLPF := A_m \cdot e^{-2.33 \cdot \beta_c}$

$HCLPF = 0.8 \cdot g$

I7.0 SUMMARY

Four failure modes of the Spent Fuel Transfer Machine (SFTM) are evaluated above: (1) structural failure of the bridge girders, (2) failure of seismic restraints of the bridge, (3) structural failure of the frame of the trolley, and (4) failure of seismic restraints of the trolley. Since the trolley's frame will also be designed to the NOG-1 criteria for Type 1 cranes, seismic fragility of the bridge girder is reported for the trolley. Similarly, seismic fragility of the trolley seismic restraint is reported for the bridge girder seismic restraint. The seismic fragilities of these failure modes are:

- Failure of bridge girders -

  A_m = 2.19g β_c = 0.47 HCLPF = 0.72g

- Failure of bridge seismic restraint

  A_m = 2.17g β_c = 0.43 HCLPF = 0.8g

- Failure of trolley frame

  A_m = 2.19g β_c = 0.47 HCLPF = 0.72g

- Failure of trolley seismic restraints

  A_m = 2.17g β_c = 0.43 HCLPF = 0.8g

APPENDIX I-A

ESTIMATE OF VERTICAL FREQUENCY OF SFTM

I-A.1 DATA OF SFTM

$E_s := 30 \cdot 10^6 \cdot psi$ Young's modulus of steel

$L_s := 65 \cdot ft$ Rail to rail distance of the SFTM (Reference I2.2.8)

$M_{SFTM} := 15 \cdot ton$ Mass of the fully loaded SFTM (Reference I2.2.8)

$W_{SFTM} := M_{SFTM} \cdot g$

$W_{SFTM} = 30 \cdot kip$

At the time this calculation was performed, detailed design of the SFTM were not available. Thus, vertical frequency of the SFTM may be estimated based on the NOG-1 allowable deflections.

$\Delta_{all} := \frac{L_s}{1000}$ Total vertical deflection of the girder under the trolley dead weight and the rated live load is limited to 1/1000 of the span (Section 4341 of NOG-1).

$\Delta_{all} = 0.78 \cdot in$

Since there is no detailed design of the SFTM, it is necessary to assume the weight of the trolley and its rated load relative to the total weight of the SFTM. This relative weight will affect the frequency estimates. Based on evaluations of other Type 1 cranes in YMSF (e.g., the Cask Transfer Trolley - Attachment D and the Cask Handling Crane - Attachment A), the combined weight of the trolley, the mast, and the lifted load is estimated to be 70% of the total SFTM weight. Thus,

$W_{trolley\_load} := 0.7 \cdot W_{SFTM}$

$W_{trolley\_load} = 21 \cdot kip$

I-A.2 Vertical Frequencies of SFTM

$I := 1 \cdot in^4$ An initial trial value of the bridge girders moment of inertia to initiate the equation solver.

Given

$\Delta_{all} = \frac{\left(W_{trolley\_load}\right) \cdot L_s^3}{48 \cdot E_s \cdot I}$ With the load at the mid-span (Page 2-298 of Reference I2.2.10).

$a := Find(I)$

$a = 8872.5 \cdot in^4$

$I := a$ Moment of inertia of the bridge girders

Deflection at midspan due to uniform weight of the girders

$w := \frac{W_{SFTM}}{L_s}$ $w = 0.46 \cdot \frac{kip}{ft}$ Uniform weight

$\Delta_1 := \frac{5 \cdot w \cdot L_s^4}{384 E_s \cdot I}$ Maximum deflection at mid-span due to uniform weight of the girders (Page 2-296 of Reference I2.2.10).

$\Delta_1 = 0.7 \cdot in$

Deflection due to concentrated weight at the mid-span of the bridge

$\Delta_2 := \frac{W_{trolley\_load} \cdot L_s^3}{48 \cdot E_s \cdot I}$ $\Delta_2 = 0.78 \cdot in$

$\Delta_{midspan} := \Delta_1 + \Delta_2$

$\Delta_{midspan} = 1.48 \cdot in$

$f_{SFTM\_midspan} := \frac{1}{2 \cdot \pi} \cdot \sqrt{\frac{g}{\Delta_{midspan}}}$ where g is the gravitational acceleration (Section 1.1 of Reference I2.2.12)

$f_{SFTM\_midspan} = 2.57 \cdot Hz$

APPENDIX I-B

DBGM-2 and BDBGM ISRS AT WHF Ground Floor (Reference I2.2.2)

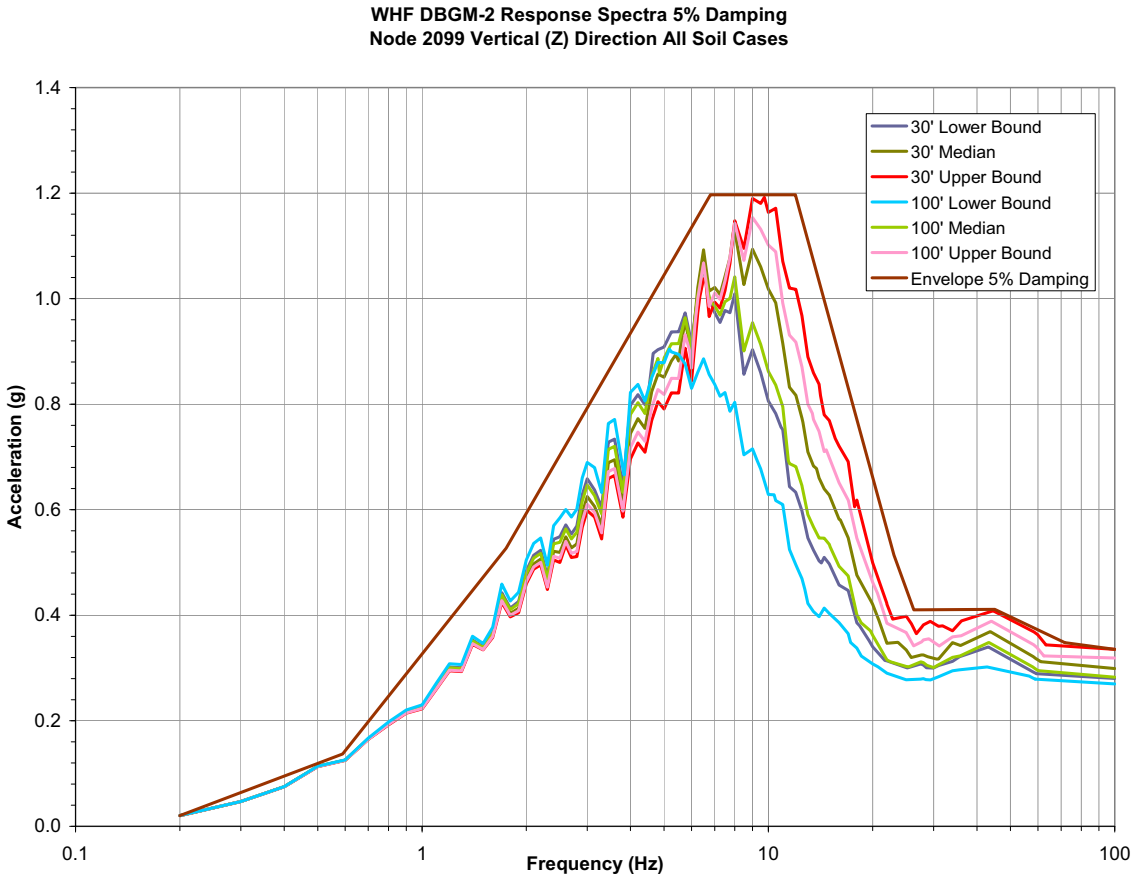

Figure I-B-1. WHF Vertical DBGM-2 5% Damped ISRS at Ground Floor (Both Design and Raw)

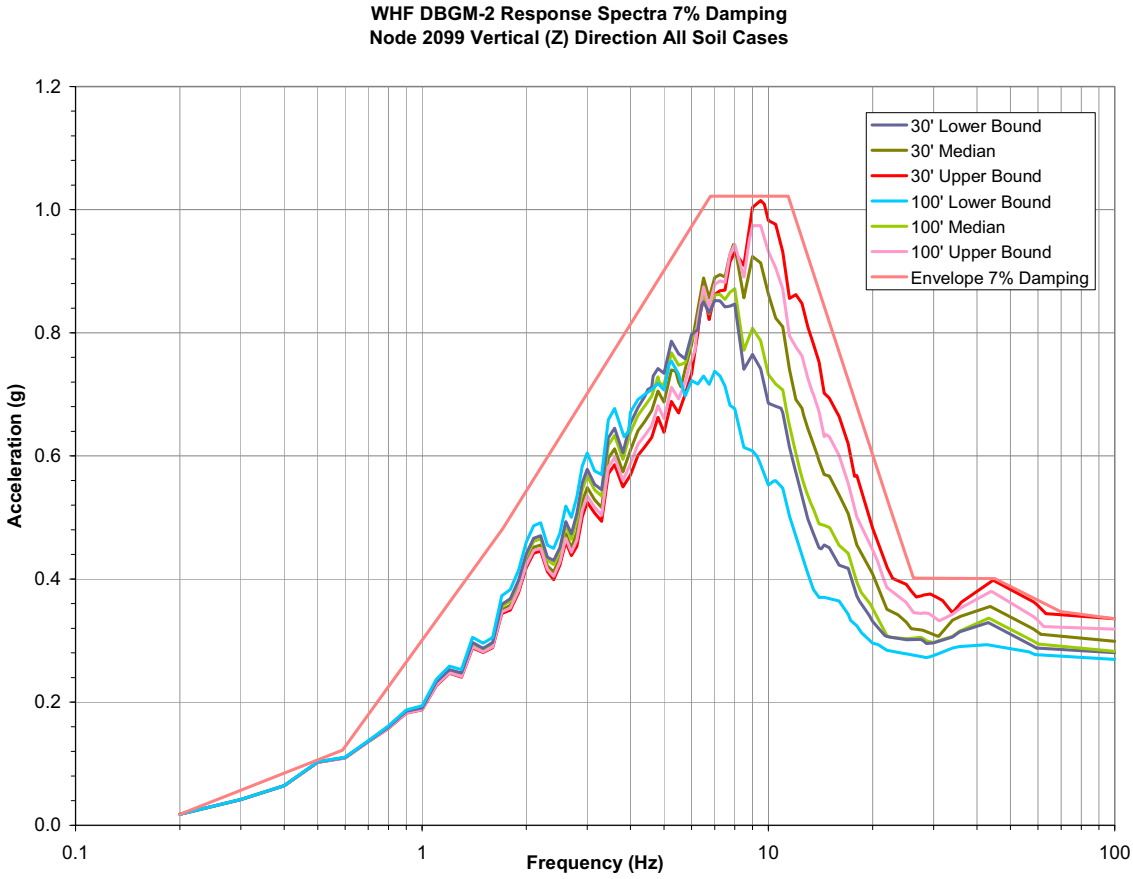

Figure I-B-2. WHF Vertical DBGM-2 7% Damped ISRS At Ground Floor

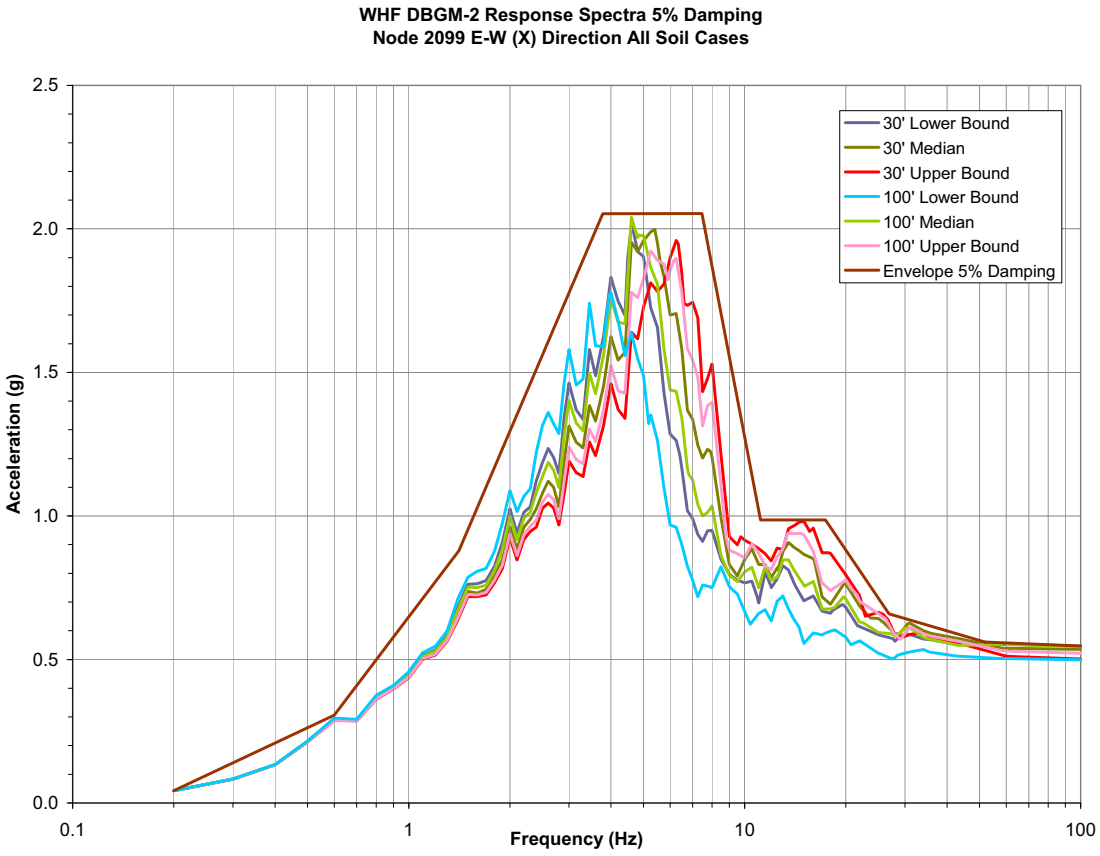

Figure I-B-3. WHF East-West DBGM-2 5% Damped ISRS (Both Design and Raw) at Ground Floor

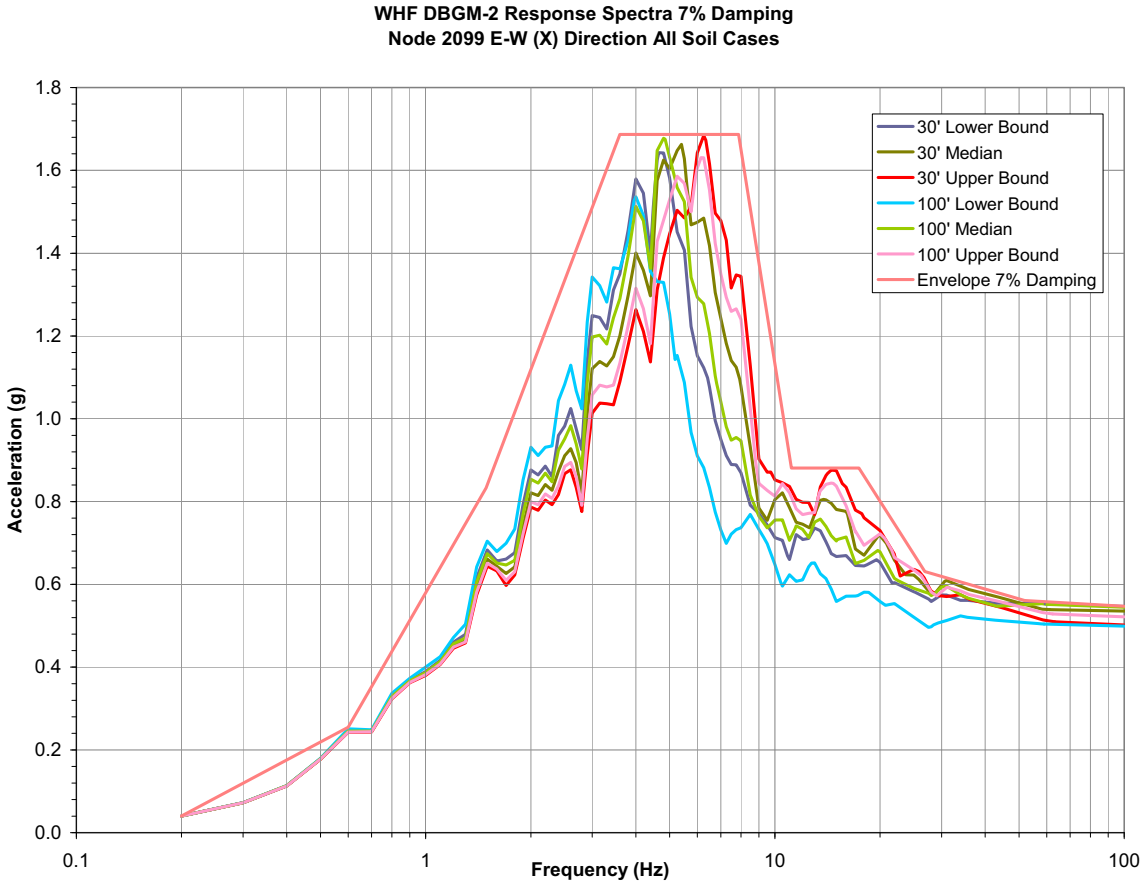

Figure I-B-4. WHF East-West DBGM-2 7% Damped ISRS (Both Design and Raw) at Ground Floor

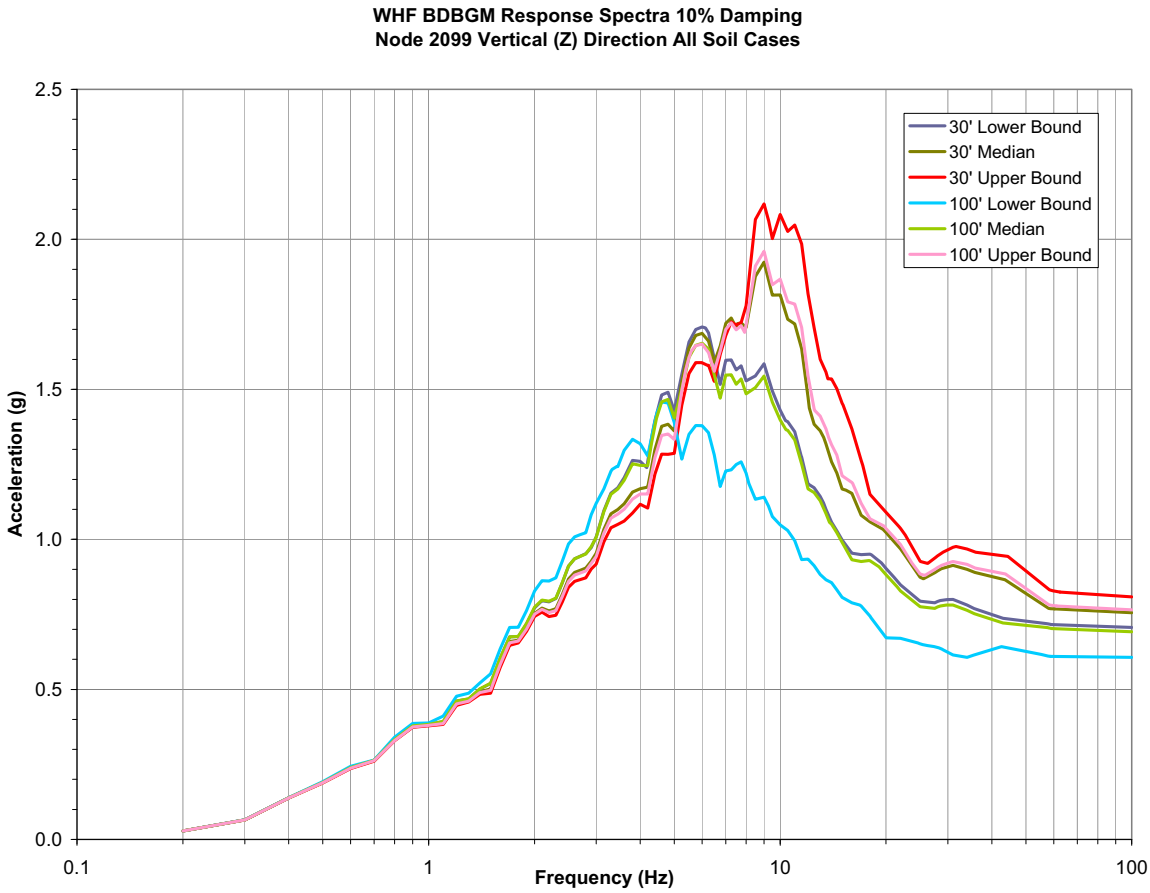

Figure I-B-5. WHF Vertical BDBGM 10% Damped ISRS at Ground Floor

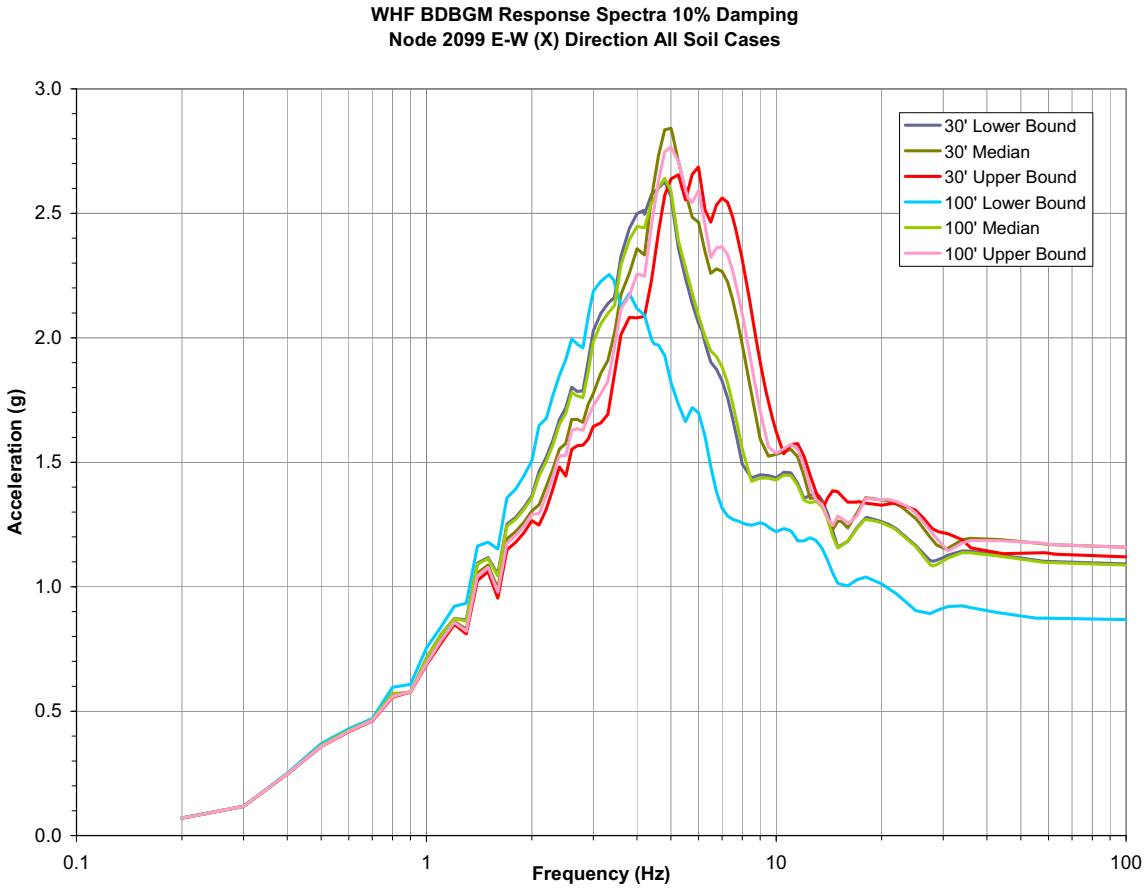

Figure I-B-6. WHF East-West BDBGM 10% Damped ISRS at Ground Floor

ATTACHMENT J
FRAGILITY FOR EQUIPMENT QUALIFIED BY TEST

Prepared By: Robert D. Campbell

ARES Check By: Gregory S. Hardy

LLNL Check By: Robert C. Murray

TABLE OF CONTENTS

ACRONYMS AND ABBREVIATIONS

ACI	American Concrete Institute
AISC	American Institute of Steel Construction
ANSI	American National Standards Insitute
AO	Aging Overpack
APE	Annual Probability of Exceedance
ASCE	American Society of Civil Engineers
ASME	American Society of Mechanical Engineers
BSC	Bechtel SAIC, LLC
BDBGM	Beyond Design Basis Ground Motion at $1x10^{-4}$ APE
CDFM	Conservative Deterministic Failure Margin
CHC	Cask Handling Crane
CIP	Cast-in-Place
CRCF	Canister Receipt and Closure Facility
CTM	Canister Transfer Machine
CTT	Cask Transfer Trolley
DBGM-2	Design Basis Ground Motion at $5x10^{-4}$ APE
DL	Dead Load
DOF	Degree of Freedom
DPC	Dual Purpose Canister
EPRI	Electric Power Research Institute
HCLPF	High Confidence of Low Probability of Failure
HVAC	Heating, Ventilation, & Air Conditioning
IEEE	Institute of Electrical and Electronics Engineers
IHF	Initial Handling Facility
ISRS	In-Structure Response Spectra

ACRONYMS AND ABBREVIATIONS (cont.)

ITS	Important to Safety
LA	License Application
LLNL	Lawrence Livermore National Laboratory
NPP	Nuclear Power Plant
PGA	Peak Ground Acceleration
RF	Receipt Facility
RRS	Required Response Spectrum
Sa	Spectral Acceleration
SFA	Surface Facilities Area
SFTM	Spent Fuel Transfer Machine
SPRA	Seismic Probabilistic Risk Assessment
SRSS	Square Root of the Sum of Squares
SSE	Safe Shutdown Earthquake (used with NPPs)
SSI	Soil Structure Interaction
SSC	Structure, System, and Component
TAD	Transportation, Aging, and Disposal canister
TEV	Transport and Emplacement Vehicle
TRS	Test Response Spectrum
UHS	Uniform Hazard Spectra
USDOE	United States Department of Energy
USNRC	United States Nuclear Regulatory Commission
WHF	Wet Handling Facility
WP	Waste Package
WPTT	Waste Package Transfer Trolley
YMSF	Yucca Mountain Surface Facilities
ZPA	Zero Period Acceleration

FRAGILITY TERMINOLOGY

Am	Median Peak Ground Motion Capacity
β_R	Log Standard Deviation of Randomness
β_U	Log Standard Deviation of Uncertainty (Lack of Knowledge)
β_C	Composite Variability = $(\beta_R^2 + \beta_U^2)^{0.5}$
F_S	Strength Factor of Safety
β_{R_S}	Strength Randomness (typical)
β_{U_S}	Strength Uncertainty (typical)
β_{C_S}	Strength Composite Variability (typical)
F_μ	Inelastic Energy Absorption Factor of Safety
F_{QM}	Qualification Factor of Safety
F_δ	Damping Factor of Safety
F_M	Modeling Factor of Safety
F_{MC}	Modal Combination Factor of Safety
F_{ECC}	Earthquake Component Combination Factor of Safety
F_{SA}	Spectral Shape Factor of Safety
F_{SSI}	Soil-Structure Interaction Factor of Safety
F_{GMI}	Ground Motion Incoherence Factor of Safety
F_{TOTAL}	Total Factor of Safety
F_{RS}	Structural Response Factor of Safety
F_{RE}	Equipment Response Factor of Safety

J1. PURPOSE

The purpose of this calculation is to develop fragilities for equipment in Yucca Mountain surface facilities that are qualified by test. Design specifications and qualification analyses are not yet available so the derivations are representaive based on the applicable BSC specifications for seismic design and applicable codes and standards.

J2.0 REFERENCES

J2.1 PROCEDURES AND DIRECTIVES

J2.1.1 EG-PRO-3DP-G04B-00037, Rev. 10. *Calculations and Analyses*. Las Vegas, Nevada: Bechtel SAIC Company. ACC: ENG.20071018.0001.

J2.1.2 IT-PRO-0011, Revision 7, ICN 0. *Software Management*. Las Vegas, Nevada: Bechtel SAIC Company. ACC: DOC.20070905.0007.

J2.2 DESIGN INPUTS

J2.2.1 EPRI (Electric Power Research Institute) 1994. *Methodology for Developing Seismic Fragilities*. EPRI TR-103959. Palo Alto, California: Electric Power Research Institute. TIC:253770. [DIRS 161329]

J2.2.2 ASCE/SEI 43-05. 2005. *Seismic Design Criteria for Structures, Systems, and Components in Nuclear Facilities*. Reston, Virginia: American Society of Civil Engineers. TIC: 257275. [DIRS 173805]

J2.2.3 IEEE Std 344-2004. 2005. *IEEE Recommended Practice for Seismic Qualification of Class 1E Equipment for Nuclear Power Generating Stations*. New York, New York: Institute of Electrical and Electronics Engineers. TIC: 258050. [DIRS 176259]

J2.2.4 BSC (Bechtel SAIC Company) 2007. *CRCF Tier-1 In-Structure Response Spectra*. 060-SYC-CR00-00900-000-00B. Las Vegas, Nevada: Bechtel SAIC Company. ACC: ENG.20071210.0008. [DIRS 184330]

J2.2.5 MO0801HCUHSSFA.001. *Mean Hazard Curves and Mean Uniform Hazard Spectra for the Surface Facilities Area*. Submittal date: 01/11/2008. [DIRS 184802]

J2.2.6 BSC (Bechtel SAIC Company) 2008. *Canister Receipt and Closure Facility 1 General Arrangement Ground Floor Plan*. 060-P10-CR00-00102-000 REV 00C. Las Vegas, Nevada: Bechtel SAIC Company. ACC: ENG.20080122.0013. [DIRS 184853]

J2.2.7 Moore, D. 2007. "*SSI Factor of Safety.*" E-mail from D. Moore to B. Murray, October 25, 2007. ACC: LLR.20080110.0145. [DIRS 184842]

J2.2.8 BSC (Bechtel SAIC Company) 2006. *Seismic Analysis and Design Approach Document.* 000-30R-MGR0-02000-000 Rev. 001. Las Vegas, Nevada: Bechtel SAIC Company. ACC: ENG.20071220.0029. [DIRS 184494]

J2.3 DESIGN CONSTRAINTS

There are no design constraints in the performance of this calculation.

J2.4 DESIGN OUTPUTS

The design outputs are representative fragilities for Yucca Mountain surface facilities ITS equipment qualified by testing for the DBGM-2 and BDBGM for function during the earthquake and function after the earthquake.

J3.0 ASSUMPTIONS

J3.1 ASSUMPTIONS REQUIRING VERIFICATION

There are no assumptions requiring verification

J3.2 ASSUMPTION NOT REQUIRING VERIFICATION

J3.2.1 In accordance with recommendations in Reference J2.2.8, Section 7.5.5, a load factor of 1.4 is to be applied to the DBGM-2 in-structure response spectra to define the minimum test level for qualification. This load factor is used in the fragility calculation to assure that the HCLPF of the tested component will be greater than the DBGM-2 in-structure response spectra.

Rationale - This is a project requirement and the load factor does not require verification.

J4. METHODOLOGY

J4.1 QUALITY ASSURANCE

This calculation is prepared in accordance with Bechtel SAIC LLC procedure EG-PRO-3DP-G04B-00037, Rev. 10, Reference J2.1.1.

J4.2 USE OF SOFTWARE

Mathcad 14 is used in this calculation. The use of this software is classified as Level 2 software per procedure IT-PRO-001, Reference J2.1.2. Therefore the software does not require separate qualification.

J5.0 LIST OF APPENDICES

APPENDIX J-A DBGM-2 In-structure Response Spectra for the Foundation Level of the Canister Receipt and Closure Facility.

APPENDIX J-B Comparison of the DBGM-2 Site-Wide Ground Motion Spectrum with the Median Soil Case for 100 Feet of Alluvium.

APPENDIX J-C Comparison of BDBGM & DBGM-2 ISRS.

J6.0 DEVELOPMENT OF FRAGILITIES

Equipment qualified by testing has an unknown fragility. In general, for lower seismicity plants, the equipment will have significantly higher capacity than the required test level. However, for higher seismicity sites such as Yucca Mountain surface facilities, this inherent margin may not exist. Reference J2.2.1, Pages 3-57 to 3-71 provides a methodology for developing seismic fragility for equipment qualified by testing. Two fragilities are developed from the test results. For function during the earthquake, a lower value is given that implies chatter of electro-mechanical contactors that could result in undesirable response in a critical electrical or control circuit such as lockout of a component, breaker trip, spurious operation of a valve motor, etc. A higher fragility can be derived from the test data for function after the earthquake. This fragility represents the condition that no significant structural damage has occurred such that the component can be expected to operate after the earthquake. Solid state circuits are generally assigned the fragility for function after the earthquake for operation both during and after the earthquake.

Anchorage fragility may or may not be covered by the shake table test. Typically, electrical cabinets are welded to embeds and if the weld to the shake table is prototypical, then the welded anchorage is qualified via the shake table testing. However, the test labs typically use high strength bolts to anchor components to the table where bolted anchorage is to be simulated. In this situation, the actual installation may use expansion anchors or low carbon steel bolting that are not representative of the behavior of the high strength bolts used in the test. In this case, the anchorage in the plant must have a separate fragility developed.

Depending upon the particular component function, the function during the earthquake fragility may not be of concern. The systems analyst is to select the appropriate fragility for the seismic event sequence analysis..

J6.1 DEVELOPMENT OF CAPACITY FACTORS AND EQUIPMENT RESPONSE FACTORS

The methodology of Reference J2.2.1 does not develop separate capacity factors and equipment response factors due to the fact that the equipment response and capacity are inherent in the equations that define the capacity above the test level and the uncertainty in this capacity. Thus, this section includes the equivalent of a capacity factor and an equipment response factor.

Modern procedures for qualifying components by test consists of subjecting them to broad banded multi-axis input motion as described in Reference J2.2.3. It is required that the test response spectrum envelope the required response spectrum. On the basis of past SPRA results, it is recommended in Reference J2.2.2, and required by Reference J2.2.8, Section 7.5.5, that an over test factor of 1.4 be applied to obtain the same reliability as structures and equipment qualified by analysis. In the development of fragilities for equipment qualified by testing, the 1.4 factor is incorporated.

In accordance with Reference J2.2.1, Equation 3-38, the median ground motion acceleration capacity, A_m, is defined as:

$$A_m = \frac{TRS_c}{RRS_c} F_D \cdot F_{RS} \cdot PGA$$

where

$$TRS_c = TRS \cdot C_T \cdot C_I$$

$$RRS_c = RRS \cdot C_{C.} \cdot D_R$$

TRS = Test Response Spectrum

RRS = Required Response Spectrum

C_T = Clipping factor for narrow banded TRS (Reduces Narrow TRS Spikes)

C_C = Clipping factor for narrow banded RRS (Reduces Narrow RRS Spikes)

F_D = Broad Frequency Input Spectrum Capacity Factor

F_{RS} = Structural Response Factor

PGA = Reference peak ground acceleration for the DBGM-2 earthquake used in producing the RRS = 0.453g

D_R = Demand reduction factor (conservatism in deterministic response versus probabilistic response)

C_I = Capacity increase factor (consideration of low probability that the RRS peak will coincide with TRS valley)

The required test response spectra for the equipment in question are the site wide broadened and smoothed floor response spectra for the DBGM-2 at the equipment location. These spectra define the minimum test input motion. For the generic fragility calculation, the required test response spectra can be taken at any reference location since the fragility is a direct function of the test response spectra. Most equipment is located on the ground floor and the floor response spectra of the CRCF ground floor are used as the required response spectra. The actual test response spectra are to be a factor of 1.4 times the required spectra in accordance with the project requirements of Reference J2.2.8, Section 7.5.5.

The median required response spectra for fragility calculations are considered to be the median soil case unbroadened spectra. The 100 foot soil depth with median soil properties is used to define the median spectra. Note that the spectra provided are based on a mean UHS rather than a median UHS. Typically, the spectral amplification is similar in both cases so it is immaterial what the ground motion reference (mean or median) is for development of fragilities.

Since the test response spectra are an envelope of the broadened and smoothed site wide spectra, they can't be clipped. However, the raw required response spectra have narrow peaks and can be clipped. For purposes of this fragility derivation, the ground floor spectra for the Canister Receipt and Closure Facility, represented by node 22, are used in order to develop a typical ratio of the TRSc to RRSc. Most equipment will be mounted on the ground floor. The ground floor layout is shown in Reference J2.2.6. This is conservative for equipment mounted higher in the structure since the in-structure spectra at higher elevations tend to have narrower peaks and clipping is more effective for the narrower peaks. The ground floor spectra are shown in Appendix J-A. The process of clipping is shown in Figure J6-1 and proceeds as follows.

At 80% of the peak of the spectrum, determine the width of the spectral peak, $\Delta f_{0.8}$.

Calculate the factor B = $\Delta f_{0.8}$/fc where fc is the central frequency at the peak.

Then, the median and uncertainty values of C_C are (Reference J2.2.1, page 3-64):

$C_C = 0.30 + 0.86B$ B equal to or < 0.4

$C_C = 0.50 + 0.36B$ B > 0.

$\beta_U = 0.37 - 0.5B$ B equal to or < 0.4

$\beta_U = 0.24 - 0.17B$ B > 0.4

Typically 5% damped spectra are provided for the required response spectrum. It does not matter what damping is specified since the TRS and RRS are to be defined at the same damping. 5% damped spectra are used for this fragility calculation.

From Appendix J-A, determine the clipping factor for the raw median soil case, 100 foot depth of alluvium spectra for the three direction of motion. Use the digitized spectral values in Reference J2.2.4.

The RRS in the three directions have several peaks and when clipping, the $\Delta f_{0.8}$ must include all spectral accelerations above 80% of the highest peak. Table J6-1 summarizes the clipping of the Appendix J-A spectra.

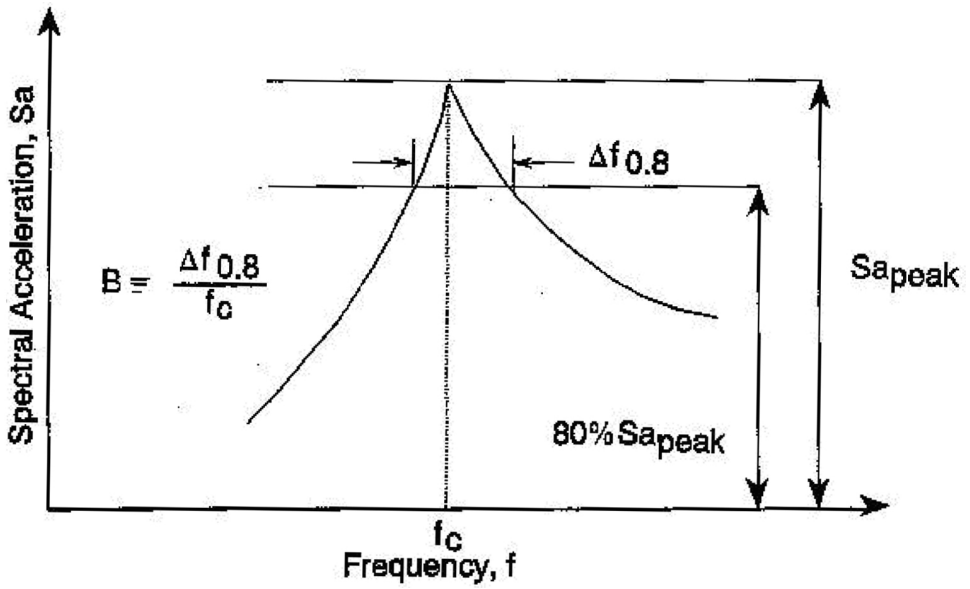

Figure J6-1 Clipping of Narrow Banded Peaks

Table J6-1 Clipping of RRS

Spectrum	Peak Sa (g)	0.8 Peak Sa	fc Hz	$\Delta f_{0.8}$	B	C_c
X	1.49	1.19	4.6	3.48	0.76	0.77
Y	1.41	1.13	4.6	4.65	1.01	0.86
Z	0.95	0.76	8.5	6.92	0.81	0.79

The clipped peaks, (Cc x Peak Sa), of the three spectra are:

SaX = 1.15
SaY = 1.21
SaZ = 0.75

Determine the ratio of the broad banded TRS to the clipped RRS as a function of frequency. Modern equipment qualified for seismic events will likely have fundamental frequencies in the 5 to 25 Hz range. For purposes of developing a fragility, we will examine frequencies from 3 to 30 Hz.

Table J6-2 Comparison of TRS to RRS
(X, Y and Z Directions)

Direction X			
Frequency	Sa TRS	Sa RRS_c	TRS/RRS_c
3	1.32	1.15	1.15
4	1.49	1.15	1.30
5	1.49	1.15	1.30
7	1.49	1.11	1.34
10	1.09	0.72	1.51
15	0.95	0.84	1.13
30	0.70	0.59	1.19

Direction Y			
Frequency	Sa TRS	Sa RRS_c	TRS/RRS_c
3	1.42	1.21	1.17
4	1.55	1.21	1.28
5	1.55	1.21	1.28
7	1.55	1.08	1.44
8.5	1.42	0.86	1.65
10	1.02	0.64	1.59
15	0.88	0.71	1.24
30	0.68	0.52	1.31

Direction Z			
Frequency	Sa TRS	Sa RRS_c	TRS/RRS_c
3	0.71	0.62	1.15
4	0.80	0.62	1.29
5	0.89	0.68	1.31
7	1.01	0.75	1.35
8.5	1.01	0.75	1.35
10	1.01	0.75	1.35
15	0.89	0.70	1.27
30	0.42	0.30	1.40

All three directions have a low ratio of TRS/RRS$_C$ at some frequency. For purposes of developing a bounding case fragility, use the X direction TRS and RRS$_c$ at 15 Hz which has a minimum ratio of 1.13.

Per requirements in Reference J2.2.8, Section 7.5.5, the TRS target will be 40% over the required demand.

$TRS := 0.95g \cdot 1.4 = 42.791 \frac{ft}{s^2}$ (1.33g)

$RRS := 0.84g$

$C_T := 1.0$ No clipping of TRS

$C_I := 1.1$ Factor to acknowledge that RRS peak will likely not line up with a TRS valley. Ref. J2.2.1, Page 3-65

$C_C := 1.0$ No clipping of RRS at 15 Hz.

$D_R := 1.0$ D_R represents the difference between probabilistic spectra and median deterministic spectra. At the ground floor level, D_R = 1.0. Ref. J2.2.1, Page 3-66.

$TRS_c := TRS \cdot C_T \cdot C_I = 47.071 \frac{ft}{s^2}$ (1.46g)

$RRS_c := RRS \cdot C_C \cdot D_R = 27.026 \frac{ft}{s^2}$ (0.84g)

The factor F_D and uncertainties β_R and β_U depend on the source of the type of qualification testing and whether function during or after the DBGM-2 is required. From Reference J2.2.1, Table 3-14:

$F_{D\_D} := 1.4$ Function during the earthquake for qualification by test

$F_{D\_A} := 1.95$ Function after the earthquake for qualification by test

$\beta_{R\_FD} := 0.09$ For both function during and after the earthquake

$\beta_{U\_FD\_D} := 0.22$ Function during the earthquake

$\beta_{c\_FD\_D} := \left(\beta_{R\_FD}^{2} + \beta_{U\_FD\_D}^{2}\right)^{0.5}$ Function during the earthquake

$\beta_{c\_FD\_D} = 0.238$

$\beta_{U\_FD\_A} := 0.28$ Function after the earthquake,

$\beta_{c\_FD\_A} := \left(\beta_{R\_FD}^{2} + \beta_{U\_FD\_A}^{2}\right)^{0.5}$ Function after the earthquake

$\beta_{c\_FD\_A} = 0.294$

$\beta_{U\_CI} := 0.05$ Ref. J2.2.1, Page 3-65

$\beta_{c\_CI} := \beta_{U\_CI} = 0.05$

Clipping is not applicable for TRS and RRS so Betas are 0 for C_T and $C_{C,}$

D_R is 1.0 so Beta is 0.

The combined capacity factor and equipment response factor for function during and function after the earthquake are:

$$F_{C\_RE\_D} := \frac{TRS_c}{RRS_c} \cdot F_{D\_D} = 2.438$$

$$F_{C\_RE\_A} := \frac{TRS_c}{RRS_c} F_{D\_A} = 3.396$$

J6.2 STRUCTURAL RESPONSE FACTOR

J6.2.1 Spectral Shape Factor

This factor accounts for conservatism in the site-wide DBGM-2 design spectrum. The depth of alluvium at the Surface Facilities Area (SFA) varies from 30 feet to 200 feet. Uniform hazard spectra at the surface are calculated from site response analyses for alluvium depths of 30', 70', 100' and 200'. The site-wide design ground response spectrum is the envelope of the surface spectra of these four alluvium depths (Reference J2.2.5; also Section 6.2.2.1 for source information).

The best-estimate horizontal dominant frequency of the soil-structure system is 5.2 Hz for the CRCF at 100-feet of alluvium and median soil properties (Appendix J-A from Reference J2.2.4). At this frequency:

$SA_{site} := 1.14g$ 5% damped site-wide spectral acceleration (Appendix J-B)

$SA_{100} := 1.06 \cdot g$ 5% damped spectral acceleration of the 100-foot best-estimate alluvium depth case in the northeast area where the preclosure surface facilities are located (Appendix J-B)

$$F_{SA} := \frac{SA_{site}}{SA_{100}}$$

$$F_{SA} = 1.075$$

Since uncertainty in the UHS is derived from uncertainty in the seismic hazard curves which will be included in the final risk quantification, no uncertainty is included under the spectral shape factor to avoid double-counting the hazard uncertainty, hence

$\beta_{U\_SA} := 0$

$\beta_{R\_SA} := 0.20$ Random variability to account for peak-to-valley variability of the smoothed UHS, Ref. J2.2.1, Table 3-2.

$$\beta_{c\_SA} := \sqrt{\beta_{U\_SA}^2 + \beta_{R\_SA}^2} = 0.2$$

J6.2.2 Damping Factor

This factor is to account for conservatism in the hysteresis damping of the building structure used in the seismic response analysis. Due to the high radiation damping of the foundation media, the effect of structure damping is insignificant. Thus,

$F_{\delta} := 1.0$

$\beta_{U\_\delta} := 0$ Since a conservative median factor of safety is used for structure damping, no value is assigned to the uncertainty logarithmic standard deviation.

$\beta_{R\_\delta} := 0$

$$\beta_{c\_\delta} := \sqrt{\beta_{U\_\delta}^2 + \beta_{R\_\delta}^2} = 0$$

J6.2.3 Modeling Factor

The Tier 1 lumped mass multiple-stick model of the CRCF includes the stiffness of various reinforced concrete walls and distribution of mass at each floor. The floors are assumed to be rigid diaphragms tying the different sticks together. Torsional response of the structure is captured through modeling eccentricity between the center of mass and center of rigidity of each floor. The foundation media underneath the buildings are modeled with soil springs and dashpots based on elastic half space theory with adjustment to account for layering effect of alluvium overlying tuff. Per Reference J2.2.7, BSC recognizes that final design will be accomplished by a more explicit finite element model and it is acceptable to consider the modeling factor to be median centered in these seismic fragility evaluations, thus:

$F_M := 1.0$

$\beta_{R\_M} := 0$ Since there is no randomness in modeling.

Uncertainty of structure frequencies predicted from mathematical modeling varies from 0.15 to 0.35 depending on the sophistication of the model (Reference J2.2.1, page 3-15). The value of 0.35 is for fairly approximate model and the value 0.15 is appropriate for detailed models. Based on the complexity of the CRCF structure and the mathematical model used for the Tier 1 ISRS analysis, it is judged that the calculated CRCF frequency has a logarithmic standard deviation of 0.25.

$\beta_f := 0.25$ Uncertainty in building frequency.

$f_m := 5.2 \cdot Hz$ Best-estimate frequency

$f_{upper} := f_m \cdot e^{\beta_f}$ Upper bound frequency

$f_{upper} = 6.677 \cdot Hz$

$SA_{upper} := 1.05g$ 5% damped spectral acceleration at f_{upper} read off from the mean 5E-4 UHS of the 100-foot alluvium depth case (Appendix J-B). This value is less than the value at the best-estimate frequency.

$f_{lower} := f_m \cdot e^{-\beta_f}$ Lower bound frequency

$f_{lower} = 4.05 \cdot Hz$

$SA_{lower} := 1.02 \cdot g$ 5% damped spectral acceleration at f_{lower} read off from the mean 5E-4 UHS of the 100-foot alluvium depth case. This value is less than the value at the best-estimate frequency.

$\beta_{U\_f} := 0$ Since the spectral value at the best-estimate frequency is greater than that at either the lower bound or upper bound frequency.

$\beta_{U\_ms} := 0.15$ Uncertainty of mode shape (Reference J2.2.1, page 3-18)

$$\beta_{U\_M} := \sqrt{\beta_{U\_f}^2 + \beta_{U\_ms}^2}$$

$$\beta_{U\_M} = 0.15$$

$$\beta_{c\_M} := \sqrt{\beta_{R\_M}^2 + \beta_{U\_M}^2}$$

$$\beta_{c\_M} = 0.15$$

J6.2.4 Modal Combination

Since the direct integration time history method is used in the Tier 1 ISRS analysis (Reference J2.2.4), the modal combination method factor of safety is unity and there is no variability associated with modal combination.

$$F_{MC} := 1$$

$$\beta_{R\_MC} := 0$$

$$\beta_{U\_MC} := 0$$

$$\beta_{c\_MC} := \sqrt{\beta_{R\_MC}^2 + \beta_{U\_MC}^2} = 0$$

J6.2.5 Soil-Structure Interaction

The Tier 1 seismic response analyses of the CRCF use the site-wide $5*10^{-4}$ mean uniform hazard spectra as the DBGM-2 input motion. Spectrum compatible time histories are used as the input motion for the time history analyses. The conservatism in the site-wide spectra was accounted for in the spectral shape factor above. Strain compatible soil properties of 100-foot and 200-foot deep alluvium are used to calculate frequency-independent soil springs and soil damping coefficients. Soil radiation damping is introduced into the model by using dashpots. Damping coefficients equal to 75% of the computed values for translational degrees of freedom and to the full computed rotational damping values are used in the response analyses (Reference J2.2.4). Conservatism or un-conservatism in SSI will be minimized in the final SSI analysis used to develop equipment design seismic input. Before the final SSI analyses

are completed, the Tier 1 SSI analysis is considered to represent the best-estimate responses per BSC recommendations in Reference J2.2.7.

$F_{SSI\_1} := 1.0$

$\beta_{R\_SSI\_1} := 0$

$\beta_{U\_SSI\_1} := 0.25$ Uncertainty of the median-centered state-of-the-art SSI methodology based on past probabilistic seismic response analyses using the same method.

$$\beta_{c\_SSI\_1} := \sqrt{\left(\beta_{R\_SSI\_1}\right)^2 + \beta_{U\_SSI\_1}{}^2} = 0.25$$

It is judged that the median seismic capacity of the equipment, expressed in terms of peak ground acceleration, is close to that of BDBGM. Due to soil nonlinearity, amplification of the input ground motion at BDBGM will be different from that of DBGM-2. The second factor of safety is to account for this difference and is estimated using the DBGM-2 raw spectra and the BDBGM raw spectra at different frequencies as shown in Table J6-3.

Table J6-3
Comparison of Amplification of ZPA for DBGM-2 and BDBGM Spectra

A	B	C	D	E	F
Freq (Hz)	5% Damped DBGM-2 Spectral Accel, Sa_DBGM (g), Note 1	Sa_DBGM to ZPA_{DBGM} Ratio, Note 2	BDBGM Spectral Accel, Sa_BDBGM (g), Note 3	Sa_BDBGM to ZPA_{BDBGM} Ratio, Note 4	Ratio of Col. E to Col. C
1	0.44	0.95	1.04	1.08	1.14
2	0.96	2.07	1.83	1.91	0.92
3	1.24	2.68	2.37	2.47	0.92
4	1.43	3.09	2.74	2.85	0.92
5	1.41	3.05	2.79	2.91	0.95
6	1.23	2.66	2.52	2.63	0.99
8	0.99	2.14	1.69	1.76	0.82
11	0.62	1.34	1.24	1.29	0.96
15	0.84	1.81	1.35	1.41	0.78
20	0.63	1.36	1.29	1.34	0.99
30	0.59	1.27	1.08	1.13	0.88
Notes:					
1. Figure J-A-1 of Appendix J-A					
2. ZPA value of DBGM-2 100' median soil case is 0.463g (Figure J-A-1)					
3. Figure J-C-1 of Appendix J-C					

The governing case for equipment qualified by test was for a 15 Hz comparison of TRS to RRS. Consider a range from 8 Hz to 30 Hz to determine an average value of F_{SSI_2} for the probable range of equipment qualified by test.

$$\text{Factor} := \text{mean}(0.82, 0.96, 0.78, 0.99, 0.88)$$

$$\text{Factor} = 0.886$$

$$F_{SSI\_2} := \frac{1}{\text{Factor}}$$

$$F_{SSI\_2} = 1.129$$

$$F_{SSI} := F_{SSI\_1} \cdot F_{SSI\_2}$$

$$F_{SSI} = 1.129$$

$$\sigma := \text{Stdev}(0.82, 0.96, 0.78, 0.99, 0.88)$$

$\sigma = 0.089$

$\beta_{c\_SSI\_2} := \frac{\sigma}{\text{Factor}}$

$\beta_{c\_SSI\_2} = 0.101$

$\beta_{c\_SSI} := \sqrt{\beta_{c\_SSI\_1}^{2} + \beta_{c\_SSI\_2}^{2}}$

$\beta_{c\_SSI} = 0.27$

J6.2.6 Ground Motion Incoherence

$L1 := 327 \cdot ft$	East-west dimension of the CRCF excluding the 49'-6" and 43' extensions at the east and west ends, respectively (Reference J2.2.6).
$L2 := 336 \cdot ft$	North-south dimension of the CRCF excluding the 56' extension at the south end.
$L_{eq} := \sqrt{L1 \cdot L2}$	Equivalent foundation dimension of the CRCF
$L_{eq} = 331.469\ ft$	

The ground motion incoherence reduction factor is a function of foundation size and frequency of response. For a 150 foot plan dimension foundation, the following reduction factors are presented in Reference J2.2.1 in page 3-22. Interpolation or extrapolation may be used to calculate the reduction factor for different dimensions and/or frequencies.

$L_{std} := 150 \cdot ft$	Foundation dimension the reduction factors in Reference J2.2.1 are calculated.
$f_5 := 5$	Frequency in cycle/sec (Hz)
$RF_5 := 1$	Reduction factor for response frequency at 5 Hz
$f_{10} := 10$	Frequency in Hz
$RF_{10} := 0.9$	Reduction factor for response frequency at 10 Hz
$RF_{5\_eq} := RF_5$	Reduction factor at 5 Hz, given the CRCF equivalent foundation dimension

$$RF_{10\_eq} := 1 - \left[\left(1 - RF_{10}\right) \cdot \frac{L_{eq}}{L_{std}} \right]$$ Linear extrapolation

$RF_{10\_eq} = 0.779$ Reduction factor at L_{eq} dimension and 10 Hz frequency of response.

At 5.2 Hz which is the fundamental frequency of horizontal response of the CRCF

$f_6 := 5.2$ Frequency in Hz

Calculate the reduction factor at 5.2 Hz frequency by interpolation

$RF_{6\_eq} := 0.4$ An arbitrary value to initiate the equation solver below.

Given

$$\frac{\log\left(RF_{10\_eq}\right) - \log\left(RF_{5\_eq}\right)}{\log\left(RF_{6\_eq}\right) - \log\left(RF_{5\_eq}\right)} = \frac{\log\left(f_{10}\right) - \log\left(f_5\right)}{\log\left(f_6\right) - \log\left(f_5\right)}$$

$a := \text{Find}\left(RF_{6\_eq}\right)$

$a = 0.986$ Reduction factor

Thus, the ground motion incoherence factor of safety is

$$F_{GMI} := \frac{1}{a}$$

$F_{GMI} = 1.014$

$$\beta_{U\_GMI} := \frac{1}{2} \cdot \ln\left(\frac{1}{a}\right)$$ A reduction factor of 1.0 (i.e., no reduction) is estimated to be two standard deviation from the calculated median factor of 0.91 (Reference J2.2.1, Page 3-23).

$\beta_{U\_GMI} = 0.01$

$\beta_{R\_GMI} := 0$

$$\beta_{c\_GMI} := \sqrt{\beta_{R\_GMI}^2 + \beta_{U\_GMI}^2}$$

$\beta_{c\_GMI} = 0.01$

J6.2.7 Structural Response Factor

$$F_{RS} := F_{SA} \cdot F_{\delta} \cdot F_{M} \cdot F_{MC} \cdot F_{SSI} \cdot F_{GMI}$$

$$F_{RS} = 1.231$$

$$\beta_{c\_RS} := \sqrt{\beta_{c\_SA}^{2} + \beta_{c\_\delta}^{2} + \beta_{c\_M}^{2} + \beta_{c\_MC}^{2} + \beta_{c\_SSI}^{2} + \beta_{c\_GMI}^{2}}$$

$$\beta_{c\_RS} = 0.368$$

J6.3 FRAGILITY

J6.3.1 Fragility for Qualification for DBGM-2

Fragility is referenced to peak ground acceleration for the DBGM-2.

$$PGA := 0.453g$$

The composite fragility for equipment qualified by testing for function during the earthquake is:

$$A_{m\_D} := \frac{TRS_c}{RRS_c} \cdot F_{D\_D} \cdot F_{RS} \cdot PGA$$

$$A_{m\_D} = 43.752 \frac{ft}{s^2} \qquad (1.36g)$$

$$\beta_{c\_D} := \left[\beta_{c\_FD\_D}^{2} + \beta_{c\_CI}^{2} + \left(\beta_{c\_RS}\right)^{2} \right]^{0.5}$$

$$\beta_{c\_D} = 0.441$$

$$HCLPF\_D := A_{m\_D} \cdot e^{-2.33 \cdot \beta_{c\_D}}$$

$$HCLPF\_D = 15.669 \frac{ft}{s^2} \qquad (0.49g)$$

The composite fragility for function after the earthquake is:

$$A_{m\_A} := \frac{TRS_c}{RRS_c} \cdot F_{D\_A} \cdot F_{RS} \cdot PGA$$

$$A_{m\_A} = 60.94 \frac{ft}{s^2} \qquad (1.89g)$$

$$\beta_{c\_A} := \left(\beta_{c\_FD\_A}^{2} + \beta_{c\_CI}^{2} + \beta_{c\_RS}^{2}\right)^{0.5}$$

$$\beta_{c\_A} = 0.474$$

$$HCLPF\_A := A_{m\_A} \cdot e^{-2.33 \cdot \beta_{c\_A}}$$

$$HCLPF\_A = 20.219 \frac{ft}{s^2} \qquad (0.63g)$$

The fragilities for function during and function after the earthquake for equipment qualified by test are summarized in Table J6-4.

Table J6-4
Fragility for Equipment Qualified by Test for DBGM-2

Reference Earthquake Design Basis	Function During the Earthquake			Function After the Earthquake		
	A_m (g)	β_c	HCLPF (g)	A_m (g)	β_c	HCLPF (g)
DBGM-2	1.36	0.441	0.49	1.89	0.474	0.63

6.3.2 Fragility for Qualification for BDBGM

Reference J2.2.8 requires that ITS components be evaluated for BDBGM and that the HCLPF should be a factor of at least 1.1 times the BDBGM. There are currently no specific design measures being taken for ITS equipment at the BDBGM level. As can be observed from Table J6-1, the HCLPF values exceed the 0.453g DBGM-2 PGA for function during and function after the earthquake. If a HCLPF of at least the 0.914g BDBGM PGA is to be achieved, it is clear that the limiting cases summarized in Table J6-1 for qualification only to DBGM-2 would not achieve this goal and qualification at higher ground motion would be required. As a sensitivity study for use within the PSA analyses, an additional set of fragilities has been estimated wherein the ITS equipment design basis is considered to be the BDBGM. Such a design would use exactly the same design codes and standards as used for design to DBGM-2. In addition, in-structure response spectra would be enveloped and broadened in the exact same manner. Differences would be only that the ground motion would be higher and soil nonlinearites in the soil-structure interaction analyses may result in different spectral shapes between the BDBGM and the DBGM-2 ISRS.

Review of the BDBGM and the DBGM-2 ISRS in Appendix J-C indicates that there is no significant difference in the peak spectral amplification (average of 2.02). As a result, the fragilities for BDBGM design are 2.02 times the DBGM-2 fragilities as shown in the calculation below and in Table J6-5.

$$PGA\_BDBGM := 0.914g$$

$$SF := \frac{PGA\_BDBGM}{PGA}$$

$$SF = 2.018$$

Table J6-5
Fragility for Equipment Qualified by Test for BDBGM

Reference Earthquake Design Basis	Function During the Earthquake			Function After the Earthquake		
	Am (g)	βc	HCLPF (g)	Am (g)	βc	HCLPF (g)
BDBGM	2.75	0.441	0.98	3.82	0.474	1.27

The HCLPF exceeds the BDBGM PGA of 0.914g for function during and function after the earthquake.

J7. SUMMARY AND CONCLUSIONS

Fragilities for function during and function after the earthquake were developed for equipment qualified by test for the DBGM-2 earthquake. A scale factor was developed to convert these fragilities for a case where the testing was conducted for a BDBGM.

Table J7-1 summarizes the fragility of equipment qualified by test for the DBGM-2 and for BDBGM.

Table J7-1
Fragility for Equipment Qualified by Test for DBGM-2 and BDBGM

Reference Earthquake Design Basis	Function During the Earthquake			Function After the Earthquake		
	Am	βc	HCLPF	Am	βc	HCLPF
DBGM-2	1.36	0.441	0.49	1.89	0.474	0.63
BDBGM	2.75	0.441	0.98	3.82	0.474	1.27

This fragility calculation has shown that the HCLPF for function during the earthquake is about 8% higher than the reference earthquake design basis and that the HCLPF for function after the earthquake is about 39% greater than the reference earthquake design basis. If function after the earthquake is the only concern, the HCLPF for function after the earthquake for a DBGM-2 design basis is about 69% of the BDBGM PGA of 0.914g.

The seismic event sequence analysis team will have to determine if function during the earthquake is important and if testing at a higher level than the DBGM-2 is necessary for some or all of the SSCs that are ITS in order to achieve the desired safety goal.

APPENDIX J-A
DBGM-2 IN-STRUCTURE RESPONSE SPECTRA FOUNDATION LEVEL OF CANISTER RECEIPT AND CLOSURE FACILITY

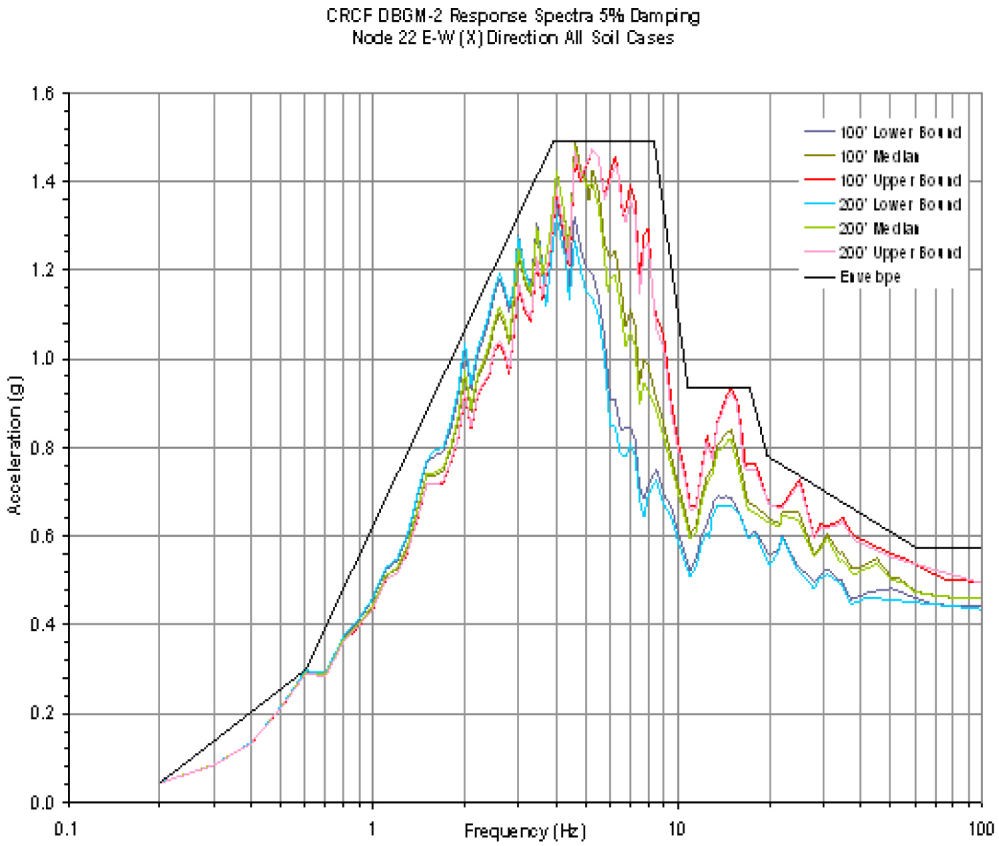

Figure J-A-1
5% Damped DBGM-2 Spectra Node 22 Foundation Level
Direction X

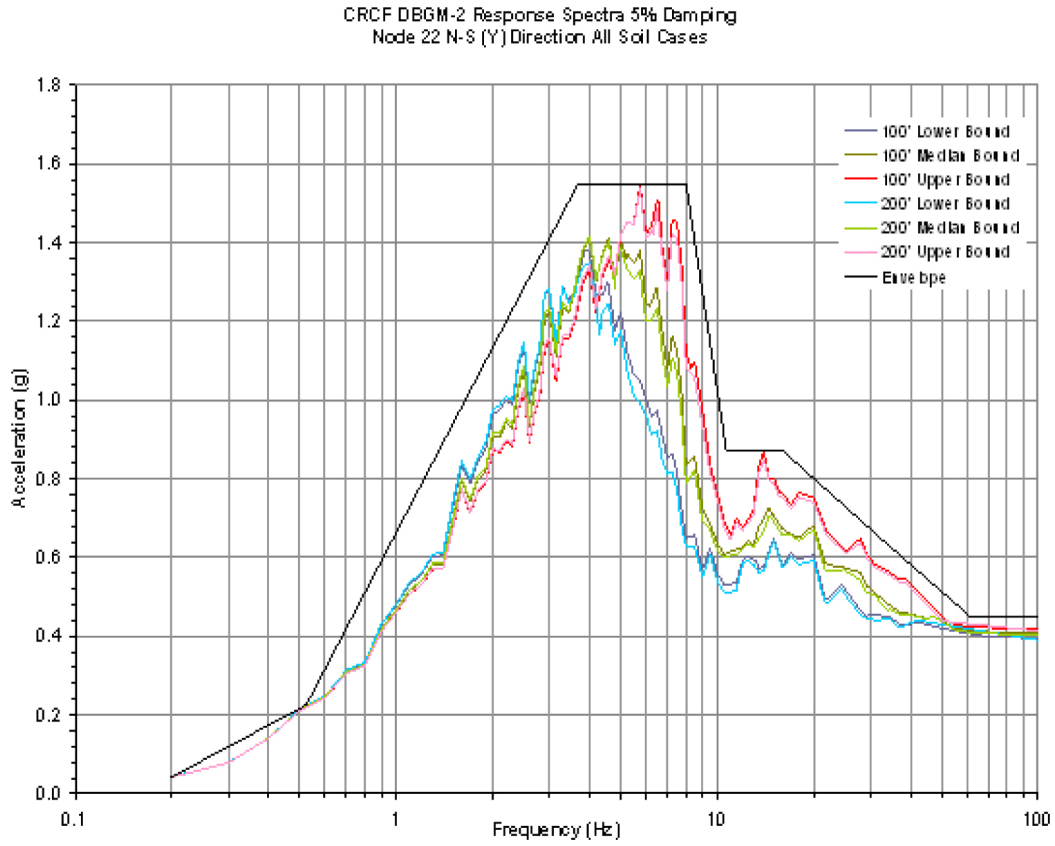

Figure J-A-2
5% Damped DBGM-2 Spectra Node 22 Foundation Level
Direction Y

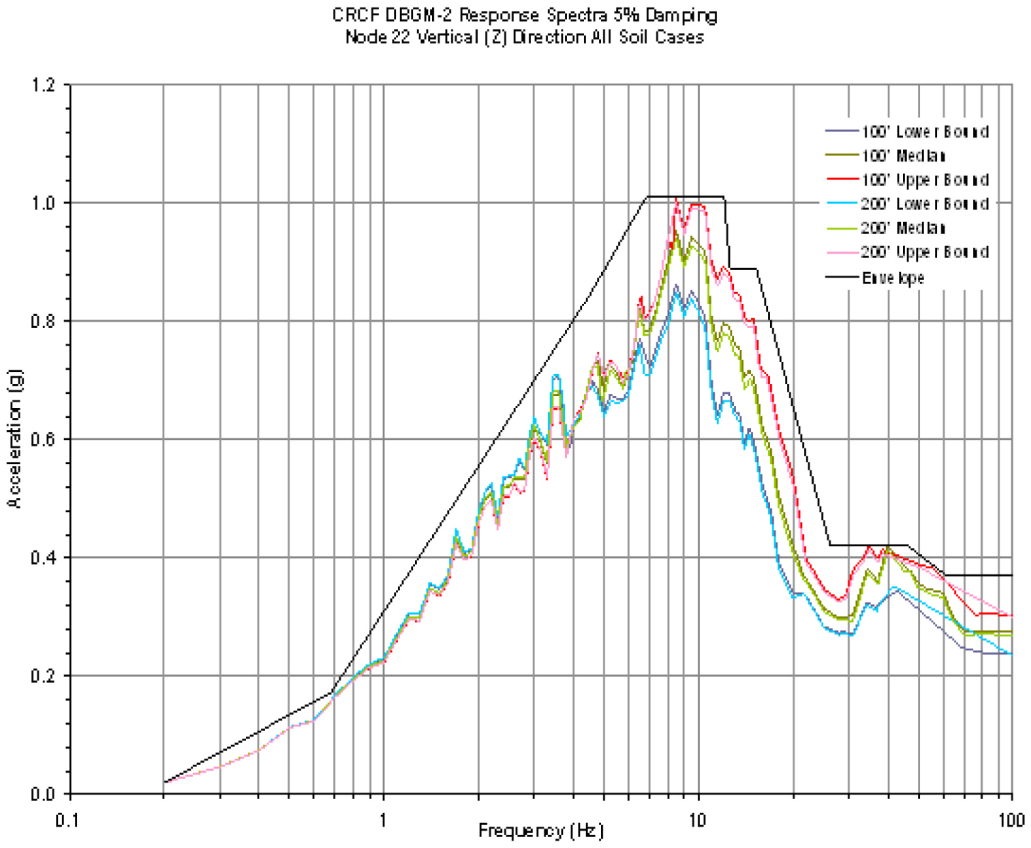

Figure J-A-3
5% Damped DBGM-2 Spectra Node 22 Foundation Level
Direction Z

APPENDIX J-B
COMPARISON OF DBGM-2 SITE-WIDE GROUND MOTION SPECTRUM WITH THE MEDIAN SOIL CASE FOR 100 FEET OF ALLUVIUM

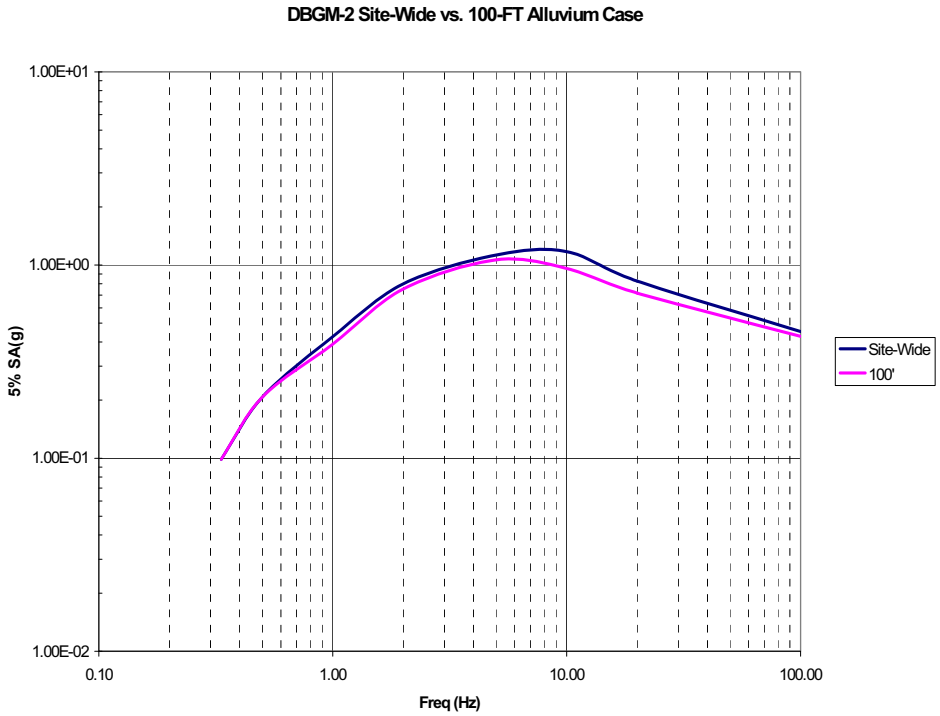

Figure J-B-1
DBGM-2 Site-Wide Horizontal Ground Motion Spectrum vs 100 Foot Alluvium Median Soil Spectrum (See Section 6.2.2.1 for source information)

APPENDIX J-C
COMPARISON OF BDBGM & DBGM-2 ISRS

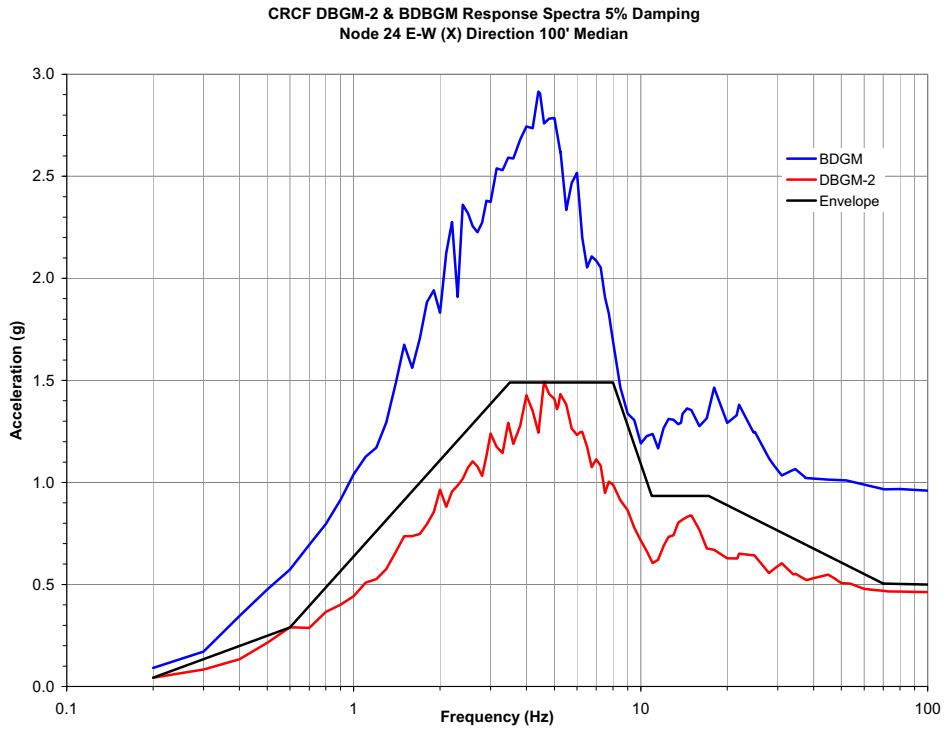

Figure J-C-1. 5% Damped 100' Alluvium Depth ISRS for BDBGM and DBGM-2 at Ground Floor (X-Direction)

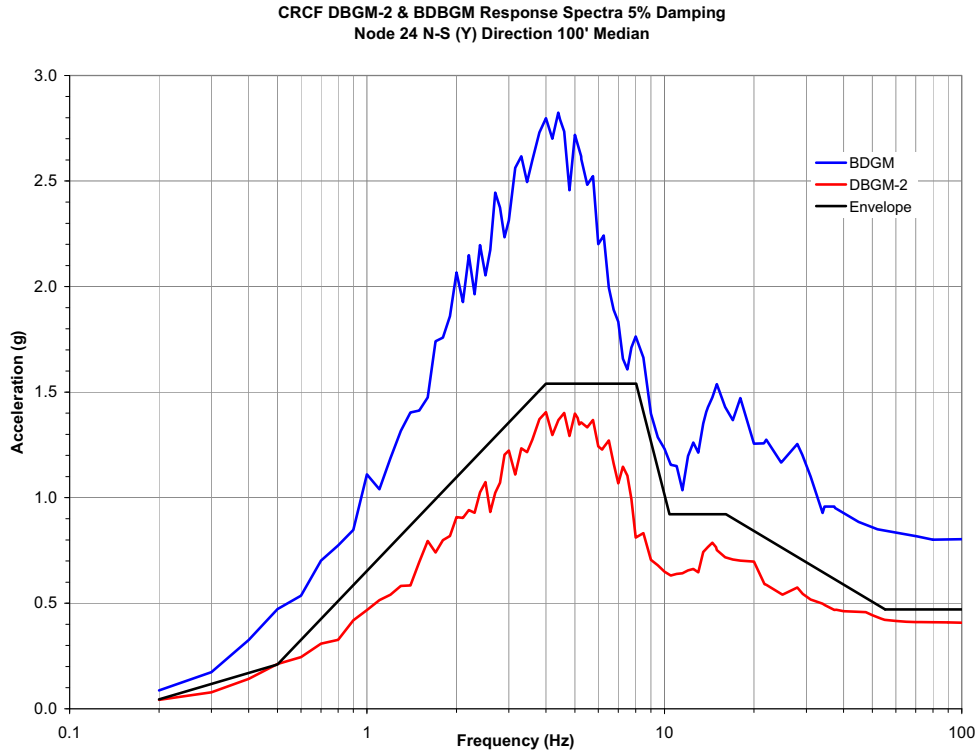

Figure J-C-2. 5% Damped 100' Alluvium Depth ISRS for BDBGM and DBGM-2 at Ground Floor (Y-Direction)

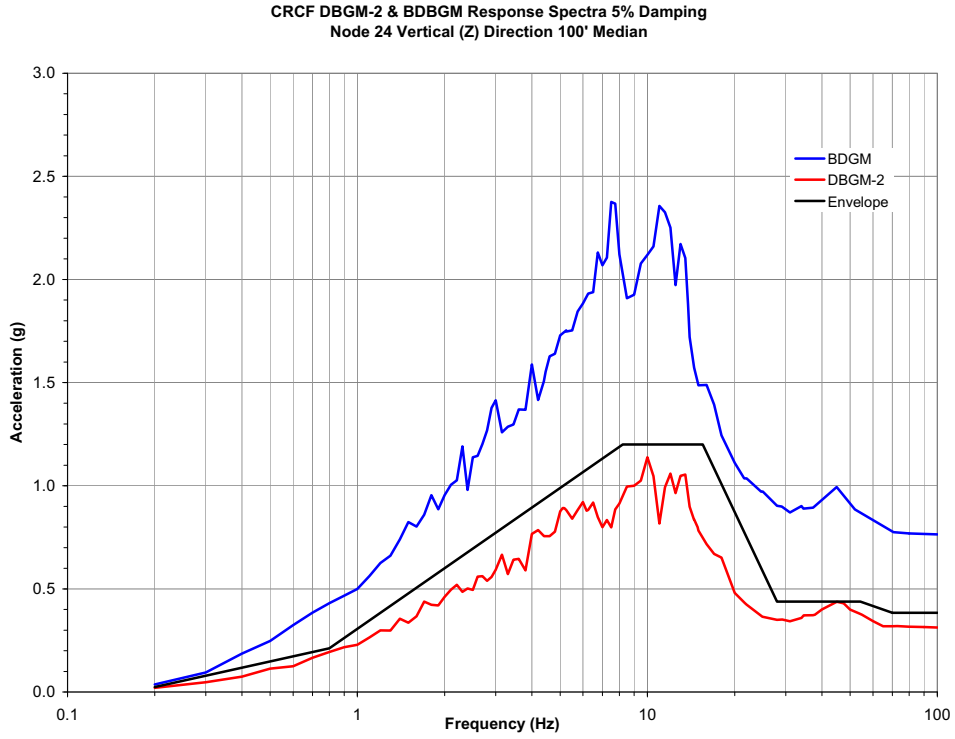

Figure J-C-3. 5% Damped 100' Alluvium Depth ISRS for BDBGM and DBGM-2 at Ground Floor (Z-Direction)

ATTACHMENT K
FRAGILITY FOR TYPICAL EQUIPMENT AND SUBSYSTEMS QUALIFIED BY ANALYSIS

Prepared By: Robert D. Campbell

ARES Check By: Wen H. Tong

LLNL Check By: Robert C. Murray

TABLE OF CONTENTS

ACRONYMS AND ABBREVIATIONS

ACI	American Concrete Institute
AISC	American Institute of Steel Construction
ANSI	American National Standards Insitute
AO	Aging Overpack
APE	Annual Probability of Exceedance
ASCE	American Society of Civil Engineers
ASME	American Society of Mechanical Engineers
BSC	Bechtel SAIC, LLC
BDBGM	Beyond Design Basis Ground Motion at $1x10^{-4}$ APE
CDFM	Conservative Deterministic Failure Margin
CHC	Cask Handling Crane
CIP	Cast-in-Place
CRCF	Canister Receipt and Closure Facility
CTM	Canister Transfer Machine
CTT	Cask Transfer Trolley
DBGM-2	Design Basis Ground Motion at $5x10^{-4}$ APE
DL	Dead Load
DOF	Degree of Freedom
DPC	Dual Purpose Canister
EPRI	Electric Power Research Institute
HCLPF	High Confidence of Low Probability of Failure
HVAC	Heating, Ventilation, & Air Conditioning
IEEE	Institute of Electrical and Electronics Engineers
IHF	Initial Handling Facility
ISRS	In-Structure Response Spectra

ACRONYMS AND ABBREVIATIONS (cont.)

ITS	Important to Safety
LA	License Application
LLNL	Lawrence Livermore National Laboratory
NPP	Nuclear Power Plant
PGA	Peak Ground Acceleration
RF	Receipt Facility
RRS	Required Response Spectrum
Sa	Spectral Acceleration
SFA	Surface Facilities Area
SFTM	Spent Fuel Transfer Machine
SPRA	Seismic Probabilistic Risk Assessment
SRSS	Square Root of the Sum of Squares
SSE	Safe Shutdown Earthquake (used with NPPs)
SSI	Soil Structure Interaction
SSC	Structure, System, and Component
TAD	Transportation, Aging, and Disposal canister
TEV	Transport and Emplacement Vehicle
TRS	Test Response Spectrum
UHS	Uniform Hazard Spectra
USDOE	United States Department of Energy
USNRC	United States Nuclear Regulatory Commission
WHF	Wet Handling Facility
WP	Waste Package
WPTT	Waste Package Transfer Trolley
YMSF	Yucca Mountain Surface Facilities
ZPA	Zero Period Acceleration

FRAGILITY TERMINOLOGY

Am	Median Peak Ground Motion Capacity
β_R	Log Standard Deviation of Randomness
β_U	Log Standard Deviation of Uncertainty (Lack of Knowledge)
β_C	Composite Variability = $(\beta_R^2 + \beta_U^2)^{0.5}$
F_S	Strength Factor of Safety
β_{R_S}	Strength Randomness (typical)
β_{U_S}	Strength Uncertainty (typical)
β_{C_S}	Strength Composite Variability (typical)
F_μ	Inelastic Energy Absorption Factor of Safety
F_C	Capacity Factor of Safety
F_{QM}	Qualification Factor of Safety
F_δ	Damping Factor of Safety
F_M	Modeling Factor of Safety
F_{MC}	Modal Combination Factor of Safety
F_{ECC}	Earthquake Component Combination Factor of Safety
F_{SA}	Spectral Shape Factor of Safety
F_{SSI}	Soil-Structure Interaction Factor of Safety
F_{GMI}	Ground Motion Incoherence Factor of Safety
F_{TOTAL}	Total Factor of Safety
F_{RS}	Structural Response Factor of Safety
F_{RE}	Equipment Response Factor of Safety

K1. PURPOSE

The purpose of this calculation is to develop fragilities of equipment and subsystems in Yucca Mountain Project surface facilities that are ITS and qualified for seismic events by analysis. Design specifications and design analyses are not yet available so the derivations are representative based on the applicable BSC specifications for seismic design and applicable codes and standards.

K2. REFERENCES

K2.1 PROCEDURES AND DIRECTIVES

K2.1.1 EG-PRO-3DP-G04B-00037, Rev. 10. *Calculations and Analyses*. Las Vegas, Nevada: Bechtel SAIC Company. ACC: ENG.20071018.0001.

K2.1.2 IT-PRO-0011, Revision 7, ICN 0. *Software Management*. Las Vegas, Nevada: Bechtel SAIC Company. ACC: DOC.20070905.0007.

K2.2 DESIGN INPUTS

K2.2.1 EPRI (Electric Power Research Institute) 1994. *Methodology for Developing Seismic Fragilities*. EPRI TR-103959. Palo Alto, California: Electric Power Research Institute. TIC:253770. [DIRS 161329]

K2.2.2 ASCE/SEI 43-05. 2005. *Seismic Design Criteria for Structures, Systems, and Components in Nuclear Facilities*. Reston, Virginia: American Society of Civil Engineers. TIC: 257275. [DIRS 173805]

K2.2.3 BSC (Bechtel SAIC Company) 2007. *CRCF Tier-1 In-Structure Response Spectra*. 060-SYC-CR00-00900-000-00B. Las Vegas, Nevada: Bechtel SAIC Company. ACC: ENG.20071210.0008. [DIRS 184330]

K2.2.4 AISC (American Institute of Steel Construction) 1991. *Manual of Steel Construction, Allowable Stress Design.* 9th Edition, 1st Revision. Chicago, Illinois: American Institute of Steel Construction. TIC: 4254. [DIRS 127579]

K2.2.5 ACI 349-01. 2001. *Code Requirements for Nuclear Safety Related Concrete Structures (ACI 349-01).* Farmington Hills, Michigan: American Concrete Institute. TIC: 252732. [DIRS 158833].

K2.2.6 ANSI/AISC N690-1994. 1994. *American National Standard Specification for the Design, Fabrication, and Erection of Steel Safety-Related Structures for Nuclear Facilities*. Chicago, Illinois: American Institute of Steel Construction. TIC: 252734. [DIRS 158835]

K2.2.7 EPRI (Electric Power Research Institute) 1991. *A Methodology for Assessment of Nuclear Power Plant Seismic Margin (Revision 1).* EPRI NP-6041-SL, Rev. 1. Palo Alto, California: Electric Power Research Institute. TIC: 253771. [DIRS 161330]

K2.2.8 ASME B31.3-2004. 2005. *Process Piping.* New York, New York: American Society of Mechanical Engineers. TIC: 258076. [DIRS 176242]

K2.2.9 Newmark, N.M. and Hall, W.J. 1978. *Development of Criteria for Seismic Review*

of Selected Nuclear Power Plants. NUREG/CR-0098. Washington, D.C.: U.S. Nuclear Regulatory Commission, Office of Nuclear Reactor Regulation. ACC: NNA.19890327.0045. [DIRS 177216]

K2.2.10 MO0801HCUHSSFA.001. *Mean Hazard Curves and Mean Uniform Hazard Spectra for the Surface Facilities Area*. Submittal date: 01/11/2008. [DIRS 184802]

K2.2.11 BSC (Bechtel SAIC Company) 2008. *Canister Receipt and Closure Facility 1 General Arrangement Ground Floor Plan*. 060-P10-CR00-00102-000 REV 00C. Las Vegas, Nevada: Bechtel SAIC Company. ACC: ENG.20080122.0013. [DIRS 184853]

K2.2.12 Moore, D. 2007. "*SSI Factor of Safety.*" E-mail from D. Moore to B. Murray, October 25, 2007. ACC: LLR.20080110.0145. [DIRS 184842]

K2.2.13 BSC (Bechtel SAIC Company) 2006. *Seismic Analysis and Design Approach Document.* 000-30R-MGR0-02000-000 Rev. 001. Las Vegas, Nevada: Bechtel SAIC Company. ACC: ENG.20071220.0029. [DIRS 184494]

K2.3 DESIGN CONSTRAINTS

There are no design constraints in the performance of this calculation

K2.4 DESIGN OUTPUTS

The design outputs are representative fragilities for Yucca Mountain Surface Facilities ITS equipment that are similar to typical nuclear power plant equipment and its anchorage qualified by analysis and including piping and supports, cable trays and supports, and HVAC ducting and supports.

K3. ASSUMPTIONS

K3.1 ASSUMPTIONS REQUIRING VERIFICATION

There are no assumptions in this calculation that require verification.

K3.2 ASSUMPTIONS NOT REQUIRING VERIFICATION

K3.2.1 Design specifications have not been developed for individual equipment qualified by analysis or for piping, cable raceways and ducting including their supports. The general guidance for seismic design in Reference K2.2.13 is utilized to determine what codes and standards will likely govern and what criteria will be used for design of ITS equipment for DBGM-2 and evaluation for BDBGM.

Rationale - The Seismic Analysis and Design Approach requirements will be passed through to equipment designers, and are thus applicable for this calculation.

K4. METHODOLOGY

K4.1 QUALITY ASSURANCE

This calculation is prepared in accordance with Bechtel SAIC LLC procedure

EG-PRO-3DP-G04B-00037, Rev. 10, Reference K2.1.1.

K4.2 USE OF SOFTWARE

Mathcad 14 is used in this calculation. The use of this software is classified as Level 2 software per procedure IT-PRO-0011, Ref. K2.1.2. Therefore the software does not require separate qualification.

K5. LIST OF APPENDICES

APPENDIX K-A 5% Damped In-Structure Response Spectra for CRCF

APPENDIX K-B UHS for 5E-4 APE

APPENDIX K-C Comparison of BDBGM & DBGM-2 ISRS

K6. DEVELOPMENT OF FRAGILITIES

Representative fragilities are developed for typical equipment and subsystems qualified by analysis. The fragilities do not include cranes, and other cask transfer equipment which will have more specific fragilities developed. Most ITS equipment, which is similar to the typical nuclear power plant equipment, will be located at grade level. For purposes of developing representative fragilities, the ground floor of the CRCF will be the reference point for seismic demand.

Passive equipment and anchorage will be qualified by analysis per Reference K2.2.13 requirements. The demand is to be defined by a dynamic analysis or an equivalent static analysis. Reference K2.2.13 requires that ITS equipment be designed for the DBGM-2 and that an evaluation be performed for the BDBGM to show adequate margin. For purposes of this calculation, fragilities for design to DBGM-2 will be developed for each anchorage type and subsystem. A minimum representative fragility is also developed as a sensitivity study for the seismic event sequence analysis to consider if a design is required for BDBGM. The HCLPF from these fragilities are then compared to the BDBGM.

K6.1 DEVELOPMENT OF CAPACITY FACTORS

Capacity factors will be developed for different types of anchorage typically used for equipment and for piping and supports, cable raceways and supports, and for ducting and supports. The passive ITS equipment will be qualified by analysis. In most cases, there will be a substantial margin in passive equipment due to its inherent ruggedness, thus anchorage will typically govern the fragility. For piping, cable raceways and ducting, supports will typically be the governing failure modes.

K6.1.1 Cast in Place Anchor Bolts

Cast-in-place (CIP) anchor bolts are to be designed per the requirements of ACI-349-01, Reference K2.2.5. This category will also include headed studs. Per ACI-349-01, CIP anchor bolts shall be designed so that the bolt will fail before concrete failure. As required by Ref. K2.2.13, Section 11.5, only ductile failure modes of anchorage are permitted in ITS structures. The capacity of cast in place anchor bolts and headed studs is then based on ultimate strength of the steel bolts. Anchor bolts are typically loaded in tension and shear, and interaction equations are used to determine the margin. Per ACI-349 (Sections B.5.1.2 and B.4.4), the design strength for CIP anchor bolts is 0.8 of the specified ultimate tensile strength. Median ultimate strength is 1.1 times

the specified ultimate strength, per Reference K2.2.1.

Per Reference K2.2.1, Tables 3-9 and 3-10, the median tensile ultimate strength in a threaded joint is 90% of the theoretical ultimate strength due to strain concentrations in the threaded region. The minimum strength factor in tension for CIP anchor bolts or headed studs can then be estimated as:

Let Ftu be a typical minimum specified ultimate tensile strength value for say A-36 steel

$Ftu := 58ksi$ Reference K2.2.4

$Pult := 0.9 \cdot 1.1 \cdot Ftu$ Median tensile capacity of bolt

$Pult = 57.42 \cdot ksi$

For equipment mounted on the floors, the dead load negates the seismic-induced tensile load on anchor bolts, i.e., the seismic overturning moment has to overcome the restoring moment before putting uplift force in the anchor bolts. Per past experience with equipment of nuclear power plants located in high seismicity areas, this dead load effect amounts to 10% to 15% of the design allowable. Use 10% of the design allowable as a conservative estimate of dead load stress. It is conservatively assumed in the fragility calculation that (1) the beneficial dead load effect is not considered in the anchorage design and (2) the anchorage is designed such that the seismic stress is at the code design strength, i.e., Pseismic = Pall.

$Pall := 0.8 \cdot Ftu$ Code design strength (Sections B.4.4 and B.5.1.2 of Reference K2.2.5)

$Pall = 46.4 \cdot ksi$

$NL := 0.1 \cdot Pall$ Dead load effects

$NL = 4.64 \cdot ksi$

$F_{S\_t} := \frac{Pult + NL}{Pall}$ Median strength factor

$F_{S\_t} = 1.337$

Next consider a case of pure shear on the full body of the anchor bolt.

$Vall := (0.75) \cdot (0.6 \cdot Ftu)$ Where 0.75 is the strength reduction factor of a ductile steel element in shear (Section B.4.4 of Reference K2.2.5) and 0.6Ftu is the nominal shear strength for cast-in headed bolt anchors (Section B.6.1.2(b) of Reference K2.2.5).

$Vult := 0.62 \cdot Ftu \cdot 1.1$ Reference K2.2.1, Table 3-10.

$F_{S\_v} := \frac{Vult}{Vall}$

$F_{S\_v} = 1.516$

The pure shear case has slightly higher margin to failure considering the applied stress to be equal to the design strength.

$$F_{S\_CIP} := \frac{F_{S\_v} + F_{S\_t}}{2}$$

$$F_{S\_CIP} = 1.427$$

From Reference K2.2.1, Table 3-10

$\beta_{U\_v} := 0.10$ For pure shear failure

$\beta_{U\_t} := 0.13$ For tensile failure

$$\beta_{c\_CIP} := \frac{\beta_{U\_v} + \beta_{U\_t}}{2} \qquad \beta_{c\_CIP} = 0.115$$

The failure is ductile locally, but on a system ductility basis, there would be little ductility. Thus no credit is taken for ductility (Page 8-16 of Reference K2.2.1) Hence, the Capacity Factor and variability are equal to the Strength Factor and its variability.

$F_{\mu\_CIP} := 1.0$

$\beta_{\mu c\_CIP} := 0$

K6.1.2 Welded Anchorage

Equipment such as electrical cabinets are typically welded to embeds using fillet welds. The welds are loaded primarily in transverse shear due to overturning and shear normal to the weld line. In some cases, short heavy equipment welded to embeds primarily loads the welds in longitudinal shear along the line of weld and transverse shear normal to the line of weld. Per Reference K2.2.1, Table 3-10, fillet welds in longitudinal shear have a median ultimate strength of 0.84 times the median ultimate tensile strength of the weld rod. Fillet welds loaded on transverse shear have an ultimate strength of 1.26 times the ultimate tensile strength of the weld rod. In both cases, the weld area is based on the throat of the fillet weld. Thus, the governing case would be when there is virtually equal shear in two horizontal directions and very little shear from overturning. If the 100-40-40 earthquake phasing rule (Reference K2.2.9) is applied, the governing shear would be 100% longitudinal and 40% transverse. Typically E-70 electrodes are used with an ultimate tensile strength of 70ksi. The median ultimate tensile strength would then be 1.1 times this specified value (Table 3-9 of Ref. K2.2.1). The average ultimate shear strength would then be:

$Fv\_ult\_long := 0.84 \cdot 70ksi \cdot 1.1$

$Fv\_ult\_tran := 1.26 \cdot 70ksi \cdot 1.1$

The failure depends upon the angle of the shear vector. For 100-40 phasing of two equal horizontal earthquakes, the shear vector angle, θ, is defined as:

$$\tan(\theta) := \frac{0.4}{1}$$

$$\theta := 0.3806$$

$V := \left(1^2 + 0.4^2\right)^{0.5}$ shear vector at angle θ

$R := 0.5 \cdot \sin(\theta)^{1.5} + 1$ Per Reference K2.2.7, Appendix P, Eq. P-10

Thus for a 100% load longitudinal and 40% load tangential the ultimate shear capacity is R times the Fv_ult_long of the weld for comparison to the vector shear.

The allowable weld stress per Ref. K2.2.6 is:

$fv\_all := 1.6 \cdot (0.3 \cdot 70)ksi$ 0.3 brings the ultimate electrode stress of 70ksi to the allowable of 21ksi, and 1.6 is the stress limit coefficient for extreme loads per Reference K2.2.6

$$F_{S\_weld} := R \cdot \frac{Fv\_ult\_long}{fv\_all}$$

$F_{S\_weld} = 2.143$

Per Ref. K2.2.1, Table 3-10,

$\beta_{U\_weld} := 0.19$

$\beta_{c\_weld} := \beta_{U\_weld}$

Welds are a brittle failure mode, thus the ductility factor is 1.0 and the Capacity Factor and its variability are equal to the Strength Factor and its variability.

$F_{\mu\_weld} := 1.0$

$\beta_{\mu c\_weld} := 0$

K6.1.3 Post-Installed Anchors

Reference K2.2.13 specifies in Section 11.5, only ductile failures are permitted in ITS structures. Slip failures and concrete failures are not permitted. Thus, if expansion anchors are used, they must be of the undercut type. Reference K2.2.13 also states that the allowable design capacities should be based on the manufacturers recommendations and include a minimum factor of safety of 4 applied to the mean ultimate capacity. The manufacturer's test data should be current and approved by an independent approval authority. Expansion anchor test data tend to be normally distributed. On this basis, it is considered that the median factor of safety is 4.0 for governing cases where all load is seismic.

It should be noted that the specification of a minimum factor of safety of 4 does not follow current

practice for the design of post-installed anchors. Post-installed anchors are currently designed following ACI-349-01 (Ref. K2.2.5) with the only difference with CIP anchor design being that post-installed anchors shall be tested before use to verify that they are capable of sustaining their design strength in cracked concrete under seismic loads (Section B.3.3 of Ref. K2.2.5). The Reference K2.2.5 provisions and commentary do not mention a required factor of safety of 4. The factor of safety of 4 is used based on its specification in Reference K2.2.13, Section 11.5.

There can be cases though for supports of piping, cable raceways, wall panels, etc where dead load can result in tension. Also, for floor mounted equipment, the dead load negates the seismic-induced tensile load on anchor bolts, i.e., the seismic overturning moment has to overcome the restoring moment before putting uplift force in the anchor bolts. As discussed in Section K6.1.1, per past experience with equipment of nuclear power plants located in high seismicity areas, this dead load effect amounts to 10% to 15% of the design allowable. In both of these cases, the median factor of safety relative to seismic loading would be higher. Consider a conservative case where the dead load effect is only 10% of the allowable capacity of 0.25 Pult and seismic is 90% of the allowable capacity.

$$F_{S\_exp} := \frac{Pult + \frac{0.10 \cdot Pult}{4}}{0.9 \cdot \frac{Pult}{4}} \qquad F_{S\_exp} = 4.6$$

Note that when the dead weight is 15% of the allowable capacity and seismic is 85% of the allowable capacity, the resulting strength factor is 4.9.

Expansion anchor capacities have large uncertainty. Use the uncertainty in Ref. K2.2.1, Table 9-3 for cracks being unlikely (consistent with quality installation with special inspection). Note that this uncertainty is consistent with expansion anchors designed with a factor of safety of 4 against test data. For ductile undercut anchors designed per current criteria, (Reference K2.2.5), this uncertainty would be expected to be similar to that for cast in place anchors.

$$\beta_{U\_exp} := 0.42$$ Reference K2.2.1, Table 9-3

There can be cases where the margin is less where only vertical weight and seismic loading contribute to failure. Likewise, when expansion anchors are used to anchor equipment to the floor, dead weight counteracts seismic induced tensile loading. Consider a case where tension from dead weight is 0 and all load is seismic. Then, the FS would be 4. Let FS = 4 be a 95th percentile case (-1.65 log standard deviations)

$$\beta_{U\_load} := \frac{1}{1.65} \cdot \ln\left(\frac{4.6}{4}\right) \qquad \beta_{U\_load} = 0.085$$

$$\beta_{c\_exp} := \left(\beta_{U\_exp}^{2} + \beta_{U\_load}^{2}\right)^{0.5}$$

$$\beta_{c\_exp} = 0.428$$

The failure is ductile locally but on a system ductility basis, there would be little ductility, thus no credit is taken for ductility. Hence, the Capacity Factor & β are equal to the Strength Factor and its β.

$F\mu\_exp := 1.0$

$\beta\mu c\_exp := 0$

K6.1.4 Piping and Supports

Welded steel piping is very ductile and historically it does not fail in earthquakes unless there are large seismic anchor movements such as a tank sliding to which the piping is attached. In development of fragilities, it has always been found that piping supports are theoretically more vulnerable than piping. Therefore, the representative fragility for piping will be based on piping support failure. For critical piping in the CRCF, it is assumed that it is designed to the ASME B31.3 code for process piping (Reference K2.2.8). Supports would typically be designed as structural steel members using common structural profiles of low carbon steel, thus supports are assumed to be designed to the ANSI/AISC N-690 code. For low carbon steel such as A-36, the working stress allowable is 0.6 of the yield strength. For extreme loads, N-690 allows a 1.6 increase in load.

$Fu := 58ksi$

$Fy := 36ksi$

$S := 0.6 \cdot 1.6 \cdot Fy \qquad S = 34.56 \cdot ksi$ Stress limit for extreme loads

Consider that pipe supports would typically be loaded in bending and may be open sections. The plastic shape factors for these open section would be less than for a solid section. Let the plastic shape factor be about 1.25. A plastic hinge would form when the section was fully plastic. Per Ref. K2.2.1, median yield for structural steel such as A-36 is 1.2 times specified.

$F\_hinge := 1.25 \cdot 1.2 \cdot Fy$

$F\_hinge = 54 \cdot ksi$

For cantilevered supports, some capacity is used up by dead weight.

Let DW = 20% of S Based on experience

$DW := 0.2 \cdot S$

Thus, the strength factor of safety can be computed as

$$F_{S\_supp} := \frac{F\_hinge - DW}{S - DW}$$

$F_{S\_supp} = 1.703$

The failure mode is considered to be ductile. ASCE/SEI-43, Reference K2.2.2 has guidance on ductility factors appropriate for different limit states in equipment and supports. At just less than ultimate failure, limit state A ductility factors can be used. The limit state A ductility factor for equipment supports is 2.0 from Table 8-1 of Ref. K2.2.2.

$F_{\mu\_supp} := 2.0$

$$F_{C\_supp} := F_{S\_supp} \cdot F_{\mu\_supp}$$

$$F_{C\_supp} = 3.406$$

This is greater than the strength factor developed for welds but the uncertainty would be higher. Use FC_supp for the capacity of piping and compute an appropriate uncertainty. Let the onset of code yield be a 99 percentile value (-2.33βc). Then the factor to code yield is:

$$F_{C\_yield} := \frac{Fy - DW}{S - DW}$$

$$F_{C\_yield} = 1.052$$

$$\beta_{c\_supp} := \frac{1}{2.33} \cdot \ln\left(\frac{F_{C\_supp}}{F_{C\_yield}}\right) \qquad \beta_{c\_supp} = 0.504$$

K6.1.5 Cable Raceways

Reference K2.2.13 does not specifically address cable raceways. Typically in nuclear plants with engineered cable raceways, they are supported by steel structural members and designed to the AISC structural steel code. For the Yucca Mountain Project it is specified that structural steel would be designed to ANSI/AISC N-690. Working stress levels would nominally be 0.6 times Fy. Stress limit for seismic design would be 1.6 times this value. For typical support structures, low carbon steel such as A36, would be used.

$$S\_CT := 1.6 \cdot 0.6 \cdot Fy \qquad S\_CT = 34.56 \cdot ksi$$

Consider cantilevered supports where dead load would use up some of the stress limit. As discussed above in piping support, dead load effect on the supports is estimated to be about 20% of the stress limit per past experience on nuclear power plant piping.

$$DL := 0.2 \cdot S\_CT$$

Thus, the strength factor of safety can be computed as

$$F_{S\_CT} := \frac{F\_hinge - DL}{S\_CT - DL}$$

$$F_{S\_CT} = 1.703$$

Per Ref. K2.2.2, Table 8-1, the limit state A ductility for equipment supports is 2.0

$$F_{\mu\_CT} := 2.0$$

Consider the plastic hinge capacity to be the same as derived for piping supports

$$F_{C\_CT} := F_{S\_CT} \cdot F_{\mu\_CT}$$

$$F_{C\_CT} = 3.406$$

Consider the onset of code yield as a 99 percentile confidence value (-2.33 βc)

$$F_{C\_y} := \frac{Fy - DL}{S\_CT - DL}$$

$$\beta_{c\_CT} := \frac{1}{2.33} \cdot \ln\left(\frac{F_{C\_CT}}{F_{C\_y}}\right)$$

$$\beta_{c\_CT} = 0.504$$

K6.1.6 Ducting

Engineered ITS ducting would have supports constructed of steel profiles that are welded to embeds, to steel structural members or to base plates that are attached to concrete structures with expansion anchors. The ducting itself would be standard construction detail used in NPPs. Typically, if the supports don't fail, the ducting would not fail. Reference K2.2.13 does not specifically address ducting. It is implied that structural supports would be designed to the requirements of ANSI/AISC N-690, Ref. K2.2.6, and the capacity factor would be the same as derived for cable tray supports.

$$F_{C\_duct} := F_{C\_CT}$$

$$\beta_{c\_duct} := \beta_{c\_CT}$$

K6.2 EQUIPMENT RESPONSE

The equipment response factor will vary depending upon the frequency of the equipment and the method of analysis. The demand spectra for the CRCF at the ground floor will be used for all equipment locations for the purposes of this representative calculation. NPP equipment is typically fairly stiff with a fundamental frequency of 8 Hz or greater. For engineered piping, the fundamental frequency range is typically less than 5 Hz but greater than 1 Hz. For cable trays and ducting that are ITS, and designed for the seismic event, the fundamental frequency is estimated to be in the in the 4 to 8 Hz range. Cable trays and ducting with engineered supports would tend to be stiffer than piping since the supports are generally spaced closer together. It is not known how the cable trays and ducting will be evaluated for seismic events. They will likely be designed using equivalent static coefficient methods but response spectrum analysis may also be conducted in some cases or as a benchmark to verify the static coefficient methods. For purposes of this fragility calculation, the demand will be based on envelope response spectrum analysis or an equivalent static coefficient analysis as specified in Reference K2.2.13.

The variables to consider for equipment response are:

- Qualification method
- Damping
- Modeling
- Mode combination
- Earthquake Direction

K6.2.1 Equipment Response For Anchorage

As stated in K6.2, the equipment is considered to have a fundamental frequency of 8 Hz or greater. Most equipment will likely be evaluated for seismic events using static coefficient methods using either the peak of the response spectrum (conservative) or the spectral acceleration at a calculated fundamental frequency. For purposed of this calculation the less conservative option of calculating a fundamental frequency is used. The demand is defined as the DBGM-2 site wide spectral acceleration at the calculated fundamental frequency.

K6.2.1.1 Qualification Method

Since some form of dynamic analysis will be conducted to define the fundamental frequency of the component. Consequently there is no bias in the qualification method.

$$F_{QM\_1} := 1.0$$

$$\beta_{c\_QM\_1} := 0$$

The other factor of safety to be considered under the qualification method is the conservatism in the broadened and smoothed design floor response spectra. Nodes 22 and 24 represent the base mat and the resulting response spectra at each node are similar. Use node 24 spectra as shown in Appendix K-A. The median response case is taken as the 100 foot soil depth case using median soil properties. Uncertainty is determined from the difference between upper bound, median and lower bound soil properties. The following tables (K6-1, K6-2, and K6-3) present comparison of the site wide broadened and smoothed spectra to the average median soil spectra. Digitized 5% damped spectra for node 24 of the CRCF from Reference K2.2.3 are used. See Appendix K-A for spectra plots.

Table K6-1 5% Damped Design ISRS and 100' and 200' Alluvium Depths ISRS at Ground Floor (X-Direction)

Direction X			
Frequency	Sa Des	Sa Med	Des/Med
1	0.64	0.44	1.45
2	1.11	0.96	1.16
3	1.39	1.24	1.12
4	1.49	1.43	1.04
5	1.49	1.41	1.06
6	1.49	1.23	1.21
8	1.49	0.99	1.51
10.9	0.93	0.62	1.50
15	0.93	0.84	1.11
20	0.88	0.63	1.40
30	0.76	0.59	1.29

Table K6-2 5% Damped Design ISRS and 100' and 200' Alluvium Depths ISRS at Ground Floor (Y-Direction)

Direction Y			
Frequency	Sa Des	Sa Med	Des/Med
1	0.65	0.47	1.38
2	1.10	0.91	1.21
3	1.36	1.22	1.11
4	1.54	1.41	1.09
5	1.54	1.40	1.10
6	1.54	1.24	1.24
8	1.54	0.81	1.90
10.4	0.92	0.64	1.44
15	0.92	0.75	1.23
20	0.84	0.70	1.20
30	0.69	0.53	1.30

Table K6-3 5% Damped Design ISRS and 100' and 200' Alluvium Depths ISRS at Ground Floor (Z-Direction)

Direction Z			
Frequency	Sa Des	Sa Med	Des/Med
1	0.31	0.23	1.35
2	0.60	0.46	1.30
3	0.77	0.59	1.31
4	0.89	0.77	1.16
5	0.99	0.88	1.13
6	1.07	0.92	1.16
8.22	1.20	0.96	1.25
10	1.20	1.14	1.05
15	1.20	0.78	1.54
20	0.87	0.48	1.81
30	0.44	0.35	1.26

The equipment is considered to be rigid in the vertical direction. Anchorage demand is primarily governed by horizontal demand. From the above tables, The minimum margin in spectral shape above 8 Hz is 1.11 in the X direction

$$F_{QM\_2} := 1.11$$

Let the broadened and smoothed design floor response spectra be a 95th percentile demand (-1.65 βc)

$$\beta_{c\_QM\_2} := \frac{1}{1.65} \cdot \ln(1.11)$$

$$\beta_{c\_QM\_2} = 0.063$$

$$F_{QM} := F_{QM\_1} \cdot F_{QM\_2} \qquad F_{QM} = 1.11$$

$$\beta_{c\_QM} := \sqrt{\beta_{c\_QM\_1}{}^2 + \beta_{c\_QM\_2}{}^2} \qquad \beta_{c\_QM} = 0.063$$

K6.2.1.2 Damping

Design damping is stated in Reference K2.2.13 to be as defined in ASCE/SEI 43-05, Reference K2.2.2. For electrical and other equipment at level 2 response, the damping is 4%. This is slightly conservative. Per Ref. K2.2.1, median damping for electrical cabinets and equipment would be 5% with a minus 1β of 3.5%.

The minimum structural response factor was for direction X at 15 Hz. Compare damping at 15 Hz.

$Sa\_5\% := 0.93g$ Design Spectra

$Sa\_4\% := 0.99g$

$$F_\delta := \frac{Sa\_4\%}{Sa\_5\%}$$

$F_\delta = 1.065$

$Sa\_5 := 0.84g$ These are 5%, 4%, and 3% damped spectral values at 15 Hz from the median ISRS (Ref. K2.2.3).

$Sa\_4 := 0.89g$

$Sa\_3 := 0.95g$

$$Sa\_1\beta := \frac{Sa\_4 + Sa\_3}{2}$$ 3.5% damped spectral acceleration

$$\beta_{c\_\delta} := \ln\left(\frac{Sa\_1\beta}{Sa\_5}\right)$$

$\beta_{c\_\delta} = 0.091$

K6.2.1.3 Modeling

Modeling is assumed to be median centered. Often for equipment, very simple models are used to determine the fundamental frequency. Let the 1β uncertainty in frequency be 0.15. (The resulting β is within the range of Ref. K2.2.1 on Pages 3-17, 3-18, and 3-49).

$F_M := 1.0$

$fn\_\beta := 15 \cdot e^{-.15} Hz \qquad fn\_\beta = 12.911 \cdot Hz$

Use median soil spectra for modeling uncertainty.

$Sa\_\beta := 0.75g$

$Sa\_15 := 0.84g$

$$\beta_{c\_M} := \ln\left(\frac{Sa\_15}{Sa\_\beta}\right) \qquad \beta_{c\_M} = 0.113$$

K6.2.1.4 Mode Combination

Equipment is considered to be primarily a single mode. Some contribution from higher modes is likely.

$$F_{MC} := 1.0$$

$$\beta_{c\_MC} := 0.10$$

K6.2.1.5 Earthquake Component Combination

The 100-40-40 rule is specified in Ref. K2.2.13. This is considered to be median centered. Geometry of the anchorage pattern determines the random variability in response to random phasing of earthquake components. Consider that the two horizontal direction demands are equal and in phase and are a $-3\beta_R$ case and that the anchorage pattern is square. The in phase demand is the vector of two equal components, whereas the vector demand for 100-40 phasing is median (only two components are included since the vertical component does not appreciably affect the anchorage).

$$F_{ECC} := 1.0$$

$$Vector\_med := \left(1.00^2 + 0.40^2\right)^{0.5}$$

$$Vector\_inphase := 1.414$$

$$\beta_{c\_ECC} := \frac{1}{3}\cdot\ln\left(\frac{Vector\_inphase}{Vector\_med}\right)$$

$$\beta_{c\_ECC} = 0.091$$

K6.2.1.6 Equipment Response for Anchorage

$$F_{RE} := F_{QM}\cdot F_{\delta}\cdot F_{M}\cdot F_{MC}\cdot F_{ECC}$$

$$F_{RE} = 1.182$$

$$\beta_{c\_RE} := \left(\beta_{c\_QM}^2 + \beta_{c\_\delta}^2 + \beta_{c\_M}^2 + \beta_{c\_MC}^2 + \beta_{c\_ECC}^2\right)^{0.5}$$

$$\beta_{c\_RE} = 0.208$$

K6.2.2 Equipment Response for Piping

Piping systems are more complex and at a lower frequency than most equipment. It is a common practice that piping is designed by dynamic response spectrum modal analysis using the envelope of the support point spectra and that damping is in accordance with Ref. K2.2.2 at 5%.

K6.2.2.1 Qualification Method

The envelope response spectrum analysis method is generally quite conservative relative to multi support time history analysis. However, for a case where all input spectra at the support points are the same, there should be no bias in the method itself.

$$F_{QM\_1} := 1.0$$

$$\beta_{c\_QM\_1} := 0$$

Consider the dominant frequency range of piping qualified by dynamic analysis to be 1 to 5 Hz. From the comparison tables of site wide broadened and smoothed spectra to median soil response spectra (Section K6.2.1.1), the conservatism in the range of 1-5 Hz is 1.04 to 1.45. Use the average.

$$F_{QM\_2} := \frac{1.04 + 1.45}{2}$$

$$F_{QM\_2} = 1.245$$

Let the range be plus to minus 95% confidence bounds (plus or minus 1.65 β)

$$\beta_{c\_QM\_2} := \frac{1}{2 \cdot 1.65} \cdot \ln\left(\frac{1.45}{1.04}\right)$$

$$\beta_{c\_QM\_2} = 0.101$$

$$F_{QM} := F_{QM\_1} \cdot F_{QM\_2} \qquad F_{QM} = 1.245$$

$$\beta_{c\_QM} := \sqrt{\beta_{c\_QM\_1}^{2} + \beta_{c\_QM\_2}^{2}} \qquad \beta_{c\_QM} = 0.101$$

K6.2.2.2 Damping

5% damping used for design is considered to be median centered. The uncertainty is the same as for equipment.

$$F_{\delta\_pipe} := 1.0$$

$$\beta_{c\_\delta\_pipe} := \beta_{c\_\delta}$$

$$\beta_{c\_\delta\_pipe} = 0.091$$

K6.2.2.3 Modeling

Current methods of modeling piping are considered to be median centered. Uncertainty is greater though due to the complexity of the modeling and due to the fact that the dominant frequencies are on a steep slope of the response spectrum from 1-5 Hz. Let the uncertainty be 0.2 to cover frequency and mode shape uncertainty.

$$F_{M\_pipe} := 1.0$$

$$\beta_{c\_M\_pipe} := 0.2$$

K6.2.2.4 Mode Combination

Many modes participate in piping response. The typical combination of modes in modern piping programs is by SRSS with various options for closely spaced modes and missing mass. These method are considered to be median centered. The random variability of mode combination for complex systems per Ref. K2.2.1 is 0.15.

$$F_{MC\_pipe} := 1.0$$

$$\beta_{c\_MC\_pipe} := 0.15$$

K6.2.2.5 Earthquake Component Combination

All three directions can have significant contribution to piping response. Consider the vector of 100-40-40 response to be median demand with vertical response at 2/3 of horizontal. Consider the vector of in-phase response to be a 3β extreme.

$$F_{ECC\_pipe} := 1.0$$

$$Vec\_med := \left[1^2 + 0.4^2 + \left(0.4 \cdot \frac{2}{3}\right)^2\right]^{0.5}$$

$$Vec\_inphase := \left[1^2 + 1^2 + \left(\frac{2.}{3}\right)^2\right]^{0.5}$$

$$\beta_{c\_ECC\_pipe} := \frac{1}{3} \cdot \ln\left(\frac{Vec\_inphase}{Vec\_med}\right)$$

$$\beta_{c\_ECC\_pipe} = 0.114$$

K6.2.2.6 Response for Piping

$$F_{RE\_pipe} := F_{QM} \cdot F_{\delta\_pipe} \cdot F_{M\_pipe} \cdot F_{MC\_pipe} \cdot F_{ECC\_pipe}$$

$$F_{RE\_pipe} = 1.245$$

$$\beta_{c\_RE\_pipe} := \left(\beta_{c\_QM}^2 + \beta_{c\_M\_pipe}^2 + \beta_{c\_MC\_pipe}^2 + \beta_{c\_ECC\_pipe}^2\right)^{0.5}$$

$$\beta_{c\_RE\_pipe} = 0.293$$

K6.2.3 Equipment Response for Cable Trays

Cable tray systems are typically designed by static coefficient methods whereas typical spans and support designs are generically derived from limited dynamic analyses of representative systems. The static coefficient method for complex systems is specified in Ref. K2.2.13 and requires that 1.5 times the peak of the spectrum be used as the equivalent static demand. Damping specified in Ref. K2.2.13 is as defined in Ref. K2.2.2 and would be 10% for level 2 response. At or near failure, Level 3 response at 15% damping would be considered median. Also, Ref. K2.2.1 suggests that 15% is median.

K6.2.3.1 Qualification Method

The static coefficient method using 1.5 times the peak of the spectrum is considered to be very conservative. Numerous studies have been conducted of piping systems to determine the peak response for comparison to static coefficient methods. The peak response relative to the peak spectral acceleration of the applicable spectra varies considerably for support loads, maximum moment and maximum acceleration. In general, using a static coefficient of 1.0 times the peak of the spectrum is somewhat conservative relative to a median response. Use 1.0 times the peak of the spectrum as median and 1.5 as a 98% confidence level (2β case)

$$F_{QM\_cable\_1} := 1.5$$

$$\beta_{c\_QM\_cable\_1} := \frac{1}{2}\cdot\ln(1.5)$$

$$\beta_{c\_QM\_cable\_1} = 0.203$$

Consider that bias in the design response spectra is already incorporated into the qualification method factor and uncertainty.

$$F_{QM\_cable\_2} := 1.0$$

$$\beta_{c\_QM\_cable\_2} := 0$$

$$F_{QM\_cable} := F_{QM\_cable\_1}\cdot F_{QM\_cable\_2} \qquad F_{QM\_cable} = 1.5$$

$$\beta_{c\_QM\_cable} := \sqrt{\beta_{c\_QM\_cable\_1}^{2} + \beta_{c\_QM\_cable\_2}^{2}}$$

$$\beta_{c\_QM\_cable} = 0.203$$

K6.2.3.2 Damping

10% is used for design and 15% is used for median. The in-structure spectra in Ref. K2.2.3 only extend out to 10%. Use the amplifications in Reference K2.2.9 to determine the relative amplified accelerations for 10% and 15% damping. Per Ref. K2.2.9, Table 2, for the amplified acceleration range:

$Amp\_10 := 3.21 - 0.68\cdot\ln(10)$ 10% damped amplification factor

$Amp\_15 := 3.21 - 0.68\cdot\ln(15)$ 15% damped amplification factor

$$F_{\delta\_cable} := \frac{Amp\_10}{Amp\_15}$$

$$F_{\delta\_cable} = 1.201$$

Per Ref. K2.2.1, 10% damping is $-1\beta U$

$$\beta_{c\_\delta\_cable} := \ln\left(\frac{Amp\_10}{Amp\_15}\right)$$

$$\beta_{c\_\delta\_cable} = 0.184$$

K6.2.3.3 Modeling

Any uncertainties in modeling when using the static coefficient method are included in the Qualification Method.

$F_{M\_cable} := 1.0$

$\beta_{c\_M\_cable} := 0$

K6.2.3.4 Mode Combination

Mode combination is included in the static coefficient factor and uncertainty.

$F_{MC\_cable} := 1.0$

$\beta_{c\_MC\_cable} := 0$

K6.2.3.5 Earthquake Component Combination

The design is by use of the median centered 100-40-40 combination. The response to the phasing of the three direction of earthquake is similar to that for piping.

$F_{ECC\_cable} := 1.0$

$\beta_{c\_ECC\_cable} := \beta_{c\_ECC\_pipe}$

K6.2.3.6 Equipment Response for Cable Trays

$F_{RE\_cable} := F_{QM\_cable} \cdot F_{\delta\_cable} \cdot F_{M\_cable} \cdot F_{MC\_cable} \cdot F_{ECC\_cable}$

$F_{RE\_cable} = 1.802$

$\beta_{c\_RE\_cable1} := \beta_{c\_QM\_cable}^2 + \beta_{c\_\delta\_cable}^2$

$\beta_{c\_RE\_cable2} := \beta_{c\_M\_cable}^2 + \beta_{c\_MC\_cable}^2 + \beta_{c\_ECC\_cable}^2$

$\beta_{c\_RE\_cable} := \left(\beta_{c\_RE\_cable1} + \beta_{c\_RE\_cable2}\right)^{0.5}$

$\beta_{c\_RE\_cable} = 0.296$

K6.2.4 Equipment Response for Ducting

Ducting is typically designed by equivalent static methods the same as for cable trays. The only significant difference in the ducting response versus cable tray response is in the damping. Ducting will generally remain elastic. There is no guidance on damping for ducting in Reference K2.2.13 or K2.2.2. Ducting would remain elastic and elastic damping values would typically be used for design which would conservatively be considered median at failure of ducting supports, thus the damping factor is 1.0. The uncertainty in response due to damping is considered the same as for piping.

$F_{\delta\_duct} := 1.0$

$\beta_{c\_\delta\_duct} := \beta_{c\_\delta\_pipe}$

$F_{RE\_duct} := \frac{F_{RE\_cable} \cdot F_{\delta\_duct}}{F_{\delta\_cable}}$

$F_{RE\_duct} = 1.5$

$\beta_{c\_RE\_duct} := \left(\beta_{c\_RE\_cable}^{2} - \beta_{c\_\delta\_cable}^{2} + \beta_{c\_\delta\_duct}^{2}\right)^{0.5}$

$\beta_{c\_RE\_duct} = 0.25$

K6.3 STRUCTURAL RESPONSE

K6.3.1 Spectral Shape Factor

This factor accounts for conservatism in the site-wide DBGM-2 design spectrum. The depth of alluvium at the Surface Facilities Area (SFA) varies from 30 feet to 200 feet. Uniform hazard spectra at the surface are calculated from site response analyses for alluvium depths of 30', 70', 100' and 200'. The site-wide design ground response spectrum is the envelope of the surface spectra of these four alluvium depths (Reference K2.2.10; also Section 6.2.2.1 for source information).

The best-estimate horizontal dominant frequency of the soil-structure system is 5.2 Hz for the CRCF at 100-foot alluvium of median properties (Attachment 1 of Reference K2.2.3). At this frequency:

$SA_{site} := 1.14g$ 5% damped site-wide spectral acceleration (Appendix K-B).

$SA_{100} := 1.06 \cdot g$ 5% damped spectral acceleration of the 100-foot best-estimate alluvium depth case in the northeast area where the preclosure surface facilities are located.

$F_{SA} := \frac{SA_{site}}{SA_{100}}$

$F_{SA} = 1.075$

Since uncertainty in the UHS is derived from uncertainty in the seismic hazard curves which will be included in the final risk quantification, no uncertainty is included under the spectral shape factor to avoid double-counting the hazard uncertainty, hence

$\beta_{U\_SA} := 0$

$\beta_{R\_SA} := 0.20$ Random variability to account for peak-to-valley variability of the smoothed UHS (Reference K2.2.1, Table3-2).

$\beta_{c\_SA} := \sqrt{\beta_{U\_SA}^{2} + \beta_{R\_SA}^{2}}$ $\beta_{c\_SA} = 0.2$

K6.3.2 Damping Factor

This factor is to account for conservatism in the hysteresis damping of the building structure used in the seismic response analysis. Due to the high radiation damping of the foundation media, the effect of structure damping is insignificant. Thus,

$F_{\delta} := 1.0$

$\beta_{U\_\delta} := 0$ Since a conservative median factor of safety is used for structure damping, no value is assigned to the uncertainty logarithmic standard deviation.

$\beta_{R\_\delta} := 0$

$\beta_{c\_\delta} := \sqrt{\beta_{U\_\delta}^{2} + \beta_{R\_\delta}^{2}}$

$\beta_{c\_\delta} = 0$

K6.3.3 Modeling Factor

The Tier 1 lumped mass multiple-stick model of the CRCF includes the stiffness of various reinforced concrete walls and distribution of mass at each floor. The floors are assumed to be rigid diaphragms tying the different sticks together. Torsional response of the structure is captured through modeling eccentricity between the center of mass and center of rigidity of each floor. The foundation media underneath the buildings are modeled with soil springs and dashpots based on elastic half space theory with adjustment to account for layering effect of alluvium overlying tuff. Per Reference K2.2.12, BSC recognizes that final design will be accomplished by a more explicit finite element model and it is acceptable to consider the modeling factor to be median centered in these seismic fragility evaluations, thus

$F_{M} := 1.0$

$\beta_{R\_M} := 0$ Since there is no randomness in modeling.

Uncertainty of structure frequencies predicted from mathematical modeling varies from 0.15 to 0.35 depending on the sophistication of the model (Reference K2.2.1). The value of 0.35 is for a fairly approximate model and the value 0.15 is appropriate for a detailed model. Based on the complexity of the CRCF structure and the mathematical model used for the Tier 1 ISRS analysis, it is judged that the calculated CRCF frequency has a logarithmic standard deviation of 0.25.

$\beta_{f} := 0.25$ Uncertainty in building frequency.

$f_{m} := 5.2 \cdot Hz$ Best-estimate frequency

$f_{upper} := f_{m} \cdot e^{\beta_{f}}$ Upper bound frequency

$f_{upper} = 6.677 \cdot Hz$

$SA_{upper} := 1.05g$ 5% damped spectral acceleration at f_{upper} read off from the mean 5E-4 UHS of the 100-foot alluvium depth case (Appendix K-B). This value is less than the value at the best-estimate frequency.

$f_{lower} := f_m \cdot e^{-\beta_f}$ Lower bound frequency

$f_{lower} = 4.05 \cdot Hz$

$SA_{lower} := 1.02 \cdot g$ 5% damped spectral acceleration at f_{lower} read off from the mean 5E-4 UHS of the 100-foot alluvium depth case. This value is less than the value at the best-estimate frequency.

$\beta_{U\_f} := 0$ Since the spectral value at the best-estimate frequency is greater than that at either the lower bound or upper bound frequency.

$\beta_{U\_ms} := 0.15$ Uncertainty of mode shape (Reference K2.2.1, page 3-18)

$\beta_{U\_M} := \sqrt{\beta_{U\_f}^2 + \beta_{U\_ms}^2}$

$\beta_{U\_M} = 0.15$

$\beta_{c\_M} := \sqrt{\beta_{R\_M}^2 + \beta_{U\_M}^2}$

$\beta_{c\_M} = 0.15$

K6.3.4 Modal Combination

Since the direct integration time history method is used in the Tier 1 ISRS analysis (Reference K2.2.3), the modal combination method factor of safety is unity and there is no variability associated with modal combination.

$F_{MC} := 1$

$\beta_{R\_MC} := 0$

$\beta_{U\_MC} := 0$

$\beta_{c\_MC} := \sqrt{\beta_{R\_MC}^2 + \beta_{U\_MC}^2}$

$\beta_{c\_MC} = 0$

K6.3.5 Soil-Structure Interaction

The Tier 1 seismic response analyses of the CRCF used the site-wide $5*10^{-4}$ mean uniform hazard spectra as the DBGM-2 input motion. Spectrum compatible time histories are used as the input motion for the time history analyses. The conservatism in the site-wide spectra was accounted for in the spectral shape factor above. Strain compatible soil properties of 100-foot and 200-foot deep alluvium are used to calculate frequency-independent soil springs and soil damping coefficients. Soil radiation damping is introduced into the model by using dashpots. Damping coefficients equal to 75% of the computed values for translational degrees of freedom

and to the full computed rotational damping values are used in the response analyses (Reference K2.2.3). Conservatism or unconservatism in SSI will be minimized for final SSI analyses used to develop equipment design seismic input. Before the final SSI analyses are completed, the Tier 1 SSI analysis is taken to represent the best-estimate responses per BSC recommendations in Reference K2.2.12.

$F_{SSI\_1} := 1.0$

$\beta_{R\_SSI\_1} := 0$

$\beta_{U\_SSI\_1} := 0.25$ Uncertainty of the median-centered state-of-the-art SSI method based on past probabilistic seismic response analyses using the same method.

$\beta_{c\_SSI\_1} := \sqrt{\beta_{R\_SSI\_1}^{2} + \beta_{U\_SSI\_1}^{2}}$

$\beta_{c\_SSI\_1} = 0.25$

It is judged that the median seismic capacity of the equipment, expressed in terms of peak ground acceleration, is close to that of BDBGM. Due to soil nonlinearity, amplification of the input ground motion at BDBGM will be different from that of DBGM-2. The second factor of safety is to account for this difference and is estimated using the DBGM-2 raw spectra and the BDBGM raw spectra at different frequencies as shown in the table below.

Table K6-4 Comparison of Spectral Amplification Factors of DBGM-2 vs. BDBGM

A	B	C	D	E	F
Freq (Hz)	5% Damped DBGM-2 Spectral Accel, Sa_DBGM (g), Note 1	Sa_DBGM to ZPA_{DBGM} Ratio, Note 2	5% Damped BDBGM Spectral Accel, Sa_BDBGM (g), Note 3	Sa_BDBGM to ZPA_{BDBGM} Ratio, Note 4	Ratio of Col. E to Col. C
1	0.44	0.95	1.04	1.08	1.14
2	0.96	2.07	1.83	1.91	0.92
3	1.24	2.68	2.37	2.47	0.92
4	1.43	3.09	2.74	2.85	0.92
5	1.41	3.05	2.79	2.91	0.95
6	1.23	2.66	2.52	2.63	0.99
8	0.99	2.14	1.69	1.76	0.82
11	0.62	1.34	1.24	1.29	0.96
15	0.84	1.81	1.35	1.41	0.78
20	0.63	1.36	1.29	1.34	0.99
30	0.59	1.27	1.08	1.13	0.88
Notes:					
1. Figure K-A-1 of Appendix K-A.					
2. ZPA value of DBGM-2 100' median case is 0.463g (Figure K-A-1).					
3. Figure K-C-1 of Appendix K-C.					
4. ZPA value of BDBGM 100' median case is 0.96g (Figure K-C-1).					

For equipment with frequency above 8 Hz

$Factor := mean(0.82, 0.96, 0.78, 0.99, 0.88)$

$Factor = 0.886$

$F_{SSI\_2\_8Hz} := \frac{1}{Factor}$

$F_{SSI\_2\_8Hz} = 1.129$

$F_{SSI\_8Hz} := F_{SSI\_1} \cdot F_{SSI\_2\_8Hz}$

$F_{SSI\_8Hz} = 1.129$

$\sigma := Stdev(0.82, 0.96, 0.78, 0.99, 0.88)$

$\sigma = 0.089$

$\beta_{c\_SSI\_2} := \frac{\sigma}{Factor}$

$\beta_{c\_SSI\_2} = 0.101$

$\beta_{c\_SSI\_8Hz} := \sqrt{\beta_{c\_SSI\_1}^{2} + \beta_{c\_SSI\_2}^{2}}$

$\beta_{c\_SSI\_8Hz} = 0.27$

For distribution systems

$Factor := mean(0.92, 0.92, 0.92, 0.95, 0.99)$

$Factor = 0.94$

$F_{SSI\_2\_dist} := \frac{1}{Factor}$

$F_{SSI\_2\_dist} = 1.064$

$F_{SSI\_dist} := F_{SSI\_1} \cdot F_{SSI\_2\_dist}$

$F_{SSI\_dist} = 1.064$

$\sigma := Stdev(0.92, 0.92, 0.92, 0.95, 0.99)$

$\sigma = 0.031$

$\beta_{c\_SSI\_2} := \frac{\sigma}{Factor}$

$\beta_{c\_SSI\_2} = 0.033$

$\beta_{c\_SSI\_dist} := \sqrt{\beta_{c\_SSI\_1}^{2} + \beta_{c\_SSI\_2}^{2}}$

$\beta_{c\_SSI\_dist} = 0.252$

K6.3.6 Ground Motion Incoherence

$L1 := 327 \cdot ft$	East-west dimension of the CRCF excluding the 49'-6" and 43' extensions at the east and west ends, respectively (Reference K2.2.11).
$L2 := 336 \cdot ft$	North-south dimension of the CRCF excluding the 56' extension at the south end.
$L_{eq} := \sqrt{L1 \cdot L2}$	Equivalent foundation dimension of the CRCF
$L_{eq} = 331.5\ ft$	

The ground motion incoherence reduction factor is a function of foundation size and frequency of response. For a 150 foot plan dimension foundation, the following reduction factors are presented in Reference K2.2.1 in page 3-22. Interpolation or extrapolation may be used to calculate the reduction factor for different dimensions and/or frequencies.

$L_{std} := 150 \cdot ft$	Foundation dimension for which the reduction factors in Reference K2.2.3 are calculated.
$f_5 := 5$	Frequency in cycle/sec (Hz)
$RF_5 := 1$	Reduction factor for response frequency at 5 Hz
$f_{10} := 10$	Frequency in Hz
$RF_{10} := 0.9$	Reduction factor for response frequency at 10 Hz
$RF_{5\_eq} := RF_5$	Reduction factor at 5 Hz, given the CRCF equivalent foundation dimension
$RF_{10\_eq} := 1 - \left[\left(1 - RF_{10}\right) \cdot \frac{L_{eq}}{L_{std}} \right]$	Linear extrapolation
$RF_{10\_eq} = 0.779$	Reduction factor at L_{eq} dimension and 10 Hz frequency of response.

At 5.2 Hz which is the fundamental frequency of horizontal response of the CRCF

$f_6 := 5.2$ Frequency in Hz

Calculate the reduction factor at 5.2 Hz frequency by interpolation

$RF_{6\_eq} := 0.4$ An arbitrary value to initiate the equation solver below.

Given

$$\frac{\log(RF_{10\_eq}) - \log(RF_{5\_eq})}{\log(RF_{6\_eq}) - \log(RF_{5\_eq})} = \frac{\log(f_{10}) - \log(f_5)}{\log(f_6) - \log(f_5)}$$

$a := \text{Find}(RF_{6\_eq})$

$a = 0.986$ Reduction factor

Thus, the ground motion incoherence factor of safety is

$$F_{GMI} := \frac{1}{a}$$

$F_{GMI} = 1.014$

$$\beta_{U\_GMI} := \frac{1}{2} \cdot \ln\left(\frac{1}{a}\right)$$ A reduction factor of 1.0 (i.e., no reduction) is estimated to be two standard deviation from the calculated median factor of 0.91 (Reference K2.2.1, Page 3-23).

$\beta_{U\_GMI} = 0.01$

$\beta_{R\_GMI} := 0$

$$\beta_{c\_GMI} := \sqrt{\beta_{R\_GMI}^2 + \beta_{U\_GMI}^2}$$

$\beta_{c\_GMI} = 0.01$

K6.3.7 Structural Response Factors

For equipment with frequency greater than 8 Hz

$F_{RS\_8Hz} := F_{SA} \cdot F_{\delta} \cdot F_M \cdot F_{MC} \cdot F_{SSI\_8Hz} \cdot F_{GMI}$

$F_{RS\_8Hz} = 1.231$

$$\beta_{c\_RS\_8Hz} := \sqrt{\beta_{c\_SA}^2 + \beta_{c\_\delta}^2 + \beta_{c\_M}^2 + \beta_{c\_MC}^2 + \beta_{c\_SSI\_8Hz}^2 + \beta_{c\_GMI}^2}$$

$\beta_{c\_RS\_8Hz} = 0.368$

For distribution systems

$$F_{RS\_dist} := F_{SA} \cdot F_{\delta} \cdot F_{M} \cdot F_{MC} \cdot F_{SSI\_dist} \cdot F_{GMI}$$

$$F_{RS\_dist} = 1.16$$

$$\beta_{c\_RS\_dist} := \sqrt{\beta_{c\_SA}^{2} + \beta_{c\_\delta}^{2} + \beta_{c\_M}^{2} + \beta_{c\_MC}^{2} + \beta_{c\_SSI\_dist}^{2} + \beta_{c\_GMI}^{2}}$$

$$\beta_{c\_RS\_dist} = 0.355$$

K6.4 FRAGILITIES FOR DBGM-2 DESIGN

Fragility is the product of the capacity factor, equipment response factor, structural response factor and PGA of the DBGM-2. The composite uncertainty, βc, is the SRSS of the uncertainties for capacity, equipment response and structural response.

Table K6-5 lists the fragilities for each of the six categories.

Table K6-5 Fragilities for SSCs Designed for DBGM-2

Component	F_C	F_{RE}	F_{RS}	Am (g)	β_{c_C}	β_{c_RE}	β_{c_RS}	β_c	HCLPF(g)
CIP Bolt	1.43	1.182	1.231	0.94	0.115	0.208	0.368	0.44	0.34
Weld	2.14	1.182	1.231	1.41	0.19	0.208	0.368	0.46	0.48
P-I Anchors	4.6	1.182	1.231	3.03	0.428	0.208	0.368	0.60	0.75
Piping	3.41	1.25	1.16	2.24	0.5	0.293	0.355	0.68	0.46
Cable Trays	3.41	1.8	1.16	3.23	0.5	0.296	0.355	0.68	0.66
Ducts	3.41	1.5	1.16	2.69	0.5	0.25	0.355	0.66	0.57

The HCLPF exceeds the DBGM-2 PGA of 0.453g in all cases except for CIP bolts. This implies that the ACI-349 design requirements for anchorage to concrete may not be conservative enough. This will be determined as a result of the ongoing seismic probabilistic risk assessment. Note that if the factor of safety of 4 was not imposed for post-installed anchors in Ref. K2.2.13, the fragility of post-installed anchors that are ductile undercut anchors would be similar to that of CIP bolts.

K6.5 FRAGILITIES FOR BDBGM DESIGN

Reference K2.2.13 requires that ITS components be evaluated for BDBGM and that the HCLPF should be a factor of 1.1 times the BDBGM. There are currently no specific design measures being taken for ITS equipment at the BDBGM level. As can be observed from Table K6-5, the HCLPF values exceed the 0.453g DBGM-2 PGA in all cases except for CIP anchor bolts. If a HCLPF of at least the 0.914g BDBGM PGA is to be achieved, it is clear that the limiting cases summarized in Table K6-5 for design only to DBGM-2 would not achieve this goal and a design at higher ground motion would be required. As a sensitivity study for use within the PSA analyses, an additional set of fragility has been estimated wherein the ITS equipment design basis is considered to be the BDBGM. Such a design would use exactly the same design codes and standards as used for design to DBGM-2. In

addition, in-structure response spectra would be enveloped and broadened in the exact same manner. Differences would be only that the ground motion would be higher and soil nonlinearities in the soil-structure interaction analyses may result in different spectral shapes between the BDBGM and the DBGM-2 ISRS.

Review of the BDBGM and the DBGM-2 ISRS in Appendix K-C indicates that there is no significant difference in the peak spectral amplification (average of 2.02). As a result, the fragilities for BDBGM design are 2.02 times the DBGM-2 fragilities as shown in Table K6-6.

Table K6-6 Fragilities for SSCs Designed for BDBGM

Component	F_C	F_{RE}	F_{RS}	Am (g)	β_{c_C}	β_{c_RE}	β_{c_RS}	β_c	HCLPF(g)
CIP Bolt	1.43	1.182	1.231	1.90	0.115	0.208	0.368	0.44	0.69
Weld	2.14	1.182	1.231	2.85	0.19	0.208	0.368	0.46	0.97
P-I Anchors	4.6	1.182	1.231	6.12	0.428	0.208	0.368	0.60	1.51
Piping	3.41	1.25	1.16	4.52	0.5	0.293	0.355	0.68	0.93
Cable Trays	3.41	1.8	1.16	6.51	0.5	0.296	0.355	0.68	1.33
Ducts	3.41	1.5	1.16	5.42	0.5	0.25	0.355	0.66	1.16

From the above table it may be seen that the HCLPF capacity is greater than the BDBGM PGA of 0.914g except for CIP bolts. (Note that this same conclusion may also be true for ductile undercut post-installed anchors). For CIP bolts, either a reduced allowable stress or a load factor on demand may be required to assure a HCLPF value greater than the design demand.

K7. SUMMARY

Representative fragilities have been developed for typical anchorage, piping, cable raceways and ducting designed to the generalized seismic requirements of Reference K2.2.13. Two design cases have been considered. The first case is that the designs are based on the DBGM-2 demand and that BDBGM has not been designed for. Results are given in Table K6-5.

As a sensitivity study for use in the PSA analyses, fragilities were also estimated for a higher design level. The sensitivity study considers that the design is conducted for BDBGM using the same codes and standards specified in Reference K2.2.13 for design to DBGM-2.

The SPRA team will have to determine if the second criterion is required for all ITS SSCs or only for a limited scope of ITS SSCs.

The fragilities developed in this calculation are based on limiting cases where the demand is equal to the design capacity. In actual designs, this is typically not the situation, thus the limiting case fragilities developed in this calculation are generally conservative. Also, it is conservatively implied that if a support fails in a piping system, cable raceway system or ducting system, that the system will fail. It is rare that a support failure in a distribution system will result in collapse and functional or structural failure of the distribution system. Thus, this limiting case is also considered to be very conservative. When actual designs or detailed specifications are available, more refined fragilities could be developed that would not be as conservative as the limiting case values developed herein.

It is noted that in the case of cast-in-place anchor bolts designed to the requirements of ACI-349, that the margin to failure is less than for other components. The margin is also less than for bolting failure in AISC and ASME applications. Depending upon the results of the risk analysis, it may be prudent to restrict the stresses in CIP anchor bolts to values less than allowed by ACI-349. As noted, this may also be necessary for post-installed ductile undercut anchors if the design guidance in Ref. K2.2.13, Section 11.5 is updated. In all other cases, the limiting case HCLPF is greater than the demand.

If HCLPFs equal to or exceeding the BDBGM are required, then the vendor must design for the BDBGM or even more. If only the DBGM-2 demand is specified, the margin on BDBGM will not be achieved unless the designer increases the capacity..

Table K7-1 compares the medians and HCLPFs achieved by designing for DBGM-2 with the minimum HCLPF that can be assured by designing to BDBGM as discussed in Section K6.5.

Table K7-1 Comparison of Limiting Case Medians and HCLPFs for Design to DBGM-2 to Limiting Case Medians and HCLPFS for Design to BDBGM

Component	Design to DBGM-2 (g)		Min Values for Design to BDBGM (g)		HCLPF for DBGM-2 Exceeds BDBGM
	Am	HCLPF	Am	HCLPF	
CIP Bolts	0.94	0.34	1.90	0.69	no
Fillet Weld	1.41	0.48	2.85	0.97	no
Post-Installed Anchors	3.03	0.75	6.12	1.51	no
Piping Supports	2.24	0.46	4.52	0.93	no
Cable Tray Supports	3.23	0.66	6.51	1.33	no
HVAC Supports	2.69	0.57	5.42	1.16	no

APPENDIX K-A
5% Damped In-Structure Response Spectra for CRCF (Reference K2.2.3)

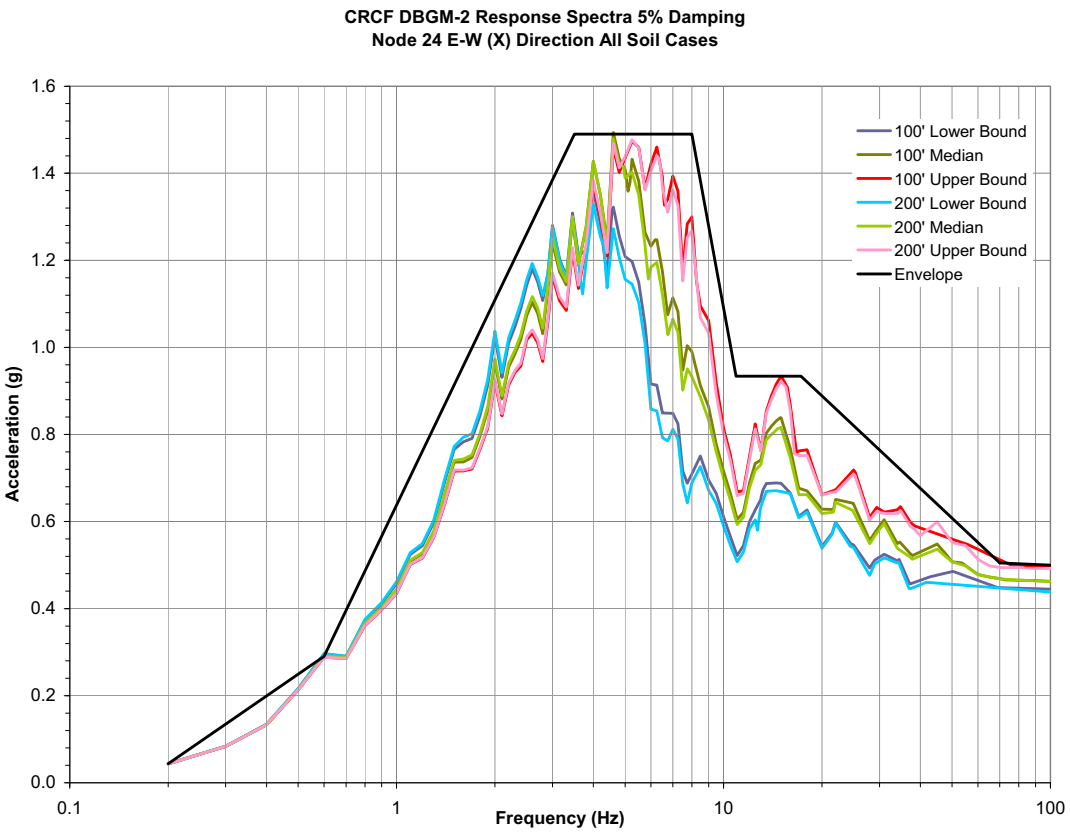

Figure K-A-1. 5% Damped Design ISRS and 100' and 200' Alluvium Depths ISRS at Ground Floor (X-Direction)

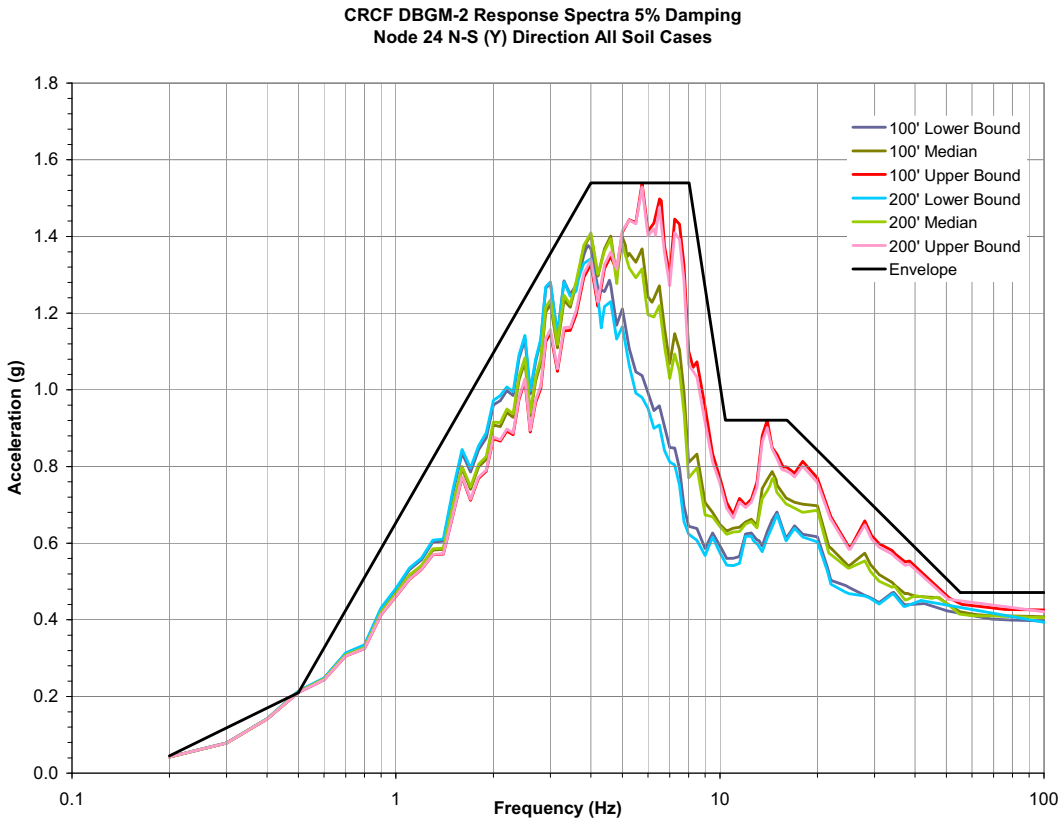

Figure K-A-2. 5% Damped Design ISRS and 100' and 200' Alluvium Depths ISRS at Ground Floor (Y-Direction)

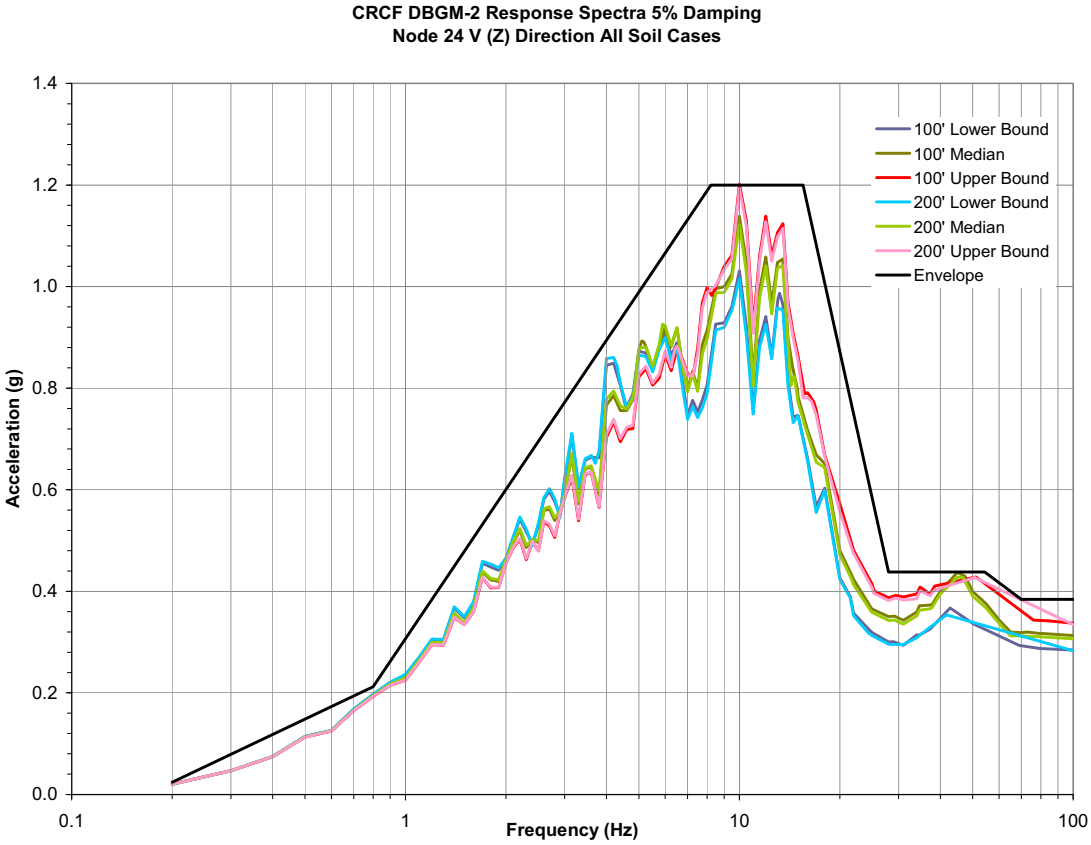

Figure K-A-3. 5% Damped Design ISRS and 100' and 200' Alluvium Depths ISRS at Ground Floor (Z-Direction)

APPENDIX K-B
UHS for 5E-4 APE

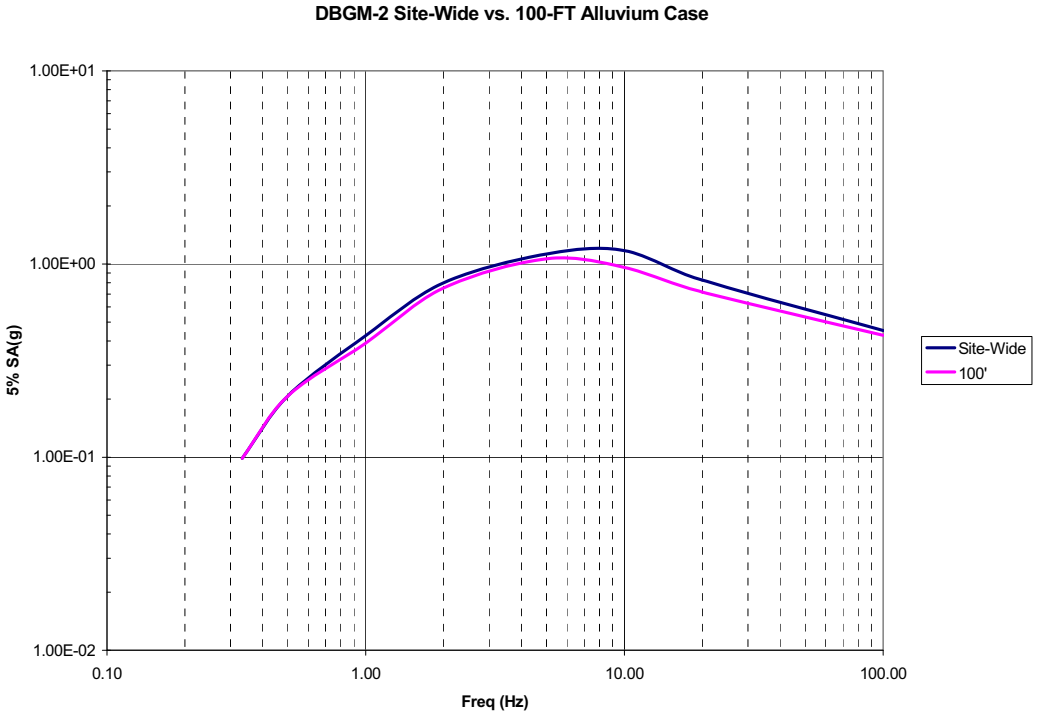

Figure K-B-1. UHS of Site-Wide and 100 Foot Alluvium Cases (See Section 6.2.2.1 for source information)

APPENDIX K-C
Comparison OF BDBGM & DBGM-2 ISRS
(Reference K2.2.3)

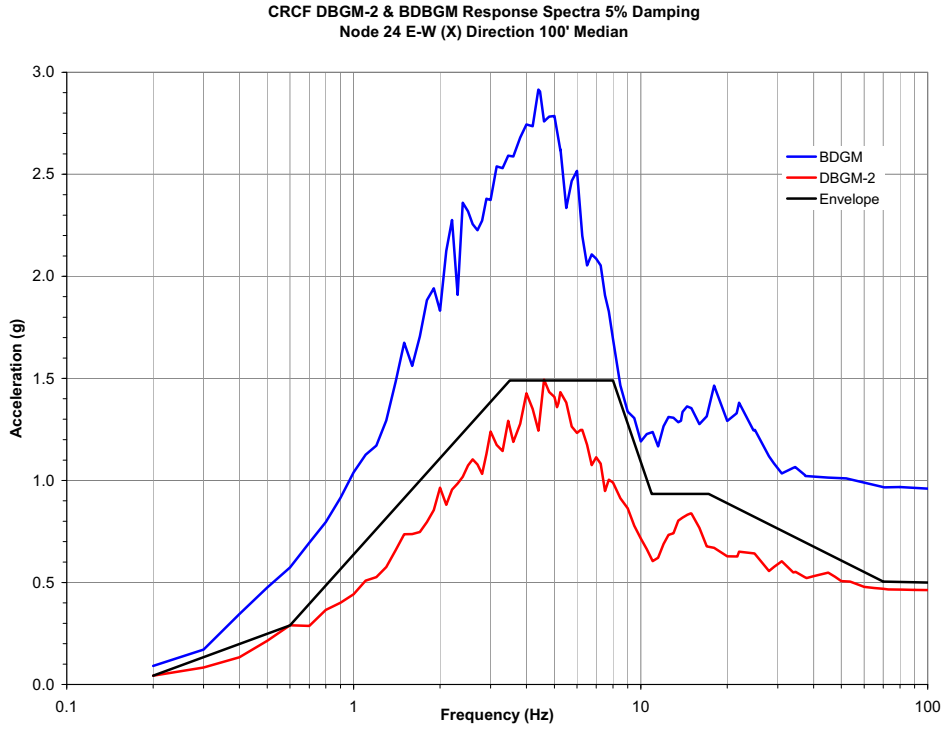

Figure K-C-1. 5% Damped 100' Alluvium Depth ISRS for BDBGM and DBGM-2 at Ground Floor (X-Direction)

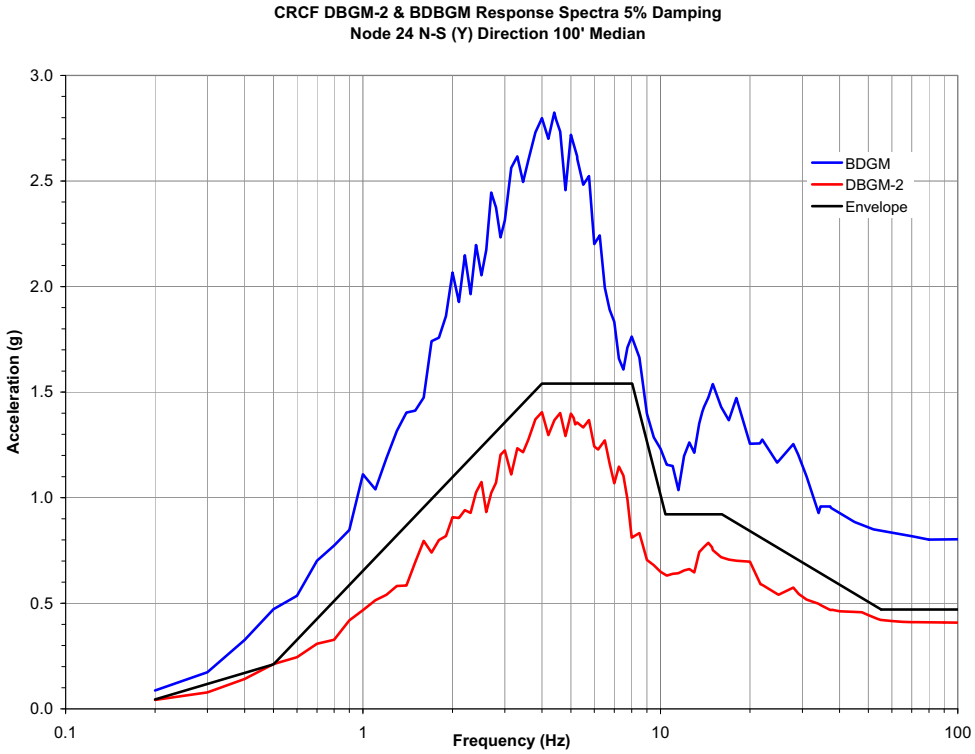

Figure K-C-2. 5% Damped 100' Alluvium Depth ISRS for BDBGM and DBGM-2 at Ground Floor (Y-Direction)

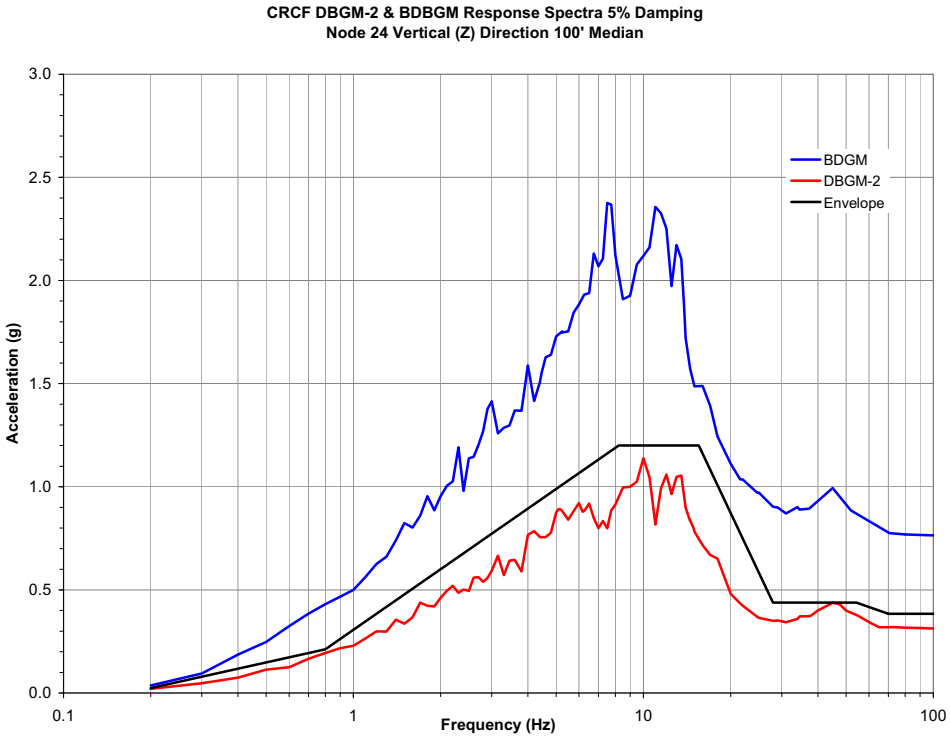

Figure K-C-3. 5% Damped 100' Alluvium Depth ISRS for BDBGM and DBGM-2 at Ground Floor (Z-Direction)

ATTACHMENT L
FRAGILITY FOR STRUCTURAL FAILURE OF CRCF EQUIPMENT SHIELD DOORS

Prepared By: Stephen A. Short

ARES Check By: Wen H. Tong

LLNL Check By: Robert C. Murray

TABLE OF CONTENTS

ACRONYMS AND ABBREVIATIONS

ACI	American Concrete Institute
AISC	American Institute of Steel Construction
ANSI	American National Standards Insitute
AO	Aging Overpack
APE	Annual Probability of Exceedance
ASCE	American Society of Civil Engineers
ASME	American Society of Mechanical Engineers
BSC	Bechtel SAIC, LLC
BDBGM	Beyond Design Basis Ground Motion at $1x10^{-4}$ APE
CDFM	Conservative Deterministic Failure Margin
CHC	Cask Handling Crane
CIP	Cast-in-Place
CRCF	Canister Receipt and Closure Facility
CTM	Canister Transfer Machine
CTT	Cask Transfer Trolley
DBGM-2	Design Basis Ground Motion at $5x10^{-4}$ APE
DL	Dead Load
DOF	Degree of Freedom
DPC	Dual Purpose Canister
EPRI	Electric Power Research Institute
HCLPF	High Confidence of Low Probability of Failure
HVAC	Heating, Ventilation, & Air Conditioning
IEEE	Institute of Electrical and Electronics Engineers
IHF	Initial Handling Facility
ISRS	In-Structure Response Spectra

ACRONYMS AND ABBREVIATIONS (cont.)

ITS	Important to Safety
LA	License Application
LLNL	Lawrence Livermore National Laboratory
NPP	Nuclear Power Plant
PGA	Peak Ground Acceleration
RF	Receipt Facility
RRS	Required Response Spectrum
Sa	Spectral Acceleration
SFA	Surface Facilities Area
SFTM	Spent Fuel Transfer Machine
SPRA	Seismic Probabilistic Risk Assessment
SRSS	Square Root of the Sum of Squares
SSE	Safe Shutdown Earthquake (used with NPPs)
SSI	Soil Structure Interaction
SSC	Structure, System, and Component
TAD	Transportation, Aging, and Disposal canister
TEV	Transport and Emplacement Vehicle
TRS	Test Response Spectrum
UHS	Uniform Hazard Spectra
USDOE	United States Department of Energy
USNRC	United States Nuclear Regulatory Commission
WHF	Wet Handling Facility
WP	Waste Package
WPTT	Waste Package Transfer Trolley
YMSF	Yucca Mountain Surface Facilities
ZPA	Zero Period Acceleration

FRAGILITY TERMINOLOGY

Am	Median Peak Ground Motion Capacity
β_R	Log Standard Deviation of Randomness
β_U	Log Standard Deviation of Uncertainty (Lack of Knowledge)
β_C	Composite Variability = $(\beta_R^2 + \beta_U^2)^{0.5}$
F_S	Strength Factor of Safety
β_{R_S}	Strength Randomness (typical)
β_{U_S}	Strength Uncertainty (typical)
β_{C_S}	Strength Composite Variability (typical)
F_μ	Inelastic Energy Absorption Factor of Safety
F_{QM}	Qualification Factor of Safety
F_δ	Damping Factor of Safety
F_M	Modeling Factor of Safety
F_{MC}	Modal Combination Factor of Safety
F_{ECC}	Earthquake Component Combination Factor of Safety
F_{SA}	Spectral Shape Factor of Safety
F_{SSI}	Soil-Structure Interaction Factor of Safety
F_{GMI}	Ground Motion Incoherence Factor of Safety
F_{TOTAL}	Total Factor of Safety
F_{RS}	Structural Response Factor of Safety
F_{RE}	Equipment Response Factor of Safety

L1. PURPOSE

The purpose of this calculation is to estimate the seismic fragility of equipment shield doors located in the Canister Receipt and Closure Facility (CRCF). Detailed design specifications and detailed design analyses are not yet available so the derivations are representative based on the applicable BSC specifications for seismic design and applicable codes and standards. The mean seismic fragility curve of the equipment shield doors will be convolved with the mean site-specific seismic hazard curve to calculate risk of seismic-induced equipment shield door failure.

L2. REFERENCES

L2.1 PROCEDURES AND DIRECTIVES

L2.1.1 EG-PRO-3DP-G04B-00037, Rev. 10. *Calculations and Analyses*. Las Vegas, Nevada: Bechtel SAIC Company. ACC: ENG.20071018.0001.

L2.1.2 IT-PRO-0011, Revision 7, ICN 0. *Software Management*. Las Vegas, Nevada: Bechtel SAIC Company. ACC: DOC.20070905.0007.

L2.2 DESIGN INPUTS

L2.2.1 EPRI (Electric Power Research Institute) 1994. *Methodology for Developing Seismic Fragilities*. EPRI TR-103959. Palo Alto, California: Electric Power Research Institute. TIC:253770. [DIRS 161329]

L2.2.2 ASCE/SEI 43-05. 2005. *Seismic Design Criteria for Structures, Systems, and Components in Nuclear Facilities*. Reston, Virginia: American Society of Civil Engineers. TIC: 257275. [DIRS 173805]

L2.2.3 BSC (Bechtel SAIC Company) 2007. *CRCF Tier-1 In-Structure Response Spectra*. 060-SYC-CR00-00900-000-00B. Las Vegas, Nevada: Bechtel SAIC Company. ACC: ENG.20071210.0008. [DIRS 184330]

L2.2.4 BSC (Bechtel SAIC Company) 2008. *Mechanical Handling Design Report: Shield Doors, Gates and Windows*. 000-30R-MR00-00100-000 REV 001. Las Vegas, Nevada: Bechtel SAIC Company. ACC: ENG.20080206.0065..

L2.2.5 ACI 349-01. 2001. *Code Requirements for Nuclear Safety Related Concrete Structures (ACI 349-01).* Farmington Hills, Michigan: American Concrete Institute. TIC: 252732. [DIRS 158833].

L2.2.6 ANSI/AISC N690-1994. 1994. *American National Standard Specification for the Design, Fabrication, and Erection of Steel Safety-Related Structures for Nuclear Facilities*. Chicago, Illinois: American Institute of Steel Construction. TIC: 252734. [DIRS 158835]

L2.2.7 [Reserved].

L2.2.8 BSC (Bechtel SAIC Company) 2007. *Nuclear Facilities Equipment Shield Door-Type 1 Mechanical Equipment Envelope*. 000-MJ0-H000-00701-000 REV 00C. Las Vegas, Nevada: Bechtel SAIC Company. ACC: ENG.20071205.0016; ENG.20080213.0003. [DIRS 184352]

L2.2.9 BSC (Bechtel SAIC Company) 2007. *Nuclear Facilities Equipment Shield*

Door—Type 2 Mechanical Equipment Envelope. 000-MJ0-H000-00801-000 REV 00C. Las Vegas, Nevada: Bechtel SAIC Company. ACC: ENG.20071205.0017. [DIRS 184358]

L2.2.10 BSC (Bechtel SAIC Company) 2007. *Nuclear Facilities Equipment Shield Door-Type 3 Mechanical Equipment Envelope*. 000-MJ0-H000-00901-000 REV 00C. Las Vegas, Nevada: Bechtel SAIC Company. ACC: ENG.20071205.0018. [DIRS 184359]

L2.2.11 BSC (Bechtel SAIC Company) 2007. *Nuclear Facilities Equipment Shield Door-Type 4 Mechanical Equipment Envelope*. 000-MJ0-H000-01001-000 REV 00B. Las Vegas, Nevada: Bechtel SAIC Company. ACC: ENG.20071205.0019; ENG.20080131.0008. [DIRS 184360]

L2.2.12 BSC (Bechtel SAIC Company) 2007. *Nuclear Facilities Equipment Shield Door-Type 5 Mechanical Equipment Envelope*. 000-MJ0-H000-01101-000 REV 00B. Las Vegas, Nevada: Bechtel SAIC Company. ACC: ENG.20071205.0020. [DIRS 184361]

L2.2.13 Blevins, R.D. 2001. *Formulas for Natural Frequency and Mode Shape*. 1st Edition. Malabar, Florida: Krieger Publishing Company. ISBN 1-57524-184-6. 506 pp.

L2.2.14 MO0801HCUHSSFA.001. *Mean Hazard Curves and Mean Uniform Hazard Spectra for the Surface Facilities Area*. Submittal date: 01/11/2008. [DIRS 184802]

L2.2.15 BSC (Bechtel SAIC Company) 2008. *Canister Receipt and Closure Facility 1 General Arrangement Ground Floor Plan*. 060-P10-CR00-00102-000 REV 00C. Las Vegas, Nevada: Bechtel SAIC Company. ACC: ENG.20080122.0013. [DIRS 184853]

L2.2.16 Moore, D. 2007. "*SSI Factor of Safety.*" E-mail from D. Moore to B. Murray, October 25, 2007. ACC: LLR.20080110.0145. [DIRS 184842]

L2.2.17 BSC (Bechtel SAIC Company) 2006. *Canister Receipt and Closure Facility (CRCF) Seismic Analysis.* 060-SYC-CR00-00400-000-00A. Las Vegas, Nevada: Bechtel SAIC Company. ACC: ENG.20061220.0029. [DIRS 178793]

L2.2.18 BSC (Bechtel SAIC Company) 2007. *Basis of Design for the TAD Canister-Based Repository Design Concept*. 000-3DR-MGR0-00300-000-001. Las Vegas, Nevada: Bechtel SAIC Company. ACC: ENG.20071002.0042; ENG.20071026.0033; ENG.20071108.0002; ENG.20071109.0001; ENG.20071120.0023; ENG.20071126.0049; ENG.20071214.0009; ENG.20071213.0005; ENG.20071227.0018; ENG.20080207.0004; ENG.20080212.0003. [DIRS 182131]

L2.2.19 BSC (Bechtel SAIC Company) 2006. *Seismic Analysis and Design Approach Document.* 000-30R-MGR0-02000-000 Rev. 001. Las Vegas, Nevada: Bechtel SAIC Company. ACC: ENG.20071220.0029. [DIRS 184494]

L2.3 DESIGN CONSTRAINTS

There are no design constraints in the performance of this calculation

L2.4 DESIGN OUTPUTS

The calculated seismic fragility of structural failure of equipment shield doors in the CRCF, expressed in terms of a median seismic capacity and an associated combined variability, will be convolved with the site-specific seismic hazard curve to calculate risk of seismic-induced failure of CRCF equipment shield doors. This is performed to support information in the License

Application (LA).

L3. ASSUMPTIONS

L3.1 ASSUMPTIONS REQUIRING VERIFICATION

There are no assumptions in this calculation that require verification.

L3.2 ASSUMPTIONS NOT REQUIRING VERIFICATION

L3.2.1 Equipment shield door detailed designs and detailed design specifications have not been developed at the time of this seismic fragility calculation. The general guidance for seismic design in References L2.2.18 and L2.2.19 are utilized to determine what codes and standards will likely govern and what criteria will be used for design of the equipment shield doors for DBGM-2 and evaluation for BDBGM.

L4. METHODOLOGY

L4.1 QUALITY ASSURANCE

This calculation is prepared in accordance with Bechtel SAIC LLC procedure EG-PRO-3DP-G04B-00037, Rev. 10, Reference L2.1.1.

L4.2 USE OF SOFTWARE

Mathcad 14 is used in this calculation. The use of this software is classified as Level 2 software per procedure IT-PRO-0011, Ref. L2.1.2. Therefore the software does not require separate qualification.

L4.3 APPROACH

The Separation-of-Variable method documented in EPRI TR-103959 (Reference L2.2.1, Section 3) is followed in calculating seismic fragility of this ITS equipment component.

L5. LIST OF APPENDICES

APPENDIX L-A 5% Damped In-Structure Response Spectra for CRCF

APPENDIX L-B UHS for 5E-4 APE

APPENDIX L-C Comparison of BDBGM & DBGM-2 ISRS

L6. DEVELOPMENT OF FRAGILITIES

A representative seismic fragility of equipment shield doors located in the CRCF is calculated here. The calculation considers shield door failure when it loses structural integrity and falls from its fixed position where it can impact the structure or an ITS item. The shield doors are large components weighing hundreds of tons that can cause significant collateral damage if they fall.

L6.1 EQUIPMENT SHIELD DOORS

Equipment shield doors are located between adjacent operation rooms (or areas). The doors are opened to allow the transfer of equipment (including waste forms) from one room (or area) to another, and subsequently closed for purposes of radiation shielding. There are five types of ITS equipment shield doors. Types 1 and 4 and Types 2 and 5 are single-sliding and double-sliding doors, respectively. The doors are of steel construction, and incorporate sufficient steel thickness (and polyethylene for neutron absorbing purposes if required) to provide adequate radiation shielding for facility personnel. These doors are supported by rollers mounted in a recessed channel in the floor, and utilize a wall mounted track at the top of each door for stabilization. The doors move horizontally and are powered by an electric motor. In the closed position the doors have a central overlap to prevent radiation shine. These doors are shown conceptually on References L2.2.8, L2.2.9, L2.2.11, and L2.2.12

Type 3 doors are used exclusively in the Initial Handling Facility (IHF) and may be used in the CRCF, and consist of two hinged, vertical axis of rotation doors (powered by electric motors) that overlap at the center when closed. The door hinges are attached to embedded plates in the wall. Type 3 doors are shown conceptually on Reference L2.2.10.

A representative seismic fragility of equipment shield doors is developed herein because design details are not currently available. The Type 1 single sliding door was chosen specifically for this representative seismic fragility calculation.

In accordance with Reference L2.2.4, the Type-1 equipment shield door remains closed until a transportation cask, secured in the Cask Transfer Trolley, has been prepared for transfer to the cask unloading room. The shield door then opens (actuated locally or from the operations room) and the Cask Transfer Trolley moves the transportation cask into the cask unloading room, positioning the cask beneath the cask port slide gate. The shield door subsequently closes.

Requirements for Equipment Shield Doors are stated in Reference L2.2.4 that, in turn cites the Basis for Design (Reference L2.2.18). One basic requirement is for the door to maintain integrity to reduce frequency of collapse onto waste containers.

To meet the above requirement, Reference L2.2.4 states "The equipment shield doors and their supports are designed in accordance with the applicable provisions of ANSI/AISC N690-1994, *American National Standard Specification for the Design, Fabrication, and Erection of Steel Safety-Related Structures for Nuclear Facilities* (Reference L2.2.6), for loads and accelerations associated with a DBGM-2 seismic event. They are also analyzed for more severe events, including the BDBGM seismic event, to provide assurance that under such loading and accelerations they will not collapse onto a waste container. Dynamic seismic analysis for the equipment shield doors is performed in accordance with ASCE/SEI 43- 05, 2005, *Seismic Design Criteria for Structures, Systems, and Components in Nuclear Facilities,* (Reference L2.2.2)."

L6.2 POTENTIAL FAILURE MODES

Equipment shield doors are thick steel flat plate structures that are attached at the top and bottom by rollers that set in steel brackets. The steel brackets are then welded to embedded plates that are anchored to the concrete walls by cast-in-place bolts. From the thickness and weights shown on References L2.2.8 and L2.2.11, it may be determined that the flat plate door spanning the opening is all steel with no voids. The door thickness shown on the drawings is 1 foot, four inches. The door plate of this thickness is likely made up of thick plates (i.e., a few inches) that are keyed together to obtain shear transfer such that the plate structurally spans the door opening at its full thickness (i.e., 1 foot, four inches).

During an earthquake, the door is subject to transverse lateral inertial loads spanning one way vertically to supports at the top and bottom. Assuming simply supported one way behavior of the door, the fundamental frequency may be computed using relations in Reference L2.2.13.

Take the door aperture height to be the vertical span and consider a unit width door strip. From Reference L2.2.8 for the Type 1 door in the CRCF cask unloading room, door properties are:

$h := 28.5\,ft$ $t := 16\,in$ $b := 1\,in$

$W_{steel} := 490\,\frac{lbf}{ft^3}$ $E_{steel} := 29000000\,psi$

$I_{door} := \frac{b \cdot t^3}{12}$ $I_{door} = 341.333 \cdot in^4$ Moment of inertia

$w_{steel} := W_{steel} \cdot b \cdot t$ $w_{steel} = 4.537 \cdot \frac{lbf}{in}$ Door weight per unit length

From Ref. L2.2.8, there is additional neutron absorbing material on the face of the door. This material is non-structural but does add mass. The added mass is estimated to be 10 percent.

$w := 1.1 \cdot w_{steel}$ $w = 4.991 \cdot \frac{lbf}{in}$

From Table 8-1 of Reference L2.2.13, the fundamental frequency of a simply supported beam with a uniform load is given by:

$$f_{door} := \frac{\pi}{2 \cdot h^2} \cdot \sqrt{\frac{E_{steel} \cdot I_{door} \cdot g}{w}} \qquad f_{door} = 11.752 \cdot Hz$$

This door is very stiff but it is still in the amplified range of earthquake response. Furthermore, it is understood that the door thickness could be reduced in the future when radiation shielding requirements are better defined. At any rate, it is anticipated that the door will be designed on the basis of a dynamic seismic response analysis.

The thick door plates will be very lowly stressed during earthquake response. For the door to fail and impact nearby waste containers, there would have to be a failure of the door supports and anchorage. The door supports and anchorage are comprised of steel supports (wheels, brackets, etc.), welded anchorage to embedded plates, and cast-in place bolts anchoring the embeds to the concrete structure.

Hence, this seismic fragility calculation will consider the door support load path including:

1. cast in place anchor bolts
2. welded anchorage
3. steel supports

L6.3 DEVELOPMENT OF CAPACITY FACTORS

Capacity factors will be developed for cast-in-place anchor bolts attaching embedded plates to the concrete structure, welded anchorage of the steel supporting structure to the embedded plates, and the steel supports themselves. The door plate is judged to be lowly stressed and not close to the governing seismic fragility.

L6.3.1 Cast-in-Place Anchor Bolts

Cast-in-place (CIP) anchor bolts for equipment shield door embedded support plates are to be designed per the requirements of ACI 349-01, Reference L2.2.5. This category will also include headed studs. Per ACI 349-01, CIP anchor bolts shall be designed so that the bolt will fail before concrete failure. As required by Ref. L2.2.19, Section 11.5, only ductile failure modes of anchorage are permitted in ITS structures. The capacity of cast-in-place anchor bolts and headed studs is then based on ultimate strength of the steel bolts. Anchor bolts are typically loaded in tension and shear, and interaction equations are used to determine the margin. Per ACI-349 (Sections B.5.1.2 and B.4.4), the design strength for CIP anchor bolts is 0.8 of the specified ultimate tensile strength. Median ultimate strength is 1.1 times the specified ultimate strength, per Reference L2.2.1.

Per Reference L2.2.1, Tables 3-9 and 3-10, the median tensile ultimate strength in a threaded joint is 90% of the theoretical ultimate strength due to strain concentrations in the threaded region. The minimum strength factor in tension for CIP anchor bolts or headed studs can then be estimated as:

Let Ftu be a typical minimum specified ultimate tensile strength value for say A-36 steel

$Ftu := 58ksi$ Reference L2.2.6

$Pult := 0.9 \cdot 1.1 \cdot Ftu$ Median tensile capacity of bolt

$Pult = 57.42 \cdot ksi$

For shield doors mounted on the walls, the dead load does not affect the seismic-induced tensile load on anchor bolts. It is conservatively assumed in the fragility calculation that (1) the dead load effect is not considered in the anchorage design and (2) the anchorage is designed such that the seismic stress is at the code design strength, i.e., Pseismic = Pall.

$Pall := 0.8 \cdot Ftu$ Code design strength (Sections B.4.4 and B.5.1.2 of Reference L2.2.5)

$Pall = 46.4 \cdot ksi$

$F_{S\_t} := \frac{Pult}{Pall}$ Median strength factor

$F_{S\_t} = 1.237$

Next consider a case of pure shear on the full body of the anchor bolt.

$Vall := (0.75)\cdot(0.6\cdot Ftu)$ Where 0.75 is the strength reduction factor of a ductile steel element in shear (Section B.4.4 of Reference L2.2.5) and 0.6Ftu is the nominal shear strength for cast-in-place headed bolt anchors (Section B.6.1.2(b) of Reference L2.2.5).

$Vult := 0.62\cdot Ftu\cdot 1.1$ Reference L2.2.1, Table 3-10.

$F_{S\_v} := \frac{Vult}{Vall}$

$F_{S\_v} = 1.516$

The pure shear case has slightly higher margin to failure considering the applied stress to be equal to the design strength. However, the failure mode of interest is tension on the embedded plate and anchor bolt

$F_{S\_CIP} := F_{S\_t}$

$F_{S\_CIP} = 1.237$

From Reference L2.2.1, Table 3-10

$\beta_{U\_t} := 0.13$ For tensile failure

$\beta_{c\_CIP} := \beta_{U\_t} = 0.13$

The failure is ductile locally, but on a system ductility basis, there would be little ductility. Thus no credit is taken for ductility (Page 8-16 of Reference L2.2.1). Hence, the Capacity Factor and variability are equal to the Strength Factor and its variability.

$F_{\mu\_CIP} := 1.0$

$\beta_{\mu c\_CIP} := 0$

The capacity factor is then given by:

$F_{C\_CIP} := F_{S\_CIP} = 1.237$

$\beta_{c\_CIP} = 0.13$

L6.3.2 Welded Anchorage

Equipment shield door support brackets are welded to embeds using fillet welds. For the failure mode of interest, welds are loaded in transverse shear normal to the weld line as the door experiences out-of-plane seismic inertial loads. For the equipment shield doors, it is judged that this is the only significant load on the welds due to multiple components of motion. The welds to the embedded plates do not restrain the door due to the horizontal and vertical in-plane components of earthquake motion. Per Reference L2.2.1, Table 3-10, fillet welds in longitudinal shear have a median ultimate strength of 0.84 times the median ultimate tensile strength of the weld rod. Fillet welds loaded in transverse shear have an ultimate strength of 1.26 times the ultimate tensile strength of the weld rod. In both cases, the weld area is based on the throat of the fillet weld. For these doors, the governing case would be 100% of transverse shear with no contributions from other components. Typically E-70 electrodes are used with an ultimate tensile strength of 70ksi. The median ultimate tensile strength would then be 1.1 times this specified value (Table 3-9 of Ref. L2.2.1). The average ultimate shear strength would then be:

$$Fv\_ult\_long := 0.84 \cdot 70ksi \cdot 1.1$$

$$Fv\_ult\_tran := 1.26 \cdot 70ksi \cdot 1.1$$

For the failure mode of out-of-plane seismic response of the door, the ultimate shear capacity is equal to the Fv_ult_tran of the weld for comparison to the seismic response shear.

The allowable weld stress per Ref. L2.2.6 is:

$$fv\_all := 1.6 \cdot (0.3 \cdot 70)ksi$$

0.3 brings the ultimate electrode stress of 70ksi to the allowable of 21ksi, and 1.6 is the stress limit coefficient for extreme loads per Reference L2.2.6

$$F_{S\_weld} := \frac{Fv\_ult\_tran}{fv\_all}$$

$$F_{S\_weld} = 2.888$$

Per Ref. L2.2.1, Table 3-10,

$$\beta_{U\_weld} := 0.19$$

$$\beta_{c\_weld} := \beta_{U\_weld}$$

Welds are a brittle failure mode, thus the ductility factor is 1.0 and the Capacity Factor and its variability are equal to the Strength Factor and its variability.

$$F_{\mu\_weld} := 1.0$$

$$\beta_{\mu c\_weld} := 0$$

$$F_{C\_weld} := F_{S\_weld} = 2.888 \qquad \beta_{c\_weld} = 0.19$$

L6.3.4 Equipment Shield Door Steel Supports

Shield door supports would typically be designed as structural steel members using common structural profiles of low carbon steel. Per Reference L2.2.19, such supports are to be designed to the ANSI/AISC N-690 code. For low carbon steel such as A-36, the working stress allowable is 0.6 of the yield strength. For extreme loads, N-690 allows a 1.6 increase in allowable stress.

$Fu := 58ksi$

$Fy := 36ksi$

$S := 0.6 \cdot 1.6 \cdot Fy \qquad S = 34.56 \cdot ksi$ Stress limit for extreme loads

Consider that door supports would typically be loaded in bending and may be open sections. The plastic shape factors for these open section would be less than for a solid section. Let the plastic shape factor be about 1.25. A plastic hinge would form when the section was fully plastic. Per Ref. L2.2.1, median yield for structural steel such as A-36 is 1.2 times specified.

$F\_hinge := 1.25 \cdot 1.2 \cdot Fy$

$F\_hinge = 54 \cdot ksi$

For equipment shield door supports, no capacity is used up by dead weight. Therefore:

$DW := 0.0$

Thus, the strength factor of safety can be computed as

$$F_{S\_supp} := \frac{F\_hinge - DW}{S - DW}$$

$F_{S\_supp} = 1.563$

The failure mode is considered to be ductile. ASCE/SEI-43, Reference L2.2.2 has guidance on ductility factors appropriate for different limit states in equipment and supports. At just less than ultimate failure, limit state A ductility factors can be used. The limit state A ductility factor for equipment supports is 2.0 from Table 8-1 of Ref. L2.2.2.

$F_{\mu\_supp} := 2.0$

$F_{C\_supp} := F_{S\_supp} \cdot F_{\mu\_supp}$

$F_{C\_supp} = 3.125$

Uncertainty is computed using F_{C_supp} for the capacity of door supports. Let the onset of code yield be a 99 percentile value ($-2.33\beta c$). Then the factor to code yield is:

$$F_{C\_yield} := \frac{Fy - DW}{S - DW} \qquad F_{C\_yield} = 1.042$$

$$\beta_{c\_supp} := \frac{1}{2.33} \cdot \ln\left(\frac{F_{C\_supp}}{F_{C\_yield}}\right) \qquad \beta_{c\_supp} = 0.472$$

L6.4 EQUIPMENT RESPONSE FACTOR

The equipment response factor will vary depending upon the frequency of the equipment and the method of analysis. The demand spectra for the CRCF at the ground floor and at a height of 32 feet will be used for all equipment locations for the purposes of this representative calculation. Door seismic input is introduced at the top and bottom of the door and all CRCF doors extend from the ground floor up to the 32 foot elevation. Furthermore, the doors are all aligned with the same orientation in the CRCF such that the x direction seismic input results in out-of-plane door behavior that is the focus of this seismic fragility evaluation. Door seismic input is taken to be the average of the input motion at the top and bottom of the door in the X-direction. As shown earlier, equipment shield doors are fairly stiff with a fundamental frequency of 10 Hz or greater. It is not known how the shield doors will be evaluated for seismic events. They will likely be designed using response spectrum analysis but equivalent static coefficient methods may also be employed. For purposes of this fragility calculation, the demand will be based on envelope response spectrum analysis or an equivalent static coefficient analysis as specified in Reference L2.2.18.

The variables to consider for equipment response are:

- Qualification method
- Damping
- Modeling
- Mode combination
- Earthquake Direction

As shown in L6.2, the equipment shield doors has a fundamental frequency of 10 Hz or greater. These doors will be evaluated based on the spectral acceleration at a calculated fundamental frequency. The demand is defined as the average DBGM-2 in-structure spectral accelerations at the top and bottom of the doors at the calculated fundamental frequency.

L6.4.1 Qualification Method

Since some form of dynamic analysis will be conducted to define the fundamental frequency of the component. Consequently there is no bias in the qualification method.

$$F_{QM\_1} := 1.0$$

$$\beta_{c\_QM\_1} := 0$$

The other factor of safety to be considered under the qualification method is the conservatism in the broadened and smoothed design floor response spectra. Nodes 22 and 24 (Ref. L2.2.17) represent the base mat and the resulting response spectra at each node are similar. Node 224 (Ref. L2.2.17) represents the floor level that is 32 feet above the ground floor. The average of the node 24 and node 224 spectra as shown in APPENDIX L-A are used. The median response case is taken as the 100 foot soil depth case using median soil properties. Uncertainty is determined from the difference between upper bound, median and lower bound soil properties. Table L6.4-1 presents comparison of the site wide broadened and smoothed spectra to the average median soil spectra for the X-direction. Digitized 5% damped spectra for nodes 24 and

224 of the CRCF from Reference L2.2.3 are used. See APPENDIX L-A for spectra plots.

Table L6.4-1 Comparison of 5% Damped Median & Design Spectral Amplification Factors

Freq. (Hz)	24 Median	224 Median	Door Median	24 Design	224 Design	Door Design	Des/Med
10	0.72	1.16	0.94	1.08	1.95	1.51	1.61
11	0.61	1.00	0.80	0.93	1.86	1.40	1.74
12	0.69	0.82	0.76	0.93	1.61	1.27	1.68
13	0.74	0.82	0.78	0.93	1.39	1.16	1.49
14	0.82	0.72	0.77	0.93	1.18	1.06	1.37
15	0.84	0.73	0.78	0.93	1.00	0.97	1.24

Seismic demand is primarily governed by horizontal demand in the X direction. Considering a door fundamental frequency of 12 Hz as computed in Section L6.2, from the above table, the margin in spectral shape at 12 Hz is 1.68 in the X direction.

$$F_{QM\_2} := 1.68$$

Uncertainty in frequency will be treated with the modeling factor such that:

$$\beta_{c\_QM\_2} := 0$$

$$F_{QM} := F_{QM\_1} \cdot F_{QM\_2} \qquad F_{QM} = 1.68$$

$$\beta_{c\_QM} := \sqrt{\beta_{c\_QM\_1}^{2} + \beta_{c\_QM\_2}^{2}} \qquad \beta_{c\_QM} = 0$$

L6.4.2 Damping

Design damping is stated in Reference L2.2.18 to be as defined in ASCE/SEI 43-05, Reference L2.2.2. For welded metal structures at level 2 response, the damping is 4%. This is slightly conservative. Per Ref. L2.2.18, median damping for metal structures at Response Level 3 is 7%. It is judged that 4% would be a minus 1β.

Door frequency was evaluated to be 12 Hz in Section L6.2. Therefore, damping will be evaluated at 12 Hz from Reference L2.2.3 median or raw spectra.

$$Sa24\_7 := 0.66g \qquad Sa224\_7 := 0.80g$$

$$Sa24\_4 := 0.71g \qquad Sa224\_4 := 0.83g$$

These are 7% and 4% damped spectral values at 12 Hz from the 100' median ISRS (Ref. L2.2.3).

$$Sa\_7 := \frac{Sa24\_7 + Sa224\_7}{2} \qquad Sa\_7 = 0.73 \cdot g$$

$$Sa\_4 := \frac{Sa24\_4 + Sa224\_4}{2} \qquad Sa\_4 = 0.77 \cdot g$$

$$F_{\delta} := \frac{Sa\_4}{Sa\_7} \qquad F_{\delta} = 1.055$$

$$\beta_{c\_\delta} := \ln\left(\frac{Sa\_4}{Sa\_7}\right) \qquad \beta_{c\_\delta} = 0.053$$

L6.4.3 Modeling

Modeling is assumed to be median centered. For these shield doors, a very simple model is used to determine the fundamental frequency. Say that 12 Hz as computed in Section L6.2 is the best estimate frequency. Let the 1β uncertainty in frequency be plus or minus 2 Hz. (The resulting β is within the range of Ref. L2.2.1 on Pages 3-17, 3-18, and 3-49).

$$F_M := 1.0$$

$$fn\_minus\beta := 10Hz \qquad fn\_plus\beta := 14Hz$$

Use median soil spectra for modeling uncertainty. From Table L6.4-1:

$$S_{a\_10} := 0.94g \qquad S_{a\_12} := 0.76g \qquad S_{a\_14} := 0.77g$$

$$\beta_{c\_M1} := \ln\left(\frac{S_{a\_10}}{S_{a\_12}}\right) \qquad \beta_{c\_M1} = 0.213$$

$$\beta_{c\_M2} := \ln\left(\frac{S_{a\_14}}{S_{a\_12}}\right) \qquad \beta_{c\_M2} = 0.013$$

$$\beta_{c\_M} := \frac{\beta_{c\_M1} + \beta_{c\_M2}}{2} \qquad \beta_{c\_M} = 0.113$$

L6.4.4 Mode Combination

Equipment shield door response is considered to be primarily a single mode. Some contribution from higher modes is likely.

$$F_{MC} := 1.0$$

$$\beta_{c\_MC} := 0.10$$

L6.4.5 Earthquake Component Combination

Equipment shield door response is dominated by one horizontal direction of shaking. Therefore:

$$F_{ECC} := 1.0$$

$$\beta_{c\_ECC} := 0$$

L6.4.6 Equipment Response Summary

$$F_{RE} := F_{QM} \cdot F_{\delta} \cdot F_{M} \cdot F_{MC} \cdot F_{ECC}$$

$$F_{RE} = 1.772$$

$$\beta_{c\_RE} := \left(\beta_{c\_QM}^{2} + \beta_{c\_\delta}^{2} + \beta_{c\_M}^{2} + \beta_{c\_MC}^{2} + \beta_{c\_ECC}^{2} \right)^{0.5}$$

$$\beta_{c\_RE} = 0.16$$

L6.5 STRUCTURAL RESPONSE FACTOR

L6.5.1 Spectral Shape Factor

This factor accounts for conservatism in the site-wide DBGM-2 design spectrum. The depth of alluvium at the Surface Facilities Area (SFA) varies from 30 feet to 200 feet. Uniform hazard spectra at the surface are calculated from site response analyses for alluvium depths of 30', 70', 100' and 200'. The site-wide design ground response spectrum is the envelope of the surface spectra of these four alluvium depths (Reference L2.2.14; also Section 6.2.2.1 for source information).

The best-estimate horizontal dominant frequency of the soil-structure system is 5.2 Hz for the CRCF at 100-foot alluvium of median properties (Attachment 1 of Reference L2.2.3). At this frequency:

$SA_{site} := 1.14g$ 5% damped site-wide spectral acceleration (APPENDIX L-B).

$SA_{100} := 1.06 \cdot g$ 5% damped spectral acceleration of the 100-foot best-estimate alluvium depth case in the northeast area where the preclosure surface facilities are located.

$$F_{SA} := \frac{SA_{site}}{SA_{100}}$$

$$F_{SA} = 1.075$$

Since uncertainty in the UHS is derived from uncertainty in the seismic hazard curves which will be included in the final risk quantification, no uncertainty is included under the spectral shape factor to avoid double-counting the hazard uncertainty, hence

$$\beta_{U\_SA} := 0$$

$\beta_{R\_SA} := 0.20$ Random variability to account for peak-to-valley variability of the smoothed UHS (Reference L2.2.1, Table 3-2).

$$\beta_{c\_SA} := \sqrt{\beta_{U\_SA}^{2} + \beta_{R\_SA}^{2}} \qquad \beta_{c\_SA} = 0.2$$

L6.5.2 Damping Factor

This factor is to account for conservatism in the hysteresis damping of the building structure used in the seismic response analysis. Due to the high radiation damping of the foundation media, the effect of structure damping is insignificant. Thus,

$F_{\delta} := 1.0$

$\beta_{U\_\delta} := 0$ Since a conservative median factor of safety is used for structure damping, no value is assigned to the uncertainty and random logarithmic standard deviation.

$\beta_{R\_\delta} := 0$

$\beta_{c\_\delta} := \sqrt{\beta_{U\_\delta}^{2} + \beta_{R\_\delta}^{2}}$

$\beta_{c\_\delta} = 0$

L6.5.3 Modeling Factor

The Tier 1 lumped mass multiple-stick model of the CRCF includes the stiffness of various reinforced concrete walls and distribution of mass at each floor. The floors are assumed to be rigid diaphragms tying the different sticks together. Torsional response of the structure is captured through modeling eccentricity between the center of mass and center of rigidity of each floor. The foundation media underneath the buildings are modeled with soil springs and dashpots based on elastic half space theory with adjustment to account for layering effect of alluvium overlying tuff. Per Reference L2.2.16, BSC recognizes that final design will be accomplished by a more explicit finite element model and it is acceptable to consider the modeling factor to be median centered in these seismic fragility evaluations, thus

$F_{M} := 1.0$

$\beta_{R\_M} := 0$ Since there is no randomness in modeling.

Uncertainty of structure frequencies predicted from mathematical modeling varies from 0.15 to 0.35 depending on the sophistication of the model (Reference L2.2.1). The value of 0.35 is for a fairly approximate model and the value 0.15 is appropriate for a detailed model. Based on the complexity of the CRCF structure and the mathematical model used for the Tier 1 ISRS analysis, it is judged that the calculated CRCF frequency has a logarithmic standard deviation of 0.25.

$\beta_{f} := 0.25$ Uncertainty in building frequency.

$f_{m} := 5.2 \cdot Hz$ Best-estimate frequency

$f_{upper} := f_{m} \cdot e^{\beta_{f}}$ Upper bound frequency

$f_{upper} = 6.677 \cdot Hz$

$SA_{upper} := 1.05g$

5% damped spectral acceleration at f_{upper} read off from the mean 5E-4 UHS of the 100-foot alluvium depth case (APPENDIX L-B). This value is less than the value at the best-estimate frequency.

$f_{lower} := f_m \cdot e^{-\beta_f}$

Lower bound frequency

$f_{lower} = 4.05 \cdot Hz$

$SA_{lower} := 1.02 \cdot g$

5% damped spectral acceleration at f_{lower} read off from the mean 5E-4 UHS of the 100-foot alluvium depth case. This value is less than the value at the best-estimate frequency.

$\beta_{U\_f} := 0$

Since the spectral value at the best-estimate frequency is greater than that at either the lower bound or upper bound frequency.

$\beta_{U\_ms} := 0.15$

Uncertainty of mode shape (Reference L2.2.1, page 3-18)

$\beta_{U\_M} := \sqrt{\beta_{U\_f}^2 + \beta_{U\_ms}^2}$

$\beta_{U\_M} = 0.15$

$\beta_{c\_M} := \sqrt{\beta_{R\_M}^2 + \beta_{U\_M}^2}$

$\beta_{c\_M} = 0.15$

L6.5.4 Modal Combination

Since the direct integration time history method is used in the Tier 1 ISRS analysis (Reference L2.2.3), the modal combination method factor of safety is unity and there is no variability associated with modal combination.

$F_{MC} := 1$

$\beta_{R\_MC} := 0$

$\beta_{U\_MC} := 0$

$\beta_{c\_MC} := \sqrt{\beta_{R\_MC}^2 + \beta_{U\_MC}^2}$

$\beta_{c\_MC} = 0$

L6.5.5 Soil-Structure Interaction

The Tier 1 seismic response analyses of the CRCF used the site-wide $5*10^{-4}$ mean uniform hazard spectra as the DBGM-2 input motion. Spectrum compatible time histories are used as the input motion for the time history analyses. The conservatism in the site-wide spectra was accounted for in the spectral shape factor above. Strain compatible soil properties of 100-foot and 200-foot deep alluvium are used to calculate frequency-independent soil springs and soil damping coefficients. Soil radiation damping is introduced into the model by using dashpots. Damping coefficients equal to 75% of the computed values for translational degrees of freedom and to the full computed rotational damping values are used in the response analyses (Reference L2.2.3). Conservatism or unconservatism in SSI will be minimized for final SSI analyses used to develop equipment design seismic input. Before the final SSI analyses are completed, the Tier 1 SSI analysis is taken to represent the best-estimate responses per BSC recommendations in Reference L2.2.16.

$F_{SSI\_1} := 1.0$

$\beta_{R\_SSI\_1} := 0$

$\beta_{U\_SSI\_1} := 0.25$

Uncertainty of the median-centered state-of-the-art SSI method based on past probabilistic seismic response analyses using the same method.

$\beta_{c\_SSI\_1} := \sqrt{\beta_{R\_SSI\_1}^{2} + \beta_{U\_SSI\_1}^{2}}$ $\beta_{c\_SSI\_1} = 0.25$

It is judged that the median seismic capacity of the equipment, expressed in terms of peak ground acceleration, is close to that of BDBGM. Due to soil nonlinearity, amplification of the input ground motion at BDBGM will be different from that of DBGM-2. The second factor of safety is to account for this difference and is estimated using the DBGM-2 raw spectra and the BDBGM raw spectra at different frequencies as shown in Table L6.5-1.

For equipment shield doors with frequency in the range of 10 to 15 Hz

$Factor := mean(0.79, 0.95, 0.95, 0.85, 0.84, 0.81)$ Table L6.5-1

$Factor = 0.865$

$F_{SSI\_2\_8Hz} := \frac{1}{Factor}$

$F_{SSI\_2\_8Hz} = 1.156$

$F_{SSI\_8Hz} := F_{SSI\_1} \cdot F_{SSI\_2\_8Hz}$

$F_{SSI\_8Hz} = 1.156$

$\sigma := Stdev(0.79, 0.95, 0.95, 0.85, 0.84, 0.81)$ Table L6.5-1

$\sigma = 0.069$

$$\beta_{c\_SSI\_2} := \frac{\sigma}{Factor}$$

$\beta_{c\_SSI\_2} = 0.08$

$$\beta_{c\_SSI} := \sqrt{\beta_{c\_SSI\_1}^{2} + \beta_{c\_SSI\_2}^{2}}$$

$\beta_{c\_SSI} = 0.262$

Table L6.5-1 Comparison of 5% Damped Spectral Amplification Factors of DBGM-2 vs. BDBGM

	DBGM-2			
Freq.	24 Median	224 Median	Door Median	Median Amplif.
10	0.72	1.16	0.94	1.88
11	0.61	1.00	0.80	1.61
12	0.69	0.82	0.76	1.52
13	0.74	0.82	0.78	1.56
14	0.82	0.72	0.77	1.54
15	0.84	0.73	0.78	1.57
ZPA	0.46	0.53	0.50	
	BDBGM			
Freq.	24 Median	224 Median	Door Median	Median Amplif.
10	1.19	1.83	1.51	1.48
11	1.24	1.87	1.56	1.52
12	1.27	1.68	1.47	1.44
13	1.31	1.40	1.35	1.32
14	1.34	1.30	1.32	1.29
15	1.35	1.26	1.31	1.28
ZPA	0.96	1.08	1.02	
Freq.	Ratio of BDGM to DBGM-2 Amplif.			
10	0.79			
11	0.95			
12	0.95			
13	0.85			
14	0.84			
15	0.81			

Note that the DBGM-2 spectral values come from Figures L-A-1 and L-A-2 of Appendix L-A and the BDBGM spectral values come from Figures L-C-1 and L-C-2 of Appendix L-C. The median amplification is the door median spectral acceleration divided by the ZPA value. The door median accelerations are the average of the Node 24 and Node 224 values. For the very thick shield doors, elastic behavior is expected at the BDBGM such that the same damping is appropriate for DBGM-2 and BDBGM.

L6.5.6 Ground Motion Incoherence

$L1 := 327 \cdot ft$ East-west dimension of the CRCF excluding the 49'-6" and 43' extensions at the east and west ends, respectively (Reference L2.2.15).

$L2 := 336 \cdot ft$ North-south dimension of the CRCF excluding the 56' extension at the south end.

$L_{eq} := \sqrt{L1 \cdot L2}$ Equivalent foundation dimension of the CRCF

$L_{eq} = 331.5\ ft$

The ground motion incoherence reduction factor is a function of foundation size and frequency of response. For a 150 foot plan dimension foundation, the following reduction factors are presented in Reference L2.2.1 in page 3-22. Interpolation or extrapolation may be used to calculate the reduction factor for different dimensions and/or frequencies.

$L_{std} := 150 \cdot ft$ Foundation dimension for which the reduction factors in Reference L2.2.3 are calculated.

$f_5 := 5$ Frequency in cycle/sec (Hz)

$RF_5 := 1$ Reduction factor for response frequency at 5 Hz

$f_{10} := 10$ Frequency in Hz

$RF_{10} := 0.9$ Reduction factor for response frequency at 10 Hz

$RF_{5\_eq} := RF_5$ Reduction factor at 5 Hz, given the CRCF equivalent foundation dimension

$RF_{10\_eq} := 1 - \left[\left(1 - RF_{10}\right) \cdot \frac{L_{eq}}{L_{std}} \right]$ Linear extrapolation

$RF_{10\_eq} = 0.779$ Reduction factor at L_{eq} dimension and 10 Hz frequency of response.

At 5.2 Hz which is the fundamental frequency of horizontal response of the CRCF

$f_6 := 5.2$ Frequency in Hz

Calculate the reduction factor at 5.2 Hz frequency by interpolation

$RF_{6\_eq} := 0.4$ An arbitrary value to initiate the equation solver below.

Given

$$\frac{\log(RF_{10\_eq}) - \log(RF_{5\_eq})}{\log(RF_{6\_eq}) - \log(RF_{5\_eq})} = \frac{\log(f_{10}) - \log(f_5)}{\log(f_6) - \log(f_5)}$$

$a := \text{Find}(RF_{6\_eq})$

$a = 0.986$ Reduction factor

Thus, the ground motion incoherence factor of safety is

$$F_{GMI} := \frac{1}{a}$$

$F_{GMI} = 1.014$

$\beta_{U\_GMI} := \frac{1}{2} \cdot \ln\left(\frac{1}{a}\right)$ A reduction factor of 1.0 (i.e., no reduction) is estimated to be two standard deviation from the calculated median factor of 0.91 (Reference L2.2.1, Page 3-23).

$\beta_{U\_GMI} = 0.01$

$\beta_{R\_GMI} := 0$

$\beta_{c\_GMI} := \sqrt{\beta_{R\_GMI}^2 + \beta_{U\_GMI}^2}$

$\beta_{c\_GMI} = 0.01$

L6.5.7 Structural Response Factors

$F_{RS} := F_{SA} \cdot F_{\delta} \cdot F_M \cdot F_{MC} \cdot F_{SSI\_8Hz} \cdot F_{GMI}$

$F_{RS} = 1.261$

$\beta_{c\_RS} := \sqrt{\beta_{c\_SA}^2 + \beta_{c\_\delta}^2 + \beta_{c\_M}^2 + \beta_{c\_MC}^2 + \beta_{c\_SSI}^2 + \beta_{c\_GMI}^2}$

$\beta_{c\_RS} = 0.363$

L6.6 FRAGILITIES FOR DBGM-2 DESIGN

Fragility is the product of the capacity factor, equipment response factor, structural response factor and PGA of the DBGM-2. The composite variability, βc, is the SRSS of the uncertainties for capacity, equipment response and structural response.

$PGA := 0.453g$ Peak ground acceleration of the DBGM-2 design spectrum (Reference L2.2.14; also Section 6.2.2.1 for source information).

Capacity Factors for Cast-in-Place Anchorage of Embedded Plates

$F_{C\_CIP} = 1.237$ $\beta_{c\_CIP} = 0.13$

Capacity Factors for Welds to Embedded Plates

$F_{C\_weld} = 2.888$ $\beta_{c\_weld} = 0.19$

Capacity Factors for Shield Door Steel Supports

$F_{C\_supp} = 3.125$ $\beta_{c\_supp} = 0.472$

Equipment Response Factor

$F_{RE} = 1.772$ $\beta_{c\_RE} = 0.16$

Structural Response Factor

$F_{RS} = 1.261$ $\beta_{c\_RS} = 0.363$

Embedded Plate Anchorage

$F_{total} := F_{C\_CIP} \cdot F_{RS} \cdot F_{RE}$

$F_{total} = 2.765$

$A_m := F_{total} \cdot PGA$

$A_m = 1.253 \cdot g$ Median seismic capacity in terms of PGA

$\beta_c := \sqrt{\beta_{c\_CIP}^2 + \beta_{c\_RS}^2 + \beta_{c\_RE}^2}$

$\beta_c = 0.417$

$HCLPF := A_m \cdot e^{-2.33 \cdot \beta_c}$

$HCLPF = 0.474 \cdot g$

Embedded Plate Weld

$F_{total} := F_{C\_weld} \cdot F_{RS} \cdot F_{RE}$

$F_{total} = 6.452$

$A_m := F_{total} \cdot PGA$

$A_m = 2.923 \cdot g$ Median seismic capacity in terms of PGA

$\beta_c := \sqrt{\beta_{c\_weld}^2 + \beta_{c\_RS}^2 + \beta_{c\_RE}^2}$

$\beta_c = 0.439$

$HCLPF := A_m \cdot e^{-2.33 \cdot \beta_c}$

$HCLPF = 1.05 \cdot g$

Door Steel Supports

$F_{total} := F_{C\_supp} \cdot F_{RS} \cdot F_{RE}$

$F_{total} = 6.983$

$A_m := F_{total} \cdot PGA$

$A_m = 3.163 \cdot g$ Median seismic capacity in terms of PGA

$\beta_c := \sqrt{\beta_{c\_supp}^2 + \beta_{c\_RS}^2 + \beta_{c\_RE}^2}$

$\beta_c = 0.616$

$HCLPF := A_m \cdot e^{-2.33 \cdot \beta_c}$

$HCLPF = 0.753 \cdot g$

L7. SUMMARY

Three failure modes of the equipment shield doors in the CRCF are evaluated above: (1) anchorage failure of the embedded plates used for door support, (2) weld failure of door supports to the embedded plates, and (3) failure of structural steel door supports. Note that the very thick door plate is expected to be very lowly stressed due to earthquake and a seismic fragility is not computed for this failure mode. The seismic fragilities of these failure modes are summarized in Table L7-1:

Table L7-1 Fragilities for SSCs Designed for DBGM-2

Component	F_C	F_{RE}	F_{RS}	Am (g)	β_{c_C}	β_{c_RE}	β_{c_RS}	β_c	HCLPF(g)
CIP Bolt	1.237	1.772	1.261	1.25	0.13	0.16	0.363	0.42	0.47
Weld	2.89	1.772	1.261	2.92	0.19	0.16	0.363	0.44	1.05
Door Supports	3.13	1.772	1.261	3.16	0.472	0.16	0.363	0.62	0.75

The HCLPF exceeds the DBGM-2 PGA of 0.453g in all cases. The HCLPF for embedded plate anchored by cast-in-place (CIP) bolts exceeds the DBGM-2 PGA by only 4%. This implies that the ACI-349 design requirements for anchorage to concrete may not be conservative enough. This will be determined as a result of the ongoing seismic probabilistic risk assessment. Depending upon the results of the risk analysis, it may be prudent to restrict the stresses in CIP anchor bolts to values less than allowed by ACI-349.

The fragilities developed in this calculation are based on limiting cases where the demand is equal to the design capacity. In actual designs, this is typically not the situation, thus the limiting case fragilities developed in this calculation are generally conservative. When actual designs or detailed specifications are available, more refined fragilities could be developed that would not be as conservative as the limiting case values developed herein.

APPENDIX L-A
5% Damped In-Structure Response Spectra for CRCF (Reference L2.2.3)

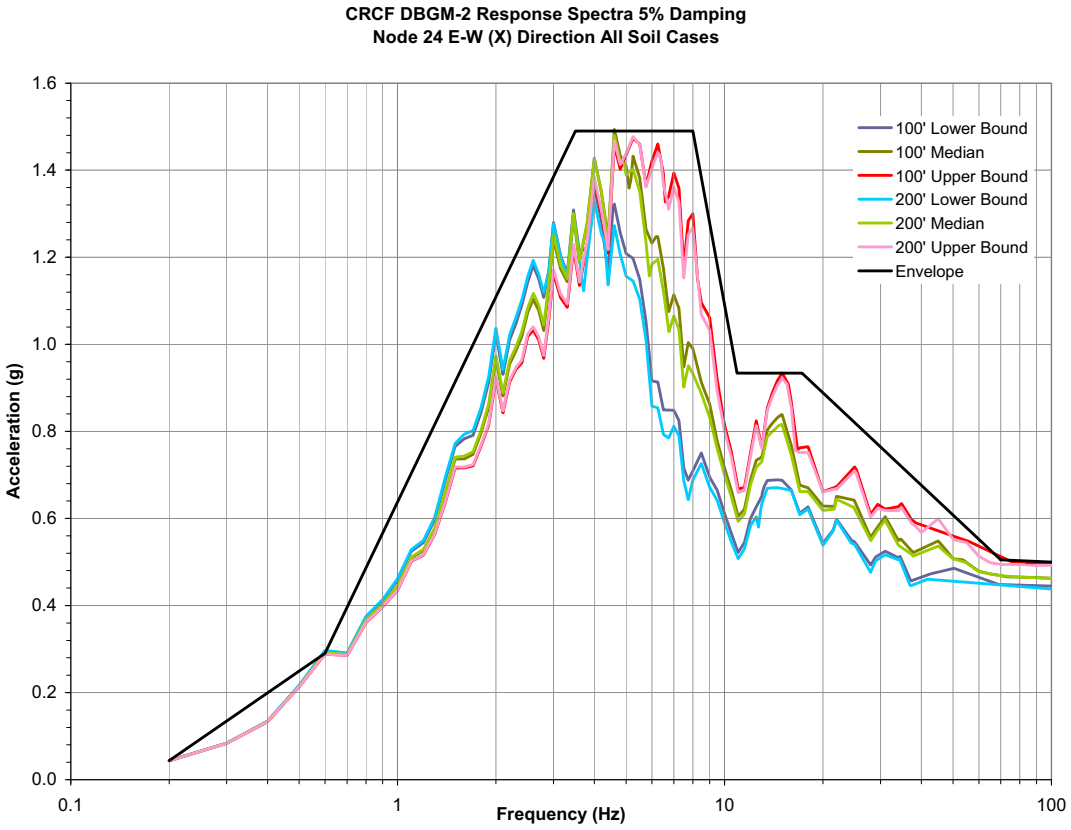

Figure L-A-1. 5% Damped Design ISRS and 100' and 200' Alluvium Depths ISRS at Ground Floor (X-Direction)

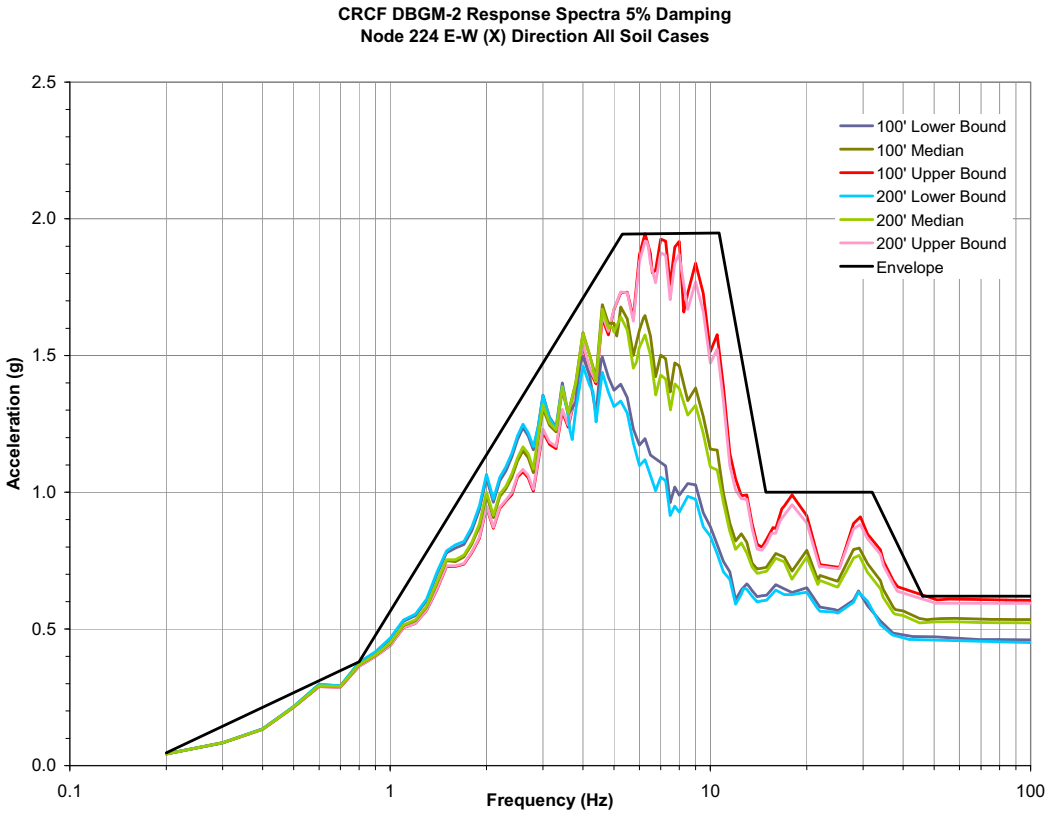

Figure L-A-2. 5% Damped Design ISRS and 100' and 200' Alluvium Depths ISRS at 32 foot Building Elevation (X-Direction)

APPENDIX L-B
UHS for 5E-4 APE

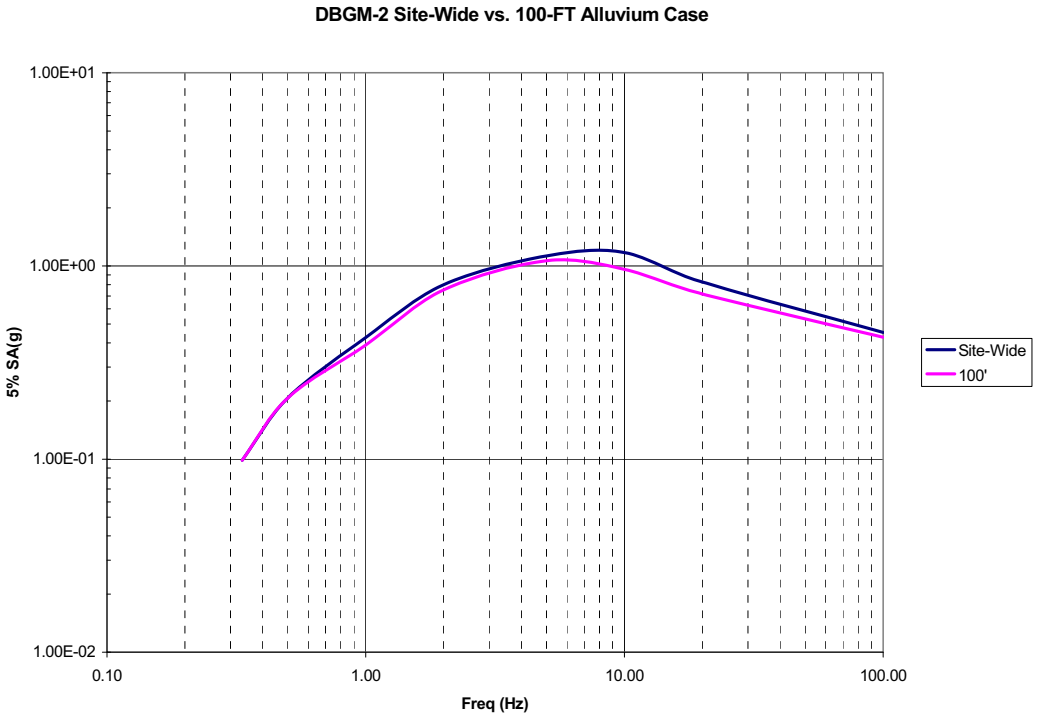

Figure L-B-1. UHS of Site-Wide and 100 Foot Alluvium Cases (See Section 6.2.2.1 for source information)

APPENDIX L-C
Comparison OF BDBGM & DBGM-2 ISRS
(Reference L2.2.3)

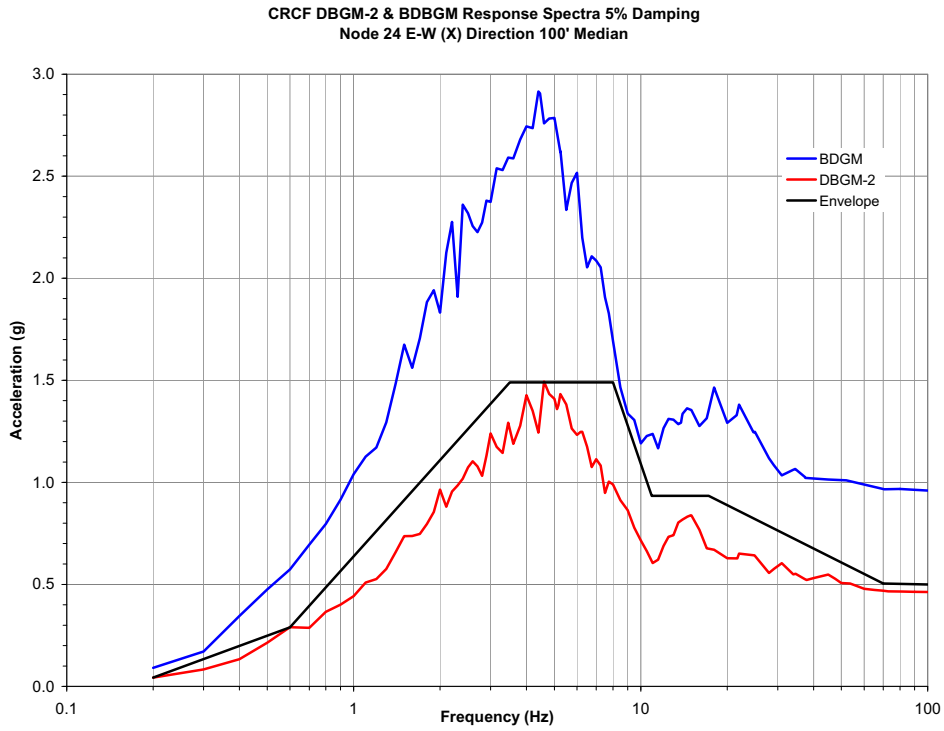

Figure L-C-1. 5% Damped 100' Alluvium Depth ISRS for BDBGM and DBGM-2 at Ground Floor (X-Direction)

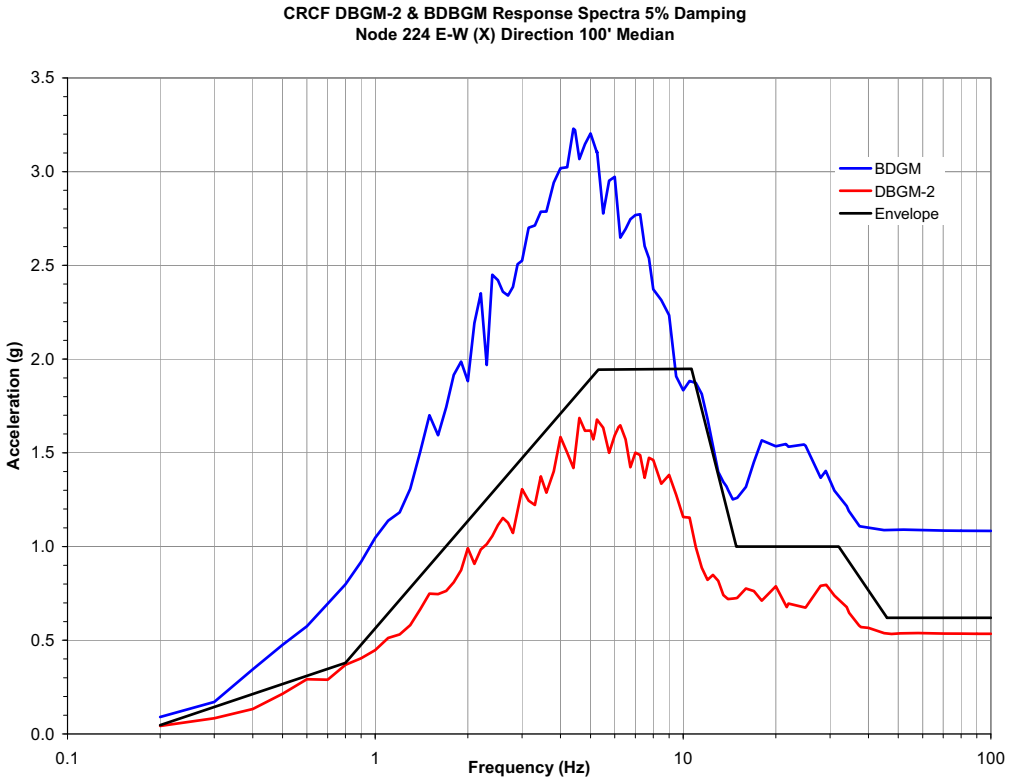

Figure L-C-2. 5% Damped 100' Alluvium Depth ISRS for BDBGM and DBGM-2 at 32 Foot Building Elevation (X-Direction)

ATTACHMENT M
FRAGILITY FOR OFFSITE POWER

Prepared by: **Greg S. Hardy**

ARES Check By: **Robert D. Campbell**

LLNL Check By: **Robert C. Murray**

TABLE OF CONTENTS

ACRONYMS AND ABBREVIATIONS

ACI	American Concrete Institute
AISC	American Institute of Steel Construction
ANSI	American National Standards Insitute
AO	Aging Overpack
APE	Annual Probability of Exceedance
ASCE	American Society of Civil Engineers
ASME	American Society of Mechanical Engineers
BSC	Bechtel SAIC, LLC
BDBGM	Beyond Design Basis Ground Motion at $1x10^{-4}$ APE
CDFM	Conservative Deterministic Failure Margin
CHC	Cask Handling Crane
CIP	Cast-in-Place
CRCF	Canister Receipt and Closure Facility
CTM	Canister Transfer Machine
CTT	Cask Transfer Trolley
DBGM-2	Design Basis Ground Motion at $5x10^{-4}$ APE
DL	Dead Load
DOF	Degree of Freedom
DPC	Dual Purpose Canister
EPRI	Electric Power Research Institute
HCLPF	High Confidence of Low Probability of Failure
HVAC	Heating, Ventilation, & Air Conditioning
IEEE	Institute of Electrical and Electronics Engineers
IHF	Initial Handling Facility
ISRS	In-Structure Response Spectra

ACRONYMS AND ABBREVIATIONS (cont.)

ITS	Important to Safety
LA	License Application
LLNL	Lawrence Livermore National Laboratory
NPP	Nuclear Power Plant
PGA	Peak Ground Acceleration
RF	Receipt Facility
RRS	Required Response Spectrum
Sa	Spectral Acceleration
SFA	Surface Facilities Area
SFTM	Spent Fuel Transfer Machine
SPRA	Seismic Probabilistic Risk Assessment
SRSS	Square Root of the Sum of Squares
SSE	Safe Shutdown Earthquake (used with NPPs)
SSI	Soil Structure Interaction
SSC	Structure, System, and Component
TAD	Transportation, Aging, and Disposal canister
TEV	Transport and Emplacement Vehicle
TRS	Test Response Spectrum
UHS	Uniform Hazard Spectra
USDOE	United States Department of Energy
USNRC	United States Nuclear Regulatory Commission
WHF	Wet Handling Facility
WP	Waste Package
WPTT	Waste Package Transfer Trolley
YMSF	Yucca Mountain Surface Facilities
ZPA	Zero Period Acceleration

FRAGILITY TERMINOLOGY

Am	Median Peak Ground Motion Capacity
β_R	Log Standard Deviation of Randomness
β_U	Log Standard Deviation of Uncertainty (Lack of Knowledge)
β_C	Composite Variability = $(\beta_R^2 + \beta_U^2)^{0.5}$
F_S	Strength Factor of Safety
β_{R_S}	Strength Randomness (typical)
β_{U_S}	Strength Uncertainty (typical)
β_{C_S}	Strength Composite Variability (typical)
F_μ	Inelastic Energy Absorption Factor of Safety
F_{QM}	Qualification Factor of Safety
F_δ	Damping Factor of Safety
F_M	Modeling Factor of Safety
F_{MC}	Modal Combination Factor of Safety
F_{ECC}	Earthquake Component Combination Factor of Safety
F_{SA}	Spectral Shape Factor of Safety
F_{SSI}	Soil-Structure Interaction Factor of Safety
F_{GMI}	Ground Motion Incoherence Factor of Safety
F_{TOTAL}	Total Factor of Safety
F_{RS}	Structural Response Factor of Safety
F_{RE}	Equipment Response Factor of Safety

M1. PURPOSE

The purpose of this calculation is to develop a seismic fragility for the offsite power system at Yucca Mountain.

M2. REFERENCES

M2.1 PROCEDURES AND DIRECTIVES

M2.1.1 EG-PRO-3DP-G04B-00037, Rev. 10. *Calculations and Analyses*. Las Vegas, Nevada: Bechtel SAIC Company. ACC: ENG.20071018.0001.

M2.1.2 IT-PRO-0011, Revision 7, ICN 0. *Software Management*. Las Vegas, Nevada: Bechtel SAIC Company. ACC: DOC.20070905.0007.

M2.2 DESIGN INPUTS

M2.2.1 EPRI (Electric Power Research Institute) 1994. *Methodology for Developing Seismic Fragilities*. EPRI TR-103959. Palo Alto, California: Electric Power Research Institute. TIC:253770. [DIRS 161329]

M2.2.2 Budnitz, R.J.; Lambert, H.E.; Apostolakis, G.; Salas, J.K.; Wu, J.S.; and Ravindra, M.K. 1998. *A Methodology for Analyzing Precursors to Earthquake-Initiated and Fire-Initiated Accident Sequences*. NUREG/CR-6544. Washington, D.C.: U.S. Nuclear Regulatory Commission. ACC: MOL.20080122.0254. [DIRS 184644]

M2.2.3 Campbell, R.D., Ravindra, M.K., Bhatia, A., and Murray, R.C. 1985. *Compilation of Fragility Information from Available Probabilistic Risk Assessments*. UCID-20571. Livermore, CA: Lawrence Livermore National Laboratory. ACC: MOL.20080207.0023. [DIRS 184646]

M2.3 DESIGN CONSTRAINTS

None

M2.4 DESIGN OUTPUTS

The design output is the seismic fragility for failure modes that could result in damage to the offsite power system and result in loss of external AC power.

M3. ASSUMPTIONS

M3.1 ASSUMPTIONS REQUIRING VERIFICATION

None

M3.2 ASSUMPTIONS NOT REQUIRING VERIFICATION

None

M4. METHODOLOGY

M4.1 QUALITY ASSURANCE

This calculation is prepared in accordance with Bechtel SAIC LLC procedure EG-PRO-3DP-GO4B-00037, Rev. 10, Reference M2.1.1.

M4.2 USE OF SOFTWARE

Mathcad 14 is used in this calculation. The use of this software is classified as Level 2 software per procedure IT-PRO-0011, Rev. 7, Ref. M2.1.2. Therefore the software does not require separate qualification.

M5. LIST OF APPENDICES

None

M6. DEVELOPMENT OF FRAGILITY

Offsite power fragilities are traditionally developed directly from earthquake experience data. This is different from most of the fragilities that are developed from individual response and capacity factors as described in Reference M2.2.1. The fragility for offsite power is defined as the earthquake level at which the offsite AC power will not be available to the YMSF following the earthquake. Since the offsite power system is not safety related, it has not necessarily been designed (or will not be designed for the portions that are not yet built) for seismic loads. Failure of offsite power can occur due to a variety of failure modes, including the following:

1) Transmission line failures
2) Transformer Bushing Failures
3) Circuit Breaker Leakage
4) Ceramic Insulator Damage and Failure
5) Electrical Panel Failure

These failures could occur within the switchyard at the Yucca Mountain site, within the transmission lines away from the site or in the substations that feed power to the YMSF. As a result, it is extremely resource intensive to determine a fragility for the specific offsite power system (substations, transmission systems and switchyards) that will be utilized at Yucca Mountain. As a result, generic fragilities based on earthquake experience will be the basis for this fragility.

References M2.2.2 and M2.2.3 both report generic fragilities for the offsite power systems based on the performance of the grid following earthquakes at various peak ground accelerations. Reference M2.2.2 (Table 6-1) recommends the following for offsite power fragility parameters:

$$A_m := 0.3g$$

$$\beta_R := 0.3$$

$$\beta_U := 0.45$$

$$\beta_c := \sqrt{\beta_R^{\,2} + \beta_U^{\,2}} = 0.541$$

$$HCLPF := A_m \cdot e^{-2.33 \cdot \beta_c} = 0.085 \cdot g$$

Reference M2.2.3 (Table 1) summarizes the fragilities from a wide number of past Seismic Probabilistic Risk Assessments (SPRAs) and supports the use of this fragility. The values utilized within those past SPRAs for offsite power fragility ranged from a median of 0.2 g (PGA) to a median of 0.4 g (PGA). The HCLPF value for all of the generic fragilities within Reference M2.2.3 was approximately 0.1 g. Thus, the range of offsite power fragilities reported in nuclear plant SPRAs supports the median value of 0.3 g for A_m and also the HCLPF of 0.085 g.

M7. SUMMARY OF RESULTS AND CONCLUSIONS

The offsite power fragility recommended for use at Yucca Mountain is defined above. That fragility is based on earthquake experience and is the best source of data with which to develop the offsite power median capacity and variabilities. There has been some evidence that more modern switchyard components for higher KV systems, such as the one that will be designed for the Yucca Mountain site, have a somewhat higher seismic capacity than this general fragility defined above, but that higher capacity would not necessarily apply to the transmission lines, the cabinet fragility nor the substation component fragilities (all of which are integral to the overall offsite power fragility). Therefore, the generic fragility above is judged to be appropriate for Yucca Mountain.

ATTACHMENT N
FRAGILITY FOR STRUCTURAL FAILURE OF CRCF CANISTER STAGING RACKS

Prepared By: Stephen A. Short

ARES Check By: Wen H. Tong

LLNL Check By: Robert C. Murray

TABLE OF CONTENTS

ACRONYMS AND ABBREVIATIONS

ACI	American Concrete Institute
AISC	American Institute of Steel Construction
ANSI	American National Standards Insitute
AO	Aging Overpack
APE	Annual Probability of Exceedance
ASCE	American Society of Civil Engineers
ASME	American Society of Mechanical Engineers
BSC	Bechtel SAIC, LLC
BDBGM	Beyond Design Basis Ground Motion at $1x10^{-4}$ APE
CDFM	Conservative Deterministic Failure Margin
CHC	Cask Handling Crane
CIP	Cast-in-Place
CRCF	Canister Receipt and Closure Facility
CTM	Canister Transfer Machine
CTT	Cask Transfer Trolley
DBGM-2	Design Basis Ground Motion at $5x10^{-4}$ APE
DL	Dead Load
DOF	Degree of Freedom
DPC	Dual Purpose Canister
EPRI	Electric Power Research Institute
HCLPF	High Confidence of Low Probability of Failure
HVAC	Heating, Ventilation, & Air Conditioning
IEEE	Institute of Electrical and Electronics Engineers
IHF	Initial Handling Facility
ISRS	In-Structure Response Spectra

ACRONYMS AND ABBREVIATIONS (cont.)

ITS	Important to Safety
LA	License Application
LLNL	Lawrence Livermore National Laboratory
NPP	Nuclear Power Plant
PGA	Peak Ground Acceleration
RF	Receipt Facility
RRS	Required Response Spectrum
Sa	Spectral Acceleration
SFA	Surface Facilities Area
SFTM	Spent Fuel Transfer Machine
SPRA	Seismic Probabilistic Risk Assessment
SRSS	Square Root of the Sum of Squares
SSE	Safe Shutdown Earthquake (used with NPPs)
SSI	Soil Structure Interaction
SSC	Structure, System, and Component
TAD	Transportation, Aging, and Disposal canister
TEV	Transport and Emplacement Vehicle
TRS	Test Response Spectrum
UHS	Uniform Hazard Spectra
USDOE	United States Department of Energy
USNRC	United States Nuclear Regulatory Commission
WHF	Wet Handling Facility
WP	Waste Package
WPTT	Waste Package Transfer Trolley
YMSF	Yucca Mountain Surface Facilities
ZPA	Zero Period Acceleration

FRAGILITY TERMINOLOGY

Am	Median Peak Ground Motion Capacity
β_R	Log Standard Deviation of Randomness
β_U	Log Standard Deviation of Uncertainty (Lack of Knowledge)
β_C	Composite Variability = $(\beta_R^2 + \beta_U^2)^{0.5}$
F_S	Strength Factor of Safety
β_{R_S}	Strength Randomness (typical)
β_{U_S}	Strength Uncertainty (typical)
β_{C_S}	Strength Composite Variability (typical)
F_μ	Inelastic Energy Absorption Factor of Safety
F_{QM}	Qualification Factor of Safety
F_δ	Damping Factor of Safety
F_M	Modeling Factor of Safety
F_{MC}	Modal Combination Factor of Safety
F_{ECC}	Earthquake Component Combination Factor of Safety
F_{SA}	Spectral Shape Factor of Safety
F_{SSI}	Soil-Structure Interaction Factor of Safety
F_{GMI}	Ground Motion Incoherence Factor of Safety
F_{TOTAL}	Total Factor of Safety
F_{RS}	Structural Response Factor of Safety
F_{RE}	Equipment Response Factor of Safety

N1. PURPOSE

The purpose of this calculation is to estimate the seismic fragility of canister staging racks located in the Canister Receipt and Closure Facility (CRCF). Detailed design specifications and detailed design analyses are not yet available so the derivations are representative based on the applicable BSC specifications for seismic design and applicable codes and standards. The mean seismic fragility curve of the canister staging racks will be convolved with the mean site-specific seismic hazard curve to calculate risk of seismic-induced canister staging rack failure.

N2. REFERENCES

N2.1 PROCEDURES AND DIRECTIVES

N2.1.1 EG-PRO-3DP-G04B-00037, Rev. 10. *Calculations and Analyses*. Las Vegas, Nevada: Bechtel SAIC Company. ACC: ENG.20071018.0001.

N2.1.2 IT-PRO-0011, Revision 7, ICN 0. *Software Management*. Las Vegas, Nevada: Bechtel SAIC Company. ACC: DOC.20070905.0007.

N2.2 DESIGN INPUTS

N2.2.1 EPRI (Electric Power Research Institute) 1994. *Methodology for Developing Seismic Fragilities*. EPRI TR-103959. Palo Alto, California: Electric Power Research Institute. TIC:253770. [DIRS 161329]

N2.2.2 ASCE/SEI 43-05. 2005. *Seismic Design Criteria for Structures, Systems, and Components in Nuclear Facilities*. Reston, Virginia: American Society of Civil Engineers. TIC: 257275. [DIRS 173805]

N2.2.3 BSC (Bechtel SAIC Company) 2007. *CRCF Tier-1 In-Structure Response Spectra*. 060-SYC-CR00-00900-000-00B. Las Vegas, Nevada: Bechtel SAIC Company. ACC: ENG.20071210.0008. [DIRS 184330]

N2.2.4 BSC (Bechtel SAIC Company) 2008. *CRCF 1 DOE Canister Staging Rack Mechanical Equipment Envelope*. 060-MJ0-HTC0-00501-000 REV 00B. Las Vegas, Nevada: Bechtel SAIC Company. ACC: ENG.20080128.0002. [DIRS 184908]

N2.2.5 BSC (Bechtel SAIC Company) 2008. *CRCF 1 TAD Canister Staging Rack Mechanical Equipment Envelope*. 060-MJ0-HTC0-00601-000 REV 00B. Las Vegas, Nevada: Bechtel SAIC Company. ACC: ENG.20080128.0003. [DIRS 184909]

N2.2.6 ANSI/AISC N690-1994. 1994. *American National Standard Specification for the Design, Fabrication, and Erection of Steel Safety-Related Structures for Nuclear Facilities*. Chicago, Illinois: American Institute of Steel Construction. TIC: 252734. [DIRS 158835]

N2.2.7 [Reserved]

N2.2.8 Blevins, R.D. 2001. *Formulas for Natural Frequency and Mode Shape*. 1st Edition. Malabar, Florida: Krieger Publishing Company. ISBN 1-57524-184-6. 506 pp.

N2.2.9 MO0801HCUHSSFA.001. *Mean Hazard Curves and Mean Uniform Hazard Spectra for the Surface Facilities Area*. Submittal date: 01/11/2008. [DIRS 184802]

N2.2.10 BSC (Bechtel SAIC Company) 2008. *Canister Receipt and Closure Facility 1 General Arrangement Ground Floor Plan*. 060-P10-CR00-00102-000 REV 00C. Las Vegas, Nevada: Bechtel SAIC Company. ACC: ENG.20080122.0013. [DIRS 184853]

N2.2.11 Moore, D. 2007. "*SSI Factor of Safety.*" E-mail from D. Moore to B. Murray, October 25, 2007. ACC: LLR.20080110.0145. [DIRS 184842]

N2.2.12 BSC (Bechtel SAIC Company) 2006. *Canister Receipt and Closure Facility (CRCF) Seismic Analysis*. 060-SYC-CR00-00400-000-00A. Las Vegas, Nevada: Bechtel SAIC Company. ACC: ENG.20061220.0029. [DIRS 178793]

N2.2.13 AISC (American Institute of Steel Construction) 1991. *Manual of Steel Construction, Allowable Stress Design.* 9th Edition, 1st Revision. Chicago, Illinois: American Institute of Steel Construction. TIC: 4254. [DIRS 127579]

N2.2.14 Moore, D. 2007. "Staging Racks." E-mail from D. Moore to S. Short (ARES Corp.), November 28, 2007. ACC: LLR.20080128.0004. [DIRS 184928]

N2.2.15 BSC (Bechtel SAIC Company) 2007. *Basis of Design for the TAD Canister-Based Repository Design Concept*. 000-3DR-MGR0-00300-000-001. Las Vegas, Nevada: Bechtel SAIC Company. ACC: ENG.20071002.0042; ENG.20071026.0033; ENG.20071108.0002; ENG.20071109.0001; ENG.20071120.0023; ENG.20071126.0049; ENG.20071214.0009; ENG.20071213.0005; ENG.20071227.0018; ENG.20080207.0004; ENG.20080212.0003. [DIRS 182131]

N2.2.16 BSC (Bechtel SAIC Company) 2006. *Seismic Analysis and Design Approach Document.* 000-30R-MGR0-02000-000 Rev. 001. Las Vegas, Nevada: Bechtel SAIC Company. ACC: ENG.20071220.0029. [DIRS 184494]

N2.3 DESIGN CONSTRAINTS

There are no design constraints in the performance of this calculation

N2.4 DESIGN OUTPUTS

The calculated seismic fragility of structural failure of canister staging racks in the CRCF, expressed in terms of a median seismic capacity and an associated combined variability, will be convolved with the site-specific seismic hazard curve to calculate risk of seismic-induced failure of CRCF canister staging racks. This is performed to support information in the License Application (LA).

N3. ASSUMPTIONS

N3.1 ASSUMPTIONS REQUIRING VERIFICATION

There are no assumptions in this calculation that require verification.

N3.2 ASSUMPTIONS NOT REQUIRING VERIFICATION

N3.2.1 Canister staging rack detailed designs and design specifications have not been developed at the time of this seismic fragility calculation. The general guidance for seismic design in References N2.2.15 and N2.2.16 are utilized to determine what codes and standards will likely govern and what criteria will be used for design of the canister staging racks for DBGM-2 and evaluation for BDBGM.

Rationale - The fragility is based on the well established design methods given in References N2.2.15 and N2.2.16 and does not require any further verification.

N3.2.2 The development of representative fragilities is based on the methodology in Reference N2.2.1.

Rationale - The methodology is well established and quoted in Reference N2.2.15 and does not require any further verification.

N4. METHODOLOGY

N4.1 QUALITY ASSURANCE

This calculation is prepared in accordance with Bechtel SAIC LLC procedure EG-PRO-3DP-G04B-00037, Rev. 10, Reference N2.1.1.

N4.2 USE OF SOFTWARE

Mathcad 14 is used in this calculation. The use of this software is classified as Level 2 software per procedure IT-PRO-0011, Ref. N2.1.2. Therefore the software does not require separate qualification.

N5. LIST OF APPENDICES

APPENDIX N-A 5% Damped In-Structure Response Spectra for CRCF

APPENDIX N-B UHS for 5E-4 APE

APPENDIX N-C Comparison of BDBGM & DBGM-2 ISRS

N6. DEVELOPMENT OF FRAGILITIES

A representative seismic fragility of canister staging racks located in the CRCF is calculated here. The calculation considers staging rack failure when it loses structural integrity and fails to hold canisters in an upright and separated position.

N6.1 CANISTER STAGING RACKS

Canister staging racks are located on the ground floor in four rooms of the CRCF. These racks are shown conceptually in References N2.2.4 and N2.2.5 for DOE and TAD canisters respectively. Sketches of the rack concepts are shown in Figures N6.2-1 and N6.2-2.

The weight of the racks is 6.5 tons per References N2.2.4 and N2.2.5. DOE canisters stored in the racks weigh up to 21 tons and TAD canisters stored in the racks weigh up to 55 tons.

The canister staging racks appear to be substantial braced frame structures made of tubular steel. The braced frame structure containing the canisters is anchored to the floor by bolts or welds. In addition, this structure is braced at two elevations by steel members that extend out to all four canister staging room walls. These horizontal seismic supports are attached to the walls by welds or bolts. It is likely that the attachment is in all directions at one wall and only for vertical support at the opposite wall. In this manner, the supports may be designed to accommodate thermal expansion.

To achieve structural integrity of the racks during earthquakes, the racks will be designed as steel members following allowable stress design in accordance with the applicable provisions of ANSI/AISC N690-1994, *American National Standard Specification for the Design, Fabrication, and Erection of Steel Safety-Related Structures for Nuclear Facilities* (Reference N2.2.6), for loads and accelerations associated with a DBGM-2 seismic event. They are also analyzed for more severe events, including the BDBGM seismic event, to provide assurance that under such loading and accelerations they will not collapse.

Seismic design criteria is specified in Reference N2.2.16, for steel allowable stress design. By these criteria, earthquake loads are combined with non-seismic concurrent loads with load factors of unity. In addition, stresses due to the combined loads are limited to the allowable stress multiplied by a stress increase factor, k. For compression in members, shear in members, and bolted connections, k is 1.4, for all others k is 1.6 (Section 8.3.3 of Reference N2.2.16).

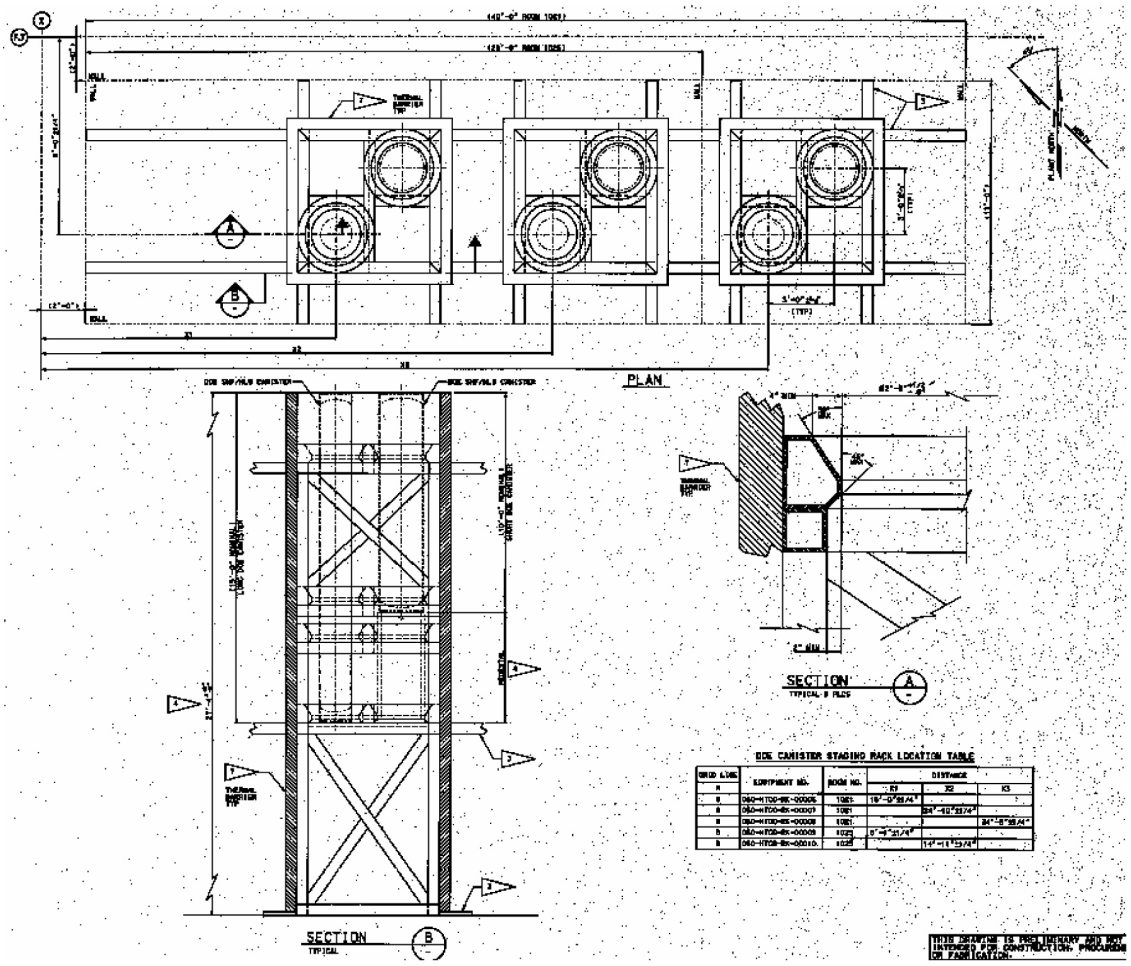

Figure N6.1-1 DOE Canister Staging Rack
NOTE: Legibility of figure does not affect the technical content of the document. See source for detail

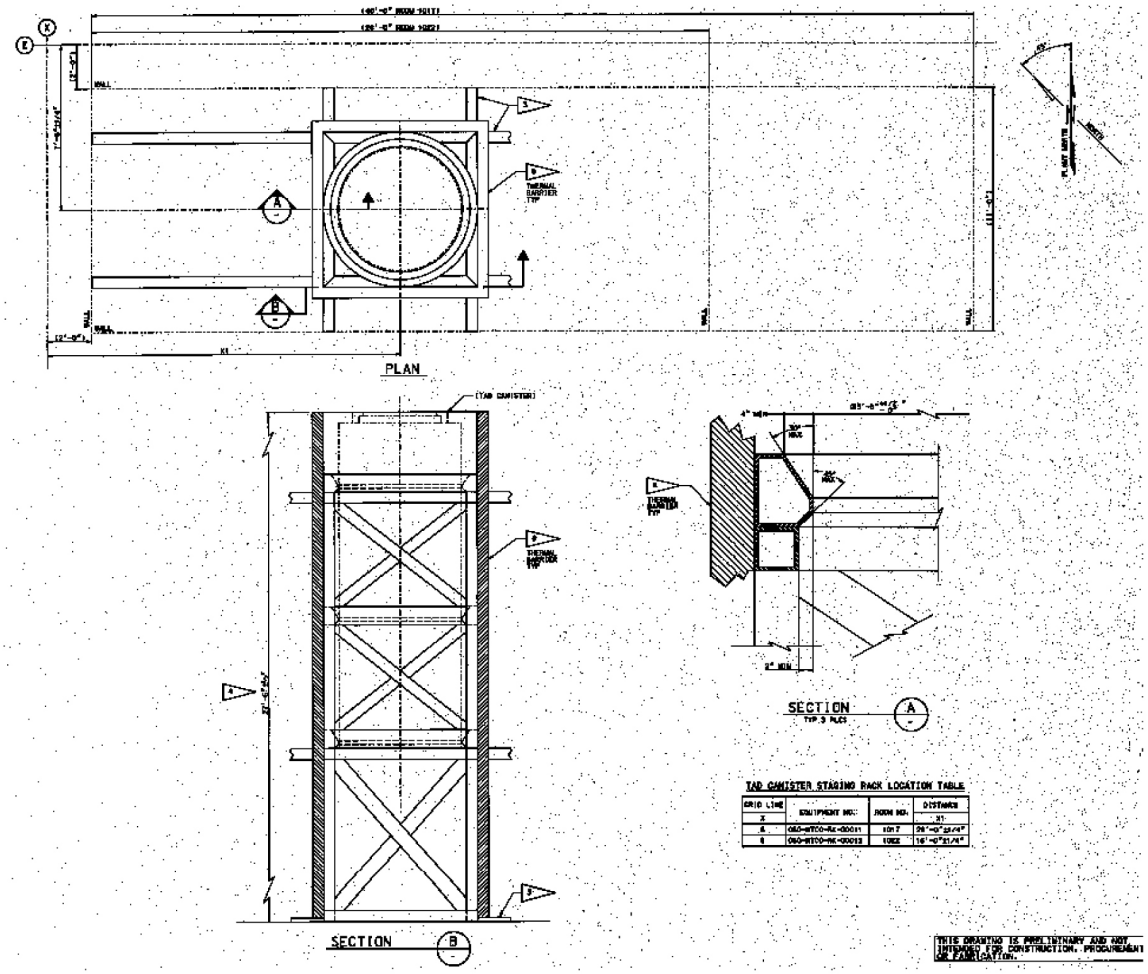

Figure N6.1-2 TAD Canister Staging Rack

N6.2 POTENTIAL FAILURE MODES

Canister staging racks are very stiff steel structures whose stiffness is derived from axial behavior of horizontal supporting members and of diagonal bracing members in vertical planes. With both braced frame behavior and horizontal supports at two elevations to all four walls, this structure has a great deal of redundancy and is likely to have very high seismic capacity. However, detailed designs are not currently available such that it must be assumed that all members are designed to their full capacity.

Seismic inertial loads will be resisted by members in proportion to their relative rigidities. For this fragility calculation, these forces will be determined by a detailed structural analysis and members will be designed such that the seismic demand in all members will be just equal to the member capacity. In fact, there is always margin between the demand and the capacity and for these racks that margin would be expected to be larger than is typical because of the redundancy of this design concept with multiple load paths.

It is likely that the stiffest load path is through the horizontal supporting members transferring seismic inertial loads out to the building four foot thick walls. During earthquake shaking, horizontal supports on one side of the canisters go into tension and the horizontal supports on the opposite side of the canisters go into compression. One potential failure mode is buckling of these horizontal supports in compression.

Following horizontal support buckling, the horizontal supports would become ineffective in carrying load and all load would be transferred down through the braced frame to the floor. However, this braced frame is already designed with no margin and the additional load transferred from buckled horizontal supports would produce collapse of the rack.

Even if the rack braced frame that is supported from the floor were the stiffest load path, the staging racks could not fail until the horizontal strut members failed in buckling. When the braced frame has seismic loads in excess of its capacity, it would lose stiffness and load would be transferred to the horizontal struts. Failure would not occur until buckling of the horizontal struts occurs.

Hence, the governing failure mode of the CRCF canister staging racks will be taken to be buckling of horizontal support steel members.

N6.3 DEVELOPMENT OF CAPACITY FACTORS

A capacity factor will be developed for buckling of the horizontal strut members supporting the staging rack braced frame.

Staging rack members and supports would typically be designed as structural steel members using common structural profiles of low carbon steel. Per References N2.2.4 and N2.2.5, the supporting members appear to be steel tubing members on the order of 6 by 6 inch member size. Per Reference N2.2.16, such supports are to be designed to the ANSI/AISC N-690 code (Ref. N2.2.6). For members in compression, the working stress allowable includes a factor of safety that varies between 5/3 = 1.67 and 23/12 = 1.92, depending on the member slenderness ratio, (Section CQ1.5.1.3.1 of Ref. N2.2.6). For extreme loads, Section 8.3.3 of Reference N2.2.16 allows a 1.4 increase in working stress allowable for compression in members.

Following ANSI/AISC N-690 (Ref. N2.2.6), the allowable compression capacity of a steel structural member depends on the unbraced length, the stiffness, and the material strength. From References N2.2.4 and N2.2.5, the largest unbraced lengths appear to be about 134 inches for the DOE canister and 252 inches for the TAD canister, respectively. As mentioned above, for both types of canisters, the structural members appear to be 6 inch square hollow structural sections (HSS). It is specified that A500 steel will be used for the rack structural members for which minimum specified yield strength and the elastic modulus are:

$F_y := 46ksi$ $E := 29000ksi$

From References N2.2.4 and N2.2.5:

$L_{DOE} := 134in$ $L_{TAD} := 252in$

$W_{rack} := 6.5tonf$ $W_{rack} = 13 \cdot kip$ References N2.2.4 and N2.2.5

$W_{DOE} := 21tonf$ $W_{DOE} = 42 \cdot kip$ Reference N2.2.4

$W_{T\_DOE} := W_{rack} + W_{DOE}$ $W_{T\_DOE} = 55 \cdot kip$

$W_{TAD} := 55tonf$ $W_{TAD} = 110 \cdot kip$ Reference N2.2.5

$W_{T\_TAD} := W_{rack} + W_{TAD}$ $W_{T\_TAD} = 123 \cdot kip$

Suppose the 6 inch square HSS members are an intermediate size from the AISC code with 3/8 inch wall thickness (Reference N2.2.13) for the TAD support. In this case:

$A_{HSS\_6\_TAD} := 8.08in^2$ Member cross section area

$r_{TAD} := 2.27in$ radius of gyration

It is logical that the support members for the DOE canisters are lighter as loads are less and unbraced lengths are shorter. Suppose the 6 inch square HSS members are an intermediate size from the AISC code with 1/4 inch wall thickness (Reference N2.2.13) for the DOE support. In this case:

$A_{HSS\_6\_DOE} := 5.59in^2$ Member cross section area

$r_{DOE} := 2.33in$ radius of gyration

For this braced rack configuration the effective length, KL is equal to the actual length L.

For the configuration shown in References N2.2.4 and N2.2.5 and the member sizes shown above, the axial stiffness of the racks for the DOE and TAD canisters may be computed. In this computation, the stiffness is derived from 4 braces acting in compression as the tensile side is taken to be a vertical support only.

$$k_{DOE} := \frac{4A_{HSS\_6\_DOE}\cdot E}{L_{DOE}} = 4839.1\cdot\frac{kip}{in} \qquad k_{TAD} := \frac{4A_{HSS\_6\_TAD}\cdot E}{L_{TAD}} = 3719.4\cdot\frac{kip}{in}$$

From Table 6-2 of Ref. N2.2.8, the fundamental frequency of the rack may be estimated.

$$f_{DOE} := \frac{1}{2\cdot\pi}\cdot\sqrt{\frac{k_{DOE}\cdot g}{W_{T\_DOE}}} = 29.334\cdot Hz \qquad f_{TAD} := \frac{1}{2\cdot\pi}\cdot\sqrt{\frac{k_{TAD}\cdot g}{W_{T\_TAD}}} = 17.197\cdot Hz$$

These frequencies are lower bound values as they don't consider the stiffness of the braced frame part of the rack supported off the floor. The longest braces considered herein extend in the east west direction and are thus subject to earthquake excitation in the x-direction. Input is through the supporting walls which may be estimated as the average of the ground floor and first floor (Elevation 32 feet) in-structure response spectra (ISRS). From Figures N-A-1 and N-A-2, it may be seen that spectral accelerations are between about 0.7 and 0.9g at the ground floor and about 1.0g at the first floor in the 20 to 30 Hz range.

By Reference N2.2.6, the allowable compression capacity depends on the slenderness ratio (kL/r) where for this case K=1 and the parameter C_c as defined below:

$$\frac{L_{DOE}}{r_{DOE}} = 57.511 \qquad \frac{L_{TAD}}{r_{TAD}} = 111.013$$

$$C_c := \sqrt{\frac{2\cdot\pi^2\cdot E}{F_y}} \qquad C_c = 111.554$$

$$\lambda_{DOE} := \frac{\frac{L_{DOE}}{r_{DOE}}}{C_c} = 0.516 \qquad \lambda_{TAD} := \frac{\frac{L_{TAD}}{r_{TAD}}}{C_c} = 0.995$$

Where kl/r is less than C_c , the allowable buckling stress is given by:

$$F_{a\_DOE} := \frac{\left(1 - \frac{\lambda_{DOE}^{2}}{2}\right)\cdot F_y}{\frac{5}{3} + \frac{3}{8}\cdot\lambda_{DOE} - \frac{1}{8}\cdot\lambda_{DOE}^{3}}$$ Equation Q1.5-1 of Ref. N2.2.6

$$F_{a\_DOE} = 21.644\cdot ksi$$

$$F_{a\_TAD} := \frac{\left(1 - \frac{\lambda_{TAD}^{2}}{2}\right)\cdot F_y}{\frac{5}{3} + \frac{3}{8}\cdot\lambda_{TAD} - \frac{1}{8}\cdot\lambda_{TAD}^{3}}$$ Equation Q1.5-1 of Ref. N2.2.6

$$F_{a\_TAD} = 12.116\cdot ksi$$

By Section 8.3.3 of Reference N2.2.16, these allowable stresses may be increased by a factor of 1.4 for design of members in compression and subject to seismic loads. The denominator of the above equations is the factor of safety between allowable stress of the code and the buckling capacity (As noted above this factor ranges from 1.67 to 1.92 depending on the value of λ. For seismic design, the strength factor against buckling is reduced by 1.4. Also, per Ref. N2.2.1, median yield for structural steel such as A500 is 1.2 times the minimum specified level. Hence.

$$F_{S\_DOE} := \left(\frac{5}{3} + \frac{3}{8}\cdot\lambda_{DOE} - \frac{1}{8}\cdot\lambda_{DOE}^{3}\right)\cdot\frac{1.2}{1.4} = 1.58$$

$$F_{S\_TAD} := \left(\frac{5}{3} + \frac{3}{8}\cdot\lambda_{TAD} - \frac{1}{8}\cdot\lambda_{TAD}^{3}\right)\cdot\frac{1.2}{1.4} = 1.643$$

$$F_S := \frac{F_{S\_DOE} + F_{S\_TAD}}{2} = 1.611$$

The numerators of the equations for allowable stress are close to median capacity for λ value of about 0.4 and above [i.e., (1-λ^2/2)Fy]. Hence:

$$F_\mu := 1.0$$

$$F_C := F_S\cdot F_\mu$$

$$F_C = 1.611$$

Uncertainty is computed using F_C for the capacity of the rack supports. Let the onset of code buckling be a 99 percentile value (-2.33 βc). Then the factor to code yield is:

$$\beta_{c\_C} := \frac{1}{2.33} \cdot \ln\left(F_C\right) \qquad \beta_{c\_C} = 0.205$$

N6.4 EQUIPMENT RESPONSE

The equipment response factor will vary depending upon the frequency of the equipment and the method of analysis. The demand spectra for the CRCF at the ground floor and at a height of 32 feet will be used for staging rack locations for the purposes of this representative calculation. Rack seismic input is introduced at the walls between the ground and first floors. Furthermore, the rack support compression strut considered in this calculation are all aligned with the same orientation in the CRCF such that the x direction seismic input results in axial strut behavior that is the focus of this seismic fragility evaluation. Rack seismic input is taken to be the average of the input motion at the ground and 1st floors in the X-direction. As shown earlier, CRCF canister staging racks are very stiff with a fundamental frequency of about 20 Hz or greater. It is not known how the staging racks will be evaluated for seismic events. They will likely be designed using response spectrum analysis but equivalent static coefficient methods may also be employed. For purposes of this fragility calculation, the demand will be based on envelope response spectrum analysis or an equivalent static coefficient analysis as specified in Reference N2.2.15.

The variables to consider for equipment response are:

- Qualification method
- Damping
- Modeling
- Mode combination
- Earthquake Direction

As shown in N6.2, the canister staging racks have a fundamental frequency of 20 to 30 Hz. These racks will be evaluated based on the spectral acceleration from this calculated fundamental frequency range. The demand is defined as the average DBGM-2 in-structure spectral accelerations at the ground and first floors at the calculated fundamental frequency range.

N6.4.1 Qualification Method

Since some form of dynamic analysis will be conducted to define the fundamental frequency of the component. Consequently there is no bias in the qualification method.

$$F_{QM\_1} := 1.0$$

$$\beta_{c\_QM\_1} := 0$$

The other factor of safety to be considered under the qualification method is the conservatism in the broadened and smoothed design floor response spectra. Nodes 22 and 24 (Ref. N2.2.12) represent the base mat and the resulting response spectra at each node are similar. Node 224 (Ref. N2.2.12) represents the floor level that is 32 feet above the ground floor. The average of the node 24 and node 224 spectra, as shown in APPENDIX N-A, are used. The median response case is taken as the 100 foot soil depth case using median soil properties. Uncertainty is determined from the difference between upper bound, median and lower bound soil properties. Table N6.4-1 presents comparison of the site wide broadened and smoothed spectra to the average median soil spectra for the X-direction. Digitized 5% damped spectra for nodes 24 and 224 of the CRCF from Reference N2.2.3 are used. See APPENDIX N-A for spectra plots.

Table N6.4-1 Comparison of 5% Damped Median & Design Spectral Amplification Factors

Freq. (Hz)	24 Median	224 Median	Rack Median	24 Design	224 Design	Rack Design	Des/Med
16	0.77	0.77	0.77	0.93	1.00	0.97	1.26
18	0.67	0.71	0.69	0.92	1.00	0.96	1.39
20	0.63	0.79	0.71	0.89	1.00	0.94	1.33
25	0.64	0.68	0.66	0.82	1.00	0.91	1.38
28	0.56	0.79	0.67	0.79	1.00	0.89	1.32
31	0.60	0.74	0.67	0.75	1.00	0.88	1.31
34	0.55	0.68	0.61	0.73	0.94	0.83	1.36

Seismic demand is primarily governed by horizontal demand in the X direction. Considering rack fundamental frequencies of 18 Hz for TAD canisters and 31 Hz for DOE canisters as computed in Section N6.3, from the above table, the margin in spectral shape at 18 Hz is 1.39 and at 31 Hz is 1.31 in the X direction

$$F_{QM\_2} := \frac{1.39 + 1.31}{2} = 1.35$$

Uncertainty in frequency will be treated with the modeling factor such that:

$$\beta_{c\_QM\_2} := 0$$

$$F_{QM} := F_{QM\_1} \cdot F_{QM\_2} \qquad F_{QM} = 1.35$$

$$\beta_{c\_QM} := \sqrt{\beta_{c\_QM\_1}^{2} + \beta_{c\_QM\_2}^{2}} \qquad \beta_{c\_QM} = 0$$

N6.4.2 Damping

Design damping is stated in Reference N2.2.15 to be as defined in ASCE/SEI 43-05, Reference N2.2.2. For welded metal structures at level 2 response, the damping is 4%. This is slightly conservative. Per Ref. N2.2.15, median damping for metal structures at Response Level 3 is 7%. It is judged that 4% would be a minus 1β .

Rack frequencies were evaluated to be about 18 and 31 Hz in Section N6.3. Therefore, the damping factor of safety and variability will be evaluated at these frequencies from Reference N2.2.3 median or raw spectra.

$Sa24\_7 := 0.623g$ $Sa224\_7 := 0.679g$

$Sa24\_4 := 0.707g$ $Sa224\_4 := 0.772g$

These are 7% and 4% damped spectral values at 18 Hz from the 100' median ISRS (Ref. N2.2.3).

$$Sa\_7 := \frac{Sa24\_7 + Sa224\_7}{2} \qquad Sa\_7 = 0.651 \cdot g$$

$$Sa\_4 := \frac{Sa24\_4 + Sa224\_4}{2} \qquad Sa\_4 = 0.739 \cdot g$$

$$F_{\delta\_18} := \frac{Sa\_4}{Sa\_7} \qquad F_{\delta\_18} = 1.136$$

$$\beta_{c\_\delta 18} := \ln\left(\frac{Sa\_4}{Sa\_7}\right) \qquad \beta_{c\_\delta 18} = 0.127$$

$Sa24\_7 := 0.568g$ $Sa224\_7 := 0.711g$

$Sa24\_4 := 0.628g$ $Sa224\_4 := 0.749g$

These are 7% and 4% damped spectral values at 31 Hz from the 100' median ISRS (Ref. N2.2.3).

$$Sa\_7 := \frac{Sa24\_7 + Sa224\_7}{2} \qquad Sa\_7 = 0.639 \cdot g$$

$$Sa\_4 := \frac{Sa24\_4 + Sa224\_4}{2} \qquad Sa\_4 = 0.688 \cdot g$$

$$F_{\delta\_28} := \frac{Sa\_4}{Sa\_7} \qquad F_{\delta\_28} = 1.077$$

$$\beta_{c\_\delta 28} := \ln\left(\frac{Sa\_4}{Sa\_7}\right) \qquad \beta_{c\_\delta 28} = 0.074$$

$$F_{\delta} := \frac{F_{\delta\_18} + F_{\delta\_28}}{2} = 1.106$$

$$\beta_{c\_\delta} := \frac{\beta_{c\_\delta 18} + \beta_{c\_\delta 28}}{2} = 0.101$$

N6.4.3 Modeling

Modeling is assumed to be median centered. For these staging racks, a relatively straightforward model is used to determine the fundamental frequency. Say that 18 Hz is the best estimate frequency for TAD canisters and 31 Hz is the best estimate frequency for DOE canisters as computed in Section N6.3. Let the 1 β uncertainty in frequency be plus or minus 2 Hz for TAD canisters and plus or minus 3 Hz for DOE canisters. (The resulting β is within the range of Ref. N2.2.1 on Pages 3-17, 3-18, and 3-49).

$F_M := 1.0$

For the TAD canisters

$fn\_minus\beta := 16Hz$ $fn\_plus\beta := 20Hz$

Use median soil spectra for modeling uncertainty. From Table N6.4-1:

$S_{a\_16} := 0.77g$ $S_{a\_18} := 0.69g$ $S_{a\_20} := 0.71g$

$\beta_{c\_M1} := \ln\left(\frac{S_{a\_16}}{S_{a\_18}}\right)$ $\beta_{c\_M1} = 0.11$

$\beta_{c\_M2} := \ln\left(\frac{S_{a\_20}}{S_{a\_18}}\right)$ $\beta_{c\_M2} = 0.029$

$\beta_{c\_MTAD} := \frac{\beta_{c\_M1} + \beta_{c\_M2}}{2}$ $\beta_{c\_MTAD} = 0.069$

For the DOE canisters

$fn\_minus\beta := 28Hz$ $fn\_plus\beta := 34Hz$

Use median soil spectra for modeling uncertainty. From Table N6.4-1:

$S_{a\_28} := 0.67g$ $S_{a\_31} := 0.67g$ $S_{a\_34} := 0.61g$

$\beta_{c\_M1} := \ln\left(\frac{S_{a\_28}}{S_{a\_31}}\right)$ $\beta_{c\_M1} = 0$

$\beta_{c\_M2} := \ln\left(\frac{S_{a\_31}}{S_{a\_34}}\right)$ $\beta_{c\_M2} = 0.094$

$$\beta_{c\_MDOE} := \frac{\beta_{c\_M1} + \beta_{c\_M2}}{2} \qquad \beta_{c\_MDOE} = 0.05$$

$$\beta_{c\_M} := \frac{\beta_{c\_MTAD} + \beta_{c\_MDOE}}{2} = 0.058$$

N6.4.4 Mode Combination

Horizontal strut response of the staging racks is considered to be primarily a single mode. Some contribution from higher modes is likely. Reference N2.2.1, page 3-50 suggests a range of 0.05 to 0.15 for Beta R depending on the model complexity. There is no Beta U.

$$F_{MC} := 1.0$$

$$\beta_{c\_MC} := 0.10$$

N6.4.5 Earthquake Component Combination

CRCF staging rack response is dominated by one horizontal direction of shaking. Therefore:

$$F_{ECC} := 1.0$$

$$\beta_{c\_ECC} := 0$$

N6.4.6 Equipment Response Summary

$$F_{RE} := F_{QM} \cdot F_{\delta} \cdot F_{M} \cdot F_{MC} \cdot F_{ECC}$$

$$F_{RE} = 1.493$$

$$\beta_{c\_RE} := \left(\beta_{c\_QM}^{2} + \beta_{c\_\delta}^{2} + \beta_{c\_M}^{2} + \beta_{c\_MC}^{2} + \beta_{c\_ECC}^{2}\right)^{0.5}$$

$$\beta_{c\_RE} = 0.153$$

N6.5 STRUCTURAL RESPONSE

N6.5.1 Spectral Shape Factor

This factor accounts for conservatism in the site-wide DBGM-2 design spectrum. The depth of alluvium at the Surface Facilities Area (SFA) varies from 30 feet to 200 feet. Uniform hazard spectra at the surface are calculated from site response analyses for alluvium depths of 30', 70', 100' and 200'. The site-wide design ground response spectrum is the envelope of the surface spectra of these four alluvium depths (Reference N2.2.9; also Section 6.2.2.1 for source information).

The best-estimate horizontal dominant frequency of the soil-structure system is 5.2 Hz for the CRCF at 100-foot alluvium of median properties (Attachment 1 of Reference N2.2.3). At this frequency:

$SA_{site} := 1.14g$ 5% damped site-wide spectral acceleration (APPENDIX N-B).

$SA_{100} := 1.06 \cdot g$ 5% damped spectral acceleration of the 100-foot best-estimate alluvium depth case in the northeast area where the preclosure surface facilities are located.

$$F_{SA} := \frac{SA_{site}}{SA_{100}}$$

$F_{SA} = 1.075$

Since uncertainty in the UHS is derived from uncertainty in the seismic hazard curves which will be included in the final risk quantification, no uncertainty is included under the spectral shape factor to avoid double-counting the hazard uncertainty, hence

$\beta_{U\_SA} := 0$

$\beta_{R\_SA} := 0.20$ Random variability to account for peak-to-valley variability of the smoothed UHS (Reference N2.2.1, Table 3-2).

$\beta_{c\_SA} := \sqrt{\beta_{U\_SA}^2 + \beta_{R\_SA}^2}$ $\beta_{c\_SA} = 0.2$

N6.5.2 Damping Factor

This factor is to account for conservatism in the hysteresis damping of the building structure used in the seismic response analysis. Due to the high radiation damping of the foundation media, the effect of structure damping is insignificant. Thus,

$F_{\delta} := 1.0$

$\beta_{U\_\delta} := 0$ Since a conservative median factor of safety is used for structure damping, no value is assigned to the uncertainty logarithmic standard deviation.

$\beta_{R\_\delta} := 0$

$\beta_{c\_\delta} := \sqrt{\beta_{U\_\delta}^2 + \beta_{R\_\delta}^2}$

$\beta_{c\_\delta} = 0$

N6.5.3 Modeling Factor

The Tier 1 lumped mass multiple-stick model of the CRCF includes the stiffness of various reinforced concrete walls and distribution of mass at each floor. The floors are assumed to be rigid diaphragms tying the different sticks together. Torsional response of the structure is captured through modeling eccentricity between the center of mass and center of rigidity of each floor. The foundation media underneath the buildings are modeled with soil springs and dashpots based on elastic half space theory with adjustment to account for layering effect of alluvium overlying tuff. Per Reference N2.2.11, BSC recognizes that final design will be accomplished by a more explicit finite element model and it is acceptable to consider the modeling factor to be median centered in these seismic fragility evaluations, thus

$F_M := 1.0$

$\beta_{R\_M} := 0$ Since there is no randomness in modeling.

Uncertainty of structure frequencies predicted from mathematical modeling varies from 0.15 to 0.35 depending on the sophistication of the model (Reference N2.2.1). The value of 0.35 is for a fairly approximate model and the value 0.15 is appropriate for a detailed model. Based on the complexity of the CRCF structure and the mathematical model used for the Tier 1 ISRS analysis, it is judged that the calculated CRCF frequency has a logarithmic standard deviation of 0.25.

$\beta_f := 0.25$ Uncertainty in building frequency.

$f_m := 5.2 \cdot Hz$ Best-estimate frequency

$f_{upper} := f_m \cdot e^{\beta_f}$ Upper bound frequency

$f_{upper} = 6.677 \cdot Hz$

$SA_{upper} := 1.05g$ 5% damped spectral acceleration at f_{upper} read off from the mean 5E-4 UHS of the 100-foot alluvium depth case (APPENDIX N-B). This value is less than the value at the best-estimate frequency.

$f_{lower} := f_m \cdot e^{-\beta_f}$ Lower bound frequency

$f_{lower} = 4.05 \cdot Hz$

$SA_{lower} := 1.02 \cdot g$ 5% damped spectral acceleration at f_{lower} read off from the mean 5E-4 UHS of the 100-foot alluvium depth case. This value is less than the value at the best-estimate frequency.

$\beta_{U\_f} := 0$ Since the spectral value at the best-estimate frequency is greater than that at either the lower bound or upper bound frequency.

$\beta_{U\_ms} := 0.15$ Uncertainty of mode shape (Reference N2.2.1, page 3-18)

$$\beta_{U\_M} := \sqrt{\beta_{U\_f}^2 + \beta_{U\_ms}^2}$$

$$\beta_{U\_M} = 0.15$$

$$\beta_{c\_M} := \sqrt{\beta_{R\_M}^2 + \beta_{U\_M}^2}$$

$$\beta_{c\_M} = 0.15$$

N6.5.4 Modal Combination

Since the direct integration time history method is used in the Tier 1 ISRS analysis (Reference N2.2.3), the modal combination method factor of safety is unity and there is no variability associated with modal combination.

$$F_{MC} := 1$$

$$\beta_{R\_MC} := 0$$

$$\beta_{U\_MC} := 0$$

$$\beta_{c\_MC} := \sqrt{\beta_{R\_MC}^2 + \beta_{U\_MC}^2}$$

$$\beta_{c\_MC} = 0$$

N6.5.5 Soil-Structure Interaction

The Tier 1 seismic response analyses of the CRCF used the site-wide $5*10^{-4}$ mean uniform hazard spectra as the DBGM-2 input motion. Spectrum compatible time histories are used as the input motion for the time history analyses. The conservatism in the site-wide spectra was accounted for in the spectral shape factor above. Strain compatible soil properties of 100-foot and 200-foot deep alluvium are used to calculate frequency-independent soil springs and soil damping coefficients. Soil radiation damping is introduced into the model by using dashpots. Damping coefficients equal to 75% of the computed values for translational degrees of freedom and the full computed rotational damping values are used in the response analyses (Reference N2.2.3). Conservatism or unconservatism in SSI will be minimized for final SSI analyses used to develop equipment design seismic input. Before the final SSI analyses are completed, the Tier 1 SSI analysis is taken to represent the best-estimate responses per BSC recommendations in Reference N2.2.16.

$$F_{SSI\_1} := 1.0$$

$$\beta_{R\_SSI\_1} := 0$$

$$\beta_{U\_SSI\_1} := 0.25$$

Uncertainty of the median-centered state-of-the-art SSI method based on past probabilistic seismic response analyses using the same method.

$$\beta_{c\_SSI\_1} := \sqrt{\beta_{R\_SSI\_1}^2 + \beta_{U\_SSI\_1}^2} \qquad \beta_{c\_SSI\_1} = 0.25$$

It is judged that the median seismic capacity of the equipment, expressed in terms of peak ground acceleration, is close to that of BDBGM. Due to soil nonlinearity, amplification of the input ground motion at BDBGM will be different from that of DBGM-2. The second factor of safety is to account for this difference and is estimated using the DBGM-2 raw spectra and the BDBGM raw spectra at different frequencies as shown in Table N6.5-1.

For canister staging racks with frequency in the range of 16 to 34 Hz

$Factor := mean(0.83, 1.07, 0.97, 1.05, 1.03, 0.90, 0.85, 0.91)$ Table N6.5-1

$Factor = 0.951$

$F_{SSI\_2} := \frac{1}{Factor}$

$F_{SSI\_2} = 1.051$

$F_{SSI} := F_{SSI\_1} \cdot F_{SSI\_2}$

$F_{SSI} = 1.051$

$\sigma := Stdev(0.83, 1.07, 0.97, 1.05, 1.03, 0.90, 0.85, 0.91)$ Table N6.5-1

$\sigma = 0.092$

$\beta_{c\_SSI\_2} := \frac{\sigma}{Factor}$

$\beta_{c\_SSI\_2} = 0.097$

$\beta_{c\_SSI} := \sqrt{\beta_{c\_SSI\_1}^2 + \beta_{c\_SSI\_2}^2}$

$\beta_{c\_SSI} = 0.268$

Table N6.5-1 Comparison of Spectral Amplification Factors of DBGM-2 vs. BDBGM

	DBGM-2			
Freq.	24 Median	224 Median	Rack Median	Median Amplif.
16	0.77	0.77	0.77	1.54
18	0.67	0.71	0.69	1.39
20	0.63	0.79	0.71	1.42
22	0.65	0.70	0.67	1.35
25	0.64	0.68	0.66	1.32
28	0.56	0.79	0.67	1.35
31	0.60	0.74	0.67	1.35
34	0.55	0.68	0.61	1.23
ZPA	0.46	0.53	0.50	
	BDBGM			
Freq.	24 Median	224 Median	Rack Median	Median Amplif.
16	1.28	1.32	1.30	1.27
18	1.46	1.57	1.52	1.48
20	1.29	1.53	1.41	1.38
22	1.38	1.53	1.46	1.42
25	1.25	1.54	1.40	1.37
28	1.12	1.37	1.25	1.22
31	1.03	1.30	1.17	1.14
34	1.06	1.22	1.14	1.12
ZPA	0.96	1.08	1.02	
Freq.	Ratio of BDGM to DBGM-2 Amplif.			
16		0.83		
18		1.07		
20		0.97		
22		1.05		
25		1.03		
28		0.90		
31		0.85		
34		0.91		

Note that the DBGM-2 spectral values come from Figures N-A-1 and N-A-2 of Appendix N-A and the BDBGM spectral values come from from Figures N-C-1 and N-C-2 of Appendix N-C. The median amplification is the rack median spectral acceleration divided by the ZPA value. The rack median accelerations are the average of the Node 24 and Node 224 values.

N6.5.6 Ground Motion Incoherence

$L1 := 327 \cdot ft$ — East-west dimension of the CRCF excluding the 49'-6" and 43' extensions at the east and west ends, respectively (Reference N2.2.10).

$L2 := 336 \cdot ft$ — North-south dimension of the CRCF excluding the 56' extension at the south end.

$L_{eq} := \sqrt{L1 \cdot L2}$ — Equivalent foundation dimension of the CRCF

$L_{eq} = 331.5\ ft$

The ground motion incoherence reduction factor is a function of foundation size and frequency of response. For a 150 foot plan dimension foundation, the following reduction factors are presented in Reference N2.2.1 in page 3-22. Interpolation or extrapolation may be used to calculate the reduction factor for different dimensions and/or frequencies.

$L_{std} := 150 \cdot ft$ Foundation dimension for which the reduction factors in Reference N2.2.3 are calculated.

$f_5 := 5$ Frequency in Hz

$RF_5 := 1$ Reduction factor for response frequency at 5 Hz

$f_{10} := 10$ Frequency in Hz

$RF_{10} := 0.9$ Reduction factor for response frequency at 10 Hz

$RF_{5\_eq} := RF_5$ Reduction factor at 5 Hz, given the CRCF equivalent foundation dimension

$$RF_{10\_eq} := 1 - \left[\left(1 - RF_{10}\right) \cdot \frac{L_{eq}}{L_{std}} \right]$$ Linear extrapolation

$RF_{10\_eq} = 0.779$ Reduction factor at L_{eq} dimension and 10 Hz frequency of response.

At 5.2 Hz which is the fundamental frequency of horizontal response of the CRCF

$f_6 := 5.2$ Frequency in Hz

Calculate the reduction factor at 5.2 Hz frequency by interpolation

$RF_{6\_eq} := 0.4$ An arbitrary value to initiate the equation solver below.

Given

$$\frac{\log\left(RF_{10\_eq}\right) - \log\left(RF_{5\_eq}\right)}{\log\left(RF_{6\_eq}\right) - \log\left(RF_{5\_eq}\right)} = \frac{\log\left(f_{10}\right) - \log\left(f_5\right)}{\log\left(f_6\right) - \log\left(f_5\right)}$$

$a := \text{Find}\left(RF_{6\_eq}\right)$

$a = 0.986$ Reduction factor

Thus, the ground motion incoherence factor of safety is

$$F_{GMI} := \frac{1}{a}$$

$$F_{GMI} = 1.014$$

$$\beta_{U\_GMI} := \frac{1}{2}\cdot\ln\left(\frac{1}{a}\right)$$

A reduction factor of 1.0 (i.e., no reduction) is estimated to be two standard deviation from the calculated median factor of 0.91 (Reference N2.2.1, Page 3-23).

$$\beta_{U\_GMI} = 0.01$$

$$\beta_{R\_GMI} := 0$$

$$\beta_{c\_GMI} := \sqrt{\beta_{R\_GMI}^{2} + \beta_{U\_GMI}^{2}}$$

$$\beta_{c\_GMI} = 0.01$$

N6.5.7 Structural Response Factors

$$F_{RS} := F_{SA}\cdot F_{\delta}\cdot F_{M}\cdot F_{MC}\cdot F_{SSI}\cdot F_{GMI}$$

$$F_{RS} = 1.147$$

$$\beta_{c\_RS} := \sqrt{\beta_{c\_SA}^{2} + \beta_{c\_\delta}^{2} + \beta_{c\_M}^{2} + \beta_{c\_MC}^{2} + \beta_{c\_SSI}^{2} + \beta_{c\_GMI}^{2}}$$

$$\beta_{c\_RS} = 0.367$$

N6.6 FRAGILITIES FOR DBGM-2 DESIGN

Fragility is the product of the capacity factor, equipment response factor, structural response factor and PGA of the DBGM-2. The composite uncertainty, βc, is the SRSS of the uncertainties for capacity, equipment response and structural response.

$PGA := 0.453g$ Peak ground acceleration of the DBGM-2 design spectrum (Reference N2.2.9; also Section 6.2.2.1 for source information).

Capacity Factors for CRCF Staging Rack Steel Supports

$F_C = 1.611$ $\beta_{c\_C} = 0.205$

Equipment Response Factor

$F_{RE} = 1.493$ $\beta_{c\_RE} = 0.153$

Structural Response Factor

$F_{RS} = 1.147$ $\beta_{c\_RS} = 0.367$

Canister Staging Rack Horizontal Strut Fragility

$F_{total} := F_C \cdot F_{RS} \cdot F_{RE}$

$F_{total} = 2.759$

$A_m := F_{total} \cdot PGA$

$A_m = 1.25 \cdot g$ Median seismic capacity in terms of PGA

$\beta_c := \sqrt{\beta_{c\_C}^2 + \beta_{c\_RS}^2 + \beta_{c\_RE}^2}$

$\beta_c = 0.447$

$HCLPF := A_m \cdot e^{-2.33 \cdot \beta_c}$

$HCLPF = 0.441 \cdot g$

N6.7 FRAGILITIES FOR SCALED BDBGM DESIGN

Reference N2.2.14 notes that the canister staging racks are a problem for the preclosure safety analysis (PCSA) if the median capacity is less than 3.5 g. As can be observed from Section N6.6, the median capacity is 1.25 g given that the racks are designed to the DBGM-2 input level. Hence, design to DBGM-2 may not achieve this goal and a design at higher ground motion would be required. As a sensitivity study for use within the PSA analyses, an additional fragility has been estimated wherein the ITS equipment design basis is considered to be the BDBGM scaled by an additional factor. Such a design would use exactly the same design codes and standards as used for design to DBGM-2. In addition, in-structure response spectra would be enveloped and broadened in the exact same manner. Differences would be only that the ground motion would be higher and soil nonlinearities in the soil-structure interaction analyses may result in different spectral shapes between the BDBGM and the DBGM-2 ISRS.

Review of the BDBGM and the DBGM-2 ISRS in Appendix N-C indicates that there is no significant difference in the peak spectral amplification (average of 2.02 that is equal to the BDBGM PGA of 0.914 g divided the DBGM-2 PGA of 0.453 g). However, even this level of design may not meet the required median capacity of 3.5 g and an additional scale factor would be needed. An additional scale factor of 1.4 achieves this goal. As a result, the fragilities for scaled BDBGM design are 1.4 times 2.02 times the DBGM-2 fragilities as shown below:

$$A_{m\_BDBGM} := 2.02 \cdot A_m$$

$$A_{m\_BDBGM} = 2.525 \cdot g$$

$$A_{m\_SBDBGM} := 1.4 \cdot A_{m\_BDBGM}$$

Median seismic capacity in terms of PGA for scaled BDBGM design level

$$A_{m\_SBDBGM} = 3.535 \cdot g$$

$$\beta_c = 0.447$$

$$HCLPF_{SBDBGM} := A_{m\_SBDBGM} \cdot e^{-2.33 \cdot \beta_c}$$

$$HCLPF_{SBDBGM} = 1.247 \cdot g$$

Design to the scaled BDBGM ground motion level is one approach that will assure the required capacity of the canister staging racks. Such a design measure may turn out to not be necessary during actual design of this staging rack configuration. This configuration is expected to be highly redundant and robust when detailed design is complete. At that time it may be possible to reduce the design level and still achieve acceptable seismic capacity. Alternately, timing considerations within the PCSA could be used to potentially lower the required 3.5 g capacity.

N7. SUMMARY

The governing failure mode of the CRCF canister staging racks has been taken to be buckling of horizontal support steel members that extend out to the building walls. The staging racks cannot collapse until these members fail by buckling. The seismic fragility of the rack horizontal support members for this failure mode is summarized in Table N7-1:

Table N7-1 Fragilities for Canister Staging Racks Designed for DBGM-2

Design Level	F_C	F_{RE}	F_{RS}	Am (g)	β_{c_C}	β_{c_RE}	β_{c_RS}	β_c	HCLPF(g)
DBGM-2	1.61	1.493	1.147	1.25	0.205	0.153	0.367	0.45	0.44
Scaled (1.4) BDBGM	1.61	1.493	1.147	3.53	0.205	0.153	0.367	0.45	1.25

For DBGM-2 design, the HCLPF is less the DBGM-2 PGA of 0.453 g and the median capacity is less than the required capacity of 3.5 g. This implies that the canister staging racks are not very robust and are susceptible to earthquake shaking. However, it must be noted that fragility developed in this calculation is based on a limiting case where the demand is equal to the design capacity. In actual designs, this is typically not the situation, thus the limiting case fragility developed in this calculation is conservative. When actual designs or detailed specifications are available, a more refined fragility could be developed that would not be as conservative as the limiting case value developed herein. However, to assure that a median capacity of 3.5 g is achieved the canister staging racks could be designed to the same criteria as for DBGM-2 except for increase input excitation to 1.4 times the BDBGM motion. Table N7-1 shows that the required median capacity is achieved by this approach.

Canister staging racks are very stiff steel structures whose stiffness is derived from axial behavior of horizontal supporting members and of diagonal bracing members in vertical planes. With both braced frame behavior and horizontal supports at two elevations to all four walls, this structure has a great deal of redundancy and is likely to have very high seismic capacity. However, detailed designs are not currently available such that it must be assumed that all members are designed to their full capacity. Because of the many load paths in this design it is very likely that there will be substantial margin in the structural members.

The canister staging racks as shown in References N2.2.4 and N2.2.5 are a very robust design that is not very susceptible to earthquake shaking such that when the seismic fragility of the final rack design is computed the median capacity and HCLPF values will be much greater than those shown in the above table.

APPENDIX N-A
5% Damped In-Structure Response Spectra for CRCF (Reference N2.2.3)

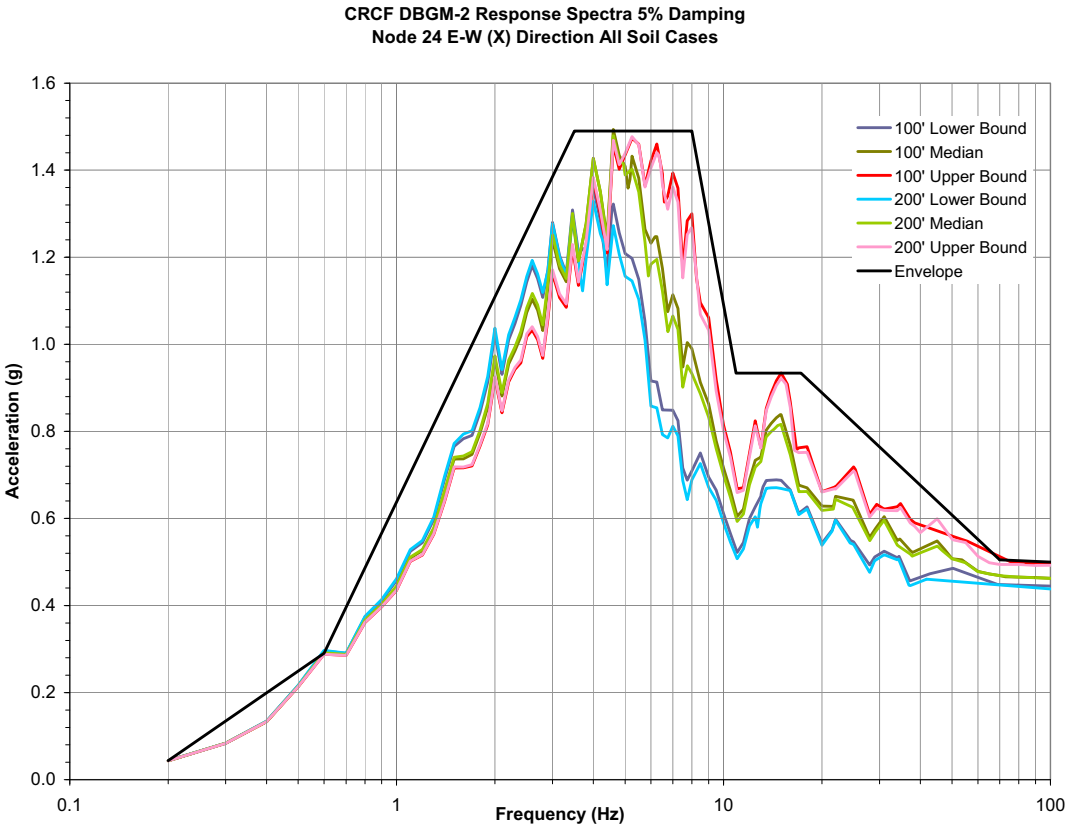

Figure N-A-1. 5% Damped Design ISRS and 100' and 200' Alluvium Depths ISRS at Ground Floor (X-Direction)

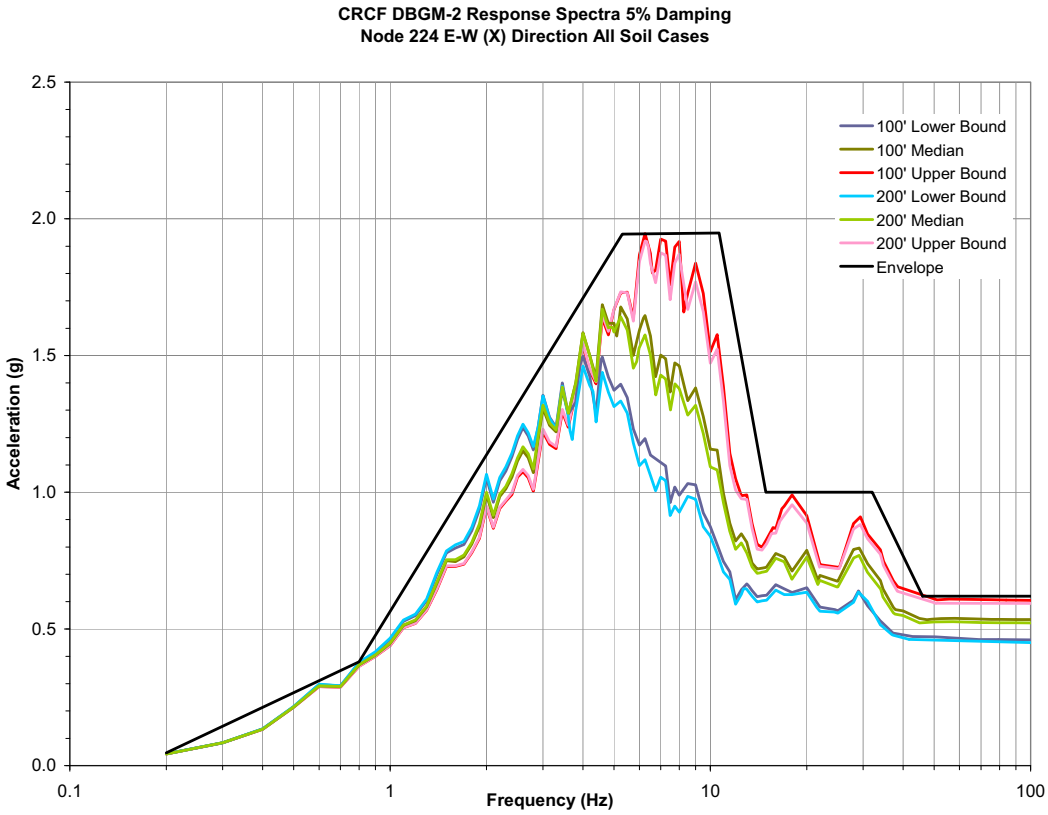

Figure N-A-2. 5% Damped Design ISRS and 100' and 200' Alluvium Depths ISRS at 32 foot Building Elevation (X-Direction)

APPENDIX N-B
UHS for 5E-4 APE

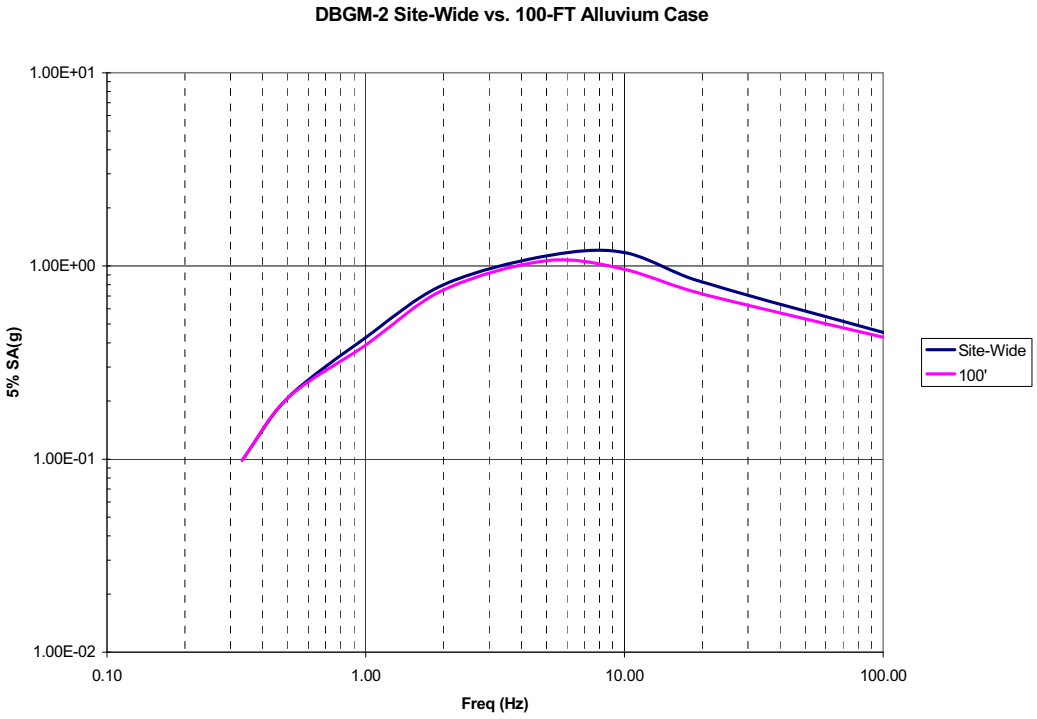

Figure N-B-1. UHS of Site-Wide and 100 Foot Alluvium Cases (See Section 6.2.2.1 for source information)

APPENDIX N-C
Comparison OF BDBGM & DBGM-2 ISRS
(Reference N2.2.3)

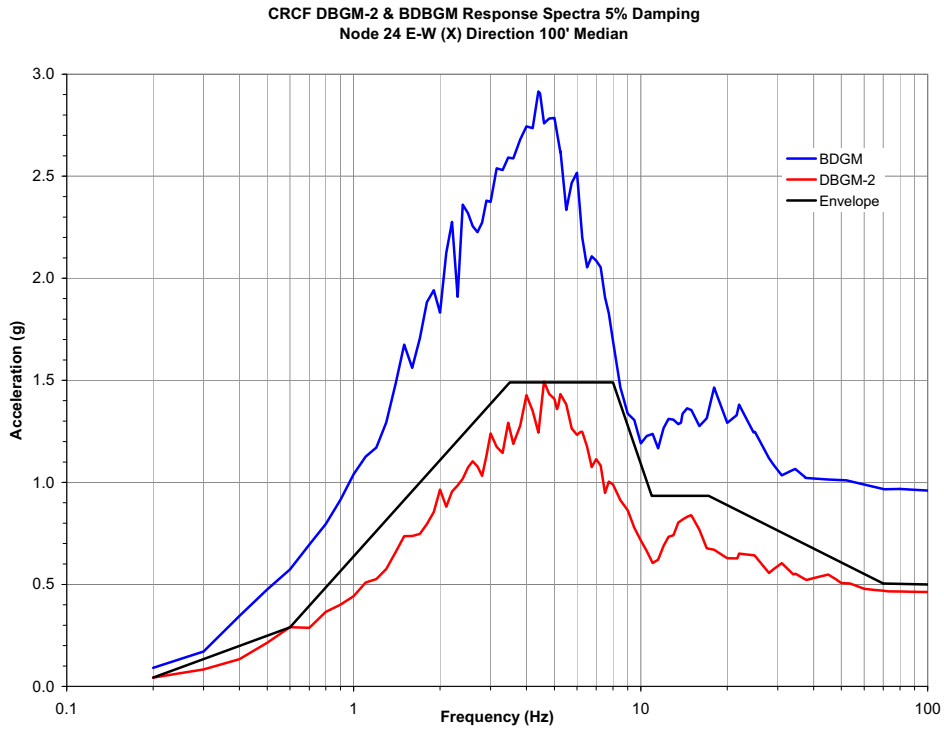

Figure N-C-1. 5% Damped 100' Alluvium Depth ISRS for BDBGM and DBGM-2 at Ground Floor (X-Direction)

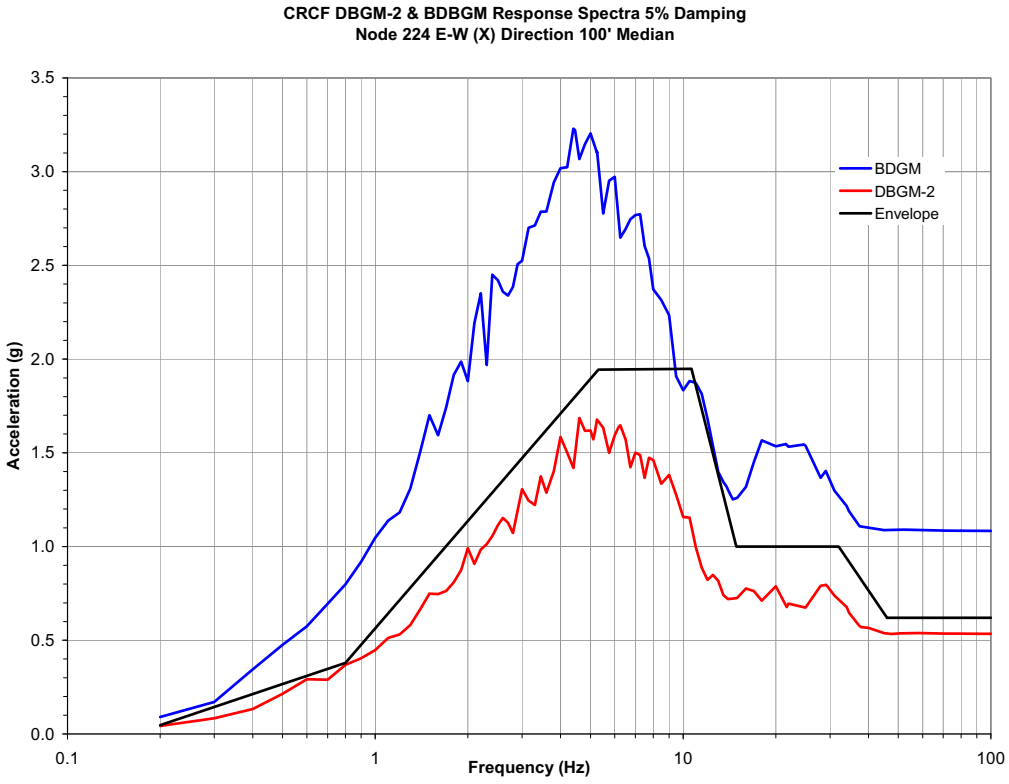

Figure N-C-2. 5% Damped 100' Alluvium Depth ISRS for BDBGM and DBGM-2 at 32 Foot Building Elevation (X-Direction)